UNIVERSITY OF TRENTO

International PhD Program in Biomolecular Sciences
26th Cycle

"RNA-based therapeutic approaches for FTDP-17"

Tutor

Prof. Michela Alessandra Denti

RNA Biology and Biotechnology

Centre for Integrative biology

Ph.D. Thesis

of

Kavitha Siva

RNA Biology and Biotechnology

Centre for Integrative biology

Academic Year 2013-2014

Declaration of Authorship

*'I **Kavitha Siva,** confirm that this is my own work and the use of all material from other sources has been properly and fully acknowledged'.*

Yours sincerely

(Kavitha Siva)

Acknowledgements

"Gratitude is the most exquisite form of courtesy." - Jacques Maritain

I take this opportunity to thank all the people who have actively contributed to the completion of this dissertation. This rewarding journey would not have been possible without the contribution of many members.

I owe my deepest gratitude to my supervisor Prof. Michela Alessandra Denti to have provided me this wonderful prospect to address multiple questions in resolving one of the puzzles in the 'neurodegenerative world'. She has provided me with the platform to learn molecular biology techniques, trained me to make meticulous observations and guided me in finding novel solutions. I extend my special thanks to her for supporting my innovative approaches and ideas during the second year of PhD and to have provided me the freedom to apply my knowledge obtained so far which has finally paved way for a patent application. Her supervision and guidance has not only enabled successful completion of this thesis but also has provided insights in to various dimensions of the biological world of science.

There are different people who have significantly played a part in this journey of getting lost in to the world of 'nowhere' to 'now- here' from 2011 to 2015.
I would like to thank the lab memebers of the laboratory of RNA biology and biotechnology Dr.Valerio Del Vescovo, Dr.Margherita Grasso and Niccolo Bacchi for their support. I also acknowledge Dr. Giuseppina Covello with acquiesce for sharing her project interests, providing training in molecular biology techniques and executing an advisory role during the years 2011-2012.

I am grateful to my collaborators at the University College London, Dr. Rohan De Silva for providing me a new scope to work in the field of neurodegeneration and to have provided guidance throughout my internship period. Dr. Roberto Simone for his continuous support in a number of ways through sharing of his skills and competence, especially during my stay at the Reta Lila Weston institute, UCL, after which he has been my external co-advisor to-date. I would also like to render my heartfelt thanks to him for providing suggestions for the write-up on the sections of collaborative project.

It is a pleasure to thank Dr. Valentina Adami and Dr.Pamela Gatto, the members of the High throughput screening facility team at the Centre Ior integrative biology (CIBIO) for their assistance in the screening analysis. Dr.Valentina Adami is a true

'கற்க கசடறக் கற்பவை கற்றபின் நிற்க அதற்குத் தக'

'கேடில் விழுச்செல்வம் கல்வி யொருவற்கு மாடல்ல மற்றை யவை'

— திருவள்ளுவர்

பிற நாட்டில் இக்கல்வியை பெற்றிருந்தாலும் என் கினிய தமிழுக்கும் என்னுடைய தமிழ் மண்ணுக்கும் இத்தனை சமர்பணிக்கின்றேன். தமிழர் நம் பங்களிப்பை இச்சமுதாயத்திற்கு பயனுறச் செய்வோம்.

— கவிதா சிவா

PREFACE

Neurodegenerative diseases are linked to altered splicing mechanisms (Mills *et al.,* 2012). Fronto temporal dementia and parkinsonism linked to chromosome 17 (FTDP-17) is one such disease that stems from the differential splicing caused due to mutations in Microtubule associated protein tau (*MAPT*) gene (Esther *et al.,* 2002).

This PhD thesis focuses on developing RNA-based therapeutic approaches to address FTDP-17.

CHAPTER 1 introduces a broad range of topics such as splicing mechanism, neurodegenerative diseases associated with splice defects, therapeutic tools to modulate such splice defects in the context of neurogenetic diseases and possible applications of available tools for FTDP-17.

CHAPTER 2 explores an exon skipping strategy to modulate splice defects in the context of FTD-17 using small nuclear RNAs **(snRNAs).**

CHAPTER 3 is based on a short interfering RNA **(siRNA)** approach to modulate post-transcriptional gene silencing of specific isoform associated to FTDP-17.

CHAPTER 4 employs long non coding RNA **(lncRNA)** to mediate post transcriptional repression of tau protein associated to FTDP-17 and deciphers its auxiliary role in splicing of exon 10

CHAPTER 5 elaborates on the future perspectives of all the above mentioned approaches to find a cure for FTDP-17.

CHAPTER 1. INTRODUCTION

1.1. RNA processing and gene expression

In 1958, Francis Crick stated that;

"In its simplest form the sequence hypothesis assumes that the specificity of a piece of nucleic acid is expressed solely by the sequence of its bases, and that this sequence is a (simple) code for the amino acid sequence of a particular protein.

According to this sequence hypothesis, which is well known as the "Central dogma" of molecular biology, a segment of DNA, called gene, is transcribed into RNA (precisely messenger-RNA, mRNA) that is then converted through a process called translation, into a protein (Crick F, 1970). The intermediate mRNA carries the essential information to form the functional protein **(Fig.1).**
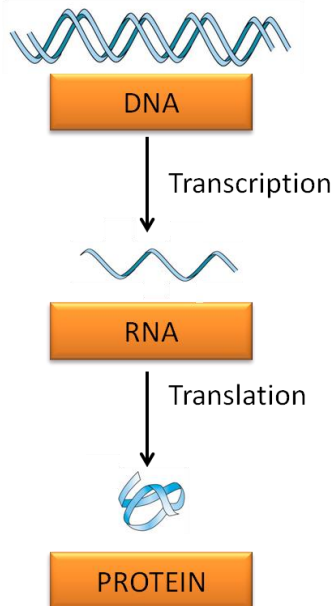
Fig. 1 | Schematic representation of the central dogma of life in which DNA is transcribed in to RNA which is translated to form proteins

The steps followed by the mRNA to allow expression of its gene are a highly complex and regulated process. Differential gene expression is crucial for growth, differentiation, development and cell survival in various situations, including environmental stress. It is therefore very important that all these processes are tightly controlled to minimise cell energy, and reduce errors that might affect survival of the cells.

Transcription is the process by which a template strand of DNA is utilized by specific RNA polymerases to generate one of the following distinct classifications of RNA (Lodish *et al.,* 2000, Cooper *et al.,* 2003, Wita *et al.,* 2006, Gueneau de Novoa, *et al.,* 2004, Vazquez, *et al.*, 2004, Watanabe, *et al.,* 2008, Amarlal *et al.,* 2008).

1. Messenger RNAs (mRNAs): A class of RNAs templates used by the translational machinery to determine the order of amino acids which forms the protein through translation.

2. Transfer RNAs (tRNAs): A class of small RNAs that interacts with the mRNAs to allow correct insertion of amino acids into the elongating polypeptide chain.

3. Ribosomal RNAs (rRNAs): A class of RNAs that cluster together with numerous ribosomal proteins, to form the ribosomes. Ribosomes attach to the mRNAs and form a catalytic domain into which the tRNAs enter with their attached amino acids.

4. Small RNAs: A class of RNAs that includes the small nuclear RNAs (snRNAs) and small nucleolar RNAs involved in RNA splicing, microRNAs (miRNAs) and short interfering RNAs (siRNAs) involved in the modulation of gene expression.

5. Long non coding RNAs (lncRNAs) involved in regulation of gene expression.

How is a functional mRNA formed? The precursor mRNAs (pre-mRNAs) are transcribed by RNA Pol II in the nucleus and undergoes various post-transcriptional modifications to form stable mature mRNAs. Along with that, the mRNAs undergo co-transcriptional events composed of: 5'-capping, 3'end-processing, splicing and RNA editing, which lead to the formation of mature transcripts (Maniatis *et al.,* 2002) **(Fig.2)**.

The matured mRNA transcript is then exported from the nucleus in to the cytoplasm where it begins to serve as a template for protein synthesis.
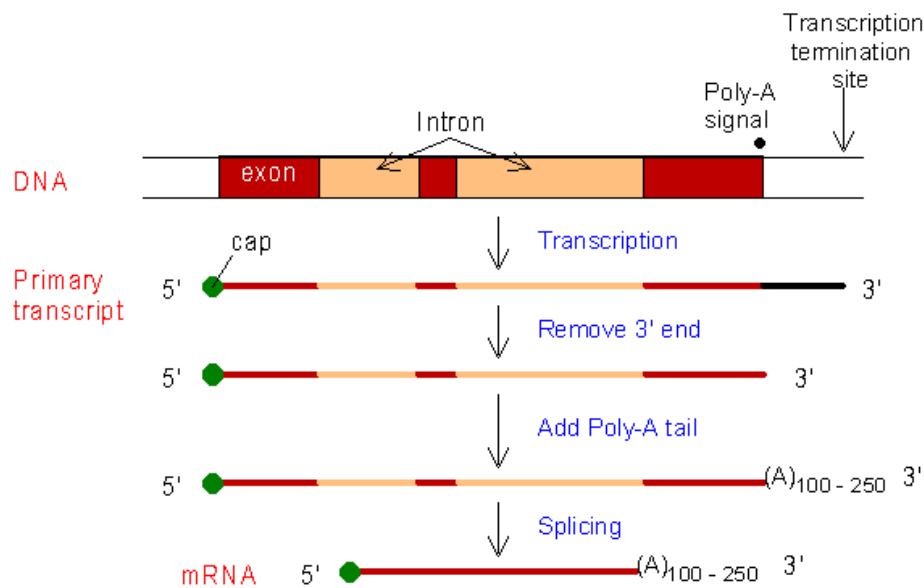
Fig. 2 | Schematic representation of RNA processing in which the primary transcript undergoes 5' end capping and 3' end processing followed by polyadenylation to form the functional mRNA.

1.1.1. 5'end capping

The capping event is comprised of the addition of 7-methylguanosine (m^{7}G) to the 5' end of the nascent pre-mRNA. This step protects the 5'-3' exonuclease mediated degradation of the pre-mRNA (Beelman *et al.*, 1995). The 5'cap further mediates export from the nucleus to the cytoplasm, thus promoting translation of the mRNA (Gross *et al.*, 2003).

1.1.2. 3'end processing

The 3' end processing is a two step reaction that comprises the following sub-steps:

(i) The pre -mRNA cleavage is mediated by the binding of the enzyme cleavage and polyadenylation specific factor (CPSF) to the AAUAAA consensus sequence (Beaudoing *et al.*, 2000) thus initiating cleavage at the 5'-CA-3' dinucleotide located 10-35 bases downstream its binding site.

10

(ii) Polyadenylation at the 3' end of the transcript which is initiated after the cleavage through the polymerase A enzyme that adds a polyA tail (composed of 200-250 adenine residues). PABII (Poly A binding protein) binds to the nascent poly A tail and stabilizes the pre-mRNA through protection from exonuclease digestion (Gromak *et al.,* 2004).

1.1.3. Splicing

In 1977, Nobel laureates, Dr. Richard Roberts and Dr. Phillip Sharp independently discovered that the genes were present in the genetic material as distinct and separate segments in the viral genome. They also hypothesised that a specific gene regulation mechanism is required for the production of proteins from the split genes.

Within half a year after the description of split genes and RNA splicing in the context of viral genome, such similarities in containing discontinuous fragments of genes were observed in eukaryotic cells as well (Rabbits *et al.*, 1978).

The majority of eukaryotic genes contain several introns and during the process of RNA synthesis, both introns and exons are transcribed from the DNA template. Before the export of mature mRNA from the nucleus to the cytoplasm, the introns need to be excised from the primary transcript followed by the joining of flanking exons. This process is called splicing in which the intervening introns are removed and the coding exons are joined together to form the correct protein reading frame (Roca *et al.*, 2013).

Splicing is mediated and regulated by the different regulatory elements located both within the exons and introns, guiding the splicing complex and auxiliary RNA binding proteins (Ward AJ *et al.*, 2010). A detailed description on pre-mRNA splicing is described in the following section.

1.1.3 (i) Evolution of alternative splicing

How did alternatively spliced exons evolve and enter in to genomes? Human-mouse comparative analyses revealed that a recent creation and/or loss of an exon is associated with alternative splice event (Maor *et al.*, 2003, Thanaraj *et al.*,

2003, Nurtdinov *et al.*, 2003). There are three known evolutionary mechanisms known to be involved in splicing (Keren *et al.*, 2013):

- Exon shuffling
- Exonisation of intronic sequences
- Transition of constitutive exon to an alternative exon.

Exon shuffling

The exon shuffling theory was proposed by Walter Gilbert in 1978 and he suggested the creation of a new chimeric protein as a result of shuffled exons provides an evolutionary advantage to the organism (Gilbert *et al.,* 1978) **(Fig.3)**. Although many studies have proved or disproved this theory, increasing evidences suggest a correlation between exon borders and protein domains (Dodlittle *et al.,* 1995, Kolkman *et al.,* 2001, Liu *et al.,* 2004). Recent analysis on exons of human and mice suggests that newly duplicated exons tend to retain the splicing status of their original exons (Peng *et al.,* 2009). The process of exon shuffling increases in proportion to the evolution of complex genome (Keren H *et al.,* 2010).
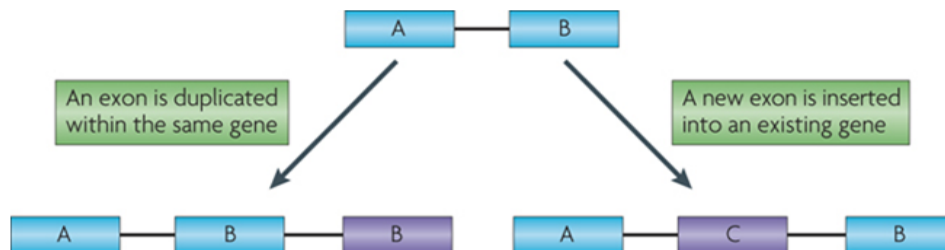
Fig. 3 | Schematic representation of exon shuffling in which the constitutive exons are represented as blue blocks, alternative exons as purple blocks and introns as solid lines. (Keren H *et al.,* 2010).

Exonisation

This process involves the transition of genomic sequence to exons. It was first suggested as a mechanism involving acquisition of 5' region in bovine thyroglobulin (TG) gene. This was further supported through many other studies in human and other vertebrate genomes.

About half of the human genome stems from the repeat forming transposable elements (TE) and are prone to exonisation. The random mutations in intronic sequences and RNA editing, both account for the creation of a true 3' or 5' splice site thus enabling spliceosome recognition and leading to exonisation of TE. This process has been extensively studied in special type of TE called *Alu* elements (Keren H *et al.,* 2010).

Transition

In the transition process, alternative cassette exons are derived from constitutively spliced exons **(Fig. 4)**. This can be accomplished through the following ways:

- Accumulation of mutations in splice sites leading to exon skipping
- Formation of a dsRNA secondary structure from 2 *Alu* exons in opposite orientations to each other thus influencing all the altered splice events in the downstream exon.

Although conserved exons maintain a specific splice pattern, reconstruction of evolution has imposed a shift from constitutive to alternative splicing. This shift arises due to mutations in the splice site that blocks binding of U1 snRNA to its proximity. Mutations in splice site also lead to creation of new splice site signals that competes with the original splice site (Keren H *et al.,* 2010).
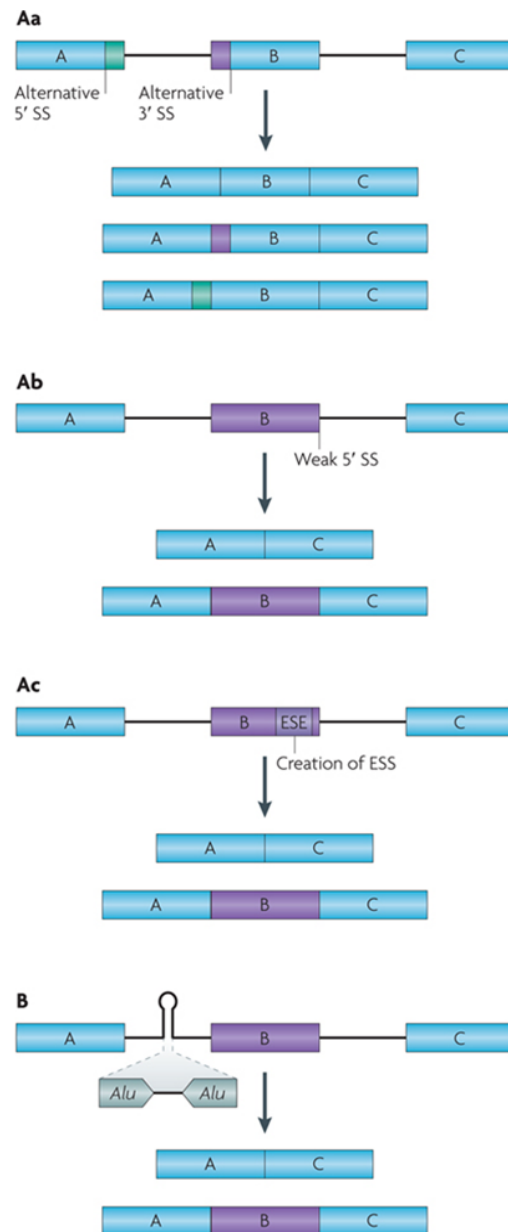
Fig. 4 | Process of conversion from constitutive to alternative splicing

A | Mutations that lead to insufficient recognition of the exon resulting in exon skipping. **A.a|** Mutations that lead to a new alternative 5′ splice site (5′ SS) or 3′ SS. **A. b|** Mutations that lead to insufficient recognition of the 5′ SS. **A. c|** Mutations in exons (or introns) that can disrupt an exonic splicing enhancer (ESE) or intronic splicing enhancer (ISE) or may create an exonic splicing silencer (ESS) or intronic silencing silencer (ISS).

B | A secondary structure, usually formed between two Alu elements in opposite orientation, thus interrupting the exon recognition. (The resulting isoforms are represented for each pathway. Constitutive exons are shown in blue, alternatively spliced regions are shown in purple, and introns are represented as solid lines) (Keren H *et al.,* 2010).

14

1.2.5. Alternative splicing

Splicing is a ubiquitous process in eukaryotes and the importance of alternative splicing (AS) can be inferred from interrogating its prevalence throughout the eukaryotic evolutionary tree. The process of AS is more abundant in higher eukaryotes than in lower eukaryotes, and the percentage of genes and exons that undergo AS is higher in vertebrates than in invertebrates (Keren *et al.,* 2010). There are several types of AS (**Fig 5**) as described by Keren *et al.,* 2010.
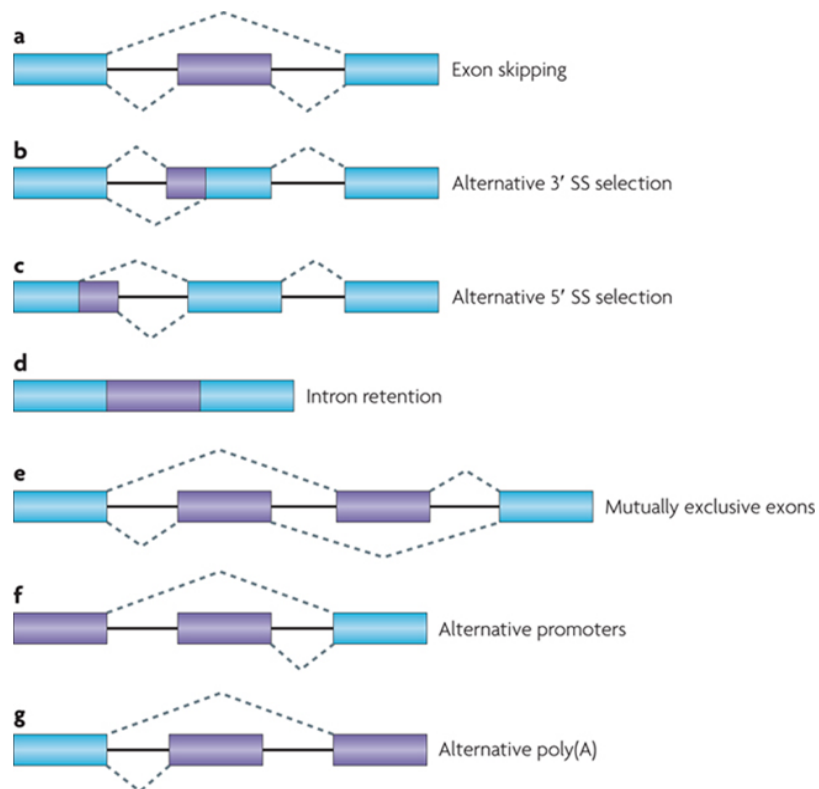
Fig. 5 | Types of alternative splicing events

a. Exon skipping in which, the cassette exon is spliced out of the transcript along with its flanking introns.

b. Alternative 3' splice site and 5' splice site selection events occur in the presence of two or more splice sites in the end of an exon.

c. Intron retention involves the inclusion of an intronic region in to the mature mRNA transcript

d. Production of an alternative transcript variant lead to the formation of mutually exclusive exons, alternative promoter usage or alternative polyadenylation.

The prevalence of exon skipping gradually increases further up the eukaryotic tree, suggesting that exon skipping is the type of AS that majorly contributes to the phenotypic complexity.

Alternative 5' and 3' splice sites are believed to be sub-families of exon skipping

1.1.3. (ii) Pre-mRNA splicing

The splicing reaction involves a rapid mechanism through which the intervening introns or the non-coding regions are excised to attach the exons or the coding regions to form the correct protein reading frame (Krainer *et al.,* 2013).

Splicing occurs via two TRANSESTERIFICATION steps **(Fig.6)**.

Step 1.

The 2′-hydroxyl group of the A residue at the branch site attacks the phosphate at the GU 5′-splice site. This reaction leads to the cleavage of 5′ exon from the intron and formation of a lariat intermediate.

Step 2.

The phosphate (p) at the 3′ end of the intron and the 3′-hydroxyl group of the detached exon, enables ligation of the two exons. This reaction further allows release of the lariat intron.
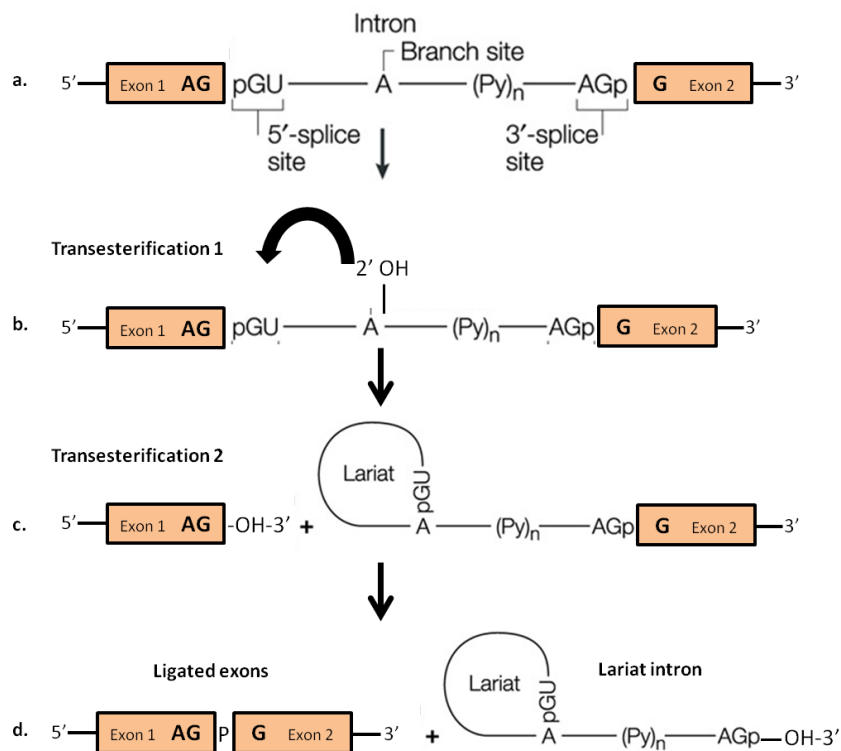
Fig. 6 | Schematic representation of splicing in two transesterfication steps.

a.| The pre-mRNA containing exons (orange boxes) and introns (lines) and the splice site signals; A= adenine residue of branch point, (Py)n = polypyrimidine tract, Splice site signals = GU and AG.

b.| In the first transesterification step, an adenine residue of the branch point attacks the phosphodiester bond at the 5'ss of exon 1.This generates two intermediates: free exon 1 and lariat –exon 2.(Modified from Pagani F et al., 2004).

c.| In the second esterfication step, the 3' OH of the detached exon attacks the phosphate at the AG 3' end of intron

d.| Splicing results in two products; The two exons joined together through a phosphodiester bond and the intron in the form of a lariat

1.2. The splicing machinery

Splicing reaction is mediated by the spliceosome- a macro-molecular machinery that assembles on to the nascent pre-mRNA transcripts. It catalyses the splicing reaction and gets released upon completion of the process.

This complex is composed of the following (Cooper A.T *et al.,* 2009);

a. Five uridine-rich (U) small nuclear ribonucleoproteins (snRNPs), each containing one or two snRNAs U1, U2, U4/U6 and U5)

b. A common set of Smith (Sm) proteins

c. Different number of complex specific protein factors including RNA binding factors (e.g.U2AF, SF1 and SRFs)

d. Enzymes such as helicases/RNPases, kinases and phosphatases.

The above mentioned factors help in modulation of structure and conformational transitions of the pre-mRNA, snRNA and protein complexes to enable splicing reaction, proof-reading and release of substrates (Nilsen *et al.,* 2003; Staley *et al.,* 1998; Will and Luhrmann *et al.,* 2001).

The spliceosome is also known to interact with several (150-300) non-snRNP proteins, such as hnRNPs and serine–arginine (SR) rich proteins (Wahl, Will *et al.,* 2009). The spliceosome assembles in a sequential manner leading to the assembly/disassembly of different snRNP and non-snRNP splicing factors on the pre-mRNA (Nilsenn TW *et al.,* 2003). The formation of mature mRNA involves several interactions such as RNA-RNA base pair, RNA-protein base-pair and protein-protein-interactions (Malca *et al.,* 2003).

The interaction between the spliceosome and the crucial motifs occurs through the following steps (Bonnal S *et al.,* 2012) **(Fig.7)**:

➢ The first step begins with the assembly of U1snRNP to the pre-mRNA. This step is mediated through an RNA-RNA base pairing between the 5' tail of the U1 snRNA and 5' ss of the intron. The complex thus formed is termed as the "early" **complex (E)** which is also known as the commitment complex interacts with the pre-mRNA through RNA-RNA base pairing and RNA- protein interaction.

➢ The branch point nucleotide A located 20-40 nucleotides upstream the acceptor splice site is bound by the branch point binding protein (BBP/SF1) (Gaur *et al.,* 1996.,Richie *et al.,* 2008).

➢ The second step in the spliceosome assembly is the formation of the **complex A** in which the BBP/SF1 is replaced by the U2 snRNP at the branch point.

➢ The third step involves transition from complex A to **complex B** in which the U4/U5 and U6 snRNPs are assembled to form the complex.

➢ The complex B contains all the necessary snRNPs to promote splicing. However, the activation of spliceosome is mediated through intricate RNA-RNA interactions, which causes a conformational change and promotes formation of **activated B* complex** (Reed *et al.,* 2000, Makarov *et al.,* 2004).

➢ The first step of transesterification reactions occurs in the B* complex generating two intermediates:

- The free 5' end of exon
- The lariat 3' of the exon

> This is followed by the formation of **C complex** in which the second esterification reaction takes place.
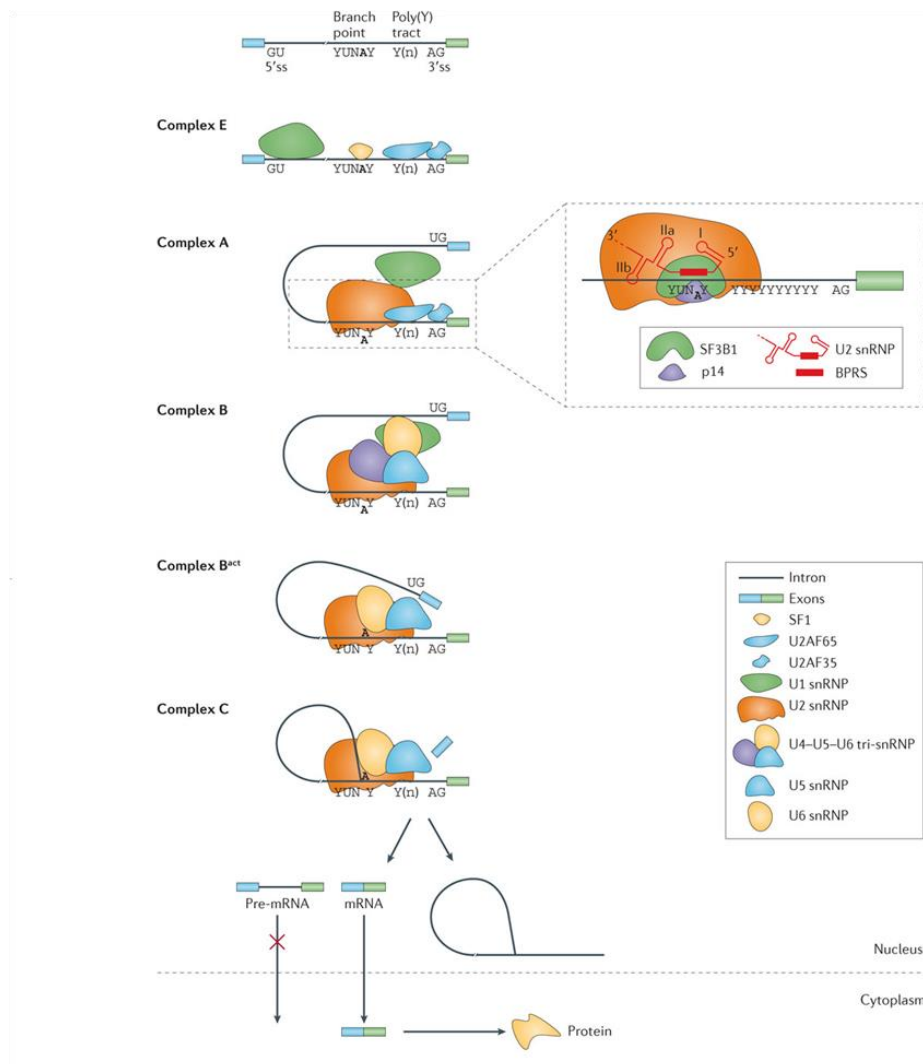
Fig. 7 | Represented at the top is a typical precursor mRNA (pre-mRNA) with intronic sequences (thin line) and exonic sequences (coloured boxes), with the consensus sequences at the intron 5′ and 3′ ends (Y = pyrimidines, N = any nucleotide and (n) = undefined number of pyrimidines). The branch point adenosine is represented in bold. The splicing factors represented in the box assemble on the pre-mRNA in a sequential manner, forming the indicated complexes (E, A and B).

Conformational rearrangements within the assembled spliceosome (complexes Bact and C) lead to splicing catalysis, generating a mature mRNA and releasing the intron in a lariat configuration. U2 small nuclear ribonucleoprotein (snRNP) binding involves base-pairing interactions between U2 small nuclear RNA (snRNA) and nucleotides flanking the branch point, as well as contacts between the U2 snRNP proteins splicing factor 3B subunit 1 (SF3B1) and p14 and the pre-mRNA. BPRS, branch point recognition sequence; SF1, splicing factor 1; ss, splice site; U2AF, U2 snRNP auxiliary factor. (Bonnal S *et al.,* 2012).

1.2.1. U snRNPs

UsnRNPs

The U snRNPs (Uridine rich small ribonucleo particles) are the constitutive elements of the splicing machinery and play an important role in the identification of the consensus signals (Will *et al.,* 2001). They contain a small nuclear U-rich RNA (U-snRNA) and different protein factors (Cooper *et al.,* 2009). The biogenesis of snRNPS is a highly complex process that involves export of the nascent pre-UsnRNAs to the cytoplasm ,where the Sm proteins assembles with the RNA and re-imported to the nucleus to aid splicing reactions (Neuenkirchen *et al.,* 2008 ;Yong *et al.,*2004).

The U1 snRNP is the first element that is involved in spliceosome assembly upon its recognition of the 5'ss in the pre-mRNA (Sperling *et al.,* 2008).
In humans, the U1 snRNP **(Fig.8)** is composed of the following:

- A 164-nucleotide long RNA molecule, U1 snRNA that recruits ten different proteins (Starke *et al.,* 2001).
- Seven of these proteins are called Sm proteins and they are common to all UsnRNPs. They are termed as Sm B, D1, D2, D3, E, F and G.
- Three other proteins are U1 specific and are termed as U1-70K, U1-A, and U1-C.
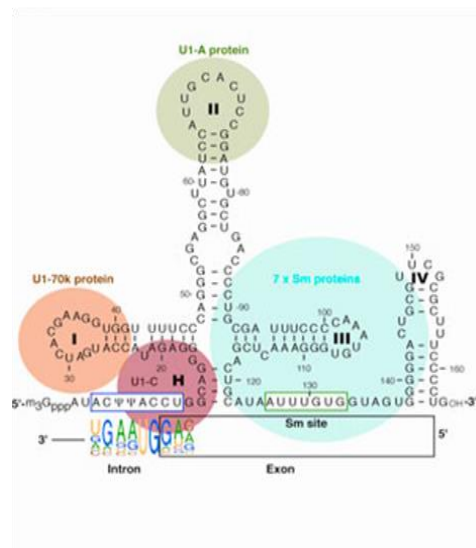
Fig.8 | Secondary structure of U1 small nuclear ribonucleic acid (snRNA) (black) and general location of the seven Sm proteins (cyan), U1-70k (peachy brown), U1-A (green),

and U1-C (maroon). A consensus 5′ splice-site is indicated, base-pairing to the single-stranded 5′ end of U1 snRNA (Krummel *et al.,* 2009).

The secondary structure of U1 snRNA is depicted by the presence of four stem loops (I, II, III, IV) and two single stranded regions. The 5' protruding tail of the U1 snRNA single strand, base-pairs with the nine bases at the 5'ss consensus motif in the pre-mRNA (Mount *et al.,* 1983). The other single stranded region between stem loops II and IV is the conserved Sm-binding site (AAUUUGUGGG). It is bound by the heteroheptameric ring composed of Sm proteins in the cytoplasm (Riker *et al.,* 1999).

The U1 specific proteins U1-70 K and U1-A interact with stem loop I and II respectively (Surowy *et al.,* 1989) U1-C enters in the U1 complex through protein-protein interaction and contributes to the following aspects (Du *et al.,* 2002): a) mediates 5' ss recognition b) stabilizes base-pairing between the 5'tail of the U1 snRNA and the donor site, thus promoting formation of the E complex. The U1 snRNP complex forms a stable interaction with nucleotides +1 to +6 of the intron at the 5' splice site promoting a suitable site for spliceosome assembly (Stakins *et al.,* 1994). U1 snRNP plays a vital role in recognition of donor splice site (Mount *et al.,* 1998), studies have also shown that recognition of 5'ss can still occur for some exons in the absence of U1 complex with a less efficient splicing process (Du *et al.,* 2002).

The U1 snRNP is also involved in targeting the U2AF to promote the polypyrimidine tract (Hoffman and Grabowski 1992), where it promotes the association of U2 snRNP complex with the branch site region (Barabino *et al.,* 1990). Although U2 snRNP can bind to the pre-mRNAs in the absence of U1 snRNP, this reaction is inefficient and seeks the assistance of U1 snRNP to establish successful binding to the pre-mRNA (Query *et al.,* 1997).

U2 snRNP interacts with the branch site at the 3' splice site with the aid of additional splice factors such as U2AF (Ruskin *et al.,* 1988), SF1 (Arning *et al.,* 1996) SF3a and SF3b, components of U2 snRNP binds upstream the branchsite of pre-mRNA and stabilizes the U2 snRNP (Gozani *et al.,* 1994). This active binding of the U2 snRNP to the branch site sequence generates the pre-spliceosome complex A.

The U5 snRNP binds to the spliceosomal complex in the form of U4/U6-U5 tri snRNP complex.

An invariant loop sequence in the U5 snRNA attaches to the nucleotide at position -1 of the first exon, before and after splice site cleavage. This loop additionally interacts with the nucleotide at position +1 of the second exon that is within the lariat intron-exon 2 intermediate.

It helps in holding the free exon 1 and intermediate in the spliceosome and aligns it with the 3' splice site for the second catalytic reaction (Sontheimer *et al.,* 1993).

The U4 and U6 snRNAs are present within a single snRNP and are associated with each other through extensive base pairing (Black *et al.,* 1986).The U4/U6 snRNP binds to U5 snRNP forming a 17S tri-snRNPs particle before binding to the complex A.

The addition of tri snRNP particle to complex A leads to the formation of spliceosomal complex or (complex B). Conformational changes further assists the formation of complex C (active spliceosome)

Thus, the base pairing between 5' splice site and U1 snRNP is disrupted and replaced by the base pairing of U6 with this region (Kandels-Lewis *et al.,* 1993) A simultaneous disruption of base pairing occurs between U4 and U6, wherein the U6 now interacts with U2 via base pairing (Madhani *et al.,* 1994). The U5 and U6 snRNAs cooperate to align the two splice sites to facilitate exon-exon ligation (Kandels-Lewis *et al.,* 1993) **(Fig.6 and 7).**

1.2.2. Canonical *cis*-acting elements in splice site selection

Three consensus sequences are found at all exon-intron junctions: the 5' splice site and 3' splice site located at the 5' and 3' ends of the introns. and the branch point sequence (BPS)that is located upstream of 3' splice site.

They recruit the spliceosome machinery through RNA-RNA and RNA-protein interactions (Cooper *et al.,* 2009, Barash *et al.,* 2010).

The following nucleotides in the consensus sequence **(Fig.9)** play a vital role in splicing:

1. The GU dinucleotide at the 5' end of splice site (5'ss)(Mount M.S *et al.,*2000).

2. The AG dinucleotide at the 3' end of splice site (3'ss)(Mount M.S *et al.,*2000).

3. A polypyrimidine tract (Py)n and the A nucleotide at the branch point both located upstream of 3' ss (Shapiro *et al.,*1987).
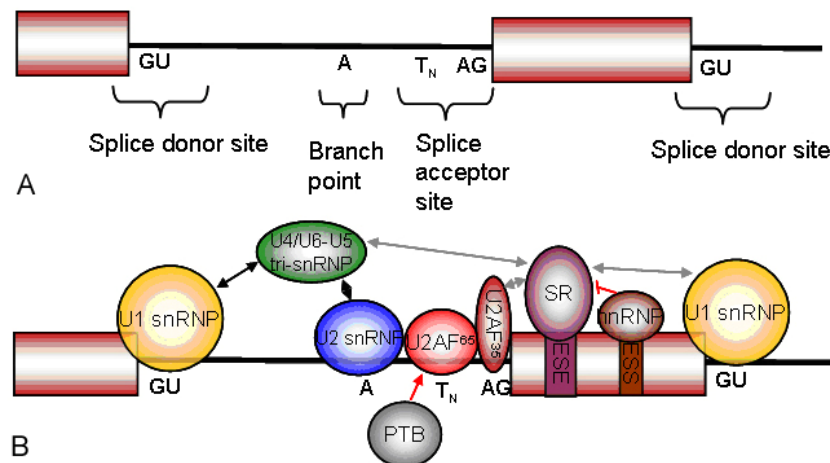
Fig. 9 | Splicing consensus sequences and its interactions.

A. Location of splice site consensus sequences. Exons are indicated by red boxes, introns by a black line. Invariant nucleotides from consensus sequences are shown in black beneath the introns. B. Interaction between the sequence elements in RNA and corresponding proteins. Grey and black arrows indicate protein-protein interactions promoting splicing, red indicates inhibitory interactions (Pettigrew *et al.,* 2008).

1.2.2. (i) The 5' splice site

The 5' splice site comprises of MAG/GURAGU (M indicates A or C and R indicates purines). An invariant dinucleotide GU located in the intron is highly conserved in eukaryotes (Baralle *et al.,* 1990; Pettigrew *et al.,* 2008).

The 5'ss is recognised by the U1 snRNA which binds through complementarity.

1.2.2. (ii). The 3' splice site

The consensus sequence at the 3' splice site is defined by three separate elements (Baralle *et al.,* 2005):

- The branch site (Branch point sequence)
- The polypyrimidine tract
- The 3' splice site dinucleotide AG

Studies have also shown that the conserved dinucleotide AG of the 3' splice site may be recognized twice during in vitro splicing of mammalian mRNA precursors. (Weiner *et al.,* 1990).

The Branch point sequence (BPS)

The mammalian branch site consensus is composed of YURAC (R = purine; Y = pyrimidine) and it is located 20-50 nucleotides downstream the 3'ss (Zhuang Y *et al.,* 1990).The U2 snRNP binds to the branch site via the U2 snRNA base pairing through RNA: RNA interaction (Will LC *et al.,* 2011).

The polypyrimidine tract

This region is located between the BPS and the AG dinucleotide at the intron/exon border. Although multiple interactions contribute to the recognition of the BPS. In metazoans, the branch adenosine is initially recognized by SF1 /mBBP, which binds along with the heteromeric dimer U2AF. The two subunits of U2AF executes the following steps (Will *et al.,* 2011):

- The 65-kDa subunit of U2AF binds to the adjacent polypyrimidine tract.
- The 35 kDa subunit contacts the 3' ss and plays a role in 3′ss recognition.

In the next step of the spliceosome assembly, the bound U2AF65 and U2AF35 facilitate substitution of SF1 for U2snRNP at the branch point to form complex A. (Fu *et al.,* 2011).

Although the effect of mutations on the classical splicing signals upstream of the 3' splice site, the polypyrimidine tract and the branch point, is less certain, many studies have shown their effect on leading to an incorrect splicing (Baralle *et al.,* 2005).

The AG dinucleotide

The AG dinucleotide located on the terminal part of the intron at the junction between intron/exon is comprised of a consensus sequence YAG/G (Y=pyrimidine) in which the AG is invariant and highly conserved. The U2AF interacts with this region through it 35 kDa subunit and assists in the formation of E complex (Wu *et al.,* 1999).

1.2.3. Auxilliary *cis*-acting sequences

In its most basic form an exon can be identified by a few *cis*-acting elements, thus recognising exons may seem a straightforward linear process. However, the sequences used as 5′ and 3′ splice sites are so diverse that many potential and similar candidates can be found in a typical mammalian transcript that match these consensus sequences as well as, and in some cases better than, the sequences at real splice sites. Therefore, raising an intriguing question in mammalian pre-mRNA splicing: how are real splice sites recognised? (Baralle *et al.*, 2005).

Evidences on literature provided so far elucidates the importance of the splice sites on mediating splicing. However, these sequences are not sufficient to define exon-intron boundaries.

Therefore additional sequences are present in the introns and exons that are known to be involved in splice site recognition and they are termed as splicing enhancers and splicing silencers **(Fig.10)** (Baralle *et al.,* 2005).
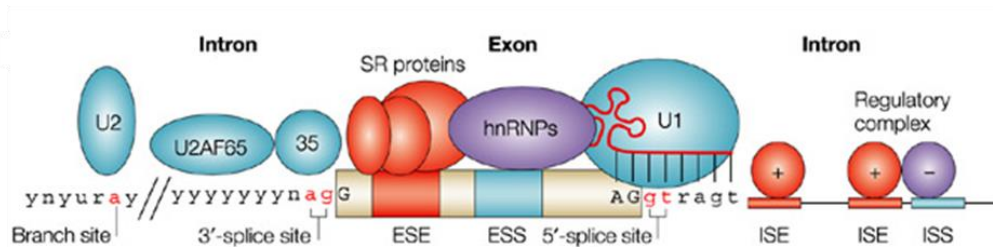
Fig. 10 | Regulatory elements in pre-mRNA splicing **a |** The essential splicing signals that define the exon boundaries are the GU and the AG dinucleotides that directly flank the exon (at the 3′ and 5′ ends, respectively) and the branch-point adenosine (all in red) are always conserved. (Pagani F et al., 2004).

Regulatory elements in the pre-mRNA splicing are reported in Fig. 10. In most cases, there is also a polypyrimidine tract of variable length (the consensus symbol 'y' represents a pyrimidine base — cytosine or thymine) upstream of the 3′-splice site. The branch point is typically located 18–40 nucleotides upstream from the polypyrimidine tract. Components of the basal splicing machinery bind to the consensus sequences and promote assembly of the splicing complex. This

multiprotein complex, known as a spliceosome, performs the correct identification of the splicing signals and catalysis of the cut-and-paste reactions Five small nuclear ribonucleoproteins (snRNPs) and more than 100 proteins make up the spliceosome. The U1 snRNP binds to the 5′-splice site, and the U2 snRNP binds the branch site through RNA–RNA interactions. Additional enhancer and silencer elements in the exons (exon splicing enhancer (ESE); exon splicing silencer (ESS)) and/or introns (intron splicing enhancer (ISE); intron splicing silencer (ISS)) allow the correct splice sites to be distinguished from the many cryptic splice sites that have identical signal sequences. Trans-acting splicing factors can interact with enhancers and silencers and can accordingly be subdivided into two main groups: members of the serine arginine (SR) family of proteins and of the heterogeneous nuclear ribonucleoprotein particles (hnRNPs). In general, SR protein binding at ESE facilitates exon recognition whereas hnRNPs are inhibitory. Protein–protein interactions in the spliceosome that modulate the recognition of the splice sites are the probable cause of splicing inhibition or activation (Pagani F *et al.*, 2004).

1.2.3 (i) Splicing enhancers

Splicing enhancer include the exonic splicing enhancer (ESE) and intronic splicing enhancer (ISE) that mediate their effects by increasing the recognition of an exon.
Most of them are recognized by proteins of the Serine-rich (SR) family. Studies on functional systematic evolution of ligands by exponential enrichment (SELEX) have identified that A/C rich enhancers play an important role in exon definition. SR proteins bind to these elements through their RNA binding domains and promote splicing by recruiting the spliceosome. However, these elements are also known to bind to other trans-acting factors apart from SR proteins. Studies have shown that GT repeat could be a possible strong intronic splicing enhancer (Gabellini *et al.,* 2001).

1.2.3 (ii) Splicing silencers

Splicing enhancer include the exonic splicing silencers (ESS) and intronic splicing silencers (ISS) and mediates their effects by decreasing the recognition of an exon.

The factors that bind to these regions have not been well characterized, however hnRNPs have been known to interact with these elements (Baralle *et al.,* 2005). Silencers are known to regulate both constitutive and alternative splicing events in mammals (Pozzuoli *et al.,* 2005).

Several studies have suggested that silencers could pose a fundamental role in preventing pseudoexon inclusion into the matured transcripts and refining the selection of constitutive exons by suppressing fake splice sites. Additionally they enable recruitment of regulatory factors to the alternatively spliced exons thus participating in regulation of alternative splicing (Pozzuoli *et al.,* 2005).

1.2.4. Trans-acting factors

1.2.4 (i) hnRNPs

The heterogenous nuclear ribonucleoproteins (*hnRNPs)* constitute a family of RNA binding proteins. They are involved in processing of heterogenous nuclear RNAs into mRNAs and act as trans-acting factors in regulation of gene expression. Studies on Hela have revealed the protein composition of hnRNP complexes. They are known to contain at-least 20 abundant major hnRNP proteins and are designated as hnRNPA1 through hnRNP U1 with varied molecular weights ranging from 34 kDa to 120 kDa. hnRNP proteins A1, A2, B1, B2, C1 and C2 were identified to be associated with nascent transcripts and were termed as "core hnRNPs" (Beyer *et al.,* 1977; Dreyfus *et al.,* 2002).

These proteins are ubiquitiously expressed in all tissues, however they show a stage-specific expression pattern.

1.2.4 (ii) SR proteins

The serine -arginine rich proteins are a highly conserved set of splicing regulators (Bradley *et al.,* 2014). They contain one or two N-terminal RNA recognition motifs (RRM) and a C terminal (RS) domain enriched in arginine and serine dipeptides. Their primary function is the regulation of splice-site selection. In alternative splicing events, these proteins function in the following ways:

- As activators facilitated by binding to the splicing enhancers (ESEs) through the RRM domain.
- Recruiting the splicing machinery to splice site via RS-domain–protein interactions.

The binding sites for SR proteins and other splice regulators are located in close proximities on the pre-mRNA suggestive of an inter-play between activation and repression that modulates exon inclusion. SELEX based techniques have identified the protein binding motifs for these proteins and ascertained degenerate purine rich sequences that resemble identified ESEs or 5' splice sites. A recent study on the regulation of alternative splicing mediated through SR proteins was performed in Drosophila (Bradley *et al.,* 2014). This study revealed that a majority of SR-regulated splice events are controlled by multiple SR proteins, wherein they can be involved in both exon inclusion and exon skipping. The binding location on the target RNA determines the positive or negative effect imposed by the SR protein. Although these proteins are known to mediate their effects by recruitment and/or stabilization of core spliceosome, they are also known to pose an effect on alternative splicing as activators/repressors (Bradley *et al.,* 2014).

1.3. Impact of splice defects in neurodegeneration

Around 50 % of human genetic diseases are linked to mutations that affect alternative splicing processes (Matlin *et al.,* 2005). Since brain has the greatest amount of alternative splicing of all tissues, the effect of altered splice events have been linked to neurodegenerative brain diseases (NBDs) that has been an important area of study in the past decade (Mills *et al.,* 2012).

1.3.1. Neurodegenerative diseases

Neurodegenerative diseases arise due to various factors including functional loss of neurons, inability of neurons to respond to changes in their internal and external environments, loss of connection in neuronal projections, all of which lead to neuronal degeneration (Courtney *et al.,* 2010).

The commonly studied neurodegenerative diseases include Alzheimers disease (AD), Parkinson's disease (PD), Huntington's disease (HD), progressive supranuclear palsy (PSP), corticobasal degeneration (CBD) and Pick's disease (PiD). The PSP, CBD and PiD are collectively classified as Fronto temporal dementia (FTD) as they share the common features of an intracellular tau-positive pathology (Mills *et al.,* 2012; Betram *et al.,* 2005) **(Fig.11).**
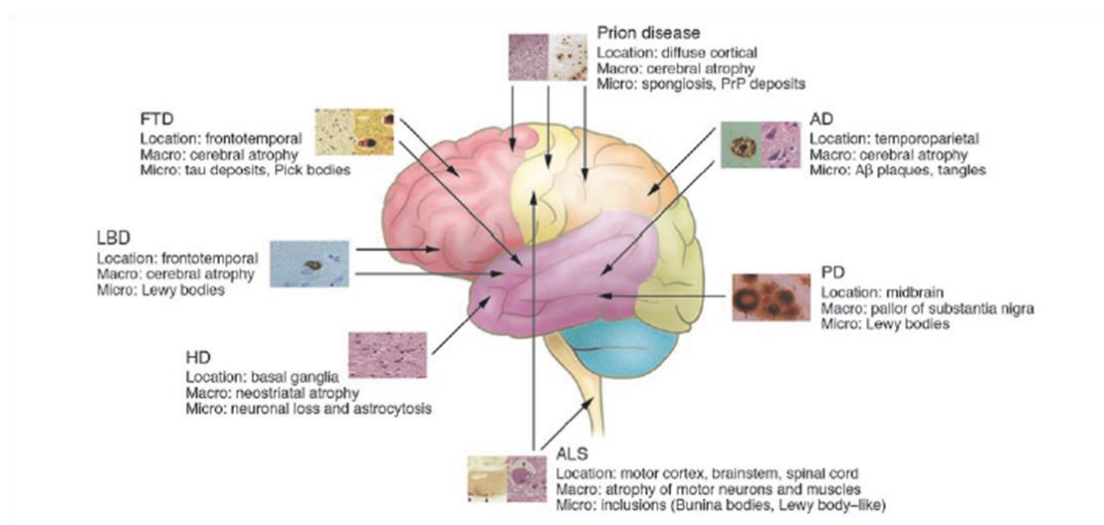
Fig. 11 | Types of neurodegeneration and the anatomical location (in brain) of macroscopic and microscopic characteristic changes involved in neurodegeneratives diseases (Betram *et al.,* 2005).

In fact, a handful of alternatively spliced genes are known to associate with the onset of these diseases (Mills *et al.,* 2012). A detailed review on association of these genes to the above mentioned diseases can be referred from Mills *et al.,* 2012 (Table 1).

Table 1
Genes alternatively spliced in the human brain that are related to neurodegenerative brain disorders

Gene symbol	Gene name	Detection technique	Reference
Alzheimer's disease			
PSEN 1	Presenilin 1	RT-PCR	(De Jonghe et al., 1999)
PSEN 2	Presenilin 2	RT-PCR	(Sato et al., 1999)
GRN	Progranulin	RT-PCR	(Cruts et al., 2006)
APP	Amyloid precursor protein	RT-PCR	(Golde et al., 1990)
			(Tang et al., 2003)
APOE	Apolipoprotein E	Illumina RNA-Seq	(Twine et al., 2011)
BACE	β-site APP-cleaving enzyme	RT-PCR	(Tanahashi and Tabira, 2001)
PIN1	Peptidyl-prolyl isomerase, NIMA-interacting 1	RT-PCR	(Maruszak et al., 2009)
Alzheimer's disease and frontotemporal dementia			
MAPT	Microtubule-associated protein tau	RT-PCR, Immunoblotting	(Goedert et al., 1989)
			(Spillantini et al., 1998)
Parkinson's disease			
PARK2	Parkin	RT-PCR	(Tan et al., 2005)
			(Sunada et al., 1998)
SNCA	α-Synuclein gene	RT-PCR	(Beyer et al., 2004)
SRRM2	Serine/arginine repetitive matrix 2	Affymetrix Exon_St1 arrays	(Shehadeh et al., 2010)
Huntington's disease			
BDNF	Brain-derived neurotrophic factor	Radioactive RT-PCR	(Zuccato et al., 2005)

Table 1 | Alternatively spliced genes in the human brain associated to neurodegenerative brain disorders (Mills *et al.,* 2012).

1.3.2. Fronto temporal lobar degeneration (FTLD)

Fronto temporal lobar degeneration (FTLD) refers to a group of progressive brain diseases that share a common feature of atrophy of frontal and temporal cortex but are heterogeneous in etiology and neuropathology. The onset of symptoms occurs before 60 years of age and the mean survival after diagnosis varies between 3 to 10 years. The prevalance is estimated to be 15 in 100,000 in the population of people in the age group between 45 and 60 years (Riedl *et al.,* 2014).

FTLD has been included in the list of orphan diseases. (Orphanet number ORPHA282 of http://www.orpha.net).

The clinical syndrome is characterized by progressive deterioration of either language or behavior. In 1892, Arnold Pick described the first patient with clinical syndrome of Pick's disease which was used interchangeably with FTLD

over a decade from then. However, now this term is referred to only a subset of FTLD with specific histopathological features.

FTLD is classified based on two functions: clinical syndromes and neuropathology.

The clinical syndromes include behavioural-variant fronto temporal dementia (bvFTD) and primary progressive aphasia (PPA).

Behavioural-variant fronto temporal dementia (bvFTD)

It is the most common clinical syndrome of FTLD and is characterized by the atrophy of mesofrontal, orbitofrontal and anterior insular cortex of the frontal lobes .It leads to progressive personality changes and behavioural disturbances. While behavioural changes dominate the initial stages, cognitive deficits appear on disease progression.

Primary progressive aphasia (PPA).

The language variants of FTLD include: a) semantic variant PPA (svPPA); also termed as semantic dementia or temporal variant dementia. b) non fluent variant PPA (nfvPPA) also referred to as progressive nonfluent aphasia (Johnson *et al.,* 2005).

Semantic variant PPA (svPPA)

It accounts for 19% of all FTLD cases and is characterized by difficulties in understanding of sensory stimuli. Loss of verbal and non-verbal skills in a progressive manner.

Non fluent variant PPA (nfvPPA)

It accounts for 24% of all FTLD cases and is characterized by reduction of speech in a progressive manner which leads to complete loss of speech in the later stages. The pathological hallmark of this disease is the atrophy of the left cerebral hemisphere.

The neuropathological subtypes are characterized as follows:

FTLD- tau

The best studied FTLD subgroups are known to contain hyperphosphorylated tau proteins in the neuron and glial cells. They represent 40 % of FTLD cases and include neuropathology observed in Pick's disease, PSP, CBD and cases of familial FTLD caused due to mutations in *MAPT*. Though these diseases share a common tau-positive pathology, each condition is characterised by an additional inclusion that enables pathological classification; Pick bodies in Pick's disease, Neuro fibrillary tangles (NFT) and tufted astrocytes in PSP and astrocytic plaques in CBD.

FTLD-U

The tau negative cases are characterized by neuronal cytoplasmic inclusions and dystrophic neurites in the layers of frontotemporal neocortex and dentate granule cells of hippocampus that were detected with ubiquitin immuno histochemistry, hence termed FTLD-U.

However, TDP-43 was identified as the ubiquitinated pathological protein hence leading to a subsequent change in the name as FTLD-TDP. The pathological form of TDP-43 consists of abnormal C-terminal fragments that are hyperphosphorylated and ubiquitinated. Around 10-20% of cases that were considered as FTLD-U did not respond to staining for either tau or TDP-43. However, discovery of FUS mutations in ALS (Amyotrophic lateral sclerosis) later led to the identification of FUS positive inclusions in this subset of tau /TDP 43 negative inclusions, hence this new group was classified and termed as FTLD-FUS. Further studies in 2004 to 2006 revealed the involvement of other genes such as Valosin containing protein (*VCP*), Chromatin modifying protein 2B (*CHMP-2B*) and Progranulin (*PGRN*) to be associated with the FTLD-U disorders (Watts *et al.,* 2004; Skbinski *et al.,* 2005; Cruts and Van Broeckhoven *et al.,* 2008).

1.4. Fronto temporal dementia and Parkinsonism linked to chromosome 17 (FTDP-17)

In 1994, the familial disease called disinhibition-dementia–parkinsonism-amyotrophy complex (DDPAC) was linked to chromosome 17q21-22 (Wilhelsmsen 1994).

This study was further followed by other reports that showed a link between number of dementing diseases and to the same region of chromosome 17. (Goedert *et al.,* 2000). In 1996, these group of diseases were termed as Fronto temporal dementia and Parkinsonism linked to chromosome 17 (FTDP-17) by a consensus conference. (Foster *et al.,* 1997).

The major clinical features include behavioral disturbances, cognitive impairment and parkinsonism (Foster *et al.,* 1997).The age for onset of disease varies between 45-65 years. (Snowden *et al.,* 1996).

A study on the Dutch population estimated its prevalence to be 1 over 1000,000 people, however clinical manifestations could account for an underestimated prevalence rate (Rosso *et al.,* 2003).

The neuropathological features include atrophy of the fronto temporal lobes of the brain accompanied by neuronal loss, gliosis and spongiosis (Pookraj *et al.,* 1998) with additional presence of proteinaceous inclusions containing hyperphosphorylated tau protein called neurofibrillary tangles (NFTs).

The behavioral changes include the following: disinhibition, apathy, compulsive behavior, negligence of personal hygiene, verbal and physical aggressiveness.

As the disease progresses, it leads to cognitive and memory deficits.

Due to the presence of motor symptoms, patients with this disease could be misdiagnosed with Parkinson's disease or progressive supra nuclear palsy (PSP).

Although a majority of FTDP-17 cases are sporadic in nature,10% to 50% of the patients have been reported to have a positive family history of the disease.

A subset of familial cases, however exhibit an autosomal dominant pattern of inheritance indicating a significant contribution to the disease onset.(Neary *et al.,*1998; Poorkaj *et al.,*1998).

Since tau gene maps to the critical interval region on chromosome 17 and hyperphosphorylated tau proteins have been characterized as neuropathological

hall-marks in in the familial fronto temporal dementia cases (Wilhelsen *et al.,* 1997), tau gene was considered a strong candidate for the FTDP-17 locus.

Further studies have led to the discovery of many mutations in tau gene and established the effect of tau dysfunction in neurodegeneration. However, it became very clear that *MAPT* gene was a candidate target gene only for FTDP-17 cases containing tau positive histopathology.

1.4.1. Microtubule associated protein tau (*MAPT)* gene

The Microtubule associated protein tau (*MAPT*) spans about 100 kb on the long arm of chromosome 17 at band position 17q21.1 (ch17q21.1). It consists of sixteen exons and has the following features (Kolarova M *et al.,* 2012):

- Exon 1 is part of the promoter and is transcribed but not translated;
- Exons 1, 4, 5, 7, 9, 11, 12 and 13 are constitutive in nature;
- Exons 2, 3 and 10 are alternatively spliced.

Alternative splicing of these exons leads to the formation of six different isoforms that are 353 to 441 amino acids long **(Fig.12)** and differentially expressed during the development of the brain. (Zhou *et al.,* 2008; Kolarova *et al.,* 2005).
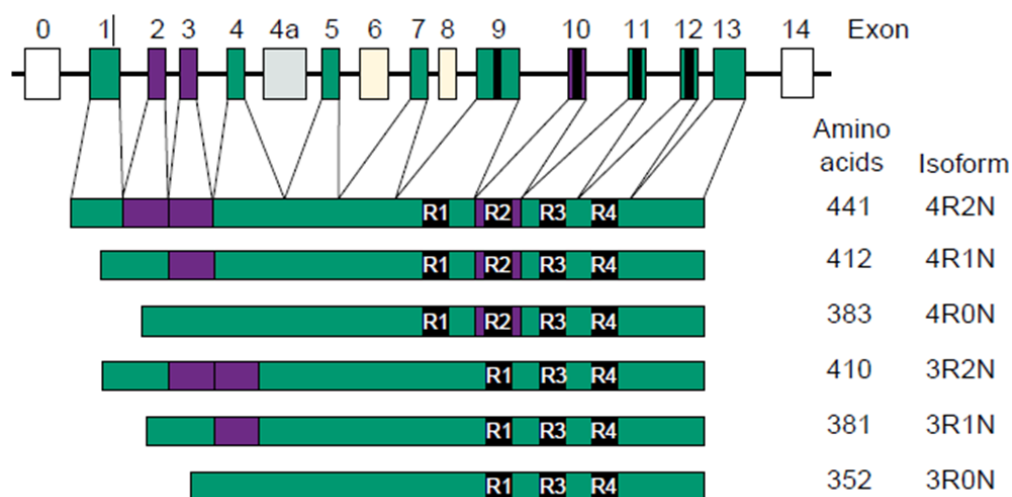
Fig.12 | Human tau gene and the six isoforms expressed in the CNS .The tau gene is composed of 16 exons of which 11 are used in the CNS (Highlighted in purple and green boxes).The alternatively spliced exons includes exons 2, 3 and 10 (purple) leads to the formation of six isoforms.The microtubule binding domain is encoded by exons 9 to 12 and labelled as R1 to R4

respectively (black bars). The isoforms are represented based on the number of repeats attained from each terminal (Esther *et al.,* 2002).

1.4.2. Tau protein: Localisation, Structure and Function

MAPT gene codes for tau protein a member of microtubule associated proteins (MAPs) family that comprises MAP 1 and MAP 2.

Localisation

Tau is localized in several parts of tissues and organs. However, it is particularly abundant in neurons of the CNS especially in their axons. A lower amount is detectable in the axons of peripheral neurons and in oligodendrocytes of glial cells. Tau expression varies in different regions of the adult brain with the frontal cortex bearing the highest level of tau followed by occipital cortex, white matter, putamen and cerebellum (Traozuni *et al.*, 2012).

Structure

Previous studies have revealed tau as a "natively unfolded" protein (Von Bergen *et al.,* 2005, Gamblin *et al.,* 2005, Jeganathan *et al.,* 2008). Since disordered proteins undergo variable conformational changes they have not been subjected to crystallographic analyses. However, nuclear magnetic resonance spectroscopic studies have enabled recovery of complete assignment of the 441 amino acid residues of the longest isoform **(Fig.13)** (Kalarova *et al.,* 2012).
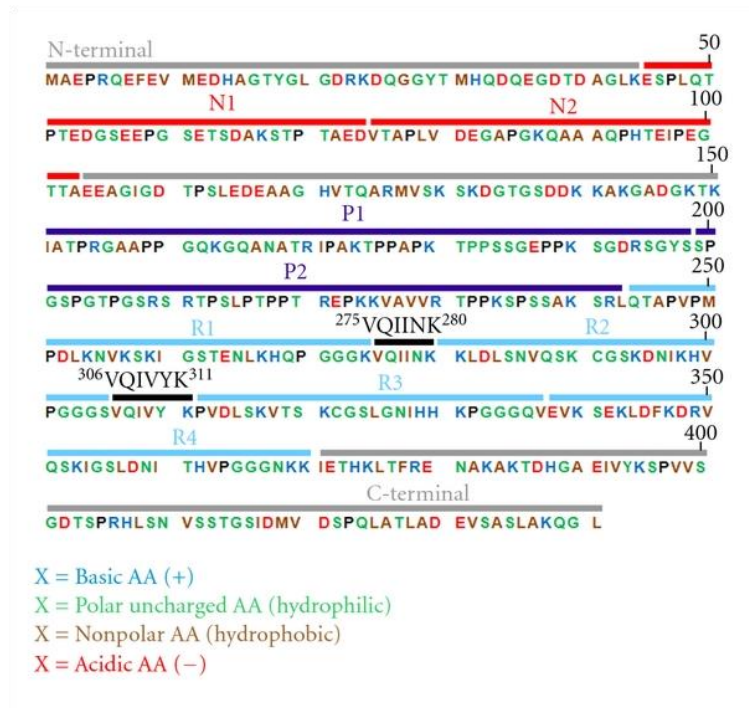
Fig. 13 | Amino acid sequence of the longest tau isoform (441 amino acids). (N1 and N2 = polypeptide sequences encoded by exons 2 and 3) (P1 and P2= proline-rich regions) (R1–R4 = microtubule-binding domains encoded by exons 9–12) (275VQIINK280 and 306VQIVYK311=sequences with β-structure) (Kalarova *et al.,* 2012).

Six isoforms of tau differ according to the contents of tubulin binding domains (R or repeats) in the C terminal designated as 4R or 3R and the number of inserts of 29 amino acids each in N-terminal portion designated as 1N, 2N or 0N.

The varied size of amino acids arises as a result of presence or absence of sequences encoded by exons 2, 3 or 10. Inclusion of exon 10 lead to the expression of tau with four repeats (**4R tau)** while exclusion results in expression of the alternative isoform with three repeats (**3R tau)** (Lee *et al.,* 2012). Skipping of both exons 2 and 3 leads to the expression of **0N isoform**, inclusion of exon 2 but not exon 3 leads to the expression of **1N isoform** and inclusion of exons 2 and 3 leads to the expression of **2N isoform** (Baker *et al.,* 2006).

The primary sequence analysis of tau shows that it consists of a half N-terminal acidic portion followed by a proline rich region and a C terminal tail. Exons 2 and 3 accounts for the acidic nature of tau protein and Exon 10 (encodes a positively charged sequence) contributes to the basic nature.

36

Thus, tau is a dipolar protein with both positive and negative charges and can be modulated by post translational modifications.

The N terminal domain is referred to as the projection domain as it projects from the microtubule surface to interact with other cytoskeletal elements and the neuronal plasma membrane. The two 29 amino acid domains encoded by exons 2 and 3 provide different lengths to the N terminal part of the tau protein. This region of tau protein is known to interact with the following molecules (Kolarova M *et al.*, 2012):

- Spectrin and actin filaments- Allows tau-stabilized microtubules to interconnect with neurofilaments
- Peptidyl-prolyl cis/trans isomerase Pin 1 – Triggers conformational changes that lead to tau dephosphorylation. Pin 1 is involved in regulation of tau and protein and protects against degeneration as a result of ageing
- Intracellular membranous elements such as mitochondria and plasma membrane
- Kinases and proteases – Helps in the maintenanace of equilibrium of both phosphorylated or dephosphorylated forms of tau protein

The proline-rich region is known to bind to Src-homology 3 (SH3) domains of several proteins. Fyn, a tyrosine kinase belongs to the class of Src-family. Studies have shown that association of tau with Fyn regulates the outgrowth of cytoplasmic processes in oligodendrocytes. Imapired interaction of Fyn kinase and hyperphosphorylated tau causes hypomyelination leading to demyelination of axons.

The repeated domains R1 to R4 encoded by exons 9-12 located in the C terminal domain enable binding of tau protein to microtubules.

Studies *in vitro* have demonstrated that tau protein increases the rate of microtubule polymerization and in parallel inhibits their rate of depolymerisation (Dreschel *et al.*, 1992).

Microtubule polymerization is stimulated by the interregion between repeats 1 and 2 (R1-R2 interregion) that codes for the peptide 275KVQIINKK280 (Sergeant *et al.*, 2005; Goode *et al.*, 1994). This is the most unique region for 4R

tau and accounts for the major difference in binding affinities between 3R and 4R tau (Sergeant *et al.*, 2005; Brandt *et al.*, 1993).

In the adult brain, the ratio of 4R and 3R is expected to be 1:1. Although the necessity for such balance between the isoforms is universally accepted, the mechanism by which an alteration causes the onset of FTDP-17 remains unclear. One of the main hypothesis is that the 4R isoform binds to different sites on microtubules as compared to its 3R counterparts. Hence, an excessive production of 4R leads to a saturation of the binding sites with a simultaneous aggregation of the unbound 4R isoforms. However, an accurate determination of the mechanism involved in the onset of FTDP-17 upon disruption of the ratios will be necessary to address potential therapeutic strategies for the treatment of tauopathies (Liu *et al.,* 2008).

The main function of tau being a promoter of tubulin polymerization depends majorly on the R domain (R). Recent studies have suggested a possible role for the R domain the modulation of phosphorylation of tau protein, wherein a direct and competitive binding has been observed between this region and microtubule on one side and the same region with PP2A (protein phosphatase 2 A) on the other side. As a result, the activity of PP2A is halted by microtubules by binding to tau protein (Sontag *et al.*, 1999).

Function

Tau functions include promotion of microtubule assembly and their stabilization, morphogenesis, axonal extension, mitosis and axonal transport (Buee *et al.*, 2000).

Microtubules are involved in diverse cellular processes such as cell morphogenesis, cell division, and intracellular trafficking (Drubin *et al.,* 1996; Goodson *et al.,* 1997). They mediate organelle transport with the help of motor proteins such as kinesin or motor dynein. These motor proteins are involved in transport of their cargoes such as mitochondria (Morris *et al.*, 1993; Tanaka *et al.*, 1998), lysosomes (Hollenback *et al.*, 1990), peroxisomes (Weimer *et al.*, 1997) towards the cell periphery or towards the microtubule organizing center (MTOC).

The tau protein is known to tightly bind to the microtubules, thus leading to intracellular trafficking, this might arise as a result of detachment of the cargoes from kinesin (Kolarova *et al.*, 2012).

1.4.3. Tau Pathology: Causes and consequences in the context of FTDP-17

Intracellular tau deposits have been observed in a number of neurodegenerative diseases (Goedert *et al.*, 2005). However, it was quite unclear whether the dysfunction of tau protein was a cause or a consequence of the disease. Studies on mutations in *MAPT* gene in 1998, however unraveled the role of tau protein and its causative role in FTDP-17. At present about 40 different mutations have been found in the gene and are known to be associated with FTDP-17 (Wszolek *et al.*, 2006).

Most of the mutations in *MAPT* gene **(Fig.13)** are missense, deletions or silent in nature. They are either located in the coding region of Exons 9 to 13 or in the first portion of the intron following exon 10.(**Table 2**) (Esther *et al.,* 2002).

Further, these mutations can be classified according to their functionality; leading to primary effects at the RNA splicing or protein levels. Mutations in exon 1 (R5H and R5L), exon 9 (K257T, L226V, and G272V), exon 11 (S320F), exon 12 (V337M, E342V and K369I) and exon 13 (G389R and R406W) have an effect on all six isoforms. Mutations in exon 10 (N279K, K280, L284L, N296, N296H, N296N, P301L, P301S, S305N and S305S) however, poses their effect on the 4R isoform.

Mutations in the coding regions of exons 9, 10 (P301L and P301S), 11, 12, and 13 of *MAPT* gene is reported to disrupt its interactions with microtubules, hence causing an improper microtubule assembly. A reduction of microtubule assembly has also been observed in R5H and R5L mutations in exon 1(Hayashi et al., 2002; Poorkaj et al., 2002).
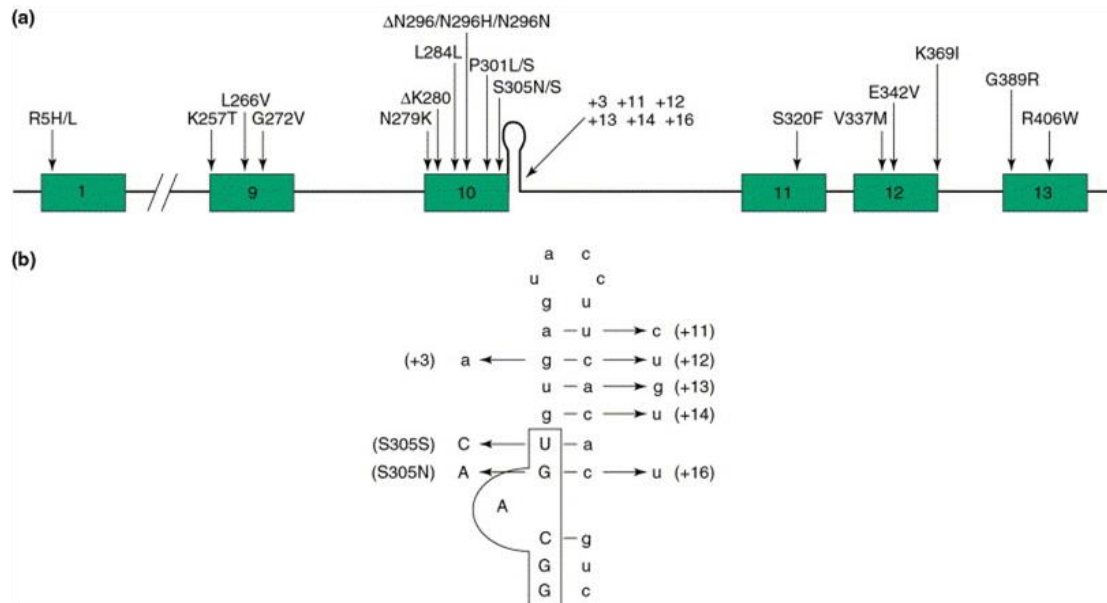
Fig. 14 | a. Mutations associated with tau gene leading to FTDP-17 are shown for exons 1 to 13. Exonic mutations are depicted according to codon number and intronic mutations according to nucleotide number. b. An enlarged version of the predicted stem loop structure located between exons 10 and 11.Exonic and intronic mutations that lead to the instability of this structure thus excessively including exon 10 are depicted in uppercase and lowercase respectively (Esther *et al.,* 2002).

Mutations that alter splicing of *MAPT* mRNA

The two types of mutations known to pose their effects on pre-mRNA splicing include:

a. Mutations within coding regions of exon 10 (N279K, 280K, N296H/N, and N296N/S305N/S).

b. Mutations in introns close to 5' splice site of exon 10 in positions +3, +11, +12,+13,+14, +16 and +19.

All of these mutations are known to increase the inclusion of exon 10 in *MAPT* mRNA, thus altering the ratios of the two isoforms of 4R and 3R. However, mutations Δ280K in exonic and +19 and +29 intronic regions lead to an opposing effect of increasing the 3R isoform (D'Souza *et al.,* 1999) **(Table 2.)**.

Location on gene	Mutation	Insoluble tau	In vitro effects
Intronic			
	E10+3	ND	↑ Exon-10 inclusion
	E10+4	Mainly 3R	↓ Exon-10 inclusion
	E10+11	Mainly 4R	↑ Exon-10 inclusion
	E10+12	Mainly 4R	↑ Exon-10 inclusion
	E10+13	Mainly 4R	↑ Exon-10 inclusion
	E10+14	Mainly 4R	↑ Exon-10 inclusion
	E10+16	Mainly 4R	↑ Exon-10 inclusion
	E10+19	Mainly 3R	↓ Exon-10 inclusion
	E10+25	Mainly 4R	↑ Exon-10 inclusion
	E10+29	Mainly 3R	↓ Exon-10 inclusion
	E10+30	Mainly 4R	↑ Exon-10 inclusion
Exonic			
	L284R	Mainly 4R	↑ Exon-10 inclusion
	ΔN296	Mainly 3R	↓ Exon-10 inclusion
	P301L	Mainly 4R	↑ Exon-10 inclusion
	P301S	ND	ND
	P301T	ND	ND
	G303V	Mainly 4R	↑ Exon-10 inclusion
	S305I	Mainly 4R	↑ Exon-10 inclusion
	N279K	Mainly 4R	↑ Exon-10 inclusion
	L284L	Mainly 4R	↑ Exon-10 inclusion
	N296N	ND	↑ Exon-10 inclusion
	S305N	ND	ND
	S305S	Mainly 4R	↑ Exon-10 inclusion
	N296H	Mainly 4R	↑ Exon-10 inclusion
	E342V	Mainly 4R	↑ Exon-10 inclusion
	ΔK280	Mainly 4R	↑ Exon-10 inclusion

Table 2 | Mutations that affect splicing of exon 10 are located both in the intronic and exonic region. (Abbreviations 4R: four repeat tau, 3R: three repeat tau, ND: Not determined, PHF: Paired helical filaments) (Modified from Esther *et al.,* 2002).
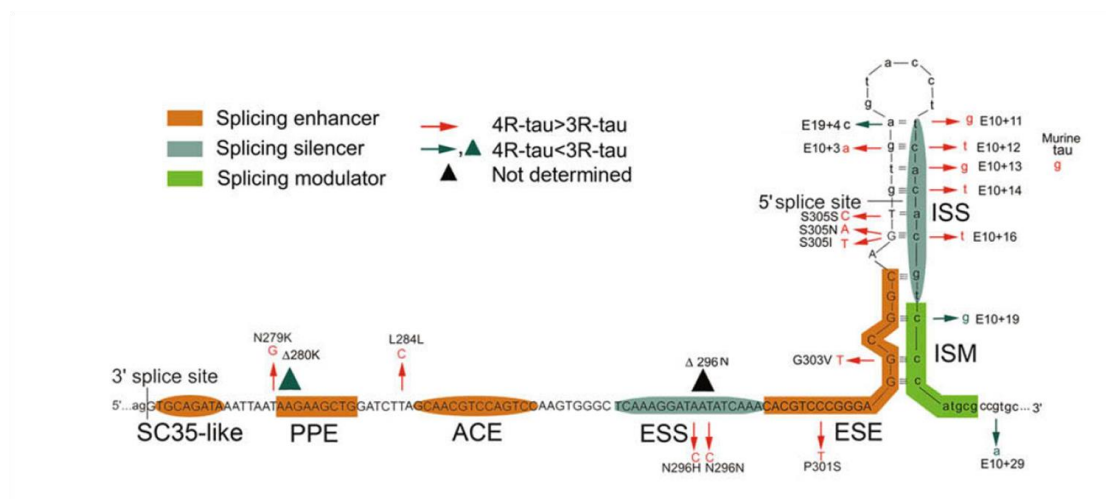
Fig. 15 | Structure of exon 10 and intron 10 of the tau gene with its regulatory elements. Exon 10 is depicted in capital letters and part of the flanking introns 9 and 10 are shown in lower case. There are three ESE (SC35-like enhancer, PPE, and ACE) at the 5' end of exon 10 and bipartite cis elements (an ESS and an ESE) at its 3' end. Intron 10 elements include an ISS and an ISM. There is a stem-loop structure at the interface between exon 10 and intron 10. Mutations that cause an

increase (red), decrease (dark green), or a not yet known change (black) in the 4R-tau: 3R-tau ratio are indicated. Triangles indicate deletion mutations. ACE, A/C-rich enhancer; ESE, exonic splicing enhancer; ESS, exonic splicing silencer; ISM, intronic splicing modulator; ISS, intronic splicing silencer; PPE, polypurine enhancer (Qian *et al.,*2010).

The N279K misense and L284L silent mutations strengthen one of the two exon splicing enhancer elements (ESEs) located at the 5' region of exon 10, thus causing an excessive accumulation of RNA containing exon 10 hence forming insoluble 4R isoforms. (D'Souza *et al.,*1999; D'Souza *et al.,*2000; Clark *et al.,* 1998, Hasegawa *et al.,* 1999). Another silent mutation N296N causes a similar effect in producing 4R transcripts that is thought to result from disruption of an existing exon splicing silencer (ESS)(Spillantini *et al.,* 2000) or through creation of an exon splicing enhancer element (ESE)(Grover *et al.,* 2002). *In vitro* studies have shown that S305N mutation changes the last amino acid of exon 10 and reduces the thermodynamic stability of a stem-loop structure (Varani *et al.*, 1999; Iijima *et al.*, 1999). Additionally, this mutation is also known to increase the binding of U1 snRNP to the 5' splice site thus causing an increased splicing of exon 10. The silent S305 mutation however is thought to disrupt the stem-loop structure without affecting the binding of U1 snRNP (Stanford *et al.*, 2000).

Mutations Delta 280, Delta 296 and N296H pose their effects at both RNA and protein levels. Like the other mutations, located in the coding regions, these reduce the ability of tau to promote MT assembly (Grover *et al.*, 2002; Yoshida *et al.*, 2002) N296H and N296N leads to excessive production of exon 10 by modulating splicing (Grover *et al.*, 2002; Yoshida *et al.*, 2002) and the K280 leads to reduced splicing in of exon 10.suggesting its primary effect on over production of 3R tau (Esther *et al.*, 2002).

Lack of available tissues however has limited the biochemical analyses of the mutations that affect splicing.

The exon-intron interface at the 3' end of exon 10 in tau pre-mRNA, (which is also a splice site junction) has been predicted to contain a stem-loop RNA structure. The two groups involved in the theoretical prediction of tau pre-mRNA for such a structure have also proposed that several tau mutations pose an effect through destabilization of the stem-loop, thereby exposing this splice site to the U1 snRNP and subsequently leading to the increased inclusion of exon 10. This

theoretical prediction has been confirmed through an indirect analysis of stem-loop in mice models: all *MAPT* mRNAs in the rodent adult brain contain exon 10, thus producing pre-dominant 4R isoforms. This enhanced inclusion of exon 10 is predicted to arise as a result of destabilization of the stem loop structure relative to the human sequence caused by a naturally occurring G at position +13 in *MAPT* intron 10 (D'Souza *et al.*, 2005) **(Fig 15).**

As previously discussed, alternative splicing is a highly regulated process therefore mutations in the essential cis acting splice regulatory elements are highly likely to induce an alteration in the splicing pattern.

Mutational studies on the region spanning Exon 10 and its adjacent introns on *MAPT* gene have shown the presence of atleast seven non redundant regulatory elements.

The first 45 nucleotides of exon 10 contain a multipartite **exonic splicing enhancer (ESE)** composed of the following:

- An SC35 –like sequence that resembles degenerate binding consensus for the SR protein SC35
- A polypurine enhancer (PPE), an exonic enhancer with a high purine content
- An AC rich enhancer (ACE), an exonic splicing enhancer rich in As and Cs.

Additionally, the sequence between the SC35-like element and the PPE element consists of a potential inhibitory element for splicing. Although the PPE element is fundamental for splicing of exon 10, additionally the other regulatory elements play a vital role in regulation of splicing. A central splicing silencer (ESS) is located between the above mentioned ESE (located at the 5' end of exon 10) and another ESE (located at the 3' end of exon 10). The downstream intron 10 sequence adjacent to the 5' splice junction is composed of a bipartite inhibitory sequence followed by an intronic splicing modulator (ISM). These regulatory elements are involved in a complex interaction to regulate splicing of exon 10, thus determining the balance between the two alternatively spliced transcripts (4R:3R) (Gao *et al.,* 2000;D'Souza *et al.*, 2005)(**Fig 15**).

Despite increasing evidences in unraveling molecular mechanisms involved in FTDP-17, there is no available cure for this disease.

1.5. Tools for manipulation of splice defects in neurodegeneration

1.5.1. Exon skipping approaches

Since exon 10 inclusion leads to FTDP-17, by posing an alteration in the balance between the two isoforms 4R and 3R, strategies to induce exon skipping or selective depletion of isoforms containing exon 10 can be utilized to recuperate the ideal equilibrium of these two isoforms.

1.5.1 (i) Antisense oligo nucleotides

The most widely studied gene therapeutic approach for correction of splice defects is through the application of antisense oligonucleotides (AONs) that target the pre-mRNA (Siva *et al.,* 2013). Antisense oligonucleotides (ASOs) with their diverse functionality, high target specificity, and relative ease of delivery in the central nervous system (CNS) are uniquely considered as potential therapies for neurological diseases (Southwell *et al.*, 2012).

Please refer to attachment for a detailed review on the use of antisense oligonucleotides in the context of neurodegenerative diseases with the following title:
Exon-skipping antisense oligonucleotides to correct missplicing in neurogenetic diseases.
Siva K, Covello G, Denti MA *Nucleic acid therapeutics* (2014).
There has been no improvement or modification in the state of the art since the above mentioned review was published.

1.5.1 (ii) Chimeric small nuclear RNA (snRNA) molecules

Although antisense oligonucleotides are used to induce exon skipping, an alternative approach is the use of suitable DNA vectors. The UsnRNPs involved in several processing of splicing appear to be attractive carriers for the antisense sequences (Wood *et al.*, 2010). They are considered to be advantageous when

compared to naked synthetic antisense oligo ribonucleotides for a number of following reasons (Glaus *et al.,* 2011);

1. They are resistant to degradation with a decreased risk of being attacked by RNA interference as they are engulfed by the RNP particles.

2. Their accumulation is specifically centred in the nucleus, the active location of splicing

3. They are continuously expressed thus avoiding repeated administrations

4. The short length of U snRNA genes (~500 bp) allows their incorporation into any transfer vector.

5. An endogenous transcriptional control of the target gene is maintained such that the protein expression is controlled by cellular regulatory elements.

6. It has the potential to rescue normal splice pattern, thus reducing the amount of mutated proteins, which is specifically relevant for the treatment of dominant diseases caused by gain of function mutations.

The most commonly used antisense molecules in this category are U1 snRNAs and U7 snRNAs (Muller et al., 1997).

U1 snRNA

The U1 snRNP is composed of a 164 bp long U1 snRNA and is known to associate to many protein factors to initiate splicing processes through Watson and crick base pairing.

In humans, the U1 snRNA gene RNU1-1 (also known as RNU1) is located on the short arm of chromosome 1, 1p36 (Naylor *et al.,* 1984).

RNAU1 is a TATA-less promoter gene which contains a) an enhancer like distal sequence element (DSE) and b) a fundamental proximal sequence (PSE) that is recognized by the snRNA gene-specific factor PTF (PSE-binding transcription factor) or SNAPc (snRNA activator protein complex) (Sadowski *et al.,*1993).

In addition, several U1 snRNA pseudogenes are present throughout the genome. There are three distinct classes of the U1 snRNA pseudogenes, that have been generated by both DNA and RNA mediated mechanisms (Denison and Weiner 1982; Bernstein *et al.,* 1985). The U1 snRNA class II and class III pseudogenes are

dispersed throughout the genome and have no homology in their flanking regions, to each other or to the U1 snRNA gene.

The U1 snRNA class I pseudogenes, in contrast, have considerable 5′ and 3′ flanking sequence homology with the U1 snRNA genes and retain good homology with the two essential promoter elements, the distal sequence element (DSE), and proximal sequence element (PSE) (Denison and Weiner 1982). Since the U1 snRNA is not translated into a protein, active pseudogenes could possibly generate variant functional snRNAs. It has been known for some time that minor U1-like snRNAs, with variation to the human U1 snRNA exist, but to date, their function remains elusive (Patton *et al*., 1987; Lund *et al*., 1988; Kyriakopoulou *et al.,* 2006).

RNU1 is polymerase II dependent and needs TBP, TFIIB, TFIIA, TFIIE and TFIIF proteins (Kuhlman *et al.,* 1999) for its transcription.

The transcription of snRNA gene follows the below mentioned pattern, (Egloff *et al*., 2008):
• snRNA gene promoters recruit gene-type-specific pre-initiation complexes;
• There are several cis acting factors and transacting factors involved in the pre-initiation complex;
• It includes, a TATA box, at –25 relative to the transcription start site, USEs (upstream sequence elements), generally located within approximately 200 bp of the start site and an Enhancer, which can be far upstream or downstream of the start site;
• TATA box is recognized by the general factor TFIID. USEs and Enhancers bind a range of sequence-specific DNA-binding factors;
• Transcription initiation may also require interaction of the pol II CTD.

The 3′ end of the U1 snRNA (Hernandez A et al., 1992) is transcribed by pol II and occurs in several steps initiated by recognition of the cis-acting 3′-box that is a 13‑16-nt-long element which directs the production of a 3′ extended pre-

snRNA. It is a specific substrate for subsequent processing that generates the mature 3′ -end after transport to the cytoplasm (Kiss T et al., 2004, Mougun A et al., 2002, Huang Q et al., 1997).

The RNU1 transcript is not spliced and its 3' end is not polyadenylated, thus preventing its association to the translation machinery (Hernandez *et al.,* 2001). The use of U1 snRNA as an antisense agent for modulation of splicing is justified as it is involved in the initiation of splicing and there are thirty functional U1 genes in human genome versus only one U7 gene. This dis-equilibrium leads to the production of $1x10^6$ U1 snRNA molecules per cell compared to only $5X10^3$ copies of U7 snRNA, suggesting that the expression of U1 snRNA per gene copy is 6 fold higher than that of U7 making U1 a more feasible carrier than the U7 snRNA (Gorman *et al.,*2000).

The U1 snRNA engineered **(Fig.16)** through the replacement of an 8 nucleotide long sequence with a complementarity to specific splicing regulatory elements was demonstrated to show an efficient expression in vivo and to accumulate stably as a small ribonucleoprotein (snRNP), hence acting as a suitable backbone for the expression of antisense sequences that induces exon skipping (De Angelis *et al.,* 2002). Antisense derivatives of U1 snRNA have been employed to induce skipping of exons in the human beta-globin pre-mRNA and (Gorman et al., 2000) and in mutated dystrophin pre-mRNA (De Angelis et al., 2002; Denti et al., 2006a, b, 2008).

A U1 snRNA modified to target mouse dystrophin gene exon 23 was systemically delivered using adeno-associated virus (AAV) vectors to the dystrophin-deficient mouse model of Duschenne muscular dystrophy (DMD) mdx (Denti et al., 2006 a and b 2008). It was observed that the treated mice successfully skipped the targeted pre-mature termination codon (PTC) containing exon 23. Although, body-wide dystrophin restoration was evident, the effect was heterogeneous throughout the skeletal muscles (Denti et al., 2006). Further to this, U1 snRNA was used to correct splicing through exon skipping in human DMD pre-mRNA in primary patient fibroblasts (Incitti *et al.,* 2010). The most efficient exon skipping was achieved from targeting splice site as well as exonic regulatory regions of exon 51.

Recent work has also shown that a single chromosome-integrated copy of ExSpe U1 induced a significant correction splicing of endogenous SMN2 E7 and resulted in the restoration of the corresponding SMN protein levels (Dal Mas et al., 2015).
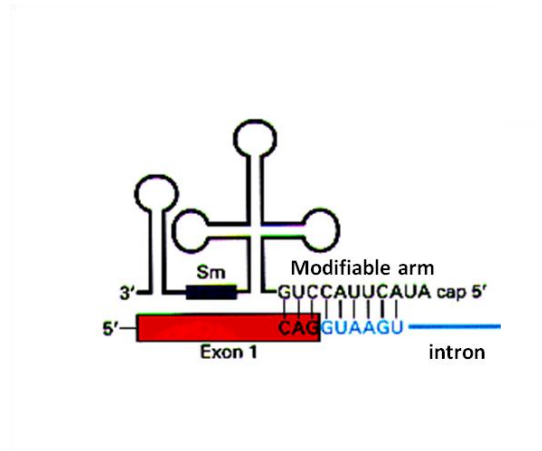
Fig.16 | Schematic representation of of U1 snRNA (black) along with its modifiable arm is shown to interact with exon 1 (red) and intron (blue) of pre mRNA at the 5'ss.

U7 snRNAs

The U7 snRNAs are involved in 3' end processing of the histone pre-mRNA (Goyanvalle A *et al.,* 2012) and is normally expressed in low levels. However they can be converted in to a versatile tool by engineering thus changing their properties and target specificities. A minor conversion of the wild type Sm binding site (AAUUUGUCUAG) into the consensus Sm-binding sequence derived from the major spliceosomal snRNPs (smOPT) was found to have beneficial effects on the U7 snRNA molecules as it increased the expression levels and enabled an efficient localization within the nucleus.

The innate 18 nt-long sequence of the modified U7snRNA (complementary to the 3' processing sites of histones) can be replaced with antisense sequences complementary to specific splicing regulatory elements, thus masking them **(Fig.17).**
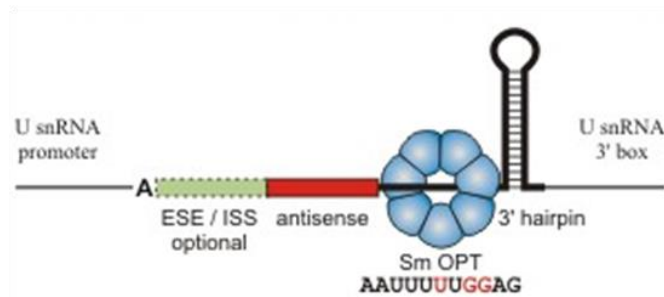
Fig. 17 | Shematic representation of modifiable U7 snRNA in which the antisense sequence (red) is embededed to target the specific sequence in the pre-mRNA to modulate splicing.The modification of wild type Sm binding site to consensus Sm binding site derived from smOPT is shown in red letters (Website:http://www.izb.unibe.ch/content/groups/schuemperli/gene_therapy_ii/index_eng.html).

In the last decade, many groups have shown that U7 snRNAs are appropriate to shuttle antisense sequences within them to correct aberrantly spliced exons in several pathologies. U7 snRNA-mediated modulation of splicing was achieved in CyPA (Cyclophillin A) that resulted in exon skipping effects and reduction of protein levels of cyclophillin A (Liu *et al.*, 2004).

It has also been applied for the dystrophin gene involved in Duchenne Muscular Dystrophy (DMD), wherein splice correction was achieved through exon skipping effects. These effects remained consistent both upon transduction in to mammalian cells and injection in to the mdx mouse model (Denti *et al.,* 2006).
A similar strategy was then successfully adapted to dystrophic immortalized mdx muscle cells wherein exon-23-skipped dystrophin mRNA rescued dystrophin protein synthesis (Brun *et al.*, 2003).
Similar effects were achieved for the SMN2 gene exon 7 implicated in Spinal Muscular Atrophy (SMA) in SMA patient-derived fibroblasts wherein the modified U7 snRNAs were able to induce exon 7 inclusion in up to 80% of transcripts (Geib *et al.*, 2009). A bifunctional U7 based snRNA was used to treat SMA mice with the modified construct through transgenic expression (Marquis *et al.*, 2007) or by lentiviral injection in to the CNS (Meyer *et al.*, 2009) both of which enabled prolonged survival in a dose dependent manner.

Recent studies have also demonstrated that U7 snRNAs can be effective in skipping of multiple exons (Goyanvalle *et al.*, 2012) in the context of Duchenne Muscular Dystrophy (DMD).

These observations prove that the antisense snRNAs embedded within AAV (Adeno-associated virus) vectors represents a promising form of gene therapy with persistent expression for treatment of several neurological disorders in the years to come (Uchikawa *et al.,* 2007).

1.5.2. Post transcriptional gene silencing (PTGS)

Only 1.5% of the mammalian genome encodes proteins (Tan L *et al.,* 2013). A significant proportion of the transcriptome that is unable to form proteins is classified as ncRNAs. They remain to be the largest class of transcripts known in the mouse and human. Based on the length, these molecules are classified as: small (<400 nucleotides) and long (>400 nucleotides) (Kornienko A.E *et al* .2013). The small ncRNAs are further divided in to:

- Infrastructural RNAs (rRNA, tRNA, and snRNA)
- Regulatory RNAs (miRNAs, siRNAs and snoRNAs)

Long noncoding RNAs can exceed 10,000 nucleotides and covers a range of regulatory molecules. This class includes Natural antisense transcripts (NATs) and RNA expansion repeats.

Transcriptional gene silencing can be achieved through both siRNAs and long noncoding RNAs (Malecova B *et al.,* 2010) thus, paving way to utilize these molecules to target diseased genes.

1.5.2 (i) siRNAs

RNA interference (RNAi) was first discovered in *Caenorhabditis elegans* by Andrew Fire and Craig Mello in 1998 (Fire *et al.,* 1998), for which they were awarded the Nobel prize in Physiology and Medicine (Chen S *et al.,* 2013).

It is a physiological gene specific silencing mechanism that is mediated by double stranded RNAs (dsRNAs) and can operate at transcriptional and post transcriptional events. (Dykxhoorn *et al.,* 2003; Meister *et al.,* 2004; Zamore *et al.,* 2005; Chapman *et al.,* 2007).

This process is initiated by an endogenous double stranded RNA (dsRNA) molecule, which is processed in the nucleus by an endonuclease, *Drosha* and exported in to the cytoplasm for a further processing by a second endonuclease *Dicer* to generate RNA duplexes that are 21-23 nucleotides in length with 2 nucleotide overhangs at the 3' termini (Miller *et al.*, 2005; Seyhan *et al.*, 2011).

These duplexes now termed as siRNAs are recognized and bound by a multi-protein complex known as RNA-induced silencing complex (RISC). The RISC unwinds the siRNA duplex; one strand termed as the "guide" / "antisense" strand hybridizes to complementary target sequence of a messenger RNA leading to its degradation (Meister *et al.,* 2004) and the other strand termed as "passenger" / "sense" strand is cut by an enzyme argonaute 2 (Ago 2) present within the RISC complex (Miller *et al.,* 2005; Seyhan *et al.,* 2011).

The guide strand directs a RISC-mediated endonucleolytic cleavage of the mRNA. This process occurs at a single phosphate across nucleotides 10 and 11 from the 5' end of the guide strand, thus triggering degradation of mRNA eventually preventing its translation in to a protein (Hamilton *et al.,* 1999; Hammond *et al.,* 2000; Zamore *et al.,* 2000; Elbashir *et al.,* 2001) **(Fig.18).**
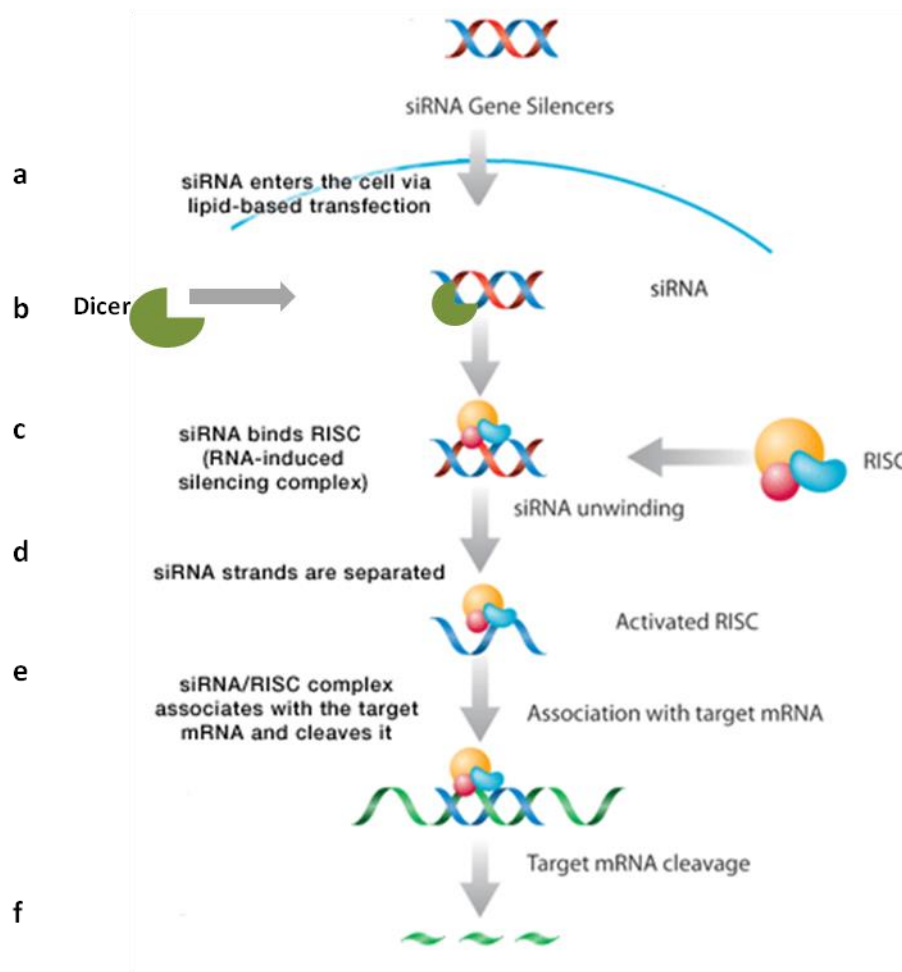
Fig. 18 | Schematic representation of the fate of double stranded siRNA a) Entry in to the cell via transfection b) The duplex binds to DICER leaving a two nucleotide long 3' overhang c)This primes binding of the dsRNA for binding to the RNA induced silencing complex (RISC) d) Binding of the RISC complex to dsRNA leads to the activation of Ago 2 enzyme and the RNAse component of RISC destroys one of the strands e) The other strand binds to the target mRNA and mediates its cleavage f) Cleaved target mRNA (Modified from Santa cruz biotechnology)

RNAi can also be triggered by exogenous delivery of dsRNAs in to cells. Once a potent and selective siRNA is identified, it can be incorporated in to short hairpin RNA (shRNA) to be expressed from plasmids or viral vectors (Seyhan *et al.,* 2011) and injected in to the cells through transfection or transduction respectively.

RNAi has been successfully used in *in vitro* and *in vivo* studies thus demonstrating its potential as a therapeutic molecule in the context of neurogenetic diseases (Seyhan A. *et al.,* 2011).

- **Amyotrophic lateral sclerosis (ALS)** is caused due to mutations in Superoxide dismutase 1 (SOD1) that leads to toxic gain of function phenotype. Selective suppression of mutant SOD1 allele using siRNAs has been shown in Drosophila lysate using reporter assays (Schwarz *et al.,* 2006).This was followed by a viral RNAi delivery in to a transgenic mouse model of ALS wherein a therapeutic benefit was observed through improved motor neuron survival, delayed disease onset and increased life span of animals (Ralph *et al*., 2005; Raoul *et al.,* 2005).

- **Spinocerebellar ataxia type 3 (SCA 3)** is caused by a dominant expression of CAG repeats in the ataxin-3 gene (Paulson *et al.,* 2000). Researches have shown that these mutations can be targeted using an AAV1 expressing shRNAs in a transgenic mouse model expressing high levels of pathogenic form of ataxin -1 with 82 CAG repeats in cerebellar cells (Burright *et al.,* 1995). Upon treatment, an improved motor coordination and cerebellar morphology was observed in the animals. Similar studies were also shown in ataxin-7 disease model (Scholefield *et al.,* 2009).

- **Huntington's disease (HD)** characterized by the poly Q proteins encoded by CAG repeats within the HTT (Huntingtin) gene was targeted with an RNAi approach using an AAV expressing shRNA, which resulted in an improvement of disease pathology and life span extension (Harper *et al*., 2005).

- **Alzheimer's disease (AD)** caused due to mutations in the Amyloid precursor protein (APP) gene. Allele specific silencing has been demonstrated in a transgenic APP mutant mouse model, in which an AAV 5 vector based delivery lead to decrease of mutant protein accumulation and an increase of psychometric performance (Rodriguez –Lebron *et al*., 2009).

- **FTDP-17** is caused due to various mutations in MAPT gene and an siRNA approach has been used to selectively target the mutant allele containing the V337M mutation in exon 12 of MAPT gene.

- **Parkinson's disease (PD)** is characterized by an over expression of alpha synuclein protein as a result of mutations such as A53T and A30P.

Lentiviral based shRNA approach was successfully employed in a rat model, in which selective suppression of the mutant allele was observed.

- Similar studies were also carried out in the **Slow channel congenital myasthenic syndrome disease (SCCMS)**, in which a selective suppression of mutant acetyl choline receptor (AChR) subunits (containing an AS226F mutation) was achieved in mammalian cells. using siRNAs and shRNAs (Croxen *et al.,* 2002).

Likewise, siRNAs have also been used as therapeutic molecules to target splice defects wherein, it is employed to specifically target and degrade disease linked mRNA isoform (Zhu *et al.,* 2005). Therefore RNAi is emerging as a valuable tool for clinical applications in the context of neurogenetic diseases. This justifies a possible approach to target the 4R isoform containing exon 10 in FTDP-17.

1.5.2 (ii) Long non coding RNAs (lncRNAs)

Long non-coding RNAs are transcripts with a varied size between 200-100,000 bases. They have little or no protein coding capacity (Schonrock *et al.,* 2012). They may or may not be spliced, or polyadenylated, they might be nuclear or cytoplasmic, and are transcribed by RNA polymerase II or III (Amaral P.P *et al.,* 2011).
Those ncRNAs engaging in RNA-RNA, RNA-DNA, and RNA-protein interactions can thus regulate processes such as chromatin remodeling, transcription, mRNA processing, stability and localization, translation and protein stability (Schonrock N *et al.,* 2012).

Long noncoding RNAs (lncRNAs) can regulate gene expression through a variety of mechanisms (Mercer, T.R. *et al*., 2009; Korneinko *et al.,* 2013) **(Fig.19)**.

Regulation *in trans*

(a) TF inactivation

7SK lncRNA
P-TEF-b
RNAPII
pc gene

(b) RNAPII inactivation

Heat shock
RNAPII
B2 lncRNA
pc gene

Regulation *in cis*

(c) X chromosome inactivation

active X chromosome

EM EM EM EM EM EM EM EM EM EM EM
inactive X chromosome
XIC   pc genes silenced

XIST lncRNA product
EM   RNAPII   EM
pc gene   XIST lncRNA transcription   pc gene

(d) Regulation by lncRNA product

EM
EM
pc gene

EM
EM
lncRNA product   RNAPII
lncRNA transcription

(e) Regulation by lncRNA product

lncRNA product   EM
RNAPII   EM
lncRNA transcription   pc gene

(f) Regulation by lncRNA transcription

lncRNA transcription
lncRNA product
RNAPII
RE   P   pc gene

G. Key

P Protein-coding gene promoter | [P_____] forward strand | [P___q] forward and reverse strand
P LncRNA promoter | (RNAPII) pc gene RNA Polymerase II | (RNAPII) lncRNA RNA Polymerase II
↳ LncRNA transcription | ⊥ Repressed functional transcription of a protein coding gene
〜 LncRNA product | EM Epigenetic Modifier guided by lncRNA product | XIC X chromosome inactivation center
☿ LncRNA EM binding site (sequence/structure) | ▬ RNA/DNA interaction element
➜ Upregulated transcription of protein-coding gene | RE *Cis*-regulatory element (enhancer, insulator)
▪ Disrupted *cis*-regulatory element-promoter interaction

Fig. 19| Long non-protein-coding RNAs (lncRNAs) act at different levels to regulate protein coding gene expression. lncRNAs can inhibit general protein-coding (pc) gene expression in trans (a) by preventing transcription factor (TF) activity (e.g. 7SK lncRNA) or (b) by inhibiting RNAPII binding to DNA (e.g: B2 lncRNA). Xist lncRNA is transcribed from the X inactivation center (XIC) and inactivates a whole chromosome in cis (c) by recruiting epigenetic modifiers (EM). lncRNAs can regulate specific genes, acting in trans (d) or in cis (e) by directly recruiting epigenetic modifiers to certain genomic loci. In both cases the lncRNA binds EMs via a specific sequence or structure and targets them to promoter regions via DNA/RNA interaction elements to influence expression of the respective pc gene. Transcription of a lncRNA through a pc gene promoter or a cis-regulatory element (RE) affects pc gene expression in cis independent of the lncRNA product.

55

Both DNA strands are shown as separate boxes to indicate lncRNA transcription over the pc gene promoter in the antisense orientation (Kornienko *et al.*, 2013).

In fact, ncRNAs have been regarded as significant regulators in orchestrating neural gene expression and function (Brosius *et al.,* 2005). Implications of ncRNAs in mediating complex biological functions such as neurogenesis, neurotransmission, neuronal patterning, synaptic plasticity, stress responses and aging of brain have been observed.

Knock out studies in mice models have shown that ncRNAs are active players in the development of nervous sytem (Guttman, M *et al.,* 2009; Mercer *et al.,* 2010; Gordon *et al.,* 2010; Bond *et al.*, 2009; Lewejohann *et al.,* 2004)

This validates the function of ncRNAs in the Central nervous system (CNS) (Cao *et al.,* 2006; Mehler *et al.,* 2007; Mercer T.R *et al.,* 2008; Tsurdome K *et al.,* 2010; Gao F.B *et al.,* 2010; Qureshi *et al.,* 2011). Thus their dysregulation could be central to the development of debilitating neurodegenerative diseases. NATs are a class of abundant ncRNAs located in the nervous system. They are transcribed from the opposite strand of either protein or non-protein coding genes and often partially overlap with the protein-coding genes thus sharing a sequence complementarity with the corresponding sense mRNA (Schonrock *et al.,* 2012).

LncRNAs have also been shown to be associated to AD, which is caused due to an accumulation of extracellular amyloid protein (Aβ42). This diseased state is thought to be associated with an elevated level of secretase enzyme, termed as β-secretase cleaving enzyme 1 (BACE1). A lncRNA, known as BACE1 antisense transcript (BACE1-AS) is known to regulate the expression of BACE1 mRNA and the protein both *in vitro* and *in vivo* (Faghihi *et al.,* 2008).

Upon exposure to Aβ42, the expression of BACE1-AS becomes elevated wherein it increases the stability of BACE1 mRNA and generates more Aβ42 through a post-transcriptional feed-forward mechanism (Faghihi *et al.,* 2008). The increased amounts of BACE1-AS was confirmed in both subjects with AD and transgenic mouse, thus proving the direct implication of lncRNA in accumulation of APP linked to AD (Massone *et al* . 2011).

Other Long ncRNAs include NEAT1and 2 that has been shown to contribute to the development of amyotrophic lateral sclerosis (ALS) (Nishimoto *et al.*, 2013).

TAR DNA-binding protein-43 (TDP-43) and fused in sarcoma/translocated in liposarcoma (FUS/TLS) (Lagier-Tourenne and Cleveland, 2009) contribute to the development of ALS. Recent studies showed that both TDP-43 and FUS/TLS are bound by and are co-localized with the long ncRNA NEAT1 and 2. This long ncRNA is vital for the formation of nuclear bodies called paraspeckles and was shown to be up-regulated in human motor neurons in early stage of ALS (Nishimoto *et al.*, 2013). Thus, NEAT1 and 2 might contribute to the development of early stage of ALS through their interaction with TDP-43 and FUS/TLS (Vucicevic *et al.*, 2014).

Long ncRNAs could also be possibly involved in the development of HD, in which long ncRNAs HAR1F and HAR1R are affected (Pollard *et al.*, 2006). Human accelerated regions (HARs) are fast evolving non-coding sequences in the human brain and are often found close to the neurodevelopmental genes like GATA3. It was postulated that they might potentially participate in unique human brain functions (Pollard *et al.*, 2006). Of these regions, the most dramatic changes were found in the HAR1 locus that codes for the two long ncRNAs HAR1F and HAR1R (Pollard *et al.*, 2006). The expression of both can be repressed by the RE-1-silencing transcriptional factor (REST) that pathologically (in HD) trans-locates to the nucleus and mediates repression of important neuronal genes in neuronal cells (Johnson *et al.*, 2010). Future studies are essential to shed light on the mechanism of HAR1 long ncRNAs and their role in development of HD (Vucicevic *et al.*, 2014).

Another lncRNA BC200 is known to exhibit abnormal sub-cellular localization and expression levels in brain regions of AD patients (Mus *et al.,* 2007).

Hence, these studies open a possible new avenue of research focusing on regulation of *MAPT* through lncRNAs for a therapeutic benefit.

CHAPTER 2. Screening for modified U1 snRNAs to modulate splicing of Exon 10 in MAPT pre-mRNA

2.2 Results

Abstract

This chapter focuses on evaluating the feasibility of a gene therapy approach using antisense sequences embedded in U1 and U7 snRNAs to modulate splicing. Since mutations in exon 10 of MAPT gene have been reported to cause an impairment of splicing leading to an altered proportion of 4R and 3R isoforms in FTDP-17, this work has been dedicated to explore modulation of splicing so as to induce skipping of exon 10 thus restoring the balance of 1:1 of the two isoforms (4R:3R).

Previous work by Covello G et al., (unpublished data) has demonstrated that antisense oligonucleotides are capable of inducing exon 10 skipping in the context of rat pheochromocytoma (PC12) cells. These oligonucleotides were further embedded in to the U1 and U7 snRNA cassettes and available in the lab prior to the beginning of sections explained below.

The first part of this project was dedicated to produce chimeric scramble constructs which were used as controls for all the following experiments.

The second part was dedicated to test the efficacy of thirteen different chimeric constructs embedded in the U1 / U7 snRNA cassette to check for their effect on regulation of MAPT exon 10 splicing.

The results were checked after 48 hours of transfection in PC12 cells using semi-quantitative Real-Time PCR assays.

2.1. Materials and methods

All the primers were synthesized by the *Eurofins* mwg/ operon company.

The following constructs were available in the Laboratory of RNA Biology and Biotechnology, CIBIO:

-pAAV2.1.-CMV eGFP3 vector, an adeno associated vector recombinant vector containing the following parts:

a. A Strong CMV promoter, that allows an high expression of foreign genes;

b. Ampicillin resistance for a positive selection of the recombined colonies and the GFP cassette for the visualization of transfected cells (Auricchio et al., 2001).

-Six different chimeric constructs, composed of the U1 snRNA cassette, coupled to specific antisense oligonucleotides, embedded in to the pAAV2.1 CMV eGFP vector **(Table 1)**.

-Six different chimeric constructs, composed of the U7 snRNA cassette, coupled to specific antisense oligonucleotides, embedded in to the pAAV2.1 CMV eGFP vector **(Table 1)**.

U1 Chimeric constructs	U7 Chimeric constructs
pAAV_GFP_U1#10_α	pAAV_GFP_U7#10_α
pAAV_GFP_U1#10_β	pAAV_GFP_U7#10_β
pAAV_GFP_U1#10_rβ	pAAV_GFP_U7#10_rβ
pAAV_GFP_U1#10_ α β	pAAV_GFP_U7#10_ α β
pAAV_GFP_U1#10_ α rβ	pAAV_GFP_U7#10_ α rβ
pAAV_GFP_U1#10_γ	pAAV_GFP_U7#10_γ

Table 1 | List of available chimeric constructs in the Lab of RNA Biology and Biotechnology (prior to 2011).

2.1.1. Construction of U snRNA chimeric scramble molecules

2.1.1.(i) Oligonucleotides phosphorylation

100 pmol of forward and reverse primers were phosphorylated in a final volume of 100 μL by using T4 polynucleotide kinase (Fermentas).

Reagent	[C]i	[C]f
Primers	100 pmol/μL	100 pmol/ 100 μL
T4 polynucleotide kinase (Fermentas)	10 U/ μL	50 U/ 100 μL
Buffer A (Fermentas)	10X	1X
ATP (Fermentas)	100 μM	1 μM
Water	-	-
Final volume: 100 μL		

After an incubation of 30 minutes at 37°C, the reaction was stopped by the addition of 1 μL of EDTA 0.5M pH=8. Oligonucleotides were purified by the addition of 100 μL of chloroform, and centrifuged for 2 minutes at 13000 rpm. The resulting supernatant containing the phosphorylated oligonucleotides was transferred in a new eppendorf.

The phosphorylated primers with a final concentration of 1 pmol/μL thus obtained were then used for the first PCR amplification reaction and /or stored at -20 °C.

2.1.1. (ii) First polymerase chain reaction

The fragments of U1#10_α scramble, U1#10_ɣ scramble, and U1#10_universal were obtained via three distinctive PCRs using the pAAV2.1.-CMV eGFP PBS U1 plasmid containing the U1 snRNA gene. Similarly, the U7#10_α scramble, and U7#10_universal were obtained via two distinctive PCRs using the pU7 smOPT containing the U7 snRNA gene.

Each individual set of PCR was carried out such that;

- 100ng of template was used with the following set of primers;
- a. U1#10_α scramble (Forward primer: U1 casup and Reverse primer: U1 antisense (α) scramble).

- b. U1#10_ý scramble (Forward primer: U1 casup and **Reverse primer**: U1 ace antisense (ý) scramble).

- c. U1#10 universal (Forward primer: U1 universal and **Reverse primer**: U1 cas down).

- d. U7#10_α scramble (Forward primer: U7 casup and Reverse primer: U7 antisense (α) scramble).

- e. U7#10 universal (Forward primer: U1 universal and **Reverse primer**: U7 cas down).

2.1.1. (iii) Ligation of the U1 fragments

The fragments were ligated such that:
- U1#10 α scramble and U1#10 universal to generate the full length U1#10 α scramble.

- U1#10 ý scramble and U1#10 universal to generate the full length U1#10 ý scramble.

- U7#10 α scramble and U7#10 universal to generate the full length U7#10 α scramble.

The ligation was performed in a final volume of 20 μL with a molar ratio of 1:2 for the U1/ U7 #10 α/ ý scramble and U1/ U7 #10 universal respectively. The reaction was incubated at 16 °C for 3 hours, according to the following protocol. The result of the ligation was checked on a 1.2% agarose gel (EtBr 5%), and subsequently used as a template for the II PCR reaction that follows.

Reagent	[C]i	[C]f
U1/ U7#10 α/ ý scramble	-	440 ng/20 μl
U1/ U7 #10 universal	-	100 ng/20 μl
T4 DNA Ligase Buffer (NEB)	10X	1X
T4 DNA Ligase (NEB)	5U/μl	3U/20 μl
Water	-	-
Final Volume = 20 μl		

2.1.1. (iv) Second polymerase chain reaction

Each of the three fragments obtained from the ligation reaction was used as a template (20ng) for a II PCR reaction, with the external U1 Cas up and U1 cas down primers to generate the full length chimeric U1 and U7 antisense scramble constructs. This reaction was performed in a final volume of 50 μL with a single series of 30 cycles, preceded by a 1 minute long pre-denaturation step, according to the below mentioned protocol:

Reagent	[C]i	[C]f
Ligation product	-	20 ng/50 μL
Cloned pfu DNA polymerase reaction buffer (Agilent)	10X	1X
dNTPs mix (Euroclone)	10 mM	0.2mM
Cloned pfu DNA polymerase (Agilent)	2U/ μL	2.5U/ 50 μL
U1 Cas up For	10 μM	0.2 μM
U1 Cas down Rev	10 μM	0.2 μM
Water	-	-
Final volume: 50 μL		

5 μL of the amplification product were loaded on a 1.2% TBE 1X agarose gel (EtBr=5%) with 1 kb plus DNA ladder (Fermentas). The electrophoresis was allowed to run for 30 minutes at 80 V. DNA products (575 bp) were purified with the QIAquick PCR purification kit (Qiagen) following manufacturer's protocol and quantified with Nanodrop ND-1000 spectrophotometer (Thermo scientific).

2.1.1. (v) Cloning in the pAAV2.1-CMV-eGFP vector

Digestion and dephosphorylation of pAAV-2.1 CMV-eGFP3 vector

The amplified product was purified using the QIAquick PCR purification kit (Qiagen). The total amount of U1/U7 #10 scrambles (α/γ) and 10 μg of pAAV2.1 CMV eGFP3 vector were digested with NheI restriction enzyme for 3 hours at 37^0 C in a final volume of 50 μL, according to the protocol described in the below mentioned table.

Reagent	[C]i	[C]f
PCR sample	-	-
NEBuffer (NEB)	10x	1x
NheI (NEB)	2U/ μL	2U/50 μL
Water	-	-
Final volume: 50 μL		

Following this, the U1 / U7 #10 scramble fragments were purified with QIAquick PCR purification kit (Qiagen), according to manufacturer's instructions. This protocol is based on an ionic exchange of columns in order to bind to DNA and elution of the sample in a final volume of 30 μL of water after a couple of washing steps, performed with appropriate buffer containing isopropanol.

In order to prevent re-circularisation of the plasmid, the digested pAAV2.1 CMV eGFP3 vector was dephosphorylated with Calf Intestine Alkaline Phosphatase (CIAP, Fermentas) at 37°C for 30 minutes, following the below mentioned protocol in table.

Reagent	[C]i	[C]f
pAAV2.1 CMV eGFP3	-	10 μg/ 100 μL
CIAP (Fermentas)	1U/ μL	0.4U/100 μL
Buffer CIAP (Fermentas)	10X	1X
Water	-	-
Final volume: 100 μL		

The dephosphorylated Nhe I- pAAV2.1 CMV eGFP3 vector was separated on 1% TAE 1X agarose gel (2.5% EtBr) in addition to 40% W/V 6X sucrose loading dye. DNA was recovered by the QIAquick Gel extraction Kit (Qiagen) according to manufacturer's instructions and quantified with Nanodrop ND-1000 Spectrophotometer (Thermo scientific).

Ligation of chimeric fragments in to the pAAV2.1 CMV eGFP3 vector
The ligation reaction was performed for three hours at 16 °C in a final volume of 20 μL by using T4 DNA ligase (NEB) and using a molar ratio of 1:3 for the vector (Nhe I- pAAV2.1 CMV eGFP3) and the chimeric scramble fragments (Nhe I- U1 / U7 #10 (α/γ)) respectively.

The exact quantity of insert to use in this reaction for 100 ng of vector was calculated with the below mentioned formula:

$$\text{ng of insert} = \frac{\text{vector (ng) x insert dimension (kb) x molar ratio (insert/vector)}}{\text{vector dimension (kb)}}$$

The protocol used for the ligation is reported in the below mentioned table.

Reagent	[C]i	[C]f
Nhe I- pAAV2.1 CMV eGFP3 vector	-	100 ng/20 μL
Nhe I- U1#10 chimeric scramble	-	35 ng/20 μL
T4 DNA Ligase Buffer (NEB)	10X	1X
T4 DNA Ligase Enzyme (NEB)	5U/ μL	5U/20 μL
Water	-	-
Final volume: 20 μL		

The result of the ligation reaction was transformed in to *E.coli* DH5 α competent cells.

2.1.1. (vi) Preparation of *E.coli* DH5α competent cells and transformation
Preparation of competent cells

An aliquot of *E.coli* DH5 α competent cells was grown in LB (25g/L, Sigma) at 37 °C until it reached the exponential growth phase, with an OD600 of 0.6. 1mL of the culture was then inoculated in 50 mL of LB (25g/L, Sigma) containing 50 μg/mL ampicillin, and incubated for 2 hours in agitation at 37 °C. DH5 α cells were then centrifuged for 5 minutes at 4000 rpm at 4°C. The pellet thus obtained was resuspended in 1/20 volume of a solution containing 25g/L LB (Sigma), 10% PEG3350, 5% DMSO, 10mM $MgCl_2$ and 10mM $MgSO_4$. 10% glycerol was added to this solution and stored at -80°C.

Transformation

Competent cells prepared as described above were thawed in ice for 10 minutes. Meanwhile, 10μL of the ligation products were mixed with 100μL of KCM solution (100mM KCL, 20 mM $Cacl_2$, 50 mM $MgCl_2$) and incubated for 5 minutes

in ice. 100μL of *DH5α* competent cells were hence added to DNA-KCM, and the resulting solution was gently mixed and incubated in ice for 20 minutes. At the end of the incubation step, *DH5α* cells were heat-shocked for 1 minute at a temperature of 42°C, and incubated for in ice for another minute. 800μL of LB (25g/L, Sigma) without ampicillin was added to the transformed cells, and the resulting solution was incubated for 1 hour at 37°C in agitation at 350 rpm. Finally, they were plated on a LB agar plate (35 g/L, Sigma) with ampicillin (50μg/mL) and incubated overnight at 37°C.

The colonies grown during the overnight incubation were picked and grown overnight in agitation at 37°C in 5 mL of 25 g/L LB (Sigma) with ampicillin (50μg/mL). On the following day, the plasmid DNA was extracted using the *QIAprep Spin Miniprep Kit* (Quiagen) following manufacturer's protocol, and its concentration was measured with *Nanodrop ND1000* spectrophotometer (Thermo scientific).

Analysis of the transformed colonies

The exact sequence and the orientation of the inserts within the PAAV-2.1CMVeGFP3 vector were confirmed by automated DNA sequencing (*BMR Genomics,* Padua) using the AAV Rev primer (5' - CCATATATGGGCTATGAACTAATG-3').

2.1.2. Selection of cell line

2.1.2. (i). PC12 cell line

Rat pheochromocytoma cells (PC12) was used as the system to study the effects of chimeric constructs on exon 10 of MAPT gene. This system has been employed as a model system to study due to its pre-dominant content of exon 10 and ability to stop division and terminally differentiate upon treatment with nerve growth factor (NGF) (Greene and Tischle, 1976). The cells were maintained in Dulbecco's Modified Eagle's Medium (DMEM) with 4.5% g/L glucose and phenol

red, supplemented with 5% Fetal Bovine serum (FBS) and 10% Horse serum (HS).Cells were plated in monolayer in a T-25 flask coated with 0.05% poly-D-lysine. They were allowed to grow until reaching a confluency of 70% after which they were transiently transfected with the chimeric constructs.

2.1.2. (ii) Optimisation of transfection efficiency

In order to optimize the best transfection efficiency, two transfection methods were adapted;

a. Lipid based transfection
b. Electroporation

These methods were optimized for transfection of DNA in PC12 cells and have been included in the manuscript with the following title:

Covello G, Siva K, Adami V, Denti MA. (2014) "An electroporation protocol for efficient DNA transfection in PC12 cells" *Cytotechnology* 66(4):543-53.

a. Lipid based transfection

The transfection reagents used in this study were: TransIT-LT1 Transfection Reagent (Mirus, Madison, WI, USA), Lipofectamine 2000 and Lipofectamine LTX (Invitrogen). 4 x 10^4 cells/well were seeded on poly-D-lysine- coated 24-well plates (Corning) a day prior to transfection and grown in supplemented DMEM at 37 °C supplied with 5 % CO_2. PC12 cells which were grown upto a 70 % confluency were then transfected with the mammalian expression vector pEGFP-C1 (Empty vector with GFP). Transfection procedures were performed as indicated by manufacturer. The ratio DNA (ng) : transfection reagent (μL) was 1:3 with all three transfection reagents.

b. Electroporation

Electroporation in PC12 cells were optimized using the pEGFP-C1 (Empty vector with GFP) as described by Covello G et al., 2014 (*Refer to attachment*).

The above mentioned optimized method was used as a standard protocol to perform transfections in PC12 cells as described below.

2.1.2. (iii) Transfection experiments in PC12 cell line

The transfection of PC12 cells with chimeric constructs was performed using the Neon transfection system MPK5000 (Invitrogen). Cells with 70% confuency were washed twice with 5mL of PBS (1X) (Lonza). 1mL of 1X Trypsin (Lonza) was added and incubated for 2 minutes at 37 °C. Trypsin was deactivated using 9mL of DMEM and cells were transferred in a 15 mL falcon and centrifuged at 400g for 5 minutes. The pellet thus obtained was re-suspended in 10 mL PBS .The number of cells were counted using the Burker chamber. Trypan blue stain exclusion test was used to determine cell viability. 10 μL of cell solution was mixed with an equal volume of 0.4% trypan blue stain and counted with the Burker chamber, using the below mentioned formula:

Cell concentration (cells/ml) =mean of the readings x titration factor x10000

Cells were further resuspended in Buffer R to reach a concentration of 10^8 cells/ mL. 10 μL of cell solution (containing ∼ 10^6 cells) plus 0.5 μg of each chimeric construct were added to 500 μL of DMEM in every well of the plate coated with poly-D-lysine.

The transient transfections of PC12 cells with chimeric constructs were performed with the following conditions: 1×10^6 cells / well, three 10ms-long pulses each with 1500 V.

Evaluation of transfection efficiency

Images of the transfected cells were acquired using Operetta High Content Imaging System (Perkin Elmer, Monza, Italy). After 48 hours of transfection, cells were washed with PBS 1X (Lonza). They were incubated for 20 minutes at 37 °C in 500 μL of supplemeted DMEM with 1mg/mL of Hoechst 3342 fluorescent dye (Sigma) to enable nuclei counterstain and subsequent total cell count. Cells were washed again with PBS 1X and replaced with supplemented medium (without red phenol).

The transfection efficiency was analysed using the Harmony High Content Imaging Software (Perkin Elmer). The 'Select Population' feature of Harmony software allowed to set a threshold of fluorescence intensity in order to identify the sub-population of transfected cells.

Images were obtained with a 20X LWD objective, with two different filter sets;
1. Filter for Hoechst 3342 stain (excitation filter: 360-400 nm, emission filter: 410-480 nm) to visualise total viable cells.
2. Filter for Alexa Fluor 488 (excitation filter 460-490 nm, emission filter: 500-550 nm) was used to count the number of transfected cells. The laser autofocus was applied and 12 image fieds were acquired for each well.

2.1.3. Semi-quantitative reverse transcriptase analysis on PC12 cell line

2.1.3. (i) RNA extraction

RNA extraction was performed using Trizol reagent (Life technologies). After the addition of 200 μL of Trizol reagent, 60 μL of chloroform was added to added to each sample and vortexed vigorously. This was followed by an incubation of 3 minutes at room temperature. The solution was then centrifuged at 12000 g for 15 minutes at 4°C. 150 μL of isopropanol was added to the mix and incubated at room temperature for 10 minutes followed by a centrifugation at 12000 g for 10 minutes at 4°C. The supernatant was discarded while the pellet was washed with 300 μL of 75% ethanol. The sample was briefly vortexed, centrifuged at 7500 g for 5 minutes at 4 °C and air-dried for 5 minutes.

The RNA was resuspended in 30 µL of RNAse free water and quantified by Nanodrop ND-1000 (Thermo scientific) spectrophotometer.

In order to remove traces of DNA, the extracted RNA was treated with DNAse by using Turbo-DNAse Kit (Ambion) following manufacturer's instructions.

2.1.3. (ii) cDNA preparation

500ng of the RNA extracted from each sample with *Trizol* reagent (Life Technologies) was reverse-transcribed to cDNA with the *RevertAidTM First Strand cDNA Synthesis Kit* (Fermentas) by using both random primers and dT18 oligonucleotides, following manufacturer's protocol. The obtained cDNA was used as template for semi-quantitative Real-Time PCR reactions, in order to evaluate the levels of the expression of the U1 chimeric molecules snRNAs and isoforms of MAPT transcripts.

2.1.3. (iii). Semi quantitative RT-PCR assay to evaluate expression of RNA of U1snRNA constructs

The expression levels of U1 snRNA chimeric constructs and their integrity was analysed using semi-quantitative reverse transcription polymerase chain reaction with appropriate primers using 5 µL of the cDNA synthesized with random primers. The amplification reaction was carried out using 35 cycles preceded by a pre-denaturation step of incubation for 1 minute at 95 °C, using the below mentioned protocol in a final volume of 25 µL. ß actin was used as a house keeping control. The dimensions of amplified U1 and U7 products are reported in the table below.

Sample	Product dimension (bp)
U1/U7 α	98
U1/U7 β	97
U1/U7 α β	130
U1/U7 αrβ	130
U1/U7 γ	98
U1/U7 α scr	98
U1 γ scr	98

Chimeric construct	Forward primer	Reverse primer
U1 α	r/h Anti 3F ATT ATC TGC ACC TTT GGT AGC C	U1+130rev gtc AGC ACA TCC GGA GTG CAA TG
U1 β	r/h Anti5F GAA GGT ACT CAC ACT GCC GCC TC	U1+130rev gtc AGC ACA TCC GGA GTG CAA TG
U1 α β	r/h Anti 3F ATT ATC TGC ACC TTT GGT AGC C	U1+130rev gtc AGC ACA TCC GGA GTG CAA TG
U1 αrβ	r/h Anti 3F ATT ATC TGC ACC TTT GGT AGC C	U1+130rev gtc AGC ACA TCC GGA GTG CAA TG
U1 γ	r/h Anti ACEF CAC TTG GAC TGG ACG TTG CTA AG	U1+130rev gtc AGC ACA TCC GGA GTG CAA TG
U1 α scramble	r/h Anti 3F ATT ATC TGC ACC TTT GGT AGC C	U1+130rev gtc AGC ACA TCC GGA GTG CAA TG
U1 γ scramble	r/hAnti ACEF CAC TTG GAC TGG ACG TTG CTA AG	U1+130rev gtc AGC ACA TCC GGA GTG CAA TG

The above mentioned forward primers were used in a combination with the U7 Reverse primer U7rev   ggg AGG GGT TTT CCG ACC GAA G for the amplification of U7 small nuclear RNAs. The primer pairs used for the amplification of the house keeping gene (HK) ß-actin is as follows:

House keeping gene	Forward primer	Reverse primer	Product length
ß actin	bACTINrt_r/mFor GAT CAA GAT CAT TGC TCC TCC TG	bACTINrt_r/mRev AGG GTG TAA AAC GCA GCT	200bp

Amplified products were allowed to run with 1 Kb plus DNA ladder (Fermentas) on a 2 % agarose gel electrophoresis (EtBr=5%) at 90 Volts in TBE 1X running buffer for about 40 minutes.

Images were acquired using the BioDoc-It Imaging (UVP) and densitometric analyses were performed on the images using Image J software.

2.1.3. (iv) Semi quantitative RT-PCR assay to evaluate expression of RNA of MAPT transcript isoforms

A semiquantitative RT-PCR amplification was performed to analyse the expression levels of MAPT and HK gene β-actin. This analysis was performed to evaluate the effects of chimeric constructs on regulation of splicing events of MAPT exon 10. The cDNA was prepared using oligo dT oligonucleotides and amplification reaction was performed in a final volume of 25 μL, with a single series of 35 cycles preceded by a 1 minute long pre-denaturation step of incubation at 95 °C, using the below mentioned protocol.

Reagent	[C]i	[C]f
cDNA	-	-
RBC reaction buffer	10X	1X
dNTPs mix (Euroclone)	10 mM	0.2 mM
RBC Taq polymerase	5U/ μL	1U /25 μL
Forward primer (Tau)	10 μM	1 μM
Reverse primer (Tau)	10 μM	1 μM
Water	-	-
Final volume: 25 μL		

Reagent	[C]i	[C]f
cDNA	-	-
RBC reaction buffer	10X	1X
dNTPs mix (Euroclone)	10 mM	0.2 mM
RBC Taq polymerase	5U/ μL	1U /25 μL
Forward primer (ß actin)	10 μM	0.5 μM
Reverse primer (ß actin)	10 μM	0.5 μM
Water	-	-
Final volume: 25 μL		

Primers used for amplification of MAPT and ß-actin gene and the PCR protocol are described as follows:

Gene	Forward primer	Reverse primer	Product dimension (bp)
Exon 10+ / Exon 10-	TAUR9F CTGAAGCACCACCAGCCGGGAGG	TAU13R TGGTCTGTCTTGGCTTTGGC	368 / 275
ß-actin	ACTIN FOR AGACGGGGTCACCCACACTGTGCCCATCTA	ACTIN REV CTAGAAGCATTTGCGGTGCACGATGGAGGG	650

PCR METHOD : 35 CYCLES (BIORAD)	
Temperature	Time
95 °C	10 minutes
95 °C	30 seconds
60 °C	40 seconds
72°C	1 minute
72°C	10 minutes
4°C	∞

The amplified products were allowed to run with 1 Kb plus DNA ladder (Fermentas) on a 2 % agarose gel electrophoresis (EtBr=5%) at 90 Volts in TBE 1X running buffer for about 40 minutes.

Images were acquired using the BioDoc-It Imaging (UVP) and densitometric analyses were performed on the images using Image J software.

2.2. Results

2.2.1. Screening of Exon specific U1 constructs (ExSpe U1s) on MAPT exon10 in the endogenous content of PC12 cell line.

A total of twelve different U1 and U7 chimeric constructs were produced and readily available in the Laboratory of RNA Biology and Biotechnology prior to my arrival.

I had produced U1 (α / γ) and U7 (α) scramble constructs. These are essential controls to validate the possible potent target specific effects of the U1 and U7 constructs on exon 10 of MAPT gene.

2.2.1. (i) Construction of U snRNA scramble chimeric molecule

For generating the U1 snRNA scramble (α / γ) constructs, as a first step, two different PCR reactions were performed using the PBS 1 plasmid as a template For the U7 snRNA scramble (γ) construct, the smOPT plasmid was used as a template (Fig 2.1).
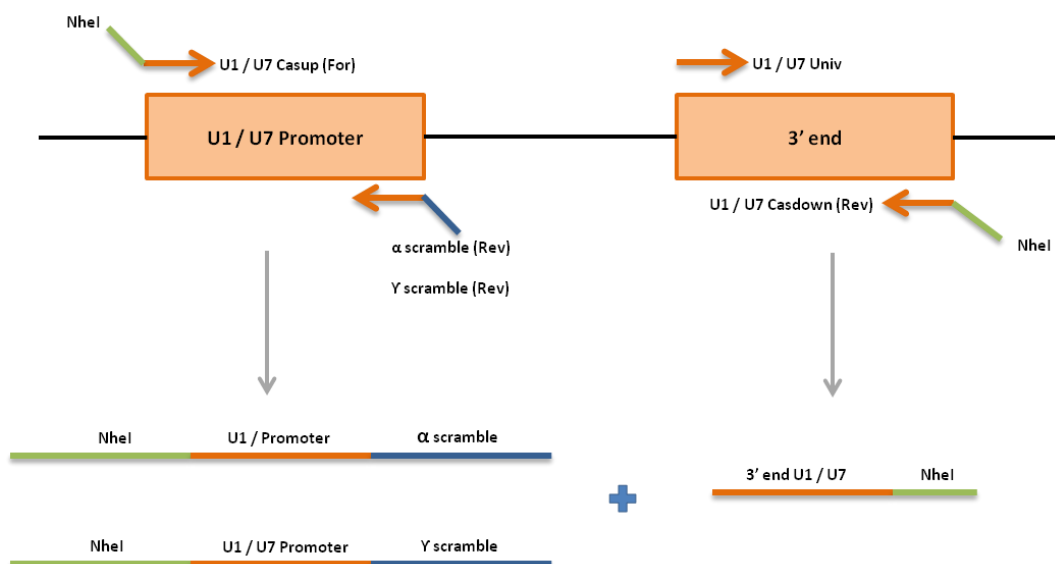
Fig. 2.1 | Schematic representation of distinct PCR reactions to amplify specific products such as U1 snRNA scramble (α / γ) constructs and the U7 snRNA scramble (γ) construct and the universal fragments for each U1 and U7 snRNA construct.(Figure is not drawn to scale).

First PCR reaction

The five different fragments obtained via distinct PCR reactions are as follows;

U1 snRNA scramble (α) fragment

A PCR reaction was set up using the PBS U1 plasmid, for which a (i) forward primer that annealed with the 5' end of the U1 snRNA promoter (U1 cas up For) with an overhanging tail coding for the NheI endonuclease site and (ii) reverse primer that annealed with the 3' end of the U1 snRNA promoter carrying additional scramble sequences specific to the 3' splice site of the Exon 10 (α scramble Rev) was used yielding a product of 360 base pairs.

U1 snRNA scramble (у́) fragment

A PCR reaction was set up using the PBS U1 plasmid, for which a (i) forward primer that annealed with the 5' end of the U1 snRNA promoter (U1 cas up For) with an overhanging tail coding for the NheI endonuclease site and a (ii) reverse primer that annealed with the 3' end of the U1 snRNA promoter carrying additional scramble sequences specific to the ACE rich region of the Exon 10 (у́ scramble Rev) was used yielding a product of 362 base pairs

U7 snRNA scramble (α) fragment

A PCR reaction was set up using the smOPT plasmid, for which a (i) forward primer that annealed with the 5' end of the U7 snRNA promoter (U7 cas up For) with an overhanging tail coding for the NheI endonuclease site and a (ii) reverse primer that annealed with the 3' end of the U7 snRNA promoter carrying additional scramble sequences specific to the 3' splice site of the Exon 10 (α scramble Rev) was used yielding a product of 364 base pairs

U1 universal fragment (U1 Univ fragment)

A PCR reaction was set up using the PBS U1 plasmid, for which a forward primer that annealed with the 5' end of the U1 snRNA (U1 Univ For) and a reverse primer that annealed with the 3' end of the U1 snRNA (U1 cas down Rev) with an overhanging tail coding for the NheI endonuclease site yielding a product of 210 base pairs.

U7 universal fragment (U7 Univ fragment)

A PCR reaction was set up using the smOPT plasmid, for which a forward primer that annealed with the 5' end of the U7 snRNA (U7 Univ For) and a reverse primer that annealed with the 3' end of the U7 snRNA (U7 cas down Rev) with an overhanging tail coding for the NheI endonuclease site yielding a product of 210 base pairs.

Ligation of constructs

The distinct products obtained via the first PCR reaction were ligated via treatment with T4 DNA ligase such that **(Fig 2.3 and Fig.2.4)**:

(i) U1 snRNA scramble (α) fragment + U1 universal fragment

(ii) U1 snRNA scramble (γ́) fragment + U1 universal fragment

(iii) U7 snRNA scramble (α) fragment + U7 universal fragment
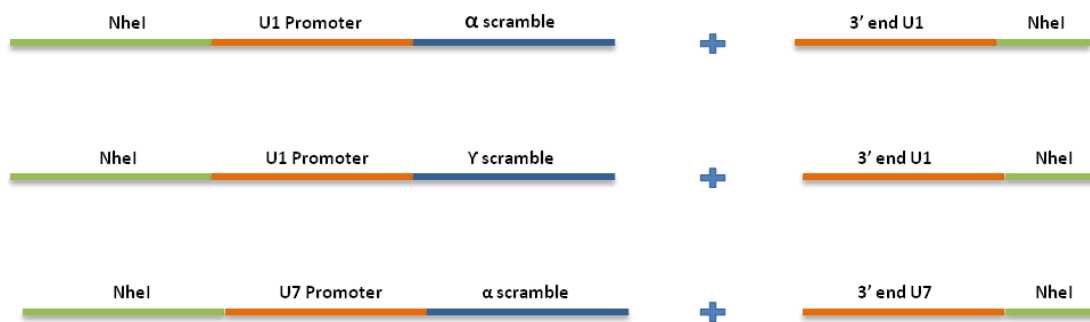
Fig. 2.2 | Schematic representation of the ligation of specific products obtained from the first PCR
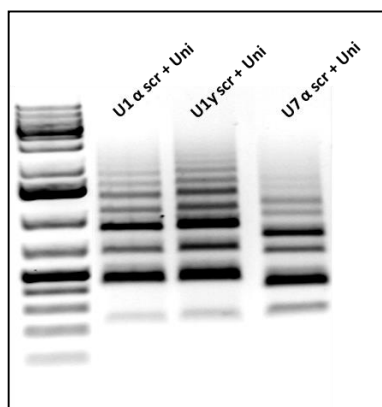
Fig.2.3 | Result of ligated products as loaded on a 1% TBE gel (Gene Ruler 1 Kb plus DNA ladder Fermentas)

Second PCR reaction

The ligated products were used as templates to initiate the second PCR reaction with the Casup forward and Casdown reverse primers (Fig.2.4) to generate the three scramble chimeric antisense constructs (U1 α scr / ɣ́ scr and U7 ɣ́ scr) **(Fig.2.5 and Fig.2.6)**.
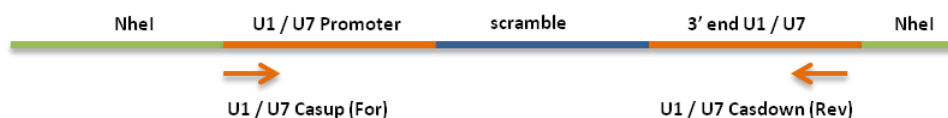
Fig. 2.4 | Schematic representation of the second PCR set up and the location of forward and reverse primers to amplify the chimeric scramble fragments.

78
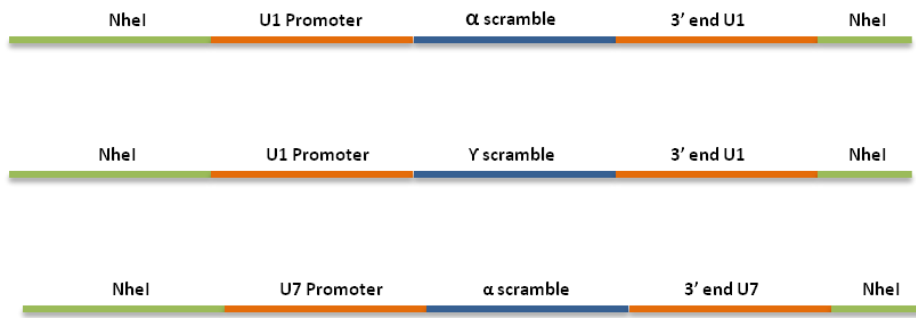
Fig. 2.5 | Schematic representation of the expected chimeric scramble fragments.after the second PCR on ligated products
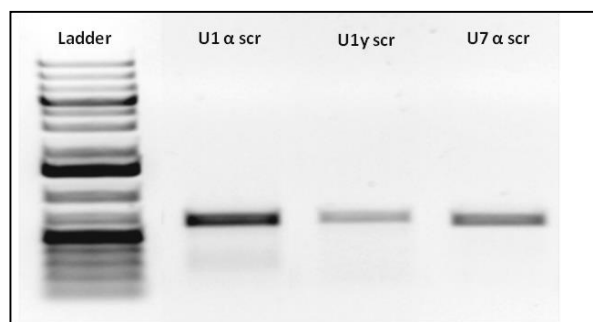
Fig. 2.6 | Result of the products after the second PCR reaction as loaded on a 1% TBE gel. Lanes 1 = U1α scramble, 2 =U1ɣ scramble and 3 = U7α scramble. (Gene Ruler 1 Kb plus DNA ladder Fermentas).

Ligation of the vector with the antisense scramble constructs

The chimeric scramble constructs thus obtained were successfully ligated with the NheI-pAAV2-2.1-CMV eGFP3 vector generating the following complete constructs **(Fig.7)**.

- Two of the U1 constructs - pAAV_GFP_U1 α and ɣ scr composed of the U1 snRNA gene, modified with the substitution of its endogenous 5' sequence responsible for recognition of the splicing donor site with an antisense scramble

- One of the U7 construct - pAAV_GFP_U7 α scr composed of the U7 snRNA gene modified with the substitution of its endogenous 5' sequence with an antisense scramble.
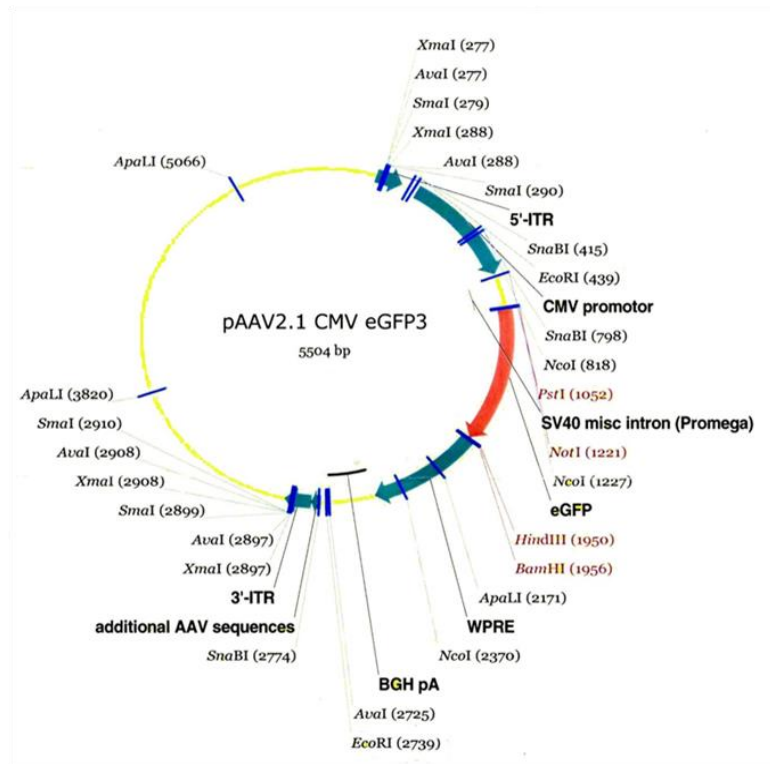
Fig. 2.7 | Schematic representation of the pAAV CMV eGFP3 vector back bone
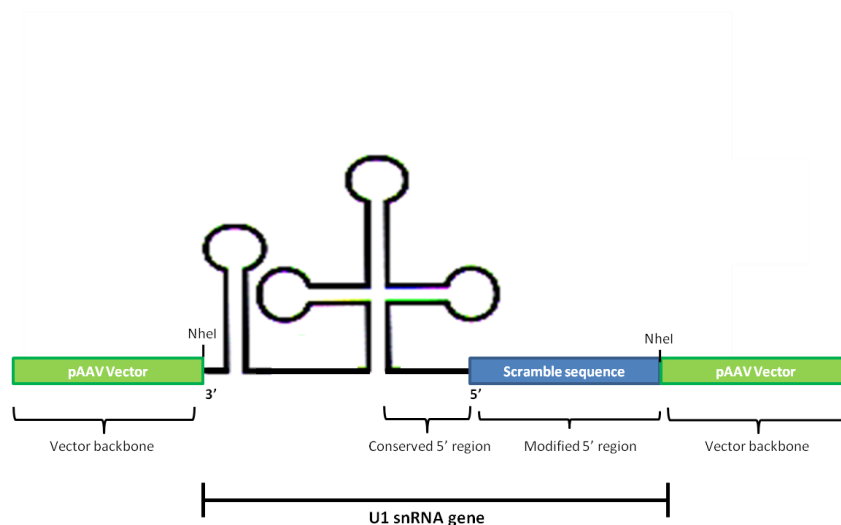
Fig. 2.8 | Schematic representation of the pAAV_GFP_U1 snRNA construct containing the modified arm with the antisense embedded within the AAV backbone.

Transformation

In order to obtain a sufficient amount of DNA (of antisense scramble constructs), the pAAV_GFP_U1 and U7 chimeric scramble construct was transformed within *E.Coli* DH5α competent cells, following which colonies were picked and inoculated in suitable volume of LB and grown overnight in agitation.

Bacterial DNA was extracted using QIAprep Spin Miniprep Kit protocol (Qiagen) and samples were digested using the NheI enzyme to check for the insertion of modified U1and U7 snRNA cassette.

Sequence analysis of the scramble constructs

The positive samples were sent for sequencing by the BMR Genomics company (Padua) using the AAV Rev primer (5' -CCATATATGGGCTATGAACTAATG-3').
The sequencing results confirmed the right nucleotide composition and correct orientation of the inserts within the pAAV2.1-CMV-eGFP3 vector.

2.2.1. (ii) PC12 cell line transfection and analysis

PC12 cells are derived from the pheochromocytoma of the adrenal medulla of rat cells. They are small cells with a limited cytoplasm and a long doubling time. They are also known to grow in culture as undifferentiated neuroblasts (Greene and Tischler 1976). It is a widely used model system for the studies on neuronal differentiation, neurotransmission and neurodegenerative disorders, as they develop in to sympathetic neuron like cells upon treatment with nerve growth factor (NGF). Additional properties such as, electrical excitability and development of synapses with muscle cells in culture makes them attractive cellular models (Grau and Greene et al., 2012). However, they posses limitations such as sensitivity to physical stress and alterations in temperature and pH.
PC12, was one of the few cells known to express 80% of Exon 10+ (4R) tau isoform, thus recapitulating the FTDP-17 pathological condition.
Since these cells are known to have limited transfection efficiency, the first experimental set up was focused on optimizing an efficient transfection protocol for introducing the pAAV_GFP_U1 and U7 chimeric constructs within the cell.

Optimisation of transfection efficiency

Lipid based transfection
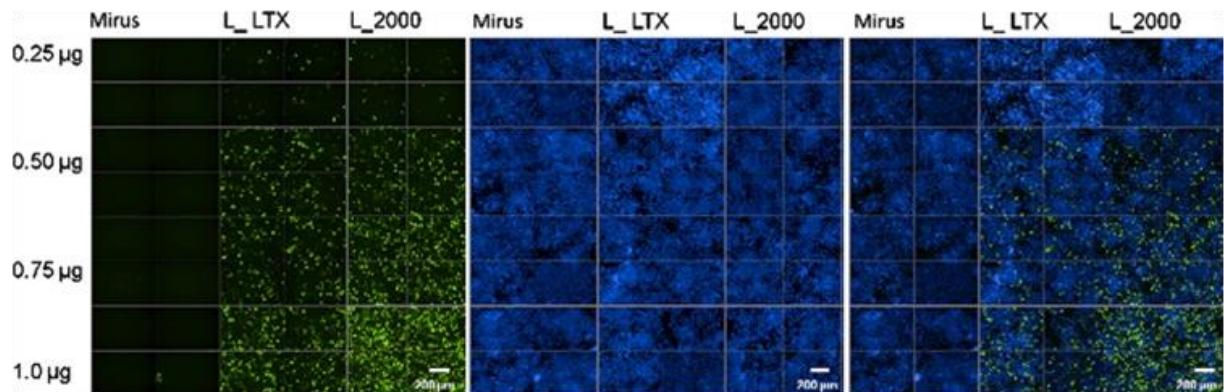
Fig. 2.9 | Transfection optimisation in PC12 cells using liposoluble agents PC12 cells were transfected using the following liposoluble agents: TransIT-LT1 Transfection Reagent (Mirus), Lipofectamine LTX (L_LTX) and Lipofectamine 2000 (L_2000) with different concentrations of plasmid encoding EGFP. Fluorescence images of transfected PC12 cells were analyzed by High-Content screening system (Operetta) after 48 h of transfection.

Fig 2.10 | A) Percentage of transfection efficiency in PC12 cells. The percentage of transfected cells was calculated by dividing the number of EGFP positive cells by the total population of cells. The best result was obtained by using 1 µg of plasmid and Lipofectamine 2000 (transfection efficiency of 45.9 %) (Data represent mean ± SEM obtained from triplicates).
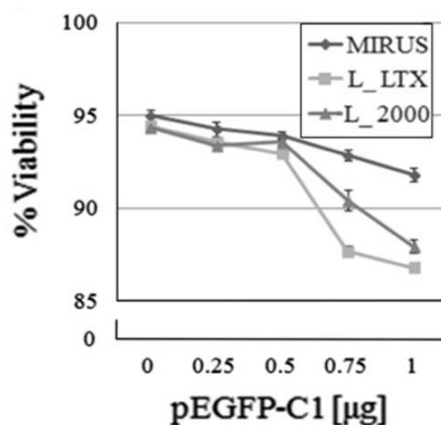
Fig 2.10 | B) Percentage of cell viability in transfected PC12 cells The percentage of viable cells after transfection was measured by the Trypan Blue assay. The optimal cell viability (93.6 %) was observed in cells transfected with 0.5 μg of plasmid and Lipofectamine 2000. (Data represent mean ± SEM obtained from triplicates).

As shown in Fig.2.9 and 2.10 the TransIT-LT1 Transfection Reagent (Mirus) was not effective in facilitating transfection of DNA in to PC12 cells, even when a higher concentration of DNA was used (However, experiments were performed in parallel on the HEY4 ovarian cancer cell line using TransIT-LT1 that showed a transfection efficiency of approximately 35 % (data not shown) thus clearly indicating that trend of efficiency depends on the cell type).

On the contrary, transfection experiments using Lipofectamine LTX and Lipofectamine 2000 enabled transfection of DNA into PC12 cells, with the respective efficiencies of 15% and 7 %, with 0.25 μg DNA; 27% and 20% with 0.5μg DNA; 30% and 40% with 0.75 μg DNA;35% and 46% with 1 μg DNA.

As expected, transfection efficiency for both reagents correlates to the amounts of DNA used. However, on comparing the transfection efficiency of the two cationic lipids, Lipofectamine LTX indicates to perform better than Lipofectamine 2000 at low DNA amounts between 0.25 – 0.5 μg, while Lipofectamine 2000 outperforms Lipofectamine LTX at higher DNA amounts between 0.5 – 1.0 μg.

On comparison of our results with those by Lee and colleagues (2008), it can be observed that upon transfection using Lipofectamine 2000 we attained 21 % transfection efficiency (with 0.5 μg of DNA in a 24-well plate) while Lee and

collaborators reported 14 % efficiency in similar conditions (1 µg of DNA in a 12-well plate).

Cell viability was measured by Trypan Blue Staining after 48 hours of transfection (Fig.2.10 B). In all cases, viability decreased as the DNA amounts increased. However, as clearly indicated there is a variation of trend for different reagents. TransIT-LT1 had a milder impact on cell viability, reaching 92 % when 1 µg of DNA was used. On the contrary, Lipofectamine 2000 and Lipofectamine LTX reached 87–88 % viability in those conditions.

Electroporation

We additionally employed optimization of transfection using the electroporation with the Neon Transfection system MPK5000 (Invitrogen) following which the most suitable condition yielding 90% of efficiency was obtained (Covello G et al., 2013). The following conditions were identified as optimal for each reaction: 3 pulses of 1500 voltage with 10 milliseconds to transfect 1×10^6 cells / well with 0.5 µg of each chimeric construct.

All the thirteen different constructs (Ten of the already available constructs plus three new scrambles) were transfected in a 24-well format. The experiments were performed in biological duplicate and technical duplicate. As the vector backbone containing the chimeric constructs contained the GFP transcriptional cassette, measure of GFP served adequate to measure efficiency of transfection.
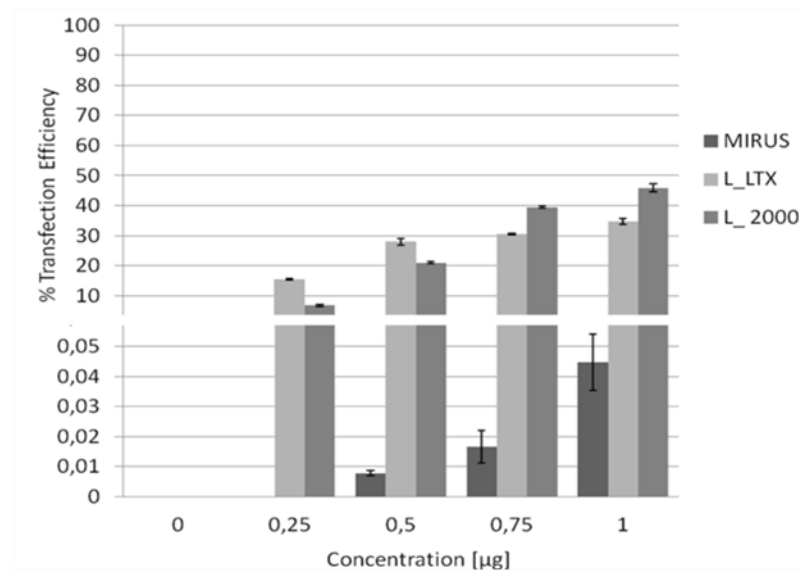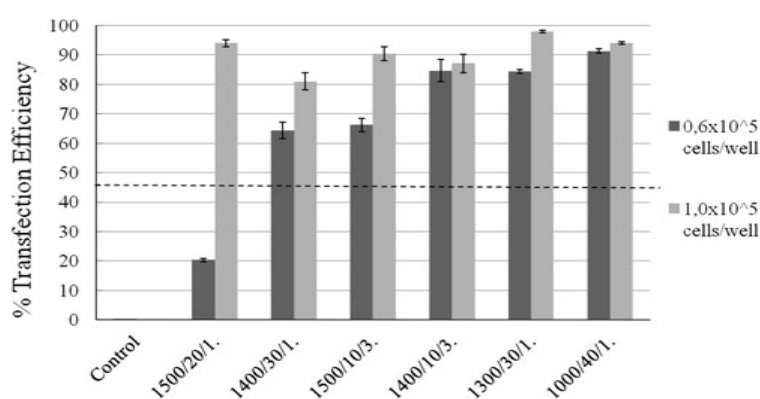

Fig 2.11 | Percentage of transfection efficiency in PC12 cells. The percentage of transfected cells was calculated by dividing the number of EGFP positive cells by the total population of cells. The best condition (99 %) was obtained by 0.5 µg of plasmid, 1×10^5 cells/well, and 3 pulses of 1,300 Volt and 10 ms. (Data represent mean ± SEM obtained from triplicates).(Refer to manuscript attached).

S2.2.1. (iii).Semi quantitative RT-PCR analysis

2.2.1. (iii) a. U1 snRNA chimeric molecule: RNA anlaysis

Following the transfection experiments, the expression of the U1 and U7 snRNA constructs in the PC12 was analysed using the RT-PCR method

RNA was extracted from each well containing cells transfected with the constructs and reverse transcribed to cDNA using both random and oligo dT-18 primers. These reactions were carried out along with the set of controls as specified by the manufacturer.

5μl of cDNA was amplified with a semi quantitative RT-PCR reaction using a forward and reverse primer designed to bind to the cDNA region of the 3' end of UsnRNA. Therefore, the cells sufficiently transfected with the chimeric constructs and enabling their expression were expected to yield amplified products. The controls such as cells with empty vector or non transfected cells were not expected to produce amplified products. ß actin served as a gene for normalization and was expected to show an endogenous expression in the all the cells (Transfected and non-transfected).
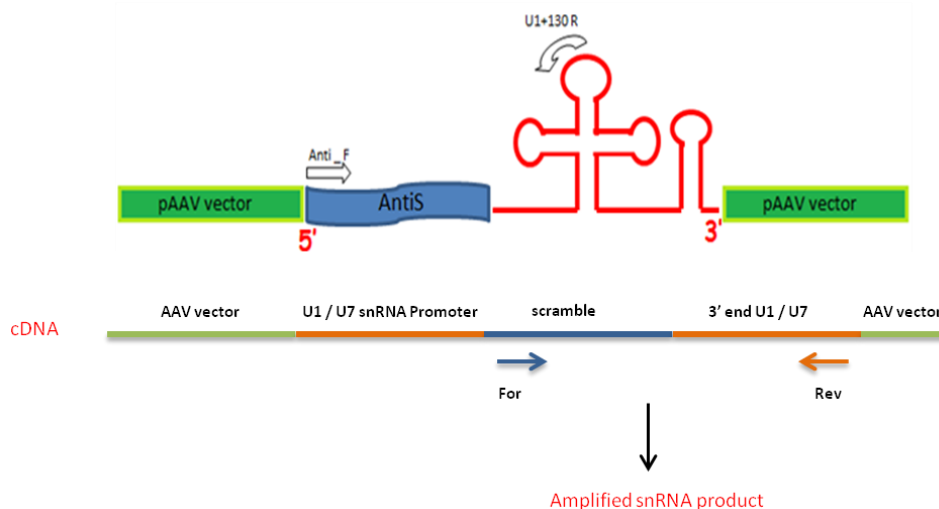
Fig 2.12 | Schematic representation of the location of forward and reverse primers used for the amplification of modified U snRNA (the figure is not drawn to scale).

Results of the semi-quantitative RT-PCR analysis on the samples containing cells transfected with the U1 snRNA constructs was checked on a 2% agarose gel. Representative results of one of the experiments are shown in **Figure 2.13.**
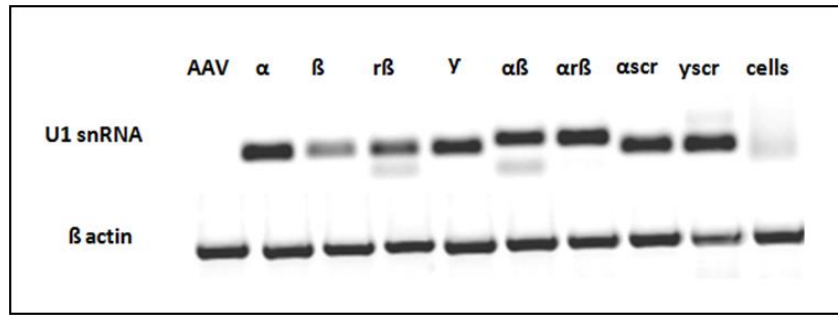
Fig 2.13 | Results of the RT-PCR amplification of the U1 snRNAs. The bands represent a) amplified product of U1 snRNA cassette possessing ∼90 bp (α, β, λ, αscr and λscr) and 130 bp (αβ and αrβ) b) amplified product of ß actin used as a house keeping gene.
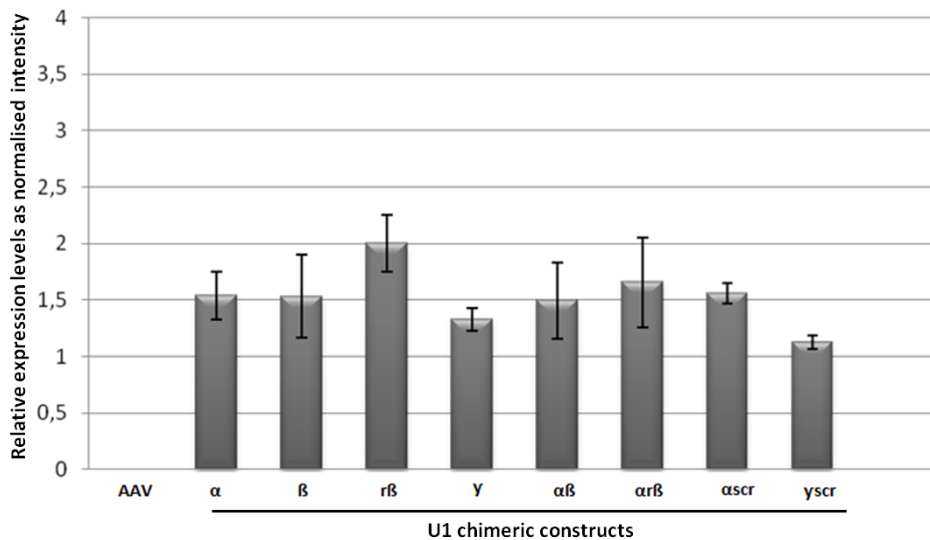
Fig 2.14 | Relative expression level of each U1 snRNA construct normalized using the ß actin as a house keeping gene.Data represent mean ± SEM obtained from biological duplicate experiments.

As expected, the samples transfected with the AAV2.1-CMV-eGFP3 vector with scramble sequences showed expression of the U1 snRNAs and corresponding amplified products of the ß actin RNA. The samples with the empty vector and non treated cells showed no bands corresponding to the amplification of U1 snRNAs but expressed ß actin. The bands of U1 αβ and αrβ appeared slightly higher than α, β, λ, αscr and λscr as they are long constructs containing double sequences. Hence, indicating a successful transfection of the constructs and their expression within the PC12 cells.

The expression analysis based on the density of each band was performed, wherein the ampflication signal from each modified U1snRNA was normalized

against that of ß actin.Means and standard deviations of the signals from the intensities are reported in **Figure 2.14.**

Results of the semi-quantitative RT-PCR analysis on the samples containing cells transfected with the U7 snRNA constructs was checked on a 2% agarose gel. Representative results of one of the experiments are shown in **Figure 2.15**.
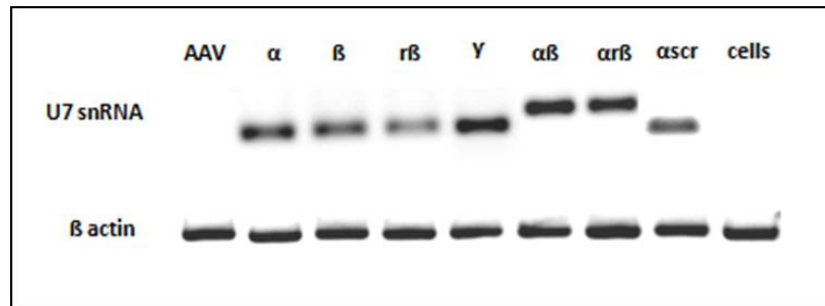
Fig 2.15 | Results of the RT-PCR amplification of the U7 snRNAs. The bands represent a) amplified product of U7 snRNA cassette cassette possessing ∼ 90 bp (α, β, λ, αscr and λscr) and 130 bp (αβ and αrβ) b) amplified product of ß actin used as a house keeping gene.
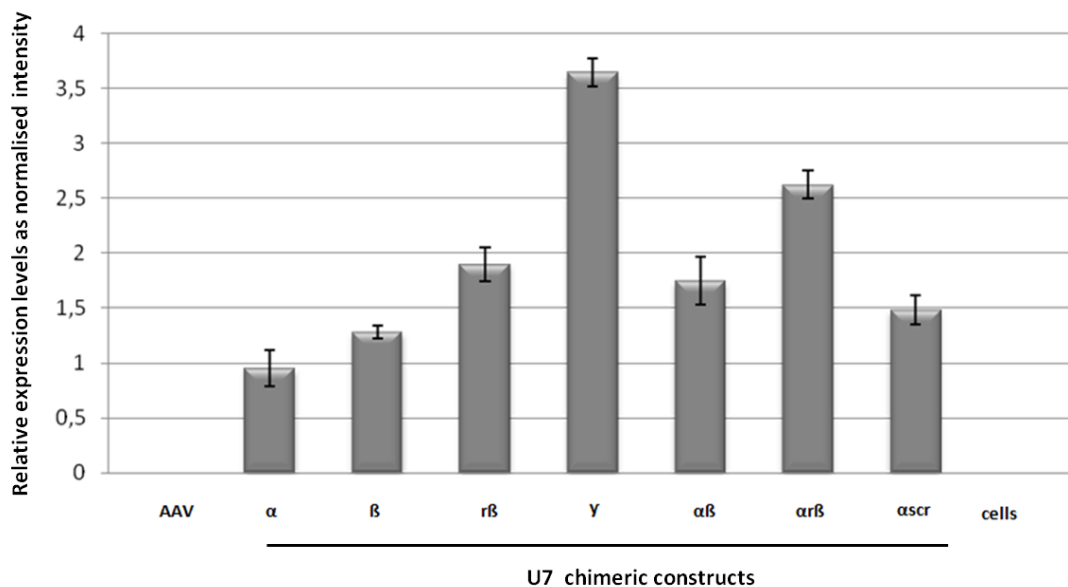
Fig 2.16 | Relative expression level of each U7 snRNA construct normalized using the ß actin as a house keeping gene. Data represent mean ± SEM obtained from biological duplicate experiments.

As expected, the samples transfected with the AAV2.1-CMV-eGFP3 vector containing scramble sequences showed expression of the U7 snRNAs and corresponding amplified products of the ß-actin RNA. The samples with the

empty vector and non treated cells showed no bands corresponding to the amplification of U7 snRNAs but expressed ß actin. The bands of U7 αβ and αrβ appeared slightly higher than α, β, λ, αscr as they are long constructs containing double sequences. Hence, indicating a successful transfection of the U7 constructs and their expression within the PC12 cells.

The expression analysis based on the density of each band was performed, wherein the ampflication signal from each modified U7snRNA was normalized against that of ß-actin. Means and standard deviations of the signals from the intensities are reported in **Figure 2.16**.

Both the U1 and U7 snRNA constructs have shown sufficient expression within the cells indicating their ability to be transcribed and expressed.

2.2.1. (iii) b. MAPT mRNA levels in the endogenous condition of PC12 cells after transfection of U1 snRNA chimeric molecule
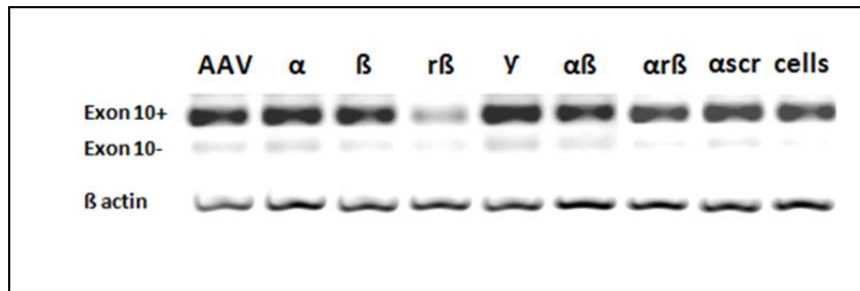
Fig 2.17 | RT-PCR analysis of MAPT cDNA of samples transfected with the U1 constructs A) The upper band corresponds to the 4R tau isoform with a length of 368 bp, whereas the lower band corresponds to the 3R tau isoforms with a length of 275 bp. B) amplified product of ß actin used as a house keeping gene.
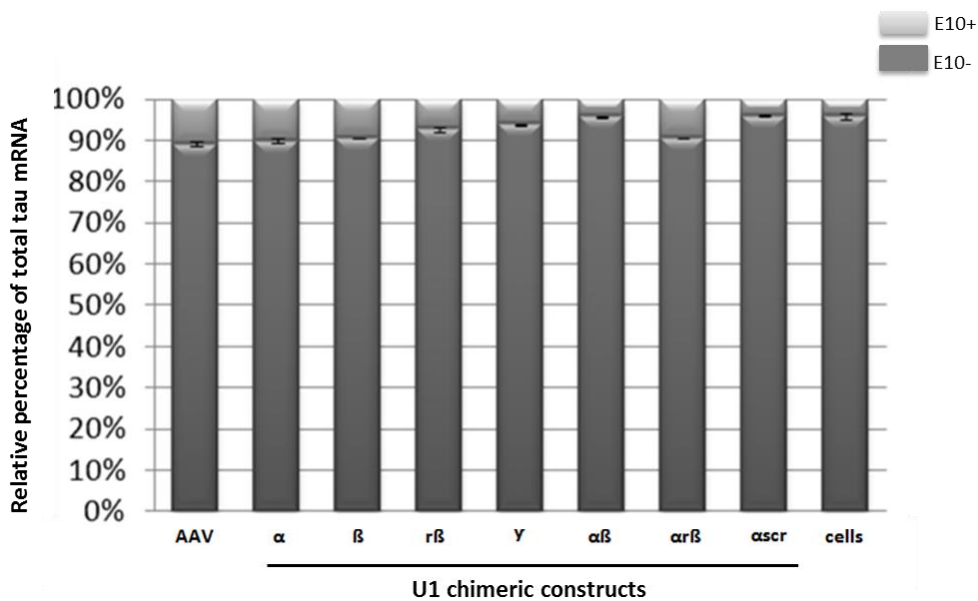
Fig 2.18 | Relative expression levels of the two different isoforms of MAPT mRNA of each sample transfected with U1 constructs Data represent mean ± SEM obtained from biological duplicate experiments.
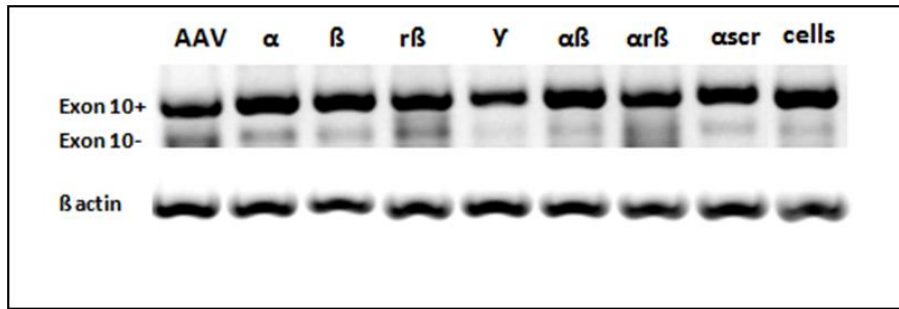
Fig 2.19 | RT-PCR analysis of MAPT cDNA of samples transfected with the U7 constructs A) The upper band corresponds to the 4R tau isoform with a length of 368 bp, whereas the lower band corresponds to the 3R tau isoforms with a length of 275 bp. B) amplified product of ß-actin is used as a house keeping gene.
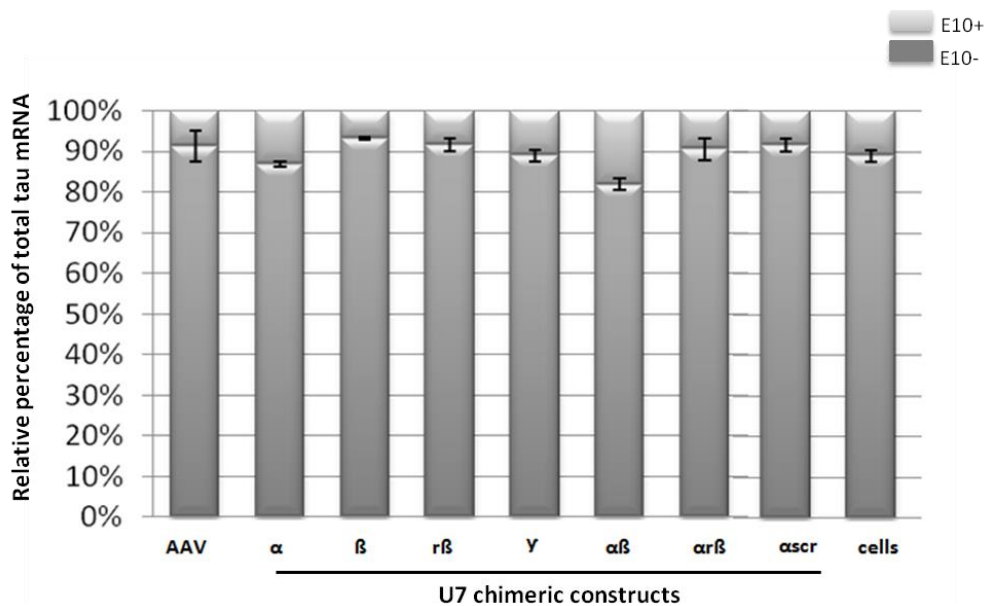
Fig.2.20 | Relative expression levels of the two different isoforms of MAPT mRNA of each sample transfected with U7 constructs Data represent mean ± SEM obtained from biological duplicate experiments.

The U1 and U7 chimeric molecules were expected to mask different *cis*-acting elements that were known to enhance inclusion of exon 10 in the MAPT transcript. Such masking was expected to induce skipping of exon 10 by inhibiting the spliceosome machinery from detecting the exon.

This would enable reduction of 4R isoforms that is known to be elevated in FTDP-17.

Although it has been demonstrated that the modified U1 and U7 snRNAs have been sufficiently expressed in the PC12 cells **(Fig.2.13-2.16)**, the graphs represent that there is no variation between the two isoforms upon treatment with the chimeric constructs. This is evident by comparison between the two isoforms of cells treated with chimeric constructs versus that of the scramble constructs or the non treated cells.

The above mentioned data indicates that the U1 and U7 chimeric constructs were not able to pose an effect of skipping on exon 10, thus did not contribute to modulating alternative splicing decisions in the context of PC12 cells.

Discussion

Design of chimeric constructs embedded in the U1 and U7 snRNA cassette

The rat neuronal pheochromocytoma PC12 cells were selected to analyse the effect of chimeric constructs on inducing skipping of exon 10. These cells predominantly express exon 10 which is most likely due to the changes in three nucleotides in the 5' splice site that resembles stem-loop-disrupting mutations in human tau.

A total of fourteen different constructs were tested for their efficiency to induce skipping of exon 10 in the context of rat PC 12 cells.

The chimeric constructs were designed and produced such that:

- Three active *cis*-acting elements in exon 10 were selected.
- Different oligonucleotides were designed to base pair with complementarities to the *cis* acting elements. This enables masking of the splice site thus preventing the assembly of the spliceosome and as a consequence, inducing skipping of exon 10.

- **AON α** is complementary to the 3' exon / intron junction , **AON ß** is complementary to the 5' exon / intron junction, **AON rß** is complementary to the 5' exon / intron junction with three nucleotide changes to make it completely complementary to the rat sequence. The U1 constructs harboring these sequences are expected to induce skipping of exon 10 as these are antisense to the canonical cis-acting elements in the splice site selection and will inhibit the recruitment of spliceosome machinery. **AON γ** is complementary to the ACE region of exon 10. **AON α ß** is a couplet formed by α and ß thus complementary to both 5' and 3' exon /intron junction. **AON α rß** is similar to AON α ß excepting the difference of the three nucleotides changes to make it complementary to the rat sequence.
- Non targeting oligonucleotides were designed to ensure the specificity of each oligonucleotide. They were composed of same nucleic acid bases in a random order and hence designated as **scrambled**
- The oligonucleotides were then embedded in to the U1 / U7 cassette to enable stable expression within the cells.
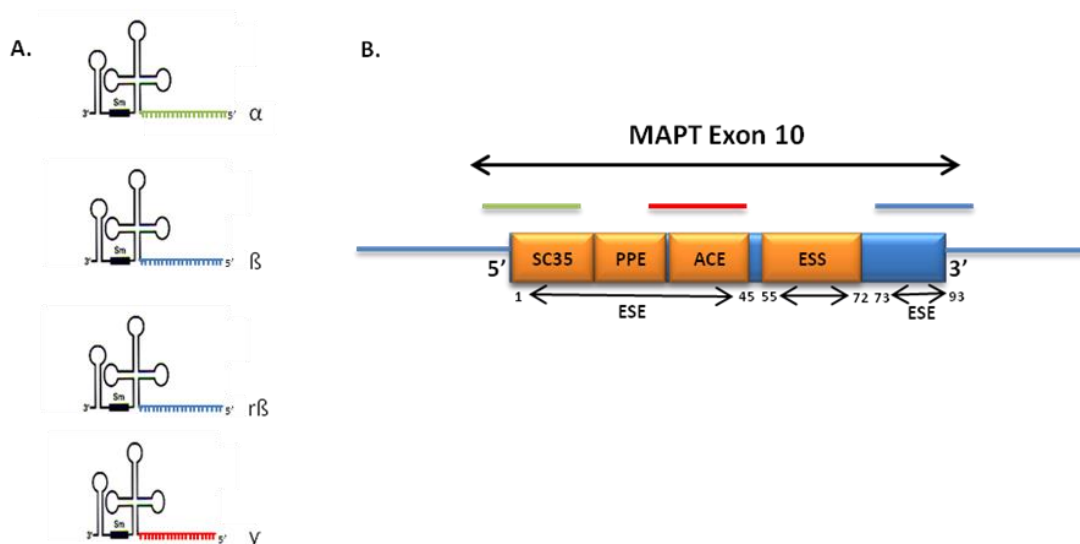
Fig 2.21 | Schematic representation of A) Modified U1 snRNA chimeric construct with specific oligonucleotides that are complementary to the *cis* acting splice sites of Exon 10 embedded in to the U1 casette. B) Exon 10 containing its specific regulatory elements involved in splicing and the location of binding of modified U1 constructs (coloured lines represents corresponding constructs).

Previous work by Covello G et al., (unpublished data) has shown that all the four oligonucleotides have induced exon 10 skipping in rat PC12 cells when transfected alone or in combination.

Therefore these oligos were embedded in the U1 and U7 snRNA cassettes for the following reasons;

The U1 snRNA is one of the prime factors involved in splice site recognition hence its utility as a vector for delivering therapeutic antisense RNA sequence is highly desirable. Since both the U1 snRNA and tau pre-mRNA co-localises within the same region (i.e: the nucleus), it should increase the effectiveness of therapeutic molecule.

Upon masking the 5' splice site, the base pairing interaction between the 5' splice site and the U1 snRNA must be shunt, thus favoring its interaction with U6 snRNA. Therefore the spliceosome's catalytic core is not formed and leads to skipping of exon 10.

Additionally, the strong pol II dependent promoter of the U1 snRNA genes ensures high levels of expression of the chimeric constructs.

These modified exon specific U1 snRNAs can also be used specifically to target the mutated splice sites by incorporating sequences complementary to the mutated region thus leaving the wild-type site unaffected. This approach offers the following advantages; (i) they do not bind directly to normal 5' ss and (ii) they are capable of correcting different types of splicing defects associated to exon skipping (Alanis et al., 2012).

The U7 snRNA functions as natural antisense sequence by hybridizing with the spacer element of histone pre-mRNA during its 3' processing. Modification of the U7 vector by converting the wild type U7 Sm binding site to the consensus Sm binding site derived from snRNPs (smOPT) provides two benefits;

The target RNA will not be cleaved by the histone 3' end processing machinery and inability of U7 smOPT particles to bind one or more U7 specific proteins prevents the RNA from binding to endogenous U7 snRNPs.

The embedded chimeric constructs are designated as U1 (α, ß, rß, ɣ, αß, αrß, αscr and ɣscr) and U7 (α, ß, rß, ɣ, αß, αrß, αscr and ɣscr).

2.3.2. Transfection efficiency was optimized for PC12 cell line

Although PC12 cells represent an important model system to study a variety of neuronal functions, they proved relatively difficult to transfect (Covello G et al., 2013). There are three different types of transfection methods; biological, chemical and physical. The biological methods include virus mediated gene delivery, Chemical method includes employment of cationic lipids, cationic polymers or calcium phosphate based delivery. The physical methods include a wide range of tools such as direct injection, biolistic particle delivery, electroporation, laser irradiation, sonoporation and magnetic nano particle. Although different methods of transfection have been developed, their applications are highly dependent on the cell type and purpose of investigation. (Kim et al., 2010).

Various methods of transfection have been attempted in PC12 cells; cationic lipids formulations have been employed to increase transfection efficiency.

Using Lipofectamine 2000 (Invitrogen) the transfection efficiency was about 14 % and was similar to the efficiency obtained with polyethyleneimine (PEI) (15 %) (Lee et al., 2008). A higher efficiency (30%) was reported with Metafectene Pro (Biontex) (Cogli et al., 2010). An increase in the transfection efficiency (40%–50 %) was observed by simultaneous treatment with Lipofectamine and 0.1 μM GALA, a pH-sensitive fusogenic peptide which accelerates the endosomal escape of the plasmid/liposome complexes to the cytosol (Futaki et al., 2005). However, this method has not encountered wide popularity thereafter.

We have compared the efficiency of three different chemical transfection reagents (Lipofectamine 2000, Lipofectamine LTX and TransIT-LT1) and of two electroporation systems (Neon and Gene Pulser Xcell) in transiently transfecting undifferentiated PC12 cells. By comparing efficiencies from replicate experiments, we conclude that electroporation (in particular Neon) is the method of choice. By optimizing different parameters (voltage, pulse width and number of pulses) we attained a high efficiency of transfection (90 %) and viability (99 %). We also demonstrated that, upon electroporation, cells do not alter and maintain their ability to differentiate.

On the process of optimization of transfection efficiency, I had contributed to the experiments on chemical transfection using three different cationic lipid reagents.

Refer to the manuscript as an attachment **M.2.**

2.3.3. The U1 and U7 ExSpe UsnRNAs did not pose an effect on skipping of exon 10 in PC12 cell line

The U1 and U7 chimeric constructs were designed to modulate splicing of exon 10 by masking the *cis*-acting elements. Although the constructs were expressed in the PC12 cells, they were unable to modulate splicing of exon 10.

2.3.4. Molecular mechanisms involved in inefficient exon skipping.

Possible hypotheses that attribute to inefficient exon skipping are described below **(Fig.2.21)**.

Inadequate expression of the chimeric constructs

A total of 0.5 µg of each construct was used. This might be too less an amount of DNA to be transcribed and produce enough amounts of transcripts to be able to mask the splice sites of exon 10. It could also be possible that the 48 hours of time after transfection was not sufficient to induce formation of enough transcripts. However, since previous studies have validated the use of chimeric small nuclear RNAs in mice, it is difficult to compare such dose and time related strategies.It could be possible that the effect might be linked to the *cis* acting regions in exon 10 that is prohibiting the effect of such therapeutic invention in the context of PC12 cells.

Contribution of *cis* acting and trans acting elements in regulation of splicing in PC12 cells

Previous studies by Freund and colleagues have reported that protein interaction between the U1 snRNP and 5' splice site is essential for splice donor

recognition (Freund et al., 2003). Additionally, experiments have demonstrated that the binding of U1 snRNA to the 5'-splice site is required, but not sufficient, to begin spliceosome assembly (Robert et al., 2005). This indicates the additional essential role of other proteins involved in the formation of U1 snRNP to initiate splicing process. It could be possible that the modified U1 snRNA constructs were not able to enter in to the integral complex due to a) insufficient expression b) complexities in their secondary structure .Thus, being unable to modulate splicing.

In vitro studies by Yamashita and colleagues have demonstrated that a new element is located in the intronic sequence that is known to possess a unique secondary structure in rodents. This element is expected to play a universal role in regulation of splicing.of exon 10. They used DNA analyzing software package ver.5 (GENETYX) to analyse the DNA sequences and secondary structures of mouse tau genes (Yamashita T et al., 2005).

In order to confirm the predicted structure, they synthesized oligo RNAs. Experiments revealed that there were two stem loop structures juxtaposed with each other suggesting a cooperative action in regulation of splicing of exon 10, thus causing an increase in the 4R isoform. In its denatured form, the mutant RNAs containing mouse intronic stem loop structure sequence was shown to move slower than its wild type counterpart (preserved set of sequence with the same A, U, G, C content as that of the mutant RNA oligo but avoiding the formation of hair pin structure). These studies indicate the existence of a possible complex secondary structure of tau mRNA containing exon 10 in PC12 cells might lead to an inaccessibility of the U1 and U7 chimeric constructs to bind to it.

Studies on antisense mediated exon skipping on exon 10 has revealed that although this strategy is successful in providing a potential therapy, the regulation of exon 10 in cells predominantly expressing 4R tau mRNA may differ from the regulation in cells expressing its alternative 3R isoform. (Sud et al., 2014). This indicates cell specific regulation and variation of dynamics involved in splicing of exon 10. Since other studies using U1 and U7 snRNAs have been

employed in different cell lines, a successful strategy to induce exon skipping was established.

An interesting work by Du and colleagues in 2002 has shown that that the U1 snRNP lacking the 5' end of its snRNA retains the 5' splice-site sequence specificity. They also propose that U1 C protein, (a component of U1 snRNP involved in splicing of mammalian sytems and known to directly interact with the 5' splice site) binds first to the pre-mRNA thus being the earliest step in splicing process followed by the canonical U1 snRNA/5' splice-site base pairing (Du et al., 2002).

Therefore, it could also be possible that there are other proteins like U1C involved in initiating the splice site recognition, hence an inability of the chimeric constructs to mask specific sites.

Another hypothesis could also result from the binding of the chimeric constructs to non specific / uncharacterized proteins thus blocking its action on the specific target on *cis* acting elements of exon 10.

Two other additional hypotheses may support the reasons why the antisense oligos had an effect on inducing exon skipping and not the U1 snRNAs; U1 constructs might rather enable and direct the recruitment of splicing machinery than blocking it, whereas the antisense oligos blocks the splice sites or PC12 cells might undergo a U1-independent splicing mechanism in MAPT gene thus not reacting to the U1 constructs. Previous studies have suggested that U1-independent splicing mechanisms could occur in cells (Raponi et al., 2008).

Having discussed the above mentioned possible suggestions leading to the ineffective exon 10 skipping in the context of PC12 cells, it is noteworthy to mention that these constructs have not been tested on other cell lines. Therefore, it would be irrational to discard the potentiality of the U1 and U7 constructs in inducing skipping of exon 10 in other cell lines.
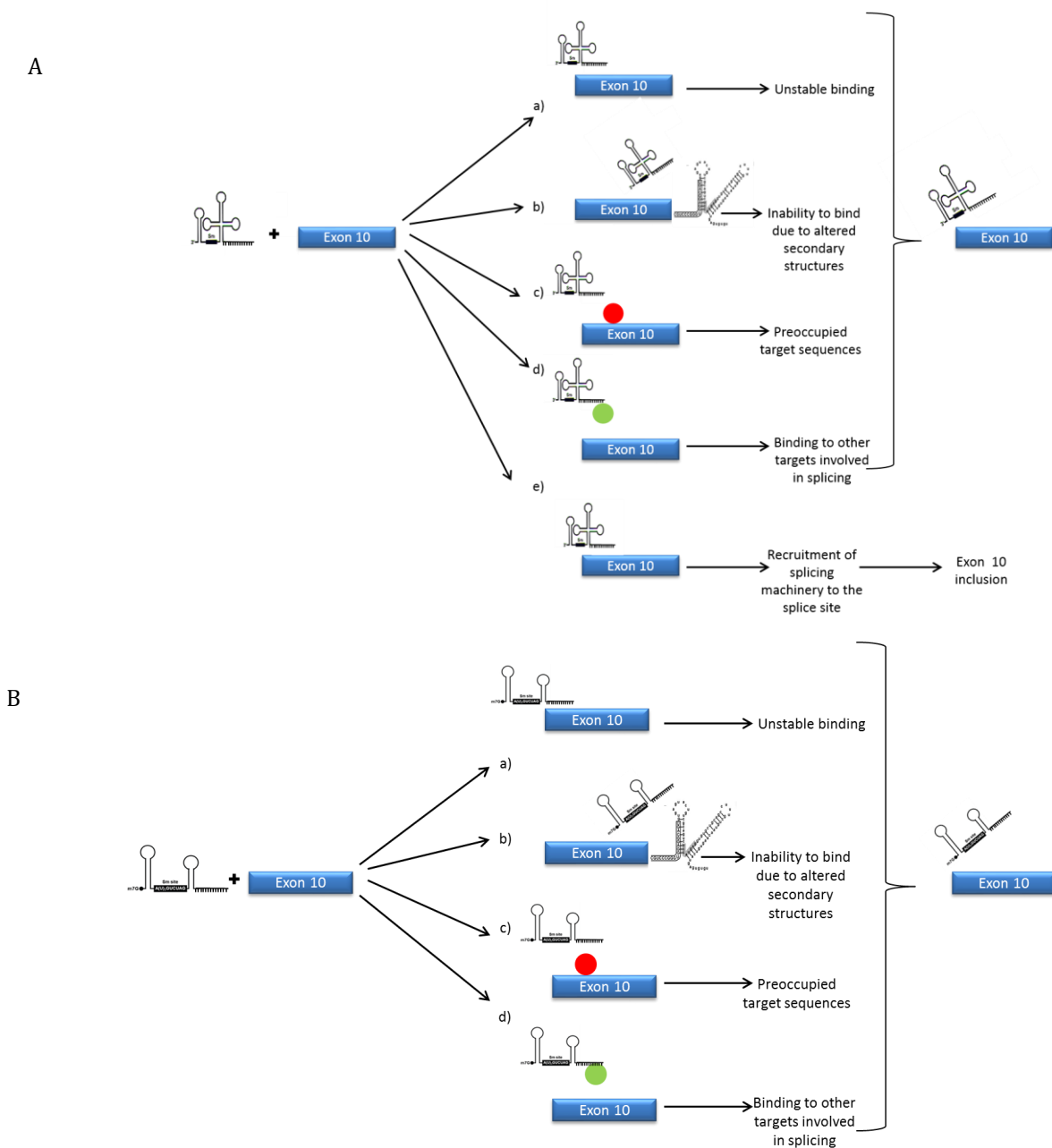
Fig 2.22 | Schematic illustration of the possible hypothesis for the inability of A) U1 and B) constructs to induce exon skipping in the context of rat PC12 cells. a) Unstable binding between the *cis* acting elements of exon 10 and the modified chimeric constructs may lead to a further dissociation of binding between them. b) Inability of the constructs to bind to active regions may be associated to a complex secondary structure arising due to the double stem loop of the intron 10 region observed in rodents. c) Pre-occupied *cis*-acting target sequences by binding to other splice regulatory elements leading to inability of the constructs to bind to the target region d) Binding of the constructs to either splice repressors or non specific targets may result in inability to bind to their targets. (The red and green circles indicate possible target elements known to interact with the *cis* acting elements and chimeric constructs respectively) e) Recruitment of splice machinery facilitated by the U1 construct may enhance splicing and inclusion of exon 10.

CHAPTER 3. Screening for siRNA molecules to mediate isoform specific target degradation of exon 10 containing MAPT pre-mRNA

3.2. Results

3.3. Discussion

Abstract

Abnormalities of microtubule associated protein tau have been shown to be linked to pathogenesis of neurodegenerative disease collectively termed as "Tauopathies. Gene mutations in tau lead to perturbation of gene splicing and tau fibrillization leading to formation of tau aggregates. A missense mutation in exon 10 at codon 279, results in an asparagine to lysine substitution (N279K). This impinges alternative splicing of exon 10 in the tau mRNA, and disturbs the normal ratio of 4R tau/3R tau. This alteration leads to an increased expression of 4R tau causing agglomeration of tau proteins eventually leading to FTDP-17.

RNA interference has proven to be an efficient strategy for silencing mutant alleles of dominant disease genes as in Alzheimer's disease, Machado-Joseph disease, Spinocerebellar ataxia type 3 and tau mutation (V337M) that causes fronto-temporal dementia (Miller V et al., 2003).

This part of project explores the feasibility of a siRNA-based gene therapy to enable post-transcriptional gene silencing of exon10 in FTDP-17. A panel of siRNAs targeting tau mRNA containing exon 10 have been designed and synthesized. They were tested in two different contexts.

A **minigene reporter system** containing N279 mutation, and an **endogenous system** of cells recapitulating FTDP-17.

The effects of siRNAs on the minigene reporter system were confirmed using an image based approach and semi quantitative RT-PCR analysis, whereas the effect on endogenous context was monitored using semi quantitative RT-PCR analysis.

3.1. Materials and Methods:

3.1.1. Design of panel of siRNAs against Exon 10

A panel of siRNAs targeting exon 10 was designed to mediate target selective depletion of the transcript **(Table 3.1)**.
The oligos were synthesized by the Eurofins / mwg operon company. The siRNAs have been designed on the basis of following rules:

- Avoid stretches of 4 or more bases such as AAAA, CCCC
- Avoid regions with GC content <30% or > 60%
- Avoid repeats and low complex sequence
- Avoid single nucleotide polymorphism (SNP) sites
- Perform BLAST homology search to avoid off-target effects on other genes or sequences

Name	Oligonucleotide sequence (5'-3')
siRNA 0	GAUAAUUAAUAAGAAGCUGTT
	CAGCUUCUUAUUAAUUAUCTT
siRNA 1	AGUCCAAGUGUGGCUCAAATT
	UUUGAGCCACACUUGGACUTT
siRNA 2	GAUAAUUAAGAAGAAGCUGTT
	CAGCUUCUUCUUAAUUAUCTT
siRNA 3	GGCUCAAAGGAUAAUAUCATT
	UGAUAUUAUCCUUUGAGCCTT
siRNA 4	CGUCCCGGGAGGCGGCAGUTT
	ACUGCCGCCUCCCGGGACGTT
siRNA 5	GCAACGUCCAGUCCAAGUGTT
	CACUUGGACUGGACGUUGCTT
siRNA control	UAAUGUAUUGGAACGCAUATT
	UAUGCGUUCCAAUACAUUATT

Table 3.1. | List of siRNA oligos targeted against exon 10. Both the sense strands and the antisense strands are reported on the right side of the panel.

3.1.2. Creation of a minigene mutant plasmid bearing N279 mutation

3.1.2. (i) Site-directed mutagenesis

The fluorescent reporter plasmid created by Peter Stoilov and colleagues (Stoilov P et al., 2008) PFLARE 5A MAPT exon 10 also referred to as the wild-type (WT) plasmid (Fig.3.1), was mutated using the Quick change II site XL site-directed mutagenesis kit following the manufacturer's instructions. The following primers were designed such that they incorporated the nucleotide change of T to G.

Forward primer	Reverse primer
CCA AAG GTG CAG ATA ATT AAG AAG	GTT GCT AAG ATC CAG CTT CTT CTT
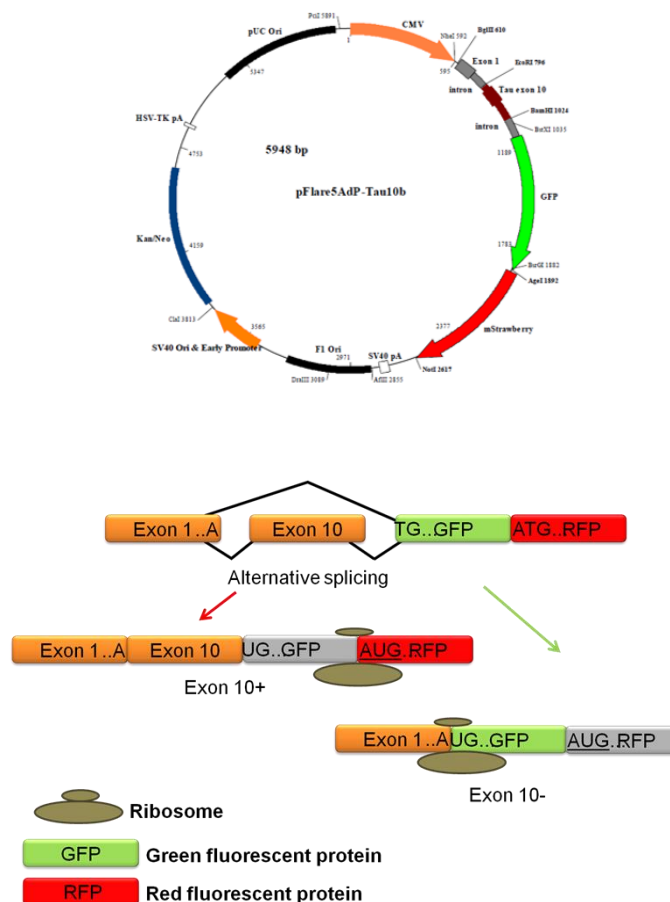
Fig. 3.1 | Schematic representation of the bichromatic reporter plasmid produced by Peter Stoilov et al., 2008. An alternative splicing of Exon 10 leads to production of two different splice isoforms. The ribosome scans for the first available AUG codon to initiate translation of specific reporter proteins such that Exon 10 results in the production of RFP and Exon 10-results in the production of GFP.

3.1.2. (ii) Preparation of competent cells and transformation

Refer to section 2.1.1.6

The resulting plasmid PFLARE 5A MAPT MUT exon 10 will be referred to as mutant N279 (Mut) plasmid.

3.1.3. SH-SY5Y cell line:

It is a thrice cloned (SK-N-SH -> SH-SY -> SH-SY5 -> SH-SY5Y) subline of the neuroblastoma cell line SK-N-SH.with a content of 15% exon 10+ and 85% of exon 10- in its transcript. The transfection efficiency (25% to 30%) in this cell line is comparitively higher than the other neuroblastoma cell lines. Therefore, this cell line was chosen to test the efficacy of siRNAs against endogenous exon 10 transcripts and for co-transfections of siRNAs with minigene reporter plasmids.

3.1.4. Co-transfection of reporter plasmid and siRNAs in SH-SY5Y cells

On the day before the experiment, 5×10^4 cells were seeded on a 24-well plate in 500 μl of complete medium without antibiotics at 37° C in 5% CO_2. The 24-well plate format has been chosen to allow the recovery of a sufficient number of cells at the end of the assay after the image-based analysis, in order to perform downstream molecular analysis, such as RT-PCR and Western Blot. Transfections were performed as instructed by the manufacturer with a ratio of DNA (ng): Lipofectamine 3000 (μl) being 1:2 in Opti-MEM medium. The plasmids were used at a concentration of 0.25μg and 0.5 μg per well in a final volume of 500 μl. Two different plasmid reporters were used for transfection namely the wild-type (WT) plasmid and the mutant type plasmid (Mut).

The siRNAs were used at the concentrations from 10nM to 100nM in a final volume of 500 μl per well. Following transfection, the cells were incubated at 37° C in 5% CO_2 for 48 hours.

3.1.5. Optimisation of high throughput screening assay to monitor effects of siRNAs on minigene

Since the out-put of read-outs are based on fluorescent intensities emitted from each of the fluorescent proteins, it was essential to optimize the screening strategy and set up threshold intensities and conditions to acquire images for a sensitive and robust analysis.

Therefore, a novel image based approach was developed to perform screening and validate the effects of siRNA on the dual fluorescent reporter plasmid.

The step-by-step approach of which has been schematically represented in **Figure 3.2**.

Work-flow for screening of plasmid reporters using high content imaging sytem
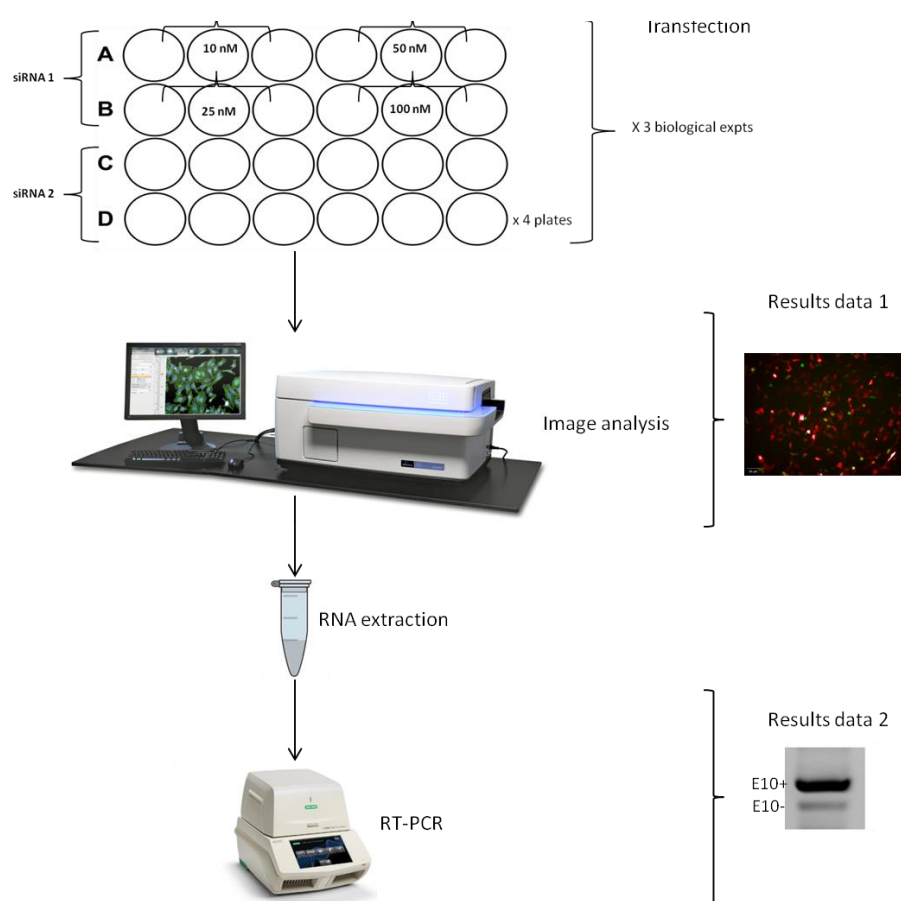
Fig.3.2 (i) | Work flow for the screening of effect of siRNAs on reporter plasmids. After transfection, the images are acquired from the 24-well plates and analysed using the high content imaging system. The samples are then subjected to downstream analyses such as RT-PCR to validate results observed through image based analysis.

3.1.5. (i) Preparation of cells for acquisition

Images of transfected cells were captured with a High content imaging system (Operetta, Perkin Elmer). After 48 hours of transfection, the cells were incubated for 20 minutes at 37° C in the presence of 1mg/ml of Hoechst 33342 fluorescent dye. This allows counter-staining the nuclei which will enable the subsequent analyses.

3.1.5. (ii) Image acquisition

Images were taken with a 20X LWD objective, in combination with different filter sets: in particular a filter for Hoechst 3342 stain (excitation filter: 360-400 nm, emission filter: 410-480 nm) is used to image the stained nuclei at 20ms exposure time, whereas a combination of filters is used to measure the reporters' intensities: GFP (excitation filter: 460-490 nm, emission filter :500-550 nm) and RFP (excitation filter: 560-630 nm , emission filter: 580-620 nm), both at 200ms exposure time.

3.1.5. (iii) Image analysis

a) For the feature extraction protocol, cells were segmented and analyzed using the following workflow;

b) The first step is the identification of Nuclei, the primary objects of interest that are segmented by using the most suitable algorithm.

c) Assuming a homogeneous distribution of both GFP and RFP in the cells, the nuclear region was selected to quantify the mean fluorescence intensity in the two channels.

d) The sub-population of transfected cells was identified using a double-threshold strategy to filter out the cells being either positive for G(GFP) or for R(RFP) or for both.

e) After restricting the analysis to the transfected cells, the ratio between the fluorescence properties G and R mean intensity is calculated on a per-cell basis. G/R is a parameter that indicates the prevalence of expression of one reporter

over the other. Specifically, a low score indicates inclusion of the cassette exon, while a high one is connected with an efficient splicing of Exon 10.

f) If allowed by the analysis software, an overview of the numerical properties of the cells can be visualized field by field in a scatter plot. Alternatively, to get a more complete representation of all the cells within a well, scatter plots or histograms of single cell properties can be created for representative wells of the WT and the Mut plasmid conditions. Such graphical representations allow a more accurate selection of an upper threshold J and a lower threshold K, distinguishing for cells preferentially expressing GFP (G/R>J), RFP (G/R<K) or equally expressing both the reporters (K<G/R<J).

g) The thresholds were then applied in a filter-based module to classify the cells in three different subpopulations.

h) Feature outputs include total cell count, transfected cells count and % calculated over the total number of cells, G/R median value of all the cells of the well, the % of cells preferentially expressing GFP (G/R>J), RFP (G/R<K) and equally expressing both the reporters (K<G/R<J).

i) Percentage of cell viability was calculated as follows: (total number of cells in transfected well/total number of cells in mock) x 100.

3.1.6. Semi-quantitative reverse transcriptase analysis on SH-SY5Y cell line

3.1.6. (i) RNA extractions
Refer to section 2.1.3. (i)

3.1.6. (ii) cDNA preparation
Refer to section 2.1.3. (ii)

3.1.6. (iii) Semi quantitative RT-PCR assay to evaluate expression of exon 10 transcript in minigene reporter

The expression levels of Exon 10 containing transcripts in the minigene were analysed with the following primers:

Gene	Forward primer (5'-3')	Reverse primer(5'-3')	Product dimension (bp)
Exon 10 / Exon 10-	AAACAGATCTACCATTGGTGCACCTGACTCC	CGTCGCCGTCCAGCTCGACCAG	300 / 207
ß-actin	GAT CAA GAT CAT TGC TCC TCC TG	AGG GTG TAA AAC GCA GCT	200

Reagent	[C]i	[C]f
cDNA	-	-
RBC reaction buffer	10X	1X
dNTPs mix (Euroclone)	10 mM	0.2 mM
RBC Taq polymerase	5U/ μL	1U /25 μL
Forward primer (ß actin)	10 μM	0.5 μM
Reverse primer (ß actin)	10 μM	0.5 μM
Water	-	-
Final volume: 25 μL		

Amplified products were allowed to run with 100bp DNA ladder (Fermentas) on a 2% Agarose gel electrophoresis (5% Ethidium Bromide) at 100 volts in 1X TBE running buffer for 40 minutes. Densitometric analyses are performed with Image J software after image acquisition with BioDoc –It imaging.

3.1.7. NSC-34 cell line and Primary cortical neurons

Mouse Motor neuron like hybrid cell line NSC-34 is produced by fusion of motor neuron enriched, embryonic mouse spinal cord cells with mouse neuroblastoma. The cultures contain two populations of cells: small, undifferentiated cells that have the capacity to undergo cell division and larger, multi-nucleate cells. These cells express many properties of motor neurons, including choline acetyltransferase, acetylcholine synthesis, storage and release and neurofilament triplet proteins. These cells can be differentiated using the all trans retinoic acid (atRA) thus establishing itself as a suitable model for the *in vitro* study of pathophysiology in motor neurons.

Primary neuronal culture on the other hand, is a powerful tool for understanding cellular and molecular mechanisms of neuronal development (Lesuisse C et al., 2001).Therefore the effects of the siRNAs can be studied on this system that is close to functional neurons.

To this end, primary cortical neurons were provided by Dr. Mauela Basso from the Laboratory of Transcriptional Neurobiology. The Primary mouse cortical neurons were obtained from C57BL/6 TG2+/− mice mated to generate male and female TG2+/+, TG2−/+, or TG2−/− embryos at day 15 (Basso M et al., 2012). Neurons were dissociated out of the cortex as described by Ratan et al., 1994 and plated in 6 well plates. After 24 hours following plating of neurons, they were supplied with neurobasal media and B27 with antioxidant. The media was changed every two days until complete maturation (DIV14). The cells at DIV 14 were subjected to further analysis.
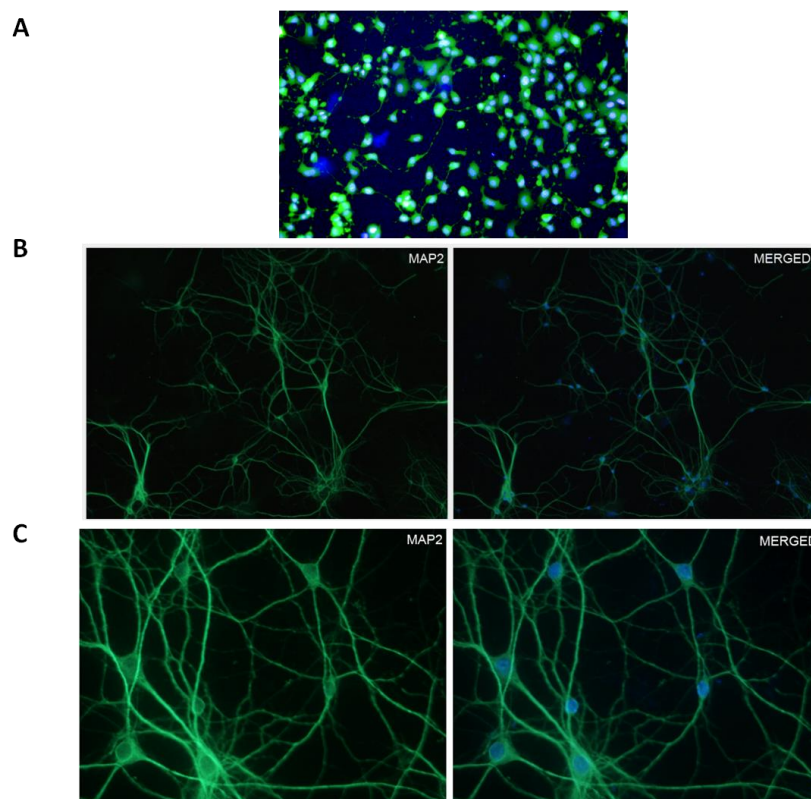
Fig. 3.2 (ii) | Representative images of A) NSC-34 cells on day 4 of differentiation with retinoic acid acquired with the Zeiss microscope at 20X stained with Hoechst and calcein. Primary cortical neurons on DIV 14 (14 Days *in vitro*) acquired with confocal microscopy at B) 40X and C) 100X after being stained with DAPI and MAP2 antibody.(Image courtesy: Dr. Lorena Zubovic and Dr. Manuela Basso).

3.1.8. Transfection of siRNAs in NSC-34 cells

On the day before the experiment, 5×10^4 cells were seeded on a 24 well plate in 500 µl of complete medium without antibiotics at 37° C in 5% CO_2. Transfections were performed as instructed by the manufacturer with 1 µl Lipofectamine 3000 for a range of siRNA concentration starting from 10nM to 100nM (in Opti-MEM medium) per well in a final volume of 500 µl.

As controls, cells were treated with Lipofectamine 3000 only (Mock) and transfected with non-targeting siRNA (Non-specific controls). Following transfection, the cells were incubated at 37° C in 5% CO_2 for 48 hours.

3.1.9. Semi-quantitative reverse transcriptase analysis on NSC34 cell line

3.1.9.(i) RNA extractions

Refer to section 2.1.3. (i)

3.1.9.(ii) cDNA preparation

Refer to section 2.1.3. (ii)

3.1.9 (iii) Semi quantitative RT-PCR assay to evaluate expression of MAPT mRNA in endogenous condition

The expression levels of Exon 10 containing transcripts were analysed with the following primers:

Gene	Forward primer (5'-3')	Reverse primer(5'-3')	Product dimension (bp)
Exon 10 / Exon 10-	CTGAAGCACCACCAGCCGGGAGG	TGGTCTGTCTTGGCTTTGGC	368 / 275
ß-actin	GAT CAA GAT CAT TGC TCC TCC TG	AGG GTG TAA AAC GCA GCT	200

Reagent	[C]i	[C]f
cDNA	-	-
RBC reaction buffer	10X	1X
dNTPs mix (Euroclone)	10 mM	0.2 mM
RBC Taq polymerase	5U/ μL	1U /25 μL
Forward primer (ß actin)	10 μM	0.5 μM
Reverse primer (ß actin)	10 μM	0.5 μM
Water	-	-
Final volume: 25 μL		

Amplified products were allowed to run with 100bp DNA ladder (Fermentas) on a 2% Agarose gel electrophoresis (5% Ethidium Bromide) at 100 volts in 1X TBE running buffer for 40 minutes. Densitometric analyses are performed with Image J software after image acquisition with BioDoc –It imaging.

3.1.10. Semi-quantitative reverse transcriptase analysis on primary cortical neurons

The semi quantitative RT-PCR analysis was performed on the primary cortical neurons at 14 DIV (Days *in vitro*) as described in section 2.1.3 and with the same set of primers.

4.1.1. Western blot analysis

For Western blot analysis, SH-SY5Y and NSC-34 cells were washed with PBS and harvested in radioimmunoprecipitation assay (RIPA) buffer (1% Nonidet P-40, 0.5% sodium deoxycholate, and 0.1% sodium dodecyl sulfate (SDS) in PBS) plus protease inhibitors (Complete, Roche Molecular Biochemicals, Indianapolis, IN, USA) and phosphatase inhibitors (New England Biolabs) at 4°C. Cell homogenates were centrifuged at 100,000 g for 30 min. Supernatants were collected, and the protein content was determined using a commercial kit (Bio-Rad, Hercules, CA, USA). Samples were separated on 4-12% gradient SDS gels and electrotransferred to nitrocellulose membrane (Millipore, Bedford, MA, USA) after dephosphorylation (NEB). Membranes were washed, blocked, and incubated overnight with rabbit anti-tau (1:10,000; Dako) antibody, followed by a second washing step before incubating with secondary antibody an Infra-red chromophore Goat anti-Rabbit 800 CW (Li-COR) for 1 h.

3.2. Results

3.2.1. Design of a panel of siRNAs targeting Exon 10

Six different siRNAs were designed to target different regions of exon 10 as shown in **Fig.3.3**.
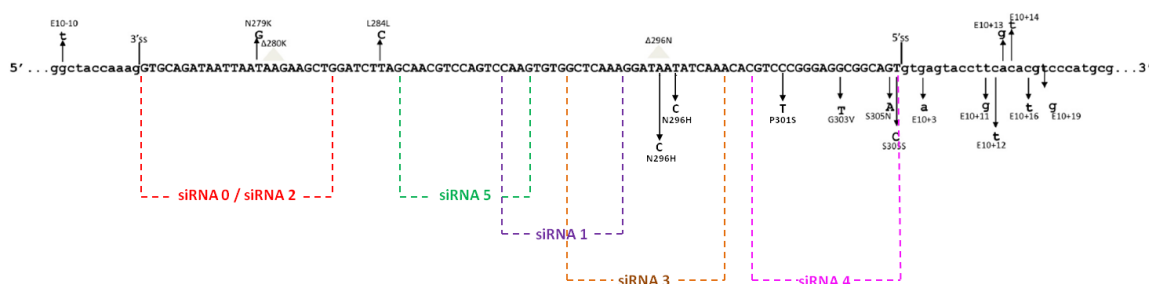
Fig 3.3 | Schematic representation of Exon 10 sequence with the mutations and design of siRNAs along the stretch of exon 10 region.

3.2.2. Analysis of fluorescent reporter plasmids transfected in SH-SY5Y cell line

One of the remarkable contributions of Stoilov and colleagues includes the production of two-colour fluorescent reporter assay with a cassette of MAPT exon 10 to test for the effect of compounds that might alter splicing (Stoilov P et al., 2008). This reporter relies on the emission of fluorescence such that: GFP (Green fluorescence protein) is transcribed upon skipping of exon 10 and RFP (Red fluorescence protein) is produced when exon 10 is included in the transcript. The plasmid was constructed on the basis of:

- ORFs of destabilized GFP and RFP are expressed from a single promoter as a bicistronic transcript.
- The start codon of GFP is split between two constitutive exons by an alternative exon cassette with its flanking introns.
- Skipping of alternative exon cassette enables the formation of start codon of GFP ORF following its expression in the mature transcript and expression of

GFP, whereas exon inclusion leads to unavailable GFP start codon and upon further scanning, the ribosome will find the first available AUG codon in Kozak sequence of RFP ORF thus translating RFP.

3.2.2. (i) Comparison of wild type and N279 mutant reporter plasmids

This dual reporter plasmid containing MAPT exon 10 (Stoilov P et al., 2008) was mutagenised by incorporating a point mutation N279 which results in asparagine to lysine substitution (T to G). This mutation affects splicing allowing exon 10 to be incorporated more frequently in tau transcripts thus causing an increase of 4R expression over 3R.

After 48 hours of transfection of the wild type and mutant plasmid in SHYS5Y cell lines, the cells were subjected to an image based analysis using the protocol On comparing the two conditions, there was an increased production of red fluorescent signal in the mutant plasmid as observed in the representative image **(Fig.3.4)** and fits well with the expected results.
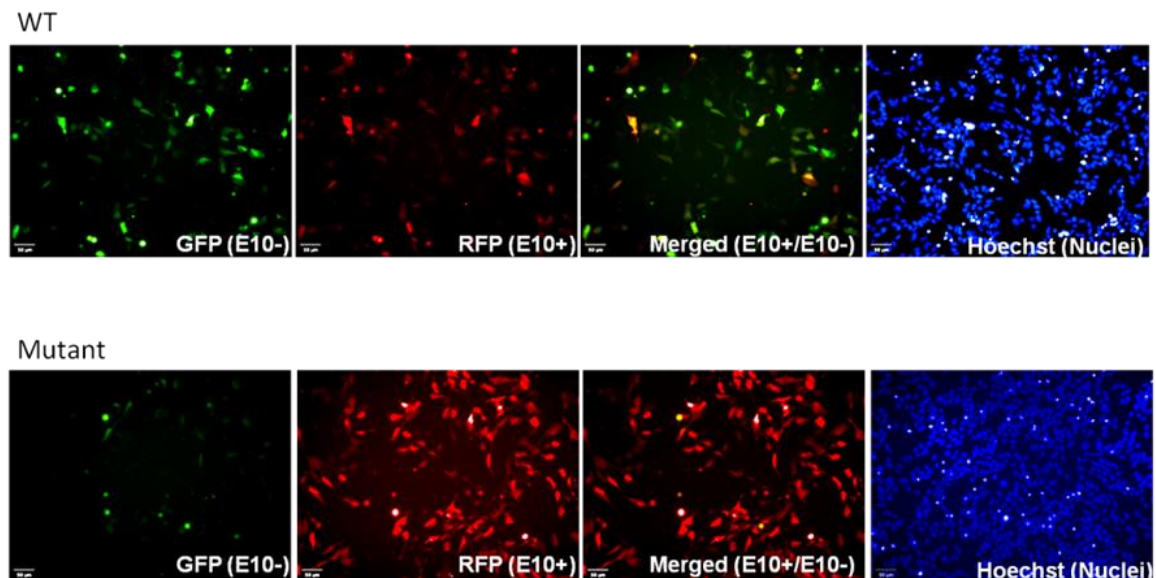
Fig.3.4 | Images of SHYS5Y cell line transfected with 0.25 µg of Wild type plasmid and Mutant plasmid. Representative Images of SH-SY5Y cells expressing the two plasmid reporters each with a different inclusion level of Exon 10: Wild type (Top panel) and Mutant N279 plasmid reporters (Bottom panel). The cells were analyzed by High-Content screening system (Operetta) after 48 h of transfection. The images were acquired using a 20× LWD objective in wide-field mode in combination with filters for Hoechst 33342 (excitation filter: 360–400 nm; emission filter: 410–480 nm) and Alexa Fluor 488 (excitation filter: 460–490 nm; emission filter: 500–550 nm).
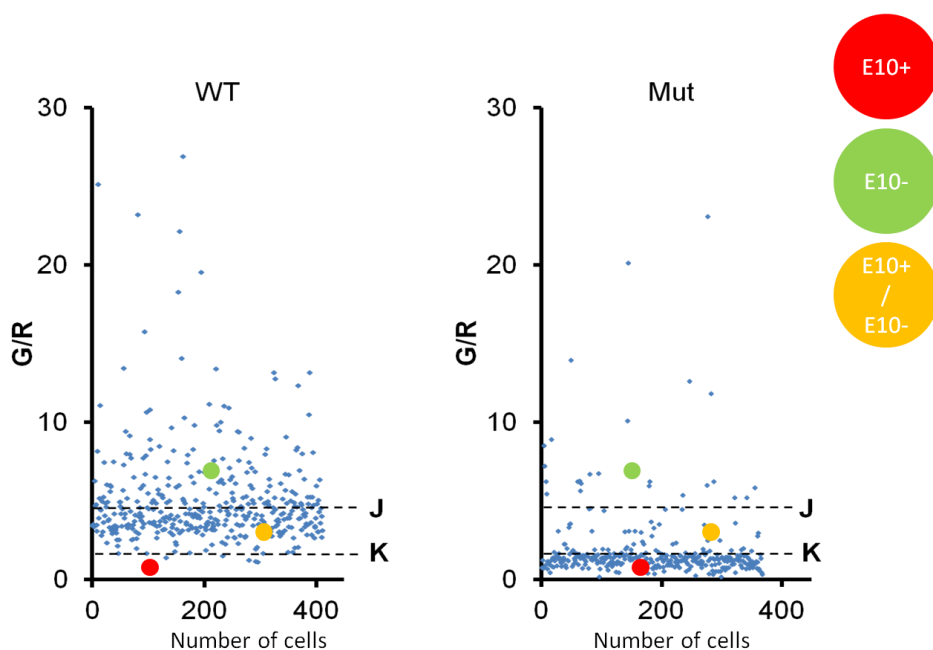
Fig.3.5 | Setting up of threshold values based on intensities of RFP and GFP. Scatter plots representing G/R values of each cell in a particular well bearing one of the dual reporter plasmids (WT and Mut, respectively). The indicated thresholds are arbitrarily selected to classify the cell population in three different classes.

Application of threshold values on these images, further allows discrimination of varied population of cells (with different intensities) within each well.

As observed from the graph, cells transfected with Wild type plasmid possesses mainly green cells (E10-) and yellow cells (E10+/E10-) with a very few red cells (E10+) **(Fig.3.5)**.

However, cells transfected with mutant plasmid indicates the shift of threshold towards a majority of red cells, and a few yellow and green cells. This confirms the production of RFP due to the introduction of N279 point mutation causing an increase of exon 10 (characteristic hall mark of FTDP-17) **(Fig.3.6)**.
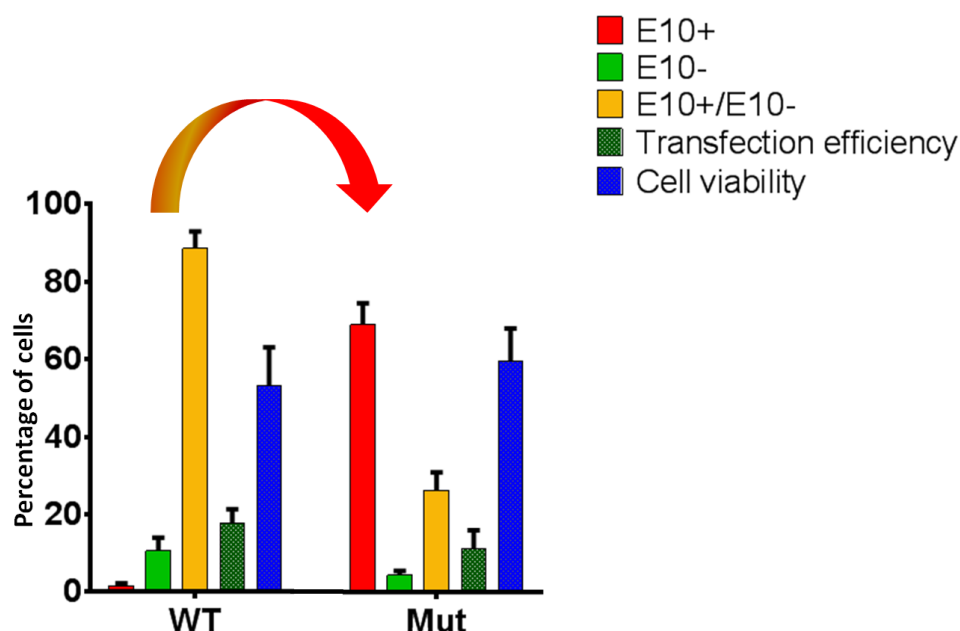
Fig.3.6 | Image based analysis of SH-SY5Y cells transfected with Wild type and Mutant reporter plasmids. Histogram represents the selected read-outs of the quantitative analysis of the two reporters, such as the relative percentages of the three sub-populations of SH-SY5Y cells classified by intensity properties, the transfection efficiency and the cell viability. Values represent mean±SD (n=3).

The image based analysis on the SH-SY5Y cells transfected with Wild type and Mutant plasmids, shows that the N279 point mutation shifts splicing of exon 10 thus altering the fluorescent signals from a relatively low level of RFP (~2%) to a very high level (~65%) due to exon 10 inclusion (exon 10+) (Fig.3.6).

Cells containing both exon 10+ and exon 10-transcripts (yellow cells) have thus shifted from ~85% to ~30% whereas cells containing only exon 10- shows a decrease from ~15% to ~5% **(Fig.3.6)**.

In both conditions of transfection, there is no variation of transfection efficiency and cell viability thus confirming that they were subjected to the same conditions and the fluorescent signals are not biased outputs, but are coherent with the N279 mutation.

In order to validate these effects at a molecular level, an RT-PCR was performed using a forward and reverse primer designed to bind to the 5' end of exon 1 and 3' end of GFP in the mutant plasmid.

Since the plasmid encodes exon 10 that undergoes alternative splicing, this reaction is expected to produce two different transcript isoforms (i) exon 10+ and (ii) exon 10-.(Fig. 3.7). The mutant is expected to show a higher amount of transcripts containing exon 10 due to the incorporated N279 mutation.
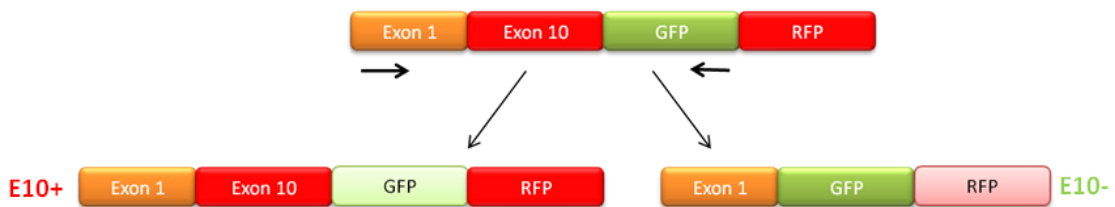
Fig.3.7 | Schematic representation of primers on WT / Mutant plasmid and the alternatively spliced transcript isoforms with and without exon 10.
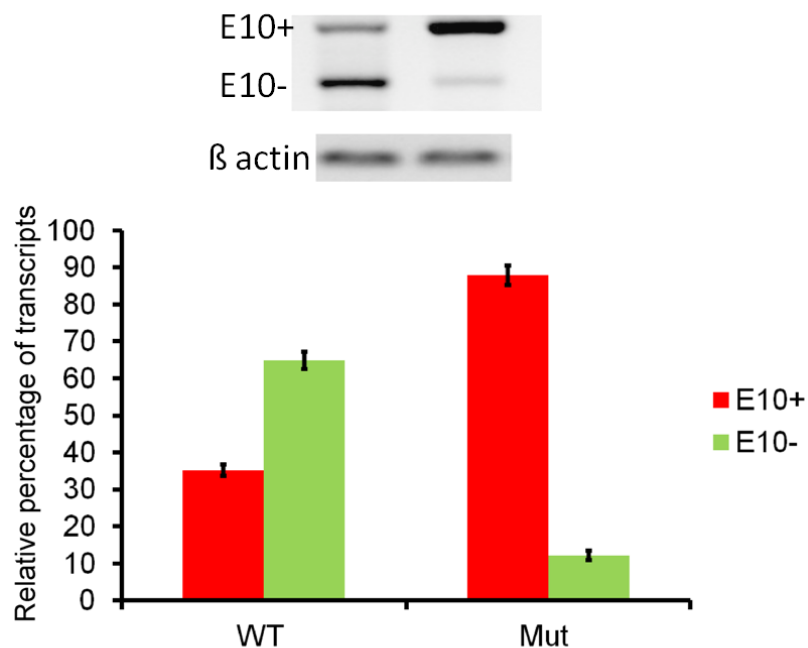
Fig.3.8 | RT-PCR analysis of Exon 10 mRNA levels in the wild type and mutant minigene plasmid transfected in SH-SY5Y cells. Gels showing the RT-PCR products of transcripts containing exon 10+ (300 bp) and exon 10-(207 bp). Histogram represents the densitometric units of each treatment condition normalised on ß actin. Values represent mean SD±(n=3).

Results of the semi quantitative PCR analysis on the samples containing cells (transfected with the WT and Mut plasmids) were checked on a 2% agarose gel. As expected, the samples showed amplification of two bands (corresponding to exon 10+ and exon 10- from the reporter plasmids) along with the expression of housekeeping gene ß-actin. **(Fig. 3.8)**.
The content of exon 10 increases from ~35% in WT to ~85% in mutant reporter plasmid, thus the observations in the image based analysis has been confirmed through RT-PCR which shows an increased inclusion of exon 10.

3.2.2 (ii) Screening for the effect of siRNAs on mutant N279 plasmid reporter

In order to assess the potentiality of suitable siRNAs to mediate transcriptional gene silencing, the following two strategies were adopted;

- An image based analysis on transfected samples;
- A subsequent RT-PCR analysis on those samples for further validation.

The six different siRNAs designed to target exon 10 was tested with varying concentrations ranging from 10 nM to 100 nM to test their efficacy in inducing transcriptional gene silencing of exon 10 containing transcripts. These effects were validated on two different concentrations of the reporter plasmids (i.e: 0.25µg and 0.5 µg) **(Fig.3.9 and 3.10)**.

The experiments were performed as biological triplicates with technical duplicates each. The samples that were subjected to image based analysis were further used for downstream analyses (i.e: RT-PCR) to quantify the amounts of exon 10 containing transcripts post-treatment with siRNAs.

The image based analysis on cells transfected with 0.25μg of mutant plasmid and varied concentrations of siRNAs confirms a variation of effects mediated through different siRNAs. **(Fig.3.9)**.

Compared to the non-treated mutant plasmid, plasmid treated with siRNA 0 and siRNA 2 shows a slight increase in inclusion of exon 10 containing transcripts whereas siRNA 1, siRNA 3 and siRNA 5 shows a decrease in exon 10 containing transcripts. siRNA 4 however shows no effect on exon 10 The control siRNA at varied concentrations does not impose any effect on exon 10.

The effect of each siRNA at specific concentration is described below **(Fig.3.9)**.

siRNAs 0, 2 and 4

siRNA 0 shows no variation in exon 10 upon treatment with 10nM and 25 nM followed by an increase of ~10% upon treatment with 50nM concentration and no effect upon treatment with a 100nM concentration.

siRNA 2 shows no difference upon treatment with concentrations 10nM and 25 nM .However, at 50nM there is an increase of ~10% of exon 10 and at 100 nM there is no effect observed. siRNA 4 showed no effects regardless of varied concentrations.

Interestingly, these data also reflects a concentration dependent effect of potential siRNAs 1, 3 and 5 on reducing exon 10.

siRNA 1

Upon treatment with 10 nM there is a slight decrease of exon 10 by ~10% .A concentration of 25 nM further reduces exon 10 by~15% and concentrations of 50 nM and 100 nM leads to a reduction by ~20%. This gradual decrease of almost ~20% of exon 10 containing cells is accompanied by a ~15% increase of cells containing both exon 10+ and exon 10- (**Fig.3.9 and 3.11)**.

siRNA 3

Upon treatment with 10 nM and 25 nM concentrations there is a decrease of exon 10 transcripts by ~20 % followed by a further reduction of ~30% with 50 nM and 100 nM concentration. This gradual decrease of almost ~30% of E10+ is accompanied by a ~30% increase of cells containing both exon 10+ and exon 10- **(Fig.3.9 and 3.11)**.

siRNA 5

Upon treatment with 10 nM and 25 nM, there is a reduction of ~15% of exon 10 transcripts and treatment with 50 nM and 100 nM led to a further decrease of 25% of exon 10 transcripts. This gradual decrease is accompanied by a ~25% increase of cells containing both exon 10+ and exon 10-**(Fig.3.9 and 3.11)**.

siRNA control

The control siRNA at varied concentrations does not impose any effect on exon 10.
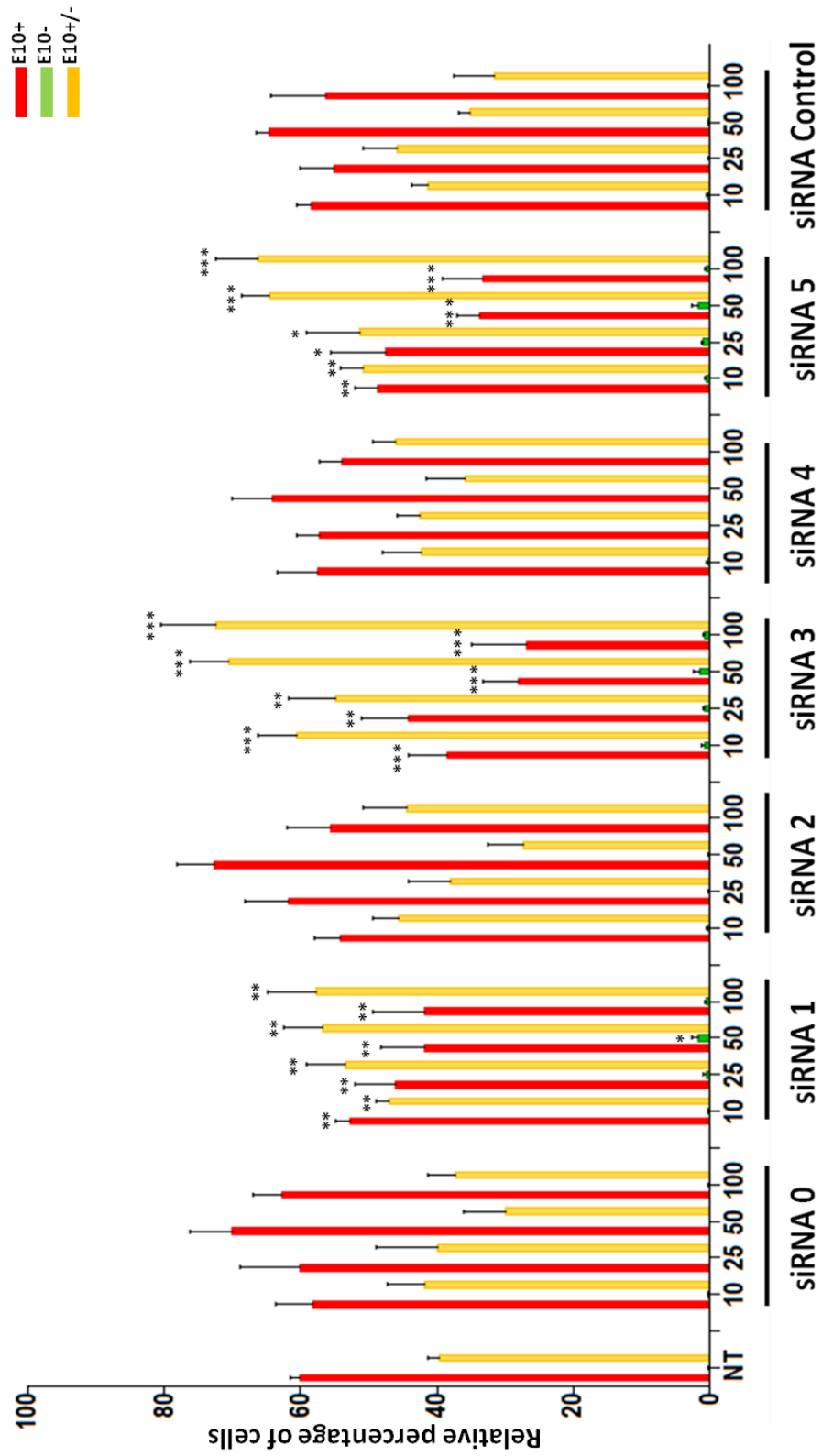
Fig.3.9 | An image based screening assay has been performed on the mutant plasmid (0.25 µg) co-transfected with varied concentrations of six different siRNAs. Values represent mean ±SD (n=3). Asteriks (*) indicate significant differences (t-test , P > 0.05, *P ≤ 0.05, **P ≤ 0.01, ***P ≤ 0.001).
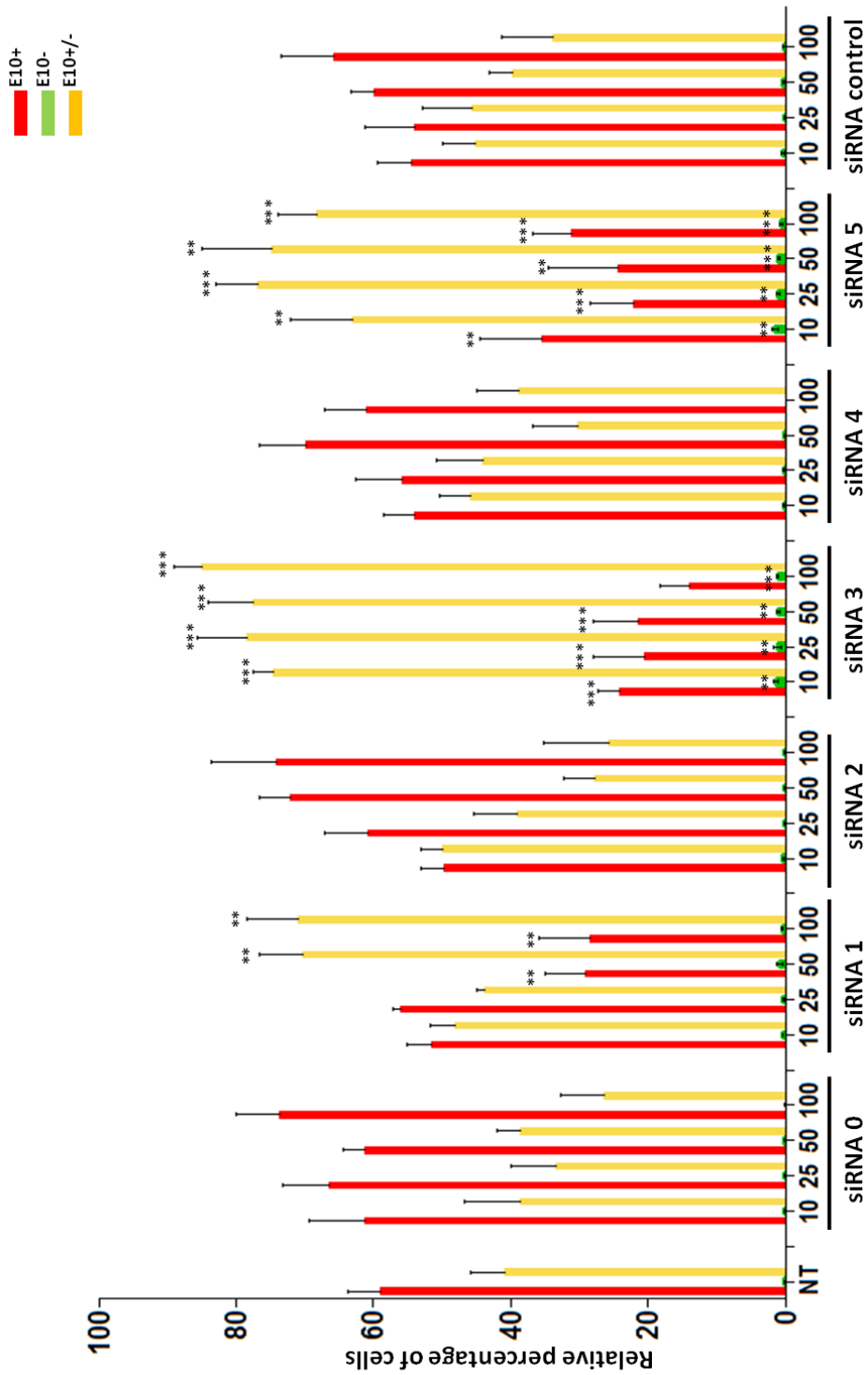
Fig.3.10 | An image based screening assay has been performed on the mutant plasmid (0.5 µg) co-transfected with varied concentrations of six different siRNAs. Values represent mean ±SD (n=3). Asteriks (*) indicate significant differences (t-test ,$P > 0.05$, *$P \le 0.05$, **$P \le 0.01$, ***$P \le 0.001$).

The image-based analysis on cells transfected with 0.5μg of mutant plasmid and varied concentrations of siRNAs confirms a variation of effects mediated through different siRNAs. **(Fig 3.10)**.

Compared to the non-treated mutant plasmid, plasmid treated with siRNA 0 and siRNA 2 shows a slight increase in inclusion of exon 10 containing transcripts whereas siRNA 1, siRNA 3 and siRNA 5 shows a decrease in exon 10 containing transcripts. siRNA 4 however shows no effect on exon 10 The control siRNA at varied concentrations does not impose any effect on exon 10.

The effect of each siRNA at specific concentration is described below.

siRNAs 0, 2 and 4

siRNA 0 shows no variation in exon 10 upon treatment with 10nM ,25 nM and 50 nM, followed by an increase of ~10% upon treatment with 100nM concentration siRNA 2 shows no difference upon treatment with concentrations 10nM and 25 nM .However, at 50nM and 100nM there is an increase of ~10%of exon 10. siRNA 4 showed no effects regardless of varied concentrations.

Interestingly, these data also reflect a concentration dependent effect of potential siRNAs 1, 3 and 5 on reducing exon 10.

siRNA 1

Upon treatment with 10 nM and 25nM there is a slight decrease of exon 10 by ~10% and concentrations of 50 nM and 100 nM leads to a further reduction of up to ~30%.

This gradual decrease of almost ~30% of exon 10+ is accompanied by a ~30% increase of cells containing both exon 10+ and without exon 10-

siRNA 3

All the different concentrations led to a decrease of ~40% of exon 10 containing transcripts. This gradual decrease of almost ~40% of exon 10+ is accompanied by a ~35% increase of cells containing both exon 10+ and exon 10-.

siRNA 5

Treatment with 10 nm led to a decrease of ~25% of exon 10 containing transcripts followed by a ~35% reduction upon treatment with 25 nM and 50 nM. A concentration of 100 nM led to a reduction of ~30% exon 10 containing transcripts. Reduction of cells expressing solely exon 10 was accompanied by an increase of cells expressing both isoforms

siRNA control

The control siRNA at varied concentrations does not impose any effect on Exon 10.

A. siRNA 1

Concentration of siRNA (nM)

Plasmid only (0.25 μg)

E10-   E10+   E10+/E10-   Nuclei

10 nM

25 nM

50 nM

100 nM

E10
+

E10
-

E10
+/-

B. siRNA 3

Concentration of siRNA (nM)

Plasmid only (0.25 μg)

E10-   E10+   E10+/E10-   Nuclei

10 nM

25 nM

50 nM

100 nM

E10
+

E10
-

E10
+/-

124
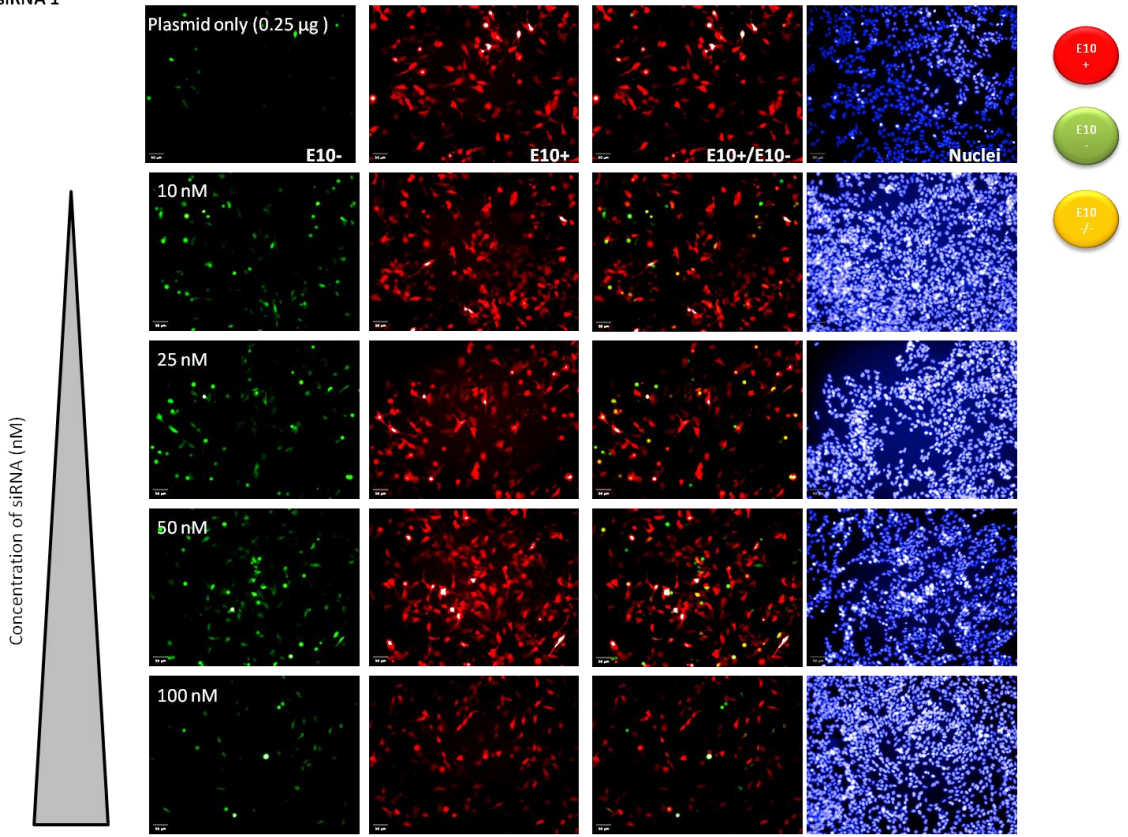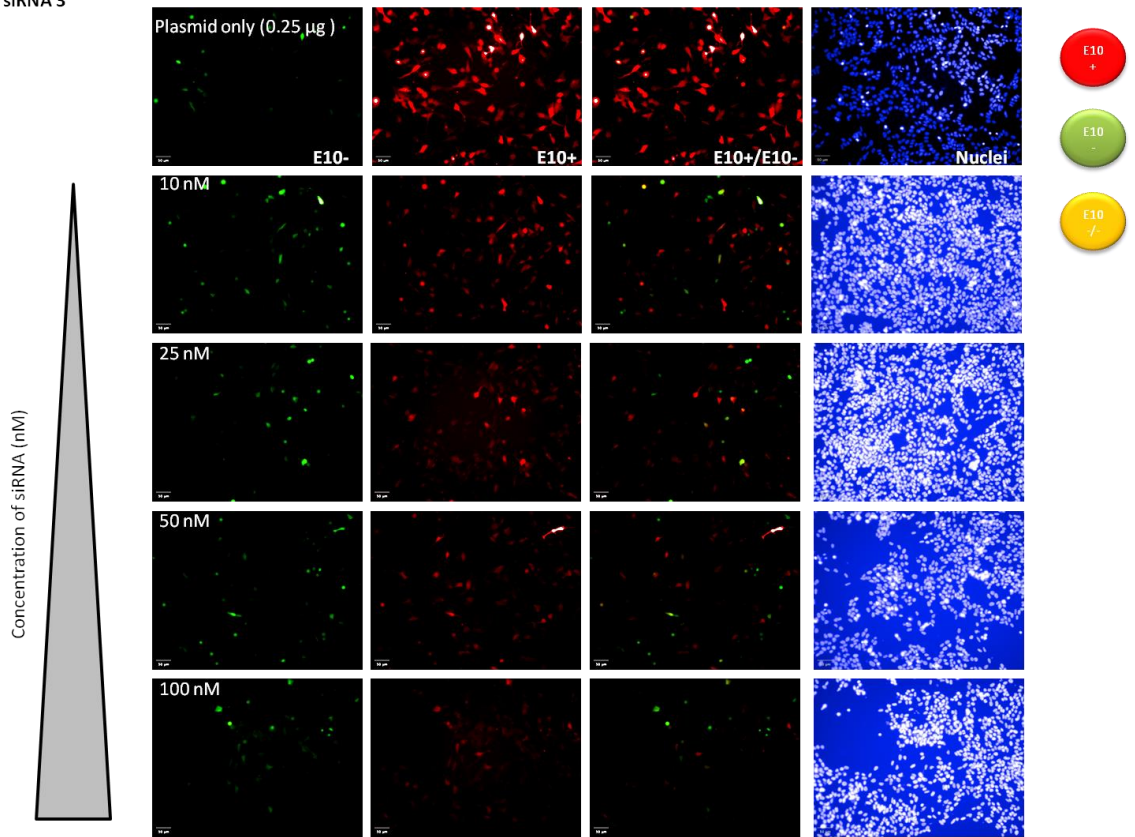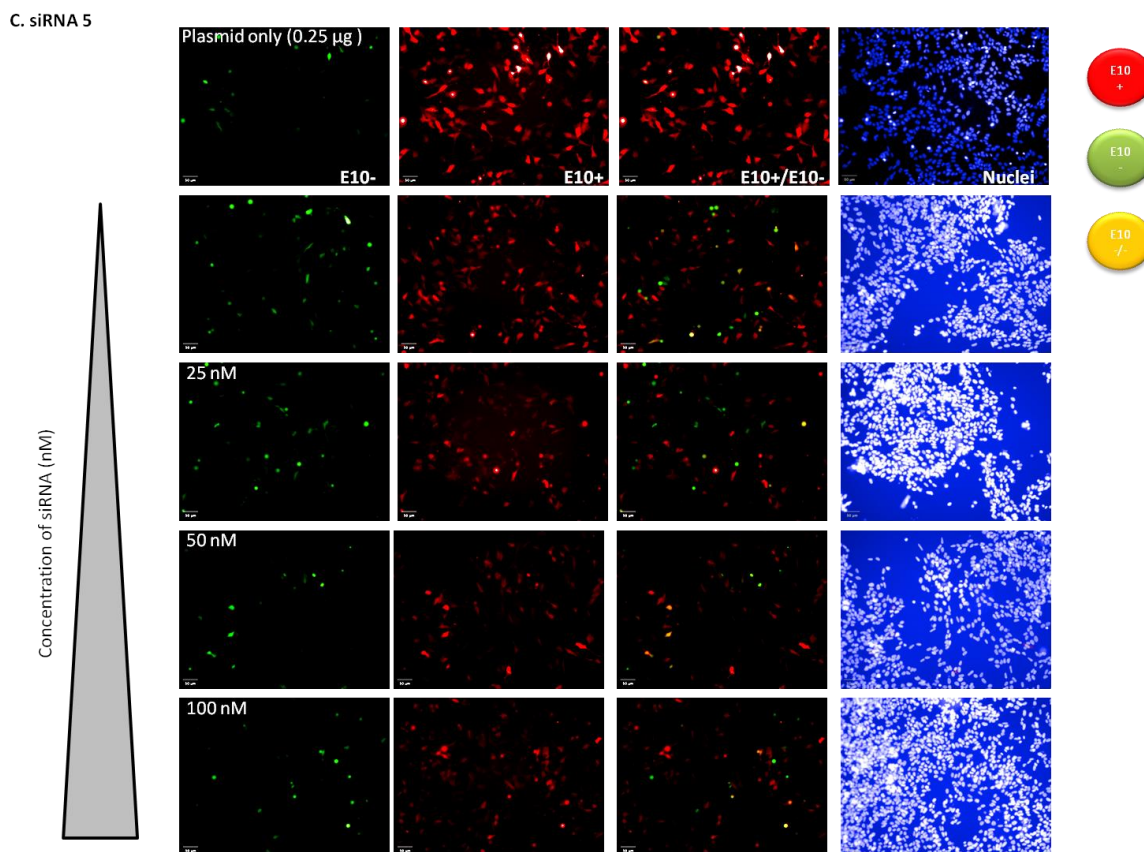
Fig. 3.11 | Images of SH-SY5Y cell line transfected with 0.25 µg of Mutant plasmid and a) siRNA 1 b) siRNA 3 c) siRNA 5 Representative Images of SH-SY5Y cells expressing the mutant plasmid reporter with varied concentrations of siRNA1 from 10nM to 100nM (Top to bottom). The cells were analyzed by High-Content screening system (Operetta) after 48 h of transfection. The images were acquired using a 20× LWD objective in wide-field mode in combination with filters for Hoechst 33342 (excitation filter: 360–400 nm; emission filter: 410–480 nm) and Alexa Fluor 488 (excitation filter: 460–490 nm; emission filter: 500–550 nm).

Representative images in **Fig.3.11** are acquired from the transfected cells containing mutant plasmid and potential siRNAs 1, 3 and 5 at varied concentrations. It can be observed that siRNA 3 is the most potent of the three siRNAs with a highest effect observed upon treatment with 50 nM and 100 nM concentrations.

3.2.3. Semi quantitative RT-PCR analysis on MAPT exon 10 of mutant minigene upon co-transfection with siRNAs

In order to evaluate and confirm the effects of the three potential siRNAs 1, 3 and 5 on inducing degradation of exon 10 containing transcripts, an RT-PCR analysis was performed as described in section 3.2.2. The non treated mutant plasmid was compared to varied treatment conditions of three siRNAs. Their relative expressions were normalised against ß-actin gene.
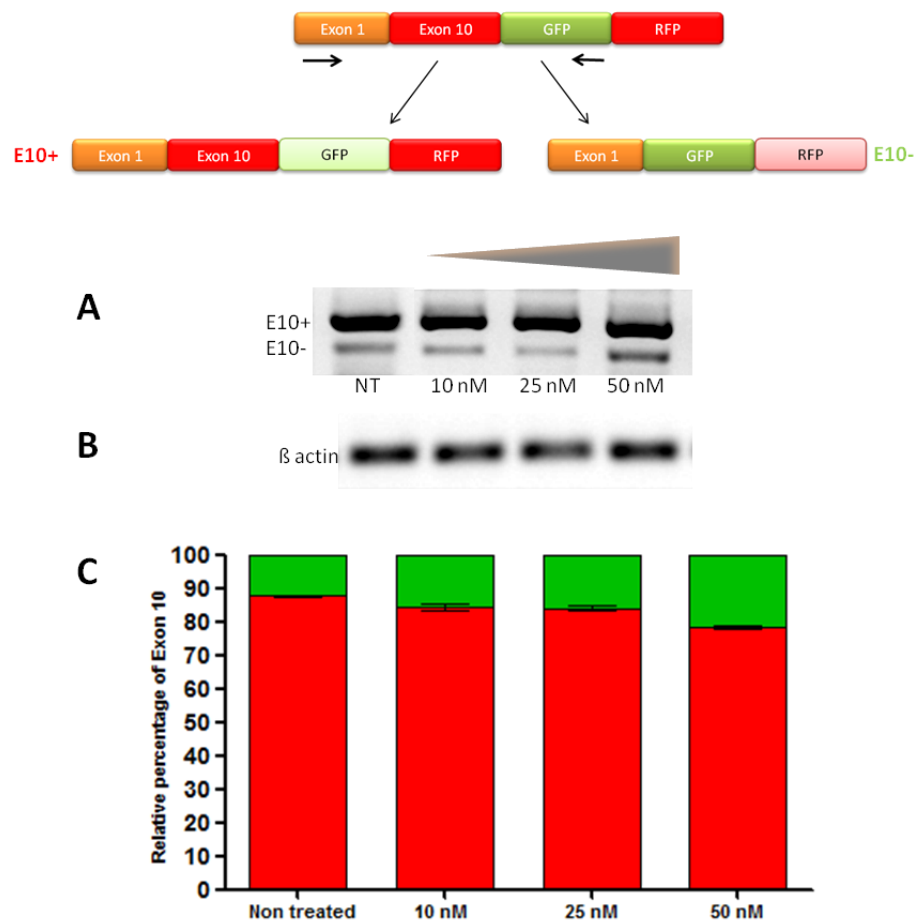
Fig 3.12 | RT-PCR analysis of SH-SY5Y cells transfected with the mutant plasmid and siRNA 1 at varied concentrations A) The upper band corresponds to the Exon 10 transcript with a length of 300 bp, whereas the lower band corresponds to the Exon 10-transcript with a length of 207 bp. B) ß actin is used as a house keeping gene (200 bp) to calculate the relative expression levels of these two isoforms. C) Relative expression levels of the two isoforms

The RT-PCR analysis further confirms that treatment with siRNA 3 leads to a ~10 % reduction of exon 10 containing transcripts at a concentration of 50 nM as observed in **Fig 3.12**.
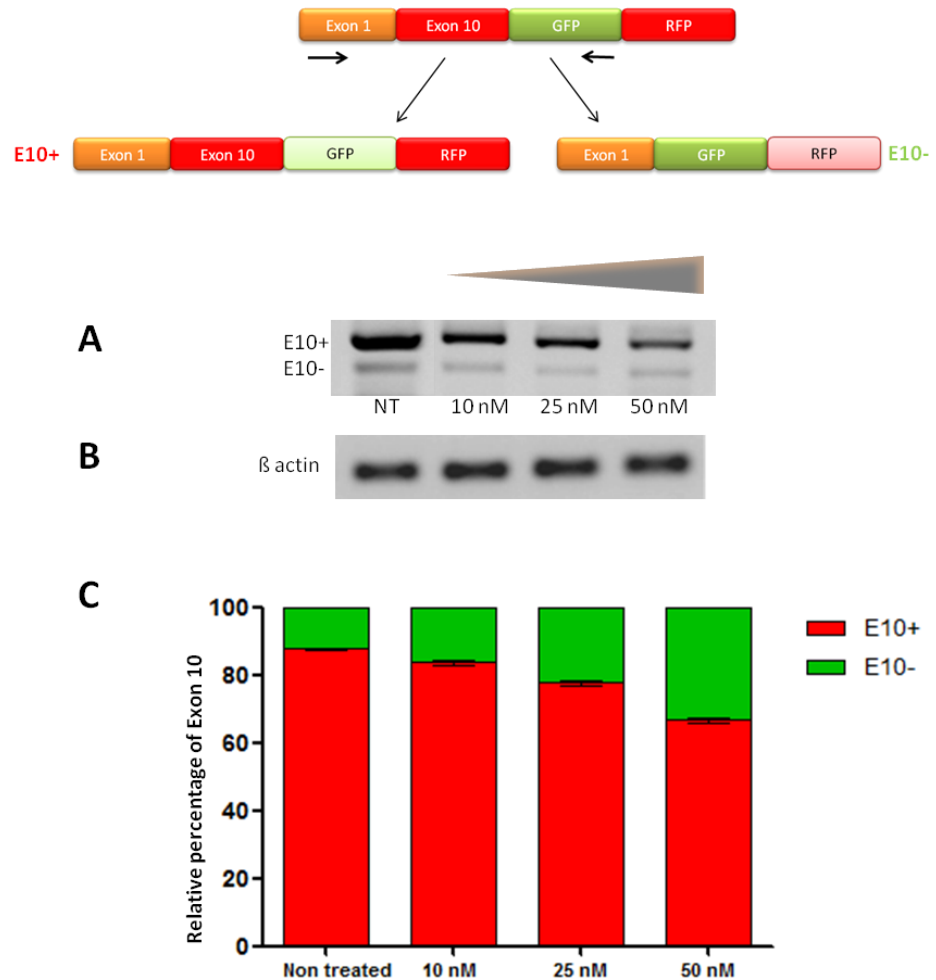
Fig 3.13 | RT-PCR analysis of SH-SY5Y cells transfected with the mutant plasmid and siRNA 3 at varied concentrations A) The upper band corresponds to the Exon 10 transcript with a length of 300 bp, whereas the lower band corresponds to the Exon 10-transcript with a length of 207 bp. ß actin is used as a house keeping gene (200 bp) to calculate the relative expression levels of these two isoforms. C) Relative expression levels of the two isoforms

The RT-PCR analysis further confirms that treatment with siRNA 3 leads to a ~25 % reduction of exon 10 containing transcripts at a concentration of 50 nM as observed in **Fig 3.13**.
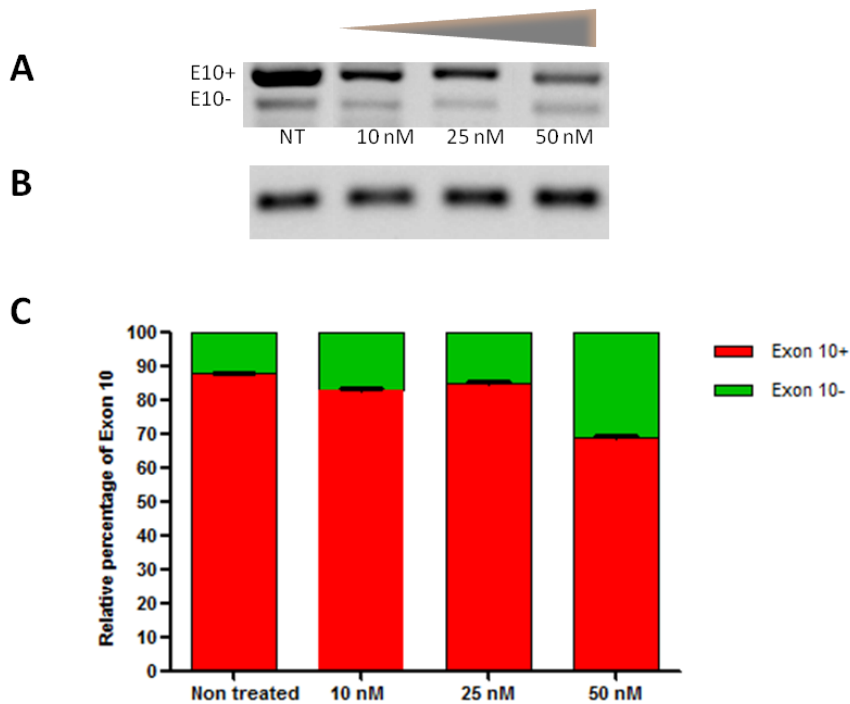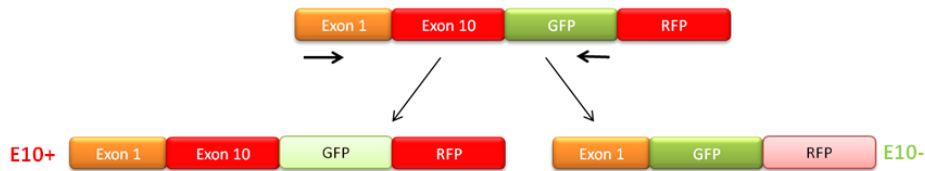
Fig 3.14 | RT-PCR analysis of SH-SY5Y cells transfected with the mutant plasmid and siRNA 5 at varied concentrations A) The upper band corresponds to the exon 10+ transcript with a length of 300 bp, whereas the lower band corresponds to the exon 10-transcript with a length of 207 bp. ß-actin is used as a house keeping gene (200 bp) to calculate the relative expression levels of these two isoforms.

The RT-PCR analysis further confirms that treatment with siRNA 3 leads to a ~20 % reduction of Exon 10 containing transcripts at a concentration of 50 nM as observed in **Fig 3.14**.

3.2.4. Selection of cell line for analyzing the effect of siRNA in an endogenous context - NSC 34 cell line

In order to evaluate the effects of siRNA on an endogenous context, an RT-PCR analysis was performed on a number of neuroblastoma cells for the presence of excessive content of Exon 10.

This was an essential step to identify a neuroblastoma model that recapitulates FTDP-17 so as to monitor the efficacies of the siRNA oligos.
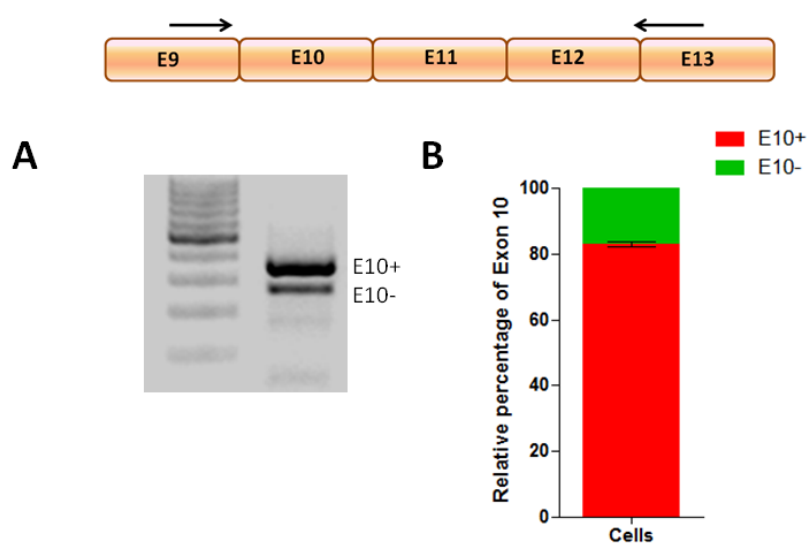
Fig.3.15 | Semi-quantitative RT-PCR shows MAPT mRNA levels in the endogenous context of Non treated NSC 34 cells A) Upper band (368 bp) represents exon 10+ transcript wheras the bottom band (275 bp) corresponds to exon 10- transcript B) Relative expression levels of two different MAPT isoforms. (Error bars represent the standard deviation of band intensities in two different biological replicates).

The primers were designed such that the forward primer detects the 3' end of exon 9 and the reverse primer detects the 5' end of exon 13.

Since exon 10 undergoes an alternative splicing, two different transcripts (Exon 10+ (368 bp) and Exon 10-(275 bp)) are produced.

Fig.3.15 shows RT-PCR on MAPT mRNA in which 83% content of Exon 10 versus 17% of transcripts without exon 10 was observed.Therefore, NSC 34 cell line was chosen as the optimal model system due to an excessive presence of exon 10 transcripts.

3.2.5. Semi quantitative RT-PCR analysis on MAPT exon 10 in endogenous context of NSC 34 cell line upon transfection with siRNAs

In order to validate the effects observed in the minigene reporter system, the three potential siRNAs 1, 3 and 5 were transfected in NSC 34 cells with a range of concentrations from 10 nM to 100 nM. As a control, a non specific siRNA was used. These treatment conditions were compared to cells treated with lipofectamine reagent as an additional control.

Semi-quantitative RT-PCR confirmed the effect of siRNAs on exon 10 transcripts in endogenous condition such that, siRNAs 1 and 3 induced a reduction from ~75% to ~65% and 30% respectively and showed a very slight dose-dependent reduction. However, siRNA 5   showed a dose dependent effect starting from a 50% when treated with a concentration of 10nM and reaching upto 40% upon treatment with 25nM, 50nM and 100nM concentrations **(Fig.3.16)**.
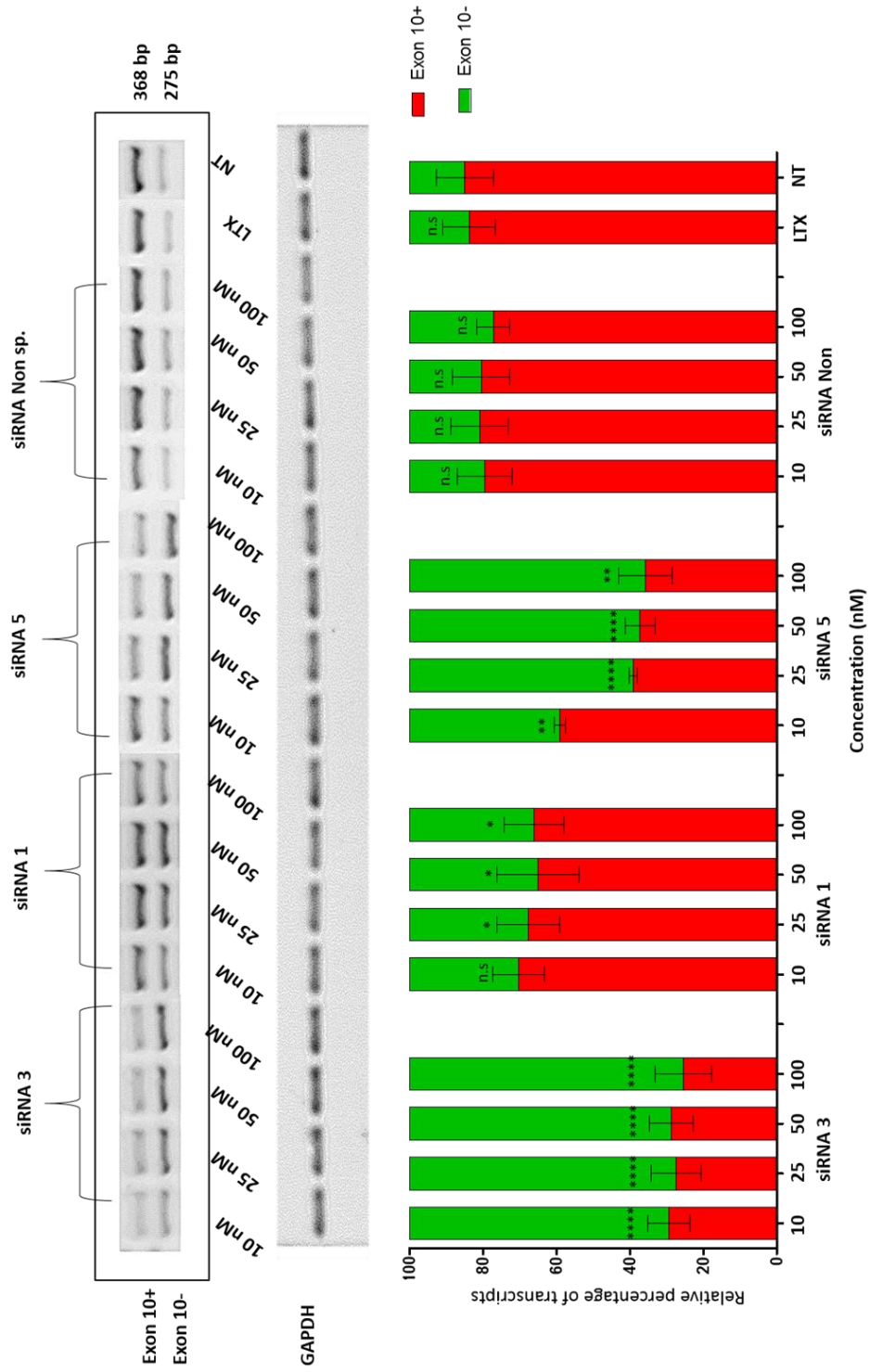
Fig.3.16 | Semi-quantitative RT-PCR shows MAPT mRNA levels in the endogenous context of NSC 34 cells treated with siRNA 3, 1, 5, non specific control and cells with lipofectamine. A) Upper band (368 bp) represents 4R tau isoforms whereas the bottom band (275 bp) corresponds to 3R tau isoforms B) Amplification of the ß-actin house keeping mRNA c) Relative expression levels of two different MAPT isoforms. (Error bars represent the standard deviation of band intensities in two different biological replicates) Asteriks (*) indicate significant differences (t-test ,P > 0.05,*P ≤ 0.05,**P ≤ 0.01,***P ≤ 0.001).

3.2.6. Semi quantitative RT-PCR analysis on MAPT exon 10 in endogenous context of primary cortical neurons
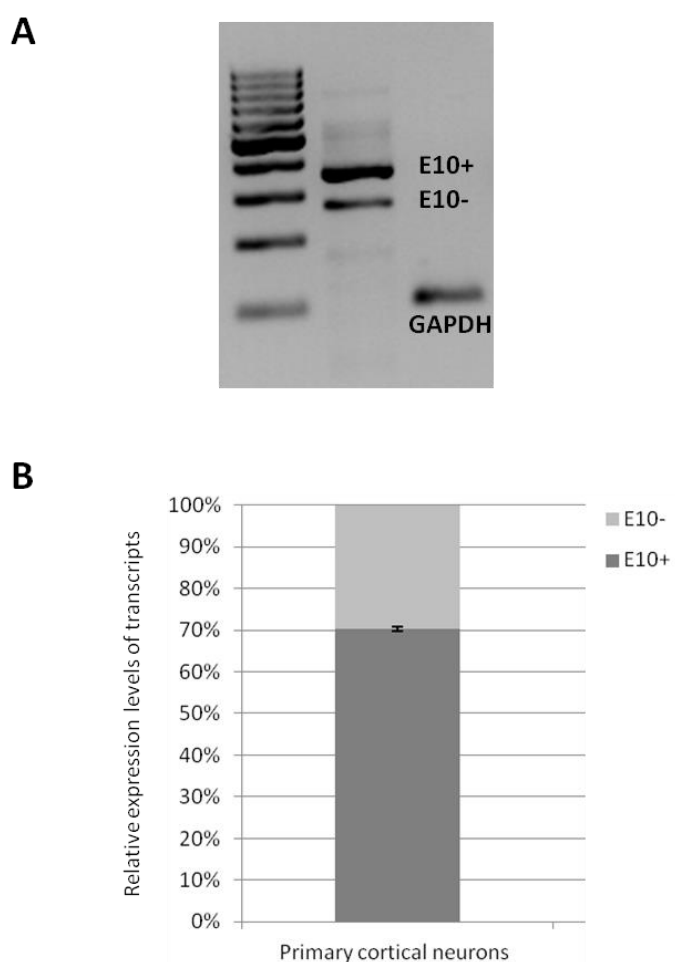
Fig.3.17 | Semi-quantitative RT-PCR shows MAPT mRNA levels in the endogenous context of primary cortical neurons at 14 DIV. A) Upper band (368 bp) represents 4R tau isoforms wheras the bottom band (275 bp) corresponds to 3R tau isoforms. GAPDH is used as a house keeping control (110 bp) B) Relative expression levels of two different MAPT isoforms. (Error bars represent the standard deviation of band intensities in two different biological replicates).

Fig.3.17 shows RT-PCR on MAPT mRNA in which 70% content of Exon 10 versus 30% of transcripts without Exon 10 was observed. Therefore, primary cortical neurons were chosen as an optimal relevant model system due to an excessive presence of Exon 10 transcripts and its neuronal nature.

3.2.7. Optimisation of Western blot analysis on SH-SY5Y cells and NSC 34 cells
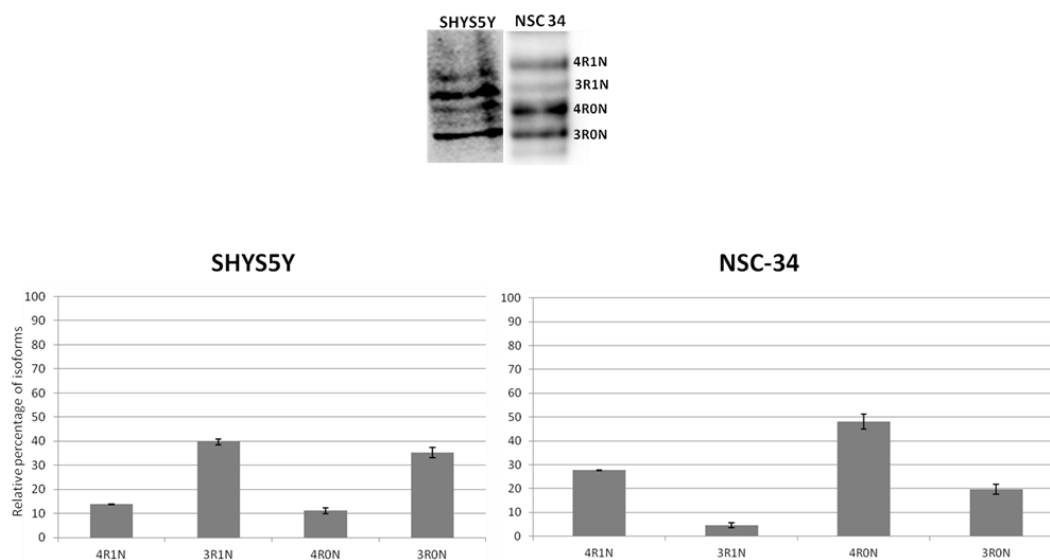
Fig.3.18 | A) Images of the western blot analysis of protein levels of tau in SH-SY5Y cells and NSC 34 cells. B) Relative expression levels of tau isoforms (4R and 3R).

The western blot confirms the presence of four different isoforms with varied sizes as compared to the literature-based evidence (Hogg et al., 2003) and the sizes of the different isoforms are reported as follows:

- 42.9 kDa represents 4R1N
- 39.7 kDa represents 3R1N
- 40.0 kDa represents 4R0N
- 36.8 kDa represents 3R0N

In the SH-SY5Y cells, the relative percentage of isoforms of 4R (4R1N and 4R0N) is ~25% and the 3R (3R1N and 3R0N) is ~75%. On the contrary, in the NSC34 cells, the relative percentage of isoforms of 4R (4R1N and 4R0N) is ~75% and the 3R (3R1N and 3R0N) is ~25% **(Fig.3.18)**.

3.2.8. Preliminary data on the effect of siRNA on the endogenous tau protein in NSC34 cells.
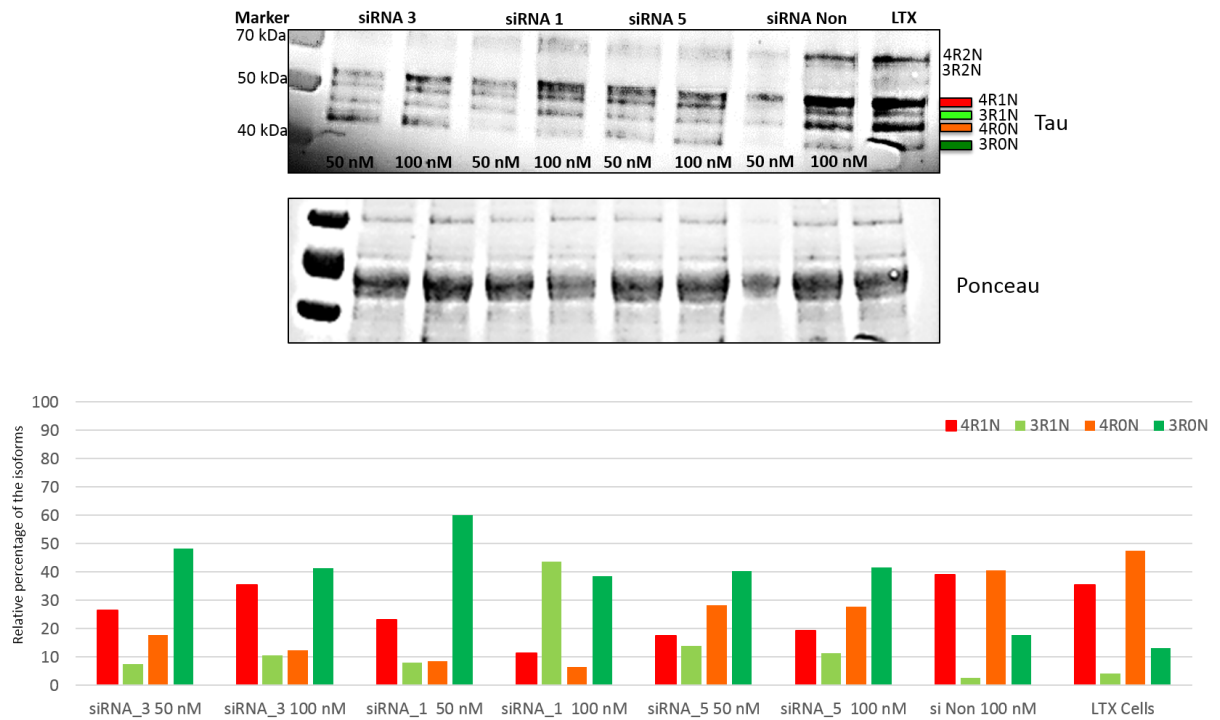
Fig.3.19 | A) Images of the western blot analysis of protein levels of NSC 34 cells and the tau isoforms (4R and 3R) after 48 hours of treatment with siRNAs 3,1 and 5. Ponceau was used as a loading control. B) Relative expression levels of the four tau isoforms.

The preliminary data on the western blot analysis indicates a reduction of 4R isoforms upon treatment with siRNAs 1, 3 and 5 with a concentration of 50nM and 100nM. Considering the percentage of 4R1N and 4R0N in NSC34 cells treated with the Non specific control and that of lipofectamine as 40% and 40% respectively. It can be observed that upon treatment with siRNA 3 there is a reduction of both these isoforms to ~30% and ~20% respectively with 50nM concentration and reaching upto 35% and 10% respectively upon treatment with 100nM concentration. siRNA 1 leads to a reduction to 20% and 10% of 4R1N and 4R0N with a 50nM concentration and 10% and 5% with a 100nM concentration. siRNA 5 shows a similar effect on both treatment conditions leading to a decrease to ~20% and ~30% respectively of 4R1N and 4R0N.

3.3. Discussion

3.3.1. Rationale behind the design of siRNAs targeting exon 10

An efficient design of siRNA oligos is a key factor in determining the efficiency of gene specific silencing (Murali R et al., 2015).

The siRNAs were designed spanning the entire region of exon 10 following certain first generation tools such as Amarzguioui method, Tuschl rules, Reynolds rules, Stockholm rules, Ui-Tei rules and Hseih rules.

Additionally certain second generation tools such as Biopredsi, DSIR, i-Score scales and My siRNA-designer were referred for possible predictions of suitable siRNAs to mediate knockdown of transcripts containing exon 10.

The following conditions were applied as a priority for the design (Ui-Tei et al., 2004):

(i) A/U at the 5' end of the antisense strand; (ii) G/C at the 5' end of the sense strand (iii) at least five A/U residues in the 5' terminal of of the antisense strands and (iv) absence of any GC stretch of more than 9 nt in length.

3.3.2. Mutant plasmid containing the N279 mutation in exon 10 was created

Alternative splicing has emerged as a promising therapeutic target in a number of human disorders. However, the discovery of compounds that target splicing has been hindered by the lack of suitable high-throughput screening assays.

This is also applicable for availability of model systems to test transcriptional gene silencing.

Previous work by Stoilov P et al (2008) has shown that the splicing of a two-color (Green/Red) fluorescent reporter plasmid with microtubule-associated protein tau (MAPT) exon 10 can be modulated using bioactive compounds.

A mutation (N279) has been introduced in this dual reporter plasmid which switches alternative splicing thus favoring the inclusion of Exon 10, in order to mimic the pathological alteration frequently observed in Fronto temporal dementia and Parkinsonism linked to chromosome 17 (FTDP-17). Further to this

135

an image-based analysis has been developed to quantify the fluorescent reporters, obtaining single cell-based read-outs using an High Content Screening system.

The content of exon 10 increases from ~35% in WT to ~85% in mutant reporter plasmid, these studies were further confirmed using the image based analysis snd RT-PCR

3.3.3. siRNAs targeting exon 10 mediates post-transcriptional gene silencing in a minigene context

The mutant plasmid thus created was co-transfected in SH-SY5Y cells along with potential siRNAs intended to induce transcriptional gene silencing.
The screening assays were performed with six different siRNAs and a non specific control wherein, three potential siRNAs were shown to induce degradation of transcripts containing exon 10.

Although there was a dose dependent effect of siRNAs 1, 3 and 5, concentrations of 50 nM and 100 nM induced degradation of transcripts containing exon 10.

Experiments with mutant plasmid (containing 60% of exon 10) of **0.25 µg** concentration, suggests that siRNA 3 posed the maximum effect with a reduction of exon 10 containing transcript reaching to ~30% followed by siRNA 5 with ~35% and siRNA 1 that induced a reduction reaching to ~40%.

Experiments with mutant plasmid of **0.5 µg** concentration (containing 60% of exon 10) suggests that siRNA 3 posed the maximum effect on the transcript with a reduction to ~15% followed by siRNA 5 with ~25% and siRNA 1 that led to ~30%.
These data suggest that there is a difference in equilibrium between the amounts of plasmid and siRNA molecules that plays an important role in determining level of silencing of gene expression and the amount of transfection reagent used as it depends upon the plasmid concentration.

However siRNA 3 seems to work the best in both conditions indicating that design of siRNAs and specific location on their target sequences do play an important role in silencing.

Cells transfected with 0.25 μg of mutant plasmid along with varied concentrations of each siRNA were further subjected to RT-PCR analysis. According to the image based analysis, a concentration of 50 nM was adequate to trigger gene silencing with all the three siRNAs 1, 3 and 5.

RT-PCR analysis confirms that siRNA 1 is able to degrade the transcripts containing exon 10 by 10% at a concentration of 50 nM, whereas siRNA 3 led to a reduction of 25% of exon 10 containing transcripts and siRNA 5 led to a 20% reduction when a concentration of 50nM was used.

These data further supports and confirms the effects observed through the image based analysis.

3.3.4. siRNAs targeting exon 10 mediates post-transcriptional gene silencing in an endogenous context

NSC-34 cells were found to have an 80% inclusion of exon 10 versus its 20% counterpart without exon 10. These cells were chosen to test the efficacy of the potential siRNAs. According to the image based analysis and RT-PCR analysis, a concentration of 50 nM was adequate to trigger gene silencing with all the three siRNAs 1, 3 and 5. However, an increasing dose of siRNAs were tested on this cell line from a starting concentration of 10nM reaching up to 100 nM.

The semi-quantitative RT-PCR analysis confirmed the potential effect of the three siRNAs on exon 10 transcripts in endogenous condition such that a maximum reduction of observed in each case was as follows: siRNA 1 induced a reduction of 10%, siRNA 3 induced a reduction of 45% and siRNA 5 led to a 40% reduction.

Thus, suggesting that all three siRNAs have a role in inducing silencing of exon 10 expression and the trend of their efficiency is similar (ie: siRNA 3>5>1) to the observations made in the minigene through both methods; image based analysis

and semi qRT-PCR. Further to this, preliminary data on the western blot indicates that all the three siRNAs have an efficient potent to downregulate exon 10 containing isoforms, however these preliminary data will need to be validated with the further experiments.

3.3.5. Molecular mechanisms at the basis of siRNA mediated post-transcriptional gene silencing

This work suggests that a meticulous and optimal designing of siRNA is an imperative step to attain best target hits. With such a rationale, we have obtained three out of six siRNAs that show efficiency in degradation of transcript containing exon 10.

Out of the three siRNAs (1, 3 and 5), siRNA 3 shows maximum efficiency. These results have been validated using a minigene recapitulating splicing mutation N279, in the SH-SY5Y (neuroblastoma cell line) system and a similar effect is exhibited on the endogenous context of NSC-34 (Hybrid of mouse spinal cord motor neurons and neuroblastoma cell line) cells.

Although three potential siRNAs have now been discovered to mediate transcriptional gene silencing in the context of exon 10, the following intriguing questions have risen:

- Why are only three siRNAs effective and what prevents the action of other siRNAs?
- Why are two other siRNAs 0 and 2 causing an increased inclusion of exon 10?
- Is a reduction of ~30% of exon 10+ adequate to restore splice defects in FTDP-17?

To address the first question, many studies have shown that although possible siRNAs can be designed against a particular target, only a fraction of them are able to induce degradation. Moreover, all siRNAs do not result in equal knockdown effects (Murali R et al., 2015).

Though we have referred to different tools to optimize an efficient designing strategy, since these tools use different features and weights in their model design (Murali R et al., 2015) the best hits are still biased.

However, additionally another prospect could be rendered to an alteration in the secondary structure of these transcripts that may not be available for binding of siRNAs 0, 2 and 4, thus preventing degradation of transcripts containing exon 10.

Additionally, proteins involved in post transcriptional regulation could be bound to the transcript containing exon 10 and inhibit binding of siRNAs 0, 1 and 2.

To this end, the Splice Aid database was referred to identify known splicing factors (proteins) bound to exon 10 (Fig.3.3.5). Although the siRNAs are known to pose an effect in the cytoplasm, knowledge of known proteins involved in the splicing of exon 10 enables identification of several of these proteins which may shuttle between nucleus and cytoplasm. These shuttling proteins still being bound to exon 10, could block specific sites targeted by siRNAs 0, 2 and 4.
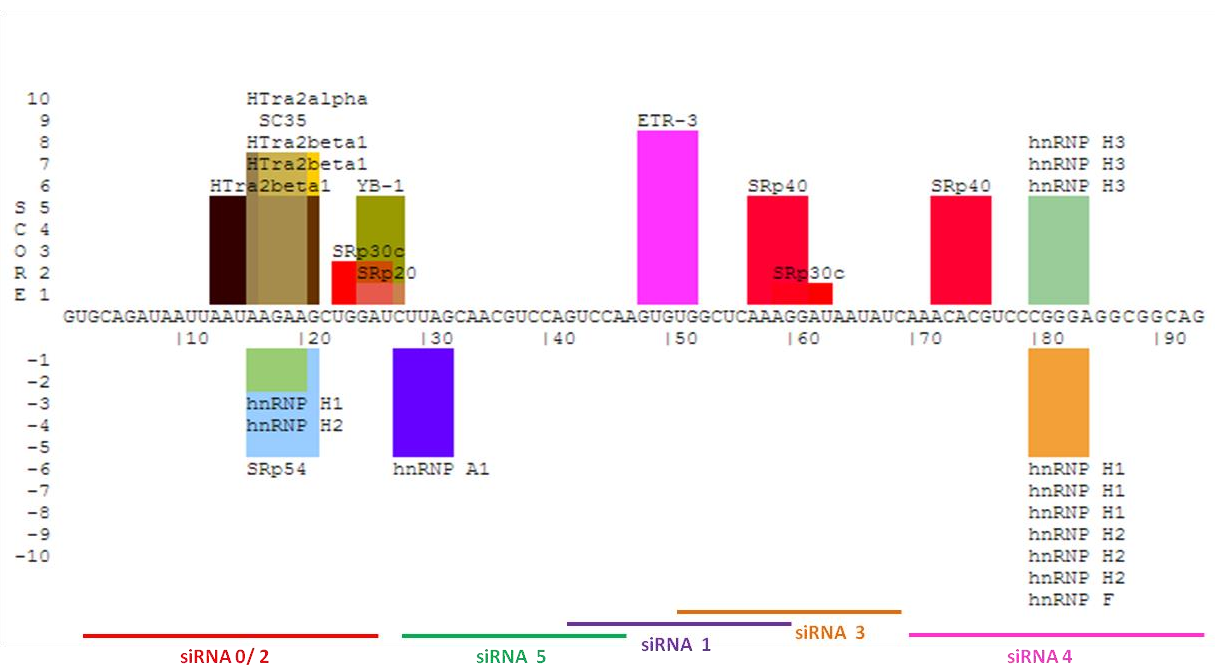
Fig.3.19 | Splice aid database highlighting the binding of splicing factors to the pre-mRNA of exon 10.(This database is constructed based on experimentally validated results) and the target sites for siRNAs 0, 1, 2, 3,4 and 5.

In **Fig.3.19** it can be observed that in the pre-mRNA of exon 10, these targets are bound by various proteins such as HTra 2 (alpha and beta 1), SC35, SRp (20, 30, 40, 54) ETR-3 and hnRNP (H1, H2 and H3). Although these proteins are mainly involved in regulation of splicing, they also have an active role in transport, stability, editing and translation of mRNA (Tacke R et al., 1998, Chaudhury et al., 2010, Twyffels et al., 2011).

A possible elucidation for the mechanism through which siRNAs 0 and 2 produced an increase in the levels of exon 10 could be supported by the studies of Jackson and colleagues. They have demonstrated that siRNAs could implicate silencing of non-targeted genes even if they have a similarity of only eleven nucleotides (Jackson AL et al., 2003). However, this is a limitation as BLAST searches close to 80% to 100% are considered to eliminate off-target effects in this study.

Thus, the genes (with partial sequence similarity) may have an essential role in splicing and could be silencers of exon 10 and be silenced by the siRNAs. Therefore, upon down-regulation of these silencers, there is an enhanced exon 10 expression. This possible hypothesis is further supported by the fact that a recent paper by Liu and colleagues have supported the activity of single stranded RNAi in nucleus where it has shown to modulate the splicing events of dystrophin gene (Liu J et al., 2015). Most of these hnRNPs are known to shuttle between the nucleus and cytoplasm. However ongoing studies are aimed at deciphering additional information such as their localization and function and these shuttling hnRNP proteins are known to define, at least in part, the nuclear history of individual mRNAs and thereby influence their cytoplasmic fate.

Therefore, it could be possible that hnRNP H1 and H2 travel along with the mRNA (containing exon 10) from nucleus to the cytoplasm and inhibiting binding of siRNAs 0, 2 and 4 all of which target the sites that are bound by these two proteins.

To address the second question, on the efficiency of transcript degradation, a simulation of the effect of the siRNA 3 on the diseased state is proposed to restore the altered ratios of 4R and 3R to its normal state **(Fig.3.20)**.

Normal Human

	E10+	E10-
Allele 1	25%	25%
Allele 2	25%	25%
Total	50%	50%

Diseased Human (E10+ = 1.8 times)

	E10+	E10-
Allele 1 (WT)	25%	25%
Allele 2 (Mut)	40%	10%
Total	65%	35%

Diseased Human + siRNA (30% efficiency) (E10+ = 1.2 times)

	E10+	E10-
Allele 1 (WT)	17.5%	25%
Allele 2 (Mut)	28%	10%
Total	45.5%	35%

Ratio of 4R:3R

Normal human 1:1

Diseased patient ~2 :1

siRNA (30% efficiency) ~1:1

Fig.3.20 | A simulation model for the effect of siRNA 3 on patient with FTDP-17

Since FTDP-17 is characterized by the altered ratio of the two isoforms, it is essential to maintain the balance between the two isoforms by enabling gene specific silencing such that the final product is in a ratio of 1:1. A complete degradation of transcript containing exon 10 would shift the ratio between the two isoforms, (4R and 3R) in such a way to possess higher amounts of 3R, a characteristic feature of Pick's disease state.

Therefore, a reduction by 30% is adequate to restore the balance between isoforms to ~1:1.

Hence the proposed work opens a novel therapeutic strategy aimed to correct splice defects in exon 10 of MAPT, especially on those inducing formation of excessive 4R isoforms, thus addressing a subtype of FTDP disease.

3.3.6. Two efficient systems to validate the functional effects of siRNAs have been established

In order to validate the functional effects of the siRNAs on inducing isoform specific target degradation, it is vital to establish an optimized method to observe all possible isoforms in the cells.

Since literature evidences have shown that the six isoforms of tau being very close in size are highly inseparable. This poses a challenge to observe modulations in the isoforms after treatment with siRNAs.

Moreover, human neuroblastoma cells have a higher expression of the 3R isoforms compared to its 4R counterpart. This trend has been observed both in the RNA levels and protein levels, thus limiting its utility in the context of this study. Therefore, considering that NSC-34 cells express higher amount of 4R compared to its 3R counterpart, in its RNA forms, this cell line was chosen as the best model system to study the effect of siRNAs in the tau proteins.

To this end, western blot analysis was optimized after repetitive applications of different experimental conditions. As a result, a well established protocol has been developed and four of the existing isoforms of SHSY5Y and NSC-34 cells can be visualized through the western blot.

The results indicate that four isoforms of tau protein can be clearly visualized in the western blot. The four isoforms are namely, 4R1N, 3R1N, 4R0N, and 3R0N. The SH-SY5Y cells predominantly expressed the 3R isoforms whereas the NSC-34 cells predominantly expressed the 4R isoforms. These results indicate the suitability of this model system to validate effects of potential siRNAs.

CHAPTER 4. Role of long non-coding RNAs in regulation of MAPT

Abstract*

The MAPT gene is known to play an important role in the broad class of neurodegenerative disorders called the tauopathies, that are characterized by the presence of abnormal fibrillar aggregates of tau protein in the affected brain. Furthermore, mutations in MAPT cause familiar frontotemporal dementia (FTLD), and common polymorphisms in MAPT (in the form of the non-inverted H1 haplotype) leads to a significant increased risk of the sporadic tauopathies, progressive supranuclear palsy (PSP), corticobasal degeneration (CBD) and Parkinson's disease (PD) (Vandrovcova J, et al., 2010).

This project is focused role of non-coding RNAs (ncRNAs) that are specific to MAPT and their roles in regulation of transcription and splicing. Many protein coding genes, including MAPT, have overlapping antisense genes that code for non-coding transcripts (natural antisense transcripts, NATs). These transcripts are co-expressed with the overlapping protein-coding gene, with either negative or positive correlations in their transcriptional levels (Gustincich *et al.*, 2006; Katayama *et al.*, 2005).

In many cases the NATs have been shown to regulate the "host" gene by several possible processes including transcription initiation, epigenetic silencing, translation or stability (Magistri M et al., 2012).

The collaborators have identified two ncRNA genes that overlap with the MAPT promoter region. These genes are termed NAT1 and NAT2, and they overlap with the MAPT core promoter and 5'UTR and extend beyond the neighboring IMP5 gene. Preliminary studies have shown that these ncRNAs significantly modulate MAPT expression level.

Further to this, a possible role in regulation of splicing of exon 10 is currently being validated using the image-based analysis.

4.1. Materials and methods

SH-SY5Y cell lines that were stably expressing the NATs both wild-types and mutants were designed and produced by Dr.Roberto Simone and available prior to the set-up described below.

Sequence of NAT transcripts

Human-NT1
GCCCCAGUCUGCGGAGAGGGAGGGCGAGGGGCGGCGGCGCAGGGGUGCACAGAGGCGGACGGCGAGGC
AGAUUUCGGAGCCGCGGCGCUUACCUGAUAGUCGACAGAGGCGAGGACGGGAGAGGACAGCGGAGGAG
GAGAAGGUGGCUGUGGUGGCGGCGGCAGAAGGAGUCAGAACAAGGACGGGCCUGUGAUGUGUCUGUC
UAUGACGAGGAGGACAAUGUCCUAAGGAAUGGAGAGGAAGAAAGUGAAGGGAACCAGGUCCCUGGAU
UCCAUGUGGAACAGUAGCCCAGGAUGUGCACUAUGGACUGUUACAAGAGAGAGACAUGAUCUUCCUU
AAGGCAUUGAUUUGUCAUGAGUCUCUUUGUUAUAGCCACUUAACGUUACCUUAAUACACCCACUUCA
UGGAUAAGUAAAACUGAGGCUUGGAGAAGCCCACAUUGACACAGC

Human-NT 2

GCGGCCGCCGAGUCCGUCCACAUCGCCAGGCCAGGACCUUGGACAGGGCCCAGCACAGGGGCCCUGGAA
UGUGGACUGUCUCAGUGGAUUCUUGUUUAUAGGAAUUAGAGGAAGGUGGAAGAAGCUCAUUCCAGA
GUGCAAUCAAUAACAGUGGAAAGAAGUCCCUGGAGCCCAGUGCAGUGGCUUGAACUGAGAAUGCACU
CACUGGCUGUUGCAGCCAAGACUCCAGUUCUCGCCUCUCUUUCCCUGACUCCCCUGUGCCCACCUUUC
CCCUGCAGGAGUCAGAACAAGGACGGGCCUGUGAUGUGUCUGUCUAUGACGAGGAGGACAAUGUCCU
AAGGAAUGGAGAGGAAGAAAGUGAAGGGAACCAGGUCCCUGGAUUCCAUGUGGAACAGUAGCCCAGG
AUGUGCACUAUGGACUGUUACAAGAGAGAGACAUGAUCUUCCUUAAGGCAUUGAUUUGUCAUGAGUC
UCUUUGUUAUAGCCACUUAACGUUACCUUAAUACACCCACUUCAUGGAUAAGUAAAACUGA

4.1.1. Western blot analysis

For Western blot analysis, SH-SY5Y cells stably expressing the NATs were washed with PBS and harvested in radioimmunoprecipitation assay (RIPA) buffer (1% Nonidet P-40, 0.5% sodium deoxycholate, and 0.1% sodium dodecyl sulfate (SDS) in PBS) plus protease inhibitors (Complete, Roche Molecular Biochemicals, Indianapolis, IN, USA) and phosphatase inhibitors (New England Biolabs) at 4°C. Cell homogenates were centrifuged at 100,000 g for 30 min. Supernatants were collected, and the protein content was determined using a commercial kit (Bio-Rad, Hercules, CA, USA). Samples were separated on 4-12% gradient SDS gels and electrotransferred to polyvinylidene difluoride (PVDF) (Millipore, Bedford, MA, USA). Membranes were washed, blocked, and incubated overnight with rabbit anti-tau (1:10,000; Dako) antibody, followed by asecond washing step before incubating with secondary antibody (an Infra-red chromophore Goat anti-Rabbit 800 CW (Li-COR) for 1 h. For each sample, ß-actin was probed as a control using a mouse anti-beta actin antibody (Sigma) as primary antibody and a Donkey anti-Mouse 680 CW IRdye secondary antibody (Li-COR). The western blot bands were acquired using an Odyssey infrared scanner.

4.1.2. Bioinformatics predictions analysis

Multiple sequence alignments (MSA) were performed followed by the use of tools such as PET cofold and intaRNA to determine the RNA: RNA interactions between the non coding antisense transcripts and splice sites of exon 10.

4.1.2. Image-based analysis of fluorescence reporter plasmid

Refer to section 3.1.5

4.2. Results

4.2.1. Non-coding RNAs regulate expression of MAPT

Non-coding RNAs that were antisense to human MAPT gene were identified computationally and examined in the Ensembl browser (http://www.ensembl.org). They were termed as Non coding antisense transcripts (NATs).

The NAT1 and NAT2 were lncRNAs that were antisense to the MAPT promoter hence, their role in regulation of MAPT was examined by establishing stable cell lines expressing either the full length or isoforms containing deleted portions of specific domains of the two NATs.

The SH-SY5Y stable cell lines were established such that it pre-dominantly expressed the following versions:

1. Empty vector carrying the NAT sequences (V5)

2. Full length NAT transcripts (NT1) and (NT2)

3. Deletion constructs lacking the 5' first exon (NT1 **Δ3'**) and (NT2 **Δ3'**)

4. Deletion of the 3' domain (NT 1 **Δ5'**) and (NT 2 **Δ5'**)

5. An artificial construct containing the non-overlapping region (NT1 Non)

6. An artificial construct containing the overlapping sequence in NAT (NT 1 Over)

7. Constructs with the flipped version of the overlapping sequence in exon 1 (NT1 flip)
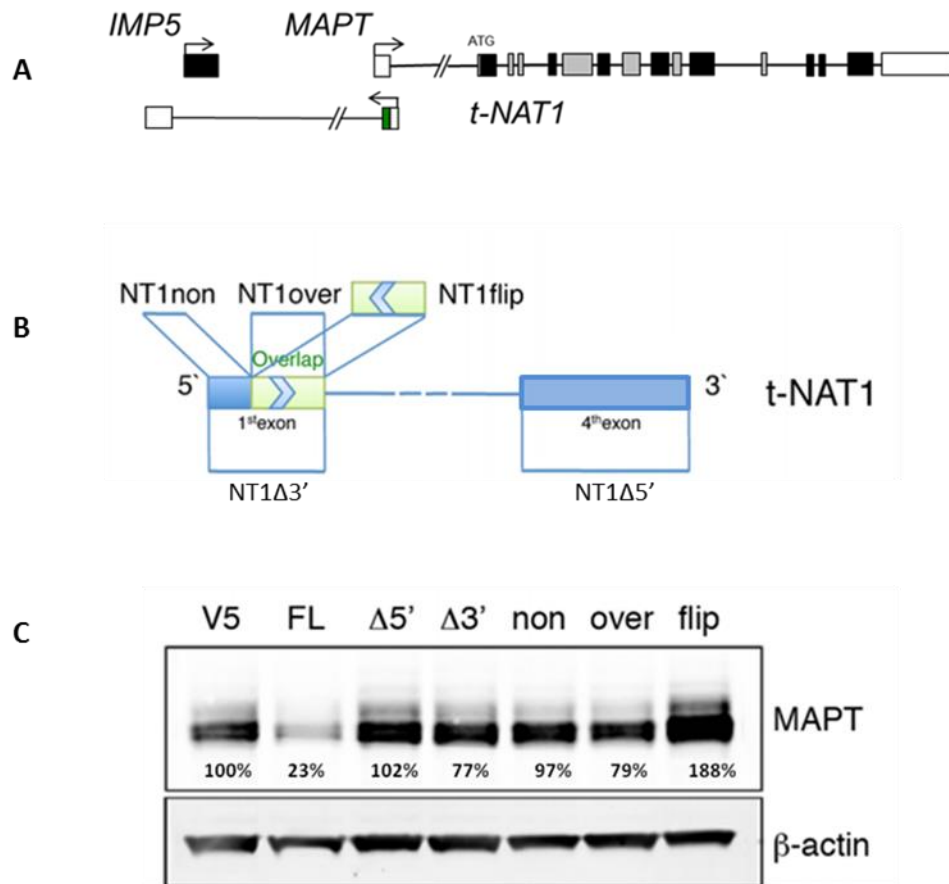
Fig. 4.1. Schematic representation of the **A)** Region of complementarity of MAPT and NAT1 **B)** different versions. of NAT 1 transcript **C)** Western blot analysis of tau in SH-SY5Y stable cell lines expressing varied forms of NAT1 transcripts.(These images were obtained in collaboration with Dr.Roberto Simone and Faiza Javad,University college London,UK).
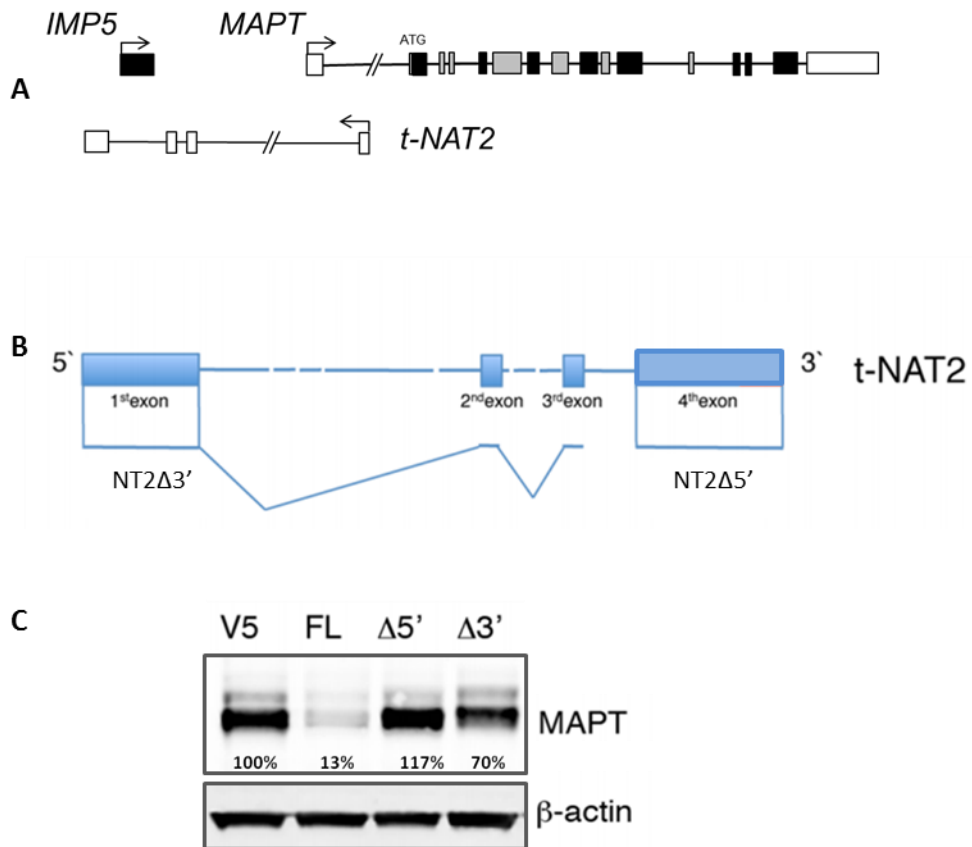
Fig. 4.2. A) Schematic representation of the **A)** Region of complementarity of MAPT and NAT2 **B)** different versions of NAT 2 transcript. **C)** Western blot analysis of tau in SH-SY5Y stable cell lines expressing varied forms of NAT2 transcripts. .(These images were obtained in collaboration with Dr.Roberto Simone and Faiza Javad,University college London,UK)

In stable cell lines expressing the NAT 1 trancripts, it can be observed that the full length NT1 induces reduction of tau protein to 23%. NT1 Δ5' and NT1 Non do not show any effect on tau protein. However, NT 1 Δ3' and NT1 over transcripts show a slight reduction to 77% and 79% respectively. On the contrary, NTflip shows an increase of tau protein levels to almost double times with 188%.

In stable cell lines expressing the NAT 2 transcripts, it can be observed that the full length NT2 induces reduction of tau protein to 13%. NT2 Δ5' does not show any effect on tau protein. However, NT 2 Δ3' shows a slight reduction to 70%.

4.2.2. Predictions reveal possible binding between splice junctions and NATs

The genomic tract spanning 147 bp upstream and 111 bp downstream of MAPT exon 10 (Exon 10 -147+111) was utilized for its homology with the NATs sequence. This region includes the splice junctions and the classical stem-loop. Bioinformatics predictions tool such as the PETcofold and inta-RNA were integrated to analyse the putative complementary regions.

Dr. Roberto Simone identified that the NT1 targets both the branch point region and the region immediately above an imperfect repeat domain (before the 3' ss) in exon 10.

Although discordance was observed in the predictions between PETcofold and inta RNA for the NAT1 transcripts, it was attributed to the possibility that PETcofold considers folding constraints using MSA, in contrast to intaRNA that does not rely on the former.

NT2 was able to target a second stem loop structure laying downstream the classical stem-loop structure at the 5' splice site.

Most of the complementary regions resided in exon 3 of the NT2 transcript.

Since the putative targets of the NATs resided on the splice site or branch point, it intrigued us to proceed further and analyze if this potential binding had an impact on splicing.

4.2.2. Effect of Non-coding RNAs in regulation of splice events
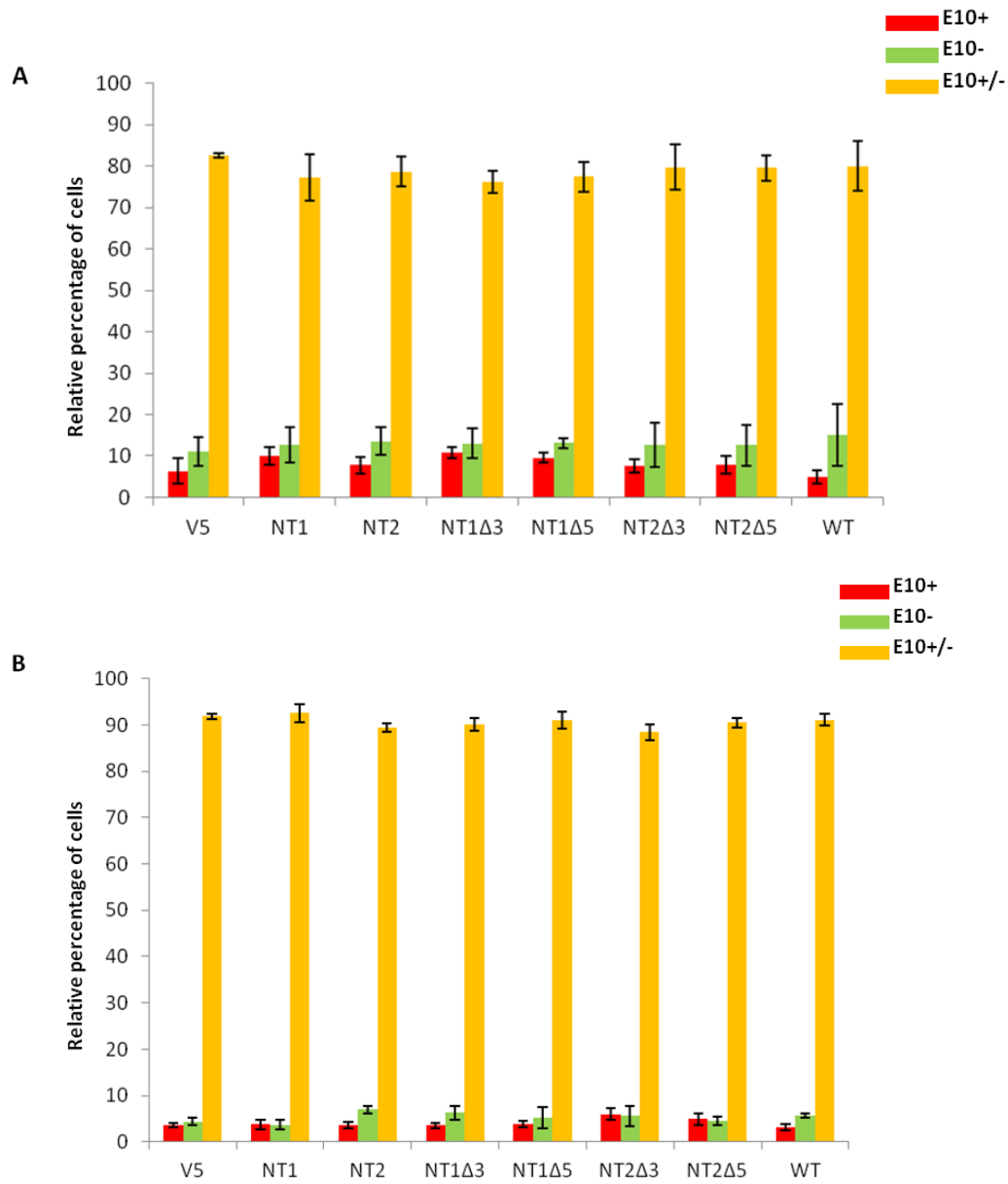
Fig.4.3. An image based screening assay has been performed on the wild type plasmid co-transfected with different concentrations of NATs (A) Wild type plasmid (0.5μg) and NATs (0.5 μg) (B) Wild type plasmid (0.5μg) and NATs (0.25 μg).

The image based analysis shows that cells treated with V5 expresses 6% of exon 10+,11% exon 10- and 83% of exon 10+/-.Treatments with the NATs plasmids shows the following trend when a ratio of 1:1 (WT:NATs) was used:

NT1= 10% of exon 10+, 13% exon 10- and 77% of exon 10+/-

NT2= 8% exon 10+, 14% of exon 10-and 78% of exon 10+/-

NT1Δ3= 11% exon 10+, 13% exon 10- and 76% exon 10+/-

NT1Δ5= 10% exon 10+, 13% exon 10- and 77% exon 10+/-

NT2Δ3= 7.5% exon 10+, 12.5% exon 10- and 80% exon 10+/-

NT2Δ5= 8% exon 10+, 12% exon 10- and 80% exon 10+/-

WT= 5% exon 10+, 15% exon 10- and 80% exon 10+/-

However, the following trend was observed upon treatment with NATs using a ratio of 2:1 (WT: NATs):

NT1= 3.5% of exon 10+, 4.5% exon 10- and 92% of exon 10+/-

NT2= 4% exon 10+, 4% of exon 10-and 92% of exon 10+/-

NT1Δ3= 3.5% exon 10+, 7% exon 10- and 89.5% exon 10+/-

NT1Δ5= 4% exon 10+, 5% exon 10- and 91% exon 10+/-

NT2Δ3= 6% exon 10+, 5% exon 10- and 89% exon 10+/-

NT2Δ5= 5% exon 10+, 4.5% exon 10- and 90% exon 10+/-

WT= 3% exon 10+, 6% exon 10- and 91% exon 10+/-
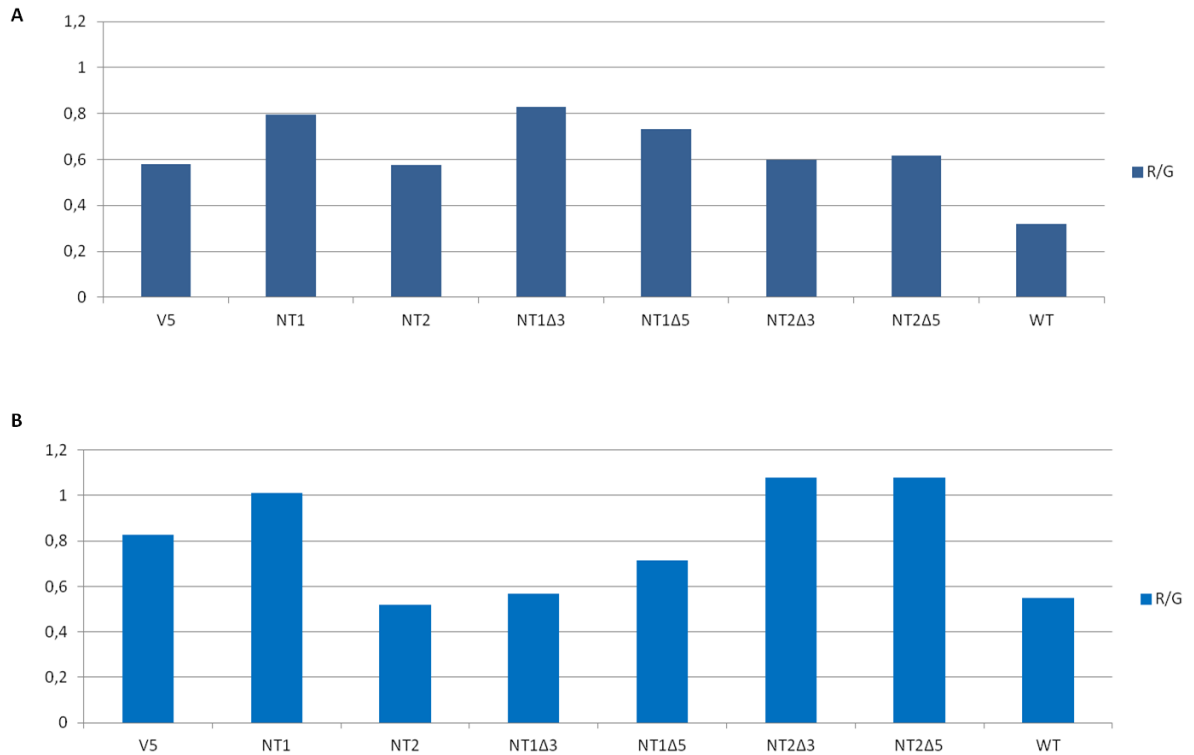
Fig. 4.4. R/G values expressing the ratio between the red cells over the green cells in (A) Wild type plasmid (0.5μg) and NATs (0.5 μg) (B) Wild type plasmid (0.5μg) and NATs (0.25 μg).

Relative expression levels of Exon 10+ and Exon 10-were calculated using the using the below mentioned formula:

$$R/G = \frac{\% \text{ of red cells}}{\% \text{ of green cells}}$$

This calculation enables an easy output to determine the type of transcript (i.e: exon 10+ or exon 10-) that undergoes a differential expression pattern upon treatment with NATs.

This ratio indicates the relative amounts of exon 10 containing cells in the total population of cells transfected with the wild type plasmid and corresponding NATs.

Treatment condition 1 (1:1 ratio of WT plasmid and NATs):

It can be observed that the R/G ratio is ~0.6 times upon treatment with the V5 which serves as a control to monitor effects upon subsequent treatment with NATs.

Upon treatment with NT1, there is an effect on exon 10 inclusion as the ratio increases to 0.8 times.

NT2 poses no effect in this condition. However, NT1Δ3' and NT1Δ5' indicate an increase of this ratio to upto 0.8 and 0.7 times respectively.

Similar to the trend observed in NT2, there is no effect upon treatment with NT2Δ3 and NT2Δ5.

However, the cells treated with only WT plasmid shows only 0.3 times exon 10.

Treatment condition 2 (2:1 ratio of WT plasmid and NATs):

The basal expression level of exon 10 upon treatment with V5 shows a ratio of 0.8 times. Upon treatment with NT1, this ratio increases to upto 1 time. Treatment with NT2 and NT1Δ3 showed a reduction of the ratio reaching up to 0.5 and 0.55 times respectively. NT1Δ5 showed no change. NT2Δ3 and NT2Δ5 showed an increase of exon 10 inclusion.

4.3. Discussion

"Nature is the source of all true knowledge. She has her own logic, her own laws, she has no effect without cause nor invention without necessity".

-Leonardo da Vinci

4.3.1. Non-coding RNAs decreases expression of MAPT protein

The Non-coding antisense transcripts (NATs) implicates a regulatory function on tau protein by mediating its expression **(Fig. 4.1 and 4.2).**

The full length transcript (NT1 FL) is shown to have a strong effect of reduction on tau protein levels. Transcripts with deletion of the first exon at the 5' end (NT1 Δ5') is unable to reduce the levels of tau protein, indicating that this domain plays an important in imposing a strong downregulation of tau. Transcripts containing only the non overlapping region (NT1 Non) also has no effect on tau indicating that this region is not a crucial player in eliciting the effect on decrease of tau protein.

However, transcripts containing deletion of the 5' domain (NT 1 Δ3') shows a slight reduction of tau protein level indicating that this region (although not complementary to the tau region mRNA) is particularly essential for the NT1 to regulate its mode of action on tau.

Transcripts containing only the overlapping region is able to induce reduction of tau but not as efficient as the full length.

On the contrary, the transcript containing the flipped version of the overlapping region (NT flip) shows an increased production of tau proteins by almost double times reaching upto 188%.

This data suggests that a domain in the first exon is crucial for the reduction of tau levels however, it is not adequate to impose the effect and its regulation is dependent on the critical sequences available on the last three exons **(Fig. 4.1)**.

In stable cell lines expressing the NAT 2 trancripts, it can be observed that the full length NT2 induces reduction of tau protein to 13%. NT1 Δ5' do not show

any effect on tau protein. However, NT 1 Δ3' shows a slight reduction to 70% (Fig.4.2).

The full length transcript (NT2 FL) is shown to have a strong effect of reduction on tau protein levels. Transcripts with deletion of the first exon at the 5' end (NT2 Δ5') is unable to reduce the levels of tau protein, indicating that this domain plays an important in imposing a strong down-regulation of tau.

However, transcripts containing deletion of the 5' domain (NT 2 Δ3') shows a slight reduction of tau protein level indicating that this region (although not complementary to the tau region mRNA)is particularly essential for the NT2 to regulate its mode of action on tau.

This data suggests that although the overlapping region confers the specificity of these NATs to regulate MAPT and the domain in the first exon is crucial for the reduction of tau levels, however, it is not adequate to impose the translational repression. Thus, suggesting that a functional element mediating the regulation of NATs is governed by other critical sequence elements.

4.3.2. Non coding RNAs may pose an effect on splicing of Exon 10

The non coding natural antisense transcripts (NATs) were expected to influence splicing based on their putative binding predictions on exon 10.

To confirm the bioinformatics prediction, a screening assay was carried out using the WT plasmid reported in section 3.1.2 to co-transfect with the NATs plasmids **(Fig.4.3)**.

Based on the preliminary observations on the R/G ratio **(Fig.4.4),** it can be seen that when the plasmid and NATs are present in equal amounts in the cell (1:1 ratio (or) 0.5μg:0.5μg), NT1, NT 1 Δ3' and NT 1 Δ5'increases the inclusion of exon 10 reaching up-to 0.8 times compared to the basal expression of 0.6 times. No effects were observed upon treatment with NT2, NT 2 Δ3' and NT 2 Δ5'.

Upon increasing the amounts of WT plasmid to a reach a ratio of 2:1,it can be observed that the NT1 still seems to increase exon 10 but the NT2, NT 1 Δ3' and NT 1 Δ5' poses an exon skipping effect by decreasing the exon 10 content. NT 2 Δ3' and NT 2 Δ5' poses effects similar to NT1 and enhance inclusion of exon 10.

In both cases, the content of exon 10+ is slightly increased in the cells treated with empty vector compared to the cells treated with only WT plasmid indicating an artefact or non specific effect exhibited by the plasmid backbone.

From these results, it is quite evident that NATs exhibit an effect on splicing of exon 10. NAT1 has implicated exon 10 inclusion regardless of the treatment conditions. NT1Δ3' and NT1Δ5' have been shown to impose similar effects when the ratio of WT plasmid and NATs is 1:1. However, they lose this tendency and begin to induce skipping of exon 10 when used in a ratio of 2:1 (WT: NATs).

NT2, NT2Δ3' and NT2Δ5' poses no effect in a ratio of 1:1.But, in a ratio of 2:1, NT2 induces exon skipping and NT2Δ3' and NT2Δ5' increase exon 10 inclusion.

Interestingly, the full length transcript, NT1 has always shown an inclusion of exon 10 regardless of the different ratios used in the study, indicating a strong relevance of this NAT in regulation of splicing.

Although lncRNAs can exhibit its role on transcriptional regulation and could work either in *cis* (when the effect is restricted to chromosome from which they are transcribed) or *trans* (effect is extended to other chromosomes) to negatively or positively control gene expression.

Here we show that the NATs which overlap with the sense strand of promoter region of MAPT is able to regulate expression of MAPT at post transcriptional level.

Additionally our preliminary data suggests that NT1 could impose an auxiliary role in splicing of exon 10 in which it aids exon 10 inclusion and NT2 induces exon skipping when there is double the amounts of WT plasmid. These observations also imply that a stoichiometric balance between the pre-mRNA and NATs could influence their mode of action.

Evidences in literature support the notion on NATs being involved in modulation of alternative splicing patterns of their overlapping genes (Krystal et al., 1990, Munroe et al., 1991, Yan et al., 2005).

The mechanism through which the effect of NT 1 and NT 2 is observed needs further investigation. However, possible processes include binding of NT1 to spliceosome machinery wherein it imparts its effect through blocking access of spliceosome to the pre-mRNA of exon 10 thus facilitating its inclusion. NT2 on the other hand could be directly involved by base-pairing with the exon 10 region leading to its skipping.

Chapter 5. Conclusions and Future perspectives

"If we examine the accomplishments of man in his most advanced endeavors, in theory and in practice, we find that the cell has done all this long before him, with greater resourcefulness and much greater efficiency".

— Albert Claude

Nobel Lecture, The Coming Age of the Cell, 12 Dec 1974

The U1 and U7 scramble constructs were successfully produced and all the available versions of the constructs were tested on PC12 cells. The drawback of low transfection efficiency was solved by employing a suitable transfection method known as electroporation.

However, these constructs were not able to induce exon 10 skipping in PC12 cells. To this end, with the utilization of available literature studies it is hypothesized that PC12 cell line may not be an appropriate model to validate effects of these constructs due to the presence of double stem loop structure which can alter the secondary structure of exon 10 (Yamashita *et al.*, 2005) and hinder the binding of U1 and U7 snRNA.

Further work should be focused on employing a suitable cell model that recapitulates FTDP-17. Since previous studies on exon skipping have validated the use of modified chimeric small nuclear RNAs to treat mice with DMD, NSC-34 cell line being a mouse cell line can be used as an alternative model to test the efficacy of these U1 and U7 constructs targeting exon 10. The underlying reasons being; (i) The presence of exon 10 has been validated in this system (as a part of the project 2) and recapitulates the diseased state and (ii) this cell line originates from mouse cells serving as an optimal choice before beginning the studies in the N279 mouse model.

In addition, analysis by Real time PCR would be an advantage to monitor slight variations upon exon 10 skipping.

In order to approach the same question from a different perspective, Post transcriptional gene silencing was employed using an siRNA based approach. As a result, six different siRNAs were designed, a plasmid reporter recapitulating FTDP-17 was created. A novel method was developed to screen the effects

observed upon treatment with siRNAs and suitable model systems were identified to validate the effects of these siRNAs on an endogenous condition. Three out of six siRNAs have been implicated to impose a therapeutic effect. Out of which one, siRNA 3 has shown the best effect of reduction of ~30% of exon 10+ transcripts.

Currently, primary cortical neurons are being analysed for the effect of siRNAs on the endogenous state. Western blot protocol has been optimised for the NSC-34 cell line, therefore, effectof siRNAs at protein level will be monitored using western blot approaches in this model and the primary cortical neurons.

The N279 mutation under this study has been shown to pose an implication only in the RNA level in which the mutation leads to an aberrant splicing thus forming excessive exon 10 containing transcripts. However it does not impose an effect on the protein level as the microtubule binding assays have revealed no alterations in the microtubule binding (Hasegawa *et al.*, 1999). There is no evidence that the missense substitution is toxic or poses a dominant effect. Although this siRNA was tested in the context of N279 mutation, this approach is also applicable to other similar mutations such as the S305N whose primary effects are at the RNA level. Future application would be directed towards employment of these siRNAs in the N279 mouse model.

The N279 mouse model developed by Dawson and colleagues (Dawson *et al.*, 2007) has been able to recapitulate several of the FTDP-17 disease hallmarks hence will serve as a suitable animal model to begin the clinical trials in vivo.

A recent review by Rettig and colleagues have summarized the possible delivery approaches of the siRNA molecules and their success in clinical trials (Rettig *et al* 2012).The current development in the field and ongoing studies establishes the significance of these synthetic siRNAs, which may serve as potential therapeutics upon suitable delivery and administration.

Direct CNS (Central nervous system) administration is used as a method of choice in neurodegenerative diseases due to restricted entry across the blood brain barrier. Options of delivery include intrathecal, intraventricular, epidural

and direct intratissue injection. Administration methods include long term infusions or through the use of mini pumps (Rettig *et al.,* 2012).

Chronic intraventricular pumps were used for the delivery of siRNAs against Amyloid precursor protein gene (*App*) to study Alzheimers related functions in adult mice. Efficient knockdowns were observed through potent siRNAs (Senechal, Y *et al.*, 2007).

By employing naked and unassisted delivery of siRNAs in buffered saline, chronic infusion was performed in non-human primates to suppress levels of α synucein. This protein is known to be associated with Parkinson's disease. Mini osmotic pumps were used for the direct infusion into the substantial niagra leading to a decrease in α-synucein both at mRNA and protein levels (McCormack *et al.*, 2010).

siRNAs with modified PS linkages and 2'F-pyrimidine residues near the ends of each strand were used for chronic infusion in to the CNS of SOD1(G93A) mouse model of amyotrophic lateral sclerosis (ALS). Significant reduction of sod1 mRNA was observed in the spinal cord. In the transgenic mouse model, an infusion over a 28 day period led to alleviated the progression of disease. The siRNAs were stable over the course of this period.

Cholestrol conjugated siRNAs were used for the direct intrastriatal injection to target mutant Huntingtin gene (*Htt*) in the context of Huntington's disease.

The above mentioned strategies highlight the different modes of delivery of siRNAs and demonstrate efficacy *in vivo*, suggesting the promising future for the siRNAs developed in this work.

As a part of collaborative project, the role of long non coding RNAs in regulation of MAPT gene have been deciphered for the first time. An additional implication in splicing of exon 10 is currently under investigation.

Transcription is pervasive throughout the eukaryotic genome giving rise to many functional ncRNAs with key roles.Although the numerous functions of lncRNAs is becoming increasingly evident, only a few of them have been fully characterised. The effect of ncRNAs in increasing the stability of BACE1 mRNA involved in AD

conditions have been recently studied thus emphasising their inevitable and predominant roles in regulation of gene expression.

Therefore identifying the mechanisms through which the regulation is employed will be the most fundamental strategy to understand their roles. Since NT1 and NT2 have been shown to regulate MAPT expression at protein levels, they can serve as therapeutic molecules for AD pathology with increased tau protein levels.

BIBLIOGRAPHY

Abdelgany, A., Wood, M., Beeson, D., 2003. Allele-specific silencing of a pathogenic mutant acetylcholine receptor subunit by RNA interference. Hum. Mol. Genet. 12, 2637–44. doi:10.1093/hmg/ddg280

Amaral, P.P., Dinger, M.E., Mercer, T.R., Mattick, J.S., n.d. as an RNA Machine 26–29.

Amaral, P.P., Mattick, J.S., 2008. Noncoding RNA in development. Mamm. Genome 19, 454–92. doi:10.1007/s00335-008-9136-7

Avila, S., Lucas, J., Pe, M.A.R., Biologı, C. De, Pé, M., 2004. Role of Tau Protein in Both Physiological and Pathological Conditions 361–384.

Baker, M., Kwok, J.B.J., Kucera, S., Crook, R., Farrer, M., Houlden, H., Isaacs, A., Lincoln, S., Onstead, L., Hardy, J., Wittenber, L., Dodd, P., Webb, S., Hayward, N., Tannenberg, T., Schofield, P., Dark, F., 1997. Localization of Frontotemporal Dementia with Parkinsonism in an Australian Kindred to Chromosome 17q2 1-22 794–798.

Barabino, SM, Blencowe, BJ, Ryder, U, Sproat, BS, Lamond, AI., 1990. Targeted snRNP depletion reveals an additional role for mammalian U1 snRNP in spliceosome assembly. Cell 63(2):293-302.

Baralle, D., Baralle, M., 2005a. Splicing in action: assessing disease causing sequence changes. J. Med. Genet. 42, 737–48. doi:10.1136/jmg.2004.029538

Baralle M, Baralle FE. 2008 Genetics and molecular biology: variations in alternative spliced pre-mRNA-protein isoforms and their role in disease. Curr Opin Lipidol. 19(4): 429-30. doi: 10.1097/MOL.0b013e328306f0b8.

Barash, Y., Calarco, J.A., Gao, W., Pan, Q., Wang, X., Shai, O., Blencowe, B.J., Frey, B.J., 2010. Deciphering the splicing code. Nature 465, 53–59. doi:10.1038/nature09000

Barbara, S., 1994. Identification of a Novel Microtubule Binding and Assembly Domain in the Developmentally Regulated Inter-repeat Region of Tau 124, 769–782.

Beaudoing, E., Freier, S., Wyatt, J.R., Claverie, J., Gautheret, D., 2000. Patterns of Variant Polyadenylation Signal Usage in Human Genes 1001–1010.

Beelman, C.A., Parker, R., 1995. Degradation of mRNA in Eukaryotes Review 179–183.

Bertram, L., Tanzi, R.E., 2005. Review series The genetic epidemiology of neurodegenerative disease 115, 1449–1457. doi:10.1172/JCI24761.The

Beyer, AL, Christensen, ME, Walker, BW, LeStourgeon, WM., 1977. Identification and characterization of the packaging proteins of core 40S hnRNP particles. Cell. 11(1):127-38.

Bird, TD, Wijsman, EM, Nochlin, D, Leehey, M, Sumi, SM, Payami, H, Poorkaj, P, Nemens, E, Rafkind, M, Schellenberg, GD.1997. Chromosome 17 and hereditary dementia: linkage studies in three non-Alzheimer families and kindreds with late-onset FAD. Neurology. 48(4):949-54.

Black, DL, Steitz, JA., 1986 Pre-mRNA splicing in vitro requires intact U4/U6 small nuclear ribonucleoprotein. Cell. 1986 Aug 29;46(5):697-704.

Bond, A.M., Vangompel, M.J.W., Sametsky, E. a, Clark, M.F., Savage, J.C., Disterhoft, J.F., Kohtz, J.D., 2009. Balanced gene regulation by an embryonic brain ncRNA is critical for adult hippocampal GABA circuitry. Nat. Neurosci. 12, 1020–7. doi:10.1038/nn.2371

Bradley, T., Cook, M.E., Blanchette, M., 2014. SR proteins control a complex network of RNA-processing events 75–92. doi:10.1261/rna.043893.113.

Brun, C, Suter, D, Pauli, C, Dunant, P, Lochmüller, H, Burgunder, JM, Schümperli, D, Weis, J., 2003. U7 snRNAs induce correction of mutated dystrophin pre-mRNA by exon skipping. Cell Mol Life Sci. 60(3):557-66.

Buratti, E., Baralle, D., 2014. Novel roles of U1 snRNP in alternative splicing regulation. RNA Biol. 7, 412–419. doi:10.4161/rna.7.4.12153

Burright, E.N., Clark, H.B., Servadio, A., Matilla, I.I.T., Duvick, L.A., Zoghbi, H.Y., 1995. SCA1 Transgenic Mice: A Model for Neurodegeneration Caused by an Expanded CAG Trinucleotide Repeat 82, 937–948.

Cartegni, L., Chew, S.L., Krainer, A.R., 2002. Listening to silence and understanding nonsense: exonic mutations that affect splicing. Nat. Rev. Genet. 3, 285–98. doi:10.1038/nrg775

Carter, J.E., Schuchman, E.H., Gene, C., Apy, T., n.d. Gene therapy for neurodegenerative diseases : fact or fiction ? 392–395.

Chapman, E.J., Carrington, J.C., 2007. Specialization and evolution of endogenous small RNA pathways. Nat. Rev. Genet. 8, 884–96. doi:10.1038/nrg2179

Chaudhury, A., Chander, P., Howe, P.H., 2010. Heterogeneous nuclear ribonucleoproteins (hnRNPs) in cellular processes : Focus on hnRNP E1 ' s multifunctional regulatory roles 1449–1462. doi:10.1261/rna.2254110.groups

Chemicals, R., 1998. letters to nature 391, 806–811.

Clancy, B.S., Education, P.D.N., 2008. RNA Splicing : Introns , Exons and Spliceosome 1.

Contribution, O., 2005. Frontotemporal Lobar Degeneration 62.

Cooper, T. a, Wan, L., Dreyfuss, G., 2009. RNA and disease. Cell 136, 777–93. doi:10.1016/j.cell.2009.02.011

Courtney, E., Kornfeld, S., Janitz, K., Janitz, M., 2010. Transcriptome profiling in neurodegenerative disease. J. Neurosci. Methods 193, 189–202. doi:10.1016/j.jneumeth.2010.08.018

Covello G, Siva K, Adami V, Denti MA. 2014 An electroporation protocol for efficient DNA transfection in PC12 cells. Cytotechnology. 66(4):543-53. doi: 10.1007/s10616-013-9608-9.

D'Souza, I., Poorkaj, P., Hong, M., Nochlin, D., Lee, V.M., Bird, T.D., Schellenberg, G.D., 1999. Missense and silent tau gene mutations cause frontotemporal dementia with parkinsonism-chromosome 17 type, by affecting multiple alternative RNA splicing regulatory elements. Proc. Natl. Acad. Sci. U. S. A. 96, 5598–603.

D'Souza, I., Schellenberg, G.D., 2000. Determinants of 4-repeat tau expression. Coordination between enhancing and inhibitory splicing sequences for exon 10 inclusion. J. Biol. Chem. 275, 17700–9. doi:10.1074/jbc.M909470199

D'Souza, I., Schellenberg, G.D., 2005. Regulation of tau isoform expression and dementia. Biochim. Biophys. Acta 1739, 104–15. doi:10.1016/j.bbadis.2004.08.009

Dal Mas, A., Rogalska, M.E., Bussani, E., Pagani, F., 2014. Improvement of SMN2 Pre-mRNA Processing Mediated by Exon-Specific U1 Small Nuclear RNA. Am. J. Hum. Genet. 96, 93–103. doi:10.1016/j.ajhg.2014.12.009

De Conti, L., Skoko, N., Buratti, E., Baralle, M., 2012. Complexities of 5'splice site definition: implications in clinical analyses. RNA Biol. 9, 911–23. doi:10.4161/rna.20386

De Souza, J.E.S., Ramalho, R.F., Galante, P. a F., Meyer, D., de Souza, S.J., 2011. Alternative splicing and genetic diversity: silencers are more frequently modified by SNVs associated with alternative exon/intron borders. Nucleic Acids Res. 39, 4942–8. doi:10.1093/nar/gkr081

Denisont, R.A., Weiner, A.M., 1982. Human Ul RNA Pseudogenes May Be Generated by Both DNA- and RNA-Mediated Mechanisms 2, 815–828.

Denti MA, Rosa A, Sthandier O, De Angelis FG, Bozzoni I. 2004 A new vector, based on the PolII promoter of the U1 snRNA gene, for the expression of siRNAs in mammalian cells. Mol Ther.10(1):191-9.

Denti, M.A., Rosa, A., Antona, G.D., Sthandier, O., Angelis, F.G. De, Auricchio, A., Nicoletti, C., Allocca, M., Pansarasa, O., Parente, V., Musaro, A., Bottinelli, R., Bozzoni, I., 2006. Body-wide gene therapy of Duchenne muscular dystrophy in the mdx mouse model 103.

Denti MA, Incitti T, Sthandier O, Nicoletti C, De Angelis FG, Rizzuto E, Auricchio A, Musarò A, Bozzoni I. 2008 Long-term benefit of adeno-associated virus/antisense-mediated exon skipping in dystrophic mice. Hum Gene Ther.19 (6):601-8. doi: 10.1089/hum.2008.012.

Ding, H., Schwarz, D.S., Keene, A., Affar, E.B., Fenton, L., Xia, X., Shi, Y., Zamore, P.D., Xu, Z., 2003. Selective silencing by RNAi of a dominant allele that causes amyotrophic lateral sclerosis 209–217.

Doolittle, R. F., 1995. The multiplicity of domains in proteins. Annu. Rev. Biochem. 64, 287–314.

Drechsel, D.N., Hyman, A.A., Cobb, M.H., Kirschner, M.W., 1992. Modulation of the Dynamic Instability of Tubulin Assembly by the Microtubule-Associated Protein Tau 3, 1141–1154.

Dreyfuss, G., Kim, V.N., Kataoka, N., 2002. Messenger-RNA-binding proteins and the messages they carry. Nat. Rev. Mol. Cell Biol. 3, 195–205. doi:10.1038/nrm760

Drubin, D.G., Nelson, W.J., 1996. Origins of Cell Polarity Review 84, 335–344.

Du, H., Rosbash, M., 2002. The U1 snRNP protein U1C recognizes the 5' splice site in the absence of base pairing 419, 1–5. doi:10.1038/nature00999.1.

Dufour BD, Smith CA, Clark RL, Walker TR, McBride JL. 2014 Intrajugular vein delivery of AAV9-RNAi prevents neuropathological changes and weight loss in Huntington's disease mice. Mol Ther. 22(4):797-810. doi: 10.1038/mt.2013.289

Dykxhoorn, D.M., Novina, C.D., Sharp, P. a, 2003. Killing the messenger: short RNAs that silence gene expression. Nat. Rev. Mol. Cell Biol. 4, 457–67. doi:10.1038/nrm1129

Egloff, S., O'Reilly, D., Murphy, S., 2008. Expression of human snRNA genes from beginning to end. Biochem. Soc. Trans. 36, 590–4. doi:10.1042/BST0360590

Elbashir, S.M., Lendeckel, W., Tuschl, T., 2001. RNA interference is mediated by 21- and 22-nucleotide RNAs 188–200. doi:10.1101/gad.862301.vents

Faghihi, M.A., Modarresi, F., Khalil, A.M., Wood, D.E., Sahagan, B.G., Morgan, T.E., Finch, C.E., St, G., Iii, L., Kenny, P.J., Wahlestedt, C., 2008. Expression of a noncoding RNA is elevated in Alzheimer ' s disease and drives rapid feed-forward regulation of b -secretase 14, 723–730. doi:10.038/nm1784

Fairbrother, W.G., Chasin, L.A., 2000. Human Genomic Sequences That Inhibit Splicing 20, 6816–6825.

Fernandez Alanis E, Pinotti M, Dal Mas A, Balestra D, Cavallari N, Rogalska ME, Bernardi F, Pagani F.2012 An exon-specific U1 small nuclear RNA (snRNA) strategy to correct splicing defects. Hum Mol Genet. 21(11):2389-98. doi: 10.1093/hmg/dds045.

Fontana F, Siva K, Denti MA. 2015 A network of RNA and protein interactions in Fronto Temporal Dementia. Front Mol Neurosci. 2015 Mar 19;8:9. doi: 10.3389/fnmol.2015.00009. eCollection 2015.

Foster, NL, Wilhelmsen, K, Sima, AA, Jones, MZ, D'Amato, CJ, Gilman, S., 1997 Frontotemporal dementia and parkinsonism linked to chromosome 17: a consensus conference. Conference Participants. Ann Neurol. 41(6):706-15.

Francisco, S., 1998. Pathogenic implications of mutations in the tau gene in pallido-ponto-nigral degeneration and related neurodegenerative disorders linked to chromosome 17 95, 13103–13107.

Froelich, S., Basun, H., Forsell, C., Lilius, L., Axelman, K., Andreadis, A., Lannfelt, L., 1997. Mapping of a Disease Locus for Familial Rapidly Progressive Frontotemporal Dementia to Chromosome 17q12-21 385, 380–385.

Fu, Y., Masuda, A., Ito, M., Shinmi, J., Ohno, K., 2011. AG-dependent 3'-splice sites are predisposed to aberrant splicing due to a mutation at the first nucleotide of an exon. Nucleic Acids Res. 39, 4396–404. doi:10.1093/nar/gkr026

Fukumura, K., Inoue, K., 2014. Role and mechanism of U1-independent pre-mRNA splicing in the regulation of alternative splicing. RNA Biol. 6, 395–398. doi:10.4161/rna.6.4.9318

Gabellini, N., 2001. A polymorphic GT repeat from the human cardiac Na 1 Ca 2 1 exchanger intron 2 activates splicing 1083, 1076–1083.

Gamblin, T.C., 2005. Potential structure/function relationships of predicted secondary structural elements of tau. Biochim. Biophys. Acta 1739, 140–9. doi:10.1016/j.bbadis.2004.08.013

Gao, F., 2010. Context-dependent functions of specific microRNAs in neuronal development 1–9.

Garcia-blanco, M.A., Baraniak, A.P., Lasda, E.L., 2004. Alternative splicing in disease and therapy 22, 535–546.

Ge, X., Chen, Y., Lv, N., 2013. Advances with RNA interference in Alzheimer ' s disease research 117–125.

Genc, S., Koroglu, T.F., Genc, K., 2004. RNA interference in neuroscience. Brain Res. Mol. Brain Res. 132, 260–70. doi:10.1016/j.molbrainres.2004.02.004

Gilbert,W., 1978. Why genes in pieces? Nature 9;271(5645):501. doi:10.1038/271501a0 4

Glaus, E., Schmid, F., Da Costa, R., Berger, W., Neidhardt, J., 2011. Gene therapeutic approach using mutation-adapted U1 snRNA to correct a RPGR splice defect in patient-derived cells. Mol. Ther. 19, 936–41. doi:10.1038/mt.2011.7

Goedert, M., 2004. Tau protein and neurodegeneration. Semin. Cell Dev. Biol. 15, 45–9. doi:10.1016/j.semcdb.2003.12.015

Goedert, M., Ghetti, B., Spillantini, M.G., 2015. Frontotemporal Dementia : Implications for Understanding Alzheimer Disease 1–22.

Goedert, M., Jakes, R., 2005. Mutations causing neurodegenerative tauopathies. Biochim. Biophys. Acta 1739, 240–50. doi:10.1016/j.bbadis.2004.08.007

Goedert, M., Spillantini, M.G., 2000. Tau mutations in frontotemporal dementia FTDP-17 and their relevance for Alzheimer ' s disease 1502, 110–121.

Gomase, VS, Tagore, S., 2008. RNAi--a tool for target finding in new drug development.Curr Drug Metab. 9(3):241-4.

Goodson, H. V, n.d. Motors and membrane traffic and Thomas 18–28.

Gordon, F.E., Nutt, C.L., Cheunsuchon, P., Nakayama, Y., Provencher, K. a, Rice, K. a, Zhou, Y., Zhang, X., Klibanski, A., 2010. Increased expression of angiogenic genes in the brains of mouse meg3-null embryos. Endocrinology 151, 2443–52. doi:10.1210/en.2009-1151

Gorman, L., Mercatante, D.R., Kole, R., 2000. Restoration of correct splicing of thalassemic beta-globin pre-mRNA by modified U1 snRNAs. J. Biol. Chem. 275, 35914–9. doi:10.1074/jbc.M006259200

Goyenvalle, A., Wright, J., Babbs, A., Wilkins, V., Garcia, L., Davies, K.E., 2012. Engineering multiple U7snRNA constructs to induce single and multiexon-skipping for Duchenne muscular dystrophy. Mol. Ther. 20, 1212–21. doi:10.1038/mt.2012.26

Gozani, O.R., Potashkin, J., Reed, R., 1998. A Potential Role for U2AF-SAP 155 Interactions in Recruiting U2 snRNP to the Branch Site 18, 4752–4760.

Grover, A., Deture, M., Yen, S., Hutton, M., 2002. Effects on splicing and protein function of three mutations in codon N296 of tau in vitro 323, 33–36.

Gross, JD, Moerke, NJ, von der Haar T, Lugovskoy, AA, Sachs, AB, McCarthy, JE, Wagner, G., 2003. Ribosome loading onto the mRNA cap is driven by conformational coupling between eIF4G and eIF4E. Cell. 12;115 (6):739-50.

Gueneau de Novoa, P., Williams, K.P., 2004. The tmRNA website: reductive evolution of tmRNA in plastids and other endosymbionts. Nucleic Acids Res. 32, D104–8. doi:10.1093/nar/gkh102

Guttman, M., Amit, I., Garber, M., French, C., Lin, M.F., Feldser, D., Huarte, M., Zuk, O., Carey, B.W., Cassady, J.P., Cabili, M.N., Jaenisch, R., Mikkelsen, T.S., Jacks, T., Hacohen, N., Bernstein, B.E., Kellis, M., Regev, A., Rinn, J.L., Lander, E.S., 2009. Chromatin signature reveals over a thousand highly conserved large non-coding RNAs in mammals. Nature 458, 223–7. doi:10.1038/nature07672

Hamilton, A.J., Baulcombe, D.C., 1999. A Species of Small Antisense RNA in Posttranscriptional Gene Silencing in Plants 213, 1997–2000.

Hammond, S.M., Bernstein, E., Beach, D., Hannon, G.J., 2000. An RNA-directed nuclease mediates post-transcriptional gene silencing in Drosophila cells 527, 524–527.

Hammond, S.M., Wood, M.J. a, 2011. Genetic therapies for RNA mis-splicing diseases. Trends Genet. 27, 196–205. doi:10.1016/j.tig.2011.02.004

Hasegawa, M., Smith, M.J., Iijima, M., Tabira, T., Y, M.G., 1999. FTDP-17 mutations N279K and S305N in tau produce increased splicing of exon 10 443, 93–96.

Hastings, M.L., Krainer, A.R., 2001. Pre-mRNA splicing in the new millennium 302–309.

Hernandez, N., 2001. Small nuclear RNA genes: a model system to study fundamental mechanisms of transcription. J. Biol. Chem. 276, 26733–6. doi:10.1074/jbc.R100032200

Heutink, P., Stevens, S.M., Rizzu, P., Bakker, E., Kros, S.J.M., 1997. Hereditary Frontotemporal Dementia Is Linked to Chromosome 17q21-q22 : A Genetic and Clinicopathological Study of Three Dutch F d e s.

Himmelstein, D.S., Ward, S.M., Lancia, J.K., Patterson, K.R., Binder, L.I., 2012. Tau as a therapeutic target in neurodegenerative disease. Pharmacol. Ther. 136, 8–22. doi:10.1016/j.pharmthera.2012.07.001

Hollenbeck, PJ, Swanson, JA., 1990 Radial extension of macrophage tubular lysosomes supported by kinesin. Nature. 30;346(6287):864-6.

Huang, Q., Jacobson, M.R., Pederson, T., 1997. 3 J Processing of Human Pre-U2 Small Nuclear RNA : a Base-Pairing Interaction between the 3 J Extension of the Precursor and an Internal Region 17, 7178–7185.

Incitti, T., De Angelis, F.G., Cazzella, V., Sthandier, O., Pinnarò, C., Legnini, I., Bozzoni, I., 2010. Exon skipping and duchenne muscular dystrophy therapy: selection of the most active U1 snRNA antisense able to induce dystrophin exon 51 skipping. Mol. Ther. 18, 1675–82. doi:10.1038/mt.2010.123

Ingram, E.M., Spillantini, M.G., 2002. Tau gene mutations : dissecting the pathogenesis of FTDP-17 8, 555–562.

Jacobson, M.R., Huang, Q., Pederson, T., 2002. JBC Papers in Press. Published on April 15, 2002 as Manuscript M202258200.

Jackson AL, Bartz SR, Schelter J, Kobayashi SV, Burchard J, Mao M, Li B, Cavet G, Linsley PS.2003 Expression profiling reveals off-target gene regulation by RNAi. Nat Biotechnol. 21(6):635-7.
Jana, S., Chakraborty, C., Nandi, S., Deb, J.K., 2004. RNA interference: potential therapeutic targets. Appl. Microbiol. Biotechnol. 65, 649–57. doi:10.1007/s00253-004-1732-1

Jeganathan S, von Bergen, M, Mandelkow, EM, Mandelkow, E., 2008. The natively unfolded character of tau and its aggregation to Alzheimer-like paired helical filaments. Biochemistry. 7;47(40):10526-39. doi: 10.1021/bi800783d.

Keren, H., Lev-Maor, G., Ast, G., 2010. Alternative splicing and evolution: diversification, exon definition and function. Nat. Rev. Genet. 11, 345–55. doi:10.1038/nrg2776

Kieffer, T., Sands, J., Cannon, B., n.d. PHYSIOLOGICAL Editor : Dennis Brown European Editorial Committee.

Kiss, T., 2004. Biogenesis of small nuclear RNPs. J. Cell Sci. 117, 5949–51. doi:10.1242/jcs.01487

Kolarova, M., García-Sierra, F., Bartos, A., Ricny, J., Ripova, D., 2012. Structure and pathology of tau protein in Alzheimer disease. Int. J. Alzheimers. Dis. 2012, 731526. doi:10.1155/2012/731526

Kolkman, J. A. & Stemmer, W. P. 2001. Directed evolution of proteins by exon shuffling. Nature Biotech. 19, 423–428.

Kornienko, A.E., Guenzl, P.M., Barlow, D.P., Pauler, F.M., 2013. Gene regulation by the act of long non-coding RNA transcription. BMC Biol. 11, 59. doi:10.1186/1741-7007-11-59

Koutsilieri, E, Rethwilm, A, Scheller, C. J., 2007. The therapeutic potential of siRNA in gene therapy of neurodegenerative disorders.Neural Transm Suppl.7;(72):43-9.

Krecic, A.M., Swanson, M.S., n.d. hnRNP complexes : and function Annette M Krecic * and Maurice S Swanson ?

Kuhlman, T.C., Cho, H., Reinberg, D., 1999. The General Transcription Factors IIA , IIB , IIF , and IIE Are Required for RNA Polymerase II Transcription from the Human U1 Small Nuclear RNA Promoter 19, 2130–2141.

Kyriakopoulou, C., Larsson, P., Liu, L.E.I., Schuster, J., Kirsebom, L.A., Virtanen, A., 2006. U1-like snRNAs lacking complementarity to canonical 5 9 splice sites 1603–1611. doi:10.1261/rna.26506.4

Lee, G., Leugers, C.J., 2013. NIH Public Access 319–335. doi:10.1016/B978-0-12-385883-2.00004-7.Tau

Lendon, CL, Lynch, T, Norton, J, McKeel, DW Jr, Busfield, F, Craddock, N, Chakraverty S, Gopalakrishnan, G, Shears, SD, Grimmett, W, Wilhelmsen, KC, Hansen, L, Morris, JC, Goate, AM., 1998. Hereditary dysphasic disinhibition dementia: a frontotemporal dementia linked to 17q21-22. Neurology 50(6):1546-55.

Lev-maor, G., Sorek, R., Shomron, N., Ast, G., 2003. The Birth of an Alternatively Spliced Exon : 3 Splice-Site Selection in Alu Exons 300, 1288–1292.

Lewandowska, M.A., 2013. The missing puzzle piece : splicing mutations 6, 2675–2682.

Lewejohann, L., Skryabin, B. V, Sachser, N., Prehn, C., Heiduschka, P., Thanos, S., Jordan, U., Dell'Omo, G., Vyssotski, a L., Pleskacheva, M.G., Lipp, H.-P., Tiedge, H., Brosius, J., Prior, H., 2004. Role of a neuronal small non-messenger RNA:

behavioural alterations in BC1 RNA-deleted mice. Behav. Brain Res. 154, 273–89. doi:10.1016/j.bbr.2004.02.015

Liebert, M.A., Denti, M.A., Rosa, A., Antona, G.D., Sthandier, O., Angelis, F.G.D.E., Nicoletti, C., Allocca, M., Pansarasa, O., Parente, V., Musarò, A., Auricchio, A., Bottinelli, R., Bozzoni, I., 2006. Nuclear RNA Effectively Rescues Dystrophin Synthesis and Muscle Function by Local Treatment of mdx Mice 574, 565–574.

Lijima, M, Tabira, T, Poorkaj, P, Schellenberg, GD, Trojanowski, JQ, Lee, VM, Schmidt, ML, Takahashi, K, Nabika, T, Matsumoto, T, Yamashita, Y, Yoshioka, S, Ishino, H., 1999. A distinct familial presenile dementia with a novel missense mutation in the tau gene. Neuroreport. 25;10(3):497-501.

Liu, F., Gong, C.-X., 2008. Tau exon 10 alternative splicing and tauopathies. Mol. Neurodegener. 3, 8. doi:10.1186/1750-1326-3-8

Liu, S., Asparuhova, M., Brondani, V., Ziekau, I., Klimkait, T., Schümperli, D., 2004. Inhibition of HIV-1 multiplication by antisense U7 snRNAs and siRNAs targeting cyclophilin A. Nucleic Acids Res. 32, 3752–9. doi:10.1093/nar/gkh715

Liu J, Hu J, Hicks JA, Prakash TP, Corey DR. 2015. Modulation of Splicing by Single-Stranded Silencing RNAs. Nucleic Acid Ther. doi: 10.1089/nat.2014.0527

Mackay, J.P., Sunde, M., Lowry, J. a., Crossley, M., Matthews, J.M., 2008. Response to Chatr-aryamontri et al.: Protein interactions: to believe or not to believe? Trends Biochem. Sci. 33, 242–243. doi:10.1016/j.tibs.2008.04.003

Madhani, HD, Guthrie, C., 1994. Dynamic RNA-RNA interactions in the spliceosome. Annu Rev Genet. 1994;28:1-26.

Makarova, O. V, Makarov, E.M., Urlaub, H., Will, C.L., Gentzel, M., Wilm, M., Lührmann, R., 2004. A subset of human 35S U5 proteins, including Prp19, function prior to catalytic step 1 of splicing. EMBO J. 23, 2381–91. doi:10.1038/sj.emboj.7600241

Malca, H., Shomron, N., Ast, G., 2003. The U1 snRNP Base Pairs with the 5 J Splice Site within a Penta-snRNP Complex 23, 3442–3455. doi:10.1128/MCB.23.10.3442

Manuscript, A., 2010. NIH Public Access 12, 214–222.

Manuscript, A., 2013. NIH Public Access 3, 34–42. doi:10.1016/j.biomed.2013.01.001.Long

Marquis, J., Meyer, K., Angehrn, L., Kämpfer, S.S., Rothen-Rutishauser, B., Schümperli, D., 2007. Spinal muscular atrophy: SMN2 pre-mRNA splicing

corrected by a U7 snRNA derivative carrying a splicing enhancer sequence. Mol. Ther. 15, 1479–86. doi:10.1038/sj.mt.6300200

Martins, H., Mao, Q., Harper, S.Q., Staber, P.D., He, X., Eliason, S.L., Yang, L., Kotin, R.M., Paulson, H.L., Davidson, B.L., 2005. RNA interference improves motor and neuropathological abnormalities in a Huntington's 102.

Masato Hasegawaa, Michael J Smitha, Masaaki Iijimab, Takeshi Tabirac, Michel Goederta, 1999. FTDP-17 mutations N279K and S305N in tau produce increased splicing of exon 10.FEBS lett.443,(2), 93–96 doi:10.1016/S0014-5793(98)01696-2.

Massone, S., Vassallo, I., Fiorino, G., Castelnuovo, M., Barbieri, F., Borghi, R., Tabaton, M., Robello, M., Gatta, E., Russo, C., Florio, T., Dieci, G., Cancedda, R., Pagano, A., 2011. 17A, a novel non-coding RNA, regulates GABA B alternative splicing and signaling in response to inflammatory stimuli and in Alzheimer disease. Neurobiol. Dis. 41, 308–17. doi:10.1016/j.nbd.2010.09.019

Matlin, A.J., Clark, F., Smith, C.W.J., 2005. Understanding alternative splicing: towards a cellular code. Nat. Rev. Mol. Cell Biol. 6, 386–98. doi:10.1038/nrm1645

McManus, C.J., Graveley, B.R., 2011. RNA structure and the mechanisms of alternative splicing. Curr. Opin. Genet. Dev. 21, 373–9. doi:10.1016/j.gde.2011.04.001

Meister, G., Tuschl, T., 2004. Mechanisms of gene silencing by double-stranded RNA 431, 343–349.

Mercer, T.R., Dinger, M.E., Mariani, J., Kosik, K.S., Mehler, M.F., Mattick, J.S., 2008. Noncoding RNAs in Long-Term Memory Formation. Neuroscientist 14, 434–45. doi:10.1177/1073858408319187

Mercer, T.R., Qureshi, I.A., Gokhan, S., Dinger, M.E., Li, G., Mattick, J.S., Mehler, M.F., 2010. Long noncoding RNAs in neuronal-glial fate specification and oligodendrocyte lineage maturation 1–15.

Meyer, K., Marquis, J., Trüb, J., Nlend Nlend, R., Verp, S., Ruepp, M.-D., Imboden, H., Barde, I., Trono, D., Schümperli, D., 2009. Rescue of a severe mouse model for spinal muscular atrophy by U7 snRNA-mediated splicing modulation. Hum. Mol. Genet. 18, 546–55. doi:10.1093/hmg/ddn382

Miller, V.M., Gouvion, C.M., Davidson, B.L., Paulson, H.L., 2004. Targeting Alzheimer's disease genes with RNA interference: an efficient strategy for silencing mutant alleles. Nucleic Acids Res. 32, 661–8. doi:10.1093/nar/gkh208

Miller, V.M., Paulson, H.L., Gonzalez-Alegre, P., 2005. RNA interference in neuroscience: progress and challenges. Cell. Mol. Neurobiol. 25, 1195–207. doi:10.1007/s10571-005-8447-4

Miller, V.M., Xia, H., Marrs, G.L., Gouvion, C.M., Lee, G., Davidson, B.L., Paulson, H.L., 2007. Allele-specific silencing of dominant disease genes 100, 7195–7200.

Mills, J.D., Janitz, M., 2012. Alternative splicing of mRNA in the molecular pathology of neurodegenerative diseases. Neurobiol. Aging 33, 1012.e11–24. doi:10.1016/j.neurobiolaging.2011.10.030

Morris, R.L., Hollenbeck, P.J., 1993. The regulation of bidirectional mitochondrial transport is coordinated with axonal outgrowth 927, 917–927.

Mount, S.M., 2000. Genomic Sequence , Splicing , and Gene Annotation 6, 788–792.

Mount, SM, Pettersson, I, Hinterberger, M, Karmas, A, Steitz, JA. The U1 small nuclear RNA-protein complex selectively binds a 5' splice site in vitro 1983 Cell. 33(2):509-18.

Muller, B., 1997. The U7 snRNP and the hairpin binding protein : Key players in histone mRNA metabolism 8.

Murrell, J.R., Koller, D., Goedert, M., Spillantini, M.G., Edenberg, H.J., Farlow, M.R., Ghetti, B., 1997. Familial Multiple-System Tauopathy with Presenile Dementia Is Localized to Chromosome 17 1131–1138.

Mus, E., Hof, P.R., Tiedge, H., 2007. Dendritic BC200 RNA in aging and in Alzheimer's disease.

Nally, M.T.M.C., 1999. U1 Small Nuclear Ribonucleoprotein and Splicing Inhibition by the Rous Sarcoma Virus Negative Regulator of Splicing Element 73, 2385–2393.

Naro, C., Sette, C., 2013. Phosphorylation-Mediated Regulation of Alternative Splicing in Cancer 2013.

Neuenkirchen, N., Chari, A., Fischer, U., 2008. Deciphering the assembly pathway of Sm-class U snRNPs. FEBS Lett. 582, 1997–2003. doi:10.1016/j.febslet.2008.03.009

Niblock, M., Gallo, J.-M., 2012. Tau alternative splicing in familial and sporadic tauopathies. Biochem. Soc. Trans. 40, 677–80. doi:10.1042/BST20120091

Nilsen, T.W., 2003. The spliceosome: the most complex macromolecular machine in the cell? Bioessays 25, 1147–9. doi:10.1002/bies.10394

Nurtdinov, R.N., 2003. Low conservation of alternative splicing patterns in the human and mouse genomes. Hum. Mol. Genet. 12, 1313–1320. doi:10.1093/hmg/ddg137

Ole, R.Y.K., 1998. Stable alteration of pre-mRNA splicing patterns by modified U7 small nuclear RNAs 95, 4929–4934.

Patton, J.R., Patterson, R.J., Pederson, T., 1987. Reconstitution of the Ul Small Nuclear Ribonucleoprotein Particle 7, 4030–4037.

Peng, T., Li, Y., 2009. Tandem exon duplication tends to propagate rather than to create de novo alternative splicing. Biochem. Biophys. Res. Commun. 383, 163–6. doi:10.1016/j.bbrc.2009.03.162

Peng KA, Masliah E. 2010 Lentivirus-expressed siRNA vectors against Alzheimer disease. Methods Mol Biol. 614:215-24. doi: 10.1007/978-1-60761-533-0_15.

Petersen, RB, Tabaton, M, Chen, SG, Monari, L, Richardson, SL, Lynch, T, Manetto, V, Lanska, DJ, Markesbery, WR, Lynch, T et al., 1995. Familial progressive subcortical gliosis: presence of prions and linkage to chromosome 17. Neurology. 45(6):1062-7.

Pomeranz Krummel, D. a, Oubridge, C., Leung, A.K.W., Li, J., Nagai, K., 2009. Crystal structure of human spliceosomal U1 snRNP at 5.5 A resolution. Nature 458, 475–80. doi:10.1038/nature07851

Poorkaj, P, Bird, TD, Wijsman, E, Nemens, E, Garruto, RM, Anderson, L, Andreadis, A, Wiederholt, WC, Raskind, M, Schellenberg, GD., 1998. Tau is a candidate gene for chromosome 17 frontotemporal dementia Ann Neurol. 43(6):815-25.

Pozzoli, U., Sironi, M., 2005. Silencers regulate both constitutive and alternative splicing events in mammals. Cell. Mol. Life Sci. 62, 1579–604. doi:10.1007/s00018-005-5030-6

Qian, W., Liu, F., 2014. Regulation of alternative splicing of tau exon 10. Neurosci. Bull. 30, 367–77. doi:10.1007/s12264-013-1411-2

Qureshi, I. a, Mehler, M.F., 2011. Non-coding RNA networks underlying cognitive disorders across the lifespan. Trends Mol. Med. 17, 337–46. doi:10.1016/j.molmed.2011.02.002

Rabbitts, T.H, Forster,A., 1978. Evidence for noncontiguous variable and constant region genes in both germ line and myeloma DNA. Cell 13(2):319-27.

Ralph, G.S., Radcliffe, P. a, Day, D.M., Carthy, J.M., Leroux, M. a, Lee, D.C.P., Wong, L.-F., Bilsland, L.G., Greensmith, L., Kingsman, S.M., Mitrophanous, K. a, Mazarakis, N.D., Azzouz, M., 2005. Silencing mutant SOD1 using RNAi protects against

neurodegeneration and extends survival in an ALS model. Nat. Med. 11, 429–33. doi:10.1038/nm1205

Raponi M, Baralle D.2008, Can donor splice site recognition occur without the involvement of U1 snRNP? Biochem Soc Trans. 3 548-50. doi: 10.1042/BST0360548.

Raoul, C., Abbas-Terki, T., Bensadoun, J.-C., Guillot, S., Haase, G., Szulc, J., Henderson, C.E., Aebischer, P., 2005. Lentiviral-mediated silencing of SOD1 through RNA interference retards disease onset and progression in a mouse model of ALS. Nat. Med. 11, 423–8. doi:10.1038/nm1207

Reed, R., 2000. Mechanisms of fidelity in pre-mRNA splicing 1–6.

Riedl, L., Mackenzie, I.R., Förstl, H., Kurz, A., Diehl-schmid, J., 2014. Frontotemporal lobar degeneration : current perspectives 297–310.

Rnas, L., Mercer, T.R., Dinger, M.E., Mattick, J.S., n.d. insights into functions.

Road, H., Kingdom, U., Adrian, E.D., Way, R., 1999. Structure of tau exon 10 splicing regulatory element RNA and destabilization by mutations of frontotemporal dementia and parkinsonism linked to chromosome 17 96, 8229–8234.

Roca, X., Krainer, A.R., Eperon, I.C., 2013. Pick one , but be quick : 5 9 splice sites and the problems of too many choices 129–144. doi:10.1101/gad.209759.112.that

Rosso, S.M., Donker Kaat, L., Baks, T., Joosse, M., de Koning, I., Pijnenburg, Y., de Jong, D., Dooijes, D., Kamphorst, W., Ravid, R., Niermeijer, M.F., Verheij, F., Kremer, H.P., Scheltens, P., van Duijn, C.M., Heutink, P., van Swieten, J.C., 2003. Frontotemporal dementia in The Netherlands: patient characteristics and prevalence estimates from a population-based study. Brain 126, 2016–22. doi:10.1093/brain/awg204

Ruskin, B, Zamore, PD, Green, MR., 1988. A factor, U2AF, is required for U2 snRNP binding and splicing complex assembly. Cell. 1988 Jan 29;52(2):207-19.

Samuels, D.C., Schon, E. a, Chinnery, P.F., 2004. Two direct repeats cause most human mtDNA deletions. Trends Genet. 20, 393–8. doi:10.1016/j.tig.2004.07.003

Sapru, M.K., Yates, J.W., Hogan, S., Jiang, L., Halter, J., Bohn, M.C., 2006. Silencing of human alpha-synuclein in vitro and in rat brain using lentiviral-mediated RNAi. Exp. Neurol. 198, 382–90. doi:10.1016/j.expneurol.2005.12.024

Scholefield, J., Greenberg, L.J., Weinberg, M.S., Arbuthnot, P.B., Abdelgany, A., Wood, M.J. a, 2009. Design of RNAi hairpins for mutation-specific silencing of

ataxin-7 and correction of a SCA7 phenotype. PLoS One 4, e7232. doi:10.1371/journal.pone.0007232

Schonrock, N., Götz, J., 2012. Decoding the non-coding RNAs in Alzheimer's disease. Cell. Mol. Life Sci. 69, 3543–59. doi:10.1007/s00018-012-1125-z

Schwarz, D.S., Ding, H., Kennington, L., Moore, J.T., Schelter, J., Burchard, J., 2006. Designing siRNA That Distinguish between Genes That Differ by a Single Nucleotide 2. doi:10.137/journal.pgen.0020140

Sciences, B., Words, K., May, R., 1992. U1 snRNP targets an essential splicing factor , U2AF65 . to the 3 ' splice site by a network interactions spanning the exon 2554–2568.

Seelaar, H., Rohrer, J.D., Pijnenburg, Y. a L., Fox, N.C., van Swieten, J.C., 2011. Clinical, genetic and pathological heterogeneity of frontotemporal dementia: a review. J. Neurol. Neurosurg. Psychiatry 82, 476–86. doi:10.1136/jnnp.2010.212225

Séraphin, B, Kandels-Lewis, S.,1993. 3' splice site recognition in S. cerevisiae does not require base pairing with U1 snRNA. Cell. 21;73(4):803-12.

Sergeant, N., Delacourte, A., Buée, L., 2005. Tau protein as a differential biomarker of tauopathies. Biochim. Biophys. Acta 1739, 179–97. doi:10.1016/j.bbadis.2004.06.020

Seyhan, A.A., 2011. RNAi : a potential new class of therapeutic for human genetic disease 583–605. doi:10.1007/s00439-011-0995-8

Sharp, P.A., 1997. A Minimal Spliceosomal Complex A Recognizes the Branch Site and Polypyrimidine Tract 17, 2944–2953.

Shuey, D.J., Mccallus, D.E., Giordano, T., 2002. RNAi : gene-silencing in therapeutic intervention 7, 1040–1046.

Siuda, J., Fujioka, S., Wszolek, Z.K., 2014. Parkinsonian syndrome in familial frontotemporal dementia. Parkinsonism Relat. Disord. 20, 957–64. doi:10.1016/j.parkreldis.2014.06.004

Siva K, Covello G, Denti MA. 2014 Exon-skipping antisense oligonucleotides to correct missplicing in neurogenetic diseases. Nucleic Acid Ther. 24(1):69-86. doi: 10.1089/nat.2013.0461

Snowden, JS, Helen L, Griffiths and Neary, D., 1996. Semantic-Episodic Memory Interactions in Semantic Dementia: Implications for Retrograde Memory Function. Cognitive Neuropsychology Vol. 13, Iss. 8.

Sontheimer, EJ, Steitz, JA., 1993. The U5 and U6 small nuclear RNAs as active site components of the spliceosome Science. 24;262(5142):1989-96.

Sperling, J., Azubel, M., Sperling, R., 2008. Structure and function of the Pre-mRNA splicing machine. Structure 16, 1605–15. doi:10.1016/j.str.2008.08.011

Spillantini, M.G., Goedert, M., 1998. Tau protein pathology in neurodegenerative diseases 2236, 428–433.

Spillantini, MG, Yoshida, H, Rizzini, C, Lantos, PL, Khan, N, Rossor, MN, Goedert, M, Brown, J., 2000. A novel tau mutation (N296N) in familial dementia with swollen achromatic neurons and corticobasal inclusion bodies. Ann Neurol. 48(6):939-43.

Spillantini, M.G., Goedert, M., 2013. Tau pathology and neurodegeneration. Lancet Neurol. 12, 609–22. doi:10.1016/S1474-4422(13)70090-5

Staknis, D., Reed, R., 1994. SR Proteins Promote the First Specific Recognition of Pre-mRNA and Are Present Together with the Ul Small Nuclear Ribonucleoprotein Particle in a General Splicing Enhancer Complex 14, 7670–7682.

Stanford, P.M., Halliday, G.M., Brooks, W.S., Kwok, J.B.J., Storey, C.E., Creasey, H., Morris, J.G.L., Fulham, M.J., Schofield, P.R., 2010. Progressive supranuclear palsy pathology caused by a novel silent mutation in exon 10 of the tau gene Expansion of the disease phenotype caused by tau gene mutations 880–893.

Taft, R.J., Pang, K.C., Mercer, T.R., Dinger, M., Mattick, J.S., 2010. Non-coding RNAs : regulators of disease 126–139. doi:10.1002/path

Tan, L., Yu, J.-T., Hu, N., Tan, L., 2013. Non-coding RNAs in Alzheimer's disease. Mol. Neurobiol. 47, 382–93. doi:10.1007/s12035-012-8359-5

Tanaka, Y., Kanai, Y., Okada, Y., Nonaka, S., Takeda, S., Harada, A., Hirokawa, N., 1998. Targeted Disruption of Mouse Conventional Kinesin Heavy Chain , kif5B , Results in Abnormal Perinuclear Clustering of Mitochondria 93, 1147–1158.

Tauopathies, O.F., Sontag, E., Nunbhakdi-craig, V., Lee, G., Brandt, R., Kamibayashi, C., Kuret, J., Iii, C.L.W., Mumby, M.C., Bloom, G.S., 1999. Molecular Interactions among Protein Phosphatase 2A , Tau , and Microtubules IMPLICATIONS FOR THE REGULATION OF TAU PHOSPHORYLATION AND THE DEVELOPMENT 274, 25490–25498.

Tazi, J., Bakkour, N., Stamm, S., 2009. Alternative splicing and disease. Biochim. Biophys. Acta 1792, 14–26. doi:10.1016/j.bbadis.2008.09.017

Uchikawa, H., Fujii, K., Kohno, Y., Katsumata, N., Nagao, K., Yamada, M., Miyashita, T., 2007. U7 snRNA-mediated correction of aberrant splicing caused by activation of cryptic splice sites. J. Hum. Genet. 52, 891–7. doi:10.1007/s10038-007-0192-8

Vazquez, F, Vaucheret, H, Rajagopalan, R, Lepers, C, Gasciolli, V, Mallory, AC, Hilbert, JL, Bartel, DP, Crété, P., 2004 Endogenous trans-acting siRNAs regulate the accumulation of Arabidopsis mRNAs Mol Cell. 16(1):69-79.

Vitro, F.I.N., Brandt, R., Lee, G., 1993. Functional Organization of Microtubule-associated Protein Tau 268, 3414–3419.

Von Bergen, M., Barghorn, S., Biernat, J., Mandelkow, E.-M., Mandelkow, E., 2005. Tau aggregation is driven by a transition from random coil to beta sheet structure. Biochim. Biophys. Acta 1739, 158–66. doi:10.1016/j.bbadis.2004.09.010

Vučićević, D., Schrewe, H., Orom, U. a, 2014. Molecular mechanisms of long ncRNAs in neurological disorders. Front. Genet. 5, 48. doi:10.3389/fgene.2014.00048

Wahl, M.C., Will, C.L., Lu, R., 2009. Review The Spliceosome : Design Principles of a Dynamic RNP Machine 701–718. doi:10.1016/j.cell.2009.02.009

Wang, J., Zhang, J., Zheng, H., Li, J., Liu, D., Li, H., Samudrala, R., Yu, J., Wong, G.K.-S., 2004. Mouse transcriptome: Neutral evolution of "non-coding" complementary DNAs. Nature 431, 26–27. doi:10.1038/nature03016

Ward, A.J., Cooper, T.A., 2010. The pathobiology of splicing 152–163. doi:10.1002/path

Ward, A.J., Cooper, T.A., 2011. NIH Public Access 220, 152–163. doi:10.1002/path.2649.The

West, S., Gromak, N., Proudfoot, N.J., 2004. Human 5' --> 3' exonuclease Xrn2 promotes transcription termination at co-transcriptional cleavage sites. Nature 432, 522–5. doi:10.1038/nature03035

Wiemer, E.A.C., Wenzel, T., Deerinck, T.J., Ellisman, M.H., Subramani, S., 1997. Visualization of the Peroxisomal Compartment in Living Mammalian Cells: Dynamic Behavior and Association with Microtubules 136, 71–80.

Wilhelmsenss, K.C., 1997. Rapidly Progressive Autosomal Dominant Parkinsonism and Dementia with Pallido-Ponto-Nigral Degeneration (PPND) and Disinhibition-Dementia-Parkinsonism- Amyotrophy Complex (DDPAC) are Clinically Distinct Conditions that are Both Linked to 17q21-22 . 3, 67–76.

Will, C.L., Lührmann, R., 2001. Spliceosomal UsnRNP biogenesis , structure and function 290–301.

Will, CL, Lührmann, R. 2005 Splicing of a rare class of introns by the U12-dependent spliceosome. Biol Chem. 386(8):713-24.

Wood, M.J. a, Gait, M.J., Yin, H., 2010. RNA-targeted splice-correction therapy for neuromuscular disease. Brain 133, 957–72. doi:10.1093/brain/awq002

Wszolek, Z.K., Tsuboi, Y., Ghetti, B., Pickering-Brown, S., Baba, Y., Cheshire, W.P., 2006. Frontotemporal dementia and parkinsonism linked to chromosome 17 (FTDP-17). Orphanet J. Rare Dis. 1, 30. doi:10.1186/1750-1172-1-30

Wu, S., Romfo, C.M., Nilsen, T.W., Green, M.R., Page, S.D.S., 1999. Functional recognition of the 3 9 splice site AG by the splicing factor U2AF 35 402.

Xu, H, Rösler, TW, Carlsson, T, Andrade, AD, Fiala, O, Hollerhage, M, Oertel, WH, Goedert, M, Aigner A, Höglinger, GU., 2014. Tau Silencing by siRNA in the P301S Mouse Model of Tauopathy. Curr Gene Ther. 14(5):343-51.

Zamore, P.D., Haley, B., 2005. Ribo-gnome : The Big World of Small RNAs 1519–1525.

Zamore, P.D., Tuschl, T., Sharp, P.A., Bartel, D.P., 2000. RNAi : Double-Stranded RNA Directs the ATP-Dependent Cleavage of mRNA at 21 to 23 Nucleotide Intervals 101, 25–33.

Zhou, J., Yu, Q., Zou, T., 2008. Alternative splicing of exon 10 in the tau gene as a target for treatment of tauopathies. BMC Neurosci. 9 Suppl 2, S10. doi:10.1186/1471-2202-9-S2-S10

Zhu, H., Gup, W., Zhang, L., Davis, J.J., Wu, S., Teraishi, F., Cao, X., Smythe, W.R., Fang, B., 2014. Enhancing TRAIL-induced apoptosis by Bcl-XL siRNA. Cancer Biol. Ther. 4, 399–403. doi:10.4161/cbt.4.4.1616

A. <u>Projects</u>

1) Screening for modified U1 snRNAs to modulate splicing of Exon 10 in MAPT pre-mRNA (Year 2011-2012).

- Produced the U1 and U7 scramble chimeric constructs that were essential to validate the specificity of exon skipping effects.

- Optimized the transfection protocol for successful delivery of DNA in PC12 cells and contributed to the results obtained via lipid-based transfection methods.

- Optimized the RT-PCR protocol for the analysis of U1 and U7 snRNA in PC12 cells.

- Validated the effect of U1 and U7 constructs on exon 10 skipping in PC12 cells.

- Proposed the utilization of another cell line NSC34 to validate effects of U1 and U7 constructs.

- Optimized the western blot protocol for validation of the effects of U1 and U7 snRNAs in neuroblastoma cells (SH-SY5Y and NSC-34).

2) Screening for siRNA molecules to mediate isoform specific target degradation of exon 10 containing MAPT pre-mRNA (Year 2013-2015).

- Postulated a novel hypothesis on the prospect of employing siRNAs in the context of FTDP-17 after being inspired by the work of Miller V et al., 2005.

- Designed a set of six siRNAs to target exon 10 of MAPT gene under the supervision of Prof. Michela Alessandra Denti.

- Designed experimental strategies to screen the effect of siRNAs on a dual fluorescent reporter plasmid provided by Stoilov P et al 2003.

- Modified the reporter plasmid via mutagenesis and developed a screening assay along with Dr. Valentina Adami to provide a high throughput read out of the observations.

- Executed screening analysis of all the siRNAs in the minigene reporter system.

- Identified a suitable model system, NSC-34 to validate the effects of these siRNAs in an endogenous context.

- Identified another model system, primary cortical neurons to validate the effects of these siRNAs on a functional neuronal model

- Optimized the western blot protocol for validation of the effects of siRNAs in neuroblastoma cells.

- Filed a patent application for the above proposed project based on the results that I obtained during my research period.

3) Role of long non-coding RNAs in regulation of MAPT (Year 2013-2015)

- Reproduced western blot assays on pre-validated stable cell lines to provide adequate replicates.

- Applied the novel method of screening to validate the effects of NATs on splicing of exon 10.

B. Manuscripts

An electroporation protocol for efficient DNA transfection in PC12 cells. *Cytotechnology* **(2013).**

Experiments on Lipid-based transfection methods were performed thus contributing to Figures 1 and 2 of the manuscript.

Antisense oligonucleotides for Exon Skipping in Neurogenetic Diseases. *Nucleic acid therapeutics* **(2014).**

All the contents in the text were written following a thorough literature search under the guidance of Prof. Michela Alessandra Denti.

A global network in Fronto Temporal Dementia: -an RNA perspective". *Frontiers in Molecular Neuroscience* **(2015).**

The following contents were contributed:
- Material of text pertaining to TDP43, MAPT and VCP
- Figures of TDP43, MAPT and VCP
- Table of contents for TDP43, MAPT and VCP

C. Patent

"RNA interference mediated therapy for neurodegenerative diseases". **EU Patent application number TO2015A000185** valid from March 2015).

The complete content of patent application was written and all the results were produced and reported as figures through independent research work.

_____   _____

Signature of PhD candidate   Signature of Tutor

(Kavitha Siva)   (Prof. Michela Alessandra Denti)

LIST OF PUBLICATIONS

1. Covello Giuseppina, **Siva Kavitha**, Michela A.Denti. "An electroporation protocol for efficient DNA transfection in PC12 cells". *Cytotechnology*. (2013). 66(4): 543–553. doi: 10.1007/s10616-013-9608-9.

2. **Siva Kavitha***, Covello Giuseppina*, Michela A. Denti. "Antisense oligonucleotides for Exon Skipping in Neurogenetic Diseases". *Nucleic acid therapeutics* (2014)(*Co-authorship). 24(1): 69–86.doi: 10.1089/nat.2013.0461.

3. Francesca Fontana*, **Siva Kavitha***, Michela A. Denti ."A global network in Fronto Temporal Dementia: -an RNA perspective". *Frontiers in Molecular Neuroscience*. (2015)(*Co-authorship). 8: 9. doi: 10.3389/fnmol.2015.00009.

4. **Siva Kavitha**, Covello Giuseppina, Michela A. Denti, "RNA interference mediated therapy for neurodegenerative diseases" (**EU Patent application number TO2015A000185** valid from March 2015).

5. **Siva Kavitha** , Adami Valentina, Zubovic L, Covello Giuseppina, Macchi P, Basso M, Michela A. Denti. "An siRNA mediated regulation of Exon 10 in FTDP-17". (Submission in progress) (2015).

6. Covello Giuseppina, **Siva Kavitha**, Michela A.Denti . Antisense RNA-induced exon-skipping for the gene therapy of Frontotemporal Dementia and Parkinsonism associated with chromosome 17 (FTDP-17) (*In preparation*) (2015).

7. Roberto Simone, Faiza Javad, Warren Emmett, **Kavitha Siva**, Victoria Kay, Geshanti Hondhamuni, Vincent Pagnol, Michela Denti, Daniah Trabzuni, Mina Ryten, Selina Wray, Elizaveth Preza, Andrew Lees, John Hardy, Thomas T Warner, Jernej Ule and Rohan de Silva. Long non-coding antisense RNA represses MAPT IRES-mediated translation through an embedded MIR repeat. (*In preparation*) (2015).

LIST OF ABBREVIATIONS

3R: Tau with 3 nucleotide binding domains

4R: Tau with 4 nucleotide binding domains

Aa: Amino acid

AAV: Adeno associated virus

ACE: A/C rich enhancer

AD: Alzheimer's disease

ALS: Amyotrophic lateral sclerosis

AS: Alternative splicing

ASOs: Antisense oligonucleotides

bp: base pairs

BPS: Branch point sequence

CBD: Cortico basal degeneration

cDNA: Complementary DNA

CHMP-2B: Chromatin modifying protein 2B

CNS: Central nervous system

DDPAC: Disinhibition-Dementia-Parkinsonism-Amyotrophy Complex

DMEM: Dulbecco's modified eagles medium

DNA: De-oxy ribonucleic acid

DSE: Distal sequence element

dsRNA: double stranded RNA

E10-:   MAPT isoform without exon 10

E10+:   MAPT isoform containing exon 10

EDTA: Ethylene diamine tetra acetic acid

ESE: Exon splicing enhancer

ESS: Exonic splicing silencer

EtBr: Ethidium bromide

FBS: Fetal bovine serum

FCS: Fetal calf serum

FTD: Fronto temporal dementia

FTDP-17:   Fronto temporal dementia and pakinsonism linked to chromosome

                  17

FTLD:	Frontotemporal lobar degeneration
FTLD-U:	FTLD with ubiquitin-positive inclusions
GFP:	Green fluorescent protein
HD:	Huntington's disease
hnRNP:	heterogenous nuclear ribonucleoprotein
HS:	Horse serum
ISE:	Intronic splicing enhancer
ISM:	Intronic splicing modulator
ISS:	Intronic splicing silencer
ITRs:	Inverted terminal repeats
Kb:	Kilobase
kDa:	Kilodalton
lncRNA:	Long non-coding RNA
lncRNAs:	Long non-coding RNAs
MAPs:	Microtubule associated proteins
MAPT:	Microtubule associated protein tau
miRNA:	micro-RNA
MND:	Motor neuron disease
mRNA:	messenger RNA
MTOC:	Microtubule organising centre
NATs:	Natural antisense transcripts
NFTs:	Neurofibrillary tangles
nfvPPA:	Non fluent variant progressive non fluent aphasia
NSC-34:	Mouse motor neuron-like hybrid cell line 34
nt:	nucleotides
PBS:	Phosphate buffer saline
PC12:	Rat pheochromocytoma cells
PCR:	Polymerase chain reaction
PD:	Parkinson's disease
PGRN:	Progranulin
PNFA:	Primary non –fluent aphasia
PPA:	Progressive non fluent aphasia
PPE:	Polypurine enhancer

PSP:	Progressive supranuclear palsy
PTB:	Polypyrimidine tract binding protein
RFP:	Red fluorescent protein
RISC:	RNA induced silencing complex
RNA Pol :	RNA polymerase I
RNA Pol II:	RNA polymerase II
RNA Pol III:	RNA polymerase III
RNA:	Ribonucleic acid
RNAi:	RNA interference
RRM:	RNA recognition motif
rRNA:	Ribosomal RNA
RS:	Arginine-serine rich motif
RT:	Reverse transcriptase
RT:	Room temperature
RT-PCR:	Reverse transcription PCR
SCA-3:	Spinocerebellar ataxia type 3
SCCMS:	Slow channel congenital myasthenic syndrome disease
SD:	Semantic dementia
sds:	splicing donor site
SDS:	Sodium dodecyl sulphate
SELEX:	Systematic evolution of ligands by exponential enrichment
shRNA:	short-hairpin RNA
SH-SY5Y:	A thrice cloned (SK-N-SH -> SH-SY -> SH-SY5 -> SH-SY5Y) subline of the neuroblastoma cell line SK-N-SH
siRNA:	small interferring RNA
SNAPc:	snRNA activator protein complex
snRNA:	small non-coding RNA
snRNP:	small non coding ribonucleoprotein
SR:	Serine-Rich
SRE:	Splicing regulatory element
ss:	Splice site
svPPA:	Semantic variant PPA
TBE:	Tris-borate-EDTA buffer

TDP-43:   Transactive response DNA binding protein 43 kDa

TE: Transposable elements

TF: Transcription factor

TG: Thyroglobulin

tRNA: Transfer RNA

U2AF: U2 snRNP auxiliary factor

UTR: Untranslated region

VCP: Valosin containing protein

Wt: Wild type

MANUSCRIPTS

"Success is not a function of the size of your title but the richness of your contribution"

-Robin Sharma

TECHNICAL NOTE

An electroporation protocol for efficient DNA transfection in PC12 cells

**Giuseppina Covello · Kavitha Siva ·
Valentina Adami · Michela A. Denti**

Abstract A wide variety of mammalian cell types is used in gene transfection studies. Establishing transfection methods that enable highly efficient DNA uptake has become increasingly important. PC12 is an established rat pheochromocytoma cell line, which responds to exposure to NGF with cessation of growth, expression of cytoplasmic processes, and differentiation into cells resembling sympathetic neurons. Although PC12 cells represent an important model system to study a variety of neuronal functions, they proved relatively difficult to transfect. We have compared the efficiency of three different chemical transfection reagents (Lipofectamine 2000, Lipofectamine LTX and TransIT-LT1) and of two electroporation systems (Neon and Gene Pulser Xcell) in transiently transfecting undifferentiated PC12 cells. By comparing efficiencies from replicate experiments we proved electroporation (in particular Neon) to be the method of choice. By optimizing different parameters (voltage, pulse width and number of pulses) we reached high efficiency of transfection (90 %) and viability (99 %). We also demonstrated that, upon electroporation, cells are not altered by the transfection and maintain their ability to differentiate.

Keywords PC12 cells · Cell culture · DNA transfection · DNA electroporation · NGF · Neural differentiation

Introduction

PC12 cells are a cell line originating from pheochromocytoma in the rat adrenal medulla (Schaefer et al. 1987) and grow in culture as undifferentiated neuroblasts. Since its characterization in 1976 (Greene and Tischler 1976) PC12 cells have become a commonly employed model system for studies of neuronal development and function (Grau and Greene 2012). One of the important features of PC12 cells is that they are small cells with a limited amount of cytoplasm and long doubling time. They possess remarkable ability to respond to nerve growth factor (NGF), a neurotrophic polypeptide, inducing morphological and biochemical changes resulting in differentiation of PC12 cells into a sympathetic neuron-like phenotype (Greene and Tischler 1976; Grau and Greene 2012; Nagase et al. 2005; Dhar et al. 2007; Park et al. 2007). For this reason PC12 cells have been regarded as a research model to study neuronal development, sympathetic

G. Covello · K. Siva · M. A. Denti (✉)
Laboratory of RNA Biology and Biotechnology, Centre for Integrative Biology (CIBIO), University of Trento, via delle Regole 101, 38123 Trento, Italy
e-mail: denti@science.unitn.it

V. Adami
High-Throughput Screening Facility, Centre for Integrative Biology (CIBIO), University of Trento, via delle Regole 101, 38123 Trento, Italy

M. A. Denti
CNR Institute of Neuroscience, Padua, Italy

neurotransmission and neurodegenerative diseases (Wang et al. 2002; Seth et al. 2002). In general, when challenged with physiological levels of NGF, these cells cease division, become electrically excitable, extend long branching neurites, and gradually acquire many characteristics of mature sympathetic neurons. Under serum-free conditions, NGF promotes not only neuronal differentiation of PC12 cells, but also their survival (Greene 1978; Fujita et al. 1989; Rukenstein et al. 1991). Several of their attributes have led to their widespread popularity in neurobiological research. These include their relatively high degree of differentiation before and after NGF treatment, homogeneous response to stimuli, availability in large numbers for biochemical studies, and suitability for genetic manipulations. However, finding transfection techniques that enable efficient DNA uptake into PC12 cells is relatively difficult. Moreover, it is important to have a good method to transfect these cells with high efficiency devoid of cellular alteration, and maintaining their ability to differentiate. An important limitation of working with PC12 cells is that they tend to be very sensitive to physical stress, alterations in temperature, pH shifts, or changes in osmolarity. Therefore, handling and manipulation during transfection is a crucial step.

Various transfection methods have been attempted to transfect this cell line. In general, cells can be gene-modified in vitro and in vivo using chemical or physical methods (Azzam and Domb 2004; Marples and Dachs 2002). Chemical methods of transfection are widely used, as they are relatively simple, cheap, and safe (Douglas 2008). They include calcium phosphate, liposomes, cationic lipids (e.g., dioleoyl trimethylammonium propane (DOTAP)), cationic polymers (e.g., polyethylenimine (PEI), dendrimers) and cationic polysaccharides (Eliyahu et al. 2005; Godbey et al. 1999a, b). In general, these reagents act via packaging mechanism to condense and deliver DNA to the cytoplasm of cells, usually by endocytosis (Vijayanathan et al. 2002). These reagents are used rapidly in high-throughput assays and can transfer DNA of various sizes (Ewert et al. 2008). However, they can be susceptible to nuclease degradation, are potentially harmful (Colombo et al. 2001) and are usually, but not always, cell cycle-dependent (Brunner et al. 2002).

In the particular case of PC12 cells, cationic lipids formulations have been employed to increase transfection efficiency. Using Lipofectamine 2000 (Invitrogen) the transfection efficiency was about 14 % and was similar to the efficiency obtained with polyethyleneimine (PEI) (15 %) (Lee et al. 2008). A higher efficiency (30 %) was reported with Metafectene Pro (Biontex) (Cogli et al. 2010). An increase in the transfection efficiency (40–50 %) was observed by simultaneous treatment with Lipofectamine and 0.1 μM GALA, a pH-sensitive fusogenic peptide which accelerates the endosomal escape of the plasmid/liposome complexes to the cytosol (Futaki et al. 2005). However, this method has not encountered wide popularity thereafter.

Physical methods, including electroporation, biolistics and injection, are used with varying success and are cell cycle-independent but may be more toxic for some cell types and usually require cell suspensions in vitro and specialized equipment (Villemejane and Mir 2009). However, the electroporation methods enable efficient transfer of exogenous DNA to a large number of cells and serve ideal in terms of material and time consumption. As with chemical methods of transfection, high-efficiency electroporation protocols for PC12 cells are not available. The literature reports efficiencies between 10 and 20 % (Darchen et al. 1995; Akamatsu et al. 1999) and 35 % (Lombardi et al. 2001), which increases to 50 % when parameters are carefully optimized (Espinet et al. 2000).

The aim of this work was to find a protocol ensuring high transfection efficiency in PC12 cells, while retaining viability and ability to differentiate. We compared two electroporation systems (Neon transfection and Gene Pulser Xcell) and three chemical transfection methods (Lipofectamine 2000, Lipofectamine LTX, TransIT-LT1).

Materials and methods

Plasmid

DNA plasmid used for transfection or electroporation was pEGFP-C1 (BD Biosciences Clontech, Palo Alto, CA, USA) driving the expression of an enhanced green fluorescent protein (EGFP) under the control of the CMV promoter. Plasmid was amplified in *Escherichia coli* DH5α; it was isolated and purified using Endo-Maxi Free Kit from QIAGEN. DNA purity and integrity were determined spectroscopically (OD_{260nm}/OD_{280nm} = 1.90–2.00), (OD_{260nm}/OD_{230nm} > 2.00).

Culture of PC12 cells

Rat PC12 cells (ATCC entry CRL-1721) were grown at 37 °C (5 % CO_2) in supplemented DMEM: Dulbecco's modified Eagle's medium with 4.5 % glucose (Lonza, Visp, Switzerland) supplemented with 10 % fetal bovine serum (Gibco, Grand Island, NY, USA), 5 % horse serum (Gibco), 1 mM glutamine (Gibco), 1 mM Penicillin/Streptomycin (Gibco). Cells were seeded onto T-75 cm^2 flasks (Corning, NY, USA) coated with 50 ng/ml poly-D-lysine hydrobromide (Sigma, St. Louis, MO, USA), to achieve 70 % confluence. Cells from passages 8–10 were used. Cells were split every other day at a ratio of about 2:3. A Pasteur pipette was used to de-aggregate cell clusters.

Viable cells counts

A Trypan Blue Stain exclusion test (Invitrogen, Carlsbad, CA, USA) was used to distinguish viable from nonviable cells. The suspended cells (9 μl) were mixed with 1 μl of 0.4 % Trypan Blue Stain and analyzed in the Countess™ Automated Cell Counter (Invitrogen) chamber slide. The percentage of viable cells was calculated as follows: (number of viable cells/total number of cells) × 100.

Lipid-mediated DNA transfection

The transfection reagents used in this study were: TransIT-LT1 Transfection Reagent (Mirus, Madison, WI, USA), Lipofectamine 2000 and Lipofectamine LTX (Invitrogen).

4×10^4 cells/well were seeded on poly-D-lysine-coated 24-well plates (Corning) one day before transfection and grown in supplemented DMEM at 37 °C and 5 % CO_2. PC12 cells grown to 70 % confluence were transfected with the mammalian expression vector pEGFP-C1. Transfection procedures were performed as indicated by manufacturer. The ratio DNA (μg) : transfection reagent (μl) was always 1:3.

Transfection by electroporation

DNA electroporation was performed with the Neon® Transfection System MPK5000 (Invitrogen) or the Gene Pulser Xcell System (BIORAD, Hercules, CA, USA).

For the electroporation with the Neon System, PC12 cells were grown to 70 % confluence in a poly-D-lysine-coated T-25 flask and washed twice with 10 ml Phosphate-Buffered Saline without Ca^{2+} and Mg^{2+}(PBS) (Lonza). This was followed by addition of 1 ml 1× trypsin (Lonza) and incubation for 2 min at 37 °C. After adding 9 ml of supplemented DMEM, the cells were resuspended, transferred in a 15 ml polypropylene tube (Sarstedt, Verona, Italy) and centrifuged at $2.200 \times g$ for 10 min. The pellet was resuspended in 10 ml of PBS and cells were counted in a Bürker chamber (PAUL MARIENFELD GmbH). Cells were pelleted again and re-suspended in Resuspension Buffer R (Neon 10 μl kit Invitrogen) to a final concentration of 1×10^7 cells ml^{-1}. 0.6×10^5 and 1×10^5 cells were transferred to a sterile 1.5 ml microcentrifuge tube (Sarstedt), brought to 10 μl final volume of cell suspension with Buffer R, and mixed with 500 ng of pEGFP-C1 vector. To optimize the best condition of transfection, electroporation was then carried out with different voltage, pulse and time parameters, according to manufacturer's instructions, as reported in Results and Discussion. Cells were seeded in a 24- well poly-D-lysine-coated cell plate with 0.5 ml of pre-warmed supplemented DMEM without antibiotics.

For the electroporation with the Gene Pulser Xcell System, PC12 cells were grown to 70 % confluence in a poly-D-lysine-coated T-75 flask and washed and trypsinized as described above. After adding supplemented DMEM, the cells were resuspended, transferred in a polypropylene tube and centrifuged at $400 \times g$ for 5 min. The pellet was resuspended and counted as above, and re-suspended in an appropriate amount of PBS. 0.4 ml of cell suspension containing 6×10^5 or 1×10^6 cells and 8 μg of DNA (pEGFP-C1 vector), were incubated on ice for 10 min, and transferred into a 4-mm electroporation cuvette (BTX). The Gene Pulser Xcell System (BIORAD) was used for single-cuvette electroporation. Electroporations were carried out with different voltage and capacitance parameters, according to manufacturer's instructions, as reported in Results and Discussion. Cells were seeded in a 12- well poly-D-lysine-coated cell plate with 1 ml of pre-warmed supplemented DMEM without antibiotics.

High-content image acquisition and analysis

Upon chemical transfection or electroporation of pEGFP-C1 vector, EGFP expression and cell nuclei were

visualized using Operetta High Content Imaging System (PERKIN ELMER, Monza, Italy). To count total cell numbers, nuclei were counterstained with Hoechst 33342 (Invitrogen). Forty-eight hours after transfection, cells were washed once with PBS and incubated in 0.5 ml of supplemented DMEM containing 1 mg/ml of Hoechst 33342, for 20 min at 37 °C and 5 % CO_2. Cells were washed once with PBS and replaced with supplemented DMEM without phenol red (Gibco) for imaging. Images were acquired on an Operetta System using a $20\times$ LWD objective in wide-field mode in combination with filters for Hoechst 33342 (excitation filter: 360–400 nm; emission filter: 410–480 nm) and Alexa Fluor 488 (excitation filter: 460–490 nm; emission filter: 500–550 nm). The laser autofocus was applied and 10 image fields were acquired per well. For quantitative analyses, individual cells were segmented based on the Hoechst 33342 nuclear stain using the Find Nuclei building block in the Harmony® High Content Imaging and Analysis Software (PERKIN ELMER) and GFP intensity was quantified within the Hoechst-defined boundaries for each cell. The Select Population module of Harmony allowed to set a fluorescence intensity threshold in order to identify the sub-population of transfected cells and to determine the transfection efficiency. The average and standard error mean (SEM) were calculated from biological experimental triplicates and technical duplicates.

Cell differentiation

Electroporated PC12 cells were plated at a density of 1×10^5 cells/well on poly-D-Lysine-coated 12-well plates and grown in supplemented DMEM without antibiotics at 37 °C in 5 % CO_2. After 24 h the medium was replaced with differentiation medium (Dulbecco's modified Eagle's medium with 4.5 % glucose supplemented with 0.3 % fetal bovine serum, 0.7 % horse serum, 1 mM glutamine) containing 75 ng/ml of NGF 2.5S (Invitrogen). The cells were maintained at 37 °C and 5 % CO_2 and the differentiation medium was replenished every 2nd day for 7 days.

Neurite analysis

Neuronal differentiation was estimated every day, for 7 days, after exposure to NGF 2.5S, by measurement of morphological parameters. Images were acquired using a fluorescence microscope (DFC420C, Leica, Milan,

Italy) and a 20X objective (magnification). Filter A (Exciter BP340–380 nm; Dichromatic Mirror 400 nm) and I3 (Exciter BP450–490 nm; Dichromatic Mirror 510 nm) were used and the images were analysed with ImageJ software (http://imagej.nih.gov/ij/) to determine the neurite length (ImageJ plugin NeuronJ) and to quantify the percentage of differentiated cells. A neurite was defined as a process of length equal to or greater than one time the diameter of the cell body. Triplicate wells were used routinely for each experimental condition. Images of three different fields were taken per well. The experiment was repeated two times.

Statistical analysis

All statistical analyses were performed using Graphpad Prism software package (GraphPad Software, San Diego, CA, USA). Student's t test and One-way analysis of variance (ANOVA) with Bonferroni's multiple comparison were adopted. A single level of 0.05 ($*p < 0.05$) was used, unless otherwise stated. Data are shown with the standard error of the mean (mean ± SEM, n = 3).

Results and discussion

Comparison of transfection chemical methods in PC12 cells

We compared transfection efficiencies obtained in PC12 cells with the lipopolyplex transfection reagent TransIT-LT1 (Mirus) and the cationic lipids Lipofectamine 2000 and LTX (Invitrogen). Cells were grown in conditions promoting proliferation including use of an enriched medium, but the transfections were carried out in a serum- and antibiotic- free environment. We performed these experiments with different amounts of pEGFP-C1 DNA (Clontech), a plasmid driving the expression of an enhanced green fluorescent protein (EGFP) under the control of the CMV promoter. The ratio DNA (μg): transfection reagent (μl) was 1:3 and we transfected increasing amounts of plasmid (0.25, 0.5, 0.75 and 1 μg).

Forty-eight hours after transfection, nuclei were stained with the viable Hoechst 33342 fluorescent dye and images were acquired on an Operetta System, which combines fluorescence microscopy in a multi-well format with automated image acquisition and

quantitative analysis (Fig. 1). Data analysis for transfection efficiency was performed by using the Harmony® High-Content Imaging Software (Perkin Elmer), comparing the number of EGFP-positive cells (detected with an Alexa Fluor 488 filter) to the total number of cells (detected with an Hoechst 33342 filter). Mock transfection controls using the transfection reagent without DNA had an auto-fluorescence background in both the Hoechst 33342 or Alexa Fluor 488 channels comparable to un-transfected PC12 cells (data not shown).

As shown in Fig. 2a, the TransIT-LT1 Transfection Reagent (Mirus) was not effective in facilitating transfection of DNA in PC12 cells, even when a higher concentration of DNA was used. However, in parallel experiments performed on the HEY4 ovarian cancer cell line, TransIT-LT1 had a transfection efficiency of approximately 35 %, thereby indicating that efficiency depends on the cell type (data not shown).

On the contrary, when we performed the transfection experiments by using Lipofectamine LTX and Lipofectamine 2000 we managed to transfect DNA into PC12 cells, with efficiencies that ranged from 7 and 15 % respectively, with 0.25 μg DNA, to 35 and 46 % respectively, when 1 μg of DNA was used.

As expected, transfection efficiency for both reagents correlates with the amounts of DNA used. However, in comparing the transfection efficiency of the two cationic lipids, Lipofectamine LTX seems to perform better than Lipofectamine 2000 at low DNA amounts, while Lipofectamine 2000 outperforms Lipofectamine LTX at higher DNA amounts.

In particular, comparing our results with those by Lee and colleagues (2008), with Lipofectamine 2000 we reached 21 % transfection efficiency (with 0.5 μg of DNA in a 24-well plate) while Lee and collaborators reported 14 % efficiency in similar conditions (1 μg of DNA in a 12-well plate).

Cell viability was measured by Trypan Blue Staining 48 h after transfection (Fig. 2b). Mock-transfected cells had a viability comparable to the non-transfected cells with either of the three transfection reagents (approx. 95 %). For all methods, viability decreased as the DNA amounts increased. However, as clearly indicated in Fig. 2b, there is a variation of trend for different reagents. TransIT-LT1 had a milder impact on cell viability, reaching 92 % when 1 μg of DNA was used. On the contrary, Lipofectamine 2000 and Lipofectamine LTX reached 87–88 % viability in those conditions.

DNA electroporation in PC12 cells

As the transfection efficiency obtained with Lipofectamine 2000 was not sufficient for our purposes, we investigated if we could obtain a higher percentage of transfected PC12 cells with an electroporation method (Neon Transfection System, Invitrogen).

To optimize conditions, 0.5 μg of plasmid DNA and two different cell densities (6×10^4 or 1×10^5 cells/well) were used. Moreover, a range of voltage, pulse width and pulse number combinations were tested (Table 1).
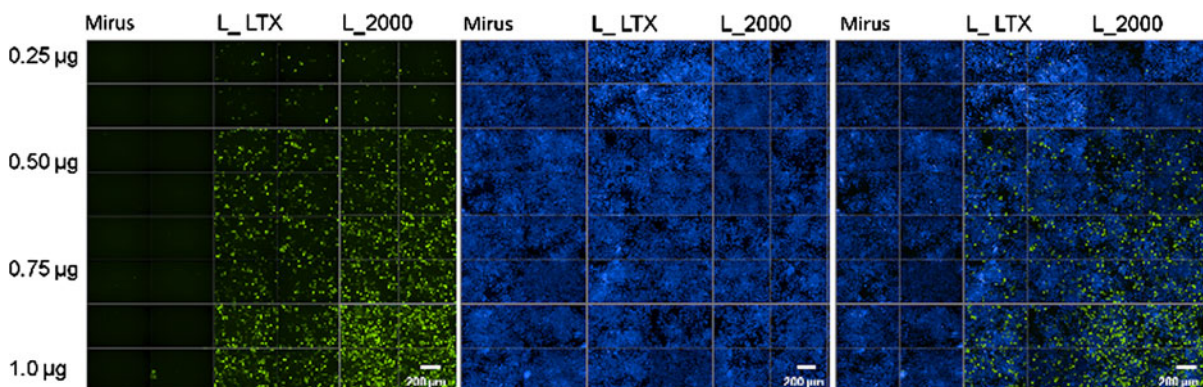
Fig. 1 Transfection of rat PC12 cells. PC12 cells were transfected by liposoluble agents (TransIT-LT1 Transfection Reagent [Mirus], Lipofectamine LTX [L_LTX] and Lipofectamine 2000 [L_2000]) and different concentrations of a plasmid encoding EGFP. Fluorescence images of transfected PC12 cells were analyzed by High-Content screening system (Operetta) 48 h after transfection. The panel shows photographs taken with a *green filter* (*left*) and a *blue filter* (*center*), and the merged images (*right*). Original magnification ×20 (*Scale bars* = 200 μm). (Color figure online)
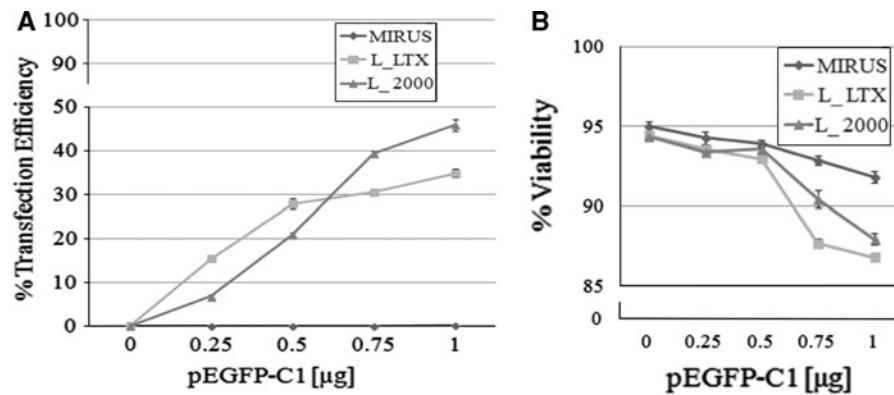
Fig. 2 Transfection efficiency and viability of rat PC12 cells. **a** The percent of transfected cells was calculated by dividing the number of EGFP positive cells by the total population. The best result was obtained by using 1 μg of plasmid and Lipofectamine 2000 (efficiency of transfection 45.9 %). **b** The percentage of viable cells after transfection was measured by a Trypan Blue assay. The best cell viability (93.6 %) was obtained with 0.5 μg of plasmid and Lipofectamine 2000. Data represent mean ± SEM obtained from triplicates

Forty-eight hours after transfection, nuclei were stained with Hoechst 33342 and images were acquired on an Operetta System (Fig. 3). Data analysis of transfection efficiency was carried out as detailed above and revealed that the density of the cells in the suspension is one of the most important variables affecting transfection efficiency in our electroporation protocols (Fig. 4a). In fact, with higher cell density, any electroporation condition tested yields high transfection efficiency, ranging between 80 and 98 %. On the contrary, when a lower cell density was used, conditions can be separated into two classes, based on the effect they have on transfection efficiency: a high-efficiency class (84–91 %) and a low-efficiency class (20–66 %).

It has to be pointed out, however, that all conditions, except one (6×10^4 cells, 1,500 V, 20 ms, 1 pulse), yielded a transfection efficiency higher than

that one obtained by the use of Lipofectamine 2000 (dashed line in Fig. 4a).

The method shows high reproducibility, as determined by comparing efficiencies from several replicate experiments.

Cell viability was measured by Trypan Blue Staining 48 h after transfection (Table 1). Mock-electroporated cells were manipulated as the electroporated cells but did not receive DNA nor an electrical pulse, and had a viability comparable to the non-electroporated cells (approx. 90 %). In the case of cell viability, there was no clear correlation with cell density, although in general cells at higher density performed better (Fig. 4b). Furthermore, different electroporation conditions worked better for the different cell densities, and a general trend could not be inferred from the graph in Fig. 4b. In general, the electroporation protocol appeared to be more pernicious to PC12 cells than the

Table 1 Parameters for DNA electroporation by Neon transfection System, transfection efficiency and cell viability

Pulse voltage (V)	Pulse width (ms)	Pulse no.	Transfection Efficiency (%)		Cell viability (%)	
			0.6×10^5 cells/well	1×10^5 cells/well	0.6×10^5 cells/well	1×10^5 cells/well
Control without electroporation			–	–	90.00	90.00
1,500	20	1	20.33	93.94	63.30	86.70
1,400	30	1	64.37	80.97	38.40	67.70
1,500	10	3	66.20	90.37	54.70	99.00
1,400	10	3	84.63	87.07	64.20	79.70
1,300	30	1	84.37	97.83	86.70	62.87
1,000	40	1	91.32	94.03	24.90	51.70

Fig. 3 Representative images of PC12 cells 48 h after electroporation. Electroporation was carried out using different conditions of voltage (1000, 1300, 1400 or 1500 Volts), pulse width (10, 20, 30 or 40 ms) and pulse number (1 or 3 pulses), as indicated on the left side of the panels. Pictures were taken with the high-content operetta system with a *blue filter* (Hoechst) and a *green filter* (EGFP), and merged (MERGE). Original magnification: ×20 (*Scale bars* = 50 μm). (Color figure online)
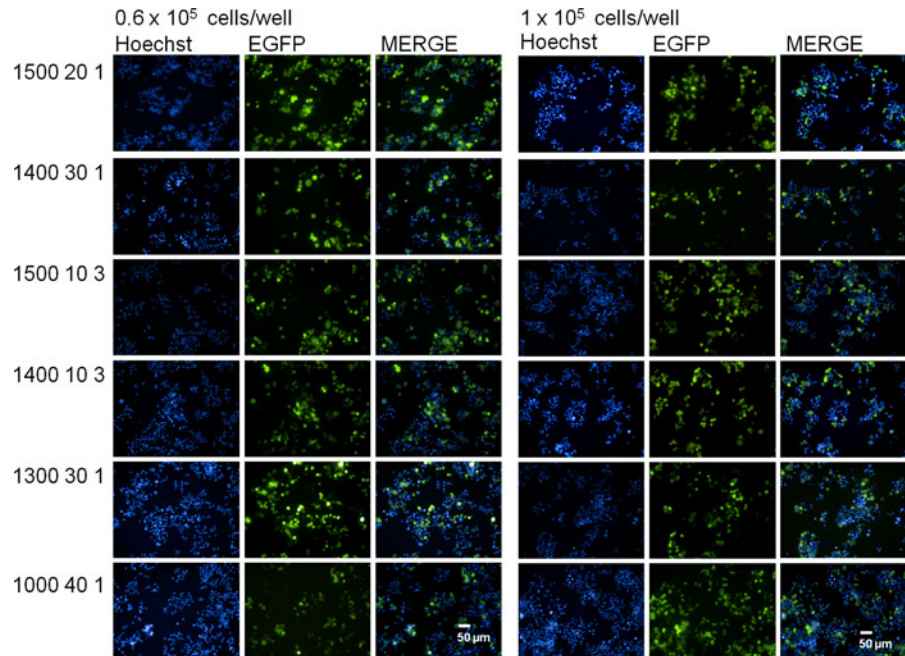
lipofection protocols, as only few conditions provided a cell viability comparable or higher than that one obtained by Lipofectamine LTX and 1 μg of DNA (dashed line in Fig. 4b).

In order to establish if electroporation in general is a better method than lipofection, or if the Neon System in particular has a high performance in transfecting PC12 cells, we performed electroporation with a different system, namely Gene Pulser Xcell (Bio-Rad). 8 μg of plasmid DNA and two different cell densities (6×10^5 or 1×10^6 cells/well) were used. The increase in DNA and cell amounts, compared to Neon System, is due to the fact that, while the Neon system is miniaturized to use electroporation tips and 10 μl transfection volumes, the Gene Pulser XCell requires specific 400 μl cuvettes. For each cell density we tested three different voltage and capacitance combinations (Table 2), in triplicate experiments. Namely, we tried 240 V/1,000 μF (Murphy et al. 2008), 250 V/960 μF (Yaron et al. 2001) and 300 V/500 μF (Lombardi et al. 2001). Analysis of the transfection efficiency and cell viability was carried out as described above. As visible in Fig. 4c and in Table 2, in our hands the Gene Pulser Xcell system outperformed lipofection methods, reaching efficiencies higher than the ones reported in the literature. However, when comparing Gene Pulser Xcell with Neon System, the latter remained the method of choice for the transfection of PC12 cells (Fig. 4a, c). As far as

viability is concerned, though, Gene Pulser Xcell compared to lipofection (Fig. 4d) and was better than Neon System in the majority of conditions.

For our purposes, the best electroporation conditions were obtained with Neon transfection System, 1×10^5 cells/well and 3 pulses of 1,500 V and 10 ms each. These conditions, in fact, yielded 90 % transfection efficiency and 99 % viability. We have chosen these conditions for the subsequent experiments.

Cell differentiation and neurite analysis

With the aim of investigating whether the electroporated PC12 cells retain the ability to differentiate into neuron-like cells, we transfected the cells using the conditions reported above, and treated them with NGF 2.5S (75 ng/ml) starting 24 h after transfection (day 0) and for the subsequent 7 days (Fig. 5a).

Images were taken at 8 h and every 24 h after transfection, in bright field and with a green fluorescence filter (Fig. 5b). NGF-treated PC12 cells showed increase in neurite length and generation during time (Fig. 5b). The total number of cells and the number of cells presenting neurites was counted in the bright-field images. Differentiated PC12 cells progressively increased reaching 23 % of total cells 4 days after induction. At later times the percentage of differentiated cells remained stable (Fig. 5c).
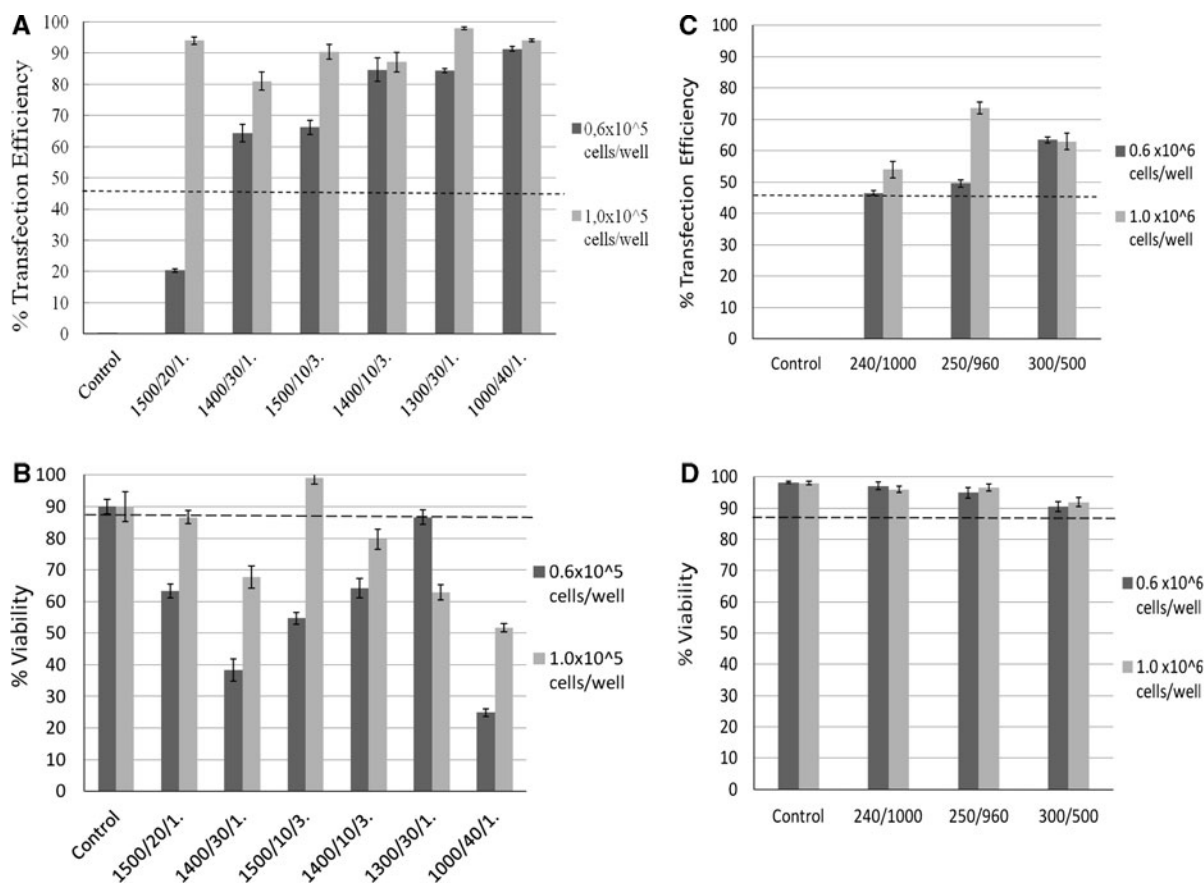
Fig. 4 Optimization of PC12 cells transfection by electroporation. Electroporation was carried out in different conditions which are indicated on the panels' x-axes in the format "voltage (V)/pulse width (ms)/pulse number" for panels A and B, and in the format "pulse voltage (V)/capacitance (μF)" for panels C and D. **a** Histograms of percentages of transfected PC12 cells show an increase of efficiencies comparing Neon electroporation with lipofecting agents. *Dashed line* represents the best transfection efficiency obtained in lipofection experiments as shown in Fig. 2. The best condition (99 %) was obtained by 0.5 μg of plasmid, 1×10^5 cells/well, and 1 pulse of 1,300 Volt and 30 ms. **b** The percentage of viable cells after Neon

electroporation was measured by Trypan Blue Staining. The best cell viability (97.8 %) was obtained with 0.5 μg of plasmid, 1×10^5 cells/well, and 3 pulses of 1,500 Volt and 10 ms each. *Dashed line* represents worst viability percentage obtained in lipofection experiments as shown in Fig. 2. **c** Transfection efficiency of electroporation experiments performed using Gene Pulser Xcell. *Dashed line* represents the best transfection efficiency obtained in lipofection experiments as shown in Fig. 2. **d** Viability of cells electroporated with Gene Pulser Xcell. *Dashed line* represents worst viability percentage obtained in lipofection experiments as shown in Fig. 2. Data represent mean ± SEM obtained from triplicates

Table 2 Electroporation parameters applied for DNA transfection by Gene Pulser Xcell, transfection efficiency and cell viability

Pulse voltage (V)	Capacitance (μF)	Transfection efficiency (%)		Cell viability (%)	
		0.6×10^6 cells/well	1×10^6 cells/well	0.6×10^6 cells/well	1×10^6 cells/well
Control without electroporation		–	–	98.22	97.94
240	1,000	46.54	54.01	97.08	95.98
250	960	49.56	73.58	94.88	96.56
300	500	63.44	62.98	90.42	91.91
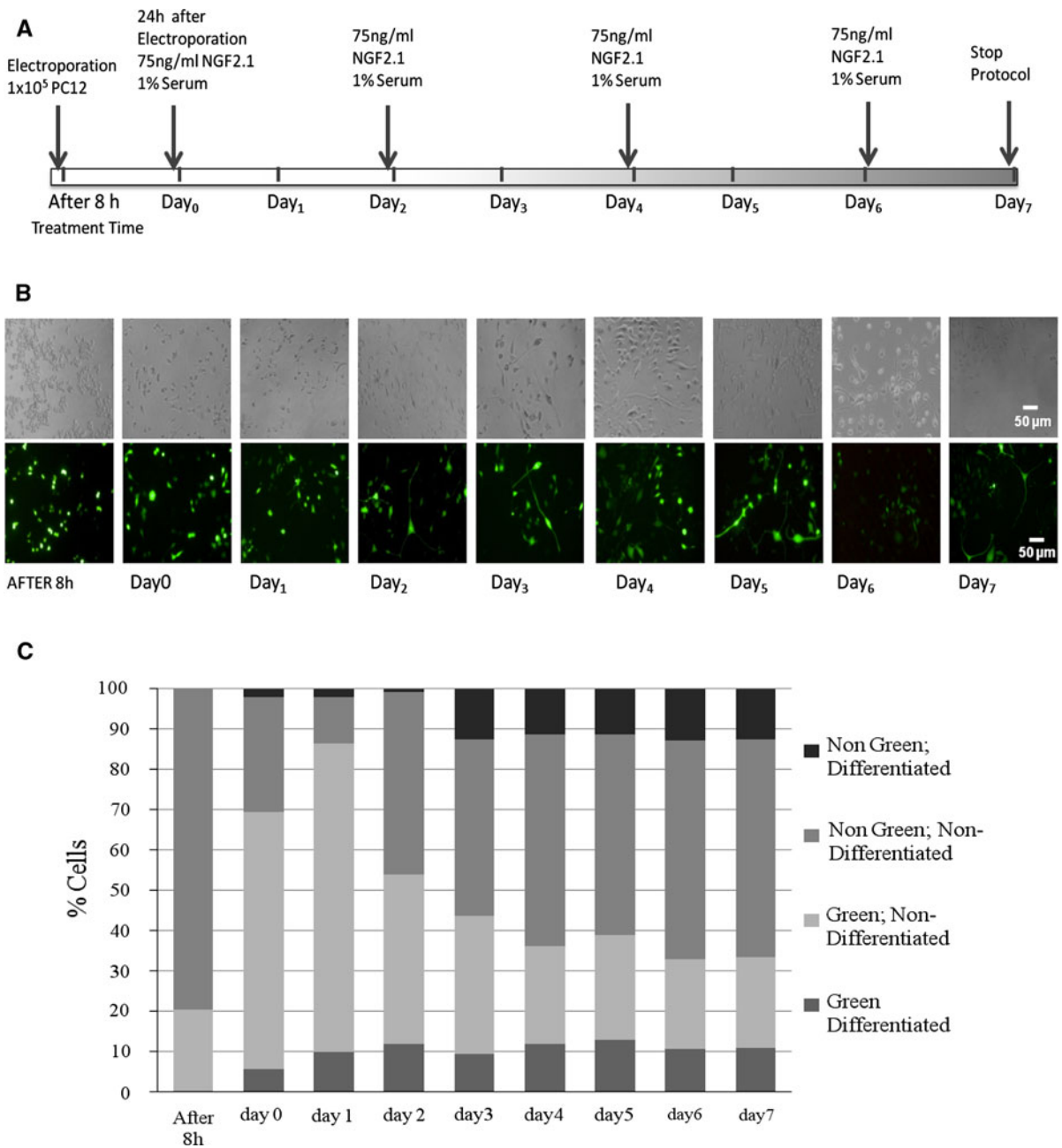
Fig. 5 Differentiation of electroporated PC12 cells. **a** Time course of PC12 differentiation. At each indicated time point, pictures were taken in bright field and in *green* fluorescence, and cells were counted. **b** Representative images of PC12 cells treated with NGF for the indicated time. Original magnification: ×20 (*Scale bars* = 50 μm). **c** Histogram of cell numbers after transfection and differentiation. Cells were grouped in four categories: *green*, differentiated cells; *green*, non-differentiated cells; *non-green*, differentiated cells; *non-green*, non-differentiated cells. Data represent images of three different fields taken per each well. The experiment was repeated two times. (Color figure online)

EGFP expression was observed both in differentiated and non-differentiated cells. The intensity of EGFP signal increased over time. At the initial time point, the intracellular expression of EGFP in NGF-differentiated PC12 cells was located in the nucleus. At later time points, it was around cytoplasm and

inside the nucleus. On the 7th day post-transfection, EGFP was seen throughout the entire cell, spreading out to the tips of the neurite extensions (not shown).

The number of transfected cells was counted in pictures taken with the GFP filter. Already 8 h after electroporation 20 % of cells showed EGFP signal. When NGF was added, 24 h after electroporation, 69 % of cells were EGFP-positive. The maximum transfection efficiency was reached 48 h after electroporation (86 %), and rapidly decreased to reach 33 % at days 6 and 7.

The discrepancy between the maximum transfection efficiency in these experiments and the results described in the previous paragraph (where 90 % of transfection efficiency was obtained) might reflect the change in serum percentages in the growth medium and the addition of NGF, 24 h after transfection.

Electroporation posed no impairment on differentiation ability of PC12 cells, since about half of the differentiated cells were green. On the contrary, our observations suggest that electroporation might even induce PC-12 cells to differentiate. It is remarkable in fact, that approximately 30 % of green cells were presenting neurite outgrowth, from day 4 onwards, while the percentage of differentiated cells in non-green PC-12 cells was about 20 %.

This stimulus to differentiate might explain why at days 0, 1 and 2, green differentiated cells were already present (6, 10 and 12 % of the total cells) while non-green differentiated cells reached comparable percentages (12 %) only at day 3.

Moreover, looking at the actual cell numbers, it appears that at day 2 non-green, non-differentiated cells started outnumbering green, non-differentiated cells, possibly indicating a higher proliferation rate of non-transfected cells, compared to non-transfected cells.

References

Akamatsu W, Okano HJ, Osumi N, Inoue T, Nakamura S, Sakakibara S-I, Miura M, Matsuo N, Darnell RB, Okano H (1999) Mammalian ELAV-like neuronal RNA-binding proteins HuB and HuC promote neuronal development in both the central and the peripheral nervous systems. Proc Natl Acad Sci USA 96:9885–9890

Azzam T, Domb AJ (2004) Current developments in gene transfection agents. Curr Drug Deliv 1:165–193

Brunner S, Furtbauer E, Sauer T, Kursa M, Wagner E (2002) Overcoming the nuclear barrier: cell cycle independent nonviral gene transfer with linear polyethylenimine or electroporation. Mol Ther 5:80–86

Cogli L, Progida C, Lecci R, Bramato R, Kruuttgen A, Bucci C (2010) CMT2B-associated Rab7 mutants inhibit neurite outgrowth. Acta Neuropathol 120:491–501

Colombo MG, Citti L, Basta G, De Caterina R, Biagini A, Rainaldi G (2001) Differential ability of human endothelial cells to internalize and express exogenous DNA. Cardiovasc Drugs Ther 15:25–29

Darchen F, Senyshyn J, Brondyk WH, Taatjes DJ, Holz RW, Henry J-P, Denizot J-P, Macara IG (1995) The GTPase Rba3a is associated with large dense core vesicles in bovine chromaffin cells and rat PC12 cells. J Cell Sci 108:1639–1649

Dhar S, McConnell MP, Gharibjanian NA, Young CM, Rogers JM, Nguyen TD, Evans GR (2007) Herpes simplex virus-thymidine kinase-based suicide gene therapy as a molecular switch off for nerve growth factor production in vitro. Tissue Eng 13:2357–2365

Douglas KL (2008) Toward development of artificial viruses for gene therapy: a comparative evaluation of viral and non-viral transfection. Biotechnol Prog 24:871–883

Eliyahu H, Barenholz Y, Domb AJ (2005) Polymers for DNA delivery. Molecules 10:34–64

Espinet C, Gómez-Arbonés X, Egea J, Comella JX (2000) Combined use of the green and yellow fluorescent proteins and fluorescence-activated cell sorting to select populations of transiently transfected PC12 cells. J Neurosci Methods 100:63–69

Ewert KK, Ahmad A, Bouxsein NF, Evans HM, Safinya CR (2008) Non-viral gene delivery with cationic liposome-DNA complexes. Methods Mol Biol 433:159–175

Fujita K, Lazarovici P, Guroff G (1989) Regulation of the differentiation of PC12 pheochromocytoma cells. Environ Health Perspect 80:127–142

Futaki S, Masui Y, Nakase I, Sugiura Y, Nakamura T, Kogure K, Harashima H (2005) Unique features of a pH-sensitive fusogenic peptide that improves the transfection efficiency of cationic liposomes. J Gene Med 7(11):1450–1458

Godbey WT, Wu KK, Mikos AG (1999a) Poly (ethylenimine) and its role in gene delivery. J Control Release 60:149–160

Godbey WT, Wu KK, Mikos AG (1999b) Tracking the intracellular path of poly (ethylenimine)/DNA complexes for gene delivery. Proc Natl Acad Sci USA 96:5177–5181

Grau CM, Greene LA (2012) Use of PC12 cells and rat superior cervical ganglion sympathetic neurons as models for neuroprotective assays relevant to Parkinson's disease. Methods Mol Biol 846:201–211

Greene LA (1978) Nerve growth factor prevents the death and stimulates the neuronal differentiation of clonal PC12 pheochromocytoma cells in serum-free medium. J Cell Biol 78:747–755

Greene LA, Tischler AS (1976) Establishment of a noradrenergic clonal line of rat adrenal pheochromocytoma cells which respond to nerve growth factor. Proc Natl Acid Sci USA 73:2424–2428

Lee JH, Ahn HH, Kim KS, Lee JY, Kim MS, Lee B, Khang G, Lee HB (2008) Polyethyleneimine-mediated gene delivery into rat pheochromocytoma PC-12 cells. J Tissue Eng Regen Med 2:288–296

Lombardi D, Palescandolo E, Giordano A, Paggi MG (2001) Interplay between the antimetastatic nm23 and the Retinoblastoma-related Rb2/130 genes in promoting neuronal differentiation of PC12 cells. Cell Death Diff 8:470–476

Marples B, Dachs GU (2002) Cancer gene therapy: "delivery, delivery, delivery". Front Biosci 7:d1516–d1524

Murphy KL, Zhang X, Gainetdinov RR, Beaulieu J-M, Caron MG (2008) A regulatory domain in the N-terminus of tryptophan hydroxylase 2 controls enzyme expression. J Biol Chem 283:13216–13224

Nagase H, Yamakuni T, Matsuzaki K, Kasahara J, Hinohara Y, Kondo S, Mimaki Y, Sashida Y (2005) Mechanism of neurotrophic action of nobiletin in PC12D cells. Biochemistry 25:13683–13691

Park IK, Lasiene J, Chou SH, Horner PJ, Pun SH (2007) Neuron-specific delivery of nucleic acids mediated by Tet1-modified poly(ethylenimine). J Gene Med 9:691–702

Rukenstein A, Rydel R, Greene L (1991) Multiple agents rescue PC12 cells from serum-free cell death by translation- and transcription independent mechanisms. J Neurosci 11:2552–2563

Schaefer T, Karli UO, Scweizer FE, Burger MM (1987) Docking of chromaffin granules-a necessary step in exocytosis? Biosci Rep 7:269–279

Seth K, Agrawal AK, Aziz MH, Ahmad A, Shukla Y, Mathur N, Seth PK (2002) Induced expression of early response genes/oxidative injury in rat Pheochromocytoma (PC12) cell line by 6-hydroxydopamine: implication for Parkinson's disease. Neurosci Lett 330:89–93

Vijayanathan V, Thomas T, Thomas TJ (2002) DNA nonaparticles and development of DNA delivery vehicles for gene therapy. Biochemistry 41:14085–14094

Villemejane J, Mir LM (2009) Physical methods of nucleic acid transfer: general concepts and applications. Br J Pharmacol 157:207–219

Wang R, Zhou J, Tang XC (2002) Tacrine attenuates hydrogenperoxide-induced apoptosis by regulating expression of apoptosis-related genes in rat PC12 cells. Brain Res Mol Brain Res 107:1–8

Yaron Y, McAdara JK, Lynch M, Hughes E, Gasson JC (2001) Identification of novel functional regions important for the activity of HOXB7 in mammalian cells. J Immunol 166:5058–5067

Exon-Skipping Antisense Oligonucleotides to Correct Missplicing in Neurogenetic Diseases

Kavitha Siva,[1,*] Giuseppina Covello,[1,*] Michela A. Denti[1,2]

Alternative splicing is an important regulator of the transcriptome. However, mutations may cause alteration of splicing patterns, which in turn leads to disease. During the past 10 years, exon skipping has been looked upon as a powerful tool for correction of missplicing in disease and progress has been made towards clinical trials. In this review, we discuss the use of antisense oligonucleotides to correct splicing defects through exon skipping, with a special focus on diseases affecting the nervous system, and the latest stage achieved in its progress.

Introduction

ALTERNATIVE SPLICING IS THE PROCESS by which exons of primary transcripts can be spliced into alternative arrangements to produce structurally and functionally different messenger RNA (mRNA) and protein variants. The splicing process can be regulated by different *cis*- and *trans*-acting factors that influence splice site selection (Johnson et al., 2009). Point mutations in a gene may weaken or strengthen splice sites; enhancer or silencer elements or lead to their destruction. This in turn causes alteration of splicing events and consequent disease.

Additionally, most eukaryotic genes contain several pseudoexons, sequences resembling perfect exons, which are nonetheless ignored by the splicing machinery (Dhir and Buratti, 2010). Aberrant pseudoexon inclusion due to deep intronic mutations has been uncovered in recent years as a frequent cause of human diseases. When a pseudoexon inclusion leads to premature insertion of a termination codon in the mRNA, the term ''nonsense exon'' is used, also indicating that the mRNA undergoes rapid degradation by nonsense-mediated decay (NMD) pathways (Dhir and Buratti, 2010).

It has been observed that 50% of human genetic diseases arise due to mutation that affect the splicing process, including numerous that are associated with neurogenetic diseases (Matlin et al., 2005; Mills et al., 2012). The brain, in fact, being the most complex organ, expresses a relatively higher number of alternatively spliced genes, some of which were found to be linked to neurological and neurodegenerative diseases. Because these diseases cannot presently be cured and are degenerative, they place a great burden on caregivers and represent some of the most costly diseases for society.

Antisense Oligonucleotide-Mediated Splicing Modulation

The most widely studied gene therapy approach for the correction of aberrant splicing is the use of antisense oligonucleotides (AONs) that target the pre-mRNA. AONs are short synthetic modified nucleic acids that bind RNA through base pairing and enable modulation of its expression (Southwell et al., 2012). (For a thorough overview on the applications of antisense-mediated exon skipping, see van Roon-Mom and Aartsma-Rus, 2012).

Design of AONs that can bind to splice sites or to exonic or intronic enhancing *cis*-regulatory sequences in the pre-mRNA [exonic splice enhancers (ESEs) or intronic splice enhancers (ISEs)] leads to masking of these regions and the inability of *trans*-splicing regulatory factors to bind effectively, thus inducing switching between alternative splice isoforms via exon skipping (Fig. 1). In the same way, by masking of cryptic splice sites, AONs have been used for the correction of cryptic splicing.

As point mutation or deletions can disrupt the open reading frame in a transcript, AONs have also been used to induce the skipping of one or more additional exons, to restore the transcript reading frame, allowing the production of an internally deleted, but sometimes (partially) functional protein (Turczynski et al., 2012). This strategy has its most advanced examples in the exon skipping approaches to the treatment of Duchenne muscular dystrophy (DMD, Aartsma-Rus, 2012).

Further, AONs-mediated exon skipping can also be used to induce reading frame disruption and protein knockdown (Disterer and Khoo, 2012). However, to achieve a robust therapeutic effect, it is essential that sufficient amounts of AONs are taken up specifically by the tissue affected by the

FIG. 1. Methods of antisense oligonucleotide-mediated modification of splicing: **(A)** Alternative exon: antisense oligonucleotides (AONs) directed toward splice sites or exonic enhancers induce exon skipping. **(B)** Pseudoexon: AONs directed toward cryptic splice sites restore the normal transcript. **(C)** Nonsense exon: AONs targeting cryptic splice sites of nonsense exons restore normal transcripts. **(D)** Exonic cryptic splice site: AONs, targeting the exonic cryptic splice site, restore normal splicing.
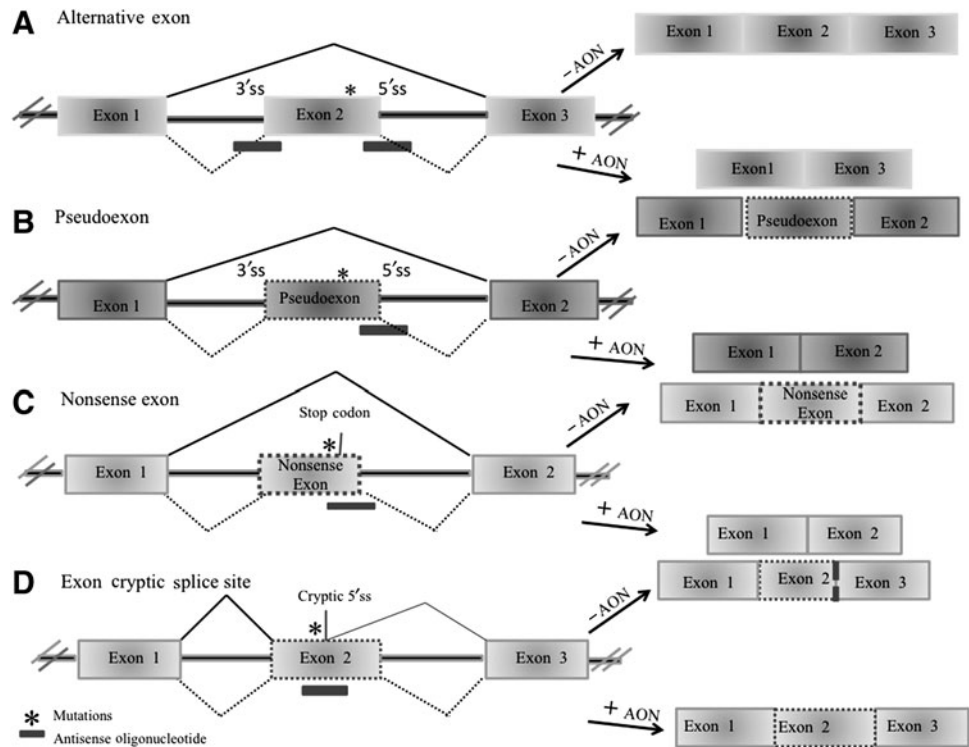
disease, which is often not the case. Moreover, other techniques such as RNA interference have shown higher efficacy and feasibility. On the other hand, protein knockdown via exon skipping may exhibit advantages over other techniques that simply knock down gene expression: the alternative isoforms may have dominant negative behavior towards the normal isoform, present additional therapeutic properties, or may avoid side effects that are associated with near total downregulation of the normal isoform.

In principle, AONs appropriately targeted to block exonic or intronic splicing silencers (ESSs or ISSs) can also restore exon inclusion in the context of disease-associated exon skipping. The exon-inclusion strategy has proven effective *in vitro* and *in vivo* as a possible therapy for spinal muscular atrophy (SMA), as extensively described in recent reviews (Hua and Krainer, 2012; Douglas and Wood, 2013).

Notably, most advanced AON-mediated exon skipping approaches are clinical phase 3 trials for DMD (Arechavala-Gomeza et al., 2012) and earlier clinical trials are in preparation for SMA (Porensky and Burges, 2013).

Different Oligonucleotide Chemistries are Available for the Correction of Splicing

The currently used AONs are rarely regular RNA or DNA oligonucleotide, as alternative AON chemistries have been developed to improve affinity, boost stability in the circulation and in target cells, and enhance cell penetration and nuclear accumulation. This issue will be here only briefly outlined and the reader is referred to (Saleh et al., 2012) for a more complete discussion of AON chemistry.

The non-bridging oxygen in the phosphate backbone has been replaced with a sulfur atom, generating phosphorothioate (PS) AONs (De Clercq et al., 1969). This modifi-

cation enhances cellular uptake and improves resistance to nucleases but reduces the affinity of the AON to the target RNA. Moreover, the PS modification does not abrogate the ability, proper of DNA oligos, to induce RNase H cleavage of the target RNA.

Addition of a methyl or a methoxyethyl group to the 2′-O atom of the ribose sugar (2′OMe and 2′OMOE, respectively) renders the AON–target RNA hybrid RNase H-resistant and increases the affinity of the AON for the target RNA (Sproat et al., 1989; Manoharan et al., 1999). Most AONs currently under study for splicing corrections have both the 2′O and the phosphorothioate (PS) modification (2′OMe-PS and 2′OMOE-PS), probably because they have a good safety profile and their synthesis is relatively inexpensive.

2′OMe-PS were the first AONs to be used for exon skipping (Sierakowska et al., 1996; Khang et al., 1998) and the first to be used for dystrophin exon skipping in cultured primary muscle cells from *mdx* dystrophic mice (Dunckley et al., 1998). Some years later, exon skipping and dystrophin protein recovery was demonstrated upon delivery of 2′OMe-PS into *mdx* mice, aided by the nonionic block copolymer pluronic F127, and injected either locally in skeletal muscles (Lu et al., 2003) or systemically via tail vein (Lu et al., 2005). 2′OMe-PS AONs targeting dystrophin exon 51 (GSK-2402968/PRO051/drisapersen) have proven successful in intramuscular clinical trials in DMD patients (van Deutekom et al., 2007) and have demonstrated significant dystrophin restoration, good safety and tolerance in systemic clinical trials (Goemans et al., 2011).

2′OMOE-PS AONs have been used in cell lines to redirect splicing of murine interleukin-5 receptor alpha chain (il5rα, Karras et al., 2000) and of myD88 (Vickers et al., 2006) and to correct aberrantly spliced reporter enhanced green fluorescent protein (EGFP; Sazani et al., 2001). Importantly,

2′OMOE-PS have been recently used successfully for exon inclusion of the *SMN2* gene as a potential approach for the treatment of SMA in cultured cells (Hua et al., 2007) and *in vivo* by intracerebroventricular (ICV) infusion or injection in a mouse model of SMA (Hua et al., 2010). In this latter work, a side-by-side comparison was also made between an 18-mer 2′OMOE-PS and an overlapping 20-mer 2′OMe-PS AON. The 2′OMOE-PS was found to be more effective after ICV infusion into adult mice central nervous system (CNS) and to elicit less unwanted proinflammatory effects (Hua et al., 2010).

In a different available oligonucleotide chemistry, a methylene bridge connects the 2′-O and the 4′-C of the ribose, forcing the nucleotide in the "endo" conformation, in what has been dubbed "locked nucleic acid" (LNA; Obika et al., 1998). This modification leads to a very high affinity for the target nucleic acid.

Aartsma-Rus and colleagues (2004) reported that an AON completely made of LNA was very effective for exon skipping in cells derived from an exon 45-deleted DMD patient. However, this AON also showed reduced specificity, probably due to the very high affinity of the 14-mer LNA with the target (Aartsma-Rus et al., 2004). In the applications that use oligonucleotides as steric inhibitors, the specificity issues associated with LNA have been solved by using a mixmer of LNA and DNA backbone sequence (Elayadi et al., 2002) or LNA and 2′OMe backbone (Arzumanov et al., 2001; Fabani and Gait, 2008). Roberts and colleagues (2006) have shown that upon intraperitoneal (IP) injection in the EGFP splice-switching mouse model, a 16-mer LNA/DNA mixmer containing 8 LNA units alternating with the DNA units, and with an all-PS backbone, showed much higher potency in the liver, colon, and small intestine than an overlapping 2′OMe 18-mer AON (Roberts et al., 2006).

In addition to the described negatively charged oligonucleotides (2′OMe-PS, 2′OMOE-PS, and LNA), two more oligonucleotide chemistries have been used in attempts to modulate splicing: peptide nucleic acids (PNAs) and phosphorodiamidate morpholino oligomers (PMOs). Both these types of charge-neutral oligonucleotides are resistant to exo- and endonucleases and RNase H cleavage.

PNAs have a 2-aminoethyl glycine backbone linked to nucleobases (Larsen et al., 1999) and show high affinity to both RNA and DNA targets and good sequence specificity (Egholm et al., 1993). It is common to incorporate additional cationic lysine residues in the PNA oligonucleotide, to get good water solubility, and to improve cell entry by facilitating the binding to the negatively charged surface of cells. Karras and colleagues have shown that a 15-mer PNA containing a single C-terminal Lys residue had similar efficiency as a 2′OMOE-PS AON in modulating the splicing of the IL5R-α pre-mRNA when electroporated into BCL1 lymphoma cells (Karras et al., 2001). In the absence of a transfection agent, an 18-mer PNA containing four Lys residues (PNA-4Lys) was shown to be taken up by HeLa cells better than a PNA of identical sequence with one Lys residue only and to modulate reporter EGFP splicing (Sazani et al., 2001). In the same conditions, 2′OMe-PS and 2′OMOE-PS AONs of identical sequence were not able to induce splicing correction (Sazani et al., 2001). The same PNA-4Lys 18-mer, when IP-injected in the splice-switching EGFP mouse, was very effective in inducing EGFP production in a number of organs,

such as kidney, liver, heart, and lung, whereas the PNA with only a single Lys residue was inactive (Sazani et al., 2002).

However, a PNA-4Lys 14-mer was not effective in inducing dystrophin exon skipping in exon-45-deleted DMD patient myoblasts (Aartsma-Rus et al., 2004), probably due to its short length.

A 20-mer PNA without Lys addition was shown to be moderately effective in dystrophin exon skipping in the *mdx* mouse model upon local muscle injection (Yin et al., 2008a). The same authors showed recently that, upon tail vein injection into *mdx* mice, a 25-mer PNA without Lys is more effective than the 20-mer PNA in dystrophin exon skipping and doses up to 100 mg/kg were well tolerated (Yin et al., 2010).

PMOs consist of morpholine rings that are connected through phosphorodiamidate groups (Summerton and Weller, 1997). Generally, PMOs used are longer than 2O′Me-PS AONs due to their slightly lower affinity. Schmajuk and colleagues (1999) have shown that a PMO 18-mer was 20-fold more effective than a corresponding 2′OMe-PS 18-mer in modulating splicing in free uptake in cell culture (Schmajuk et al., 1999).

As PMOs are charge neutral, they are difficult to transfect. Gebski and colleagues (2003) successfully transfected PMOs in *mdx* mouse muscle cells in combination with a sense oligo (leash) and Lipofectin, to allow formation of a cationic lipoplex. In these cells they showed efficient dystrophin exon skipping with a 25-mer PMO, and exon skipping and dystrophin production was also observed by intramuscular injection of the cationic lipoplex in the *mdx* mouse (Gebski et al., 2003). The same PMO 25-mer was also effective in generating dystrophin in a number of muscle types when injected intravenously and uncomplexed in mdx mice (Alter et al., 2006). Direct comparisons in the *mdx* mouse of the PMO 25-mer to a 2′OMe-PS of identical sequence and length, suggested that PMO generates higher exon skipping and dystrophin production upon both local and systemic delivery than 2′OMe-PS (Fletcher et al., 2006). However, leash transfection of a 22-mer PMO into exon 45-deleted DMD patient's muscle cells did not result in as good exon skipping as for a 20-mer 2′OMe-PS ON (Aartsma-Rus et al., 2004). The reason for these discrepancies might be different effectiveness of 2′OMe-PS and PMO AONs depending on the target exon sequence as well as on AON length, as also suggested by exon skipping studies in a range of human exons in humanized DMD mice (Heemskerk et al., 2009).

A PMO 30-mer targeting dystrophin exon 51 (AVI-4658/eteplirsen) has proven successful in intramuscular clinical trials (Kinali et al., 2009). In recent systemic studies, eteplirsen has demonstrated significant dystrophin restoration, good safety, and tolerance (Cirak et al., 2011).

To facilitate delivery into cells *ex vivo* and *in vivo,* different cell-penetrating peptides (CPPs) have been conjugated to PMOs, yielding pPMOs (peptide-conjugated PMOs). While toxicity has been associated with moderate doses of the peptide conjugates (Abes et al., 2006; Burrer et al., 2007), pPMOs have been used *in vivo* for effective oligo delivery at doses below those causing observed toxicity (Amantana et al., 2007). The systemic injection of a pPMO conjugated to different Arg-rich peptides and targeting exon 23 led to dramatic enhancement of dystrophin production and exon skipping in the skeletal muscles and heart of *mdx* mouse

(Jearawiriyapaisarn et al., 2008; Wu et al., 2008; Yin et al., 2008b, 2009, 2011; Wu et al., 2012).

In a different approach, a non-peptidic cell-penetrating moiety, consisting in an octaguanidinium dendrimer, has been attached to the 3′ end of a PMO (Li and Morcos, 2008). Such delivery-enabled PMOs, called ''vivo-morpholinos,'' are efficiently uptaken in cells (Li and Morcos, 2008) and have been successfully injected systemically in *mdx* mice showing good activity in exon skipping and dystrophin production and no signs of toxicity at the injected doses (Wu et al., 2009).

Success in the preclinical studies involving exon-skipping treatment of DMD has prompted studies aimed at extending the range of application of these antisense oligonucleotides from neuromuscular to many other genetic diseases. In the following pages, we will review AON-mediated exon skipping treatments that have been studied in relation to the central nervous system (CNS) and for neurogenetic diseases.

Exon Skipping as a Therapeutic Approach for Neurogenetic Diseases

Ataxia telangiectasia

Ataxia telangiectasia (AT) is a progressive autosomal recessive neurodegenerative disorder resulting from mutations in the ataxia telangiectasia mutated (*ATM*) gene (Perlman et al., 2003). To date, close to 600 ATM mutations have been identified (www.hgmd.cf.ac.uk/ac/gene.php?gene=ATM). The phenotypic changes include progressive cerebellar ataxia, increased cancer incidence, and chromosome instability (Teraoka et al., 1999). Worldwide incidence for this disease is estimated at 1 in 40,000 to 1 in 100,000 individuals. Disease onset is in early childhood, usually before age 5.

The *ATM* gene (located on chromosome 11q22.3) includes 66 exons and encodes a 13-kb mature transcript with an open reading frame of 9,168 nt. The first two exons, 1a and 1b, are spliced differentially in alternative transcripts. The ATM protein is a serine/threonine kinase with 30 phosphorylation targets (Bakkenist et al., 2003) constitutively expressed in all tissues, primarily in the nucleus. It has a role in the control of cell cycle checkpoints, repair of double-stranded DNA breaks, responses to oxidative stress and apoptosis, and is a potent tumor suppressor.

Approximately half of the mutations in AT have been reported as splicing mutations (Teraoka et al., 1999; Nakamura et al., 2012; Cavalieri et al., 2013) that either create new cryptic splice sites or interfere with splice regulatory elements. Some of these mutations elicit the activation of 5′ or 3′ cryptic splice sites within exonic regions, leading to the deletion of a part of the exon. Du and colleagues designed a customized mutation-based approach for AT by transfecting antisense PMOs in immortalized lymphoblastoid cell lines from three different AT patients (Du et al., 2007). Cell line TAT[C] is homozygous for the mutation 7865C>T (A2622V) that creates a new 5′ splice site in exon 55. This, in turn, results in the deletion of 64 nt in the spliced mRNA, frameshifting, and the appearance of a premature stop codon. The ATM protein produced is therefore shorter and possibly the mutated mRNA would undergo NMD. Cell line IRAT9 is homozygous for the mutation 513C>T (Y171Y), which activates a stronger 3′ cryptic splice site within exon 8, resulting in a deletion of the first 22 nt of exon 8, frameshifting and the appearance of a premature stop codon. This in turn causes the ATM protein to be truncated. Cell line AT203LA carries in heterozygosis the mutation IVS28-159 A>G, that results in the insertion of a 112-nt segment of intron 28 in the mRNA, frameshifting, and premature translation termination (Fig. 2).

For TAT[C] and IRAT9 cells, PMOs were designed to mask the aberrantly activated cryptic splice sites (Fig. 2A, B), and correction was observed at transcriptional level with a 40% of pre-mRNA being spliced in the normal manner. PMOs could redirect aberrant splicing as early as 8 hours after treatment and this effect lasted at least 84 hours. The maximum effect, however, occurred at 48 hours. At the protein level, less than 10% ATM protein was induced at 24 hours of treatment, as compared with the ATM protein level in controls and as measured by western blots on nuclear extracts. However, the ATM protein level continued to increase until 84 hours, and the restored ATM protein was functional for kinase activity, as evaluated by ATM autophosphorylation and downstream transactivation of ATM substrates p53 and SMC1.

For the AT203LA cell line, two different PMOs were designed, one targeting the 3′splice site and one targeting the 5′ splice site of the pseudoexon (Fig. 2C). Only the latter PMO showed effective blocking of pseudoexon inclusion and almost completely restored normal splicing, as evaluated both at the mRNA and protein levels.

The most debilitating feature of AT is the progressive loss of Purkinje cells in the cerebellum and the accompanying progressive ataxia. Therefore, for any compound to be effective in treating AT patients, it will have to cross the blood–brain barrier (BBB) and target brain cells, particularly Purkinje cells. Following their study in cells, Du and colleagues further extended the exon skipping strategy into preclinical studies, by investigating whether the coupling of an arginine-rich CPP to PMOs could enable their delivery to brain and cerebellum (Du et al., 2011). They showed that the targeting efficiency of these pPMOs is greatly improved in *ex-vivo* experiments, compared with PMOs of identical sequence: when the pPMO were tested on previously established cell lines (TAT[C], AT203LA) a complete abolishment of mutant transcripts along with 80% correction of ATM protein level was observed. This work was extended to the *in vivo* systemic administration of fluorescent pPMOs in wild type mice, via tail vein injection, which showed efficient uptake in the brain, and in Purkinje cells in particular (Du et al., 2011). However, no report is presently available on the *in vivo* exon-skipping efficacy of these pPMOs.

Nakamura and colleagues studied *ATM* mutations in eight families of Japanese AT patients (JPAT) where 16 different mutations were found. Six of these mutations were involved in splicing, four of which were novel (Nakamura et al., 2012). Their exon-skipping analysis was performed on lymphoblastoid cell lines of patients JPAT 11/12 bearing a splicing mutation (c.2639-384A>G) in heterozygosity with a large deletion (c.6807+272_7516-275del5350). Mutation c.2639-384A>G creates a cryptic 5′ splice site resulting in the inclusion of a 58-nt pseudoexon (Fig. 2D). This leads to a frameshift and a predicted secondary premature stop codon. They used a PMO (AMO-J11) to target the cryptic 5′ splice site, and delivered it to patient's lymphoblastoid cell line via the Endo-Porter system (Summerton, 2005). A complete ablation of mutant transcript was observed by reverse
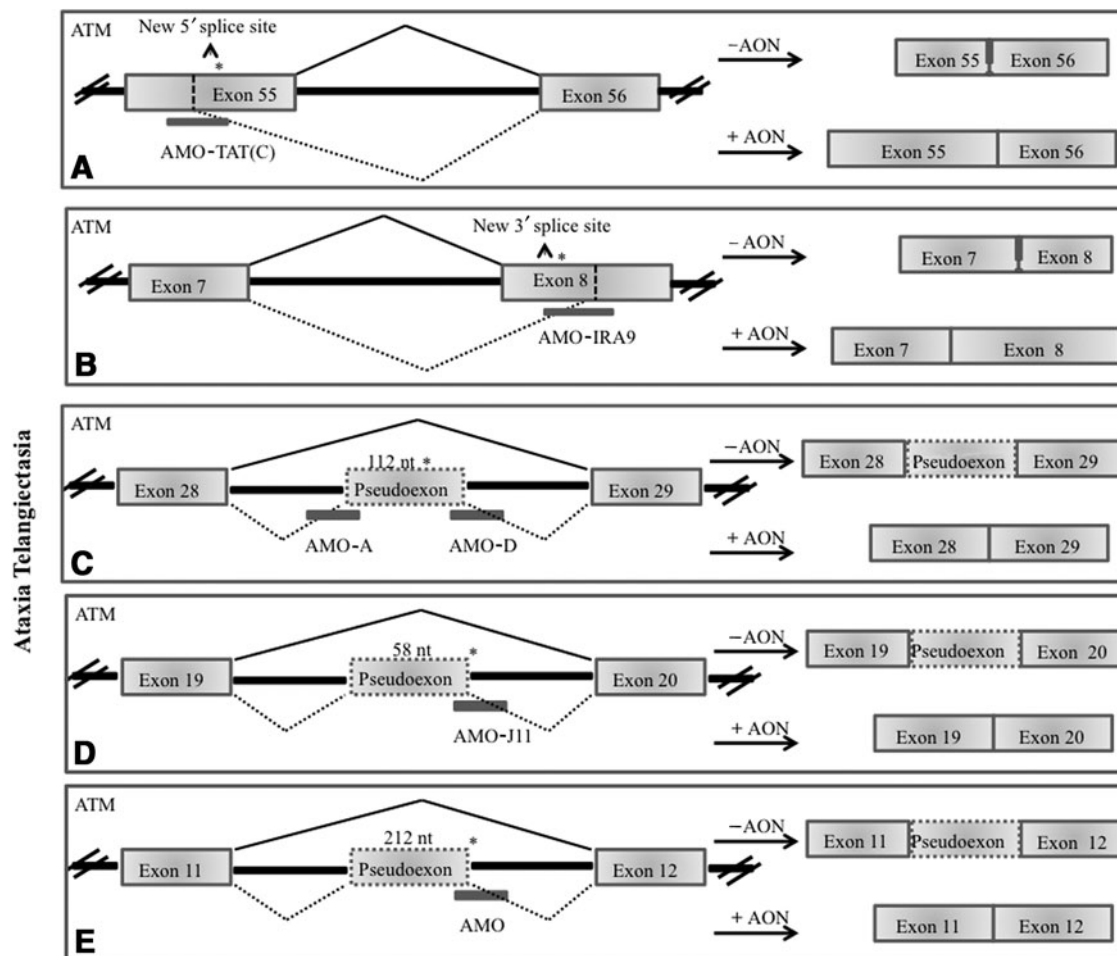
FIG. 2. Schematic representation of five splicing mutations identified in the ataxia telangiectasia mutated (*ATM*) gene, and locations of blocking antisense oligonucleotides that restore normal splicing (Du et al., 2007, 2011; Nakamura et al., 2012; Cavalieri et al., 2013).

transcription–polymerase chain reaction (RT-PCR), in a PMO dose-dependent manner, and the full-length ATM protein was recovered. They also used a vivo-morpholino of identical sequence, which was able to induce a significant amount of functional protein at lower concentrations than the PMO, as validated by the western blot (Nakamura et al., 2012). However, authors report possible cytotoxic effects of the vivo-morpholino at the used concentration, on the lymphoblastoid cell line.

In a recent work, Cavalieri and colleagues identified a new *ATM* mutation c.1236-405C>T located in intron 11, which affects splicing by creating a novel cryptic 5′ splice site, thus including a pseudoexon (Cavalieri et al., 2013). Patients bear the mutation in heterozygosis with the known missense mutation c.6326G>A. Cavalieri and colleagues (2013) used a PMO to mask the 5′ cryptic splice site created by the mutation (Fig. 2E) in patient's lymphoblasts and reported a 26% increase of the correctly spliced mRNA as observed by RT-PCR, when cells were treated with 50 μM PMO. Moreover, they used a vivo-morpholino of identical sequence and showed in patient's lymphoblasts an exon skipping efficiency of 50% to 95%, depending on AON concentrations used (1 μM or 2 μM). At these concentrations, the authors also report a cytotoxic effect of vivo-morpholinos, after 84 hours

of treatment. The functional protein activity determined through kinase activity was 50% of wild-type levels. Since AT patients with 5% to 20% of functional ATM have a mild AT phenotype, and *ATM* heterozygotes having 40% to 50% of normal ATM protein levels do not show any sign of disease, Cavalieri and colleagues have hypothesized that even a minimal rescue of functional ATM protein levels could provide therapeutic benefit to these patients.

Congenital disorder of glycosylation

Congenital disorder of glycosylation (CDG) is an autosomal recessive disorder that affects glycan synthesis. The most prevalent form of CDG, type 1a, has an incidence of 1 in 50,000 to 1 in 100,000 individuals, and is caused by mutations in *PMM2* gene, which is located on chromosome 16p13 and gene encodes phosphomannomutase 2 (PMM2), a key enzyme that controls the synthesis of GDP-mannose and is essential for the generation of N-glycans. Mutations in the *PMM2* gene lead to the hypoglycosylation of different proteins in different tissues (Dupré et al., 2000). CDG involves multi organ failure, but also leads to neurologic deficits including cognitive impairment, ataxia, pigmentary retinal degeneration, and neuropathy (Pearl et al., 2001). Clinical

presentation and course are highly variable, ranging from infants who die in the first year of life to mildly involved adults. N-glycosylation defect of cerebrospinal fluid β-trace protein, (a glycoprotein synthesized by glia-rich fractions of the brain) were observed in CDG type 1a patients (Pohl et al., 1997; Grünewald et al., 1999).

Since the total lack of the *PMM2* gene product is lethal, no patient with two copies of any inactivating mutation has ever been recorded. Patients are usually compound heterozygous. Though 95% of the mutations are missense in nature, there are yet a few mutations that cause pre-termination codons and splicing mutations (Vuillaumier-Barrot et al., 2006; Schollen et al., 2007; Vega et al., 2009). One such mutation has been targeted by Vega and colleagues, who reported the use of PMOs to revert a deep intronic mutation (c.640-15479C > T) that leads to the activation of a cryptic 5′ splice site in intron 7 (Vega et al., 2009).

Two different 25-nt-long PMOs were designed, complementary to the 5′ or 3′ cryptic splice sites of the pseudoexon in intron 7 (Fig. 3) and both these PMOs were transfected at the same time into patient's fibroblasts carrying the c.640-15479C > T mutation in heterozygosity with missense mutation c.691G > A, via the Endo-Porter reagent (Summerton, 2005). There was a 100% restoration of the correctly spliced mRNA. The levels of PMM2 protein after transfection increased from 9% to 23% of the quantity detected for the control cell line. PMM2 enzymatic activity was rescued almost to 50% that of the control fibroblasts.

Fronto-temporal dementia and Parkinsonism linked to chromosome 17

Fronto-Temporal Dementia and Parkinsonism linked to chromosome 17 (FTDP-17) is an autosomal dominant neurodegenerative disorder showing cognitive impairment, behavioral and personality changes and motor symptoms. The incidence of FTDP-17 is unknown; however, it is an extremely rare condition. It is caused by mutations in the *MAPT* gene on chromosome 17q21, which encodes microtubule-associated protein tau. Over 100 families with 44 different mutations in the *MAPT* gene have been identified worldwide. The symptoms and onset age of FTDP-17 vary not only between families carrying different mutations but also between and within families carrying the same mutations. Pathological hallmarks of the disease are aggregation of tau into

neurofibrillary tangles (NFT) in neurons and/or glial cells. The pathogenetic mechanisms underlying the disorder are related to the altered proportion of tau isoforms or to the ability of tau to bind microtubules and to promote microtubule assembly. There is currently no cure for FTDP-17 and treatment is only symptomatic and supportive. The prognosis and rate of the diseases progression vary considerably among individual patients, ranging from life expectancies of several months to several years, and, in exceptional cases, as long as two decades after diagnosis (Tsuboi et al., 2009).

Tau is constitutively and abundantly expressed in both the central (CNS) and the peripheral nervous system (PNS). In the CNS, tau is enriched in the axons of mature and growing neurons, though low levels of tau are also present in oligo-dendrocytes and astrocytes.

Tau functions in microtubule (MT) assembly, influences MT stability, and is important for neurogenesis, axonal maintenance, and axonal transport. The human *MAPT* gene consists of 16 exons and its expression is regulated by complex alternative splicing (Andreadis, 2012). Exons 9–12 each encode a 31- to 32-amino-acid imperfect repeat that comprises the MT-binding domain of tau. In adult human brain, exons 2, 3, and 10 are alternatively spliced to produce six different tau isoforms. Exon 10 (E10) inclusion generates isoforms with four microtubule repeats called 4R tau. When E10 is skipped, the result is 3R tau isoforms. In fetal brain, only the shortest 3R tau isoform is expressed because of constitutive exclusion of exons 2, 3, and 10.

While several missense mutations in *MAPT* are known, approximately one-half of the mutations observed in FTDP-17 alter the relative levels of 4R versus 3R tau by affecting alternative splicing of E10 (Andreadis, 2012). These mutations include missense (N279K, N296H, G303V, and S305N), silent (L284L, N296N), and deletion mutations (Delta280K, Delta296N) in E10, and intronic mutations (E10–10, E10 + 3, E10 + 11, E10 + 12, E10 + 13, E10 + 14, E10 + 16, and E10 + 19) in introns 9 and 10. Most of these mutations increase E10 inclusion. The result is that the 4R/3R ratio, which is normally 1, is increased to 2–3. These mutations demonstrate that the 4R/3R ratio is crucial to the correct functioning of tau, although the mechanism by which this alteration leads to neurodegeneration and FTDP-17 is presently unclear.

Kalbfuss and his colleagues have shown that AONs directed against *MAPT* exon 10 splice sites could suppress
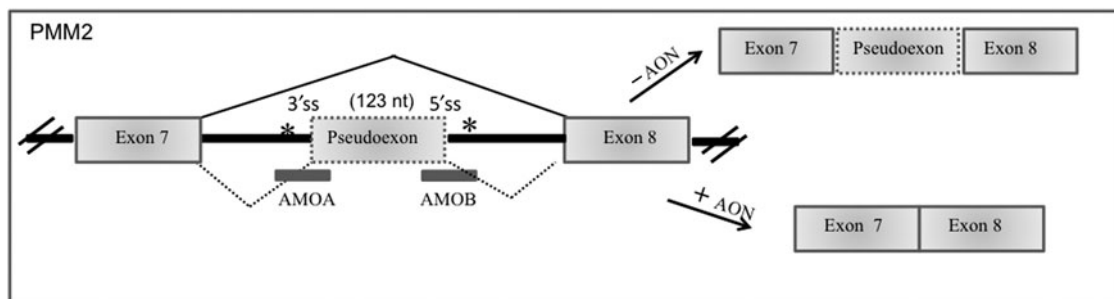
FIG. 3. Congenital disorder of glycosylation type 1A. Diagram of splicing mutations and antisense oligonucleotides locations that rescue the aberrant transcript in congenital disorder of glycosylation type 1a causal gene *PMM2* (for phosphomannomutase 2) (Vega et al., 2009).

inclusion of E10 (Kalbfuss et al., 2001). The experiment was performed on COS-1 green monkey kidney cells by co-transfecting reporter minigenes (with a single point mutations either at position −1, +3, or +14 relative to E10) with 17- to 21-nt-long 2′OMe PS AONs targeting either the 5′ or the 3′ splice site of E10 (Fig. 4). Both these AONs were successful in skipping E10 in the three minigenes, as assessed by RT-PCR. They further proved these results in rat pheochromo-cytoma PC12 cells, in which both AONs effectively excluded exon 10 from the endogenous wild type *MAPT* mRNA, as observed through RT-PCR. Western blots confirmed the reduction of tau 4R isoform. Furthermore, they observed that exon skipping-inducing AONs had a significant and specific physiological effect by destabilizing the microtubule cyto-skeleton and altering cell morphology, when transfected in rat AR42J pancreatic acinar cells.

Donahue and colleagues have validated the use of the 5′ splice site-targeting 2′OMe-PS AON described by Kalbfuss, in HeLa cells cotransfected with luciferase reporter mini-genes, in the wild-type and mutant E10 + 14 versions (Donahue et al., 2006). Transfection of the AONs resulted in a decrease in luciferase expression of about 50%, relative to cells transfected with a control oligoribonucleotide. Real-time RT-PCR confirmed an increase of approximately 15 time of the 3R/4R mRNA ratio, relative to control treatment.

The work of Kalbfuss and colleagues (Kalbfuss et al., 2001) has been further extended by Peacey and colleagues by targeting E10 5′ splice site with a bipartite 2′OMe-PS AON and comparing its efficiency in inducing E10 skipping to that of Kalbfuss' ''continuous'' 5′ splice site-targeting 2′OMe-PS oligonucleotide (Peacey et al., 2012). The bipartite 2′OMe-PS AON was designed to interact with the 5′ and 3′ regions immediately flanking an hairpin located at the junction between exon 10 and intron 10, and consists of 10 bases complementary to the 3′ flank, a linker of one adenosine, and 9 bases complementary to the 5′ flank.

Cotransfection of the bipartite 2′OMe-PS or the ''continuous'' 2′OMe-PS along with wild-type minigene in SK-N-SH neuroblastoma cells induced exon skipping with a reduction in 4R of 68% and 66%, respectively. In addition, bipartite 2′OMe-PS and ''continuous'' 2′OMe-PS significantly increased expression of 3R tau by 37 and 65%, respectively. When tested on a E10 + 14 mutant form of the minigene, the bipartite 2′OMe-PS and the ''continuous'' 2′OMe-PS significantly reduced expression of 4R tau by 57 and 61%, respectively with concomitant increase in 3R tau expression. The effect of bipartite 2′OMe-PS AON on endogenous tau mRNA was verified in HEK 293 cells that showed 42% reduction of E10 inclusion.

Niemann-Pick disease type C

Niemann-Pick disease Type C (NPC) is an autosomal recessive disorder due to mutations in genes *NPC1* or *NPC2*, with an incidence of 1 in 150,000 individuals. NPC is involved in a significant reduction of life expectancy (Miao et al., 2012) and is mainly associated with progressive neurodegeneration and neurological, psychiatric, and hepatic manifestations. Approximately 50% of cases present before 10 years of age, but manifestations may first be recognized as late as the sixth decade. Neurological symptoms vary with age accompanied by hypotonia, delay in developmental motor milestones, learning difficulties, ataxia with cognitive deficits, and psychosis (Kheder et al., 2013).

In the NPC neurons, there is a gross alteration in the overall amounts of cholesterol and an accumulation of unesterified cholesterol and glycosphingolipids in the lysosome-like storage organelles in the cell bodies (Mukherjee et al., 2004).

Though most of the mutations in *NPC1* are missense, some splicing mutations have been found (Rodríguez-Pascau et al., 2009; Macías-Vidal et al., 2011). Work by Rodríguez-Pascau and colleagues focused on mutation c.1554-1009G > A, located in intron 9 of *NPC1* gene, leading to the insertion of a 194-nt pseudoexon, both in HeLa cells transfected with a mutant minigene and in patient fibroblasts, which carry the mutation in heterozygosis with in-frame deletion-insertion p.N961_F966delinsS (Rodríguez-Pascau et al., 2009). A PMO complementary to the cryptic 5′ splice site was used to block the access of the splicing machinery to the pre-mRNA thus avoiding the formation of the aberrantly spliced transcript (Fig. 5). The PMO was able to prevent the inclusion of the pseudoexon and restored normal splicing upon delivery to patients' fibroblasts via the Endo-Porter system (Summerton, 2005). RT-PCR analysis shows the complete disappearance of the amplicon corresponding to the aberrant splicing, upon 48 hours of treatment with 10μM PMO (Rodríguez-Pascau et al., 2009).

Neurofibromatosis type 1

Neurofibromatosis type 1 (NFT 1) is an autosomal dominant disorder characterized by café-au-lait spots, cutaneous
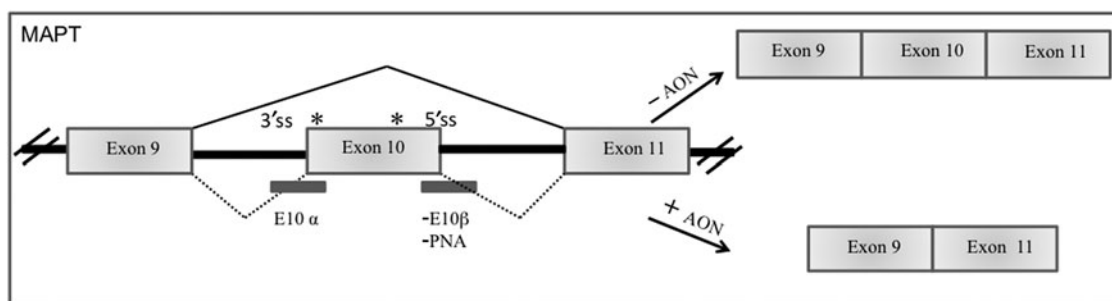
FIG. 4. Frontotemporal dementia and Parkinson's disease. Schematic representation of Exon 10 splicing mutations in *MAPT* gene, which encodes microtubule-associated protein tau, and of the locations of antisense oligonucleotides that induce skipping of exon 10 (Kalbfuss et al., 2001; Peacey et al., 2012).
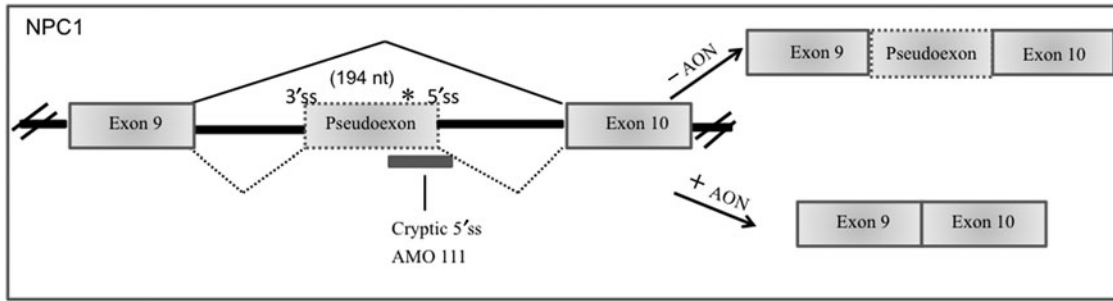
FIG. 5. Niemann Pick disease type C (NPC1). Scheme of splicing mutations and location of antisense oligonucleotides that restore the aberrant transcript in *NPC1* (Rodriguez-Pascau et al., 2009).

neurofibromas, Lisch nodules, inguinal and axillary freckling, and a high predisposition to develop certain types of tumors. It affects 1 in 3,000 individuals, especially targeting young children (Friedman et al., 1999). Affected individuals develop glial neoplasms (optic gliomas, malignant astrocytomas) and neuronal dysfunction leading to learning disabilities and attention deficits (Gutmann et al., 2012).

NFT1 is caused by mutations in the *NF1* gene, which is located on chromosome 17q11.2, contains 57 constitutive exons and encodes for an 11- to 13-kb mRNA transcript. The gene product neurofibromin negatively regulates Ras and acts as a tumor suppressor. Neurofibromin also plays important roles in cell growth, neuronal activity and bone metabolism (Hseuh et al., 2012).

About 44% of the mutations found in *NF1* are splicing mutations (Pros et al., 2008). A small subset of these mutations (20%) are deep intronic single nucleotide changes that, creating either a novel 5′ or 3′ site, increase pseudoexon inclusion into mature mRNA.

Work by Pros and colleagues aimed at restoring normal splicing using PMOs in primary fibroblast and lymphocyte cell lines derived from six NFT1 patients bearing three different deep intronic mutations (c.288+2025T>G, c.5749+332A>G and c.7908-321C>G) (Pros et al., 2009). PMOs were designed against the mutant cryptic 5′ splice sites, and delivered via Endo-porter reagent (Summerton, 2005) (Fig. 6). PMO treatment effectively restored normal *NF1* splicing at the mRNA level for the three mutations
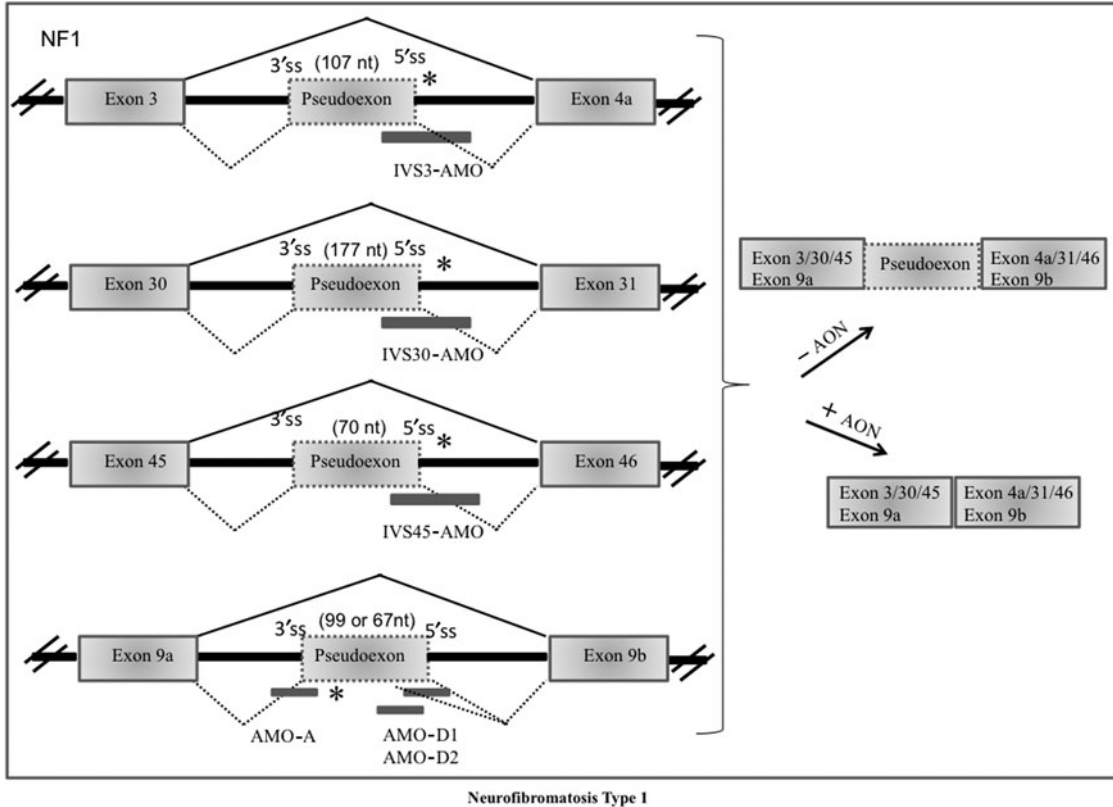
FIG. 6. Neurofibromatosis type 1 (NF1). Schematic representation of four *NF1* deep intronic mutations and of the location of specific phosphorodiamidate morpholino oligomers (PMOs) used to restore the correct splicing (Pros et al., 2009; Fernández-Rodríguez et al., 2011).

studied in the different cell lines analyzed. The efficiency of *NF1* splicing correction in fibroblasts after 24 hours of treatment ranged from 87 to 100% in the different mutations. These authors also found that PMOs had a rapid effect in fibroblasts that lasted for several days, acting in a sequence-specific manner and interfering with the splicing mechanism. A lower degree of aberrant splicing correction (30%–70%) was observed in lymphocyte cell lines, and a higher concentration of PMO, together with a longer time of exposure, was needed to produce similar effects to those seen in fibroblasts. These differences are probably due to the greater difficulty of lymphocyte transfection. To test whether the correction of aberrant NF1 splicing also restored neurofibromin function to wild-type levels, the authors measured the amount of Ras-GTP after PMO treatment in primary fibroblasts, as an indirect indication of the GTPase activity of neurofibromin. The results clearly show a PMO-dependent decrease in Ras-GTP levels, which is consistent with the restoration of neurofibromin function.

Fernández-Rodríguez and colleagues analysed the genetic basis of a benign phenotype observed in a NFT1 patient carrying the mutation c.3198-314G>A in intron 19a of the *NF1* gene (Fernández-Rodríguez et al., 2011). This deep intronic mutation creates a new cryptic 3′ splice site that uses two different 5′ splice sites present in the wild type sequence, generating two aberrantly spliced transcripts leading to the inclusion of two different pseudoexons, both of which would generate the same putative truncated protein. A minigene construct containing mutation c.3198-314G>A indicated the production of both mutated and wild type transcripts, with a low proportion of the mutated form due to leaking in the splicing mechanism, contributing to the benign nature of *NF1* mutation and consequent mild phenotypic effect observed in the patient.

As a personalized therapeutic approach for *NF1* mutations, PMOs were delivered in patient's fibroblasts. Three different PMOs were designed, which the authors named antisense morpholino oligomers (AMOs): AMO-A, blocking the 3′ splice site; AMO-D1, blocking the first 5′ (donor 1) splice site; and AMO-D2, blocking the second 5′ (donor 2) splice site (Fig. 6). Reduction of the mutant transcripts was validated by RT-PCR. However, a complete correction was observed only when a combination of the three PMOs was used. In order to provide insights into the functional validation, and in agreement with the results obtained by Pros and colleagues (Pros et al., 2009), a significant reduction of Ras-GTP was observed in fibroblasts treated with specific PMOs.

Neurofibromatosis type 2

Neurofibromatosis type 2 (NFT 2) is an autosomal dominant disorder that affects about 1 in 33,000 newborns, characterized by tumors of the nervous system and ocular abnormalities. The presence of bilateral vestibular nerve schwannomas is the most distinctive feature of NFT 2, but patients can develop other clinical manifestations such as schwannomas in other cranial, spinal and peripheral nerves, and also other types of tumors, like meningiomas (both intracranial and intraspinal) and ependymomas (low-grade CNS malignancies). This cancer syndrome is caused by mutations in the tumor suppressor *NF2* gene that is located on chromosome 22q12 and that codes for the tumor suppressor protein merlin.

Human merlin mainly located in adherens junctions and is predominantly found in nervous tissue, but also in several other fetal tissues. Merlin links receptors at the plasma membrane to their cytoplasmic kinases to promote contact-mediated growth inhibition. It is also involved in interaction with other cytoplasmic and nuclear proteins that affect cell cycle progression (Beltrami et al., 2013). Around 85% of the germline *NF2* mutations are point mutations, among which approximately 25% seem to affect splicing. In the recent work by Castellanos and colleagues, a patient with a deep intronic mutation (g.74409T>A, NG_009057.1) was identified (Castellanos et al., 2013). This mutation leads to the inclusion of a nonsense pseudoexon of 167 nt in the mature mRNA, between exon 13 and exon 14, thus resulting in a truncated Merlin protein. Castellanos and colleagues have been successful in devising a therapeutic strategy for the first time for an NFT 2 case, using a PMO targeting the deep intronic mutation (Fig. 7).

Patient-derived fibroblasts were treated with three different PMO concentrations (5, 10, and 20 μM) for 24 hours, and a complete inhibition of pseudoexon inclusion was already observed at the lowest concentration tested. PMOs were delivered via the Endo-porter system (Summerton, 2005). Merlin protein levels, although starting to recover at 24 hours, were not significantly increased until 48 hours after PMO delivery. Merlin transcript levels were not affected by control PMO treatment in patient-derived fibroblasts or in fibroblast derived from a non-NF2 individual treated with PMO, further supporting the sequence-specific effect of PMO treatment. Based on the role that Merlin has in contact-dependent inhibition of proliferation, the functionality of
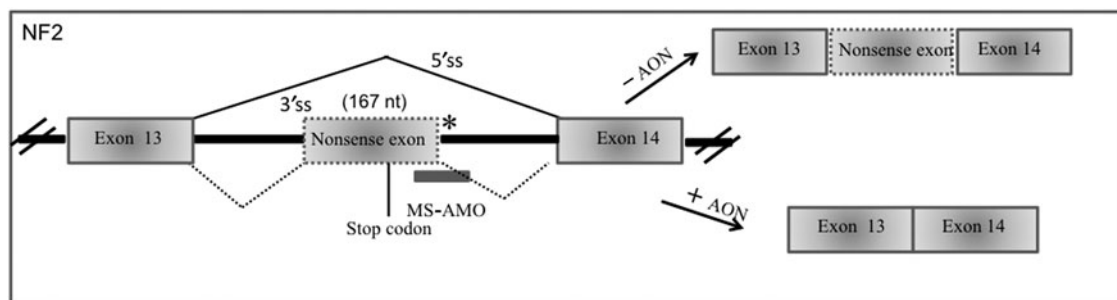
FIG. 7. Neurofibromatosis type 2. Schematic representation of the identified *NF2* deep intronic mutation and PMO location (Castellanos et al., 2013).

recovered Merlin protein was tested by BrdU incorporation assay. Cell proliferation was reduced by 41% at 24 hours and by 67% at 48 hours when compared with control PMO-treated cells. Functional restoration of Merlin was also proven, by showing that F-acting polymerization abnormalities were eliminated in PMO-treated cells (Castellanos et al., 2013).

Megalencephalic leukoencephalopathy with subcortical cysts type 1

Megalencephalic leukoencephalopathy with subcortical cysts type 1 (MLC1) is a rare type of leukodystrophy (incidence ∼ 1 in 500,000 individuals) associated with mutations in *MLC1* gene. The essential features of this disease include macrocephaly (large head) with onset in infancy, motor delay followed by motor disability in the form of progressive spasticity and ataxia, seizures and cognitive decline. MLC1 is an oligomeric plasma membrane (PM) protein, mainly expressed in glial cells and neurons. Most disease-causing missense mutations dramatically reduce the total and PM MLC1 expression levels in mammalian cells (Duarri et al., 2008).

In a recent work, Mancini and colleagues have described a homozygous *MLC1* deep intronic mutation (c.895-226T > G), which leads to the reduction of transcripts due to the inclusion of a 264 nt nonsense exon between exons 10 and 11 (Mancini et al., 2012). Studies performed with the mutated minigene transfected in HeLa cells showed only a partial inclusion of the pseudoexon, suggesting a ''leaky'' mechanism of the mutation. A PMO was used to mask the cryptic 5′ splice splice site activated by this mutation in a patient's lymphoblastoid cell line (Fig. 8). This led to complete abrogation of the 264-nt pseudoexon, as analyzed by RT-PCR.

Pelizaeus-Merzbacher disease

Pelizaeus-Merzbacher disease (PMD) is a recessive X-linked dysmyelinating disorder of the CNS. PMD affects 1 in 400,000 individuals and its onset is usually in early infancy. The most characteristic early signs are nystagmus (rapid, involuntary, rhythmic motion of the eyes) and hypotonia (low muscle tone). Motor abilities are delayed or never acquired, mostly depending upon the severity of the mutation.

Causes of PMD include *PLP1* deletions, duplications, and point mutations. While deletions are reported only rarely, duplications account for 60%–70% of cases, and point mutations have been identified in 20% of cases. Mutations in the *PLP1* gene can also give rise to spastic paraplegia type 2

(SPG2), which is an allelic form of the disease. A spectrum of CNS disorders from mild SPG2 to severe connatal PMD is associated with the mutations in this gene.

Various types of *PLP1* mutations result in missplicing: Bonnet-Dupeyron et al. (2008) reported that of the 33 mutation they detected, 7 were splicing mutations, including one considered as a missense in exon 2 and a nucleotide substitution in intron 3 outside the classical donor and acceptor splicing sites; Hobson et al. (2002) reportered a 19-bp deletion in intron 3 causing missplicing of PLP1; Hübner et al. (2005) described a nucleotide exchange (c.762G > T) at the 3′ border of exon 6 that resulted in partial skipping of exon 6 in the PLP1 mRNA; Lassuthová et al. (2013), finally, recently described three new PLP1 splicing mutations.

PLP1 encodes proteolipid protein (PLP), a major four-pass transmembrane protein in CNS myelin, and is abundantly expressed in oligodendrocytes (Woodward et al., 2008).

The *PLP 1* gene undergoes alternative splicing and produces the PLP protein and a shorter protein isoform DM20, which lacks 35 amino acids from the intracellular domain. Two competing 5′splice sites residing within the 3′ portion of exon 3 are responsible for the alternative splicing of the gene transcript (Nave et al., 1987; Gabern et al., 2007).

Recent work by Regis and colleagues has focused on an exonic missense mutation c.436C > G in the *PLP1* gene of a patient affected by Pelizaeus-Merzbacher disease (Regis et al., 2013). This mutation led to introduction of regulatory motifs that perturb splicing, leading to a loss of the major PLP transcript. An antisense-based approach was used for *in vitro* correction and restoration of PLP transcript in the murine oligodendrocyte precursor cell line Oli-neu transfected with mutated reporter minigenes (Regis et al., 2013) (Fig. 9). A PMO was designed to target the mutated region in a co-transfection experiment of the mutant minigene along with the PMO in Oli-neu cells. Using real-time PCR the authors estimated the increase of the PLP/(DM20 + PLP) mRNA ratio as 58% of the wild-type ratio. It remains to be estimated the PMO effect at the protein level, and whether the recovered PLP protein, which bears a mutated amino acid, is functional.

Concluding Remarks

As AONs-induced exon skipping is proving a powerful tool for the correction of DMD and progress has been made towards clinical trials, the scientific community is learning the principles of successful oligonucleotide design and
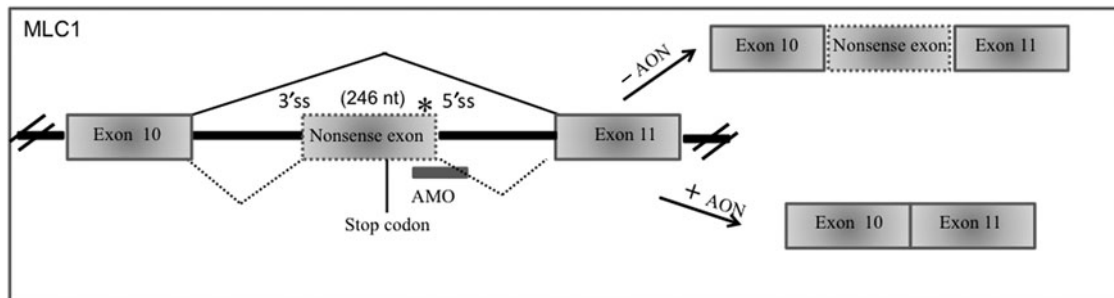
FIG. 8. Megalencephalic leukoencephalopathy with subcortical cysts type 1 (MLC1). Schematic representation of the identified *MLC1* deep intronic mutation and specific PMO location (Mancini et al., 2012).
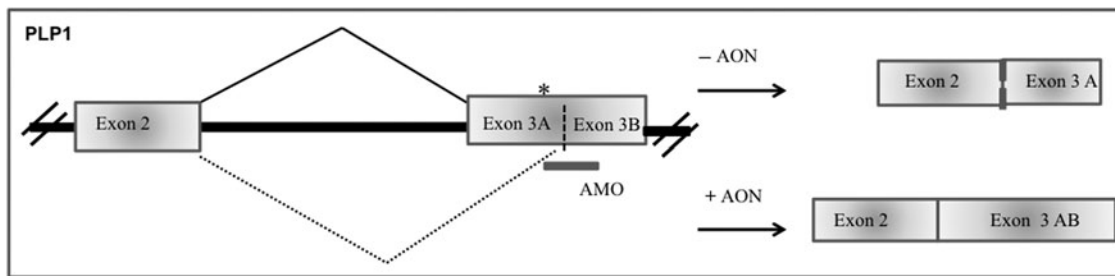
FIG. 9. Pelizaeus-Merzbacher disease. Schematic representation of the identified *PLP1* gene mutation and specific PMO location (Regis et al., 2013).

delivery to skeletal and cardiac muscles. Parallel to the development of exon skipping strategies for DMD, the ability to investigate and identify the genetic causes of other genetic diseases has been improving, thanks to new sequencing methodologies. The number of identified splicing mutations and deep intronic mutations inducing inclusion of pseudoexons is accordingly increasing.

The time appears therefore ripe for extending exon-skipping strategies to many other diseases. In this review, we cover, to the best of our knowledge, the use of antisense oligonucleotides to correct splicing defects through exon skipping, with a special focus on diseases affecting the nervous system. The papers presented here for nine different neurogenetic diseases provide proofs of principle that exon skipping can become a therapy for many neurogenetic diseases. However, all the reviewed papers show efficacy either on reporter minigenes in transfected cells or in patient-derived cells in culture (Table 1). To move this therapeutic approach towards clinical application, *in vivo* preclinical studies will be needed, which will be made possible by the availability of animal models of these diseases, bearing splicing mutations. For FTDP-17, for example, two such mouse models are available: the T279 mouse (Dawson et al., 2007) that expresses human N279K mutated tau protein from a minigene, which allows alternative splicing of exon 10 and is under the regulation of the human TAU promoter; and the E10 + 16C > T mouse, which bears a transgenic human tau minigene with the intronic mutation E10 + 16C > T (Umeda et al., 2013). Both models show progressive neurodegeneration and tau accumulation.

Since the treatment of neurogenetic disorders with AONs may require life-long repeated dosing, it would be preferable to be able to administer such agents systemically. AONs, indeed, have a relatively long half-life and do not elicit immunogenic responses.

The principal obstacle that hampers the systemic delivery of therapeutic AONs to the CNS is the blood-brain barrier (BBB) (Chen et al., 2012; Wong et al., 2012). Molecules can only enter the brain interstitial fluid by transport through the brain capillary endothelial cells. However, modified AONs are taken up extremely fast in neurons and glial cells with a long residence, once inside the blood brain barrier (BBB).

It has been demonstrated that AONs with a PS backbone have a saturable BBB transport system, which allows them to easily access the CNS when systemically administered *in vivo*. A PS 42-mer injected in the tail vein of mice overexpressing amyloid precursor protein entered the cerebrospinal fluid (CSF) and the parenchymal space of the brain; transport was especially high in the hippocampus (Banks et al., 2001; Erickson et al., 2012). However, as many studies indicated lately that BBB is altered in a wide spectrum of brain diseases, care should be taken when extending studies on wild-type animals or specific disease models, to other disease models.

In *mdx* mice, nanoparticles have been used to deliver 2′OMe-PS AONs to muscles by intraperitoneal injections (Rimessi et al., 2009; Ferlini et al., 2010). Notably, the AON doses needed for exon skipping and dystrophin restoration were much lower than with 2′OMe-PS alone. Several studies have been recently focused at the development of nanoparticles for brain drug delivery (reviewed in Masserini, 2013) in general and for the delivery of nucleic acids in particular (reviewed in Pérez-Martínez et al., 2011). It is likely, therefore, that future attempts to systemic delivery of exon-skipping AONs to the brain will take advantage of the knowledge on nanoparticles that is currently accumulating.

Extracellular vesicles in the form of exosomes, the focus of much ongoing research, might also prove capable of delivering AONs across the BBB (Lee et al., 2012). Research in drug delivery to the brain is also attempting transient BBB opening, via bacterial proteins, ultrasounds, or small molecules (such as mannitol or bradykinin).

Delivering AONs via the nasal passages could provide a noninvasive way to bypass the BBB and avoid toxicity due to systemic administration (Dhuria et al., 2010). Small interfering RNAs, for example, have been delivered intranasally to the olfactory bulbs of mice via the olfactory nerve pathway, either naked (Renner et al., 2012) or in cell-penetrating peptide-modified nanomicelles (Kanazawa et al., 2013). Partially destroying the BBB.

Even if systemic delivery would represent a less invasive therapeutic protocol, it still has several disadvantages: the majority of AONs end up in the liver and kidney for each of the different AON chemistries (Sazani et al., 2002; Fluiter et al., 2003; Swayze et al., 2007; Aartsma-Rus and van Ommen, 2009). Moreover, although some AONs have been shown to cross the BBB, approximately 100-fold higher doses must be delivered systemically to achieve AONs concentrations similar to those achieved by intra-CNS delivery (Banks et al., 2001; Erickson et al., 2012) increasing the risk of toxicity.

Many animal studies have therefore employed alternative routes of administration (intraparenchimal injections in specific brain areas, intracerebroventricular injections, intrathecal injections), sometimes administering the AONs

TABLE 1. CURRENT USE OF ANTISENSE OLIGONUCLEOTIDES FOR MISSPLICING CORRECTION IN NEUROGENETIC DISEASES

Disorder	Prevalence	Target gene	Target site	System in which efficacy has been tested	Oligo type	References
Ataxia telangiectasia	1/40,000 to 100,000	ATM	Intronic and exonic cryptic splice sites	Patient-derived lymphoblastoid cell lines homozygous for mutation c.7865C>T or c513C>T or heterozygous for mutation IVS28-159A>G	PMO pPMO	Du et al., 2007 Du et al., 2011
				Patient-derived lymphoblastoid cell lines with mutation c.2639-384A>G (in heterozygosis with large deletion c.6807+272_7516-275del5350)	PMO vivo-morpholino	Nakamura et al., 2012
				Patient-derived lymphoblastoid cell lines with mutation c.1236-405C>T (in heterozygosis with missense mutation c.6326G>A)	PMO vivo-morpholino	Cavalieri et al., 2013
Congenital disorder of glycosylation	1/50,000 to 100,000	PMM2	Intronic 5′ and 3′ cryptic splice sites	Patient fibroblasts with intronic mutation c.640-15479C>T (in heterozygosis with missense mutation c.691G>A)	PMO	Vega et al., 2009
Frontotemporal dementia and Parkinsonism linked to chromosome 17	Incidence rate unknown	MAPT	Exon 10 5′ and 3′ splice sites	Green monkey kidney COS-1, SK-N-SH, or HeLa cell lines transfected with minigenes containing mutations S305S; E10+3; E10+14. Rat PC12 cell line	2′OMe-PS	Kalbfuss et al., 2001; Donahue et al., 2006; Peacey et al., 2012
Niemann Pick disease type C	1/150,000	NPC1	Intronic cryptic 5′ splice site	Patient fibroblasts with intronic mutation c.1554-1009G>A (in heterozygosis with in-frame deletion insertion p.N961_F966delinsS)	PMO	Rodríguez-Pascau et al., 2009
Neurofibromatosis type 1	1/3000	NF1	Intronic cryptic 5′ splice site	Patient fibroblasts and lymphocytes with intronic mutations c.288+2025T>G; c.5749+332A>G; c.7908-321C>G	PMO	Pros et al., 2009
				Patient fibroblasts with intronic mutation c.3198-314G>A	PMO	Fernández-Rodríguez et al., 2011
Neurofibromatosis type 2	1/33,000	NF2	Intronic cryptic 5′ splice site	Patient fibroblasts with mutation g.74409T>A	PMO	Castellanos et al., 2013
Megalencephalic leukoencephalopathy with subcortical cysts type 1	1/500,000	MLC1	Intronic cryptic 5′ splice site	Patient-derived lymphoblastoid cell lines homozygous for mutation c.895-226T>G	PMO	Mancini et al., 2012
Pelizaeus-Merzbacher disease	1/400,000	PLP1	Exonic cryptic 5′ splice site	Murine oligodendroglial Oli-neu cell lines transfected with minigene containing mutation c.436C>G	PMO	Regis et al., 2013

AONs, antisense oligonucleotides; PMO, phosphorodiamidate morpholino oligomer; 2′OMe-PS, 2′ O-methyl phosphorothioate antisense oligonucleotides; pPMO, peptide conjugated PMO.

through the use of micro-osmotic pumps (Smith et al., 2006; Hua et al., 2010).

In recent years, oligonucleotides have being successfully employed in preclinical studies on neurodegenerative diseases and for some diseases are being tested in clinical trials. For the therapy of Huntington's disease (HD), AONs that catalyze RNase H-mediated degradation of huntingtin mRNA were proven effective by intraparenchymal bolus delivery directly to the striatum of mice (Carroll et al., 2011) and by transient infusion into the CSF of symptomatic HD mouse models and nonhuman primates (Kordasiewicz et al., 2012). For Alzheimer's disease, AONs directed against the Aβ region of amyloid precursor protein (APP) were injected intracerebroventricular (Kumar et al., 2000; Banks et al., 2001; Chauhan et al., 2002; Chauhan et al., 2007; Fiorini et al., 2013), or systemically in the tail vein (Banks et al., 2001). In amyotrophic lateral sclerosis (ALS) AONs continuously infused intraventricularly have been demonstrated to distribute widely throughout the CNS of rodents and primates (Smith et al., 2006; Winer et al., 2013). Results of a phase 1 clinical trial with an AON against superoxide dismutase 1 (SOD1), delivered intrathecally in patients with SOD1 familial ALS have been recently reported (Miller et al., 2013). For SMA, AONs have been ICV infused in the mouse model by means of a micro-osmotic pump and have been observed to be uptaken from CSF by motoneurons of both upper and lower spinal regions (Hua et al., 2011; Passini et al., 2011). A single ICV injection was sufficient to rescue SMA in embryonic or neonate mice (Porensky et al., 2012). On these premises, a phase 1 clinical trial for SMA has been started, which consists in a single AON intratechal injection (ClinicalTrials.gov identifier NCT01494701).

In proceeding toward oligonucleotide-based exon-skipping therapies for neurogenetic diseases, several issues must be considered. Not only effective AON chemistry and design should be found, but the chemistry should be such that the AON can be synthesized easily and cost effectively on at least gram scale or higher and under good manufacturing practice. Moreover, the best delivery route should be found for the specific disease, aiming at the affected part of the CNS or PNS and keeping in mind that the disease itself could alter the normal physiology, including the BBB.

Finally, as we are dealing often with rare diseases and with patient-specific mutations, we are confronted with issues affecting the development and implementation of personalized medicine and placing new demands upon the regulatory frameworks that control the licensing of medicinal products. For example, at present, each AON for each specific mutation need its own approval procedure from the European Medicines Agency or from the U.S. Food and Drug Administration.

The lessons learned in the delivery of oligonucleotides to the brain for the cure of the above-mentioned neuromuscular and neurodegenerative disorders, together with the experience gained in the successful design of exon-skipping AONs for the cure of DMD will hopefully make personalized exon-skipping therapies for several neurogenetic disorders a reality in the next few years.

Acknowledgments

Author Disclosure Statement

No competing financial interests exist.

References

AARTSMA-RUS, A., KAMAN, W.E., BREMMER-BOUT, M., JANSON, A.A., DEN DUNNEN, J.T., VAN OMMEN, G.and VAN DEUTEKOM, J.C. (2004). Comparative analysis of antisense oligonucleotide analogs for targeted DMD exon 46 skipping in muscle cells. Gene Ther **11,** 1391–1398.

AARTSMA-RUS, A., and VAN OMMEN, G.J. (2009). Antisense-mediated exon skipping: a versatile tool with therapeutic and research applications. RNA. **13,** 1609–1624.

AARTSMA-RUS, A. (2012). Overview on DMD exon skipping. In: Exon Skipping. A. Aartsma-Rus, ed. Methods Mol. Biol. **867,** 97–116.

ABES, S., MOULTON, H.M., CLAIR, P., PREVOT, P., YOUNGBLOOD, D.S., WU, R.P., IVERSEN, P.L., and LEBLEU, B. (2006). Vectorization of morpholino oligomers by the (R-Ahx-R)(4) peptide allows efficient splicing correction in the absence of endosomolytic agents. J. Control. Release **116,** 304–113.

ALTER, J., LOU, F., RABINOWITZ, A., YIN, H., ROSENFELD, J., WILTON, S.D., PARTRIDGE, T.A., and LU, Q.L. (2006). Systemic delivery of morpholino oligonucleotide restores dystrophin expression bodywide and improves dystrophic pathology. Nat. Med. **12,** 175–177.

AMANTANA, A., MOULTON, H.M., CATE, M.L., REDDY, M.T., WHITEHEAD, T., HASSINGER, J.N., YOUNGBLOOD, D.S., and IVERSEN, P.L. (2007). Pharmacokinetics, Biodistribution, stability and toxicity of a cell-penetrating peptide-morpholino oligomer conjugate. Bioconjug. Chem. **18,** 1325–1331.

ANDREADIS, A. (2012). Tau splicing and the intricacies of dementia. J. Cell. Physiol. **227,** 1220–1225.

ARECHAVALA-GOMEZA, V., ANTHONY, K., MORGAN, J., and MUNTONI, F. (2012). Antisense oligonucleotide-mediated exon skipping for Duchenne muscular dystrophy: progress and challenges. Curr. Gene Ther. **12,** 52–60.

ARZUMANOV, A., WALSH, A.P., RAJWANSHI, V.K., KUMAR, R., WENGEL, J., and GAIT, M.J. (2001). Inhibition of HIV-1 Tat-dependent trans-activation by steric block chimeric 2′-O-methyl/LNA oligoribonucleotides. Biochemistry **40,** 14645–14654.

BAKKENIST, C.J., and KASTAN, M.B. (2003). DNA damage activates ATM through intermolecular autophosphorylation and dimer dissociation. Nature. **421,** 499–506.

BANKS, W.A., FARR, S.A., BUTT, W., KUMAR, V.B., FRANKO, M.W., and MORLEY, J.E. (2001). Delivery across the blood-brain barrier of antisense directed against amyloid beta: reversal of learning and memory deficits in mice overexpressing amyloid precursor protein. J. Pharmacol. Exp. Ther. **297,** 1113–1121.

BELTRAMI, S., KIM, R., and GORDON, J. (2013). Neurofibromatosis type 2 protein, NF2: an unconventional cell cycle regulator. Anticancer Res. **33,** 1–11.

BONNET-DUPEYRON, M.N., COMBES, P., SANTANDER, P., CAILLOUX, F., and BOESPFLUG-TANGUY, O. (2008). PLP1 splicing abnormalities identified in Pelizaeus-Merzbacher disease and SPG2 fibroblasts are associated with different types of mutations. Hum. Mutat. **29,** 1028–1036.

BURRER, R., NEUMAN, B.W., TING, J.P.C., STEIN, D.A., MOULTON, H.M., IVERSEN, P.L., KUHN, P., and BUCHMEIER, M.J. (2007). Antiviral effects of antisense

morpholino oligomers in murine coronavirus infection models. J. Virol. **81,** 5637–5648.

CARROLL, J.B., WARBY, S.C., SOUTHWELL, A.L., DOTY, C.N., GREENLEE, S., SKOTTE, N., HUNG, G., BENNETT, C.F., FREIER, S.M., and HAYDEN, M.R. (2011). Potent and selective antisense oligonucleotides targeting single-nucleotide polymorphisms in the Huntington disease gene/allele-specific silencing of mutant huntingtin. Mol. Ther. **19,** 2178–2185.

CASTELLANOS, E., ROSAS, I., SOLANES, A., BIELSA, I., LÁZARO, C., CARRATO, C., HOSTALOT, C., PRADES, P., ROCA-RIBAS, F., BLANCO, I., and SERRA, E; NF2 Multidisciplinary Clinics HUGTiP-ICO-IMPPC. (2013). In vitro antisense therapeutics for a deep intronic mutation causing Neurofibromatosis type 2. Eur. J. Hum. Genet. **21,** 769–73.

CAVALIERI, S., POZZI, E., GATTI, R.A., and BRUSCO, A. (2013). Deep-intronic ATM mutation detected by genomic resequencing and corrected in vitro by antisense morpholino oligonucleotide (AMO). Eur. J. Hum. Genet. **21,** 774–778.

CHAUHAN, N.B. (2002). Trafficking of intracerebroventricularly injected antisense oligonucleotides in the mouse brain. Antisense Nucleic Acid Drug Dev. **12,** 353–357.

CHAUHAN, N.B. and SIEGEL, G.J. (2007). Antisense inhibition at the b secretase-site of b-amyloid precursor protein reduces cerebral amyloid and acetyl cholinesterase activity in Tg2576. Neuroscience **146,** 143–151.

CHEN, Y., and LIU, L. (2012). Modern methods for delivery of drugs across the blood-brain barrier. Adv. Drug Deliv. Rev. **64,** 640–665.

CIRAK, S., ARECHAVALA-GOMEZA, V., GUGLIERI, M., FENG, L., TORELLI, S., ANTHONY, K., et al. (2011). Exon skipping and dystrophin restoration in patients with Duchenne muscular dystrophy after systemic phosphorodiamidate morpholino oligomer treatment: an open-label, phase 2, dose-escalation study. Lancet. **378,** 595–605.

DAWSON, H.N., CANTILLANA, V., CHEN, L., and VITEK, M.P. (2007). The tau N279K exon 10 splicing mutation recapitulates Frontotemporal Dementia and Parkinsonism linked to chromosome 17 tauopathy in a mouse model. J. Neurosci. **27,** 9155–9168.

DE CLERCQ, E., ECKSTEIN, F., STERNBACH, H., and MERIGAN, T.C. (1969). Interferon induction by and ribonuclease sensitivity of thiophosphate-substituted polyribonucleotides. Antimicrob. Agents Chemother. (Bethesda) **9,** 187–191.

DHIR, A., and BURATTI, E. (2010). Alternative splicing: role of pseudoexons in human disease and potential therapeutic strategies. FEBS J **277,** 841–855.

DHURIA, S.V., HANSON, L.R., and FREY, W.H., 2nd (2010). Intranasal delivery to the central nervous system: mechanisms and experimental considerations. J. Pharm. Sci. **99,** 1654–1673.

DISTERER, P. and KHOO, B. (2012). Antisense-mediated exon-skipping to induce gene knockdown. In: Exon Skipping. Annemieke Aartsma-Rus, ed. Methods Mol. Biol. **867,** 289–306.

DONAHUE, C.P., MURATORE, C., WU, J.Y., KOSIK, K.S., and WOLFE, M.S. (2006). Stabilization of the tau exon 10 stem loop alters pre-mRNA splicing. J. Biol. Chem. **281,** 23302–23306.

DOUGLAS A.G.L., and WOOD M.J.A. (2013). Splicing therapy for neuromuscular disease. Mol. Cell. Neurosci. **56,** 169–185.

DU, L., POLLARD, J.M., and GATTI, R.A. (2007). Correction of prototypic ATM splicing mutations and aberrant ATM function with antisense morpholino oligonucleotides. Proc. Natl. Acad. Sci. U. S. A. **104,** 6007–6012.

DU, L., KAYALI, R., BERTONI, C., FIKE, F., HU, H., IVERSEN, P.L., and GATTI, R.A. (2011). Arginine-rich cell-penetrating peptide dramatically enhances AMO-mediated ATM aberrant splicing correction and enables delivery to brain and cerebellum. Hum. Mol. Genet. **20,** 3151–3160.

DUARRI, A., TEIJIDO, O., LÓPEZ-HERNÁNDEZ, T., SCHEPER, G.C., BARRIERE, H., BOOR, I., AGUADO, F., ZORZANO, A., PALACÍN, M., MARTÍNEZ, A., et al. (2008). Molecular pathogenesis of megalencephalic leukoencephalopathy with subcortical cysts: mutations in MLC1 cause folding defects. Hum. Mol. Genet. **17,** 3728–3739.

DUNCKLEY, M.G., MANOHARAN, M., VILLIET, P., EPERON, I.C., and DICKSON, G. (1998). Modification of splicing in the dystrophin gene in cultured mdx muscle cells by antisense oligoribonucleotides. Hum. Mol. Genet. **7,** 1083–1090.

DUPRÉ, T., BARNIER, A., DE LONLAY, P., CORMIER-DAIRE, V., DURAND, G., CODOGNO, P., and SETA N. (2000). Defect in N-glycosylation of proteins is tissue-dependent in congenital disorders of glycosylation ia. Glycobiology **10,** 1277–1128.

EGHOLM, M., BUCHARDT, O., CHRISTENSEN, L., BEHRENS, C., FREIER, S.M., DRIVER, D.A. BERG, R.H., KIM, S.K., NORDÉN, B., and NIELSEN, P.E. (1993). PNA hybridizes to complementary oligonucleotides obeying the Watson-Crick hydrogen bonding rules. Nature **365,** 566–568.

ELAYADI, A.N., BRAASCH, D.A., and COREY, D.R. (2002). Implications of high-affinity hybridization by locked nucleic acid oligomers for inhibition of human telomerase. Biochemistry **41,** 9973–9981.

ERICKSON, M.A., NIEHOFF, M.L., FARR, S.A., MORLEY, J.E., DILLMAN, L.A., LYNCH, K.M., and BANKS, W.A. (2012). Peripheral administration of antisense oligonucleotides targeting the amyloid-ß protein precursor reverses AßPP and LRP-1 overexpression in the aged SAMP8 mouse brain. J. Alzheimers Dis. **28,** 951–960.

FABANI, M., and GAIT, M.J. (2008). miR-122 targeting with LNA/2′-O-methyl oligonucleotide mixmers, peptide nucleic acids (PNA), and PNA peptide conjugates. RNA **14,** 336–346.

FERLINI, A., SABATELLI, P., FABRIS, M., BASSI, E., FALZARANO, S., VATTEMI, G., PERRONE, D., GUALANDI, F., MARALDI, N.M., MERLINI, L., et al. (2010). Dystrophin restoration in skeletal, heart and skin arrector pili smooth muscle of mdx mice by ZM2 NP-AON complexes. Gene Ther. **17,** 432–438.

FERNÁNDEZ-RODRÍGUEZ, J., CASTELLSAGUÉ, J., BENITO, L., BENAVENTE, Y., CAPELLÁ, G., BLANCO, I., SERRA, E. and LÁZARO, C. (2011). A mild neurofibromatosis type 1 phenotype produced by the combination of the benign nature of a leaky *NF1*-splice mutation and the presence of a complex mosaicism. Hum. Mutat. **32,** 705–709.

FIORINI, A., SULTANA, R., FÖRSTER, S., PERLUIGI, M., CENINI, G., CINI C., CAI, J., KLEIN, J.B., FARR, S.A., NIEHOFF, M.L., et al. (2013). Antisense directed against PS-1 gene decreases brain oxidative markers in aged senescence accelerated mice (SAMP8) and reverses learning and memory impairment: A proteomics study. Free Radic. Biol. Med. **15,** 65C:1–14.

FLETCHER, S., HONEYMAN, K., FALL, A.M., HARDIN, P.L., JOHNSEN, R.D., and WILTON, S.D. (2006). Dystrophin expression in the mdx mouse after localised and systemic administration of a morpholino antisense oligonucleotide. J. Gene Med. **8,** 207–216.

FLUITER, K., TEN ASBROEK, A.L., DE WISSEL, M.B., JAKOBS, M.E., WISSENBACH, M., OLSSON, H., OLSEN, O., OERUM, H., and BAAS, F. (2003). In vivo tumor growth inhibition and biodistribution studies of locked nucleic acid (LNA) antisense oligonucleotides. Nucl. Acids Res. **31,** 953–962.

FRIEDMAN, J.M. (1999). Epidemiology of neurofibromatosis type 1. Am. J. Med. Genet. **89,** 1–6.

GARBERN, J.Y. (2007). Pelizaeus-Merzbacher disease: genetic and cellular pathogenesis. Cell. Mol. Life Sci. **64,** 50–65.

GEBSKI, B.L., MANN, C.J., FLETCHER, S., and WILTON, S.D. (2003). Morpholino antisense oligonucleotide induced dystrophin exon 23 skipping in mdx mouse muscle. Hum. Mol. Genet. **12,** 1801–1811.

GOEMANS, N.M., TULINIUS, M., VAN DEN AKKER, J.T., BURM, B.E., EKHART, P.F., HEUVELMANS, N,. et al. (2011). Systemic administration of PRO051 in Duchenne's muscular dystrophy. N. Engl. J. Med. **364,** 1513–1522.

GRÜNEWALD, S., HUYBEN, K., DE JONG, J.G., SMEI-TINK, J.A., RUBIO, E., BOERS, G.H, CONRADT, HS., WENDEL, U., and WEVERS, R.A. (1999). Beta-trace protein in human cerebrospinal fluid: a diagnostic marker for N-glycosylation defects in brain. Biochim. Biophys. Acta. **1455,** 54–60.

GUTMANN, D.H., PARADA, L.F., SILVA, A.J., and RAT-NER, N. (2012). Neurofibromatosis type 1: modeling CNS dysfunction. J. Neurosci. **32,** 14087–14093.

HEEMSKERK, H.A., DE WINTER, C.L., DE KIMPE, S.J., VAN KUIK-ROMEIJN, P., HEUVELMANS, N., PLATEN-BURG, G., VAN OMMEN, G.J., VAN DEUTEKOM, J.C., and AARTSMA-RUS, A. (2009). In vivo comparison of 2′-O-methyl phosphorothioate and morpholino antisense oligo-cleotides for Duchenne muscular dystrophy exon skipping. J. Gene Med. **11,** 257–266.

HOBSON GM, HUANG Z, SPERLE K, STABLEY DL, MARKS HG, and CAMBI F. (2002). A PLP splicing ab-normality is associated with an unusual presentation of PMD. Ann. Neurol. **52,** 477–488.

HOYER, J., and NEUNDORF, I. (2012). Peptide vectors for the nonviral delivery of nucleic acids. Acc. Chem. Res. **45,** 1048–1056.

HSUEH, Y.P. (2012). From neurodevelopment to neurodegen-eration: the interaction of neurofibromin and valosin-con-taining protein/p97 in regulation of dendritic spine formation. J. Biomed. Sci. **19,** 33.

HUA, Y., VICKERS, T.A., BAKER, B.F., BENNETT, C.F., and KRAINER, A.R. (2007). Enhancement of SMN2 Exon 7 inclusion by antisense oligonucleotides targeting the exon. PLoS Biol **5,** e73.

HUA, Y., SAHASHI, K., RIGO, F., HUNG, G., HOREV, G., BENNETT, C.F., and KRAINER, A.R. (2011). Peripheral SMN restoration is essential for long-term rescue of a severe spinal muscular atrophy mouse model. Nature **478,** 123–126.

HUA, Y., SAHASHI, K., HUNG, G., RIGO, F., PASSINI, M.A., BENNETT, C.F., and KRAINER, A.R. (2010). Antisense correction of SMN2 splicing in the CNS rescues necrosis in a type III SMA mouse model. Genes Dev. **24,** 1634–1644.

HUA Y., and KRAINER A.R. (2012). HUA Y., and KRAINER A.R. (2012). Antisense-mediated exon inclusion. In Exon Skipping: Methods and Protocols. Aartsma-Rus A., ed. Methods in Molecular Biology, **867,** 307–323.

HÜBNER CA, SENNING A, ORTH U, ZERRES K, URBACH H, GAL A, and RUDNIK-SCHÖNEBORN S. (2002). Mild Pelizaeus-Merzbacher disease caused by a point mutation affecting correct splicing of PLP1 mRNA. Neuroscience. **132,** 697–701.

JEARAWIRIYAPAISARN, N., MOULTON, H.M., BUCK-LEY, B., ROBERTS, J., SAZANI, P., FUCHAROEN, S., IVERSEN, P.L., and KOLE, R. (2008). Sustained dystrophin expression induced by peptide-conjugated morpholino olig-omers in the muscles of mdx mice. Mol Ther **16,** 1624–1629.

JOHNSON, M.B., KAWASAWA, Y.I., MASON, C.E., KRSNIK, Z., COPPOLA, G., BOGDANOVIĆ, D., GESCH-WIND, D.H., MANE, S.M., STATE, M.W., and SESTAN, N. (2009). Functional and evolutionary insights into human brain development through global transcriptome analysis. Neuron **62,** 494–509.

KALBFUSS, B., MABON, S.A., and MISTELI, T. (2001). Correction of alternative splicing of tau in frontotemporal dementia and parkinsonism linked to chromosome 17. J. Biol. Chem. **276,** 42986–42993.

KANAZAWA, T., AKIYAMA, F., KAKIZAKI, S., TAKA-SHIMA, Y., and SETA, Y. (2013). Delivery of siRNA to the brain using a combination of nose-to-brain delivery and cell-penetrating peptide-modified nano-micelles. Biomaterials **34,** 9220–9226.

KANG, S.-H., CHO, M.-J., and KOLE, R. (1998). Up-regulation of luciferase gene expression with antisense oligonucleotides: implications and applications in functional assay development. Biochemistry **37,** 6235–6239.

KARRAS, J.G., MCKAY, R.A., DEAN, N.M., and MONIA, B.P. (2000). Deletion of individual exons and induction of soluble murine interleukin-5 receptor alpha chain expression through antisense oligonucleotide-mediated redirection of premRNA splicing. Mol. Pharmacol. **58,** 380–387.

KARRAS, J.G., MAIER, M.A., LU, T., WATT, A., and MANOHARAN, M. (2001). Peptide nucleic acids are potent modulators of endogenous pre-mRNA splicing of the murine interleukin-5 receptor-α chain. Biochemistry **40,** 7853–7859.

KHEDER, A., SCOTT, C., OLPIN, S., and HADJIVASSI-LIOU, M. (2013). Niemann-Pick type C: a potentially treat-able disorder? Pract. Neurol. **13,** 382–385. doi: 10.1136/practneurol-2013-000525.

KINALI, M., ARECHAVALA-GOMEZA, V., FENG, L., CIRAK, S., HUNT, D., ADKIN, C., et al. (2009). Local restoration of dystrophin expression with the morpholino oligomer AVI-4658 in Duchenne muscular dystrophy: a single-blind, placebo-controlled, dose-escalation, proof-of-concept study. Lancet Neurol. **8,** 918–928.

KORDASIEWICZ, H.B., STANEK, L.M., WANCEWICZ, E.V., MAZUR, C., MCALONIS, M.M., PYTEL, K.A., AR-TATES, J.W., WEISS, A., CHENG, S.H., SHIHABUDDIN, L.S., et al. (2012). Sustained therapeutic reversal of Hun-tington's disease by transient repression of huntingtin syn-thesis. Neuron **74,** 1031–1044.

KUMAR, V.B., FARR, S.A., FLOOD, J.F., KAMLESH, V., FRANKO, M., BANKS, W.A., and MORLEY, J.E. (2000). Site-directed antisense oligonucleotide decreases the expres-sion of amyloid precursor protein and reverses deficits in learning and memory in aged SAMP8 mice Peptides **21,** 1769–1775.

LARSEN, H.J., BENTIN, T., and NIELSEN, P.E. (1999). An-tisense properties of peptide nucleic acid. Biochim. Biophys. Acta **1489,** 159–166.

LASSUTHOVÁ, P., ZALIOVÁ, M., INOUE, K., HABERLOVÁ, J., SIXTOVÁ, K., SAKMARYOVÁ, I., PADEROVÁ, K., MAZANEC, R., ZÁMECNÍK, J., SISKOVÁ, D., et al. (2013). Three new PLP1 splicing mutations demonstrate pathogenic and

phenotypic diversity of Pelizaeus-Merzbacher disease. J. Child Neurol. 2013, Jun 14. [Epub ahead of print]

LEE, Y., EL ANDALOUSSI, S., and WOOD, M.J. (2012). Exosomes and microvesicles: extracellular vesicles for genetic information transfer and gene therapy. Hum. Mol. Genet. **21,** R125–R134.

LI, Y.F., and MORCOS, P.A. (2008). Design and synthesis of dendritic molecular transporter that achieves efficient in vivo delivery of morpholino antisense oligo. Bioconjug. Chem. **19,** 1464–1470.

LU, Q.L., MANN, C.J., LOU, F., BOU-GHARIOS, G., MORRIS, G.E., XUE, S.A., FLETCHER, S., PARTRIDGE, T.A., and WILTON, S.D. (2003). Functional amounts of dystrophin produced by skipping the mutated exon in the mdx dystrophic mouse. Nat Med. **9,** 1009–1014.

LU, Q.L., RABINOWITZ, A., CHEN, Y.C., YOKOTA, T., YIN, H., ALTER, J., JADOON, A., BOU-GHARIOS, G., and PARTRIDGE, T. (2005). Systemic delivery of antisense oligoribonucleotide restores dystrophin expression in body-wide skeletal muscles. Proc. Natl. Acad. Sci. U. S. A. **102,** 198–203.

MACÍAS-VIDAL, J., RODRÍGUEZ-PASCAU, L., SÁNCHEZ-OLLÉ, G., LLUCH, M., VILAGELIU, L., GRINBERG D., and COLL, M.J.; SPANISH NPC WORKING GROUP. (2011). Molecular analysis of 30 Niemann-Pick type C patients from Spain. Clin. Genet. **80,** 39–49.

MANCINI, C., VAULA, G., SCALZITTI, L., CAVALIERI, S., BERTINI, E., AIELLO, C., LUCCHINI, C., GATTI, R.A., BRUSSINO, A., and BRUSCO, A. (2012). Megalencephalic leukoencephalopathy with subcortical cysts type 1 (MLC1) due to a homozygous deep intronic splicing mutation (c.895-226T > G) abrogated in vitro using an antisense morpholino oligonucleotide. Neurogenetics **13,** 205–14.

MANOHARAN, M. (1999). 2′-Carbohydrate modifications in antisense oligonucleotide therapy: importance of conformation, configuration and conjugation. Biochim. Biophys. Acta **1489,** 117–130.

MASSERINI, M. (2013). Nanoparticles for Brain Drug Delivery. ISRN Biochemistry. doi:10.1155/2013/238428

MATLIN, A.J., CLARK, F., and SMITH, C.W.J. (2005). Understanding alternative splicing: Towards a cellular code. Nat. Rev. Mol. Cell Biol. **6,** 386–398.

MIAO, N., LU X., O'GRADY, N.P., YANJANIN, N., PORTER, F.D., and QUEZADO, Z.M. (2012). Niemann-pick disease type C: implications for sedation and anesthesia for diagnostic procedures. J. Child Neurol. **27,** 1541–1546.

MILLER, T.M., PESTRONK, A., DAVID, W., ROTHSTEIN, J., SIMPSON, E., APPEL, S.H., ANDRES, P.L., MAHONEY, K., ALLRED, P., ALEXANDER, K., et al. (2013). An antisense oligonucleotide against SOD1 delivered intrathecally for patients with SOD1 familial amyotrophic lateral sclerosis: a phase 1, randomised, first-in-man study. Lancet Neurol. **5,** 435–442.

MILLS, J.D., and JANITZ, M. (2012). Alternative splicing of mRNA in the molecular pathology of neurodegenerative diseases. Neurobiol. Aging **33,** 1012.e11–1012.e24.

MUKHERJEE, S., and MAXFIELD, F.R. (2004). Lipid and cholesterol trafficking in NPC. Biochim. Biophysic. Acta **1685,** 28–37.

NAKAMURA, K., DU, L., TUNUGUNTLA, R., FIKE, F., CAVALIERI, S., MORIO, T., MIZUTANI, S., BRUSCO, A., and GATTI, R.A. (2012). Functional characterization and targeted correction of ATM mutations identified in Japanese patients with ataxia-telangiectasia. Hum. Mutat. **33,** 198–208.

NAVE, K.A., LAI, C., BLOOM, F.E., and MILNER, R.J. (1987). Splice site selection in the proteolipid protein (PLP) gene transcript and primary structure of the DM-20 protein of central nervous system myelin. Proc. Natl. Acad. Sci. U. S. A. **84,** 5665–5669.

OBIKA, S., NANBU, D., HARI, Y. ANDOH, I., MORIO, K., DOI, T. and IMANISHI, T. (1998). Stability and structural features of the duplexes containing nucleoside analogues with fixed N-type conformation, 2′-O,4′-C-methyleneribonucleosides. Tetrahedron Lett. **39,** 5401–5404.

PASSINI, M.A, BU, J., RICHARDS A.M, KINNECOM, C., SARDI, S.P., STANEK, L.M., HUA, Y., RIGO F., MATSON J., HUNG, G., et al. (2011). Antisense oligonucleotides delivered to the mouse CNS ameliorate symptoms of severe spinal muscular atrophy. Sci. Transl. Med.**3,** 72ra18.

PEACEY, E., RODRIGUEZ, L., LIU, Y., and WOLFE, M.S. (2012). Targeting a pre-mRNA structure with bipartite antisense molecules modulates tau alternative splicing. Nucleic Acids Res. **40,** 9836–9849.

PEARL, P.L., and KRASNEWICH, D. (2001). Neurologic course of congenital disorders of glycosylation J. Child Neurol. **16,** 409–413.

PÉREZ-MARTÍNEZ, F.C., GUERRA, J., POSADAS, I., and CEÑA, V. (2011). Barriers to non-viral vector-mediated gene delivery in the nervous system. Pharm Res. **28,** 1843–1858.

PERLMAN, S., BECKER-CATANIA, S., and GATTI, R.A. (2003). Ataxia-telangiectasia: diagnosis and treatment. Semin. Pediatr. Neurol. **10,** 173–182.

POHL, S., HOFFMANN, A., RÜDIGER, A., NIMTZ, M., JAEKEN, J., and CONRADT, H.S. (1997). Hypoglycosylation of a brain glycoprotein (β-trace protein) in CDG syndromes due to phosphomannomutase deficiency and N-acetylglucosaminyl-transferase II deficiency. Glycobiology **7,** 1077–1084.

PORENSKY, P., and BURGHES, A. (2013). Antisense oligonucleotides for the treatment of Spinal Muscular Atrophy. Hum. Gene Ther. **24,** 489–498.

PORENSKY, P.N., MITRPANT, C., MCGOVERN, V.L., BEVAN, A.K., FOUST, K.D., KASPAR, B.K., WILTON, S.D., and BURGHES, A.H. (2012). A single administration of morpholino antisense oligomer rescues spinal muscular atrophy in the mouse. Hum. Mol. Genet. **21,** 1625–1638.

PROS, E., GÓMEZ, C., MARTÍN, T., FÁBREGAS, P., SERRA, E., and LÁZARO, C. (2008). Nature and mRNA effect of 282 different NF1 point mutations: focus on splicing alterations. Hum. Mutat. **29,** 173–193.

PROS, E., FERNÁNDEZ-RODRÍGUEZ,J., CANET, B., BENITO, L., SÁNCHEZ, A., BENAVIDES, A., RAMOS, F.J., LÓPEZ-ARIZTEGUI, M.A., CAPELLÁ, G., BLANCO, I., et al. (2009). Antisense therapeutics for neurofibromatosis type 1 caused by deep intronic mutations. Hum. Mutat. **30,** 454–462.

REGIS, S., CORSOLINI, F., GROSSI, S., TAPPINO, B., COOPER, D.N., and FILOCAMO, M. (2013). Restoration of the normal splicing pattern of the PLP1 gene by means of an antisense oligonucleotide directed against an exonic mutation. PLoS One **8,** e73633.

RENNER, D.B., FREY, W.H. 2nd, and HANSON, L.R. (2012). Intranasal delivery of siRNA to the olfactory bulbs of mice via the olfactory nerve pathway. Neurosci. Lett. **513,** 193–197.

RIMESSI, P., SABATELLI, P., FABRIS, M., BRAGHETTA, P., BASSI, E., SPITALI, P., VATTEMI, G., TOMELLERI, G., MARI, L., PERRONE, D., et al. (2009). Cationic PMMA

nanoparticles bind and deliver antisense oligoribonucleotides allowing restoration of dystrophin expression in the mdx mouse. Mol. Ther. **17,** 820–827.

ROBERTS, J., PALMA, E., SAZANI, P., ØRUM, H., CHO, M., and KOLE, R. (2006). Efficient and persistent splice switching by systemically delivered LNA oligonucleotides in mice. Mol. Ther. **14,** 471–475.

RODRÍGUEZ-PASCAU, L., COLL, M.J., VILAGELIU, L., and GRINBERG, D. (2009). Antisense oligonucleotide treatment for a pseudoexon-generating mutation in the NPC1 gene causing Niemann-Pick type C disease. Hum. Mutat. **30,** E993–E1001.

SALEH, A.F., ARZUMANOV, A.A., and GAIT M.J. (2012). Overview of alternative oligonucleotide chemistries for exon skipping. In: Exon Skipping. A. Aartsma-Rus, ed. Methods Mol. Biol. **867,** 365–378.

SAZANI, P., KANG, S.-H., MAIER, M.A., WEI, C., DILLMAN, J., SUMMERTON, J., MANOHARAN, M., and KOLE, R. (2001). Nuclear antisense effects of neutral, anionic and cationic analogs. Nucleic Acids Res. **29,** 3965–3974.

SAZANI, P., GEMIGNANI, F., KANG, S.H., MAIER, M.A., MANOHARAN, M., PERSMARK, M., BORTNER, D., and KOLE, R. (2002). Systemically delivered antisense oligomers upregulate gene expression in mouse tissues. Nat. Biotechnol. **20,** 1228–1233.

SCHMAJUK, G., SIERAKOWSKA, H., and KOLE, R. (1999). Antisense oligonucleotides with different backbones. Modification of splicing pathways and efficacy of uptake. J. Biol. Chem. **274,** 21783–21789.

SCHOLLEN, E., KELDERMANS, L., FOULQUIER, F., BRIONES, P., CHABAS, A., SÁNCHEZ-VALVERDE, F., ADAMOWICZ, M., PRONICKA, E., WEVERS, R., and MATTHIJS, G. (2007). Characterization of two unusual truncating PMM2 mutations in two CDG-Ia patients. Mol. Genet. Metab. **90,** 408–413.

SIERAKOWSKA, H., SAMBADE, M.J., AGRAWAL, S., and KOLE, R. (1996). Repair of thalassemic human β-globin mRNA in mammalian cells by antisense oligonucleotides. Proc. Natl. Acad. Sci. U. S. A. **93,** 12840–12844.

SMITH, R.A., MILLER, T.M., YAMANAKA, K., MONIA, B.P., CONDON, T.P., HUNG, G., LOBSIGER, C.S., WARD, C.M., MCALONIS-DOWNES, M., WEI, H., et al. (2006). Antisense oligonucleotide therapy for neurodegenerative disease. J. Clin. Invest. **116,** 2290–2296.

SOUTHWELL, A.L., SKOTTE, N.H., BENNETT, C.F., and HAYDEN, M.R. (2012). Antisense oligonucleotide therapeutics for inherited neurodegenerative diseases. Trends Mol. Med. **18,** 634–643.

SPROAT, B.S., LAMOND, A.I., BEIJER, B., NEUNER, P., and RYDER, U. (1989). Highly efficient chemical synthesis of 2′-O-methyloligoribonucleotides and tetrabiotinylated derivatives; novel probes that are resistant to degradation by RNA or DNA specific nucleases. Nucleic Acids Res. **17,** 3373–3386.

SUMMERTON, J.E. (2005). Endo-Porter: a novel reagent for safe, effective delivery of substances into cells. Ann. N. Y. Acad. Sci. **1058,** 62–75.

SUMMERTON, J.E., and WELLER, D. (1997). Morpholino antisense oligomers: design, preparation, and properties. Antisense Nucleic Acid Drug Dev. **7,** 187–195.

SWAYZE, E.E., SIWKOWSKI, A.M., WANCEWICZ, E.V., MIGAWA, M.T., WYRZYKIEWICZ T.K., HUNG, G., MONIA, B.P. and BENNETT, C.F. (2007). Antisense oligonucleotides containing locked nucleic acid improve potency but cause significant hepatotoxicity in animals. Nucleic Acids Res. **35,** 687–700.

TERAOKA, S.N.,TELATAR, M., BECKER-CATANIA, S., LIANG, T., ONENGÜT, S., TOLUN, A., CHESSA, L., SANAL, O., BERNATOWSKA, E., GATTI, and R.A., CONCANNON, P. (1999). Splicing defects in the ataxia-telangiectasia gene, ATM: underlying mutations and consequences. Am. J. Hum. Genet. **64,** 1617–1631.

TSUBOI, Y. (2009). Clinical, pathological, and genetic characteristics of frontotemporal dementia and parkinsonism linked to chromosome 17 with mutations in the MAPT and PGRN. Brain Nerve. **11,** 1285–1291.

TURCZYNSKI, S., TITEUX, M., PIRONON, N., and HOVNANIAN, A. (2012). Antisense-mediated exon skipping to reframe transcripts. In: Exon Skipping. A. Aartsma-Rus. ed. Methods Mol. Biol. **867,** 221–238.

UMEDA, T., YAMASHITA, T., KIMURA. T., OHNISHI, K., TAKUMA, H., OZEKI, T., TAKASHIMA, A., TOMIYAMA, T., and MORI, H. (2013). Neurodegenerative disorder FTDP-17-related tau intron $10+16C>T$ mutation increases tau exon 10 splicing and causes tauopathy in transgenic mice. Am. J. Pathol. **183,** 211–225.

VAN DEUTEKOM, J.C., JANSON, A.A., GINJAAR, I.B., FRANKHUIZEN, W.S., AARTSMA-RUS, A., BREMMER-BOUT, M., et al. (2007). Local dystrophin restoration with antisense oligonucleotide PRO051. N. Engl. J. Med. **357,** 2677–2686.

VAN ROON-MOM W.M.C. and AARTSMA-RUS A. (2012). Overview on applications of antisense-mediated exon skipping. In: Exon Skipping. A. Aartsma-Rus, ed. Methods Mol. Biol. **867,** 79–96.

VEGA, A.I., PÉREZ-CERDÁ, C., DESVIAT, L.R., MATTHIJS, G., UGARTE, M., and PÉREZ, B. (2009). Functional analysis of three splicing mutations identified in the PMM2 gene: toward a new therapy for congenital disorder of glycosylation type 1a. Hum. Mutat. 30,795–803.

VICKERS, T.A., ZHANG, H., GRAHAM, M.J., LEMONIDIS, K.M., ZHAO, C., and DEAN, N.M. (2006). Modification of MyD88 mRNA splicing and inhibition of IL-1 signaling in cell culture and in mice with a 2′-O-methoxyethyl-modified oligonucleotide. J. Immunol. **176,** 3652–3661.

VUILLAUMIER-BARROT, S., LE BIZEC, C., DE LONLAY, P., MADINIER-CHAPPAT, N., BARNIER, A., DUPRE, T., DURAND, G., and SETA, N. (2006). PMM2 intronic branch-site mutations in CDG-Ia. Mol. Genet. Metab. **87,** 337–340.

WINER, L., SRINIVASAN, D., CHUN S. et al. (2013). SOD1 in cerebral spinal fluid as a pharmacodynamic marker for antisense oligonucleotide therapy. JAMA Neurol., **70,** 201–207

WONG, H.L., WU, X.Y., and BENDAYAN, R. (2012). Nanotechnological advances for the delivery of CNS therapeutics. Adv. Drug Deliv. Rev. **64,** 686–700.

WOODWARD, K.J. (2008). The molecular and cellular defects underlying Pelizaeus-Merzbacher disease. Expert Rev. Mol. Med. **19,** 10.

WU, B., MOULTON, H.M., P.L., IVERSEN, JIANG, J., LI, J., LI, J., SPURNEY, C.F., SALI, A., GUERRON, A.D., NAGARAJU, K., et al. (2008). Effective rescue of dystrophin improves cardiac function in dystrophin-deficient mice by a modified morpholino oligomer. Proc. Natl. Acad. Sci. U. S. A. **105,** 14814–14819.

WU, B., LU, P., CLOER, C., SHABAN, M., GREWAL, S., MILAZI, S., SHAH, S.N., MOULTON, H.M., and LU, Q.L. (2012). Long-term rescue of dystrophin expression and

improvement in muscle pathology and function in dystrophic mdx mice by peptide-conjugated morpholino. Am. J. Pathol. **181,** 392–400.

WU, B., LI, Y.-F., MORCOS, P.A., DORAN, T.J., LU, P., and LU, Q.L. (2009). Octa-guanidine morpholino restores dystrophin expression in cardiac and skeletal muscles and ameliorates pathology in dystrophic mdx mice. Mol. Ther. **17,** 864–871.

YIN, H., LU, Q., and WOOD, M.J. (2008a). Effective exon skipping and restoration of dystrophin expression by peptide nucleic acid antisense oligonucleotides in mdx mice. Mol. Ther. **16,** 38–45.

YIN, H., MOULTON, H.M., SEOW, Y., BOYD, C., BOUTI-LIER, J., IVERSON, P., and WOOD, M.J. (2008b). Cell-penetrating peptide-conjugated antisense oligonucleotides restore systemic muscle and cardiac dystrophin expression and function. Hum. Mol. Genet. **17,** 3909–3918.

YIN, H., MOULTON, H.M., BETTS, C., SEOW, Y., BOUTI-LIER, J., IVERSON, P.L., and WOOD, M.J. (2009). A fusion peptide directs enhanced systemic dystrophin exon skipping and functional restoration in dystrophin-deficient mdx mice. Hum. Mol. Genet. **18,** 4405–4414.

YIN, H., SALEH, A.F., BETTS, C., CAMILETTI, P., SEOW, Y., ASHRAF, S., ARZUMANOV, A.and WOOD, M.J. (2011). Pip5 transduction peptides direct high efficiency oligonucleotide-mediated dystrophin exon skipping in heart and phenotypic correction in mdx mice. Mol. Ther. **19,** 1295–1303.

YIN, H., BETTS, C., SALEH, A.F., IVANOVA, G.D., LEE, H., SEOW, Y., KIM, D., GAIT, M.J., and WOOD, MJ. (2010). Optimization of peptide nucleic acids antisense oligonucleotides for local and systemic dystrophin splice correction in the mdx mouse. Mol. Ther. **18,** 819–827.

Address correspondence to:
Michela A. Denti, PhD
Center for Integrative Biology (CIBIO)
University of Trento
via delle Regole, 101,
Trento 38123
Italy

E-mail: denti@science.unitn.it

A network of RNA and protein interactions in Fronto Temporal Dementia

Francesca Fontana[1][†], Kavitha Siva[1][†] and Michela A. Denti[1,2]*

[1] *Laboratory of RNA Biology and Biotechnology, Centre for Integrative Biology, University of Trento, Trento, Italy,* [2] *CNR, Institute of Neuroscience, Padua, Italy*

Frontotemporal dementia (FTD) is a neurodegenerative disorder characterized by degeneration of the fronto temporal lobes and abnormal protein inclusions. It exhibits a broad clinicopathological spectrum and has been linked to mutations in seven different genes. We will provide a picture, which connects the products of these genes, albeit diverse in nature and function, in a network. Despite the paucity of information available for some of these genes, we believe that RNA processing and post-transcriptional regulation of gene expression might constitute a common theme in the network. Recent studies have unraveled the role of mutations affecting the functions of RNA binding proteins and regulation of microRNAs. This review will combine all the recent findings on genes involved in the pathogenesis of FTD, highlighting the importance of a common network of interactions in order to study and decipher the heterogeneous clinical manifestations associated with FTD. This approach could be helpful for the research of potential therapeutic strategies.

Keywords: FTD, TDP-43, FUS, progranulin, tau, CHMP2B. C9ORF72

Frontotemporal Dementia

Despite 90% of the human genome being transcribed to RNA, only 1.2% of genomic sequence is protein-coding, indicating that a huge proportion of non-coding RNAs (ncRNAs) are likely to participate in a number of physiological processes in cell types, including neurons (Lander et al., 2001; Birney et al., 2007; Wilhelm et al., 2008; Clark et al., 2011). The transcribed precursors of messenger RNAs (pre-mRNA) undergo splicing, such that the non-coding introns are removed and exons are combined variably to produce an RNA that would code for protein (Pandit et al., 2008). The pre-mRNAs undergoes alternative splicing producing mature messenger RNAs (mRNAs) which are then expressed in specific tissues and cell types in different stages of development. These mRNAs then associate with the ribosomal machinery to be translated into proteins in the cytoplasm. Non-coding RNAs (among which microRNAs and long non-coding RNAs), might regulate the translation of specific mRNAs, thereby representing a post-transcriptional mechanism exerting a fine-tuned control in the production of specific proteins.

microRNAs (miRNAs) are a group of small non-coding RNAs of 21–22 nt with important regulatory roles on the post-transcriptional expression of target mRNAs (Bartel, 2009; Ghildiyal and Zamore, 2009). MiRNAs are generating from longer transcripts of different lengths called primary transcripts (pri-miRNAs), usually transcribed by RNA polymerase II, from intragenic or intergenic DNA regions (Lee et al., 2004; Garzon et al., 2010). The pri-miRNAs are processed in the nucleus by the micro-processor complex, formed by an RNase III enzyme, Drosha, and its cofactor DiGeorge

syndrome critical region in gene eight termed (DGCR8) (Lee et al., 2003). The process lead to the production of small hairpin structure of 70–100 nt called precursor miRNAs (pre-miRNAs). Pre-miRNAs are exported to the cytoplasm through Exportin 5 (Kim, 2004), where they are further processed by an RNase III nuclease, Dicer to produce RNA duplex (Bernstein et al., 2001; Grishok et al., 2001; Hutvagner et al., 2001). One strand is loaded on the RNA-Induced Silencing Complex (RISC) and associated with Argonaute-2 (Ago2) to interact with the target mRNA. The miRNA-RISC complex induces mRNA downregulation through two different ways: mRNA cleavage in case of perfect complementarity between miRNA and target mRNA or translation inhibition if there is an imperfect binding (Wahid et al., 2010) (**Figure 1**). In case of perfect complementarity, Ago2 is the protein involved in the cleavage of the target mRNA in humans (Liu et al., 2004). However, in animals, translational repression is the most frequent way of action for miRNAs (Huntzinger and Izaurralde, 2011; Pasquinelli, 2012), although the exact process is still unknown since is not clear if the repression occur at the initiation step or during the translation process (Wahid et al., 2010). Even the mechanisms for target regulation played by miRNAs are still unclear, the target mRNA could be repressed by the promotion of deadenylation, sequestration of miRNAs and target by stress granules and P-Bodies (Valencia-Sanchez et al., 2006), disruption of translation initiation or protein degradation caused by RISC after translation (Tang et al., 2008).

The enormous content of non-coding RNA (ncRNA) in the cell intrigues its role and function in the cells. LncRNAs are defined as transcripts longer than 200 nucleotides and lacking an appreciable open reading frame (usually less than 100 amino acids). They may be transcribed by RNA polymerase II (RNA Pol II) or RNA Pol III, and may undergo splicing or comprise of a single exon. In contrast to small ncRNAs, lncRNAs tend to be poorly conserved evolutionarily and regulate gene expression by diverse mechanisms that are not entirely understood. As a functionally diverse macromolecule, the biological roles of lncRNAs cannot be determined solely from their nucleotide sequence, secondary structures, or genomic locations (Ng et al., 2013).

Recent work has begun to elucidate the roles of some lncRNAs, such as architectural function in nuclear paraspeckles (Sunwoo et al., 2009; Souquere et al., 2010), transcriptional co-regulators (Feng et al., 2006; Bond et al., 2009), and as endogenous competing RNAs (ceRNAs) (Cesana et al., 2011; Tay et al., 2011). LncRNA expression is abundant in cells of the CNS (Mehler and Mattick, 2007; Mercer et al., 2008) and recent studies have suggested that lncRNAs play crucial roles in spatial-temporal control of gene expression in brain development (Mercer et al., 2008). They have also known to be involved in brain development, neural differentiation and maintenance, synaptic plasticity, cognitive function and memory, and in aging and neurodegenerative disorders (Wu et al., 2013b).
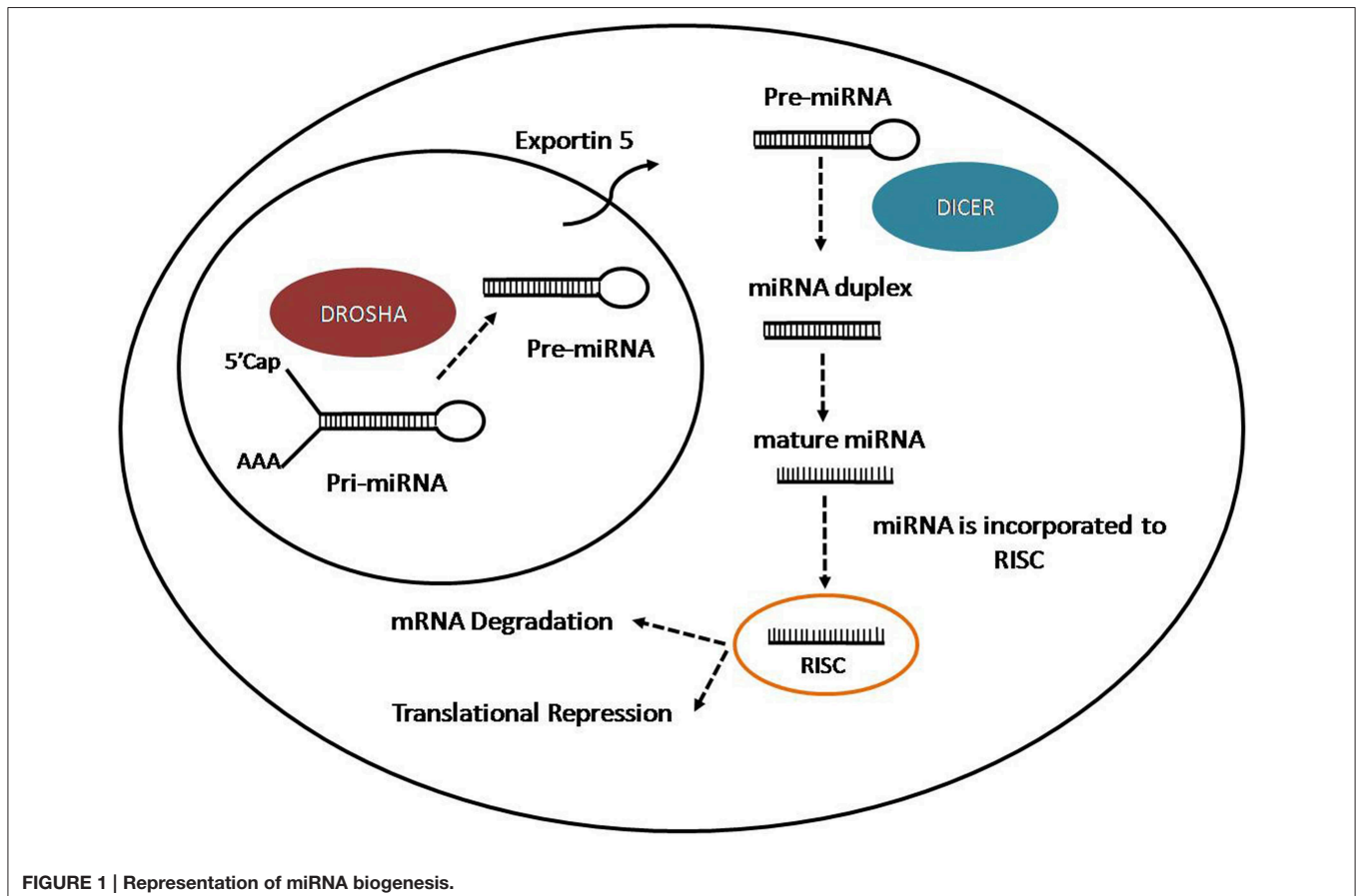
FIGURE 1 | Representation of miRNA biogenesis.

Though different mechanisms may play a role in causing neurodegenerative disorders, recent studies show increasing evidence of abnormalties in RNA processes, highlighting the possible putative role of RNA in neurodegeneration. An mRNA gain-of-toxic-function has been proposed for some neurodegenerative diseases (Osborne and Thornton, 2006; O'Rourke and Swanson, 2009; Todd and Paulson, 2010) whereas other neurodegenerative disorders are driven through altered or lost non-coding RNA, RNA splicing and RNA binding activities (Gallo et al., 2005; Cooper et al., 2009; Lagier-Tourenne et al., 2010).

Fronto temporal lobar degeneration (FTLD) is the most common cause of dementia after Alzheimer's disease. The clinico-pathological spectrum of FTLD includes frontal and temporal variants of frontotemporal dementia (FTD), primary progressive aphasia, semantic dementia, Cortico-basal degeneration (CBD), progressive supranuclear palsy (PSP), progressive subcortical gliosis (PSG) and FTD with motor neuron disease (FTD–MND) (Bugiani, 2007). Moreover, despite Amyotrophic Lateral Sclerosis (ALS) and FTD being two different neurodegenerative disorders, they often share genetic, neuropathological and clinical characteristics; therefore they are considered part of the same spectrum of diseases (Ling et al., 2013). Frontotemporal dementia symptoms can also be present along with disabling muscle weakness and osteolytic bone lesions, in IBMPFD1 (Inclusion body myopathy with early-onset Paget disease with or without Frontotemporal dementia 1).

It is estimated that one in seven people in the US might develop a neurodegenerative disorder in their lifetime, with dementia being one of the leading causes of death in US (Thies and Bleiler, 2011). Though this broad spectrum of disorders has been studied based on protein aggregation and research has been focusing on protein functions and alterations, emerging avenues in research unravels the role of RNA and RNA processing in contributing to neurodegeneration (Belzil et al., 2013).

To date, FTD has been linked to mutations in seven different genes (*TARDBP, FUS, MAPT, GRN, VCP, CHMP2B, C9ORF72*).

Findings that showed the presence of ubiquitinated protein TDP-43 in sporadic cases of ALS with FTD further linked these two diseases (Arai et al., 2006; Neumann et al., 2006). Following these findings, mutations in the gene coding for the RNA binding protein TDP-43 were discovered in ALS cases (Kabashi et al., 2008; Sreedharan et al., 2008; Van Deerlin et al., 2008) and FTD cases (Borroni et al., 2009; Kovacs et al., 2009).

With the broadening knowledge on the impact of impaired RNA binding proteins in mediating the disease process, mutations in the fused in sarcoma/translocated in liposarcoma (*FUS/TLS*) gene were found to account for an additional 5% of familial ALS and few rare cases of FTD (Kwiatkowski et al., 2009; Vance et al., 2009).

TDP-43 and FUS share similar structural and functional properties with a likely role in multiple steps of RNA processing and they are both linked to RNA metabolism. The pathological accumulation of these proteins is observed in over 90% ALS and 50% FTD patients. These studies also highlight that errors in RNA processing might be enough to initiate the disease process.

MAPT mutations were observed in several FTD families with abnormally phosphorylated tau proteins being isolated from neuroectoderm cells of patients. Mutations present in the C terminal repeat domains lead to the inhability of abnormal tau protein to bind microtubules, thus leading to its instability and accumulation and causing neuronal degeneration (Bugiani, 2007). FTD with tau inclusions was characterized as a tauopathy and dubbed FTLD-tau.

However, a different class of patients were found to have had accumulated ubiquitin and ubiquitin-associated proteins (FTLD-U). Co-localization of abnormal proteins with ubiquitin in the nucleus and perikaryon of neuronal cells, indicated the involvement of proteasome dysfunction in the pathology. Analysis of significant genes on chromosome 17, close to the MAPT locus, led to the discovery of mutations in *GRN* (Baker et al., 2006; Cruts et al., 2006). GRN is known to be involved in the cell cycle control and motility.

Studies on an ALS/FTD-affected Scandinavian family (Morita et al., 2006) and on IBMPFD1 families suggested the possible role of mutations in chromosome 9 in FTD. The disorder was associated to mutations in *VCP*, encoding the valosin-containing protein essential for ubiquitin-mediated protein degradation (Watts et al., 2004; Johnson et al., 2010).

Other FTLD mutations are located on chromosome 3 (FTD-3), in the *CHMP2B* gene, which encodes for a protein involved in degradation of surface receptor proteins and formation of endocytic multivesicular bodies (Skibinski et al., 2005).

Another link between ALS and FTD are the large intronic hexanucleotide repeat expansions in the *C9ORF72* gene located on chromosome 9 found in ALS, FTD, or ALS/FTD cases (DeJesus-Hernandez et al., 2011; Renton et al., 2011; Gijselinck et al., 2012).

This review will focus on the single genes known to have implications in FTD and their altered functions in the diseased state. The ultimate aim is to explorepossible functional connections between these seven diverse genes and describe a network in which a possible common thread might be represented through RNA mediated processes.

TARDBP (TDP 43)

Human TDP-43 was discovered in 1995 in a screen for transcriptional repressors of the trans-active response (TAR) DNA binding element of the HIV-1 virus, and thus the gene is named TARDNA Binding Protein (*TARDBP*) (Ou et al., 1995). *TARDBP* is composed of six exons and maps on chromosome 1p36.22.

The protein *TARDBP* produces is being labeled as TDP-43 due to its molecular weight of 43 KDa (Neumann et al., 2006). *TARDBP* is ubiquitously expressed in various human tissues (**Table 1**) including brain and spinal cord (Wang et al., 2008a). To date, 34 different TDP-43 mutations have been discovered in 131 different FTD and ALS families (Cruts et al., 2012). Pathogenic mutations observed in TDP-43 are highlighted in **Table 2**.

Structure
TDP-43 is a 414 amino acids protein (**Figure 2A**) containing two RNA recognition motifs (RRMs), a glycine-rich low sequence

TABLE 1 | Protein localisation of different genes associated to FTD.

Gene	Genomic location	Protein	Tissue localization in the brain	Cell type	Subcellular localization
TARDBP	Chromosome 1 p36.22	TDP-43	Cerebral cortex, hippocampus, lateral ventricle, cerebellum and spinal cord	Endothelial, neuronal, glial cells, neuropil and cell in granular and molecular layer, Purkinje cells	Nucleus and cytoplasm
FUS	Chromosome 16 p11.2	FUS	Cerebral cortex, hippocampus, lateral ventricle and cerebellum	Endothelial, neuronal, glial cells, neuropil and cell in granular and molecular layer, Purkinje cells	Nucleus and cytoplasm
MAPT	Chromosome 17 q21.3	Tau	Cerebral cortex, hippocampus, lateral ventricle and cerebellum	Neuronal, glial cells, neuropil and cell in granular and molecular layer, Purkinje cells	Cytoskeleton, cytoplasm, nucleus and plasma membrane
GRN	Chromosome 17 q21.31	Progranulin	Cerebral cortex, hippocampus, lateral ventricle and cerebellum	Neuronal, glial, endothelial cells and cell in granular layer	Vesicles, endoplasmic reticulum, golgi, extracellular space
VCP	Chromosome 9 p13.3	VCP	Cerebral cortex, hippocampus, lateral ventricle and cerebellum	Endothelial, neuronal, neuropil, glial cells and cell in granular and molecular layer, Purkinje cells	Endoplasmic reticulum, nucleus, cytoplasm
CHMP2B	Chromosome 3 p11.2	CHMP2B	Lateral ventricle	Neuronal cells	Cytosol, endosome, nucleus, mitochondria
C9ORF72	Chromosome 9 p21.2	C9ORF72	Cerebral cortex, hippocampus and lateral ventricle	Endothelial, neuropil, glial cells	Cytoplasm, nucleus, cytoskeleton

The information provided are derived through integration of two different databases (http://www.genecards.org/ and http://www.proteinatlas.org/) and literature reported in the text.

TABLE 2 | List of mutations in *TARDBP* and their characteristic phenotypes.

Subtypes of Dementia	Mutation	Change in amino acid	Type	References
FTD	g.6142C>T	p.N12	Pathogenic	Luquin et al., 2009
FTD	g.9253C>T	A90V	Pathogenic	Sreedharan et al., 2008
FTD/PSP	g.14575A>G	K263E	Pathogenic	Kovacs et al., 2009
ALS/FTD	g.14588A>G	N267S	Pathogenic	Corrado et al., 2009
FTD	g.14671G>A	G295S	Pathogenic	Benajiba et al., 2009
FTD	g.14932G>A	A382T	Pathogenic	Chiò et al., 2010

FTD, Frontotemporal Dementia; PSP, Progressive supranuclear palsy.
All the information reported in the table is derived from a cumulative study of the literature and the database: http://www.molgen.ua.ac.be/ADMutations/default.cfm?MT=0&ML=2& Page=FTD.

complexity prion-like domain (Wang et al., 2013). A nuclear localization signal motif (NLS) and a nuclear export signal motif (NES) allow TDP-43 to shuttle between the nucleus and the cytosol (Buratti and Baralle, 2001).

Localization and Function

Though TDP-43 expression is seen in the nucleus with low cytosolic localization (Ayala et al., 2005), there is a significant cytosolic TDP-43 expression especially in large motor neurons where TDP-43 has an additional role in mRNA transport as a neuronal activity responsive factor in dendrites thus promoting dendritic branching (Wang et al., 2008a; Barmada et al., 2010; Kabashi et al., 2010).

TDP-43 was found to be accumulated in cytoplasmic stress granules due to oxidative stress (Colombrita et al., 2009). Stress granules are aggregations, formed after cell insults such as oxidative stress or heat shock that temporarily store non-translating mRNAs, small ribosome subunits, RNA-binding proteins and translation initiation factors (Buchan and Parker, 2009).

Formation of stress granules protects the cells, allowing a translational block and initiation of repair processes (Anderson and Kedersha, 2008).

Upregulation of nuclear TDP-43 has also been shown to provide protection to primary neurons against glutamate induced excitotoxicity (Zheng et al., 2012). These findings also suggest that TDP-43 regulates synaptic plasticity by governing the transport and splicing of synaptic mRNAs. In a recent review, Belzil and co-authors postulate that altered TDP-43 could lead to impaired hippocampal plasticity and render neurons more vulnerable to cellular stressors (Belzil et al., 2013).

TDP-43 is highly conserved from human to *C. elegans*, both in the RNA binding motifs and in the carboxy-terminal portion (Ayala et al., 2005). *In situ* hybridization studies showed that TDP-43 is expressed very early in the brain and spinal cord of zebrafish (Shankaran et al., 2008) suggesting that it plays an important role in nervous system development.

FIGURE 2 | (A) TAR DNA-binding protein 43 (TDP-43) contains two RNA-recognition motifs (RRM1 and RRM2), a carboxy-terminal glycine-rich domain, a bipartite nuclear localization signal (NLS), and a nuclear export signal (NES). Mutations are mainly located in the glycine-rich domain. **(B)** The network of interactions of TDP-43 with proteins and RNAs. Green arrows indicate binding interactions or processes that result in activation or increased expression. Red arrows indicate binding interactions or processes that result in inhibition of activity or reduced expression. Black arrows indicate binding interactions or processes whose result can be either positive or negative. Dashed arrows indicated indirect processes. Symbols as in Legend. lncRNAs, long non-coding RNAs; IGF-1, insulin-like growth factor 1; HDAC4, histone deacetylase 4; NRXN1, neurexin 1; TDP-43, TAR DNA binding protein; FUS, fused in sarcoma; GRN, progranulin; NEAT1, nuclear-enriched autosomal transcript 1; NEAT2, nuclear-enriched autosomal transcript 1.

Implications of RNA in Pathogenesis

Many studies have linked TDP-43 to neurodegenerative disorders, including ALS and FTLD (Neumann et al., 2006; Lagier-Tourenne et al., 2010; Lee et al., 2012). Janssens and Van Broeckhoven (2013) have highlighted the increasing evidence of role of impaired RNA metabolism in TDP-43-driven neurodegeneration.

TARDBP primary transcript undergoes alternative splicing to produce eleven different mRNAs including the one encoding TDP-43. Seven of these are shorter transcripts which are generated through the seven different splicing reactions within exon 6 of *TARDBP* pre-mRNA using a combination of four different

5′ donor sites and four different 3′ acceptor sites (Wang et al., 2004a).

In few ALS cases a smaller TDP-43 isoform (~28 KDa) was observed additionally to the 43 kDa isoform, lacking exon 3 and a significant portion of exon 6-encoded amino acids (Strong et al., 2007). This smaller isoform lacks the carboxy-terminal portion of the protein and is thought to be associated with disease pathology (Neumann et al., 2006).

Converging lines of evidence in research suggest that TDP-43 regulates RNA in various ways (**Figure 2B**; Lee et al., 2012). The RRM1 domain of TDP-43 is critical for its binding to single-stranded RNA (Ou et al., 1995; Buratti and Baralle, 2001; Wang

et al., 2004a; Ayala et al., 2005). TDP-43 preferentially binds UG repeats, but is also found to be associated with non-UG repeat sequences (Buratti and Baralle, 2001; Ayala et al., 2005; Polymenidou et al., 2011; Tollervey et al., 2011).

Pathological TDP-43 aggregates are ubiquitinated and phosphorylated. Under normal conditions, these forms are not readily detectable in brain tissues, thus making them disease-specific. Over-expression of full-length TDP-43 in a variety of transgenic animal models lead to the presence of phosphorylated TDP-43 aggregates similar to ALS and FTD cases (Wegorzewska et al., 2009; Shan et al., 2010; Stallings et al., 2010; Wils et al., 2010; Xu et al., 2010a). The phosphorylated form has a longer half-life than the non-phosphorylated form thus leading to accumulation of phosphorylated proteins. Despite the progress toward describing the full spectrum of TDP-43 pathology in human neurodegenerative diseases, the fundamental question of whether TDP-43 dysfunction mediates neuro-degeneration through gain of toxic function or a loss of normal function remains unanswered (Lee et al., 2012).

Upon depletion of TDP-43 from adult mouse brain with antisense oligonucleotides, levels of 601 mRNAs, including FUS, GRN and other transcripts involved in neurodegeneration, were altered, along with 965 varied splicing events. RNAs depleted by the reduction of TDP-43 were coded by genes with long introns (Polymenidou et al., 2011).

In-vivo searches for TDP-43 RNA targets in mouse (Polymenidou et al., 2011), human brain (Tollervey et al., 2011), rat cortical neurons (Sephton et al., 2011), a mouse NSC-34 cell line (Colombrita et al., 2012), and a human neuroblastoma cell line (Xiao et al., 2011) revealed that there are more than 6000 RNA targets which constitutes to about 30% of total transcriptome. TDP-43 was found to preferentially bind to introns (including deep intronic sites), 3′ untranslated regions (UTRs), and non-coding RNAs (Polymenidou et al., 2011; Tollervey et al., 2011), indicating a multifaceted role in RNA maturation. TDP-43 can influence splice site selection by binding to exon-intron junctions and intronic regions, mRNA stability and transport by binding on 3′UTRs. A substantial amount of mRNAs regulated by TDP-43 at splicing levels were involved in neuronal development or in neurological diseases (Tollervey et al., 2011). Additional data show that when TDP-43 is reduced the levels of several other mRNAs increase. As the affected mRNAs include more than 300 mRNAs without TDP-43 binding sites, these observation point toward an indirect mechanism (Polymenidou et al., 2011) of modulation.

i-CLIP experiments have also shown that TDP-43 binds to long ncRNAs (lncRNAs), including nuclear-enriched autosomal transcript 1 (NEAT1) and metastasis-associated lung adenocarcinoma transcript 1 (MALAT1, also called NEAT 2) (Tollervey et al., 2011). Expression of both lncRNAs is elevated in FTD patients with TDP-43 inclusions, thus correlating with their increased association with TDP-43 (Tollervey et al., 2011).

The binding of TDP-43 to small (<200 base) ncRNAs and miRNAs remains largely unexplored. However, the association of TDP-43 with Drosha microprocessor (Ling et al., 2010) and Dicer complexes (Freibaum et al., 2011; Kawahara and Mieda-Sato, 2012) provides a suggestive role of TDP-43 involvement in

miRNA biogenesis. Indeed, let-7b miRNA is downregulated, whereas miR-663 is upregulated upon reduction of TDP-43 (Buratti et al., 2010). Di Carlo and collegues demonstrated that TDP-43 directly interacts with Drosha and controls its stability at different levels. Moreover, TDP-43 is also involved in the Drosha substrate recognition as in the regulation mediated by Drosha of Neurogenin 2, an important and master gene in neurogenesis (Di Carlo et al., 2013).

Fan et al. (2014) have performed CLIP-seq analysis to examine the small RNAs (pri-miRNAs, miRNAs, and piRNAs) bound to TDP-43 and found that a novel miRNA (miR-NID1), which is processed from the intron five of human neurexin 1 gene (NRXN1), interacts with TDP-43 and represses expression of NRXN1. Neurexins are cellular proteins that function as cell adhesion molecules and receptors in the vertebrate nervous system, involved in synaptic development including calcium signaling, heterogeneous cell-to-cell adhesion and synaptogenesis (Craig et al., 2006; Bottos et al., 2011) Disruptions or mutations of NRXN1 have been reported to associate with autistic spectrum disorder (ASD), mental retardation, and schizophrenia (Reichelt et al., 2012).

Recent studies by King and colleagues identified a physical interaction between TDP-43 and miR-1 family which is known to be involved in smooth muscle gene repression in heart and an opposing myogenic differentiation (King et al., 2014). TDP-43 overexpression in skeletal muscle led to decrease of miR-1 and increased protein levels of the miR-1 family targets, IGF-1 and HDAC4. These results demonstrate that TDP-43 could influence miRNA regulation through a physical interaction by limiting their bioavailability for RISC loading and offer a mechanism by which mature miRNAs can be differentially regulated.

The expression of TDP-43 is tightly autoregulated through a complex interplay between transcription, splicing, and 3′ end processing (Avendaño-Vázquez et al., 2012): TDP-43 overexpression in humans and mice leads to activation of a 3′ UTR intron which results in excision of proximal polyA site (PAS) which in turn activates a cryptic PAS and prevents TDP-43 expression through a nuclear retention mechanism.

The above mentioned studies have highlighted that TDP-43 is linked to various mRNAs and non-coding RNAs, in a neuronal context wherein it mediates effects through splicing or interaction with Drosha and Dicer complexes. It is also involved in its autoregulation mediated at the RNA level.

Additionally, TDP 43 is known to interact with MATR3, a DNA RNA binding protein. Their interaction was confirmed to be RNA based. Mutations in this gene have been linked to cases of ALS. The authors further report that the phenotype observed in patients with MATR3 was a combination of those observed in cases of ALS and myopathy. Clinical symptoms were similar to patients with VCP mutations (Johnson et al., 2014).

FUS

FUS, (fused in sarcoma, also called TLS: translocated in liposarcoma) belongs to the TET family of RNA binding proteins involved in many different cellular processes (Bertolotti et al., 1996; Law et al., 2006; Tan and Manley, 2009). FUS, located

on chromosome 16 at locus p11.2, encodes a multifunctional protein able to bind and interact with single stranded RNA and double stranded DNA, participating in different aspects of RNA metabolism (Shelkovnikova et al., 2014).

Structure

FUS is characterized by different domains (**Figure 3A**): a N-terminal domain with transcriptional activating properties mainly composed of glutamine, glycine, serine, and tyrosine residues (Law et al., 2006), a glycine rich region, a RNA binding domain, and a highly conserved C-terminus capable of binding DNA, RNA and splicing factors (Law et al., 2006).

Localization and Function

FUS is mainly localized in the nucleus (Colombrita et al., 2009; Van Blitterswijk and Landers, 2010; Kawahara and Mieda-Sato, 2012) but it is also actively implicated in other cellular processes that occur in the cytoplasm such as mRNA transport, mRNA stability and translation (Buratti and Baralle, 2010; Colombrita et al., 2011). Indeed FUS was reported to shuttle between the nucleus and the cytoplasm, exporting to the cytoplasm spliced mRNAs in ribonucleoprotein complexes (Zinszner et al., 1997). Particularly, upon stimulation in hippocampal neurons FUS was reported to accumulate in the spines of mature dendrites, where local translation occurred (Fujii and Takumi, 2005). FUS immunoreactivity was also observed in dendritic spines in mature primary cultures and in adult hippocampus *in situ* (Belly et al., 2005; **Table 1**).

The C-terminal part of FUS encodes for a non-classic nuclear localization signal (**Figure 3A**; Iko et al., 2004) that is necessary for nuclear import, as it was demonstrated through the generation of deletion mutant lacking 13 amino acids in the C-terminal part of FUS(Dormann et al., 2010).

Several papers reported that mutations and aberrations of *FUS* are linked to the pathogenesis of frontotemporal degeneration (FTD) as well as familial and sporadic ALS (Kwiatkowski et al., 2009; Vance et al., 2009), as reported in **Table 3**. Moreover, FUS accumulates in inclusions in the cytoplasm of autopsied spinal cords and brains of sporadic and familial ALS and FTD. FUS inclusions are not only observed in presence of *FUS* mutations, as they were found in patients with different or unknown genetic defects such as sporadic ALS, ALS/dementia or FTLD (with or without progranulin mutations), FUS or TDP43 mutation-linked familial ALS, SOD1-negative familial ALS. These inclusions were also positive for TDP43/ubiquitin and p62 (Deng et al., 2010).

ALS/FTD patients show mutations mainly in the Glycine rich region and C-terminal part (Lagier-Tourenne et al., 2010). The mechanism underlying the pathogenesis of FUS mutations was related to FUS nucleus/cytoplasmic imbalance since ALS mutations increase its localization in the cytoplasm, observed through immunostaining of FUS in postmortem ALS brain samples (Kwiatkowski et al., 2009), or through the analysis in neuroblastoma cell lines of the subcellular localization of recombinant mutant FUS fused either to green fluorescent protein (GFP) (Kwiatkowski et al., 2009; Morlando et al., 2012), an N-terminal hemagglutinin (HA) tag (Vance et al., 2009), a C-terminal V5-His tag, or an N-terminal myc tag in HeLa (Ito et al., 2011).

Both the loss of FUS nuclear function and the potential gain of toxic effect by FUS in the cytoplasm could explain pathogenesis (Shelkovnikova et al., 2014).

Very few studies so far reported FTD cases associated with *FUS* mutations. The first analysis of *FUS* in FTD patients showed a novel missense mutation in the glycine-rich region of FUS, predicted to be pathogenic by *in silico* analysis (Van Langenhove et al., 2010). Subsequently another study found novel missense mutations in patients with familial ALS with features of frontotemporal dementia (FALS/FTD) and one with familial ALS with parkinsonism and dementia (FALS/PD/DE) (Yan et al., 2010). Recently, another study found two novel heterozygous missense mutations in *FUS* in patients with behavioral variant FTD (bvFTD), however the pathogenicity of these mutations needs to be further investigated in other screening (Huey et al., 2012).

FUS has been reported to co-localize with TDP-43 in nuclear complexes (Kim et al., 2010b; Ling et al., 2010) and in larger cytoplasmic complexes (Kim et al., 2010b). Purified FUS has also been reported to interact with purified His-tagged TDP-43 *in vitro* in an RNA-independent manner, associated to the C-terminal region of TDP-43 (Kim et al., 2010b). These ubiquitously expressed binding proteins seem to have similar and complementary functions.

Only the mutant form of FUS was found in stress granules in reponse to translational arrest (Bosco et al., 2010). FUS and TDP-43 were observed to co-localize in cytoplasmic aggregations of ALS/FTLD-affected neurons (Da Cruz and Cleveland, 2011). Dormann and colleagues found stress granule markers such as PABP-1 and eIF4G co-deposited with FUS inclusions in sections of post-mortem brain and spinal cord tissue from familial ALS-FUS and sporadic FTDLD-U. On the contrary, TDP inclusions did not show any co-localization with stress granules proteins in HeLa transiently transfected with the mutated form of FUS, after heat shock for 1 h (Dormann et al., 2010). Another study reported that ubiquitin-positive inclusions in frozen post-mortem tissue from FTLD-TDP patients were not stained with anti-FUS antibodies (Neumann et al., 2009b), therefore FUS and TDP-43 are not always found in the same inclusions or aggregates.

The relation between FUS and TDP-43 is reported as a delicate equilibrium, where small alteration on their relative quantity and presence in nucleus/cytoplasm could very likely cause serious problem over a long period (Colombrita et al., 2012), which might be an accumulation of events due to an alteration of their targetome.

Implications of RNA in Pathogenesis

FUS is involved in pre-mRNA splicing (**Figure 3B**), by interacting with splicing factors such as SRm160, PTB, and serine/arginine rich proteins (SR proteins) (Yang et al., 1998; Meissner et al., 2003). In addition the recent sequencing approaches applied to clarify the function and identify the targets of FUS reinforced its fundamental role in splicing (Colombrita et al., 2012) by revealing its binding to intronic sequences or to splice site acceptors.

Similarly to many other splicing factors, FUS can bind the C-terminal domain of RNA polymerase II and prevent
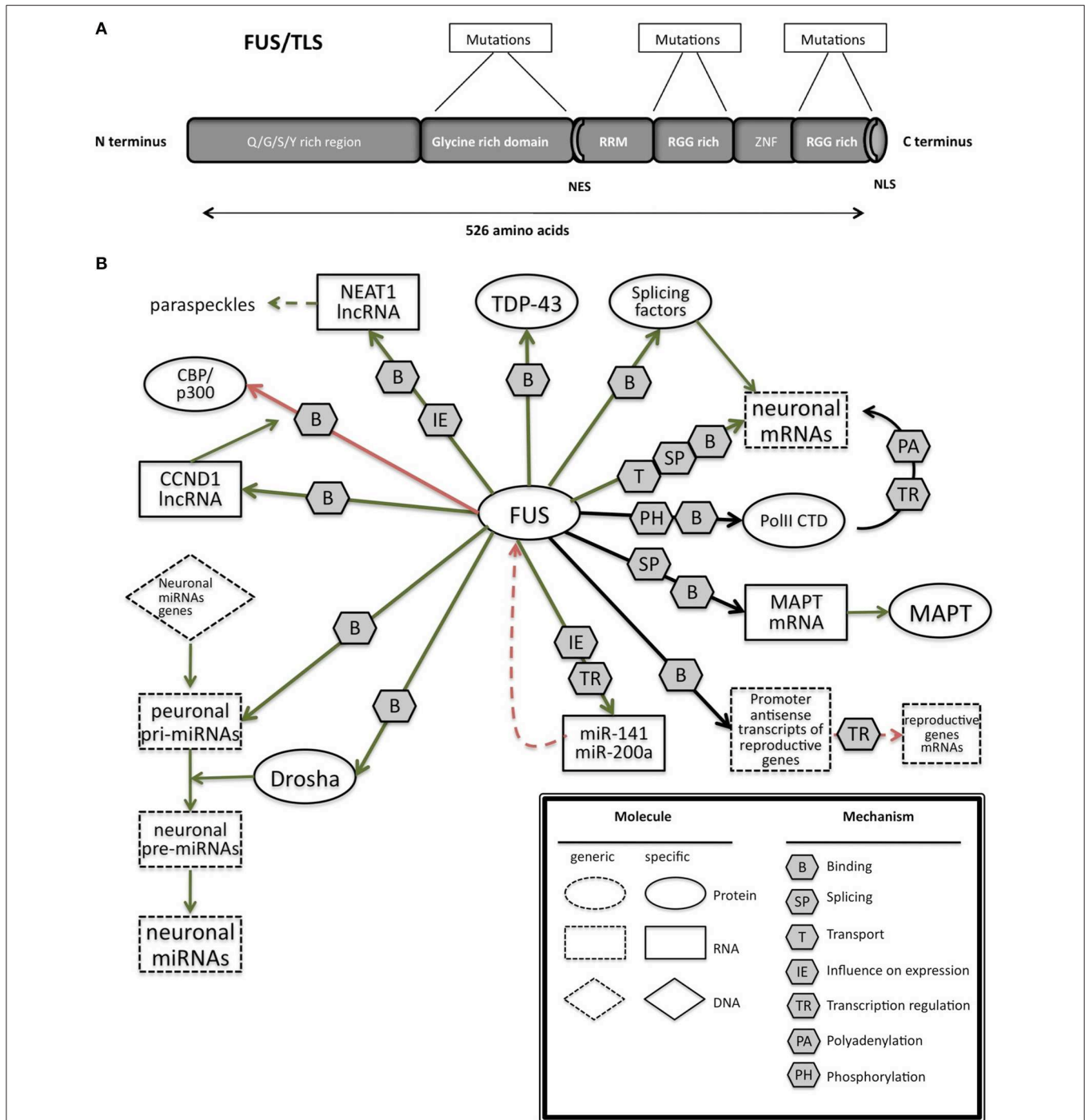
FIGURE 3 | (A) Schematic representation of the functional domains in FUS/TLS. FUS contains a N-terminal part enriched in glutamine, glycine, serine and tyrosine residues (QGSY region), a glycine-rich region, a nuclear export signal (NES), an RNA recognition motif (RRM), repeats of arginine, glycine, glycine (RGG), a zinc finger motif (ZNF), and a C-terminal nuclear localization signal (NLS). Most of the mutation are localized in the glycine rich region and in the last 17 amino acids of the NLS part. **(B)** The network of interactions of FUS with proteins and RNAs. Green arrows indicate binding interactions or processes that result in activation or increased expression. Red arrows indicate binding interactions or processes that result in inhibition of activity or reduced expression. Black arrows indicate binding interactions or processes whose result can be either positive or negative. Dashed arrows indicated indirect processes. Symbols as in Legend. lncRNAs, long non-coding RNAs; IGF-1, insulin-like growth factor 1; HDAC4, histone deacetylase 4; NRXN1, neurexin 1; TDP-43, TAR DNA binding protein; FUS, fused in sarcoma; MAPT, microtubule-associated protein tau; NEAT1, nuclear-enriched autosomal transcript 1; CCND1, G1/S-specific cyclin-D1; CBP, CREB-binding protein; p300, Histone acetyltransferase p300; PolI CTD, Carboxy-terminal Domain of the RNA polymerase II.

TABLE 3 | List of mutations in *FUS* and their characteristic phenotypes.

Subtypes of Dementia	Mutation	Change in amino acid	Type	References
FTD	g.4961A>G	M254V	Unclear	Van Langenhove et al., 2010
bvFTD	g.31183985C>T	P106L	Unclear	Huey et al., 2012
ALS/FTD	g.31185031G>A	G206S	Unclear	Yan et al., 2010
FALS/PD/DE	g.31191418C>T	R521C	Unclear	Yan et al., 2010
ALS/FTD	g.31191419G>A	R521H	Pathogenic	Broustal et al., 2010

ALS, Amyotrophic lateral sclerosis; FTD, Frontotemporal Dementia; bv FTD, behavioral variant Frontotemporal Dementia; FALS, Familial Amyotrophic lateral sclerosis; PD, Parkinson's disease; DE, Dementia.
All the information reported in the table is derived from a cumulative study of the literature and the database: http://www.molgen.ua.ac.be/ADMutations/default.cfm?MT=0&ML=2& Page=FTD.

the premature hyperphosphorylation of Ser2 in the C-terminal domain of RNA polymerase II. Moreover the lack of FUS leads to an accumulation of RNA polymerase II at the transcription start site with a shift toward abundance of mRNA isoforms with early polyadenylation (Schwartz et al., 2012).

FUS can bind to the promoter antisense strand transcript of some genes such as Ptprn2, Xrn1, Gak, or Glt1d1 and this interaction downregulates the transcription of the coding sense strand, but this effect seems to be specific for some genes enriched with GO terms connected to the reproductive process(Ishigaki et al., 2012).

As FUS was shown to regulate RNA polymerase II at many more gene promoters than the genes reported for splicing defects, its role on transcription could be a separated function in addition to the regulation on splicing (Schwartz et al., 2012). However, a small proportion of FUS target regions is localized in exonic sequences and in the 3′UTRs (Hoell et al., 2011), suggesting another potential role, such as the transport of mRNAs or the control of mRNA stability and translation (Fujii et al., 2005; Fujii and Takumi, 2005). A model was suggested, in which FUS is released from actin filaments, when cytoskeletal organization collapses, becoming free to be linked to the mRNA that is transported to the local translational machinery in the spines (Fujii and Takumi, 2005).

Recent techniques, like HITS-CLIP or RIP-CHIP were also used to identify FUS binding motif, but all the studies lead to the common assumption that FUS binds to specific secondary structures on its RNA targets and a primary sequences analysis is not sufficient (Colombrita et al., 2012; Ishigaki et al., 2012).

Interestingly, silencing of *FUS* was reported to alter splicing events in genes, such as *MAPT,* that have an important neuronal function (Ishigaki et al., 2012). This finding leads an unexpected connection between these two genes, both involved in the pathogenesis of FTD. In particular, FUS was shown to help the skipping of *MAPT* exon 10 in primary cortical neurons (Ishigaki et al., 2012). The alternative splicing of *MAPT* exon 10 is known to have a causative role in FTD as discussed later (*MAPT* paragraph).

FUS is also involved in microRNA biogenesis (Morlando et al., 2012), specifically interacting with pri-miRNAs and Drosha, and helping the recruitment of Drosha for the correct miRNA processing in neuronal cells. Several miRNAs like miR-9, miR-132, and miR-125b whose biogenesis is controlled by FUSare important for neuronal functions, neuronal differentiation, and

synaptogenesis (Morlando et al., 2012). Additionally miR-9 and miR-132 have also been shown to control neurite extension and branching through downregulation of Foxp2 (Forkhead box protein P2) (Clovis et al., 2012) Moreover this role of FUS seems to be prominent in neuronal cells compared to non-neuronal cells, such as HeLa cells, in which the proportion of miRNAs affected by *FUS* knockdown was lower. Indeed the mutations known to induce a cytoplasmic delocalization of FUS would impede its nuclear role as pri-miRNA processor. Though the balance of nuclear and cytoplasmic FUS seems necessary, the sole role of nuclear FUS should not be neglected and further investigations would be needed to clarify its biological function within this cell compartment. Recently, the same laboratory demonstrated the presence of a regulatory loop in which FUS can enhance the expression of miR-141 and miR-200a, which in turn regulate FUS, through a binding on its 3′UTR. This pathway seems to be affected in the presence of one mutation found in two ALS patients (Dini Modigliani et al., 2014).

FUS is also reported to bind lncRNAs. The binding to lncRNA CCND1 induces an allosteric change in FUS, thus in turn permits its interaction with CBP/p300. As FUS represses CBP/p300-mediated transcription by inhibiting their histone acetyltransferase (HAT) functions (Wang et al., 2008a), in the presence of ncRNA CCDN1, CBP/p300-mediated transcription is repressed.

The nuclear-enriched abundant transcript 1 (NEAT1) produces two types of lncRNAs from the same promoter NEAT1_1 and NEAT1_2 (Nishimoto et al., 2013). FUS was shown to bind NEAT1_2, known to assemble and organize the core proteins of paraspeckles (Wang et al., 2008a; Hoell et al., 2011; Lagier-Tourenne et al., 2012), which represent a storage for the rapid release of RNAs during stress condition or a nuclear retention of long hyperedited transcripts (Prasanth et al., 2005; Chen and Carmichael, 2009). According to observations and data obtained from cultured cells, transgenic mice and human postmortem tissue, paraspeckles represents an important protective cell mechanism during stress conditions (Nakagawa et al., 2011; Nakagawa and Hirose, 2012; Shelkovnikova et al., 2014).

Paraspeckels are present in almost all the cultured cells (Fox and Lamond, 2010), but in normal tissues are found only in cells that contain high levels of NEAT1_2 RNA and coherently, in neurons where NEAT1 is express at low levels, paraspeckles are not observed (Nakagawa et al., 2011).

The presence of FUS in paraspeckles was confirmed in different cell lines by three studies (Naganuma et al., 2012; Nishimoto et al., 2013; Shelkovnikova et al., 2014) Moreover, NEAT1 was shown through PAR-CLIP to be a target of both WT and mutant FUS (Hoell et al., 2011).

Paraspeckles are found in spinal motoneurons of patients at early stage of ALS. The possibility that aging induces an increase in the level of NEAT1_2 was ruled out due to the fact that human control cases were older that ALS cases of an average of 10 years. However, the process that induces an up-regulation of NEAT1_2 lncRNA during the early phases of ALS is still unknown (Nishimoto et al., 2013). Overall FUS seems to play a key role on the regulation of RNA at different levels, acting on transcription, splicing, transport, and stability of mRNA with a particular function in microRNA biogenesis and interaction with non-coding RNAs.

MAPT (Tau)

MAPT (microtubule associated protein) encodes for protein Tau and is located on chromosome 17q21.3. The gene, which is 150 kb-long, contains 16 exons, out of which 11 are expressed in CNS (Wolfe, 2012).

Structure

The protein consists of a projection domain, including an acidic and a proline-rich region, which interacts with cytoskeletal elements (**Figure 4A**). The N-terminal part is involved in signal transduction pathways by interacting with proteins such as PLC-γ and Src-kinases. The C-terminal part, referred to as the microtubule binding domain, regulates the rate of microtubules polymerization and is involved in binding with functional proteins such as protein phosphatase 2A (PP2A) or presenilin 1 (PS1) (Luna-Muñoz et al., 2013).

Localization and Function

Tau is a microtubule-associated protein which is found in abundance in the axons of Central nervous system (CNS) and Peripheral nervous system (PNS) (Binder et al., 1985; Couchie et al., 1992; **Table 1**). It is also observed in astrocytes and oligodendrocytes in the CNS. The tau pre-mRNA undergoes alternative splicing at exons 2, 3, and 10 to give six different possible isoforms. Inclusion of exon 10 generates 4-repeat or 4R tau, while exclusion forms 3-repeat or 3R tau. In neurons this ratio is controlled throughout development, emphasizing the importance of this balance for neuronal functions.

Implications of RNA in Pathogenesis

In FTD populations, *MAPT* mutation frequency ranges from 8 to 50%. To date, 44 different *MAPT* mutations, either mis-sense or splice mutations or both, have been discovered in 138 different families (Cruts et al., 2012). The list of pathogenic mutations observed in *MAPT* are reported in **Table 4**). Most missense mutations alter ability of tau to bind to microtubules, thus leading to the formation of inclusion in neurons and glia, called neurofibrillary tangles (NFT) (Lee et al., 2005).

About half of the mutations in *MAPT*, however, are associated with alteration of splicing of exon 10 and increase the ratio of 4R to 3R. The mutations near exon 10 5′ splice site enhance inclusion of exon 10 either by altering the linear *cis*-splicing elements or by

FIGURE 4 | (A) Schematic representation of the functional domains of the largest tau isoform (441 amino acids 2N4R isoform). The N-terminal projection domain, including an acidic and a proline-rich region, interacts with cytoskeletal elements. The N-terminal part is also involved in signal transduction pathways by interacting with proteins such as PLC-γ and Src-kinases. The C-terminal part, also known as the microtubule-binding domain, regulates the rate of microtubules polymerization and is involved in binding with proteins such as protein phosphatase 2A (PP2A) or presenilin 1(PS1). **(B)** Schematic representation of the progranulin structure encoded by the major human transcript containing all the 13 exons. The lettered boxes on the progranulin scheme represent the individual granulin domains containing cystein-rich motifs.

TABLE 4 | List of mutations in *MAPT* and their characteristic phenotypes.

Subtypes of dementia	Mutation	Change in amino acid	Type	References
FTD	g.75756G>A	R5H	Pathogenic	Hayashi et al., 2002
FTD	g.110018A>C	K592T	Pathogenic	Rizzini et al., 2000
FTD	g.110026A>G	I595V	Pathogenic	Grover et al., 2003
FTD	g.110044C>G	L601V	Pathogenic	Kobayashi et al., 2003
FTD	g.110063G>T	G607V	Pathogenic	Schenk, 1959
FTD	g.110065G>A	G608R	Pathogenic	Van der Zee et al., 2006
FTD	g.123725T>G	N614K	Pathogenic	Wszolek et al., 1992
FTD	g.123729_123731delAAG	DeltaK616 (alias ΔK280; ΔK281)	Unclear	Rizzu et al., 1999
FTD	g.123740T>C	L619	Pathogenic	D'Souza et al., 1999
FTD	g.123774A>C	N631H	Pathogenic	Iseki et al., 2001
FTD	g.123776T>C	N631	Pathogenic	Brown et al., 1996
FTD	g.123789C>A	P636T	Pathogenic	Lladó et al., 2007
FTD	g.123789C>T	P636S	Pathogenic	Bugiani et al., 1999
FTD	g.123790C>T	P636L	Pathogenic	Hutton et al., 1998
FTD	g.123802G>A	S640N	Pathogenic	Iijima et al., 1999
FTD	g.123802G>T	S640I	Pathogenic	Kovacs et al., 2008
FTD	g.123803T>C	S640	Pathogenic	Spillantini and Goedert, 2000
FTD/PSP	g.123806G>A	Intronic	Pathogenic	Spillantini et al., 1997
FTD	g.123814T>C	Intronic	Pathogenic	Miyamoto et al., 2001
FTD	g.123815C>T	Intronic	Pathogenic	Takamatsu et al., 1998
FTD	g.123816A>G	Intronic	Pathogenic	Hutton et al., 1998
FTD	g.123817C>T	Intronic	Pathogenic	Lynch et al., 1994
FTD	g.123819C>T	Intronic	Pathogenic	Lanska et al., 1994
FTD	g.123822C>G	Intronic	Pathogenic	Stanford et al., 2003
FTD	g.127672T>G	L650R	Pathogenic	Rosso et al., 2003
FTD	g.127673G>A	L315	Pathogenic	(Bird, 2005, Personal Communication)
FTD	g.127678A>T	K652M	Pathogenic	Zarranz et al., 2005
FTD/PD/MND	g.127687C>T	S655F	Pathogenic	Rosso et al., 2002
FTD	g.132033G>A	G670S	Pathogenic	Spina et al., 2007
FTD	g.132034G>T	G670V	Pathogenic	Neumann et al., 2005
FTD	g.137420G>A	G389R	Pathogenic	Pickering-Brown et al., 2000
FTD	g.137420G>C	G389R	Pathogenic	Murrell et al., 1999
FTD	g.137471C>T	R741W	Pathogenic	Dickson, 1997
FTD	g.137525C>A	Q424K	Pathogenic	(Brice, 2005, Personal Communication)
FTD	g.137535C>T	T762M	Pathogenic	Giaccone et al., 2004
bvFTD	c.163G>A	G55R	Pathogenic	Iyer et al., 2013
FTD	c.363T>C	V363A	Pathogenic	Rossi et al., 2014
FTD	c.363C>A	V363I	Pathogenic	Rossi et al., 2014
FTD	c.454G>A	A152T	Pathogenic	Kara et al., 2012
FTD	c.530A>T	D177V	Unclear	Kim et al., 2014
FTD	c.853A > C	S285R	Pathogenic	Ogaki et al., 2013
FTD	c.892 A>G	K298E	Pathogenic	Iovino et al., 2014
FTD	c.1090C>T	P364S	Pathogenic	Rossi et al., 2012
FTD	c.1096G>A	G366R	Pathogenic	Rossi et al., 2012
FTD	c.1228A>C	N410H	Pathogenic	Kouri et al., 2014
FTD	c.1381-74G > A	Intronic	Pathogenic	Kim et al., 2010a
FTD	c.1908G > A	P636P	Pathogenic	Kim et al., 2010a
FTD	c.1815G > A	P605P	Pathogenic	Kim et al., 2010a
FTD	c.1828-47C > A	Intronic	Pathogenic	Kim et al., 2010a
FTD	c.2002+90G > A	Intronic	Pathogenic	Kim et al., 2010a

(Continued)

TABLE 4 | Continued

Subtypes of dementia	Mutation	Change in amino acid	Type	References
FTD	c.2092G>A	V363I	Pathogenic	Bessi et al., 2010
FTD	IVS10+4A>C	Intronic	Pathogenic	Anfossi et al., 2011
FTD	IVS9-15T>C	Intronic	Pathogenic	Anfossi et al., 2011
FTD	g.132037A>G	Q336R	Pathogenic	Pickering-Brown et al., 2004

FTD, Frontotemporal Dementia; bv FTD, behavioral variant frontotemporal Dementia.

All the information reported in the table is derived from a cumulative study of the literature and the database: http://www.molgen.ua.ac.be/ADMutations/default.cfm?MT=0&ML=2&Page=FTD.

destabilizing a stem-loop structure at the exon-intron junction (D'Souza et al., 1999; Grover et al., 1999; Spillantini and Goedert, 2013). This stem-loop arises as a result of the self complementarity among bases in this region and has a putative role in masking the 5′ splice site Mutations that disrupt the stem-loop structure make the 5′ splice site accesible to splicing factors, leading to inclusion of exon 10 (Wolfe, 2012).

Though mutations lead to alteration of splicing at the mRNA level, their primary effect becomes pathogenic through changes in the protein level in about half of the cases (Goedert and Jakes, 2005).

The human *MAPT* 3′UTR, as well as that of rodents, contains two Polyadenylation Signals (PAS) in tandem and can undergo alternative polyadenylation (APA) to produce transcripts of approximately 2 or 6 kb, namely the short and long transcript variants (Poorkaj et al., 2001). Dickson and colleagues investigated the role of human *MAPT* 3′-UTR in regulating tau expression (Dickson et al., 2013). They observed that the two *MAPT* 3′UTR variants are differentially regulated and influence both mRNA stability and protein expression levels. The same authors have reported that miR-34a can bind the human *MAPT* 3′-UTR long form and reduce tau levels, whereas inhibition of endogenous miR-34 family members leads to increased tau levels, leading to a hypothesis that up-regulation of miR-34 observed during neuronal differentiation could be a compensatory mechanism to decrease the expression of tau aggregates. Recent work (Wu et al., 2013a) also confirms the finding that *MAPT* is regulated by miRNA 34c-5p and miRNA 34c-3p, which bind to its 3′UTR.

Additionally, work by Zovoilis and colleagues have suggested that miR-34c could be a marker for the onset of cognitive disturbances linked to Alzheimers disease and they also indicate that targeting miR-34c could thus be a suitable therapy (Zovoilis et al., 2011).

Studies also reported that miR-34 regulates apoptosis by blocking the SIRT1 gene (Hermeking, 2010) and astrocytic apoptosis has been observed as an early event in FTLD conditions (Broe et al., 2004). These findings suggest that miRNAs might be involved in FTD through apoptotic mechanisms.

Tau is known to spread through synaptic and non-synaptic mechanisms (Medina and Avila, 2014) and its accumulation is thought to be mediated through spreading of the protein from cell to cell. Tau has been reported to be secreted unconventionally in naked form (Chai et al., 2012) or associated to exosomes (Saman et al., 2012) and/or other membrane vesicles (Simón et al., 2012). This method of elimination of tau has been suggested

as a response mechanism to inhibit tau secretion and toxicity. Recent reports have suggested that tau is released into culture medium from neuroblastoma cells, tau-expressing non-neuronal cells, induced pluripotent stem cell-derived human neurons, and mouse primary neurons (Kim et al., 2010a; Shi et al., 2012). This has also been observed in the brain interstitial fluid of both wild-type and P301S tau-expressing mice in micro-dialysis studies (Yamada et al., 2011). Clinico-pathological studies underline the tau pathology progression from entorhinal cortex through the hippocampus and into limbic system (Arriagada et al., 1992). Recent *in vivo* studies in tauopathy transgenic mouse models have also highlighted the spreading of tau pathology through a trans-synaptic mechanism in anatomically connected neuronal networks (De Calignon et al., 2012; Liu et al., 2012). Apart from these, intracerebral inoculation of synthetic tau fibrils induced NFT (Neuro fibrillary tangles) like inclusions that propagated from injected sites to other connected regions of brain (Iba et al., 2013).

Current hypotheses also include that pathological progression of improperly folded of tau could be transferred between neuronal cells via a prion-like seeding mechanism which might lead to neurodegeneration.

The major implication observed upon mutations which lead to splice defects highlights the relevance of regulation at RNA level which decides the fate of onset of neurodegeneration. The regulation of MAPT mediated through miRNAs further indicates the role of non-coding RNAs in determining tau protein levels.

GRN (Progranulin)

GRN is located on the long arm of chromosome 17 at the locus q21.31 which is present at a distance of 1.7 Mb from *MAPT* (Baker et al., 2006; Cruts et al., 2006). *GRN* encodes for a 593 aa precursor protein of 68.5 kDa called progranulin.

Structure

Progranulin can be N-glycosylated at five potential sites and secreted as a mature protein of 88 kDa (Chen-Plotkin et al., 2010; Songsrirote et al., 2010). The protein is formed by 7.5 cysteine-rich granulin domains, separated through linker sequences that contain disulfide bridges (He and Bateman, 2003), as represented in **Figure 4B**. This characteristic structure can be cleaved at the intra-linker spacer sequences to produce seven non-identical granulins that contain cysteine-rich motifs. Different proteases can cleave progranulin, such as matrix metalloproteinase-14 (Butler et al., 2008), elastase (Zhu et al., 2002), proteinase 3, and

neutrophil elastase (NE) at the pericellular microenvironment of the neutrophil cell surface (Kessenbrock et al., 2008). The full-length progranulin, once secreted, is protected from cleavage by the high-density lipoprotein (HDL)/Apolipoprotein A-I complex (Okura et al., 2010) and the secretory leukocyte protease inhibitor (SLPI) (Zhu et al., 2002).

Localization and Function

Progranulin is present in many tissues, is highly expressed in immune system cells (Daniel et al., 2000) and in a medium level in the brain (Bhandari et al., 1996; Ahmed et al., 2007), where it is highly expressed in specific populations of neuronal cells, such as cortical neurons, and granule cells of the hippocampus (Daniel et al., 2000; **Table 1**). The subcellular location of progranulin seems to be the endoplasmic reticulum (ER) and Golgi, where it is particular abundant in mouse cortical neurons and mouse microglia (Almeida et al., 2011). Progranulin is implicated in a wide range of biological processes such as embryogenesis (Díaz-Cueto et al., 2000; Daniel et al., 2003; Bateman and Bennett, 2009), cell survival and cell growth (Plowman et al., 1992; He and Bateman, 1999), inflammation and wound repair (Zhu et al., 2002; He et al., 2003; Kessenbrock et al., 2008; Yin et al., 2010), transcriptional repression (Hoque et al., 2003, 2010) and several reports suggest its role in neuronal development (Van Damme et al., 2008). Interestingly, progranulin and the proteolytically cleaved granulins can have coherent functions, such as in the regulation of neurite outgrowth (Van Damme et al., 2008), or they can have contrasting roles, such as in inflammation processes (He and Bateman, 2003).

To date, 69 different *GRN* mutations have been discovered in 231 families (Cruts et al., 2012). A list of detailed pathogenic mutations are reported in **Table 5**. The *GRN* mutations frequency range from 1 to 11.7% in FTD patients, but the frequency rises to 12–25% in familial FTD (Cruts et al., 2006; Gass et al., 2006; Huey et al., 2006; Bronner et al., 2007; Borroni et al., 2008). There are different types of *GRN* mutations, the majority are classified as non-sense, frameshift, and splice site mutations that cause a premature stop codons (Baker et al., 2006; Cruts et al., 2006). However, the pathogenic variants include also missense mutations with a partial decrease of progranulin and a loss of its function (Mukherjee et al., 2006, 2008; Shankaran et al., 2008; Wang et al., 2010). Silent and intronic mutation with unknown pathology can also occur. Generally the pathogenic *GRN* mutations lead to a decreased *GRN* expression due to a non-sense-mediated mRNA decay, resulting in a *GRN* haploinsufficiency inherited in an autosomal dominant manner (Baker et al., 2006; Cruts et al., 2006; Gass et al., 2006; Cruts and Van Broeckhoven, 2008).

Indeed progranulin levels, measured in either the serum or cerebrospinal fluid (CSF) of patients with *GRN* mutations are ~30–50% of normal (Van Damme et al., 2008). Moreover, a decreased progranulin level can be also detected in plasma of *GRN* mutations patients (Finch et al., 2009) and a reduced GRN mRNA level can be observed in patient whole blood samples through microarray experiments (Coppola et al., 2008). In contrast an increased level of GRN mRNA was observed in the frontal cortex from post-mortem brain samples

of FTD patients with *GRN* mutations, as compared to FTD patients without *GRN* mutations (Chen-Plotkin et al., 2010). The higher level of GRN transcripts could be due to the robust microglia infiltrations, observed in the brain tissues of *GRN* mutation patients. Indeed microglia shows high level of GRN expression.

Implications of RNA in Pathogenesis

Most of the patients with FTLD-U show *GRN* mutations with presence of TDP-43 ubiquitin positive inclusions, hence bearing the term FTLD-TDP (Mackenzie et al., 2006, 2010; Sampathu et al., 2006). The relation between TDP-43 and progranulin is not fully understood, however several recent studies indicate that TDP-43 controls the expression of progranulin by binding to GRN mRNA. On a study in which TDP-43 targets were identified through a RIP-chip analysis, it is shown that TDP-43 has a post-transcriptional regulation on GRN and VEGFA (Vascular endothelial growth factor A) (Colombrita et al., 2012).

As previously mentioned, TDP-43 was shown to specifically bind GRN 3′UTR controlling GRN mRNA stability and the final quantity of progranulin protein (Polymenidou et al., 2011; Colombrita et al., 2012). Moreover a knock-down of TDP-43 in mice showed an increase in the amount of GRN mRNA level (Polymenidou et al., 2011; Colombrita et al., 2012). Depletion of TDP-43 also led to altered splicing of sortilin, the putative progranulin receptor (Polymenidou et al., 2011). The relation between GRN and TDP-43 was also demonstrated *in vitro*: cells that were treated with siRNA against GRN for 72 h, showed a caspase-dependent cleavage of TDP-43 into fragments (Zhang et al., 2007); whereas primary neuronal cultures upon knowck-down of GRN showed a re-localization of TDP-43 in the cytoplasm (Guo et al., 2010).

Through genetic association analysis, a common genetic variation localized on the 3′UTR of GRN (rs5848) was shown to represent a genetic risk factor for FTD (Rademakers et al., 2008). Progranulin levels in brain extracts from rs5848 TT homozygous FTD patients were lower than in CC carriers, as observed through western blot analyses, ELISA, and immunohistochemistry. A stronger binding of miR-659 in the 3′UTR of GRN was shown in the presence of the rs5848 T variant, and might explain the reduced progranulin levels.

It is reported that miR-107 is downregulated in presence of Alzheimer's disease at early stage (Wang et al., 2008b). Another study demonstrated through a RIP-Chip analysis performed in human H4 neuroglioma cells that the open reading frame of GRN mRNA contains many recognizing sequences elements for miR-107 (Wang et al., 2010), showing implications of miR-107 deregulation in neurodegenerative diseases. In particular miR-107 regulation of GRN seems to be relevant to glucose metabolism in cultured H4 neuroglioma cells. Previous analysis identified miR-107 as one of the microRNAs that increase their expression with glucose supplementation in cell culture medium (Tang et al., 2009). Wang and colleagues reported that glucose metabolic pathway may recruit miR-107 to regulate GRN expression. Another microRNAs that was found significantly down-regulated in brains of Alzheimer's disease patients

TABLE 5 | List of mutations in *GRN* and their characteristic phenotypes.

Subtypes of Dementia	Mutation	Change in amino acid	Type	References
FTD	delGRN[DR184]	Complete gene deletion	Pathogenic	Gijselinck et al., 2008
FTD	c.-7-20C>T	INTRON	Suggesting Pathogenic	Kim et al., 2010a
FTD	c.349 + 34C > T	INTRON	Suggesting Pathogenic	Kim et al., 2010a
FTD	IVS6+5_8delGTGA	N/A	Unclear	Marcon et al., 2011; Skoglund et al., 2011
FTD	c.1138C>G	Q380E	Unclear	Kim et al., 2014
FTD	g.2988_2989delCA	P439_R440fsX6	Pathogenic	Gabryelewicz et al., 2010
FTD	g.5215A>T	Complete protein degradation	Pathogenic	Le Ber et al., 2007
FTD	g.5217G>C	Complete protein degradation	Pathogenic	Cruts et al., 2006
FTD	g.5913A>G	INTRON	Pathogenic	Mukherjee et al., 2008
FTD/PD	g.8948_12532del	Complete protein deletion	Pathogenic	Rovelet-Lecrux et al., 2008
FTD	g.9044T>C	Predicted failed translation	Pathogenic	Baker et al., 2006
FTD	g.9045G>A	Predicted failed translation	Pathogenic	Cruts et al., 2006
FTD/MND	g.9055G>C	V5L	Unclear	Lopez de Munain et al., 2008
FTD	g.9061T>C	W7R	Unclear	Le Ber et al., 2007
FTD/PPA	g.9068C>A	A9D	Pathogenic	Mukherjee et al., 2006
FTD	g.9132_9133insCTGC	C31LfsX35	Pathogenic	Baker et al., 2006
FTD/PPA	g.9144delC	G35EfsX19	Pathogenic	Gass et al., 2006
FTD	g.9181G>A	Failed translation initiation	Pathogenic	Gass et al., 2006
FTD/AD	g.9319delA	T52HfsX2	Pathogenic	Gass et al., 2006
FTD	g.9399_9400delAG	G79DfsX39	Pathogenic	Gass et al., 2006
FTD	g.9408delC	S82VfsX174	Pathogenic	Bronner et al., 2007
FTD	g.9429G>A	E88	Unclear	Gass et al., 2006
FTD	g.9593T>C	C105R	Unclear	Gass et al., 2006
FTD	g.10129C>T	Q125X	Pathogenic	Baker et al., 2006
FTD	g.10134 C>G	C126W	Unclear	Bernardi et al., 2012
FTD	g.10136_10137delCT	P127RfsX2	Pathogenic	Cruts et al., 2006
FTD	g.10144_10147delCAGT	Q130SfsX125	Pathogenic	Baker et al., 2006
FTD	g.10319G>A	A155WfsX56	Pathogenic	Gass et al., 2006
FTD/PPA	g.10645_10646delCA	S226WfsX28	Pathogenic	Gass et al., 2006
FTD	g.10668C>A	P233Q	Unclear	Bronner et al., 2007
FTD	g.10678C>T	N236	Unclear	Gass et al., 2006
FTD	g.10679G>C	V200GfsX18	Pathogenic	Gass et al., 2006
FTD	g.10965_10966delTG	C253X	Pathogenic	Gass et al., 2006
FTD	g.11002 G>C	A266P	Unclear	Bernardi et al., 2012
FTD	g.11041_11042insCTGA	A237WfsX4	Pathogenic	Cruts et al., 2006
FTD/CBS	g.11240G>C	V279GfsX5	Pathogenic	Gass et al., 2006
FTD	g.11266G>C	E287D	Unclear	Gass et al., 2006
FTD	g.11315_11316insTG	W304LfsX58	Pathogenic	Gass et al., 2006
FTD	g.11316G>A	W304X	Pathogenic	Gass et al., 2006
FTD	g.11339G>A	V279GfsX5	Pathogenic	Baker et al., 2006
FTD/CBS	g.11639delC	T382SfsX30	Pathogenic	Baker et al., 2006
FTD	g.11651G>A	W386X	Pathogenic	Baker et al., 2006
FTD	g.11944_11945delGT	V411SfsX2	Pathogenic	Bronner et al., 2007
FTD	g.11965C>T	R418X	Pathogenic	Baker et al., 2006
FTD	g.12054C>T	H447	Unclear	Bronner et al., 2007
FTD	g.12108_12109insC	C466LfsX46	Pathogenic	Gass et al., 2006
FTD	g.12115C>T	Q468X	Pathogenic	Baker et al., 2006
FTD	g.12227C>T	C474	Unclear	Gass et al., 2006
FTD	g.12282C>T	R493X	Pathogenic	Huey et al., 2006
FTD	g.12428G>C	W541C	Unclear	Bronner et al., 2007

AD, Alzheimers disease; CBS, Corticobasal syndrome; FTD, Frontotemporal Dementia; PPA, Primary progressive aphasia; MND, Motor neuron disease; PD, Parkinsons disease.
All the information reported in the table is derived from a cumulative study of the literature and the database: http://www.molgen.ua.ac.be/ADMutations/default.cfm?MT=0&ML=2&Page=FTD.

is miR-29b, that beloged to the miR-29a/b-1 cluster (Hébert et al., 2008). Interestingly progranulin can also be regulated by miR-29b through a binding in the 3′UTR of GRN mRNA (Jiao et al., 2010). It would be useful to know if these microRNAs deregulation can contribute to the pathogenesis of dementia. So far different microRNAs seem to be important for the control of progranulin along with the role played by TDP-43 on the stability of GRN mRNA and its expression.

VCP

The VCP (Valosin-containing protein) gene is located on chromosome 9p13.3. It also called p97 or CDC48, consists of 17 coding exons.

Structure

The VCP protein is composed of four domains vital for its proper functioning, namely the N, D1 D2 and C-terminal domains (**Figure 5B**; DeLaBarre et al., 2006; Pye et al., 2007). The VCP N domain is encoded by exons 1, 2, 3, 4 and 5, while the D1 and D2 domains are encoded by exons 6, 7, 8, 9, 10 and 12, 13, 14, respectively. There are two linker domains in the protein: the N-D1 linker and the flexible D1-D2 linker.

VCP is a member of the AAA-ATPase gene superfamily (ATPase Associated with diverse cellular Activities) (Woodman, 2003; Wang et al., 2004b), and is one of the most abundant cytosolic proteins (**Table 1**) conserved throughout in mammals. The complete protein contains 806 amino acids. The N domain of VCP is responsible for the cofactor and ubiquitin binding
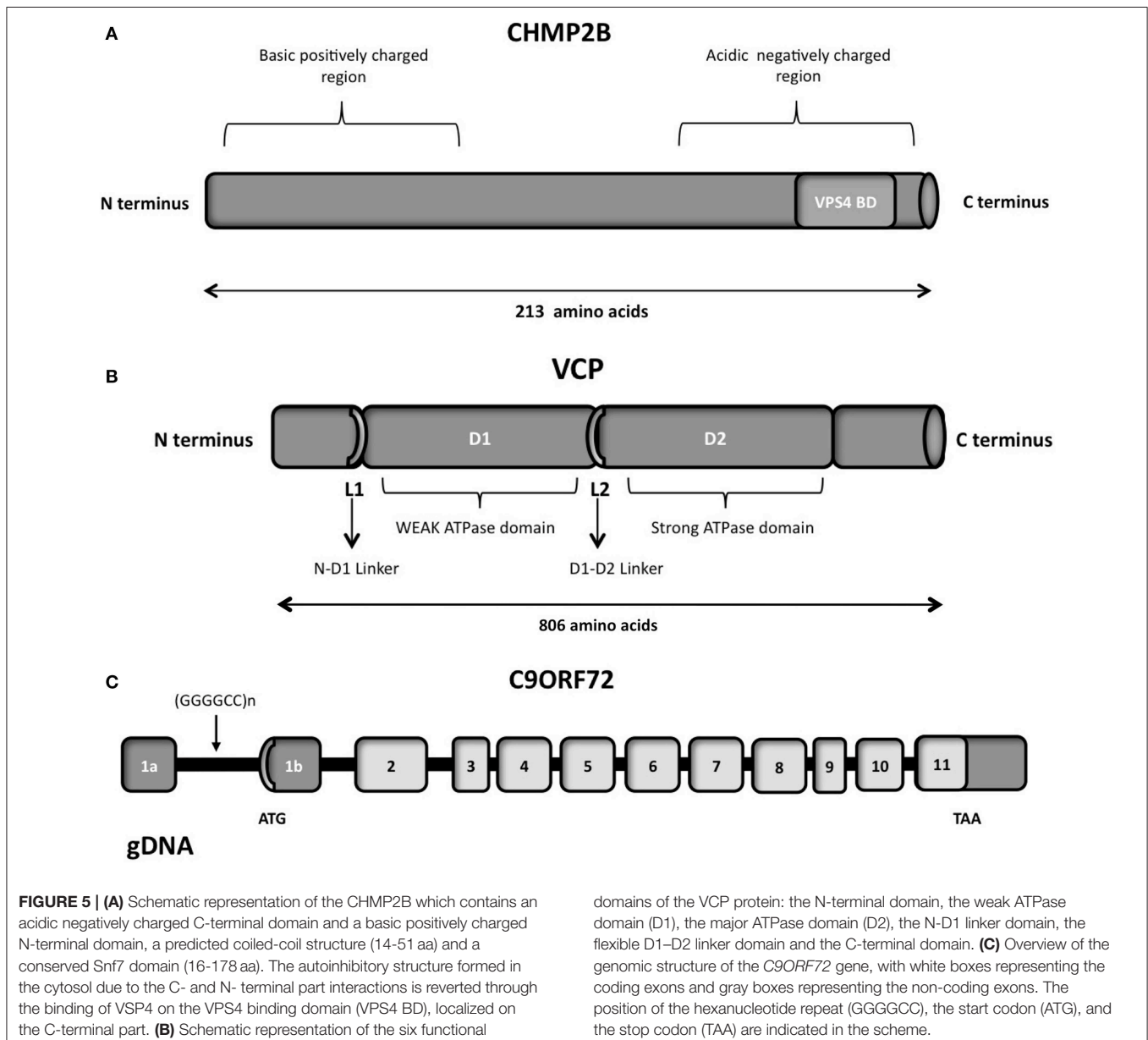
FIGURE 5 | (A) Schematic representation of the CHMP2B which contains an acidic negatively charged C-terminal domain and a basic positively charged N-terminal domain, a predicted coiled-coil structure (14-51 aa) and a conserved Snf7 domain (16-178 aa). The autoinhibitory structure formed in the cytosol due to the C- and N- terminal part interactions is reverted through the binding of VSP4 on the VPS4 binding domain (VPS4 BD), localized on the C-terminal part. **(B)** Schematic representation of the six functional

domains of the VCP protein: the N-terminal domain, the weak ATPase domain (D1), the major ATPase domain (D2), the N-D1 linker domain, the flexible D1–D2 linker domain and the C-terminal domain. **(C)** Overview of the genomic structure of the *C9ORF72* gene, with white boxes representing the coding exons and gray boxes representing the non-coding exons. The position of the hexanucleotide repeat (GGGGCC), the start codon (ATG), and the stop codon (TAA) are indicated in the scheme.

FIGURE 6 | A possible network of interactions between proteins and RNAs, at the basis of FrontoTemporal Dementia. Green arrows indicate binding interactions or processes that result in activation or increased expression. Red arrows indicate binding interactions or processes that result in inhibition of activity or reduced expression. Black arrows indicate binding interactions or processes whose result can be either positive or negative.

Purple arrows indicate binding interactions or processes which are hypotetical. Symbols as in Legend. lncRNAs, long non-coding RNA; TDP-43, TAR DNA binding protein; FUS, Fused in Sarcoma; GRN, progranulin; MAPT, Microtubule-Associated Protein Tau; VCP, Valosin Containing Protein; C9ORF72. CHMP2B, Charged multivesicular body protein 2b; Rab7, Ras-related protein 7.

function (Wang et al., 2004b). While the D1 domain mediates oligomerization-independent nucleotide binding, the D2 domain confers most of the ATPase activity (Wang et al., 2004b).

Localization and Function

This protein functions as a molecular chaperone in various distinct cellular processes including ubiquitin-dependent protein degradation, stress responses, programmed cell death, nuclear envelope reconstruction, and Golgi and endoplasmic reticulum (ER) assembly (Guinto et al., 2007).

VCP is known to be involved in protein aggregation/quality control of mitochondria and cell proliferation (Hayashi, 2013) and is vital for retro-translocation of misfolded proteins from Endoplasmic reticulum to cytoplasm (Kimonis et al., 2008). Mutation and depletion studies of VCP have provided evidence of accumulation of poly-ubiquitinated proteins (Dai and Li, 2001). Mutations in this gene may suggest the disruption of normal protein degradation pathway in the disease. This could be facilitated through the disruption of binding between the VCP and protein adaptors.

The expression of mutant VCP in myoblastic cell lines is associated with increased ubiquitin conjugated proteins (Weihl et al., 2006). Studies on overexpression of mutant VCP protein in transgenic mice implicated an age-dependent muscle weakness and Ubiquitin-positive inclusions and accumulation of high molecular weight protein aggregates (Weihl et al., 2007).

VCP functions as a homohexamer (Zhang et al., 2000; Rouiller et al., 2002) by binding to multiple proteins associated with Ubiquitin proteasome system (UPS). The VCP complex binds to polyubiquitin chains and unbounds ubiquitinated proteins from their binding partners thereby facilitating transport to the UPS.

Implications of RNA in Pathogenesis

To date, 18 different VCP mutations have been discovered in 48 different families, which include FTLD that is associated with ALS, inclusion body myopathy, and Paget disease (Cruts et al., 2012). **Table 6** high-lights the list of pathogenic mutations observed so far. The association of inclusion body myopathy and FTD was established by Kovach et al. (2001).

TABLE 6 | List of mutations in *VCP* and their characteristic phenotypes.

Subtypes of Dementia	Mutation	Change in amino acid	Type	References
IBMPFD	g.284G>A	R92H	Unclear	Kaleem et al., 2007
IBMPFD	g.410C>T	P137L	Pathogenic	Stojkovic et al., 2009
IBMPFD	g.4438C>T	R93C	Pathogenic	Guyant-Maréchal et al., 2006
IBMPFD	g.4444C>G	R95G	Pathogenic	Watts et al., 2004
IBMPFD	g.4444C>T	R95C	Pathogenic	Kimonis et al., 2008
IBMPFD	g.6990C>T	R155C	Pathogenic	Watts et al., 2004
IBMPFD	g.6991G>A	R155H	Pathogenic	Watts et al., 2004
IBMPFD	g.6991G>T	R155L	Unclear	Kumar et al., 2010
IBMPFD	g.6991G>C	R155P	Pathogenic	Watts et al., 2004
IBMPFD	g.6990C>A	R155S	Pathogenic	Stojkovic et al., 2009; Vesa et al., 2009
IBMPFD	g.6996G>C	G157R	Pathogenic	Stojkovic et al., 2009; Djamshidian et al., 2009
IBMPFD	g.7002C>T	R159C	Pathogenic	Bersano et al., 2009
IBMPFD	g.7003G>A	R159H	Pathogenic	Haubenberger et al., 2005
IBMPFD	g.7099G>A	R191Q	Pathogenic	Watts et al., 2004
IBMPFD	g.8085T>G	L198W	Pathogenic	Watts et al., 2007
IBMPFD	g.8187C>A	A232E	Pathogenic	Watts et al., 2004
IBMPFD	g.9349A>G	T262A	Pathogenic	Spina et al., 2008
IBMPFD	g.10742A>C	N387H	Pathogenic	Watts et al., 2007
IBMPFD	g.11295G>C	A439P	Pathogenic	Shi et al., 2012
IBMPFD	g.11295G>T	A439S	Pathogenic	Stojkovic et al., 2009

IBMPFD, Inclusion body myopathy with Paget's disease of the bone and frontotemporal dementia.
All the information reported in the table is derived from a cumulative study of the literature and the database: http://www.molgen.ua.ac.be/ADMutations/default.cfm?MT=0&ML=2&Page=FTD.

A recent work by Jacquin et al. (2013) has showed R155H (464 G>A) mutation of the *VCP* gene in a French family, led to the Inclusion body myopathy with Paget's disease of the bone and frontotemporal dementia (IBMPFD), with a psychiatric onset of FTD.

The expression of IMBPFD-associated *VCP* mutations in skeletal muscle cells reduced UNC-45 (a molecular chaperone involved in myosin assembly) degradation that is linked to severe myofibril disorganization in myotubules. This study suggests a possible mechanism for the selective vulnerability of skeletal muscle in IBMPFD; however, the implication for the pathogenesis of FTD still remains unknown. Studies on a *VCP*-mutant transgenic mouse have shown TDP-43 and ubiquitin positive accumulations (Custer et al., 2010) suggesting a possible interplay between these proteins. IBMPFD is known to have TDP-43 aggregation with *VCP* mutations (Nalbandian et al., 2011). Ju et al. (2009) have established a link between *VCP* and autophagosomes wherein the loss of VCP leads to accumulation of autophagosomes, thus establishing a possible cause of aggregation of proteins such as TDP-43.

VCP has been detected in a few inclusions of neurodegenerative diseases such as senile plaques in Alzheimer's disease, Lewy bodies in Parkinson's disease, neuronal intranuclear inclusions in CAG/polyglutamine diseases and ubiquitin-positive inclusions in ALS (Hirabayashi et al., 2001; Mizuno et al., 2003; Ishigaki et al., 2004).

Bartolome and colleagues have performed analyses in fibroblasts derived from patients with three different pathogenic *VCP* mutations, VCP-deficient cells, mouse cortical primary neurons and astrocytes, to conclude that reduction of VCP led to uncoupling of mitochondria and increased oxygen consumption and a subsequent decrease in ATP of cells leading to cellular toxicity and neuronal death (Bartolome et al., 2013).

VCP has been recently involved in clearance of mRNP granules (Buchan et al., 2013), thereby unraveling a new mechanism in clearance of RNPs from the cell. This might indicate why *VCP* mutations lead to accumulation of stress granule constituents or cytoplasmic inclusions. mRNP granules assemble to form stress granules as a consequence of their aggregation (Erickson and Lykke-Andersen, 2011). Wang et al. (2015) have shown a direct interaction between VCP and FUS. VCP being a key regulator of protein degradation, DNA interaction, and mitochondrial activity, its direct interaction with FUS is intriguing. Although there is no evidence which shows a direct interaction or implication of *VCP* mutations on RNA, its association with TDP-43 and FUS, both of which are RNA binding proteins may suggest their unraveled interactions in RNA metabolism.

CHMP2B

CHMP2B (Charged multivesicular body protein) is encoded by a gene located on chromosome 3 and is a component of the endosomal sorting complex required for transport-III (ESCRT-III complex).

Structure

CHMP2B is a protein of 213 amino acids, with an acid C-terminal domain and basic N-terminal domain (**Figure 5A**), and

a predicted coiled-coil structure (Skibinski et al., 2005). The negatively charged C-terminal domain interacts with the positively charged N-terminal part, creating a closed and autoinhibitory structure in the cytosol (Whitley et al., 2003; Shim et al., 2007). CHMP2B requires therefore an activation process performed by VPS4, which binds to its C-terminal domain. Indeed the C-terminal part of CHMP2B contains a binding domain for VPS4. VPS4 is a member of the AAA-ATPase family and it has a role in catalyzing the dissociation of ESCRT complexes from endosomes (Katzmann et al., 2002). The ATPase activity of VPS4 is important for endosomal sorting (Katzmann et al., 2002; Obita et al., 2007). Mutations localized in the VSP4-binding region impair the function of CHMP2B, preventing the formation of protrusions from the cell (Bodon et al., 2011).

Localization and Function

Northern-Blot analysis demonstrated that CHMP2B is expressed in all the major parts of the brain, including the temporal and frontal lobes (**Table 1**). Moreover through *in situ* hybridization of mouse brain, an enhanced expression of CHMP2B in the hippocampus, frontal and temporal lobes, and cerebellum was shown (Skibinski et al., 2005). The endosomal-sorting complex required for transport (ESCRT) is a protein complex involved in the endocytosed protein trafficking from endosome to lysosomes, playing an important role for sorting of proteins and for their efficient lysosomal degradation (Urwin et al., 2010). Moreover ESCRT complexes have a relevant role at the plasma membrane, during cytokinesis (Carlton and Martin-Serrano, 2007; Elia and Sougrat, 2011), budding of some enveloped viruses (Usami et al., 2009; Martin-Serrano and Neil, 2011), autophagy and transcriptional regulation (Roxrud et al., 2010; Schmidt and Teis, 2012). Endosomal trafficking is a key process for the internalization and transport of neuronal growth factors, secreted growth factors, signaling molecules (Bronfman et al., 2007). A dysfunction in this process could lead to an altered cell-signaling and aberrant communication between cells.

Implications of RNA in Pathogenesis

In particular ESCRT dysfunction is associated with neurodegeneration, indeed mutation in *CHMP2B* have been reported in frontotemporal dementia linked to chromosome 3 (FTD-3) (Urwin et al., 2010). FTD-3 has an onset of 48–67 years and is an autosomal dominant dementia with TDP-43 negative FTLD-U, ubiquitin positive inclusions (Urwin et al., 2010).

As reported in **Table 7**, several missense mutations are connected with FTD-3 (Skibinski et al., 2005), with familial or sporadic cases of ALS (Parkinson et al., 2006; Urwin et al., 2010), familial frontotemporal lobar degeneration (FTLD) (Ghanim et al., 2010) or CBD (Van der Zee et al., 2008), however only few studies analyzed their pathogenic features in cultured neurons.

A point mutation has been identified in the 5′ acceptor site of exon 6, causing the production of two abnormal transcripts: CHMP2B^{intron5} with retention of intron 5 and CHMP2B$^{\Delta10}$ that has a 10 bp deletion and a sequence frameshift due to the use of a criptic splice site in exon 6 (Skibinski et al., 2005). Both proteins lack 36 amino acids in the C-terminal part with the subsequent absence of VPS4-binding domain and an accumulation of CHMP2B on the endosomal membrane (Skibinski et al., 2005; Urwin et al., 2010). This accumulation suggests that the binding of mutated proteins to the endosomes prevents the recruitment of the correct proteins necessary for the fusion with lysosomes (Metcalf and Isaacs, 2010; Urwin et al., 2010). Indeed large and abnormal endosomal structures are observed in post-mortem brain tissues, in patient fibroblast cultures and in case of overexpression of CHMP2B mutant in PC12 and human neuroblastoma cell lines (Skibinski et al., 2005; Van der Zee et al., 2008; Urwin et al., 2010). Moreover CHMP2B seems to act through a gain of function mechanism in the presence of mutations, since only the transgenic mice expressing CHMP2B^{intron5} show similar neuropathology features observed in FTD-3 patients, whereas the knockout mice with the inactivation of CHMP2B do not show any pathological characteristics (Ghazi-Noori et al., 2012).

Another non-sense mutation replaces a glutamine residue with a stop codon, creating a more severe C-terminal truncation (Van der Zee et al., 2008).

TABLE 7 | List of mutations in CHMP2B and their characteristic phenotypes.

Subtypes of Dementia	Mutation	Change in amino acid	Type	References
FTD	g.13227A>G	I29V	Unclear	Cannon et al., 2006
FTD	g.18376C>A	T104N	Unclear	Cox et al., 2010
FTD	g.25885A>G	N143S	Unclear	Van der Zee et al., 2007
FTD	g.25899G>T	D148Y	Pathogenic	Skibinski et al., 2005
FTD	g.25950C>T	Q165X	Pathogenic	Van der Zee et al., 2007
FTD	g.26189G>C	p.M178VfsX2/p.M178LfsX30	Pathogenic	Skibinski et al., 2005
FTD	g.26214C>T	R186X	Unclear	Momeni et al., 2006
FTD	g.26218G>A	S187N	Unclear	Ferrari et al., 2010
FTD	g.26276A>C	Q206H	Pathogenic	Parkinson et al., 2006
FTD	c.581C>T	S194L	Unclear	Ghanim et al., 2010

FTD, Frontotemporal Dementia.

All the information reported in the table is derived from a cumulative study of the literature and the database: http://www.molgen.ua.ac.be/ADMutations/default.cfm?MT=0&ML=2&Page=FTD.

Since CHMP2B is involved in the endosomal trafficking of signal molecules, it could be interesting and possibly relevant for the pathology to check if an altered endosomal process can affect the function of other proteins involved in FTLD, such as progranulin, as is it also suggested by Urwin et al. (2010).

C9ORF72

Structure

Large expansions of the non-coding GGGGCC repeat in *C9ORF72* (Chromosome 9 open reading frame 72) were recently demonstrated to cause ALS and FTD (DeJesus-Hernandez et al., 2011; Renton et al., 2011). Indeed 20–80% of familial and 5–15% of sporadic ALS and FTD in North American and European patients show this hexanucleotide expansion with a range of 700–1600 repeats, whereas the normal population carries less than 30 repeats (DeJesus-Hernandez et al., 2011; Renton et al., 2011; Smith et al., 2012). Pathogenic mutations reported in *C9ORF72* are listed in **Table 8**. *C9ORF72* is localized on chromosome 9 and is composed of 12 exons, with two alternate non-coding first exons (**Figure 5C**, exon 1a and 1b) (DeJesus-Hernandez et al., 2011). Specifically, the polymorphic hexanucleotides repeat was identified between the two alternatively spliced non-coding exons, through a sequencing approach (DeJesus-Hernandez et al., 2011).

Depending on alternative transcription initiation, the GGGGCC repeat can be located on the promoter of transcriptional variant 1 or in the intron 1 of transcriptional variants 2 and 3. Variant 2 results from splicing of exons 1a and exons 2–5 whereas variant 3 is composed of exon 1a and exons 2–11.

Localization and Function

Expression array data showed wild type C9ORF72 RNA present in different CNS tissues, including spinal cord and higher expression in the cerebellum (Renton et al., 2011; **Table 1**).

The protein encoded by *C9ORF72* is still uncharacterized and with unknown function even if it is well-conserved across species (DeJesus-Hernandez et al., 2011).

Recently, Farg et al. (2014) demonstrated for the first time that the endogenous C9ORF72 protein has a function in the regulation of intracellular trafficking processes in the endosomal and autophagy-lysosomal compartments in neuronal cell lines. Therefore, they reported the normal cellular function of C9ORF72 that is essential to understand its role in FTD/ALS.

In particular, they found co-localization in neuronal cell lines and primary cortical neurons of C9ORF72 with four Rab

proteins, which are involved in endosomal trafficking. In motor neurons, they found 70% of colocalization with Rab7, which is a fundamental protein implicated in the biogenesis of lysosomes, the transport of endosomes and the maturation of autophagosomes (Gutierrez et al., 2004). A similar mechanism of interaction and recruitment of Rab7 was also described for CHMP2B by Urwin and collaborators. In *CHMP2B* mutant cells, an impaired recruitment of Rab7 onto endosomes was observed with a decreased fusion with lysosomes and a delayed degradation (Urwin et al., 2010).

C9ORF72 protein was also found to colocalize with lysosomes, ubiquilin-2 and autophagosomes, involved in autophagy (Farg et al., 2014). Interestingly, the ability of C9ORF72 to interact with hnRNPs and induce not yet characterized nuclear aggregates and stress granules, could link the C9ORF72 protein with RNA metabolism processes (Farg et al., 2014).

Implications of RNA in Pathogenesis

Immunocytochemistry analysis on human fibloblasts and mouse motor neuron NSC-34 cell line revealed a predominant nuclear localization of C9ORF72 protein (Renton et al., 2011). Immunohistochemical analysis showed C9ORF72 expression in neurons and in FTD- and ALS-affected regions with a predominant cytoplasmic staining and a synaptic localization, but the quantitative mRNA analysis demonstrated that the repeat expansion reduces C9ORF72 transcript variant 1 expression in lymphoblast cell lines of expanded repeats carriers and in frontal cortex samples from unrelated FTLD-TDP patients carrying expanded repeats (DeJesus-Hernandez et al., 2011). The hexanucleotide repetitions present in the C9ORF72 transcript can form G-tetrad units, called G-quartets, where G bases are rearranged in a cyclic pattern with eight hydrogen bonds (Fratta et al., 2012). The presence of RNA G-quadruplexes has been found in different organisms and has been observed *in vitro* and *in vivo* (Kikin et al., 2008; Xu et al., 2010b). Transcripts are enriched in RNA G-quadruplexes structures in the 5′UTR, 3′UTR and in the first exon (Eddy and Maizels, 2008; Huppert et al., 2008). Recently a molecular mechanism was described by which the DNA and RNA G-quadruplexes in C9ORF72 create structures that promote the formation of RNA/DNA hybrids (R-loops) (Haeusler et al., 2014). The pathological mechanism involving *C9ORF72* gene or its function are not clear, even if several studies showed a decrease in the mRNA levels of some C9ORF72 variants in ALS, which suggests a loss-of-function mechanism (DeJesus-Hernandez et al., 2011; Renton et al., 2011; Gijselinck et al., 2012; Mori et al., 2013b). Moreover, the aberrant transcripts containing

TABLE 8 | List of mutations in *C9ORF72* and their characteristic phenotypes.

Subtypes of Dementia	Mutation	Change in amino acid	Type	References
FTD/ALS	g.5321GGGGCC(?)	G4C2 hexanucleotide repeat expansion	Pathogenic	DeJesus-Hernandez et al., 2011
FTD	g.11942A>T	T66S	Pathogenic	Van der Zee et al., 2013

TD, Frontotemporal Dementia; ALS, Amyotrophic lateral sclerosis.
All the information reported in the table is derived from a cumulative study of the literature and the database: http://www.molgen.ua.ac.be/ADMutations/default.cfm?MT=0&ML=2&Page=FTD.

the hexanucleotide repeats can accumulate and form structures in the nucleus called RNA foci, which may produce neurodegeneration through a toxic effect (DeJesus-Hernandez et al., 2011). These transcripts can be aberrantly expressed through repeat-associated non-ATG (RAN) translation (Mori et al., 2013b). Several groups reported that the RAN translation of the hexanucleotide repeats produces poly(GP), poly(GA) and poly(GR) proteins, since this type of translation, without an initiation codon, can have all the possible reading frames (Ash et al., 2013; Mori et al., 2013b) and RNA can be also bidirectionally transcribed (Gendron et al., 2013). These RAN proteins can form inclusions in neurons and are considered a hallmark of the disease (Ash et al., 2013; Mori et al., 2013b). The neuronal inclusions can be detected through antibodies that recognize putative GGGGCC repeat RAN-translated peptides, therefore this type of immunoreactivity can be use as a potential biomarker for the disease (Ash et al., 2013).

It is also reported that RNA foci may sequester important RNA binding proteins, causing an alteration inside the cell and a subsequent dysfunction of RNA targets, in a process similar to the formation of RNA foci in myotonic dystrophy type 1 (DM1) (Lee et al., 2013; Mori et al., 2013a; Reddy et al., 2013; Xu et al., 2013). Specifically, one study demonstrated that hnRNP-H is sequestrated by RNA foci, reducing its available amount and its splicing efficiency on different target transcripts (Lee et al., 2013). A recent paper by Gendron et al. (2013) contains detailed descriptions of the proteins found to be sequestered on RNA foci in *in vitro* studies.

The presence of both sense and antisense RNA foci in frontotemporal dementia with the presence of *C9ORF72* repeats (C9FTLD), was demonstrated in patients, specifically in the frontal cortex, motor cortex, hippocampus, cerebellum, and spinal cord (Gendron et al., 2013; Lagier-Tourenne et al., 2013; Mizielinska et al., 2013; Zu et al., 2013). RNA foci were identified in neurons and with lower frequency in astrocytes, microglia, and oligodendrocytes; the highest concentration of foci was found in the frontal cortex region, compared to cerebellum and hippocampus (Mizielinska et al., 2013). However, another work reported that foci are localized with higher frequency in the cerebellum (Lee et al., 2013). Despite this inconsistency, the major part of RNA foci is localized at the very edge of the nucleus, but the explanation for this localization is still unknown (Mizielinska et al., 2013). The cellular toxicity associated with the longer hexanucleotide repeats and the presence of RNA foci was demonstrated using neuroblastoma cells and zebrafish embryos (Lee et al., 2013). One patient, who was homozygous for the *C9ORF72* hexanucleotide repeats, showed a higher proportion of sense and antisence foci with an early onset of FTD and severe pathological characteristics, compared to the heterozygous case (Mizielinska et al., 2013). A recent study found a mechanism for the disease in which the DNA and RNA–DNA structures formed in the repeat regions, alter the RNA transcription, with a result of transcriptional pausing and abortion. The accumulation of abortive transcripts with hexanucleotides repeats, creates G-quadruplexes, and hairpins structures with a binding of essential proteins, leading to nuclear stress, and further defects (Haeusler et al., 2014).

TDP-43 and FUS, two FTD related proteins previously decribed, are structurally related to the hnRNPs that are found to bind C9ORF72 RNA foci (Lee et al., 2013; Mori et al., 2013b), however FUS and TDP-43 do not colocalize with C9ORF72 RNA foci in cells, patient motor neuron cultures or in spinal motor neurons from patients (Lagier-Tourenne et al., 2013; Lee et al., 2013; Sareen et al., 2013). Since TDP-43 is capable to bind through its C-terminal region the hnRNP proteins (Buratti et al., 2005), the accumulation of these ribonucleoprotein on the RNA foci could indirectly influence TDP-43 function, creating a possible link of interaction between these two factors involved in FTD and ALS (Gendron et al., 2013). Indeed most of the cases with *C9ORF72* expansion show TDP-43 inclusions (FTLD-TDP) (DeJesus-Hernandez et al., 2011; Lagier-Tourenne et al., 2013; Mackenzie et al., 2014) with some exception, such as a case in UK with *C9ORF72* repeats with FTLD-tau pathology (Snowden et al., 2012). It was reported that the plasma and CSF level of phosphorylated TDP-43 is significantly higher in patients with FTD carrying *C9ORF72* expansion or *GRN* mutations compared to other FTD patients or healthy controls (Suárez-Calvet et al., 2014). This finding creates another possible link of interaction or regulation between TDP-43 and C9ORF72 that needs further analysis.

Discussion

In this review we describe the different genes involved in FTD, focusing on their possible interactions, in order to identify a common network of their combined regulations. We created this network focusing on the RNA aspect, an emerging and crucial molecule that plays critical and fundamental functions in the cells. Recently, research has increased its focus on the role of RNA in neurodegeneration (Renoux and Todd, 2012). We believe that the RNA mediated regulation plays a key role in the unique integration of all the known genes involved in FTD.

In this picture (**Figure 6**) FUS and TDP-43 RNA binding proteins are at the core of the network, since they often are associated factors that share similar features, with sometimes different but complementary roles (Colombrita et al., 2012). They interact with RNA in three main roles: as RNA binding proteins participating on the different aspects of mRNA processing (Bosco et al., 2010; Colombrita et al., 2011), as regulators of microRNAs processing, and as regulators of lncRNAs. FUS and TDP-43 were both found in aggregates in ALS/FTLD affected neurons (Da Cruz and Cleveland, 2011), nuclear complexes and in cytoplasmic RNPs (Kim et al., 2010b). TDP-43 appears to be the main regulator of this network, being able to interact with FUS pre-mRNA and regulate its splicing, and auto-regulate its own pre-mRNA, causing a reduction of its own expression (Polymenidou et al., 2011).

TDP-43 can also bind GRN pre-mRNA, negatively controlling its splicing and, accordingly, knock-down of TDP-43 was shown to increase the amount of GRN mRNA level (Polymenidou et al., 2011; Colombrita et al., 2012). In the presence of *GRN* mutations, TDP-43 regulation can be altered, causing the formation of inclusions containing TDP-43 (Mackenzie et al., 2006, 2010; Sampathu et al., 2006). Though TDP-43 aggregation is a typical hallmark of many other neurodegenerative disorders, such as Alzheimer's

disease, Guam Parkinsonism dementia complex, and Lewy body disease (Dickson, 2008), its impact on FTD in influencing the regulation of the network should not be underestimated.

On the other side, FUS acts as a splicing regulator of MAPT mRNA, indeed it was demonstrated that silencing of FUS alters the splicing of MAPT. In particular, FUS helps the skipping of exon 10 in primary cortical neurons (Ishigaki et al., 2012). The presence and the absence of exon 10 in *MAPT* gene has a fundamental role in the regulation of a delicate balance in the ratio of 4 or 3 repeats that can lead to FTD.

For the recently identified *C9ORF72* gene, large expansions of the non-coding GGGGCC repeat correlate with pathogenesis, making an RNA gain-of function mechanism possible. Indeed the aberrant C9ORF72 transcripts accumulate in nuclear RNA foci and sequester several RNA-binding proteins, including some splicing factors. However, other possible pathogenetic mechanisms are under scrutiny for *C9ORF72*, including impaired transcription of the expanded gene or repeat-associated non-ATG (RAN) translation of expanded transcripts.

In this scenario, two FTD genes code for proteins that fit in the picture not for their relation to RNA, but for their role in protein degradation.

VCP, taking part in the ubiquitin-proteasome pathway and protein turnover (Zhang et al., 2000; Rouiller et al., 2002), could be involved in the degradation of protein inclusions present in different forms of FTD. TDP-43 inclusions were found in the presence of a *VCP* mutation (Neumann et al., 2009a). A direct interaction between VCP and FUS has been observed suggesting a possible convergence in their functions (Wang et al., 2015).

CHMP2B regulates protein trafficking between endosomes and lysosomes and is involved in the protein degradation pathway through lysosomes (Urwin et al., 2010). Therefore, CHMP2B could be relevant for the internalization and transport of neuronal growth factors or signaling molecules such as progranulin.

Recently, a function for the C9ORF72 protein was uncovered, in the regulation of intracellular trafficking processes in the endosomal and autophagy-lysosomal compartments (Farg et al., 2014), providing an additional link to VCP and CHMP2B proteins.

During the preparation of this review a recent study performed by Van der Zee and colleagues have demonstrated ananalysis on a European cohort of 1808 FTLD patients revealing mutationsin SQSTM1 (Sequestosome 1) or p62. The p62 protein is a stress-responsiveubiquitin-binding protein, which is shown to have a role in degradation ofpolyubiquitinated proteins via the proteasome pathway or autophagicprocesses (Van der Zee et al., 2014). This gene was known to be associated with ALS and found as a rare mutation with a frequency of 1–3% in both ALS and FTLD cases. This further intrigued its possible role in pathogenicity with a common patho-mechanism. p62 is present in neuronal and glial ubiquitin-positive inclusions in different tauopathies and synucleinopathies (Van der Zee et al., 2014). The meta-analysis performed by Van der Zee and colleagues revealed that rare mutations clustering in the UBA domain of SQSTM1 may influence disease susceptibility by doubling the risk for FTLD. Further, histopathology analysis of autopsied brain of SQSTM1 mutation carriers demonstrated a widespread of neuronal and glial phospho-TDP-43 pathology. Therefore, this study opens up another target gene SQSTM1, which is known to have implications in FTLD/ALS and additionally associated with TDP-43. Despite further work being needed, to unravel and confirm the details of the proposed network, we foresee that the construction of a picture of the interactions between proteins and RNAs at the basis of the FTD pathology will be of invaluable importance, not only to comprehend the pathogenetic mechanisms but also to develop new and more effective therapeutical approaches. Through the network analysis proposed in this review, it can be foreseen that more genes can be linked to FTD and their roles will possibly fall in to two main categories: regulation of gene expression through RNA or protein degradation. Additionally it could be predicted that novel genes related to FTD in future will be possibly a part of the proposed network.

Acknowledgments

References

Ahmed, Z., Mackenzie, I. R., Hutton, M. L., and Dickson, D. W. (2007). Progranulin in frontotemporal lobar degeneration and neuroinflammation. *J. Neuroinflammation* 4:7. doi: 10.1186/1742-2094-4-7

Almeida, S., Zhou, L., and Gao, F.-B. (2011). Progranulin, a glycoprotein deficient in frontotemporal dementia, is a novel substrate of several protein disulfide isomerase family proteins. *PLoS ONE* 6:e26454. doi: 10.1371/journal.pone.0026454

Anderson, P., and Kedersha, N. (2008). Stress granules: the Tao of RNA triage. *Trends Biochem. Sci.* 33, 141–150. doi: 10.1016/j.tibs.2007.12.003

Anfossi, M., Vuono, R., Maletta, R., Virdee, K., Mirabelli, M., Colao, R., et al. (2011). Compound heterozygosity of 2 novel MAPT mutations in frontotemporal dementia. *Neurobiol. Aging* 32, 757.e1-757.e11. doi: 10.1016/j.neurobiolaging.2010.12.013

Arai, T., Hasegawa, M., Akiyama, H., Ikeda, K., Nonaka, T., Mori, H., et al. (2006). TDP-43 is a component of ubiquitin-positive tau-negative inclusions in frontotemporal lobar degeneration and amyotrophic lateral sclerosis. *Biochem. Biophys. Res. Commun.* 351, 602–611. doi: 10.1016/j.bbrc.2006.10.093

Arriagada, P. V., Marzloff, K., and Hyman, B. T. (1992). Distribution of Alzheimer-type pathologic changes in nondemented elderly individuals matches the pattern in Alzheimer's disease. *Neurology* 42, 1681–1688. doi: 10.1212/WNL.42.9.1681

Ash, P. E., Bieniek, K. F., Gendron, T. F., Caulfield, T., Lin, W.-L., Dejesus-Hernandez, M., et al. (2013). Unconventional translation of C9ORF72 GGGGCC expansion generates insoluble polypeptides specific to c9FTD/ALS. *Neuron* 77, 639–646. doi: 10.1016/j.neuron.2013.02.004

Avendaño-Vázquez, S. E., Dhir, A., Bembich, S., Buratti, E., Proudfoot, N., and Baralle, F. (2012). Autoregulation of TDP-43 mRNA levels involves interplay between transcription, splicing, and alternative polyA site selection. *Genes Dev.* 26, 1679–1684. doi: 10.1101/gad.194829.112

Ayala, Y. M., Pantano, S., D'Ambrogio, A., Buratti, E., Brindisi, A., Marchetti, C., et al. (2005). Human, Drosophila, and C.elegans TDP43: nucleic acid binding

properties and splicing regulatory function. *J. Mol. Biol.* 348, 575–588. doi: 10.1016/j.jmb.2005.02.038

Baker, M., Mackenzie, I. R., Pickering-Brown, S. M., Gass, J., Rademakers, R., Lindholm, C., et al. (2006). Mutations in progranulin cause tau-negative frontotemporal dementia linked to chromosome 17. *Nature* 442, 916–919. doi: 10.1038/nature05016

Barmada, S. J., Skibinski, G., Korb, E., Rao, E. J., and Wu, J. Y. (2010). Cytoplasmic mislocalization of TDP-43 is toxic to neurons and enhanced by a mutation associated with familial ALS 30. *J. Neurosci.* 30, 639–649. doi: 10.1523/JNEUROSCI.4988-09.2010

Bartel, D. P. (2009). MicroRNAs: target recognition and regulatory functions. *Cell* 136, 215–233. doi: 10.1016/j.cell.2009.01.002

Bartolome, F., Wu, H.-C., Burchell, V. S., Preza, E., Wray, S., Mahoney, C. J., et al. (2013). Pathogenic VCP mutations induce mitochondrial uncoupling and reduced ATP levels. *Neuron* 78, 57–64. doi: 10.1016/j.neuron.2013.02.028

Bateman, A., and Bennett, H. P. (2009). The granulin gene family: from cancer to dementia. *Bioessays* 31, 1245–1254. doi: 10.1002/bies.200900086

Belly, A., Moreau-Gachelin, F., Sadoul, R., and Goldberg, Y. (2005). Delocalization of the multifunctional RNA splicing factor TLS/FUS in hippocampal neurones: exclusion from the nucleus and accumulation in dendritic granules and spine heads. *Neurosci. Lett.* 379, 152–157. doi: 10.1016/j.neulet.2004.12.071

Belzil, V. V., Gendron, T. F., and Petrucelli, L. (2013). RNA-mediated toxicity in neurodegenerative disease. *Mol. Cell. Neurosci.* 56, 406–419. doi: 10.1016/j.mcn.2012.12.006

Benajiba, L., Le Ber, I., Camuzat, A., Lacoste, M., Thomas-Anterion, C., Couratier, P., et al. (2009). TARDBP mutations in motoneuron disease with frontotemporal lobar degeneration. *Ann. Neurol.* 65, 470–473. doi: 10.1002/ana.21612

Bernardi, L., Frangipane, F., Smirne, N., Colao, R., Puccio, G., Curcio, S. M., et al. (2012). Epidemiology and genetics of frontotemporal dementia: a door-to-door survey in southern Italy. *Neurobiol. Aging* 33, 2948.e1–2948.e10. doi: 10.1016/j.neurobiolaging.2012.06.017

Bernstein, E., Caudy, A. A., Hammond, S. M., and Hannon, G. J. (2001). Role for a bidentate ribonuclease in the initiation step of RNA interference. *Nature* 409, 363–366. doi: 10.1038/35053110

Bersano, A., Del Bo, R., Lamperti, C., Ghezzi, S., Fagiolari, G., Fortunato, F., et al. (2009). Inclusion body myopathy and frontotemporal dementia caused by a novel VCP mutation. *Neurobiol. Aging* 30, 752–758. doi: 10.1016/j.neurobiolaging.2007.08.009

Bertolotti, A., Lutz, Y., and Heard, D. (1996). hTAF (II) 68, a novel RNA/ssDNA-binding protein with homology to the pro-oncoproteins TLS/FUS and EWS is associated with both TFIID and RNA polymerase II. *EMBO J.* 15, 5022–5031.

Bessi, V., Bagnoli, S., Nacmias, B., Tedde, A., Sorbi, S., and Bracco, L. (2010). Semantic dementia associated with mutation V363I in the tau gene. *J. Neurol. Sci.* 296, 112–114. doi: 10.1016/j.jns.2010.06.007

Bhandari, V., Daniel, R., Lim, P. S., and Bateman, A. (1996). Structural and functional analysis of a promoter of the human granulin/epithelin gene. *Biochem. J.* 319(Pt 2), 441–447.

Binder, L. I., Frankfurter, A., and Rebhun, L. I. (1985). The distribution of tau in the mammalian central nervous system. *J. Cell Biol.* 101, 1371–1378. doi: 10.1083/jcb.101.4.1371

Birney, E., Stamatoyannopoulos, J. A., Dutta, A., Guigó, R., Gingeras, T. R., and Margulies, E. H. (2007). Identification and analysis of functional elements in 1% of the human genome by the ENCODE pilot project. *Nature* 447, 799–816. doi: 10.1038/nature05874

Bodon, G., Chassefeyre, R., Pernet-Gallay, K., Martinelli, N., Effantin, G., Hulsik, D. L., et al. (2011). Charged multivesicular body protein 2B (CHMP2B) of the endosomal sorting complex required for transport-III (ESCRT-III) polymerizes into helical structures deforming the plasma membrane. *J. Biol. Chem.* 286, 40276–40286. doi: 10.1074/jbc.M111.283671

Bond, A. M., Vangompel, M. J., Sametsky, E. A., Clark, M. F., Savage, J. C., Disterhoft J. F., et al. (2009). Balanced gene regulation by an embryonic brain ncRNA is critical for adult hippocampal GABA circuitry. *Nat. Neurosci.* 12, 1020–1027. doi: 10.1038/nn.2371

Borroni, B., Archetti, S., Alberici, A., Agosti, C., Gennarelli, M., Bigni, B., et al. (2008). Progranulin genetic variations in frontotemporal lobar degeneration: evidence for low mutation frequency in an Italian clinical series. *Neurogenetics* 9, 197–205. doi: 10.1007/s10048-008-0127-3

Borroni, B., Bonvicini, C., Alberici, A., Buratti, E., Agosti, C., Archetti, S., et al. (2009). Mutation within TARDBP leads to frontotemporal dementia without motor neuron disease. *Hum. Mutat.* 30, E974–E983. doi: 10.1002/humu.21100

Bosco, D. A., Lemay, N., Ko, H. K., Zhou, H., Burke, C., Kwiatkowski, T. J., et al. (2010). Mutant FUS proteins that cause amyotrophic lateral sclerosis incorporate into stress granules. *Hum. Mol. Genet.* 19, 4160–4175. doi: 10.1093/hmg/ddq335

Bottos, A., Rissone, A., Bussolino, F., and Arese, M. (2011). Neurexins and neuroligins: synapses look out of the nervous system. *Cell. Mol. Life Sci.* 68, 2655–2666. doi: 10.1007/s00018-011-0664-z

Broe, M., Kril, J., and Halliday, G. M. (2004). Astrocytic degeneration relates to the severity of disease in frontotemporal dementia. *Brain* 127, 2214–2220. doi: 10.1093/brain/awh250

Bronfman, F. C., Escudero, C. A., and Weis, J. K. A. (2007). Endosomal transport of neurotrophins: roles in signaling and neurodegenerative diseases. *Dev. Neurobiol.* 67, 1183–1203. doi: 10.1002/dneu.20513

Bronner, I. F., Rizzu, P., Seelaar, H., van Mil, S. E., Anar, B., Azmani, A., et al. (2007). Progranulin mutations in Dutch familial frontotemporal lobar degeneration. *Eur. J. Hum. Genet.* 15, 369–374. doi: 10.1038/sj.ejhg.5201772

Broustal, O., Camuzat, A., Guillot-Noël, L., Guy, N., Millecamps, S., Deffond, D., et al. (2010). FUS mutations in frontotemporal lobar degeneration with amyotrophic lateral sclerosis. *J. Alzheimers Dis.* 22, 765–769.

Brown, J., Lantos, P. L., Roques, P., Fidani, L., and Rossor, M. N. (1996). Familial dementia with swollen achromatic neurons and corticobasal inclusion bodies: a clinical and pathological study. *J. Neurol. Sci.* 135, 21–30. doi: 10.1016/0022-510X(95)00236-U

Buchan, J. R., Kolaitis, R.-M., Taylor, J. P., and Parker, R. (2013). Eukaryotic stress granules are cleared by autophagy and Cdc48/VCP function. *Cell* 153, 1461–1474. doi: 10.1016/j.cell.2013.05.037

Buchan, J. R., and Parker, R. (2009). Eukaryotic stress granules: the ins and outs of translation. *Mol. Cell.* 36, 932–941. doi: 10.1016/j.molcel.2009.11.020

Bugiani, O. (2007). The many ways to frontotemporal degeneration and beyond. *Neurol. Sci.* 28, 241–244. doi: 10.1007/s10072-007-0829-6

Bugiani, O., Murrell, J. R., Giaccone, G., Hasegawa, M., Ghigo, G., Tabaton, M., et al. (1999). Frontotemporal dementia and corticobasal degeneration in a family with a P301S mutation in tau. *J. Neuropathol. Exp. Neurol.* 58, 667–677. doi: 10.1097/00005072-199906000-00011

Buratti, E., and Baralle, F. E. (2001). Characterization and functional implications of the RNA binding properties of nuclear factor TDP-43, a novel splicing regulator of CFTR exon 9. *J. Biol. Chem.* 276, 36337–36343. doi: 10.1074/jbc.M104236200

Buratti, E., and Baralle, F. E. (2010). The multiple roles of TDP-43 in pre-mRNA processing and gene expression regulation. *RNA Biol.* 7, 420–429. doi: 10.4161/rna.7.4.12205

Buratti, E., Brindisi, A., Giombi, M., Tisminetzky, S., Ayala, Y. M., and Baralle, F. E. (2005). TDP-43 binds heterogeneous nuclear ribonucleoprotein A/B through its C-terminal tail: an important region for the inhibition of cystic fibrosis transmembrane conductance regulator exon 9 splicing. *J. Biol. Chem.* 280, 37572–37584. doi: 10.1074/jbc.M505557200

Buratti, E., De Conti, L., Stuani, C., Romano, M., Baralle, M., and Baralle, F. (2010). Nuclear factor TDP-43 can affect selected microRNA levels. *FEBS J.* 277, 2268–2281. doi: 10.1111/j.1742-4658.2010.07643.x

Butler, G. S., Dean, R. A., Tam, E. M., and Overall, C. M. (2008). Pharmacoproteomics of a metalloproteinase hydroxamate inhibitor in breast cancer cells: dynamics of membrane type 1 matrix metalloproteinase-mediated membrane protein shedding. *Mol. Cell. Biol.* 28, 4896–4914. doi: 10.1128/MCB.01775-07

Cannon, A., Baker, M., Boeve, B., Josephs, K., Knopman, D., Petersen, R., et al. (2006). CHMP2B mutations are not a common cause of frontotemporal lobar degeneration. *Neurosci. Lett.* 398, 83–84. doi: 10.1016/j.neulet.2005.12.056

Carlton, J. G., and Martin-Serrano, J. (2007). Parallels between cytokinesis and retroviral budding: a role for the ESCRT machinery. *Science* 316, 1908–1912. doi: 10.1126/science.1143422

Cesana, M., Cacchiarelli, D., Legnini, I., Santini, T., Sthandier, O., Chinappi, M., et al. (2011). A long noncoding RNA controls muscle differentiation by functioning as a competing endogenous RNA. *Cell* 147, 358–369. doi: 10.1016/j.cell.2011.09.028

Chai, X., Dage, J. L., and Citron, M. (2012). Constitutive secretion of tau protein by an unconventional mechanism. *Neurobiol. Dis.* 48, 356–366. doi: 10.1016/j.nbd.2012.05.021

Chen, L., and Carmichael, G. (2009). Altered nuclear retention of mRNAs containing inverted repeats in human embryonic stem cells: functional role of a nuclear noncoding RNA. *Mol. Cell* 35, 467–478. doi: 10.1016/j.molcel.2009.06.027

Chen-Plotkin, A. S., Xiao, J., Geser, F., Martinez-Lage, M., Grossman, M., Unger, T., et al. (2010). Brain progranulin expression in GRN-associated frontotemporal lobar degeneration. *Acta Neuropathol.* 119, 111–122. doi: 10.1007/s00401-009-0576-2

Chiò, A., Calvo, A., Moglia, C., Restagno, G., Ossola, I., Brunetti, M., et al. (2010). Amyotrophic lateral sclerosis-frontotemporal lobar dementia in 3 families with p.Ala382Thr TARDBP mutations. *Arch. Neurol.* 67, 1002–1009. doi: 10.1001/archneurol.2010.173

Clark, M. B., Amaral, P. P., Schlesinger, F. J., Dinger, M. E., Taft, R. J., Rinn, J. L., et al. (2011). The reality of pervasive transcription. *PLoS Biol.* 9:e1000625; discussion e1001102. doi: 10.1371/journal.pbio.1000625

Clovis, Y. M., Enard, W., Marinaro, F., Huttner, W. B., and De Pietri Tonelli, D. (2012). Convergent repression of Foxp2 3′UTR by miR-9 and miR-132 in embryonic mouse neocortex: implications for radial migration of neurons. *Development* 139, 3332–3342. doi: 10.1242/dev.078063

Colombrita, C., Onesto, E., Megiorni, F., Pizzuti, A., Baralle, F. E., Buratti, E., et al. (2012). TDP-43 and FUS RNA-binding proteins bind distinct sets of cytoplasmic messenger RNAs and differently regulate their post-transcriptional fate in motoneuron-like cells. *J. Biol. Chem.* 287, 15635–15647. doi: 10.1074/jbc.M111.333450

Colombrita, C., Onesto, E., Tiloca, C., Ticozzi, N., Silani, V., and Ratti, A. (2011). RNA-binding proteins and RNA metabolism: a new scenario in the pathogenesis of Amyotrophic lateral sclerosis. *Arch. Ital. Biol.* 149, 83–99. doi: 10.4449/aib.v149i1.1261

Colombrita, C., Zennaro, E., Fallini, C., Weber, M., Sommacal, A., Buratti, E., et al. (2009). TDP-43 is recruited to stress granules in conditions of oxidative insult. *J. Neurochem.* 111, 1051–1061. doi: 10.1111/j.1471-4159.2009.06383.x

Cooper, T. A., Wan, L., and Dreyfuss, G. (2009). RNA and disease. *Cell* 136, 777–793. doi: 10.1016/j.cell.2009.02.011

Coppola, G., Karydas, A., Rademakers, R., Wang, Q., Baker, M., Hutton, M., et al. (2008). Gene expression study on peripheral blood identifies progranulin mutations. *Ann. Neurol.* 64, 92–96. doi: 10.1002/ana.21397

Corrado, L., Ratti, A., Gellera, C., Buratti, E., Castellotti, B., Carlomagno, Y., et al. (2009).High frequency of TARDBP gene mutations in Italian patients with amyotrophic lateral sclerosis. *Hum. Mutat.* 30, 688–694. doi: 10.1002/humu.20950

Couchie, D., Mavilia, C., Georgieff, I. S., Liem, R. K., Shelanski, M. L., and Nunez, J. (1992). Primary structure of high molecular weight tau present in the peripheral nervous system. *Proc. Natl. Acad. Sci. U.S.A.* 89, 4378–4381. doi: 10.1073/pnas.89.10.4378

Cox, L. E., Ferraiuolo, L., Goodall, E. F., Heath, P. R., Higginbottom, A., Mortiboys, H., et al. (2010). Mutations in CHMP2B in lower motor neuron predominant amyotrophic lateral sclerosis (ALS). *PLoS ONE* 5:e9872. doi: 10.1371/journal.pone.0009872

Craig, A., Graf, E., and Linhoff, M. (2006). How to build a central synapse: clues from cell culture. *Trends Neurosci.* 29, 8–20. doi: 10.1016/j.tins.2005.11.002

Cruts, M., Gijselinck, I., Van der Zee, J., Engelborghs, S., Wils, H., Pirici, D., et al. (2006). Null mutations in progranulin cause ubiquitin-positive frontotemporal dementia linked to chromosome 17q21. *Nature* 442, 920–924. doi: 10.1038/nature05017

Cruts, M., Theuns, J., and Van Broeckhoven, C. (2012). Locus-specific mutation databases for neurodegenerative brain diseases. *Hum. Mutat.* 33, 1340–1344. doi: 10.1002/humu.22117

Cruts, M., and Van Broeckhoven, C. (2008). Loss of progranulin function in frontotemporal lobar degeneration. *Trends Genet.* 24, 186–194. doi: 10.1016/j.tig.2008.01.004

Custer, S. K., Neumann, M., Lu, H., Wright, A. C., and Taylor, J. P. (2010). Transgenic mice expressing mutant forms VCP/p97 recapitulate the full spectrum of IBMPFD including degeneration in muscle, brain and bone. *Hum. Mol. Genet.* 19, 1741–1755. doi: 10.1093/hmg/ddq050

D'Souza, I., Poorkaj, P., Hong, M., Nochlin, D., Lee, V. M., Bird, T. D., et al. (1999). Missense and silent tau gene mutations cause frontotemporal dementia with parkinsonism-chromosome 17 type, by affecting multiple alternative RNA splicing regulatory elements. *Proc. Natl. Acad. Sci. U.S.A.* 96, 5598–5603. doi: 10.1073/pnas.96.10.5598

Da Cruz, S., and Cleveland, D. W. (2011). Understanding the role of TDP-43 and FUS/TLS in ALS and beyond. *Curr. Opin. Neurobiol.* 21, 904–919. doi: 10.1016/j.conb.2011.05.029

Dai, R. M., and Li, C. C. (2001). Valosin-containing protein is a multi-ubiquitin chain-targeting factor required in ubiquitin-proteasome degradation. *Nat. Cell Biol.* 3, 740–744. doi: 10.1038/35087056

Daniel, R., Daniels, E., He, Z., and Bateman, A. (2003). Progranulin (acrogranin/PC cell-derived growth factor/granulin-epithelin precursor) is expressed in the placenta, epidermis, microvasculature, and brain during murine development. *Dev. Dyn.* 227, 593–599. doi: 10.1002/dvdy.10341

Daniel, R., He, Z., Carmichael, K. P., Halper, J., and Bateman, A. (2000). Cellular localization of gene expression for progranulin. *J. Histochem. Cytochem.* 48, 999–1009. doi: 10.1177/002215540004800713

De Calignon, A., Polydoro, M., Suárez-Calvet, M., William, C., Adamowicz, D. H., Kopeikina, K. J., et al. (2012). Propagation of tau pathology in a model of early Alzheimer's disease. *Neuron* 73, 685–697. doi: 10.1016/j.neuron.2011.11.033

DeJesus-Hernandez, M., Mackenzie, I. R., Boeve, B. F., Boxer, A. L., Baker, M., Rutherford, N. J., et al. (2011). Expanded GGGGCC hexanucleotide repeat in noncoding region of C9ORF72 causes chromosome 9p-linked FTD and ALS. *Neuron* 72, 245–256. doi: 10.1016/j.neuron.2011.09.011

DeLaBarre, B., Christianson, J. C., Kopito, R. R., and Brunger, A. T. (2006). Central pore residues mediate the p97/VCP activity required for ERAD. *Mol. Cell* 22, 451–462. doi: 10.1016/j.molcel.2006.03.036

Deng, H.-X., Zhai, H., Bigio, E. H., Yan, J., Fecto, F., Ajroud, K., et al. (2010). FUS-immunoreactive inclusions are a common feature in sporadic and non-SOD1 familial amyotrophic lateral sclerosis. *Ann. Neurol.* 67, 739–748. doi: 10.1002/ana.22051

Díaz-Cueto, L., Stein, P., Jacobs, A., Schultz, R. M., and Gerton, G. L. (2000). Modulation of mouse preimplantation embryo development by acrogranin (epithelin/granulin precursor). *Dev. Biol.* 217, 406–418. doi: 10.1006/dbio.1999.9564

Di Carlo, V., Grossi, E., Laneve, P., Morlando, M., Dini Modigliani, S., Ballarino, M., et al. (2013). TDP-43 regulates the microprocessor complex activity during in vitro neuronal differentiation. *Mol. Neurobiol.* 48, 952–963. doi: 10.1007/s12035-013-8564-x

Dickson, D. W. (1997). Neurodegenerative diseases with cytoskeletal pathology: a biochemical classification. *Ann. Neurol.* 42, 541–544. doi: 10.1002/ana.410420403

Dickson, D. W. (2008). TDP-43 immunoreactivity in neurodegenerative disorders: disease versus mechanism specificity. *Acta Neuropathol.* 115, 147–149. doi: 10.1007/s00401-007-0323-5

Dickson, J. R., Kruse, C., Montagna, D. R., Finsen, B., and Wolfe, M. S. (2013). Alternative polyadenylation and miR-34 family members regulate tau expression. *J. Neurochem.* 127, 739–749. doi: 10.1111/jnc.12437

Dini Modigliani, S., Morlando, M., Errichelli, L., Sabatelli, M., and Bozzoni, I. (2014). An ALS-associated mutation in the FUS 3′-UTR disrupts a microRNA-FUS regulatory circuitry. *Nat. Commun.* 5:4335. doi: 10.1038/ncomms5335

Djamshidian, A., Schaefer, J., Haubenberger, D., Stogmann, E., Zimprich, F., Auff, E., et al. (2009). A novel mutation in the VCP gene (G157R) in a German family with inclusion-body myopathy with Paget disease of bone and frontotemporal dementia. *Muscle Nerve* 39, 389–391. doi: 10.1002/mus.21225

Dormann, D., Rodde, R., Edbauer, D., Bentmann, E., Fischer, I., Hruscha, A., et al. (2010). ALS-associated fused in sarcoma (FUS) mutations disrupt transportin-mediated nuclear import. *EMBO J.* 29, 2841–2857. doi: 10.1038/emboj.2010.143

Eddy, J., and Maizels, N. (2008). Conserved elements with potential to form polymorphic G-quadruplex structures in the first intron of human genes. *Nucleic Acids Res.* 36, 1321–1333. doi: 10.1093/nar/gkm1138

Elia, N., and Sougrat, R. (2011). Dynamics of endosomal sorting complex required for transport (ESCRT) machinery during cytokinesis and its role in abscission. *Proc Natl Acad Sci U.S.A.* 108, 4846–4851. doi: 10.1073/pnas.1102714108

Erickson, S. L., and Lykke-Andersen, J. (2011). Cytoplasmic mRNP granules at a glance. *J. Cell Sci.* 1, 293–297. doi: 10.1242/jcs.072140

Fan, Z., Chen, X., and Chen, R. (2014). Transcriptome-wide analysis of TDP-43 binding small RNAs identifies miR-NID1 (miR-8485), a novel miRNA that represses NRXN1 expression. *Genomics* 103, 76–82. doi: 10.1016/j.ygeno.2013.06.006

Farg, M. A., Sundaramoorthy, V., Sultana, M. J., Yang, S., Atkinson, R. A. K., Levina, V., et al. (2014). C9ORF72, implicated in amytrophic lateral sclerosis and frontotemporal dementia, regulates endosomal trafficking. *Hum. Mol. Genet.* 23, 3579–3595. doi: 10.1093/hmg/ddu068

Feng, J., Bi, C., Clark, B. S., Mady, R., Shah, P., and Kohtz, J. D. (2006). The Evf-2 noncoding RNA is transcribed from the Dlx-5/6 ultraconserved region and functions as a Dlx-2 transcriptional coactivator. *Genes Dev.* 20, 1470–1484. doi: 10.1101/gad.1416106

Ferrari, R., Kapogiannis, D., Huey, E. D., Grafman, J., Hardy, J., and Momeni, P. (2010). Novel missense mutation in charged multivesicular body protein 2B in a patient with frontotemporal dementia. *Alzheimer Dis. Assoc. Disord.* 24, 397–401. doi: 10.1097/WAD.0b013e3181df20c7

Finch, N., Baker, M., Crook, R., Swanson, K., Kuntz, K., Surtees, R., et al. (2009). Plasma progranulin levels predict progranulin mutation status in frontotemporal dementia patients and asymptomatic family members. *Brain* 132, 583–591. doi: 10.1093/brain/awn352

Fox, A. H., and Lamond, A. I. (2010). Paraspeckles. *Cold Spring Harb. Perspect. Biol.* 2:a000687. doi: 10.1101/cshperspect.a000687

Fratta, P., Mizielinska, S., Nicoll, A. J., Zloh, M., Fisher, E. M. C., Parkinson, G., et al. (2012). C9orf72 hexanucleotide repeat associated with amyotrophic lateral sclerosis and frontotemporal dementia forms RNA G-quadruplexes. *Sci. Rep.* 2:1016. doi: 10.1038/srep01016

Freibaum, B. D., Chitta, R., High, A. A., and Taylor, J. P. (2011). Global analysis of TDP-43 interacting proteins reveals strong association with RNA splicing and translation machinery. *J. Proteome Res.* 9, 1104–1120. doi: 10.1021/pr901076y

Fujii, R., Okabe, S., Urushido, T., Inoue, K., Yoshimura, A., Tachibana, T., et al. (2005). The RNA binding protein TLS is translocated to dendritic spines by mGluR5 activation and regulates spine morphology. *Curr. Biol.* 15, 587–593. doi: 10.1016/j.cub.2005.01.058

Fujii, R., and Takumi, T. (2005). TLS facilitates transport of mRNA encoding an actin-stabilizing protein to dendritic spines. *J. Cell Sci.* 118, 5755–5765. doi: 10.1242/jcs.02692

Gabryelewicz, T., Masellis, M., Berdynski, M., Bilbao, J. M., Rogaeva, E., St George-Hyslop, P., et al. (2010). Intra-familial clinical heterogeneity due to FTLD-U with TDP-43 proteinopathy caused by a novel deletion in progranulin gene (PGRN). *J. Alzheimer Dis.* 22, 1123–1133. doi: 10.3233/JAD-2010-101413

Gallo, J.-M., Jin, P., Thornton, C. A., Lin, H., Robertson, J., D'Souza, I., et al. (2005). The role of RNA and RNA processing in neurodegeneration. *J. Neurosci.* 25, 10372–10375. doi: 10.1523/JNEUROSCI.3453-05.2005

Garzon, R., Marcucci, G., and Croce, C. (2010). Targeting microRNAs in cancer: rationale, strategies and challenges. *Nat. Rev. Drug Discov.* 9, 775–789. doi: 10.1038/nrd3179

Gass, J., Cannon, A., Mackenzie, I. R., Boeve, B., Baker, M., Adamson, J., et al. (2006). Mutations in progranulin are a major cause of ubiquitin-positive frontotemporal lobar degeneration. *Hum. Mol. Genet.* 15, 2988–3001. doi: 10.1093/hmg/ddl241

Gendron, T. F., Bieniek, K. F., Zhang, Y.-J., Jansen-West, K., Ash, P. E., Caulfield, T., et al. (2013). Antisense transcripts of the expanded C9ORF72 hexanucleotide repeat form nuclear RNA foci and undergo repeat-associated non-ATG translation in c9FTD/ALS. *Acta Neuropathol.* 126, 829–844. doi: 10.1007/s00401-013-1192-8

Ghanim, M., Guillot-Noel, L., Pasquier, F., Jornea, L., Deramecourt, V., Dubois, B., et al. (2010). CHMP2B mutations are rare in French families with frontotemporal lobar degeneration. *J. Neurol.* 257, 2032–2036. doi: 10.1007/s00415-010-5655-8

Ghazi-Noori, S., Froud, K. E., Mizielinska, S., Powell, C., Smidak, M., Fernandez de Marco, M., et al. (2012). Progressive neuronal inclusion formation and axonal degeneration in CHMP2B mutant transgenic mice. *Brain* 135, 819–832 doi: 10.1093/brain/aws006

Ghildiyal, M., and Zamore, P. D. (2009). Small silencing RNAs: an expanding universe. *Nat. Rev. Genet.* 10, 94–108. doi: 10.1038/nrg2504

Giaccone, G., Rossi, G., Di Fede, G., Marcon, G., Farina, L., Sacco, L., et al. (2004). Familial frontotemporal dementia is associated with the novel tau mutation T427M. *Neurobiol. Aging* 25, 449–450. doi: 10.1016/S0197-4580(04)81481-7

Gijselinck, I., Van der Zee, J., Engelborghs, S., Goossens, D., Peeters, K., Mattheijssens, M., et al. (2008). Progranulin locus deletion in frontotemporal dementia. *Hum. Mutat.* 29, 53–58 doi: 10.1002/humu.20651

Gijselinck, I., Van Langenhove, T., van der Zee, J., Sleegers, K., Philtjens, S., Kleinberger, G., et al. (2012). A C9orf72 promoter repeat expansion in a Flanders-Belgian cohort with disorders of the frontotemporal lobar degeneration-amyotrophic lateral sclerosis spectrum: a gene identification study. *Lancet Neurol.* 11, 54–65. doi: 10.1016/S1474-4422(11)70261-7

Goedert, M., and Jakes, R. (2005). Mutations causing neurodegenerative tauopathies. *Biochim. Biophys. Acta.* 1739, 240–250. doi: 10.1016/j.bbadis.2004.08.007

Grishok, A., Pasquinelli, A. E., Conte, D., Li, N., Parrish, S., Ha, I., et al. (2001). Genes and mechanisms related to RNA interference regulate expression of the small temporal RNAs that control C. elegans developmental timing. *Cell* 106, 23–34 doi: 10.1016/S0092-8674(01)00431-7

Grover, A., England, E., Baker, M., Sahara, N., Adamson, J., Granger, B., et al. (2003). A novel tau mutation in exon 9 (1260V) causes a four-repeat tauopathy. *Exp. Neurol.* 184, 131–140. doi: 10.1016/S0014-4886(03)00393-5

Grover, A., Houlden, H., Baker, M., Adamson, J., Lewis, J., Prihar, G., et al. (1999). *J. Biol. Chem.* 274, 15134–15143. doi: 10.1074/jbc.274.21.15134

Guinto, J. B., Ritson, G. P., Taylor, J. P., and Forman, M. S. (2007). Valosin-containing protein and the pathogenesis of frontotemporal dementia associated with inclusion body myopathy. *Acta Neuropathol.* 114, 55–61. doi: 10.1007/s00401-007-0224-7

Guo, A., Tapia, L., Bamji, S. X., Cynader, M. S., and Jia, W. (2010). Progranulin deficiency leads to enhanced cell vulnerability and TDP-43 translocation in primary neuronal cultures. *Brain Res.* 1366, 1–8. doi: 10.1016/j.brainres.2010.09.099

Gutierrez, M. G., Munafo, D. B., Beron, W., and Colombo, M. I. (2004). Rab7 is requie for the normal progression of the autophagic pathway in mammalian cells. *J. Cell Sci.* 117(Pt 13), 2687–2697. doi: 10.1242/jcs.01114

Guyant-Maréchal, L., Laquerrière, A., Duyckaerts, C., Dumanchin, C., Bou, J., Dugny, F., et al. (2006). Valosin-containing protein gene mutations: clinical and neuropathologic features. *Neurology* 67, 644–651. doi: 10.1212/01.wnl.0000225184.14578.d3

Haeusler, A. R., Donnelly, C. J., Periz, G., Simko, E. A. J., Shaw, P. G., Kim, M.-S. et al. (2014). C9orf72 nucleotide repeat structures initiate molecular cascades of disease. *Nature* 507, 195–200. doi: 10.1038/nature13124

Haubenberger, D., Bittner, R. E., Rauch-Shorny, S., Zimprich, F., Mannhalter, C., Wagner, L., et al. (2005). Inclusion body myopathy and Paget disease is linked to a novel mutation in the VCP gene. *Neurology* 65, 1304–1305 doi: 10.1212/01.wnl.0000180407.15369.92

Hayashi, S., Toyoshima, Y., Hasegawa, M., Umeda, Y., Wakabayashi, K., Tokiguchi, S., et al. (2002). Late-onset frontotemporal dementia with a novel exon 1 (Arg5His) tau gene mutation. *Ann. Neurol.* 51, 525–530. doi: 10.1002/ana.10163

Hayashi, Y. K. (2013). Inclusion body myopathy with Paget's disease of bone and frontotemporal dementia. *Rinsho Shinkeigaku* 53, 947–950. doi: 10.5692/clinicalneurol.53.947

He, Z., and Bateman, A. (1999). Progranulin gene expression regulates epithelial cell growth and promotes tumor growth *in vivo. Cancer Res.* 3222–3229.

He, Z., and Bateman, A. (2003). Progranulin (granulin-epithelin precursor, PC-cell-derived growth factor, acrogranin) mediates tissue repair and tumorigenesis. *J. Mol. Med. (Berl).* 81, 600–612. doi: 10.1007/s00109-003-0474-3

He, Z., Ong, C. H. P., Halper, J., and Bateman, A. (2003). Progranulin is a mediator of the wound response. *Nat. Med.* 9, 225–229. doi: 10.1038/nm816

Hébert, S. S., Horré, K., Nicolaï, L., Papadopoulou, A. S., Mandemakers, W., Silahtaroglu A. N., et al. (2008). Loss of microRNA cluster miR-29a/b-1 in sporadic Alzheimer's disease correlates with increased BACE1/beta-secretase expression. *Proc. Natl. Acad. Sci. U.S.A.* 105, 6415–1520. doi: 10.1073/pnas.0710263105

Hermeking, H. (2010). The miR-34 family in cancer and apoptosis. *Cell Death Differ.* 2, 193–199. doi: 10.1038/cdd.2009.56

Hirabayashi, M., Inoue, K., Tanaka, K., Nakadate, K., Ohsawa, Y., Kamei, Y., et al. (2001). VCP/p97 in abnormal protein aggregates, cytoplasmic vacuoles, and cell death, phenotypes relevant to neurodegeneration. *Cell Death Differ.* 8, 977–984. doi: 10.1038/sj.cdd.4400907

Hoell, J. I., Larsson, E., Runge, S., Nusbaum, J. D., Duggimpudi, S., Farazi, T., et al. (2011). RNA targets of wild-type and mutant FET family proteins. *Nat. Struct. Mol. Biol.* 18, 1428–1431. doi: 10.1038/nsmb.2163

Hoque, M., Mathews, M. B., and Pe'ery, T. (2010). Progranulin (granulin/epithelin precursor) and its constituent granulin repeats repress transcription

from cellular promoters. *J. Cell. Physiol.* 223, 224–233. doi: 10.1002/jcp.22031

Hoque, M., Young, T., and Lee, C. (2003). The growth factor granulin interacts with cyclin T1 and modulates P-TEFb-dependent transcription. *Cell. Biol.* 23, 1688–1702.

Huey, E. D., Ferrari, R., Moreno, J. H., Jensen, C., Morris, C. M., Potocnik, F., et al. (2012). FUS and TDP43 genetic variability in FTD and CBS. *Neurobiol. Aging* 33, 1016.e9–1016.e17. doi: 10.1016/j.neurobiolaging.2011.08.004

Huey, E. D., Grafman, J., Wassermann, E. M., Pietrini, P., Tierney, M. C., Ghetti, B., et al. (2006). Characteristics of frontotemporal dementia patients with a progranulin mutation. *Ann. Neurol.* 60, 374–380. doi: 10.1002/ana.20969

Huntzinger, E., and Izaurralde, E. (2011). Gene silencing by microRNAs: contributions of translational repression and mRNA decay. *Nat. Rev. Genet.* 12, 99–110. doi: 10.1038/nrg2936

Huppert, J. L., Bugaut, A., Kumari, S., and Balasubramanian, S. (2008). G-quadruplexes: the beginning and end of UTRs. *Nucleic Acids Res.* 36, 6260–6268. doi: 10.1093/nar/gkn511

Hutton, M., Lendon, C. L., Rizzu, P., Baker, M., Froelich, S., Houlden, H., et al. (1998).Association of missense and 5′-splice-site mutations in tau with the inherited dementia FTDP-17. *Nature* 393, 702–705. doi: 10.1038/31508

Hutvagner, G., McLachlan, J., Pasquinelli, A. E., Balint, E., Tuschl, T., and Zamore, P. D. (2001). A cellular function for the RNA-interference enzyme Dicer in the maturation of the let-7 small temporal RNA. *Science* 293, 834–838. doi: 10.1126/science.1062961

Iba, M., Guo, J. L., Mcbride, J. D., Zhang, B., Trojanowski, J. Q., and Lee, V. M. (2013). Synthetic tau fibrils mediate transmission of neurofibrillary tangles in a transgenic mouse model of Alzheimer's-like Tauopathy *J. Neurosci.* 33, 1024–1037. doi: 10.1523/JNEUROSCI.2642-12.2013

Iijima, M., Tabira, T., Poorkaj, P., Schellenberg, G. D., Trojanowski, J. Q., Lee, V. M., et al. (1999). A distinct familial presenile dementia with a novel missense mutation in the tau gene. *Neuroreport* 10, 497–501. doi: 10.1097/00001756-199902250-00010

Iko, Y., Kodama, T. S., Kasai, N., Oyama, T., Morita, E. H., Muto, T., et al. (2004). Domain architectures and characterization of an RNA-binding protein, TLS. *J. Biol. Chem.* 279, 44834–44840. doi: 10.1074/jbc.M408552200

Iovino, M., Pfisterer, U., Holton, J. L., Lashley, T., Swingler, R. J., Calo, L., et al. (2014). The novel MAPT mutation K,98E: mechanisms of mutant tau toxicity, brain pathology and tau expression in induced fibroblast-derived neurons. *Acta Neuropathol.* 127, 283–295. doi: 10.1007/s00401-013-1219-1

Iseki, E., Matsumura, T., Marui, W., Hino, H., Odawara, T., Sugiyama, N., et al. (2001). Familial frontotemporal dementia and parkinsonism with a novel N296H mutation in exon 10 of the tau gene and a widespread tau accumulation in the glial cells. *Acta Neuropathol.* 102, 285–292.

Ishigaki, S., Hishikawa, N., Niwa, J., Iemura, S., Natsume, T., Hori, S., et al. (2004). Physical and functional interaction between Dorfin and Valosin-containing protein that are colocalized in ubiquitylated inclusions in neurodegenerative disorders. *J. Biol. Chem.* 279, 51376–51385. doi: 10.1074/jbc.M406683200

Ishigaki, S., Masuda, A., Fujioka, Y., Iguchi, Y., Katsuno, M., Shibata, A., et al. (2012). Position-dependent FUS-RNA interactions regulate alternative splicing events and transcriptions. *Sci. Rep.* 2, 529. doi: 10.1038/srep00529

Ito, D., Seki, M., Tsunoda, Y., Uchiyama, H., and Suzuki, N. (2011). Nuclear transport impairment of amyotrophic lateral sclerosis-linked mutations in FUS/TLS. *Ann. Neurol.* 69, 152–162. doi: 10.1002/ana.22246

Iyer, A., Lapointe, N. E., Zielke, K., Berdynski, M., Guzman, E., Barczak, A., et al. (2013). A novel MAPT mutation, G55R, in a frontotemporal dementia patient leads to altered Tau function. *PLoS ONE* 8:e76409. doi: 10.1371/journal.pone.0076409

Jacquin, A., Rouaud, O., Soichot, P., Bejot, Y., Dygai-Cochet, I., Sarazin, M., et al. (2013). Psychiatric presentation of frontotemporal dementia associated with inclusion body myopathy due to the VCP mutation (R155H) in a French family. *Case Rep. Neurol.* 5, 187–194. doi: 10.1159/000356481

Janssens, J., and Van Broeckhoven, C. (2013). Pathological mechanisms underlying TDP-43 driven neurodegeneration in FTLD-ALS spectrum disorders. *Hum. Mol. Genet.* 22, R77–R87. doi: 10.1093/hmg/ddt349

Jiao, J., Herl, L. D., Farese, R. V., and Gao, F.-B. (2010). MicroRNA-29b regulates the expression level of human progranulin, a secreted glycoprotein

implicated in frontotemporal dementia. *PLoS ONE* 5:e10551. doi: 10.1371/journal.pone.0010551

Johnson, J. O., Mandrioli, J., Benatar, M., Van Deerlin, V. M., Trojanowski, J. Q., Mora, G., et al. (2010). Exome sequencing reveals VCP mutations as a cause of familial ALS. *Neuron* 68, 857–864. doi: 10.1016/j.neuron.2010.11.036

Johnson, J. O., Pioro, E. P., Boehringer, A., Chia, R., Feit, H., Renton, A. E., et al. (2014). Mutations in the Matrin 3 gene cause familial amyotrophic lateral sclerosis. *Nat. Neurosci.* 17, 664–666. doi: 10.1038/nn.3688

Ju, J.-S., Fuentealba, R. A., Miller, S. E., Jackson, E., Piwnica-Worms, D., Baloh, R. H., et al. (2009). Valosin-containing protein (VCP) is required for autophagy and is disrupted in VCP disease. *J. Cell Biol.* 187, 875–888. doi: 10.1083/jcb.200908115

Kabashi, E., Lin, L., Tradewell, M. L., Dion, P. A., Bercier, V., Bourgouin, P., et al. (2010). Gain and loss of function of ALS-related mutations of TARDBP (TDP-43) cause motor deficits *in vivo*. *Hum. Mol. Genet.* 19, 671–683. doi: 10.1093/hmg/ddp534

Kabashi, E., Valdmanis, P. N., Dion, P., Spiegelman, D., McConkey, B. J., Vande Velde, C., et al. (2008). TARDBP mutations in individuals with sporadic and familial amyotrophic lateral sclerosis. *Nat. Genet.* 40, 572–574. doi: 10.1038/ng.132

Kaleem, M., Zhao, A., Hamshere, M., and Myers, A. J. (2007). Identification of a novel valosin-containing protein polymorphism in late-onset Alzheimer's disease. *Neurodegener Dis.* 4, 376–381. doi: 10.1159/000105158

Kara, E., Ling, H., Pittman, A. M., Shaw, K., de Silva, R., Simone, R., et al. (2012). The MAPT p.A152T variant is a risk factor associated with tauopathies with atypical clinical and neuropathological features. *Neurobiol. Aging.* 33, 2231.e7-2231.e14. doi: 10.1016/j.neurobiolaging.2012.04.006

Katzmann, D. J., Odorizzi, G., and Emr, S. D. (2002). Receptor downregulation and multivesicular-body sorting. *Nat. Rev. Mol. Cell Biol.* 3, 893–905. doi: 10.1038/nrm973

Kawahara, Y., and Mieda-Sato, A. (2012). TDP-43 promotes microRNA biogenesis as a component of the Drosha and Dicer complexes. *Proc. Natl. Acad. Sci. U.S.A.* 109, 3347–3352. doi: 10.1073/pnas.1112427109

Kessenbrock, K., Fröhlich, L., Sixt, M., Lämmermann, T., Pfister, H., Bateman, A., et al. (2008). Proteinase 3 and neutrophil elastase enhance inflammation in mice by inactivating antiinflammatory progranulin. *J. Clin. Invest.* 118, 2438–2447. doi: 10.1172/JCI34694

Kikin, O., Zappala, Z., D'Antonio, L., and Bagga, P. S. (2008). GRSDB2 and GRS_UTRdb: databases of quadruplex forming G-rich sequences in premRNAs and mRNAs. *Nucleic Acids Res.* 36, D141-D8.(Database issue):D141-8. doi: 10.1093/nar/gkm982

Kim, E.-J., Kwon, J. C., Park, K. H., Park, K.-W., Lee, J.-H., Choi, S. H., et al. (2014). Clinical and genetic analysis of MAPT, GRN, and C9orf72 genes in Korean patients with frontotemporal dementia. *Neurobiol. Aging.* 35, 1213.e13–1213.e17. doi: 10.1016/j.neurobiolaging.2013.11.033

Kim, H.-J., Jeon, B. S., Yun, J. Y., Seong, M.-W., Park, S. S., and Lee, J.-Y. (2010a). Screening for MAPT and PGRN mutations in Korean patients with PSP/CBS/FTD. *Parkinsonism Relat. Disord.* 16, 305–306. doi: 10.1016/j.parkreldis.2010.01.004

Kim, S. H., Shanware, N. P., Bowler, M. J., and Tibbetts, R. S. (2010b). Amyotrophic lateral sclerosis-associated proteins TDP-43 and FUS/TLS function in a common biochemical complex to co-regulate HDAC6 mRNA. *J. Biol. Chem.* 285, 34097–34105. doi: 10.1074/jbc.M110.154831

Kim, V. N. (2004). MicroRNA precursors in motion: exportin-5 mediates their nuclear export. *Trends Cell Biol.* 14, 156–159. doi: 10.1016/j.tcb.2004.02.006

Kimonis, V. E., Mehta, S. G., Fulchiero, E. C., Thomasova, D., Boycott, K., Neilan, E. G., et al. (2008). Clinical studies in familial VCP myopathy associated with paget disease of bone and frontotemporal dementia. *Am. J. Med. Genet. A.* 28, 745–757. doi: 10.1002/ajmg.a.31862

King, I., Yartseva, V., Salas, D., Kumar, A., Heidersbach, A., Ando, D. M., et al. (2014). The RNA binding protein TDP-43 selectively disrupts MicroRNA-1/206 incorporation into the RNA-induced silencing complex. *J. Biol. Chem.* 289, 14263–14271. doi: 10.1074/jbc.M114.561902

Kobayashi, T., Ota, S., Tanaka, K., Ito, Y., Hasegawa, M., Umeda, Y., et al. (2003).Novel L266V mutation of the tau gene causes frontotemporal dementia with a unique tau pathology. *Ann. Neurol.* 53, 133–137. doi: 10.1002/ana.10447

Kouri, N., Carlomagno, Y., Baker, M., Liesinger, A. M., Caselli, R. J., Wszolek, Z. K., et al. (2014). Novel mutation in MAPT exon 13 (p.N410H) causes corticobasal degeneration. *Acta Neuropathol.* 127, 271–282. doi: 10.1007/s00401-013-1193-7

Kovach, M. J., Waggoner, B., Leal, S. M., Gelber, D., Khandori, R., Levenstien, M., et al. (2001). Clinical delineation and localization to chromosome 9p13.3-p12 of a unique dominant disorder in four families: hereditary inclusion body myopathy, Paget disease of bone, and frontotemporal dementia. *Mol. Genet. Metab.* 74, 458–475. doi: 10.1006/mgme.2001.3256

Kovacs, G. G., Murrell, J. R., Horvath, S., Haraszti, L., Majtenyi, K., Molnar, M. J., et al. (2009). TARDBP variation associated with frontotemporal dementia, supranuclear gaze palsy, and chorea. *Mov. Disord.* 24, 1843–1847. doi: 10.1002/mds.22697

Kovacs, G. G., Pittman, A., Revesz, T., Luk, C., Lees, A., Kiss, E., et al. (2008). MAPT S305I mutation: implications for argyrophilic grain disease. *Acta Neuropathol.* 116, 103–118. doi: 10.1007/s00401-007-0322-6

Kumar, K. R., Needham, M., Mina, K., Davis, M., Brewer, J., Staples, C., et al. (2010). Two Australian families with inclusion-body myopathy, Paget's disease of bone and frontotemporal dementia: novel clinical and genetic findings. *Neuromuscul. Disord.* 20, 330–334. doi: 10.1016/j.nmd.2010.03.002

Kwiatkowski, T. J., Bosco, D. A., Leclerc, A. L., Tamrazian, E., Vanderburg, C. R., Russ, C., et al. (2009). Mutations in the FUS/TLS gene on chromosome 16 cause familial amyotrophic lateral sclerosis. *Science* 323, 1205–1208. doi: 10.1126/science.1166066

Lagier-Tourenne, C., Baughn, M., Rigo, F., Sun, S., Liu, P., Li, H.-R., et al. (2013). Targeted degradation of sense and antisense C9orf72 RNA foci as therapy for ALS and frontotemporal degeneration. *Proc. Natl. Acad. Sci. U.S.A.* 110, E4530–E4539. doi: 10.1073/pnas.1318835110

Lagier-Tourenne, C., Polymenidou, M., and Cleveland, D. W. (2010). TDP-43 and FUS/TLS: emerging roles in RNA processing and neurodegeneration. *Hum. Mol. Genet.* 19, R46–R64. doi: 10.1093/hmg/ddq137

Lagier-Tourenne, C., Polymenidou, M., Hutt, K. R., Vu, A. Q., Baughn, M., Huelga, S. C., et al. (2012). Divergent roles of ALS-linked proteins FUS/TLS and TDP-43 intersect in processing long pre-mRNAs. *Nat. Neurosci.* 15, 1488–1497. doi: 10.1038/nn.3230

Lander, E. S., Linton, L. M., Birren, B., Nusbaum, C., Zody, M. C., Baldwin, J., et al. (2001). Initial sequencing and analysis of the human genome. *Nature* 409, 860–921. doi: 10.1038/35057062

Lanska, D. J., Currier, R. D., Cohen, M., Gambetti, P., Smith, E. E., Bebin, J., et al. (1994). Familial progressive subcortical gliosis. *Neurology* 44, 1633–1643. doi: 10.1212/WNL.44.9.1633

Law, W. J., Cann, K. L., and Hicks, G. G. (2006). TLS, EWS and TAF15: a model for transcriptional integration of gene expression. *Brief. Funct. Genomic. Proteomic.* 5, 8–14. doi: 10.1093/bfgp/ell015

Le Ber, I., Van der Zee, J., Hannequin, D., Gijselinck, I., Campion, D., Puel, M., et al. (2007). Progranulin null mutations in both sporadic and familial frontotemporal dementia. *Hum. Mutat.* 28, 846–855. doi: 10.1002/humu.20520

Lee, E. B., Lee, V. M.-Y., and Trojanowski, J. Q. (2012). Gains or losses: molecular mechanisms of TDP43-mediated neurodegeneration. *Nat. Rev. Neurosci.* 13, 38–50. doi: 10.1038/nrn3121

Lee, H.-G., Perry, G., Moreira, P. I., Garrett, M. R., Liu, Q., Zhu, X., et al. (2005). Tau phosphorylation in Alzheimer's disease: pathogen or protector? *Trends Mol. Med.* 11, 164–169. doi: 10.1016/j.molmed.2005.02.008

Lee, Y., Ahn, C., Han, J., Choi, H., Kim, J., Yim, J., et al. (2003). The nuclear RNase III Drosha initiates microRNA processing. *Nature* 425, 415–419. doi: 10.1038/nature01957

Lee, Y.-B., Chen, H.-J., Peres, J. N., Gomez-Deza, J., Attig, J., Stalekar, M., et al. (2013). Hexanucleotide repeats in ALS/FTD form length-dependent RNA foci, sequester RNA binding proteins, and are neurotoxic. *Cell Rep.* 5, 1178–1186. doi: 10.1016/j.celrep.2013.10.049

Lee, Y., Kim, M., Han, J., Yeom, K.-H., Lee, S., Baek, S. H., et al. (2004). MicroRNA genes are transcribed by RNA polymerase II. *EMBO J.* 23, 4051–4060. doi: 10.1038/sj.emboj.7600385

Ling, S. C., Albuquerque, C. P., Han, J. S., Lagier-Tourenne, C., Tokunaga, S., Zhou, H., et al. (2010). ALS-associated mutations in TDP-43 increase its stability and promote TDP-43 complexes with FUS/TLS. *Proc. Natl. Acad. Sci. U.S.A.* 107, 13318–13323. doi: 10.1073/pnas.1008227107

Ling, S.-C., Polymenidou, M., and Cleveland, D. W. (2013). Converging mechanisms in ALS and FTD: disrupted RNA and protein homeostasis. *Neuron* 79, 416–438. doi: 10.1016/j.neuron.2013.07.033

Liu, J., Carmell, M., and Rivas, F. (2004). Argonaute2 is the catalytic engine of mammalian RNAi. *Science* 305, 1437–1441. doi: 10.1126/science.1102513

Liu, L., Drouet, V., Wu, J. W., Witter, M. P., Small, S. A., Clelland, C., et al. (2012). Trans-synaptic spread of tau pathology in vivo. *PLoS ONE* 7:e31302. doi: 10.1371/journal.pone.0031302

Lladó, A., Ezquerra, M., Sánchez-Valle, R., Rami, L., Tolosa, E., and Molinuevo, J. L. (2007). A novel MAPT mutation (P301T) associated with familial frontotemporal dementia. *Eur. J. Neurol.* 14, e9–e10. doi: 10.1111/j.1468-1331.2007.01763.x

Lopez de Munain, A., Alzualde, A., Gorostidi, A., Otaegui, D., Ruiz-Martinez, J., Indakoetxea, B., et al. (2008). Mutations in progranulin gene: clinical, pathological, and ribonucleic acid expression findings. *Biol. Psychiatry* 63, 946–952. doi: 10.1016/j.biopsych.2007.08.015

Luna-Muñoz, J., Harrington, C. R., Wischik, C. M., Flores-Rodríiguez, P., Avila, J., Zamudio, S. R., et al. (2013). "Phosphorylation of tau protein associated as a protective mechanism in the presence of toxic, C-terminally truncated tau in Alzheimer's disease," in *Understanding Alzheimer's Disease*, ed I. Zerr (InTech). doi: 10.5772/54228

Luquin, N., Yu, B., Saunderson, R. B., Trent, R. J., and Pamphlett, R. (2009). Genetic variants in the promoter of TARDBP in sporadic amyotrophic lateral sclerosis. *Neuromuscul Disord.* 19, 696–700. doi: 10.1016/j.nmd.2009.07.005

Lynch, T., Sano, M., Marder, K. S., Bell, K. L., Foster, N. L., Defendini, R. F., et al. (1994). Clinical characteristics of a family with chromosome 17-linked disinhibition-dementia-parkinsonism-amyotrophy complex. *Neurology* 44, 1878–1884. doi: 10.1212/WNL.44.10.1878

Mackenzie, I. R., Baker, M., Pickering-Brown, S., Hsiung, G.-Y. R., Lindholm, C., Dwosh, E., et al. (2006). The neuropathology of frontotemporal lobar degeneration caused by mutations in the progranulin gene. *Brain* 129, 3081–3090. doi: 10.1093/brain/awl271

Mackenzie, I. R. A., Frick, P., and Neumann, M. (2014). The neuropathology associated with repeat expansions in the C9ORF72 gene. *Acta Neuropathol.* 127, 347–357. doi: 10.1007/s00401-013-1232-4

Mackenzie, I. R., Rademakers, R., and Neumann, M. (2010). TDP-43 and FUS in amyotrophic lateral sclerosis and frontotemporal dementia. *Lancet Neurol.* 9, 995–1007. doi: 10.1016/S1474-4422(10)70195-2

Marcon, G., Rossi, G., Giaccone, G., Giovagnoli, A. R., Piccoli, E., Zanini, S., et al. (2011). Variability of the clinical phenotype in an Italian family with dementia associated with an intronic deletion in the GRN gene. *J. Alzheimers Dis.* 22, 1123–1133. doi: 10.3233/JAD-2011-110332

Martin-Serrano, J., and Neil, S. J. D. (2011). Host factors involved in retroviral budding and release. *Nat. Rev. Microbiol.* 9, 519–531. doi: 10.1038/nrmicro2596

Medina, M., and Avila, J. (2014). The role of extracellular Tau in the spreading of neurofibrillary pathology. *Front. Cell. Neurosci.* 8:113. doi: 10.3389/fncel.2014.00113

Mehler, M. F., and Mattick, J. S. (2007). Noncoding RNAs and RNA editing in brain development, functional diversification, and neurological disease. *Physiol. Rev.* 87, 799–823. doi: 10.1152/physrev.00036.2006

Meissner, M., Lopato, S., Gotzmann, J., Sauermann, G., and Barta, A. (2003). Proto-oncoprotein tls/fus is associated to the nuclear matrix and complexed with splicing factors ptb, srm160, and sr proteins. *Exp. Cell Res.* 283, 184–195. doi: 10.1016/S0014-4827(02)00046-0

Mercer, T. R., Dinger, M. E., Sunkin, S. M., Mehler, M. F., and Mattick, J. S. (2008). Specific expression of long noncoding RNAs in the mouse brain. *Proc. Natl. Acad. Sci. U.S.A.* 105, 716–721. doi: 10.1073/pnas.0706729105

Metcalf, D., and Isaacs, A. M. (2010). The role of ESCRT proteins in fusion events involving lysosomes, endosomes and autophagosomes. *Biochem. Soc. Trans.* 38, 1469–1473. doi: 10.1042/BST0381469

Miyamoto, K., Kowalska, A., Hasegawa, M., Tabira, T., Takahashi, K., Araki, W., et al. (2001). Familial frontotemporal dementia and parkinsonism with a novel mutation at an intron 10+11-splice site in the tau gene. *Ann. Neurol.* 50, 117–120. doi: 10.1002/ana.1083

Mizielinska, S., Lashley, T., Norona, F. E., Clayton, E. L., Ridler, C. E., Fratta, P., et al. (2013). C9orf72 frontotemporal lobar degeneration is characterised by frequent neuronal sense and antisense RNA foci. *Acta Neuropathol.* 126, 845–857. doi: 10.1007/s00401-013-1200-z

Mizuno, Y., Hori, S., Kakizuka, A., and Okamoto, K. (2003). Vacuole-creating protein in neurodegenerative diseases in humans. *Neurosci. Lett.* 343, 77–80. doi: 10.1016/S0304-3940(03)00280-5

Momeni, P., Rogaeva, E., Van Deerlin, V., Yuan, W., Grafman, J., Tierney, M., et al. (2006). Genetic variability in CHMP2B and frontotemporal dementia. *Neurodegener. Dis.* 3, 129–133. doi: 10.1159/000094771

Mori, K., Lammich, S., Mackenzie, I. R., Forné, I., Zilow, S., Kretzschmar, H., et al. (2013a). hnRNP A3 binds to GGGGCC repeats and is a constituent of p62-positive/TDP43-negative inclusions in the hippocampus of patients with C9orf72 mutations. *Acta Neuropathol.* 125, 413–423. doi: 10.1007/s00401-013-1088-7

Mori, K., Weng, S.-M., Arzberger, T., May, S., Rentzsch, K., Kremmer, E., et al. (2013b). The C9orf72 GGGGCC repeat is translated into aggregating dipeptide-repeat proteins in FTLD/ALS. *Science (New York, NY)*, 339, 1335–1338. doi: 10.1126/science.1232927

Morita, M., Al-Chalabi, A., Andersen, P. M., Hosler, B., Sapp, P., Englund, E., et al. (2006). A locus on chromosome 9p confers susceptibility to ALS and frontotemporal dementia. *Neurology* 66, 839–844. doi: 10.1212/01.wnl.0000200048.53766.b4

Morlando, M., Dini Modigliani, S., Torrelli, G., Rosa, A., Di Carlo, V., Caffarelli, E., et al. (2012). FUS stimulates microRNA biogenesis by facilitating co-transcriptional Drosha recruitment. *EMBO J.* 31, 4502–4510. doi: 10.1038/emboj.2012.319

Mukherjee, O., Pastor, P., Cairns, N. J., Chakraverty, S., Kauve, J. S., Shears S., et al. (2006). HDDD2 is a familial frontotemporal lobar degeneration with ubiquitin-positive, taunegative inclusions caused by a missense mutation in the signal peptide of progranulin. *Ann. Neurol.* 60, 314–322. doi: 10.1002/ana.20963

Mukherjee, O., Wang, J., Gitcho, M., Chakraverty, S., Taylor-Reinwald, L., Shears, S., et al. (2008). Molecular characterization of novel progranulin (GRN) mutations in frontotemporal dementia. *Hum. Mutat.* 29, 512–521. doi: 10.1002/humu.20681

Murrell, J. R., Spillantini, M. G., Zolo, P., Guazzelli, M., Smith, M. J., Hasegawa, M., et al. (1999). Tau gene mutation G389R causes a tauopathy with abundant pick body-like inclusions and axonal deposits. *J. Neuropathol. Exp. Neurol.* 58, 1207–1226. doi: 10.1097/00005072-199912000-00002

Naganuma, T., Nakagawa, S., Tanigawa, A., Sasaki, Y. F., Goshima, N., and Hirose, T. (2012). Alternative 3′-end processing of long noncoding RNA initiates construction of nuclear paraspeckles. *EMBO J.* 31, 4020–4034. doi: 10.1038/emboj.2012.251

Nakagawa, S., and Hirose, T. (2012). Paraspeckle nuclear bodies–useful uselessness? *Cell. Mol. Life Sci.* 69, 3027–3036. doi: 10.1007/s00018-012-0973-x

Nakagawa, S., Naganuma, T., Shioi, G., and Hirose, T. (2011). Paraspeckles are subpopulation-specific nuclear bodies that are not essential in mice. *J. Cell Biol.* 193, 31–39. doi: 10.1083/jcb.201011110

Nalbandian, A., Donkervoort, S., Dec, E., Badadani, M., Katheria, V., Rana, P., et al. (2011). The multiple faces of valosin-containing protein-associated diseases: inclusion body myopathy with Paget's disease of bone, frontotemporal dementia, and amyotrophic lateral sclerosis. *J. Mol. Neurosci.* 45, 522–531. doi: 10.1007/s12031-011-9627-y

Neumann, M., Diekmann, S., Bertsch, U., Vanmassenhove, B., Bogerts, B., Kretzschmar, H. A. (2005). Novel G335V mutation in the tau gene associated with early onset familial frontotemporal dementia. *Neurogenetics* 6, 91–95. doi: 10.1007/s10048-005-0210-y

Neumann, M., Kwong, L. K., Lee, E. B., Kremmer, E., Flatley, A., Xu, Y., et al. (2009a). Phosphorylation of S409/410 of TDP-43 is a consistent feature in all sporadic and familial forms of TDP-43 proteinopathies. *Acta Neuropathol.* 117, 137–149. doi: 10.1007/s00401-008-0477-9

Neumann, M., Rademakers, R., Roeber, S., Baker, M., Kretzschmar, H. A., and Mackenzie, I. R. A. (2009b). A new subtype of frontotemporal lobar degeneration with FUS pathology. *Brain* 132(Pt 11), 2922–2931. doi: 10.1093/brain/awp214

Neumann, M., Sampathu, D. M., Kwong, L. K., Truax, A. C., Micsenyi, M. C., Chou, T. T., et al. (2006). Ubiquitinated TDP-43 in frontotemporal lobar degeneration and amyotrophic lateral sclerosis. *Science (New York, NY)* 314, 130–133. doi: 10.1126/science.1134108

Ng, S. Y., Lin, L., Soh, B. S., and Stanton, L. W. (2013). Long noncoding RNAs in development and disease of the central nervous system. *Trends Genet.* 29, 461–468. doi: 10.1016/j.tig.2013.03.002

Nishimoto, Y., Nakagawa, S., Hirose, T., Okano, H. J., Takao, M., Shibata, S., et al. (2013). The long non-coding RNA nuclear-enriched abundant transcript 1_2 induces paraspeckle formation in the motor neuron during the early phase of amyotrophic lateral sclerosis. *Mol. Brain* 6, 31. doi: 10.1186/1756-6606-6-31

Obita, T., Saksena, S., Ghazi-Tabatabai, S., Gill, D. J., Perisic, O., Emr, S. D., et al. (2007). Structural basis for selective recognition of ESCRT-III by the AAA ATPase Vps4. *Nature* 449, 735–739. doi: 10.1038/nature06171

O'Rourke, J. R., and Swanson, M. S. (2009). Mechanisms of RNA-mediated disease. *J. Biol. Chem.* 284, 7419–7423. doi: 10.1074/jbc.R800025200

Ogaki, K., Li, Y., Takanashi, M., Ishikawa, K.-I., Kobayashi, T., Nonaka, T., et al. (2013). Analyses of the MAPT, PGRN, and C9orf72 mutations in Japanese patients with FTLD, PSP, and CBS. *Parkinsonism Relat. Disord.* 19, 15–20. doi: 10.1016/j.parkreldis.2012.06.019

Okura, H., Yamashita, S., Ohama, T., Saga, A., Yamamoto-Kakuta, A., Hamada, Y., et al. (2010). HDL/apolipoprotein A-I binds to macrophage-derived progranulin and suppresses its conversion into proinflammatory granulins. *J. Atheroscler. Thromb.* 17, 568–577. doi: 10.5551/jat.3921

Osborne, R. J., and Thornton, C., a. (2006). RNA-dominant diseases. *Hum. Mol. Genet.* 15 Spec No(2), R162–R9. doi: 10.1093/hmg/ddl181

Ou, S. H., Wu, F., Harrich, D., García-Martínez, L. F., and Gaynor, R. B. (1995). Cloning and characterization of a novel cellular protein, TDP-43, that binds to human immunodeficiency virus type 1 TAR DNA sequence motifs. *J. Virol.* 69, 3584–3596.

Pandit, S., Wang, D., and Fu, X.-D. (2008). Functional integration of transcriptional and RNA processing machineries. *Curr. Opin. Cell Biol.* 20, 260–265. doi: 10.1016/j.ceb.2008.03.001

Parkinson, N., Ince, P. G., Smith, M. O., Highley, R., Skibinski, G., Andersen, P. M., et al. (2006). ALS phenotypes with mutations in CHMP2B (charged multivesicular body protein 2B). *Neurology* 67, 1074–1077. doi: 10.1212/01.wnl.0000231510.89311.8b

Pasquinelli, A. E. (2012). MicroRNAs and their targets: recognition, regulation and an emerging reciprocal relationship. *Nat. Rev. Genet.* 13, 271–282. doi: 10.1038/nrg3162

Pickering-Brown, S., Baker, M., Yen, S. H., Liu, W. K., Hasegawa, M., Cairns, N., et al. (2000). Pick's disease is associated with mutations in the tau gene. *Ann. Neurol.* 48, 859–867. doi: 10.1002/1531-8249(200012)48:6<859::AID-ANA6>3.0.CO;2-1

Pickering-Brown, S. M., Baker, M., Nonaka, T., Ikeda, K., Sharma, S., Mackenzie, J., et al. (2004). Frontotemporal dementia with Pick-type histology associated with Q336R mutation in the tau gene. *Brain* 127(Pt. 6), 1415–1426. doi: 10.1093/brain/awh147

Plowman, G. D., Green, J. M., Neubauer, M. G., Buckley, S. D., Mcdonald, V. L., Todaro, G. J., et al. (1992). The epithelin precursor encodes two proteins with opposing activities on epithelial cell growth. *J. Biol. Chem.* 267, 13073–13078.

Polymenidou, M., Lagier-Tourenne, C., Hutt, K. R., Huelga, S. C., Moran, J., Liang, T. Y., et al. (2011). Long pre-mRNA depletion and RNA missplicing contribute to neuronal vulnerability from loss of TDP-43. *Nat. Neurosci.* 14, 459–468. doi: 10.1038/nn.2779

Poorkaj, P., Kas, A., D'Souza, I., Zhou, Y., Pham, Q., Stone, M., et al. (2001). A genomic sequence analysis of the mouse and human microtubule-associated protein tau. *Mamm. Genome.* 12, 700–712. doi: 10.1007/s00335-001-2044-8

Prasanth, K. V., Prasanth, S. G., Xuan, Z., Hearn, S., Freier, S. M., Bennett, C. F., et al. (2005). Regulating gene expression through RNA nuclear retention. *Cell* 123, 249–263. doi: 10.1016/j.cell.2005.08.033

Pye, V. E., Beuron, F., Keetch, C. A, McKeown, C., Robinson, C. V., Meyer, H. H., et al. (2007). Structural insights into the p97-Ufd1-Npl4 complex. *Proc. Natl. Acad. Sci. U.S.A.* 104, 467–472. doi: 10.1073/pnas.0603408104

Rademakers, R., Eriksen, J. L., Baker, M., Robinson, T., Ahmed, Z., Lincoln, S. J., et al. (2008). Common variation in the miR-659 binding-site of GRN is a major risk factor for TDP43-positive frontotemporal dementia. *Hum. Mol. Genet.* 17, 3631–3642. doi: 10.1093/hmg/ddn257

Reddy, K., Zamiri, B., Stanley, S. Y. R., Macgregor, R. B., and Pearson, C. E. (2013). The disease-associated r(GGGGCC)n repeat from the C9orf72 gene forms tract length-dependent uni- and multimolecular RNA G-quadruplex structures. *J. Biol. Chem.* 288, 9860–9866. doi: 10.1074/jbc.C113.452532

Reichelt, A. C., Rodgers, R. J., and Clapcote, S. J. (2012). The role of neurexins in schizophrenia and autistic spectrum disorder. *Neuropharmacology* 62, 1519–1526. doi: 10.1016/j.neuropharm.2011.01.024

Renoux, A., and Todd, P. (2012). Neurodegeneration the RNA way. *Prog. Neurobiol.* 97, 173–189. doi: 10.1016/j.pneurobio.2011.10.006

Renton, A. E., Majounie, E., Waite, A., Simón-Sánchez, J., Rollinson, S., Gibbs, J. R., et al. (2011). A hexanucleotide repeat expansion in C9ORF72 is the cause of chromosome 9p21-linked ALS-FTD. *Neuron* 72, 257–268. doi: 10.1016/j.neuron.2011.09.010

Rizzini, C., Goedert, M., Hodges, J. R., Smith, M. J., Jakes, R., Hills, R., et al. (2000).Tau gene mutation K257T causes a tauopathy similar to Pick's disease. *J. Neuropathol. Exp. Neurol.* 59, 990–1001.

Rizzu, P., van Swieten, J. C., Joosse, M., Hasegawa, M., Stevens, M., Tibben, A., et al. (1999). High prevalence of mutations in the microtubule-associated protein tau in a population study of frontotemporal dementia in the Netherlands. *Am. J. Human Genet.* 64, 414–421. doi: 10.1086/302256

Rossi, G., Bastone, A., Piccoli, E., Mazzoleni, G., Morbin, M., Uggetti, A., et al. (2012). New mutations in MAPT gene causing frontotemporal lobar degeneration: biochemical and structural characterization. *Neurobiol. Aging* 33, 834.e1–834.e6. doi: 10.1016/j.neurobiolaging.2011.08.008

Rossi, G., Bastone, A., Piccoli, E., Morbin, M., Mazzoleni, G., Fugnanesi, V., et al. (2014). Different mutations at V363 MAPT codon are associated with atypical clinical phenotypes and show unusual structural and functional features. *Neurobiol. Aging* 35, 408–417. doi: 10.1016/j.neurobiolaging.2013.08.004

Rosso, S. M., Donker, K. L., Baks, T., Joosse, M., de Koning, I., Pijnenburg, Y., et al. (2003). Frontotemporal dementia in The Netherlands: patient characteristics and prevalence estimates from a population-based study. *Brain* 126, 2016–2022. doi: 10.1093/brain/awg204

Rosso, S. M., van Herpen, E., Deelen, W., Kamphorst, W., Severijnen, L. A., Willemsen, R., et al. (2002). A novel tau mutation, S320F, causes a tauopathy with inclusions similar to those in Pick's disease. *Ann. Neurol.* 51, 373–376. doi: 10.1002/ana.10140

Rouiller, I., DeLaBarre, B., May, A. P., Weis, W. I., Brunger, A. T., Milligan, R., et al. (2002). Conformational changes of the multifunction p97 AAA ATPase during its ATPase cycle. *Nat. Struct. Biol.* 9, 950–957 doi: 10.1038/nsb872

Rovelet-Lecrux, A., Deramecourt, V., Legallic, S., Maurage, C. A., Le Ber, I., Brice, A., et al. (2008). Deletion of the progranulin gene in patients with frontotemporal lobar degeneration or Parkinson disease. *Neurobiol. Dis.* 31, 41–45. doi: 10.1016/j.nbd.2008.03.004

Roxrud, I., Stenmark, H., and Malerød, L. (2010). ESCRT and Co. *Biol. Cell*, 102, 293–318. doi: 10.1042/BC20090161

Saman, S., Kim, W., Raya, M., Visnick, Y., Miro, S., Jackson, B., et al. (2012). Exosome-associated tau is secreted in tauopathy models and is selectively phosphorylated in cerebrospinal fluid in early Alzheimer disease. *J. Biol. Chem.* 287, 3842–3849. doi: 10.1074/jbc.M111.277061

Sampathu, D. M., Neumann, M., Kwong, L. K., Chou, T. T., Micsenyi, M., Truax, A., et al. (2006). Pathological heterogeneity of frontotemporal lobar degeneration with ubiquitin-positive inclusions delineated by ubiquitin immunohistochemistry and novel monoclonal antibodies. *Am. J. Pathol.* 169, 1343–1352. doi: 10.2353/ajpath.2006.060438

Sareen, D., O'Rourke, J. G., Meera, P., Muhammad, A. K., Grant, S., Simpkinson, M., et al. (2013). Targeting RNA foci in iPSC-derived motor neurons from ALS patients with a C9ORF72 repeat expansion. *Sci. Transl. Med.* 5, 208ra149. doi: 10.1126/scitranslmed.3007529

Schenk, V. W. (1959). Re-examination of a family with Pick's disease. *Ann. Hum. Genet.* 23, 325–333. doi: 10.1111/j.1469-1809.1959.tb01476.x

Schmidt, O., and Teis, D. (2012). The ESCRT machinery. *Curr. Biol.* 22, R116–R120. doi: 10.1016/j.cub.2012.01.028

Schwartz, J. C., Ebmeier, C. C., Podell, E. R., Heimiller, J., Taatjes, D. J., and Cech, T. R. (2012). FUS binds the CTD of RNA polymerase II and regulates its phosphorylation at Ser2. *Genes Dev.* 26, 2690–2695. doi: 10.1101/gad.204602.112

Sephton, C. F., Cenik, C., Kucukural, A., Dammer, E. B., Cenik, B., Han, Y., et al. (2011). Identification of neuronal RNA targets of TDP-43-containing ribonucleoprotein complexes. *J. Biol. Chem.* 286, 1204–1215. doi: 10.1074/jbc.M110.190884

Shan, X., Chiang, P.-M., Price, D. L., and Wong, P. C. (2010). Altered distributions of Gemini of coiled bodies and mitochondria in motor neurons of TDP-43 transgenic mice. *Proc. Natl. Acad. Sci. U.S.A.* 107, 16325–16330. doi: 10.1073/pnas.1003459107

Shankaran, S. S., Capell, A., Hruscha, A. T., Fellerer, K., Neumann, M., Schmid, B., et al. (2008). Missense mutations in the progranulin gene linked to frontotemporal lobar degeneration with ubiquitin-immunoreactive inclusions reduce progranulin production and secretion. *J. Biol. Chem.* 283, 1744–1753. doi: 10.1074/jbc.M705115200

Shelkovnikova, T. A., Robinson, H. K., Troakes, C., Ninkina, N., and Buchman, V. L. (2014). Compromised paraspeckle formation as a pathogenic factor in FUSopathies. *Hum. Mol. Genet.* 23, 2298–2312. doi: 10.1093/hmg/ddt622

Shi, Z., Hayashi, Y. K., Mitsuhashi, S., Goto, K., Kaneda, D., Choi, Y.-C., et al. (2012). Characterization of the Asian myopathy patients with VCP mutations. *Eur. J. Neurol.* 19, 501–509. doi: 10.1111/j.1468-1331.2011.03575.x

Shim, S., Kimpler, L. A., and Hanson, P. I. (2007). Structure/function analysis of four core ESCRT-III proteins reveals common regulatory role for extreme C-terminal domain. *Traffic* 8, 1068–1079. doi: 10.1111/j.1600-0854.2007.00584.x

Simón, D., Garcia-Garcia, E., Royo, F., Falcon-Perez, J. M., and Avila, J. (2012). Proteostasis of tau. Tau overexpression results in its secretion via membrane vesicles. *FEBS Lett.* 586, 47–54. doi: 10.1016/j.febslet.2011.11.022

Skibinski, G., Parkinson, N. J., Brown, J. M., Chakrabarti, L., Lloyd, S. L., Hummerich, H., et al. (2005). Mutations in the endosomal ESCRTIII-complex subunit CHMP2B in frontotemporal dementia. *Nat. Genet.* 37, 806–808. doi: 10.1038/ng1609

Skoglund, L., Matsui, T., Freeman, S. H., Wallin, A., Blom, E. S., Frosch, M. P., et al. (2011). Novel progranulin mutation detected in 2 patients with FTLD. *Alzheimer Dis. Assoc. Disord.* 25, 173–178. doi: 10.1097/WAD.0b013e3181fbc22c

Smith, B. N., Newhouse, S., Shatunov, A., Vance, C., Topp, S., Johnson, L., et al. (2012). The C9ORF72 expansion mutation is a common cause of ALS+/-FTD in Europe and has a single founder. *Eur. J. Hum. Genet.* 21, 102–108. doi: 10.1038/ejhg.2012.98

Snowden, J. S., Rollinson, S., Thompson, J. C., Harris, J. M., Stopford, C. L., Richardson, A. M. T., et al. (2012). Distinct clinical and pathological characteristics of frontotemporal dementia associated with C9ORF72 mutations. *Brain* 135(Pt 3), 693–708. doi: 10.1093/brain/awr355

Songsrirote, K., Li, Z., Ashford, D., Bateman, A., and Thomas-Oates, J. (2010). Development and application of mass spectrometric methods for the analysis of progranulin N-glycosylation. *J. Proteomics* 73, 1479–1490. doi: 10.1016/j.jprot.2010.02.013

Souquere, S., Beauclair, G., Harper, F., Fox, A., and Pierron, G. (2010). Highly ordered spatial organization of the structural long noncoding NEAT1 RNAs within paraspeckle nuclear bodies. *Mol. Biol. Cell* 21, 4020–4027. doi: 10.1091/mbc.E10-08-0690

Spillantini, M. G., and Goedert, M. (2000). Tau mutations in familial frontotemporal dementia. *Brain* 123, 857–859. doi: 10.1093/brain/123.5.857

Spillantini, M. G., and Goedert, M. (2013). Tau pathology and neurodegeneration. *Lancet Neurol.* 12, 609–622. doi: 10.1016/S1474-4422(13)70090-5

Spillantini, M. G., Goedert, M., Crowther, R. A., Murrell, J. R., Farlow, M. R., and Ghetti, B. (1997). Familial multiple system tauopathy with presenile dementia: a disease with abundant neuronal and glial tau filaments. *Proc. Natl. Acad. Sci. U.S.A.* 94, 4113–4118. doi: 10.1073/pnas.94.8.4113

Spina, S., Murrell, J. R., Yoshida, H., Ghetti, B., Bermingham, N., Sweeney, B., et al. (2007). The novel Tau mutation G335S: clinical, neuropathological and molecular characterization. *Acta Neuropathol.* 113, 461–470. doi: 10.1007/s00401-006-0182-5

Spina, S., Murrell, J. R., Vidal, R., and Ghetti, B. (2008). Neuropathologic and genetic characterization of frontotemporal lobar degeneration with Ubiquitin- and/or Tdp-43-positive inclusions: a large series. *Alzheimer's Dementia* 4 (Supp. 2), T431. doi: 10.1016/j.jalz.2008.05.1280

Sreedharan, J., Blair, I. P., Tripathi, V. B., Hu, X., Vance, C., Rogelj, B., et al. (2008). TDP-43 mutations in familial and sporadic amyotrophic lateral sclerosis. *Science* 319, 1668–1672. doi: 10.1126/science.1154584

Stallings, N. R., Puttaparthi, K., Luther, C. M., Burns, D. K., and Elliott, E. J. (2010). Progressive motor weakness in transgenic mice expressing human TDP-43. *Neurobiol. Dis.* 40, 404–414. doi: 10.1016/j.nbd.2010.06.017

Stanford, P. M., Shepherd, C. E., Halliday, G. M., Brooks, W. S., Schofield, P. W., Brodaty, H., et al. (2003). Mutations in the tau gene that cause an increase in three repeat tau and frontotemporal dementia. *Brain* 126, 814–826 doi: 10.1093/brain/awg090

Stojkovic, T., Hammouda, E. H., Richard, P., Munain, A. L., De Ruiz-Martinez, J., Camaño, P., et al. (2009). Clinical outcome in 19 French and Spanish patients with valosin-containing protein myopathy associated with Paget's disease of bone and frontotemporal dementia. *Neuromuscul. Disord.* 21, 316–323. doi: 10.1016/j.nmd.2009.02.012

Strong, M. J., Volkening, K., Hammond, R., Yang, W., Strong, W., Leystra-Lantz, C., et al. (2007). TDP43 is a human low molecular weight neurofilament (hNFL) mRNA-binding protein. *Mol. Cell. Neurosci.* 35, 320–327. doi: 10.1016/j.mcn.2007.03.007

Suárez-Calvet, M., Dols-Icardo, O., Lladó, A., Sánchez-Valle, R., Hernández, I., Amer, G., et al. (2014). Plasma phosphorylated TDP-43 levels are elevated in patients with frontotemporal dementia carrying a C9orf72 repeat expansion or a GRN mutation. *J. Neurol. Neurosurg. Psychiatr.* 85, 684–691. doi: 10.1136/jnnp-2013-305972

Sunwoo, H., Dinger, M. E., Wilusz, J. E., Amaral, P. P., Mattick, J. S., and Spector, D. L. (2009). MEN epsilon/beta nuclear-retained non-coding RNAs are up-regulated upon muscle differentiation and are essential components of paraspeckles. *Genome Res.* 19, 347–359. doi: 10.1101/gr.087775.108

Takamatsu, J., Kondo, A., Ikegami, K., Kimura, T., Fujii, H., Mitsuyama, Y., et al. (1998). Selective expression of Ser 199/202 phosphorylated tau in a case of frontotemporal dementia. *Dement. Geriatr. Cogn. Disord.* 9, 82–89. doi: 10.1159/000017028

Tan, A. Y., and Manley, J. L. (2009). The TET family of proteins: functions and roles in disease. *J. Mol. Cell Biol.* 1, 82–92. doi: 10.1093/jmcb/mjp025

Tang, G., Tang, X., Mendu, V., Tang, X., Jia, X., Chen, Q.-J., et al. (2008). The art of microRNA: various strategies leading to gene silencing via an ancient pathway. *Biochim. Biophys. Acta* 1779, 655–662. doi: 10.1016/j.bbagrm.2008.06.006

Tang, X., Muniappan, L., Tang, G., and Özcan, S. (2009). Identification of glucose-regulated miRNAs from pancreatic β cells reveals a role for miR-30d in insulin transcription. *RNA* 15, 287–293. doi: 10.1261/rna.1211209

Tay, Y., Kats, L., Salmena, L., Weiss, D., Tan, S. M., Ala, U., et al. (2011). Coding-independent regulation of the tumor suppressor PTEN by competing endogenous mRNAs. *Cell* 147, 344–357. doi: 10.1016/j.cell.2011.09.029

Thies, W., and Bleiler, L. (2011). 2011 Alzheimer's disease facts and figures. *Alzheimers Dement.* 7, 208–244. doi: 10.1016/j.jalz.2011.02.004

Todd, P. K., and Paulson, H. L. (2010). RNA-mediated neurodegeneration in repeat expansion disorders. *Ann. Neurol.* 67, 291–300. doi: 10.1002/ana.21948

Tollervey, J. R., Curk, T., Rogelj, B., Briese, M., Cereda, M., Kayikci, M., et al. (2011). Characterizing the RNA targets and position-dependent splicing regulation by TDP-43. *Nat. Neurosci.* 14, 452–458. doi: 10.1038/nn.2778

Urwin, H., Authier, A., Nielsen, J. E., Metcalf, D., Powell, C., Froud, K., et al. (2010). Disruption of endocytic trafficking in frontotemporal dementia with CHMP2B mutations. *Hum. Mol. Genet.* 19, 2228–2238. doi: 10.1093/hmg/ddq100

Usami, Y., Popov, S., Popova, E., Inoue, M., Weissenhorn, W., and, G Göttlinger, H. (2009). The ESCRT pathway and HIV-1 budding. *Biochem. Soc. Trans.* 37(Pt 1), 181–184. doi: 10.1042/BST0370181

Valencia-Sanchez, M. A., Liu, J., Hannon, G. J., and Parker, R. (2006). Control of translation and mRNA degradation by miRNAs and siRNAs. *Genes Dev.* 20, 515–524. doi: 10.1101/gad.1399806

Van Blitterswijk, M., and Landers, J. E. (2010). RNA processing pathways in amyotrophic lateral sclerosis. *Neurogenetics* 11, 275–290. doi: 10.1007/s10048-010-0239-4

Vance, C., Rogelj, B., Hortobagyi, T., De Vos, K. J., Nishimura, A. L., Sreedharan, J., et al. (2009). Mutations in FUS, an RNA processing protein, cause familial amyotrophic lateral sclerosis type 6. *Science* 323, 1208–1211. doi: 10.1126/science.1165942

Van Damme, P., Van Hoecke, A., Lambrechts, D., Vanacker, P., Bogaert, E., van Swieten, J., et al. (2008). Progranulin functions as a neurotrophic factor to regulate neurite outgrowth and enhance neuronal survival. *J. Cell Biol.* 181, 37–41. doi: 10.1083/jcb.200712039

Van Deerlin, V. M., Leverenz, J. B., Bekris, L. M., Bird, T. D., Yuan, W., Elman, L. B., et al. (2008). TARDBP mutations in amyotrophic lateral sclerosis with TDP-43 neuropathology: a genetic and histopathological analysis. *Lancet Neurol.* 7, 409–416. doi: 10.1016/S1474-4422(08)70071-1

Van der Zee, J., Gijselinck, I., Dillen, L., Van Langenhove, T., Theuns, J., Engelborghs, S., et al. (2013). A pan-European study of the C9orf72 repeat associated with FTLD: geographic prevalence, genomic instability, and intermediate repeats. *Hum. Mutat.* 34, 363–373. doi: 10.1002/humu.22244

Van der Zee, J., Rademakers, R., Engelborghs, S., Gijselinck, I., Bogaerts, V., Vandenberghe, R., et al. (2006). A Belgian ancestral haplotype harbours a highly prevalent mutation for 17q21-linked tau-negative FTLD. *Brain* 129(Pt 4), 841–852. doi: 10.1093/brain/awl029

Van der Zee, J., Le Ber, I., Maurer-Stroh, S., Engelborghs, S., Gijselinck, I., Camuzat, A., et al. (2007). Mutations other than null mutations producing a pathogenic loss of progranulin in frontotemporal dementia. *Hum. Mutat.* 28, 416. doi: 10.1002/humu.9484

Van der Zee, J., Urwin, H., Engelborghs, S., Bruyland, M., Vandenberghe, R., Dermaut, B., et al. (2008). CHMP2B C-truncating mutations in frontotemporal lobar degeneration are associated with an aberrant endosomal phenotype *in vitro*. *Hum. Mol. Genet.* 17, 313–322. doi: 10.1093/hmg/ddm309

Van der Zee, J., Van Langenhove, T., Kovacs, G. G., Dillen, L., Deschamps, W., Engelborghs, S., et al. (2014). Rare mutations in SQSTM1 modify susceptibility to frontotemporal lobar degeneration. *Acta Neuropathol.* 128, 397–410. doi: 10.1007/s00401-014-1298-7

Van Langenhove, T., van der Zee, J., Sleegers, K., Engelborghs, S., Vandenberghe, R., Gijselinck, I., et al. (2010). Genetic contribution of FUS to frontotemporal lobar degeneration. *Neurology* 74, 366–371. doi: 10.1212/WNL.0b013e3181ccc732

Vesa, J., Su, H., Watts, G. D., Krause, S., Walter, M. C., Martin, B., et al. (2009). Valosin containing protein associated inclusion body myopathy: abnormal vacuolization, autophagy and cell fusion in myoblasts. *Neuromuscul. Disord.* 19, 766–772. doi: 10.1016/j.nmd.2009.08.003

Wahid, F., Shehzad, A., Khan, T., and Kim, Y. Y. (2010). MicroRNAs: synthesis, mechanism, function, and recent clinical trials. *Biochim. Biophys. Acta* 1803, 1231–1243. doi: 10.1016/j.bbamcr.2010.06.013

Wang, H.-Y., Wang, I.-F., Bose, J., and Shen, C.-K. J. (2004a). Structural diversity and functional implications of the eukaryotic TDP gene family. *Genomics* 83, 130–139. doi: 10.1016/S0888-7543(03)00214-3

Wang, Q., Song, C., and Li, C.-C. H. (2004b). Molecular perspectives on p97-VCP: progress in understanding its structure and diverse biological functions. *J. Struct. Biol.* 146, 44–57. doi: 10.1016/j.jsb.2003.11.014

Wang, T., Jiang, X., Chen, G., and Xu, J. (2015). Interaction of amyotrophic lateral sclerosis/frontotemporal lobar degeneration-associated fused-in-sarcoma with proteins involved in metabolic and protein degradation pathways. *Neurobiol. Aging* 36, 527–535. doi: 10.1016/j.neurobiolaging.2014.07.044

Wang, W. X., Rajeev, B. W., Stromberg, A. J., Ren, N., Tang, G., Huang, Q., et al. (2008b). The expression of microRNA miR-107 decreases arly in Alzheimer's disease and may accelerate disease progression through regulation of beta-site amyloid precursor protein-cleaving enzyme 1. *J. Neurosci.* 28, 1213–1223. doi: 10.1523/JNEUROSCI.5065-07.2008

Wang, W.-X., Wilfred, B. R., Madathil, S. K., Tang, G., Hu, Y., Dimayuga, J., et al. (2010). miR-107 regulates granulin/progranulin with implications for traumatic brain injury and neurodegenerative disease. *Am. J. Pathol.* 177, 334–345. doi: 10.2353/ajpath.2010.091202

Wang, X., Arai, S., Song, X., Reichart, D., Du, K., Pascual, G., et al. (2008a). Induced ncRNAs allosterically modify RNA-binding proteins in cis to inhibit transcription. *Nature* 454, 126–130. doi: 10.1038/nature06992

Wang, Y. T., Kuo, P. H., Chiang, C. H., Liang, J. R., Chen, Y. R., Wang, S., et al. (2013). The Truncated C-terminal RNA recognition motif of TDP-43 protein plays a key role in forming proteinaceous aggregates. *J. Biol. Chem.* 288, 9049–9057. doi: 10.1074/jbc.M112.438564

Watts, G. D. J., Thomasova, D., Ramdeen, S. K., Fulchiero, E. C., Mehta, S. G., Drachman, D. A., et al. (2007). Novel VCP mutations in inclusion body myopathy associated with Paget disease of bone and frontotemporal dementia. *Clin. Genet.* 72, 420–426. doi: 10.1111/j.1399-0004.2007.00887.x

Watts, G. D. J., Wymer, J., Kovach, M. J., Mehta, S. G., Mumm, S., Darvish, D., et al. (2004). Inclusion body myopathy associated with Paget disease of bone and frontotemporal dementia is caused by mutant valosin-containing protein. *Nat. Genet.* 36, 377–381. doi: 10.1038/ng1332

Wegorzewska, I., Bell, S., Cairns, N. J., Miller, T. M., and Baloh, R. H. (2009). TDP-43 mutant transgenic mice develop features of ALS and frontotemporal

lobar degeneration. *Proc. Natl. Acad. Sci. U.S.A.* 106, 18809–18814. doi: 10.1073/pnas.0908767106

Weihl, C. C., Dalal, S., Pestronk, A., and Hanson, P. I. (2006). Inclusion body myopathy-associated mutations in p97/VCP impair endoplasmic reticulum-associated degradation. *Hum. Mol. Genet.* 15, 189–199. doi: 10.1093/hmg/ddi426

Weihl, C. C., Miller, S. E., Hanson, P. I., and Pestronk, A. (2007). Transgenic expression of inclusion body myopathy associated mutant p97/VCP causes weakness and ubiquitinated protein inclusions in mice. *Hum. Mol. Genet.* 16, 919–928. doi: 10.1093/hmg/ddm037

Whitley, P., Reaves, B. J., Hashimoto, M., Riley, A. M., Potter, B. V. L., and Holman, G. D. (2003). Identification of mammalian Vps24p as an effector of phosphatidylinositol 3,5-bisphosphate-dependent endosome compartmentalization. *J. Biol. Chem.* 278, 38786–38795. doi: 10.1074/jbc.M306864200

Wilhelm, B. T., Marguerat, S., Watt, S., Schubert, F., Wood, V., Goodhead, I., et al. (2008). Dynamic repertoire of a eukaryotic transcriptome surveyed at single-nucleotide resolution. *Nature* 453, 1239–1243. doi: 10.1038/nature07002

Wils, H., Kleinberger, G., Janssens, J., Pereson, S., Joris, G., Cuijt, I., et al. (2010). TDP-43 transgenic mice develop spastic paralysis and neuronal inclusions characteristic of ALS and frontotemporal lobar degeneration. *Proc. Natl. Acad. Sci. U.S.A.* 107, 3858–3863. doi: 10.1073/pnas.0912417107

Wolfe, M. S. (2012). The role of tau in neurodegenerative diseases and its potential as a therapeutic target. *Scientifica* 2012:796024. doi: 10.6064/2012/796024

Woodman, P. G. (2003). P97, a protein coping with multiple identities. *J. Cell Sci.* 116(Pt 21), 4283–4290. doi: 10.1242/jcs.00817

Wszolek, Z. K., Pfeiffer, R. F., Bhatt, M. H., Schelper, R. L., Cordes, M., Snow, B. J., et al. (1992). Rapidly progressive autosomal dominant parkinsonism and dementia with pallido-ponto-nigral degeneration. *Ann. Neurol.* 32, 312–320. doi: 10.1002/ana.410320303

Wu, H., Huang, M., Lu, M., Zhu, W., Shu, Y., Cao, P., et al. (2013a). Regulation of microtubule-associated protein tau (MAPT) by miR-34c-5p determines the chemosensitivity of gastric cancer to paclitaxel. *Cancer Chemother. Pharmacol.* 71, 1159–1171. doi: 10.1007/s00280-013-2108-y

Wu, P., Zuo, X., Deng, H., Liu, X., Liu, L., and Ji, A. (2013b). Roles of long noncoding RNAs in brain development, functional diversification and neurodegenerative diseases. *Brain Res. Bull.* 97, 69–80. doi: 10.1016/j.brainresbull.2013.06.001

Xiao, S., Sanelli, T., Dib, S., Sheps, D., Findlater, J., Bilbao, J., et al. (2011). RNA targets of TDP-43 identified by UV-CLIP are deregulated in ALS. *Mol. Cell. Neurosci.* 47, 167–180. doi: 10.1016/j.mcn.2011.02.013

Xu, Y. F., Gendron, T. F., Zhang, Y. J., Lin, W. L., D'Alton, S., Sheng, H., et al. (2010a). Wild-type human TDP-43 expression causes TDP-43 phosphorylation, mitochondrial aggregation, motor deficits, and early mortality in transgenic mice. *J. Neurosci.* 30, 10851–10859. doi: 10.1523/JNEUROSCI.1630-10.2010

Xu, Y., Suzuki, Y., Ito, K., and Komiyama, M. (2010b). Telomeric repeat-containing RNA structure in living cells. *Proc. Natl. Acad. Sci. U.S.A.* 107, 14579–14584. doi: 10.1073/pnas.1001177107

Xu, Z., Poidevin, M., Li, X., and Li, Y. (2013). Expanded GGGGCC repeat RNA associated with amyotrophic lateral sclerosis and frontotemporal dementia causes neurodegeneration. *Proc. Natl. Acad. Sci. U.S.A.* 110, 7778–7783. doi: 10.1073/pnas.1219643110

Yamada, S., Inoue, Y., Suga, A., and Iwazaki, M. (2011). Surgical risk of vessel injury: an unusual anatomical variant of the right medial basal segmental pulmonary artery. *Gen. Thorac. Cardiovasc. Surg.* 59, 301–303. doi: 10.1007/s11748-010-0655-2

Yan, J., Deng, H.-X., Siddique, N., Fecto, F., Chen, W., Yang, Y., et al. (2010). Frameshift and novel mutations in FUS in familial amyotrophic lateral sclerosis and ALS/dementia. *Neurology* 75, 807–814. doi: 10.1212/WNL.0b013e3181f07e0c

Yang, L., Embree, L. J., Tsai, S., and Hickstein, D. D. (1998). Oncoprotein TLS interacts with serine-arginine proteins involved in RNA splicing. *J. Biol. Chem.* 273, 27761–27764. doi: 10.1074/jbc.273.43.27761

Yin, F., Banerjee, R., Thomas, B., Zhou, P., Qian, L., Jia, T., et al. (2010). Exaggerated inflammation, impaired host defense, and neuropathology in progranulin-deficient mice. *J. Exp. Med.* 207, 117–128. doi: 10.1084/jem.20091568

Zarranz, J. J., Ferrer, I., Lezcano, E., Forcadas, M. I., Eizaguirre, B., Atares, B., et al. (2005). A novel mutation (K317M) in the MAPT gene causes FTDP and motor neuron disease. *Neurology* 64, 1578–1585. doi: 10.1212/01.WNL.0000160116.65034.12

Zhang, H., Wang, Q., and Kajino Kiichi, G. M. I. (2000). VCP, a weak ATPase involved in multiple cellular events, interacts physically with BRCA1 in the nucleus of living cells. *DNA Cell Biol.* 19, 253–263. doi: 10.1089/10445490050021168

Zhang, Y.-J., Xu, Y., Dickey, C. A., Buratti, E., Baralle, F., Bailey, R., et al. (2007). Progranulin mediates caspase-dependent cleavage of TAR DNA binding protein-43. *J. Neurosci.* 27, 10530–10534. doi: 10.1523/JNEUROSCI.3421-07.2007

Zheng, M., Liao, M., Cui, T., Tian, H., Fan, D. S., and Wan, Q. (2012). Regulation of nuclear TDP-43 by NR2A-containing NMDA receptors and PTEN. *J. Cell Sci.* 125(Pt 6), 1556–1567. doi: 10.1242/jcs.095729

Zhu, J., Nathan, C., Jin, W., Sim, D., Ashcroft, G. S., Wahl, S. M., et al. (2002). Conversion of proepithelin to epithelins: roles of SLPI and elastase in host defense and wound repair. *Cell* 111, 867–878. doi: 10.1016/S0092-8674(02)01141-8

Zinszner, H., Sok, J., Immanuel, D., Yin, Y., and Ron, D. (1997). TLS (FUS) binds RNA in vivo and engages in nucleo-cytoplasmic shuttling. *J. Cell Sci.* 110(Pt 1), 1741–1750.

Zovoilis, A., Agbemenyah, H. Y., Agis-Balboa, R. C., Stilling, R. M., Edbauer, D., Rao, P., et al. (2011). microRNA-34c is a novel target to treat dementias. *EMBO J.* 30, 4299–4308. doi: 10.1038/emboj.2011.327

Zu, T., Liu, Y., and Bañez-Coronel, M. (2013). RAN proteins and RNA foci from antisense transcripts in C9ORF72 ALS and frontotemporal dementia. *Proc. Natl. Acad. Sci. U.S.A.* 110, E4968–E4977. doi: 10.1073/pnas.1315438110

Description of the industrial invention with title:

"RNA interference mediated therapy for neurodegenerative diseases"

Of: Università degli Studi di Trento, Italian nationality, Via Belenzani 12 - 38122 Trento, Italia

Designated Inventors: Kavitha Siva, Giuseppina Covello, Michela Alessandra Denti

Filed on: March 25, 2015

* * *

TEXT OF THE DESCRIPTION

FIELD OF THE INVENTION

The present invention concerns RNA interference mediated therapy for neurodegenerative diseases associated with abnormalities of microtubule-associated protein tau.

BACKGROUND OF THE INVENTION

Modulation of gene expression by endogenous, non-coding RNAs have been increasingly appreciated and known to play a role in eukaryotic development, and epigenetic control. Recently, methods have been developed to trigger RNA interference (RNAi) against specific targets in mammalian cells by introducing exogenously produced or intra-cellularly expressed small interfering RNA (siRNA) molecules.

These quick, inexpensive and effective methods have proven to be effective for knockdown experiments in vitro and in vivo. The ability to attain such selective gene silencing has led to the hypothesis that siRNAs can be used to suppress gene expression for therapeutic benefit. The

ideal candidates for such an siRNA approach would be dominantly inherited diseases.

Recent studies by Miller V et al[1] have shown that siRNAs can be used to target untreatable neurodegenerative diseases such as polyglutamine (polyQ) neurodegeneration in Machado-Joseph disease, spinocerebellar ataxia type 3 (MJDSCA3) and Frontotemporal dementia with parkinsonism linked to chromosome 17 (FTDP-17). These studies have focused exclusively on selective silencing of the transcript produced by the mutant allele[1]. RNA interference has proven to be an efficient strategy for silencing mutant tau allele V337M, however, selective depletion of mutant allele was not completely achieved in the study because there was a partial depletion of the wild type allele of tau[1]. More recently, another example of MAPT-targeting siRNAs was described[2], wherein a mix of four siRNAs aimed at suppressing all tau isoforms in a mouse model of tauopathy was tested.

The MAPT (Microtubule associated protein tau) gene consists of 16 exons and its expression is regulated by complex alternative splicing. This results in the production of two types of alternatively spliced transcripts: one bearing Exon 10, also known as 4R (Four microtubule repeats) isoform and the other that lacks Exon 10 is called 3R isoform (Three microtubule repeats). Equal levels of these two isoforms are expressed in normal human adult brain. Though several mutations causing FTDP-17 are known in MAPT, a half of these affect alternative splicing of Exon 10. These include mis-sense mutations, silent mutations and point mutations which are located in Exon 10, introns 9 and 10. They are known to implicate an increase in Exon 10 causing an excessive accumulation of 4R. This

leads to the formation of neurofibrillary tangles, hence resulting in neurodegeneration.

It is worth mentioning that abnormalities of tau are linked to the pathogenesis of neurodegenerative disease collectively termed as "tauopathies", and significantly elevated levels of tau are present in AD (Alzhiemer's disease) brains.

A few approaches have been used for the correction of Exon 10 inclusion in FTDP-17:

- Small molecules: a screening has been performed which yielded cardiotonic steroids as exon 10 splicing modulator, albeit non-specific, drugs[3], and

- Antisense oligonucleotides for exon skipping: US-A-2003/0170704 by Stamm et al. relates to substances which are capable of controlling the inclusion of MAPT exon 10 (proteic splicing regulators or their cDNA, polypeptides controlling the phosphorylation of splicing regulators, or their cDNA, and antisense oligonucleotides which interact with the splice junctions of MAPT exon 10). Moreover, work by Kalbfuss et al.[4] has demonstrated that oligoribonucleotides binding to Exon 10 splicing junctions could suppress the predominant inclusion of Exon 10 in tau mRNA in the context of rat PC12 cells. However, recent work by Sud R et al[5] showed that targeting Exon 10 with antisense morpholino oligonucleotides did not yield exon-skipping in neuroblastoma cell lines. These authors claim that splicing regulation of exon 10 in cells expressing predominantly 4R isoform may vary from the neuroblastoma cell line in which the 3R isoform dominates.

- Trans-splicing of exon 10: RNA reprogramming using spliceosome-mediated RNA trans-splicing (SMaRT) was used to correct aberrant Exon 10 splicing resulting from FTDP-17

mutations in a minigene system in cells in culture[6]. This approach, however, is affected by low efficiency.

OBJECT AND SUMMARY OF THE INVENTION

The object of the present invention is to provide a therapeutic agent effective in the treatment of neurodegenerative diseases associated with abnormalities of MAPT gene encoded protein tau.

According to the invention, the above object is achieved thanks to the method specified in the ensuing claims, which are understood as forming an integral part of the present description.

In an embodiment, the instant disclosure discloses a therapeutic agent for use in the treatment of neurodegenerative diseases associated with abnormalities of MAPT gene encoded protein tau, wherein said therapeutic agent comprises one or more siRNA targeting MAPT gene exon 10 sequence (SEQ ID No.:1).

In a further embodiment, the instant disclosure provides for a method for the treatment of neurodegenerative diseases associated with abnormalities of MAPT gene encoded protein tau comprising administering to a patient who needs it of one or more siRNA, wherein the one or more siRNA comprise a sense strand comprising at least 19 continuous bases of mRNA corresponding to the MAPT exon 10 sequence of SEQ ID No.: 1 and an antisense strand comprising a sequence complementary thereto in an amount sufficient to make said treatment, wherein the one or more siRNA induce selective degradation of exon 10-containing MAPT transcripts.

In a still further embodiment, the instant disclosure

concerns a pharmaceutical composition comprising one or more siRNA, wherein the one or more siRNA comprise a sense strand comprising at least 19 continuous bases of mRNA corresponding to the MAPT exon 10 sequence of SEQ ID No.: 1 and an antisense strand comprising a sequence complementary thereto and a pharmaceutically acceptable carrier.

BRIEF DESCRIPTION OF THE DRAWINGS

The invention will now be described, by way of example only, with reference to the enclosed figures of drawing, wherein:

- **Figure 1. Semi-quantitative RT-PCR analysis of levels of exon 10 in SH-SY5Y cells transfected with wild type and N279 mutant plasmid.** The gel electrophoresis shows the RT-PCR products of transcripts of the minigenes, containing exon 10 (E10+, 290 bp) and without exon 10 (E10-, 210 bp). Histogram represents the densitometric units of each treatment condition normalised on ß actin. Values represent mean SD± (n=3).

- **Figure 2. Representative images of SH-SY5Y cell line transfected with 0.25 µg of either wild type plasmid or mutant plasmid.** A) Wild type and B) Mutant N279 reporter plasmids.

- **Figure 3. Setting up of threshold values based on intensities of RFP and GFP.** Scatter plots representing Green/Red (G/R) values of each cell in a particular well bearing one of the dual reporter plasmids (WT and Mut, respectively). The indicated thresholds are arbitrarily selected to classify the cell population in three different classes.

- **Figure 4. Image based analysis of SHYS5Y cells**

transfected with Wild type and Mutant reporter plasmids.
Histogram represents the selected read-outs of the
quantitative analysis of the two reporters, such as the
relative percentages of the three sub-populations of SHYS5Y
cells classified by intensity properties, the transfection
efficiency and the cell viability. Values represent
mean±SD (n=3)

- **Figure 5. Human tau E10 sequences (capitals) and
flanking I9 and I10 sequences (lower case).** The 5' and 3'
splice sites are denoted by 5'ss and 3'ss, respectively.
Only FTDP-17 mutations affecting E10 splicing are
indicated. Deletions are denoted by shaded triangles. The
sequences and target position of the three designed siRNAs
are indicated.

- **Figure 6. An image based screening assay has been
performed for the different siRNAs and compared to the
values obtained with a control siRNA.** siRNAs were
cotransfected in SH-SY5Y cells together with 0.25 µg of
mutant reporter minigene plasmid. The values represent mean
±SD (n=3)

- **Figure 7. An image based screening assay has been
performed for the different siRNAs and compared to the
values obtained with a control siRNA.** siRNAs were
cotransfected in SH-SY5Y cells together with 0.5 µg of
mutant reporter minigene plasmid. The values represent mean
±SD (n=3).

- **Figure 8. Semi-quantitative RT-PCR analysis of SH-
SY5Y cells transfected with the minigene reporter plasmid
and siRNA A.**

- **Figure 9. Semi-quantitative RT-PCR analysis of SH-
SY5Y cells transfected with the minigene reporter plasmid
and siRNA B.**

- Figure 10. Semi-quantitative RT-PCR analysis of SH-SY5Y cells transfected with the minigene reporter plasmid and siRNA C.

- Figure 11. Semi-quantitative RT-PCR of NSC34 cells transfected with three siRNAs or a control siRNA.

- Figure 12. PFLARE 5A MAPT Exon 10 nucleotide sequence.

- Figure 13. PFLARE 5A MAPT MUT Exon 10 nucleotide sequence.

DETAILED DESCRIPTION OF THE INVENTION

The invention will now be described in detail, by way of non limiting example, with reference to an RNA interference mediated therapy making use of a cell model recapitulating the Frontotemporal dementia with parkinsonism linked to chromosome 17 (FTDP-17) disease conditions. Nevertheless, the RNA interference mediated therapy herein disclosed can be used for the treatment of other neurodegenerative diseases associated with abnormalities in MAPT gene encoded protein tau, like for example Alzheimer's disease, Huntington's disease, type 1 myotonic dystrophy, and Parkinson's disease.

In the following description, numerous specific details are given to provide a thorough understanding of embodiments. The embodiments can be practiced without one or more of the specific details, or with other methods, components, materials, etc. In other instances, well-known structures, materials, or operations are not shown or described in detail to avoid obscuring aspects of the embodiments.

Reference throughout this specification to "one

embodiment" or "an embodiment" means that a particular feature, structure, or characteristic described in connection with the embodiment is included in at least one embodiment. Thus, the appearances of the phrases "in one embodiment" or "in an embodiment" in various places throughout this specification are not necessarily all referring to the same embodiment. Furthermore, the particular features, structures, or characteristics may be combined in any suitable manner in one or more embodiments.

The headings provided herein are for convenience only and do not interpret the scope or meaning of the embodiments.

The present description concerns a therapeutic agent for use in the treatment of neurodegenerative diseases associated with abnormalities of MAPT gene encoded protein tau, wherein said therapeutic agent comprises one or more siRNAs targeting MAPT gene exon 10. Preferably, the therapeutic agent comprise a sense strand comprising at least 19 continuous bases of mRNA corresponding to the MAPT exon 10 sequence of SEQ ID No.: 1 and an antisense strand comprising a sequence complementary thereto.

In a further embodiment, the present description provides for use in the treatment of neurodegenerative diseases associated with abnormalities of MAPT gene encoded protein tau one or more siRNAs targeting MAPT gene exon 10, wherein the one or more siRNAs comprise a sense strand of 19-29 continuous bases of mRNA corresponding to the MAPT exon 10 sequence set forth in SEQ ID No.: 1 and an antisense strand comprising a sequence complementary thereto.

In a preferred embodiment, the present description concerns one or more siRNAs targeting MAPT gene exon 10

useful in the treatment of neurodegenerative diseases associated with abnormalities of MAPT gene encoded protein tau, wherein the one or more siRNAs are selected from i) a double strand RNA composed of a sense strand comprising a base sequence set forth in SEQ ID No.: 2, 4, 6, and an antisense strand comprising a sequence complementary thereto, which optionally has an overhang at the terminal of the sense strand and/or antisense strand, and ii) a double strand RNA composed of a sense strand comprising a base sequence wherein one to several bases have been added to and/or deleted from the 5' terminal and/or 3' terminal of the base sequence described in any one of SEQ ID No.: 2, 4, 6, and an antisense strand comprising a sequence complementary thereto, which optionally has an overhang at the terminal of the sense strand and/or antisense strand.

In a still further preferred embodiment, the instant description provides for one or more siRNAs targeting MAPT gene exon 10 able to induce selective degradation of exon 10-containing MAPT transcripts.

The neurodegenerative diseases associated with abnormalities of MAPT gene encoded protein tau that can benefit from the administration of one or more siRNAs targeting MAPT gene exon 10 are selected from Alzheimer disease, Huntington disease, type 1 myotonic dystrophy, Parkinson disease, frontotemporal dementia with parkinsonism linked to chromosome 17 (FTDP-17).

In a different embodiment, the description provides for a method of treatment of a neurodegenerative disease associated with abnormalities of MAPT gene encoded protein tau comprising administering to a patient who needs it of one or more siRNAs targeting MAPT gene exon 10, wherein the one or more siRNAs comprise a sense strand comprising at

least 19 continuous bases of mRNA corresponding to the MAPT exon 10 sequence of SEQ ID No.: 1 and an antisense strand comprising a sequence complementary thereto in an amount sufficient to make said treatment, wherein the one or more siRNA induce selective degradation of exon 10-containing MAPT transcripts.

In a still further embodiment, the present description concerns a pharmaceutical composition comprising one or more siRNAs targeting MAPT gene exon 10, wherein the one or more siRNAs comprise a sense strand comprising at least 19 continuous bases of mRNA corresponding to the MAPT exon 10 sequence of SEQ ID No.: 1 and an antisense strand comprising a sequence complementary thereto and a pharmaceutically acceptable carrier.

The present disclosure shows the feasibility of an siRNA-based gene therapy to enable post-transcriptional gene silencing of Exon 10-containing MAPT transcripts in FTDP-17. A panel of siRNAs targeting tau mRNA containing Exon 10 have been designed, and tested in SH-SY5Y cells on a mutant minigene reporter plasmid in the context of N279 missense mutation (AAT to AAG) recapitulating FTDP-17 disease condition. Moreover, the 3 siRNAs were tested on NSC34 cells (a motor neuron-like cell line)[1] to validate the effects on endogenous condition with a predominant inclusion of Exon 10 (80%).

The effect of the siRNAs has been assayed using a high content imaging system. The results obtained through the screening assay have been further validated using an RT-PCR analysis. The effect on the endogenous Exon 10-containing MAPT transcripts has been tested using RT-PCR analysis.

In the instant description the Inventors designed a new approach for the restoration of a normal 4Rtau/3Rtau

ratio, based on the use of siRNAs targeting MAPT exon 10 and inducing the selective degradation of the exon 10-containing MAPT transcripts. These siRNAs provide therapeutic benefit for FTDP-17 patients bearing mutations in MAPT exon 10 causing exon 10 inclusion, as the target sequences are not affected by the mutations.

The three siRNAs herein evaluated have the following nucleotide sequences:

siRNA A':

sense strand: 5'AGUCCAAGUGUGGCUCAAA3' – SEQ ID No.:2,

antisense strand: 5'UUUGAGCCACACUUGGACU3' – SEQ ID No.: 3;

siRNA B':

sense strand: 5'GGCUCAAAGGAUAAUAUCA3' – SEQ ID No.: 4,

antisense strand: 5'UGAUAUUAUCCUUUGAGCC3' – SEQ ID No.: 5;

siRNA C':

sense strand: 5'GCAACGUCCAGUCCAAGUG3' – SEQ ID No.: 6,

antisense strand: 5'CACUUGGACUGGACGUUGC3' – SEQ ID No.: 7.

Out of the 3 tested siRNAs (A, B and C), siRNA B shows maximum efficiency in transcript degradation. These results have been validated using a minigene recapitulating splicing mutation N279, and a similar effect is exhibited on NSC34[7,8] (a hybrid of mouse spinal cord motor neurons and neuroblastoma cell line) cells.

A recent review by Rettig and colleagues[9] has summarized the possible delivery approaches of the siRNA molecules and their success in clinical trials. The current development in the field and ongoing studies establishes the significance of these synthetic siRNAs, which may serve as potential therapeutics upon suitable delivery and administration.

Direct CNS (Central nervous system) administration is used as a method of choice in neurodegenerative diseases

due to restricted entry across the blood brain barrier. Options of delivery include intrathecal, intraventricular, epidural and direct intratissue injection. Administration methods include long term infusions or through the use of mini pumps.

Chronic intraventricular pumps were used for the delivery of siRNAs against Amyloid precursor protein gene (App) to study Alzheimers related functions in adult mice. Efficient knockdowns were observed through potent siRNAs[10].

By employing naked and unassisted delivery of siRNAs in buffered saline, chronic infusion was performed in non-human primates to suppress levels of α synucein[11]. This protein is known to be associated with Parkinson's disease. Mini osmotic pumps were used for the direct infusion into the substantia nigra leading to a decrease in α synucein both at mRNA and protein levels.

siRNAs with modified PS linkages and 2'F-pyrimidine residues near the ends of each strand[12] were used for chronic infusion in to the CNS of SOD1(G93A) mouse model of amyotrophic lateral sclerosis (ALS). Significant reduction of SOD1 mRNA was observed in the spinal cord. In the transgenic mouse model, an infusion over a 28 day period led to alleviated the progression of disease. The siRNAs were stable over the course of this period.

Cholestrol conjugated siRNAs[13] were used for the direct intrastriatal injection to target mutant Huntington gene (Htt) in the context of Huntington's disease.

The above mentioned strategies highlight the different modes of delivery of siRNAs and demonstrate efficacy in vivo.

Materials and methods

siRNAs

The following siRNAs – employed in the present experiments - were designed along the stretch of Exon 10 (SEQ ID No.: 1), and produced by Eurofin Genomics, Ebersberg, Germany.

siRNA A:

sense strand: 5'AGUCCAAGUGUGGCUCAAAdTdT3' – SEQ ID No.:19, antisense strand: 5'UUUGAGCCACACUUGGACUdTdT3' – SEQ ID No.:20;

siRNA B:

sense strand: 5'GGCUCAAAGGAUAAUAUCAdTdT3' – SEQ ID No.:21, antisense strand: 5'UGAUAUUAUCCUUUGAGCCdTdT3' – SEQ ID No.:22;

siRNA C:

sense strand: 5'GCAACGUCCAGUCCAAGUGdTdT3' – SEQ ID No.:23, antisense strand: 5'CACUUGGACUGGACGUUGCdTdT3' – SEQ ID No.:24;

control siRNA:

sense strand: 5' UAAUGUAUUGGAACGCAUAdTdT3' – SEQ ID No.:8, antisense strand: 5'UAUGCGUUCCAAUACAUUAdTdT3' – SEQ ID No.:9.

The above siRNAs sequences differ from the SEQ ID NO.: 2 to 7 for the presence of an overhang consisting of two monophosphate deoxyribosylthymine (dT), which were introduced in SEQ ID No.: 2 to 7 at the 3' terminal in order to increase siRNA intracellular stability and efficiency thereof.

Figure 5 shows human tau E10 sequence (capitals – corresponding to SEQ ID No.: 1) and flanking I9 and I10 sequences (lower case); the human tau E10 sequence comprising flanking I9 (11 bases) and I10 (26 bases) sequences is provided in SEQ ID No.: 18. The 5' and 3' splice sites are denoted by 5'ss and 3'ss, respectively.

Only FTDP-17 mutations affecting Exon 10 splicing are indicated. Deletions are denoted by shaded triangles. The sequences and target position of the three designed siRNAs A, B and C are provided.

SHYS5Y cell line

The SH-SY5Y cell line (ATCC-LGC standards, Teddington, UK; #CRL-2266) used for transfection experiments is a thrice cloned (SK-N-SH -> SH-SY -> SH-SY5 -> SH-SY5Y) subline of the neuroblastoma cell line SK-N-SH with a content of 15% Exon 10+ and 85% of Exon 10- in its transcript. The transfection efficiency (25% to 30%) in this cell line is comparitively higher than the other neuroblastoma cell lines. Therefore, this cell line was chosen to test the efficacy of siRNAs against endogenous Exon 10+ transcripts and for co-transfections of siRNAs with minigene reporter plasmids.

NSC-34 cell line

Mouse Motor neuron like hybrid cell line NSC-34 (Cellutions biosystems, Burlington, Ontario, Canada; # CLU140-A) was produced by fusion of motor neuron enriched, embryonic mouse spinal cord cells with mouse neuroblastoma[7,8]. The cultures contain two populations of cells: small, undifferentiated cells that have the capacity to undergo cell division and larger, multi-nucleate cells. These cells express many properties of motor neurons, including choline acetyltransferase, acetylcholine synthesis, storage and release and neurofilament triplet proteins. These cells can be differentiated using the all trans retinoic acid (atRA) thus establishing itself as a suitable model for the in vitro study of pathophysiology in

motor neurons.

Mutagenesis of fluorescent reporter with Exon 10

The fluorescent reporter plasmid created by Peter Stoilov and colleagues[3], PFLARE 5A MAPT Exon 10 also referred to as the wild-type (WT) plasmid (SEQ ID No.: 10 – Figure 12), was mutated using the Quick change II site XL site-directed mutagenesis kit (Agilent Technologies, Santa Clara, CA, USA; #200521) following the manufacturer's instructions. The following primers were designed such that they incorporated the nucleotide change of T to G.

Forward primer:
5'CCAAAGGTGCAGATAATTAAGAAG3' – SEQ ID No.: 11

Reverse primer:
5'GTTGCTAAGATCCAGCTTCTTCTT3' – SEQ ID No.: 12

The resulting plasmid PFLARE 5A MAPT MUT Exon 10 (SEQ ID No.: 13 – Figure 13) will be referred to as mutant N279 (Mut) plasmid.

Treatment of siRNA on Endogenous condition

1.Transfection of SHYS5Y cells and NSC-34 cells with siRNAs

The transfection of SHYS5Y cells and NSC34 cells with siRNAs were performed using the Lipofectamine 3000 lipid based transfection reagent (Life Technologies-Invitrogen, Monza, Italy; #L3000-008).

1.1. Preparation of cells

1.1.1) On the day before the experiment, 5×10^4 cells were seeded on a 24 well plate in 500 µl of complete medium without antibiotics at 37° C in 5% CO_2.

1.2. Transfection of siRNAs

1.2.1) Transfections were performed as instructed by

the manufacturer with 2 (μl) Lipofectamine 3000 for a range of siRNA concentration starting from 10 nM to 100 nM - in Opti-MEM medium without phenol red (Life Technologies-Gibco, Monza, Italy; #11058-021) - per well in a final volume of 500 μl.

1.2.2) As controls, cells were treated with Lipofectamine 3000 only (Mock) and transfected with Non-targeting siRNA (Non-specific controls – SEQ ID No.: 8 and 9).

1.2.3) Following transfection, the cells are incubated at 37° C in 5% CO_2 for 48 hours.

1.2.4) The wells were then washed with PBS(1X) and Trizol reagent (Life Technologies, Monza, Italy; #15596-026) was used for the extraction of RNA following manufacturer's instructions for downstream analyses.

2. Co-transfection of reporter plasmid and siRNAs in SHYS5Y cells

2.1. Preparation of cells

1.1) On the day before the experiment, 5 x 10^4 cells were seeded on a 24 well plate in 500 μl of complete medium (i.e. 1:1 mix of EMEM (Lonza #12-125F) and F12 NUTRIENT MIX (Life technologies-Gibco #1765-054) with 10% Fetal Bovine Serum (FBS)) without antibiotics at 37° C in 5% CO_2. The 24 well plate format has been chosen to allow the recovery of a sufficient number of cells at the end of the assay after the image-based analysis, in order to perform downstream molecular analysis, such as RT-PCR and Western Blot.

2.2 Lipid-based DNA and siRNA co-transfection

2.2.1) Transfections are performed as instructed by the manufacturer with a ratio of DNA (ng):Lipofectamine 3000 (μl) being 1:2 in Opti-MEM medium (GIBCO LIfetechnologies). The plasmids (SEQ ID No.: 10 and 13) are

16

used at a concentration of 0.25 µg and 0.5 µg per well in a final volume of 500 µl.

2.2.2) Two different plasmid reporters (SEQ ID No.: 10, 13) are used for transfection namely the wild-type (WT) plasmid (SEQ ID No.: 10) and the mutant type (Mut) plasmid (SEQ ID No.: 13).

2.2.3) siRNAs (SEQ ID No.: 19 to 24) are used at the concentrations from 10 nM to 100 nM in a final volume of 500 µl per well.

3. High-content image acquisition and analysis

Preparation of cells for image acquisition

3.1) Images of transfected cells were captured with a High content imaging system (Operetta, Perkin Elmer). 48 hours after transfection, the cells are incubated for 20 minutes at 37° C in the presence of 1 mg/ml of Hoechst 33342 fluorescent dye. This allows counter-staining the nuclei which will enable the subsequent analyses.

Image acquisition

3.2) Images were taken with a 20X LWD objective (Perkin Elmer #HH12940107), in combination with different filter sets: in particular a filter for Hoechst 3342 stain (excitation filter: 360-400 nm (Perkin Elmer #HH12000301); emission filter: 410-480 nm (Perkin Elmer #HH12000401)) is used to image the stained nuclei at 20 ms exposure time, whereas a combination of filters is used to measure the reporters' intensities: GFP (excitation filter: 460-490 nm (Perkin Elmer HH1200030); emission filter :500-550 nm (Perkin Elmer #HH12000405)) and RFP (excitation filter: 520-550 nm (Perkin Elmer #HH12000305); emission filter: 560-630 nm (Perkin Elmer #HH12000410)), both at 200 ms exposure time.

Image analysis

3.3) For the feature extraction protocol, cells were segmented and analyzed using the following workflow:

3.3.1) The first step is the identification of Nuclei, the primary objects of interest that are segmented by using the most suitable algorithm (phenoLOGIC™, PerkinElmer).

3.3.2) Assuming a homogeneous distribution of both GFP and RFP in the cells, the nuclear region was selected to quantify the mean fluorescence intensity in the two channels.

3.3.3) The sub-population of transfected cells was identified using a double-threshold strategy to filter out the cells being either positive for G(GFP) or for R(RFP) or for both.

3.3.4) Restricting the analysis to the transfected cells only, the ratio between the fluorescence properties G and R mean intensity is calculated on a per-cell basis. G/R is a parameter that indicates the prevalence of expression of one reporter over the other. Specifically, a low score indicates inclusion of the cassette exon, while a high one is connected with an efficient splicing of Exon 10.

3.3.5) An overview of the numerical properties of the cells can be visualized field by field in a scatter plot. Alternatively, to get a more complete representation of all the cells within a well, scatter plots or histograms of single cell properties can be created for representative wells of the WT and the Mut plasmid conditions. Such graphical representations allow a more accurate selection of an upper threshold J and a lower threshold K, distinguishing for cells preferentially expressing GFP (G/R>J), RFP (G/R<K) or equally expressing both the reporters (K<G/R<J) (Fig. 1). Harmony[R] high content imaging software (PerkinElmer) was employed.

3.4.6) The thresholds were then applied in a filter-based module to classify the cells in three different subpopulations. In synthesis, based on intensities emitted by the fluorescence signals, 3 read-outs were measured as a result of setting specific threshold values:cells expressing mainly GFP (G/R>J), cells expressing mainly RFP (G/R<K), cells equally expressing both the reporters (K<G/R<J).

3.4.7) Feature outputs include total cell count, transfected cells count and % calculated over the total number of cells, G/R median value of all the cells of the well, the % of cells preferentially expressing GFP (G/R>J), RFP (G/R<K) and equally expressing both the reporters (K<G/R<J).

3.4.8) Percentage of cell viability was calculated as follows: (total number of cells in transfected well/total number of cells in Mock)*100

4. RNA extractions and RT-PCR

4.1) The wells were washed with 1X PBS and RNA was extracted from each well using Trizol reagent following manufacturer's instructions.

4.2) The extracted RNA was treated with DNase by using Turbo DNAse kit (Life technologies-Ambion #AM1907) according to the manufacturer's instructions.

4.3) 500 ng of the extracted RNA was reverse transcribed to cDNA with Revert Aid First Strand cDNA synthesis Kit (Thermoscientific #K1622) by using oligo dT18 oligonucleotides (a synthetic single-stranded 18-mer oligonucleotide with 5'- and 3'-hydroxyl ends, available in the kit), following manufacturer's protocol.

4.4) The cDNA obtained serves as a template for semi quantitative RT-PCR reactions to evaluate the expression of

Exon 10 in these transcripts.

PCR CYCLE:

10 min	95°C
0:30 seconds	95°C
0:40 seconds	60°C
1 min	72°C
10 min	72°C
∞	4°C

4.4) The expression levels of Exon 10 containing transcripts are analyzed with the following primers:

Endogenous condition:

TAUR9F: 5'CTGAAGCACCACCAGCCGGGAGG3' – SEQ ID No.: 14,

TAU13R: 5'TGGTCTGTCTTGGCTTTGGC3' – SEQ ID No.: 15.

Plasmid reporters:

Exon 1 Bgl For: 5'AAACAGATCTACCATTGGTGCACCTGACTCC3' – SEQ ID No.: 16,

EGFP Rev: 5'CGTCGCCGTCCAGCTCGACCAG3' – SEQ ID No.: 17.

4.5) Amplified products are allowed to run with 100bp DNA ladder (Fermentas) on a 2% Agarose gel electrophoresis (5% Ethidium Bromide) at 100 volts in 1X TBE running buffer for 40 minutes.

4.6) Densitometric analyses are performed with Image J software (an open architecture system using Java plugin) after image acquisition with BioDoc-It imaging system (UPV, Upland, CA, USA).

Results

The siRNAs were tested for their efficacy on transfected reporter minigenes. Previous work by Stoilov P et al[3] has shown that the splicing of a two-color (Green/Red) fluorescent reporter plasmid with MAPT Exon 10 can be modulated using bioactive compounds. The reporter

plasmid (SEQ ID No.: 10) was produced such that exon 10 inclusion favors the production of RFP (Red fluorescent protein) and exon 10 exclusion produces GFP (Green fluorescent protein) (Fig. 1). The reporter plasmid created by Stoilov and colleagues and termed as wild type reporter (as it recapitulated the endogenous condition of exon 10 content in the majority of neuroblastoma cell lines) was used (Fig. 1). The plasmid was further mutated to incorporate the N279 mutation to alter splicing (AAT to AAG), recapitulating FTDP-17 disease condition (SEQ ID No.: 13). This base change creates a purine-rich stretch (AAGAAGAAG), and resembles an exon splice-enhancer consensus; this alters splicing leading to exon 10 inclusion and subsequent production of RFP (Fig. 1).

With the purpose of analyzing the effects of the siRNAs on the reporter minigenes, an image-based analysis to quantify the fluorescent reporters, obtaining single cell-based read-outs using an High Content Screening system, was developed by the present inventors. In brief, SH-SY5Y cell line was transfected with either wild type plasmid or mutant plasmid. The two plasmids ensure different percentages of exon 10 inclusion in the spliced transcript, which is evident from the difference in the number of red or green cells, and in their intensity (Fig. 2). The intensity of green and red fluorescence in the transfected cells was measured by an Operetta High Content Screening instrument, and the cells were grouped in three categories: red cells in which the majority of the transcript bears exon 10, green cells in which the majority of the transcript is devoid of exon 10, and yellow cells in which the proportion of the two splicing isoforms is around 1:1 (Fig. 3). By this analysis the point mutation in the

reporter minigene (SEQ ID No.: 13) was assessed to shift splicing of Exon 10 thus altering the fluorescent signals from a relatively low level of RFP (2%) to a very high level (65%) due to Exon 10 inclusion (Fig. 3 and Fig. 4). Transfection efficency was about 20% and cell viability about 60% (Fig. 4).

Three different exon 10-targeting siRNAs (SEQ ID Nos 19 to 24) spanning the exon 10 sequence have been designed on the basis of following rules: stretches of 4 or more bases (such as AAAA or CCCC), regions with GC content <30% or > 60%, repeats and low complexity sequences, single nucleotide polymorphism (SNP) sites were avoided; a BLAST homology search was performed to avoid off-target effects on other genes or sequences (Fig. 5).

The efficacy of the three designed siRNAs was tested at increasing concentrations upon their co-transfection with either 0.5 µg (Fig. 6) or 0.25 µg of the mutant reporter minigene (Fig. 7). In both experimental designs siRNA A (SEQ ID No.: 19 and 20), siRNA B (SEQ ID No.: 21 and 22) and siRNA C (SEQ ID No.: 23 and 24) were effective in reducing the exon 10-containing transcript. siRNA B (SEQ ID No.: 21 and 22) appeared to be the most efficient siRNA, decreasing the red cells from 60% to 15% and increasing the yellow cells from 40% to 80% (Fig. 7). Semi-quantitative RT-PCR analysis confirmed the reduction of Exon 10 upon treatment with siRNA A (SEQ ID No.: 19 and 20, Fig. 8), siRNA B (SEQ ID No.: 20 and 22, Fig. 9) and siRNA C (SEQ ID No.: 23 and 24, Fig. 10) reaching ~10%, 25% and 20% reduction, respectively, upon treatment with a 50 nM concentration.

The effect of siRNA A (SEQ ID No.: 19 and 20), siRNA B (SEQ ID No.: 20 and 22) and siRNA C (SEQ ID No.: 23 and 24)

on the endogenous MAPT transcript was tested upon their transfection in NSC34 cell line (Fig. 11). In NSC34 cells 83% of the endogenous MAPT transcript contains exon 10 and the remaining 17% is devoid of exon 10, thus serving as a suitable model for the study of effects of siRNA on Exon 10 containing transcripts in endogenous conditions (Fig. 11). RT-PCR analysis shows reduction of Exon 10+ endogenous transcripts upon treatment with siRNAs A (SEQ ID No.: 19 and 20)(6%), B (SEQ ID No.: 20 and 22)(28%) and C (SEQ ID No.: 23 and 24)(12%) at 50 nM concentration. In this model system, therefore, siRNA B appears the most effective siRNA in the selective degradation of exon 10-containing transcripts.

Naturally, while the principle of the invention remains the same, the details of construction and the embodiments may widely vary with respect to what has been described and illustrated purely by way of example, without departing from the scope of the present invention.

REFERENCES

1. Miller et al. Targeting Alzheimer's disease genes with RNA interference: an efficient strategy for silencing mutant alleles. *Nucl Acids Res* (2004) 32(2): 661-668

2. Xu et al. Tau Silencing by siRNA in the P301S Mouse model of Tauopathy. *Curr Gene Ther* (2014); 14(5):343-351.

3. Stoilov et al. A high-throughput screening strategy identifies cardiotonic steroids as alternative splicing modulators. *Proc Natl Acad Sci U S A* (2008) 105(32): 11218-23.

4. Kalbfuss et al. Correction of alternative splicing of tau in frontotemporal dementia and parkinsonism linked to chromosome 17. *J Biol Chem* (2001) 276: 42986-42993.

5.Sud et al. Antisense-mediated Exon Skipping Decreases Tau Protein Expression: A Potential Therapy For Tauopathies. *Mol Ther Nucleic Acids* (2014) Jul 29; 3: e180

6. Rodriguez-Martin et al. Correction of tau mis-splicing caused by FTDP-17 MAPT mutations by spliceosome-mediated RNA trans-splicing. *Hum Mol Genet* (2009) 18(17): 3266-73.

7. Cashman et al. Neuroblastoma x spinal cord (NSC) hybrid cell lines resemble developing motor neurons. *Dev Dyn* (1992); 194(3):209-21.

8. Maier et al. Differentiated NSC-34 motoneuron-like cells as experimental model for cholinergic neurodegeneration. *Neurochem Int* (2013) 62(8): 1029-38

9. Rettig GR, Behlke MA Progress toward in vivo use of siRNAs-II *Mol Ther.* (2012) Mar;20(3):483-512.

10. Senechal et al. (2007). Amyloid precursor protein knockdown by siRNA impairs spontaneous alternation in adult mice. *J Neurochem* 102: 1928-1940.

11. McCormack et al. (2010). Alpha-synuclein suppression by targeted small interfering RNA in the primate substantia nigra. *PLoS ONE* 5: e12122.

12. Wang et al. (2008). Therapeutic gene silencing delivered by a chemically modified small interfering RNA against mutant SOD1 slows amyotrophic lateral sclerosis progression. *J Biol Chem* 283: 15845-15852.

13. DiFiglia et al. Therapeutic silencing of mutant huntingtin with siRNA attenuates striatal and cortical neuropathology and behavioral deficits. *Proc Natl Acad Sci USA* (2007) 104: 17204-17209.

CLAIMS

1. Therapeutic agent for use in the treatment of neurodegenerative diseases associated with abnormalities of MAPT gene encoded protein tau, wherein said therapeutic agent comprises one or more siRNAs targeting MAPT gene exon 10.

2. Therapeutic agent for use according to claim 1, wherein the one or more siRNAs comprise a sense strand comprising at least 19 continuous bases of mRNA corresponding to the MAPT gene exon 10 sequence set forth in SEQ ID No.: 1 and an antisense strand comprising a sequence complementary thereto.

3. Therapeutic agent for use according to claim 1 or claim 2, wherein the one or more siRNAs comprise a sense strand of 19-29 continuous bases of mRNA corresponding to the MAPT gene exon 10 sequence set forth in SEQ ID No.: 1 and an antisense strand comprising a sequence complementary thereto.

4. Therapeutic agent for use according to any one of claims 1 to 3, wherein the one or more siRNAs are selected from i) a double strand RNA composed of a sense strand comprising a base sequence set forth in SEQ ID No.: 2, 4, or 6, and an antisense strand comprising a sequence complementary thereto, which optionally has an overhang at the terminal of the sense strand and/or antisense strand, and ii) a double strand RNA composed of a sense strand comprising a base sequence wherein one to several bases have been added to and/or deleted from the 5' terminal

and/or 3' terminal of the base sequence described in any one of SEQ ID No.: 2, 4, or 6, and an antisense strand comprising a sequence complementary thereto, which optionally has an overhang at the terminal of the sense strand and/or antisense strand.

5. Therapeutic agent for use according to any one of claims 1 to 4, wherein the one or more siRNAs induce selective degradation of exon 10-containing MAPT transcripts.

6. Therapeutic agent for use according to any one of claims 1 to 5, wherein the neurodegenerative diseases associated with abnormalities of MAPT gene encoded protein tau are selected from Alzheimer disease, Huntington disease, type 1 myotonic dystrophy, Parkinson disease, and frontotemporal dementia with parkinsonism linked to chromosome 17 (FTDP-17).

7. A method for the treatment of a neurodegenerative diseases associated with abnormalities of MAPT gene encoded protein tau comprising administering to a patient who needs it of one or more siRNA, wherein the one or more siRNAs comprise a sense strand comprising at least 19 continuous bases of mRNA corresponding to the MAPT exon 10 sequence set forth in SEQ ID No.: 1 and an antisense strand comprising a sequence complementary thereto in an amount sufficient to make said treatment, wherein the one or more siRNAs induce selective degradation of exon 10-containing MAPT transcripts.

8. A pharmaceutical composition comprising one or more

siRNAs, wherein the one or more siRNAs comprise a sense strand comprising at least 19 continuous bases of mRNA corresponding to the MAPT exon 10 sequence set forth in SEQ ID No.: 1 and an antisense strand comprising a sequence complementary thereto, and a pharmaceutically acceptable carrier.

ABSTRACT

Therapeutic agent for use in the treatment of neurodegenerative diseases associated with abnormalities of MAPT gene encoded protein tau, wherein said therapeutic agent comprises one or more siRNAs targeting MAPT exon 10 sequence.
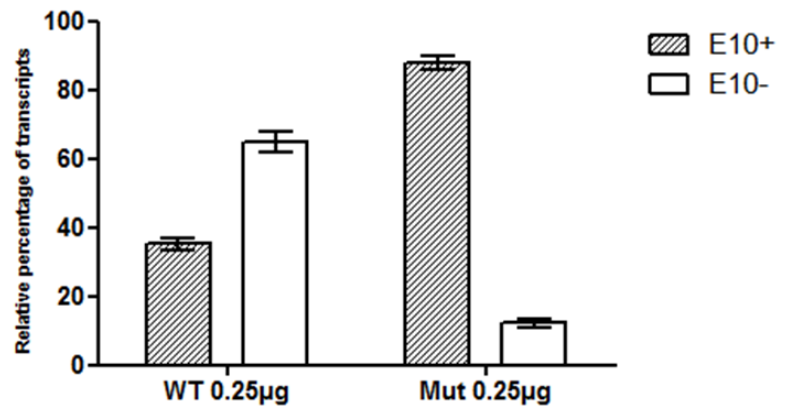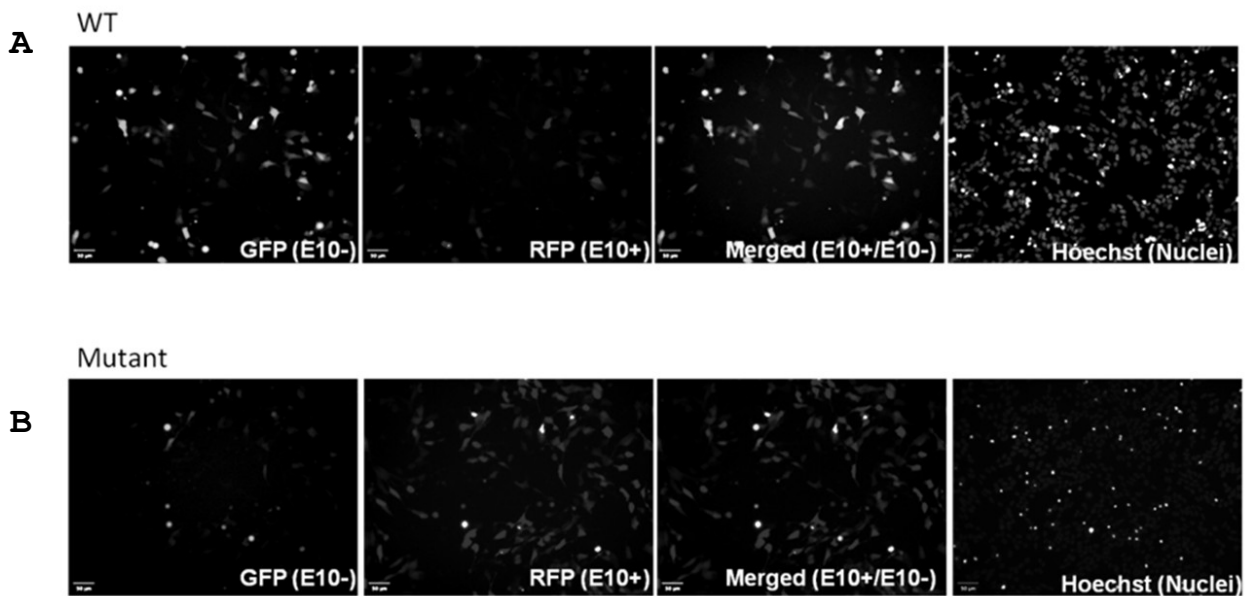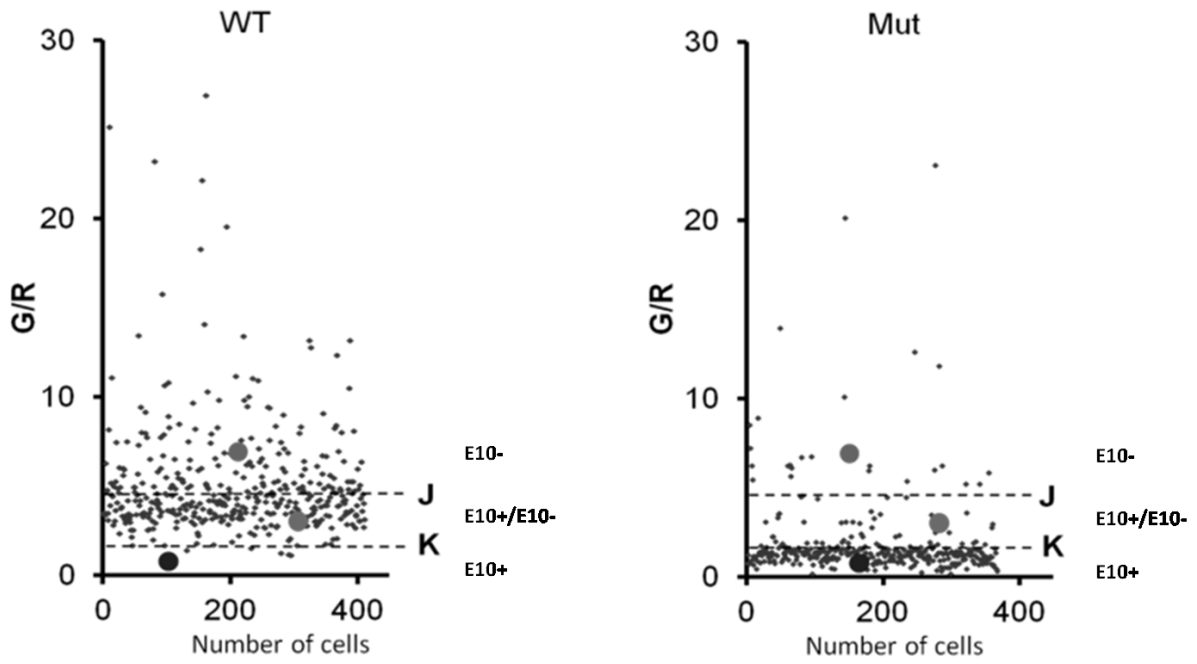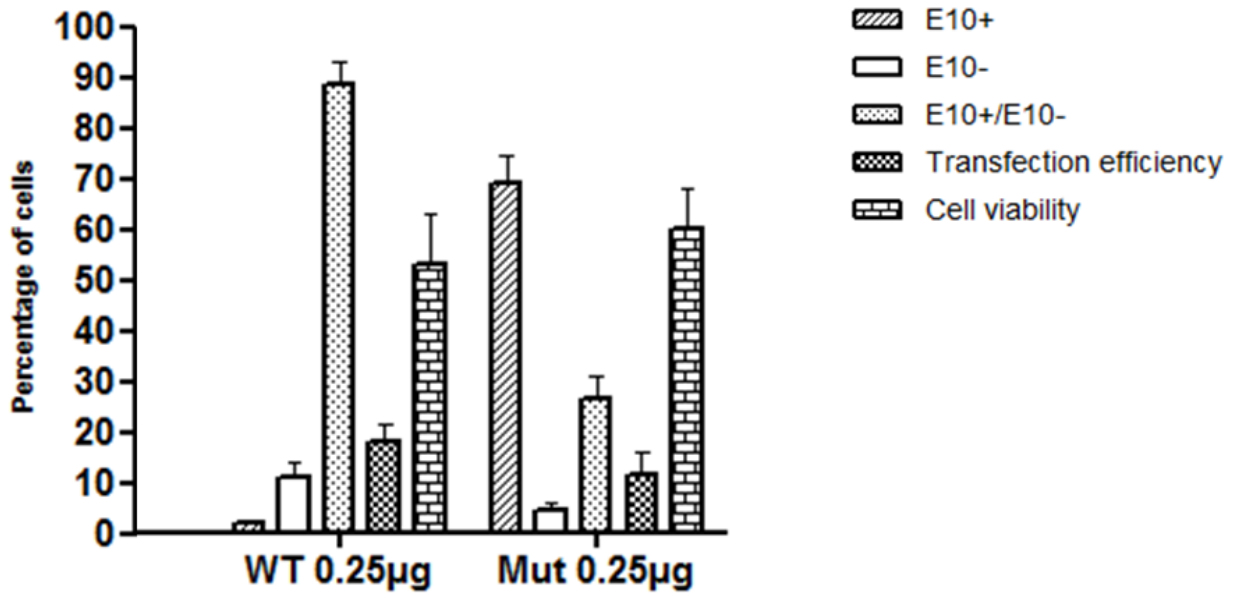
Figure 1

Figure 2

Figure 3

Figure 4
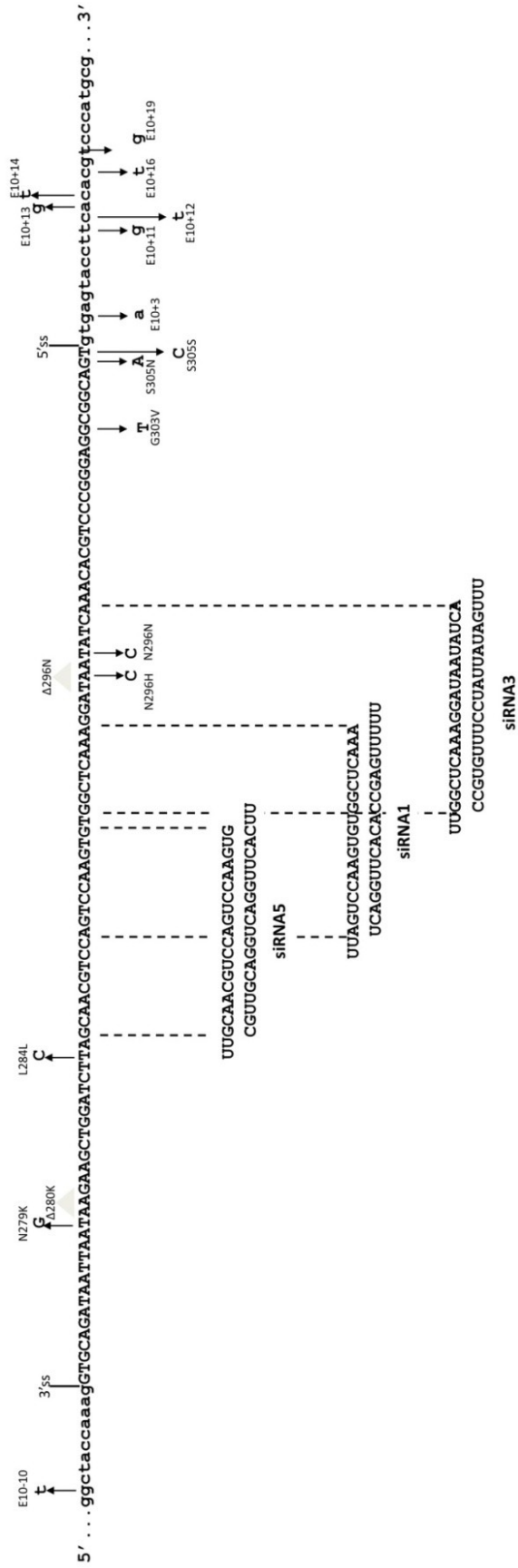
Figure 5
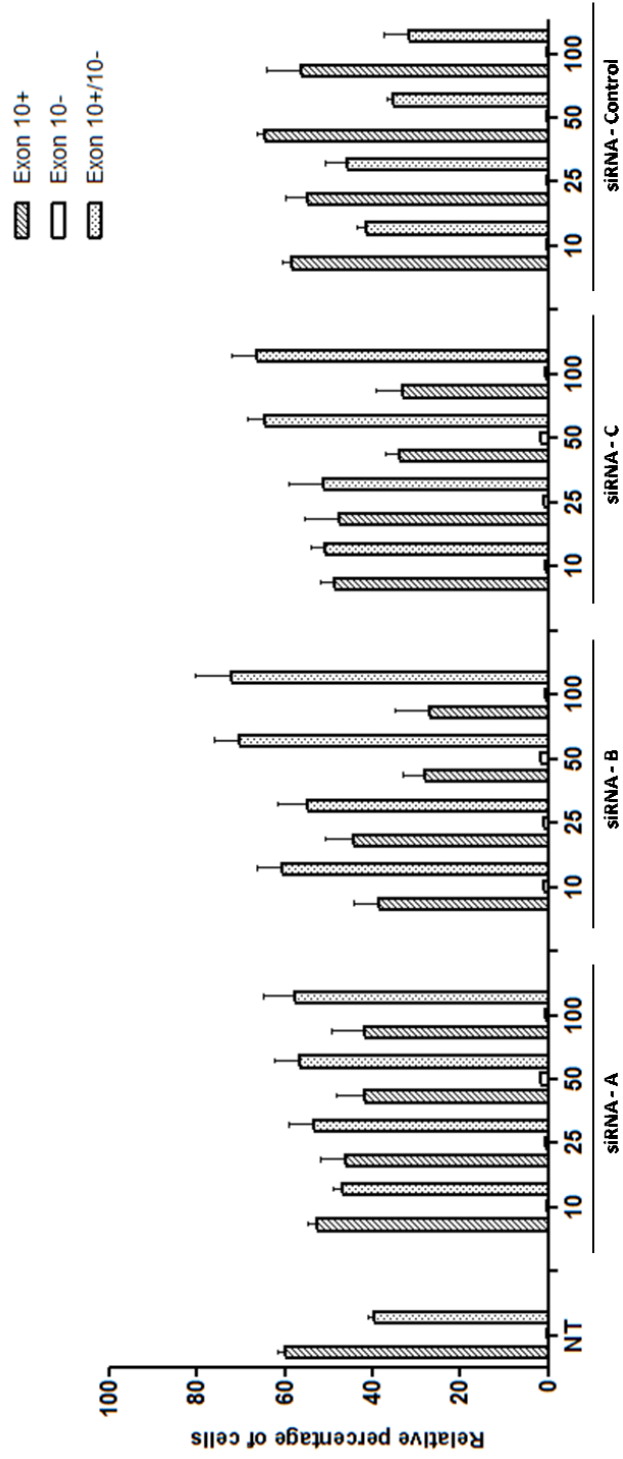
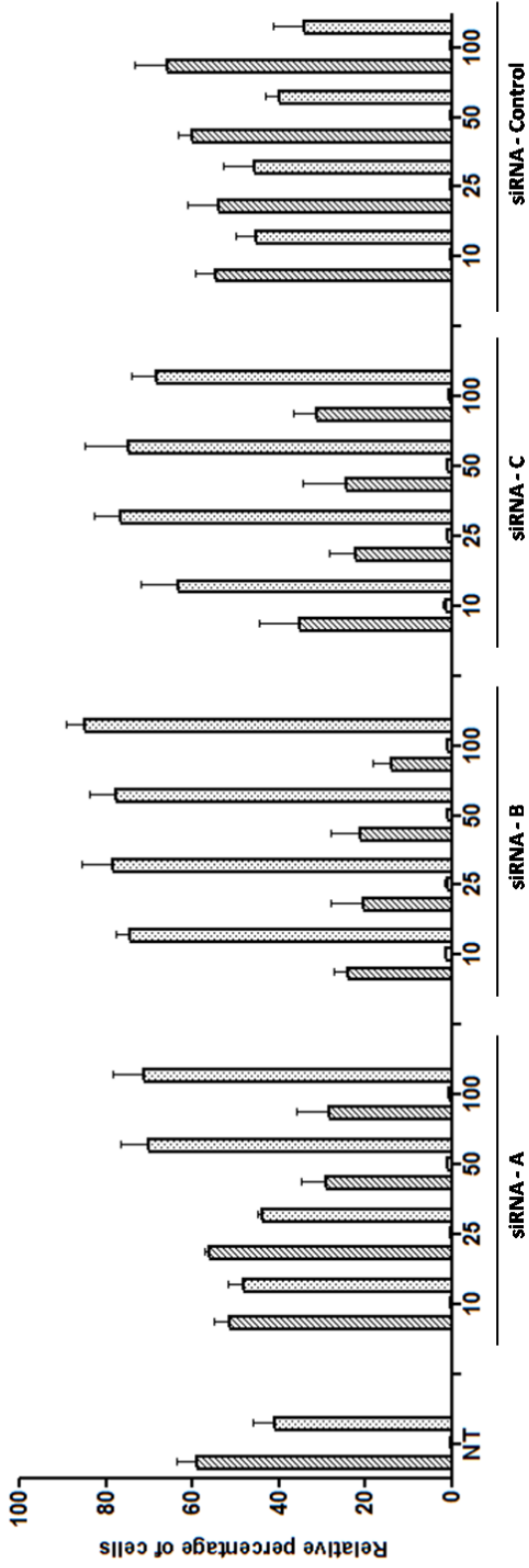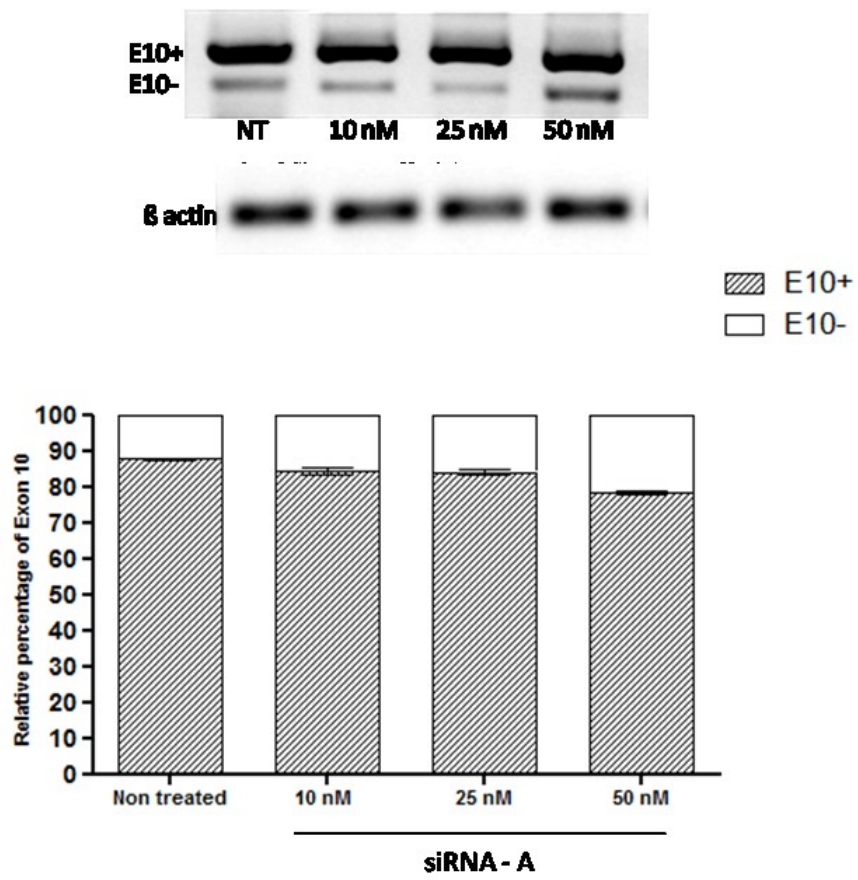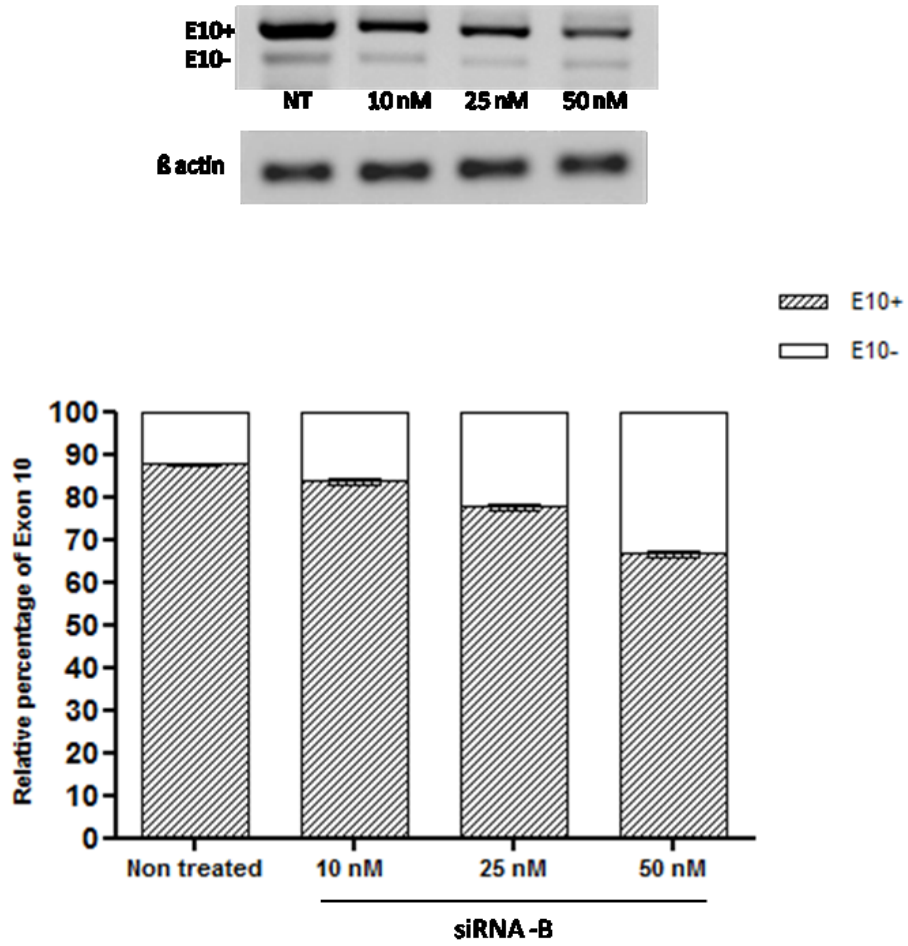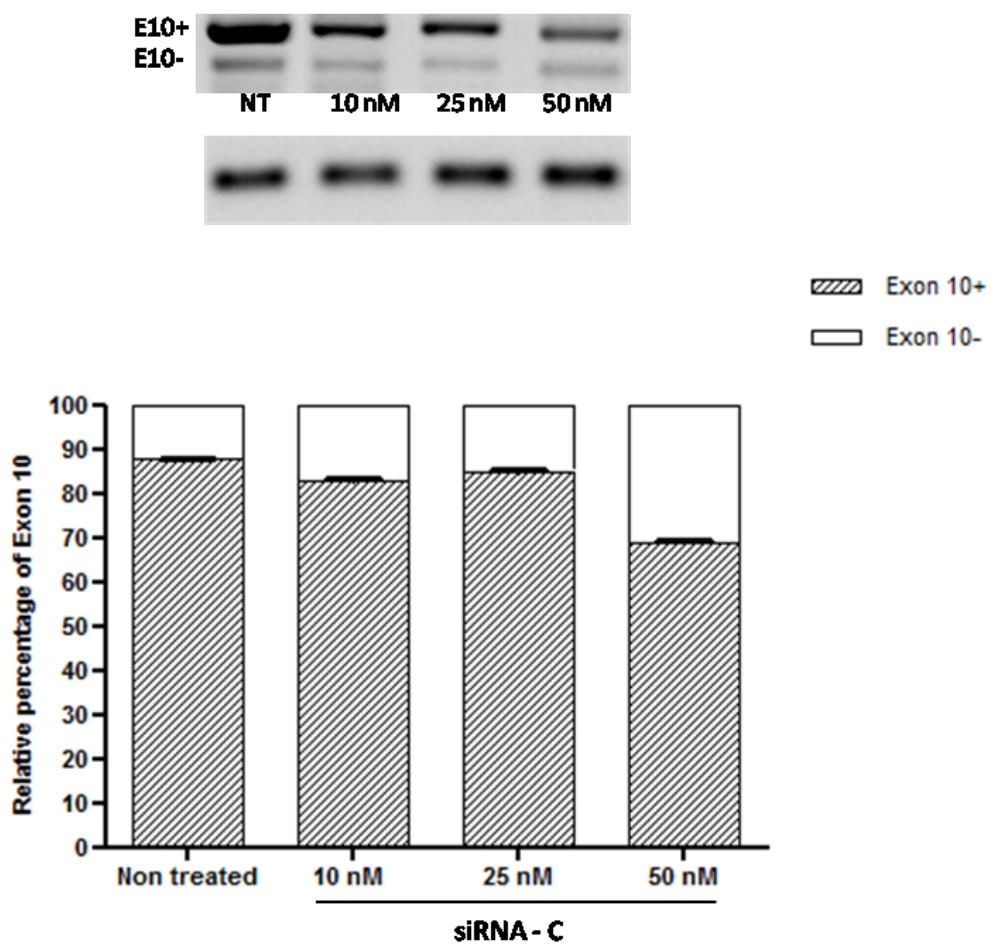Figure 6

Figure 7

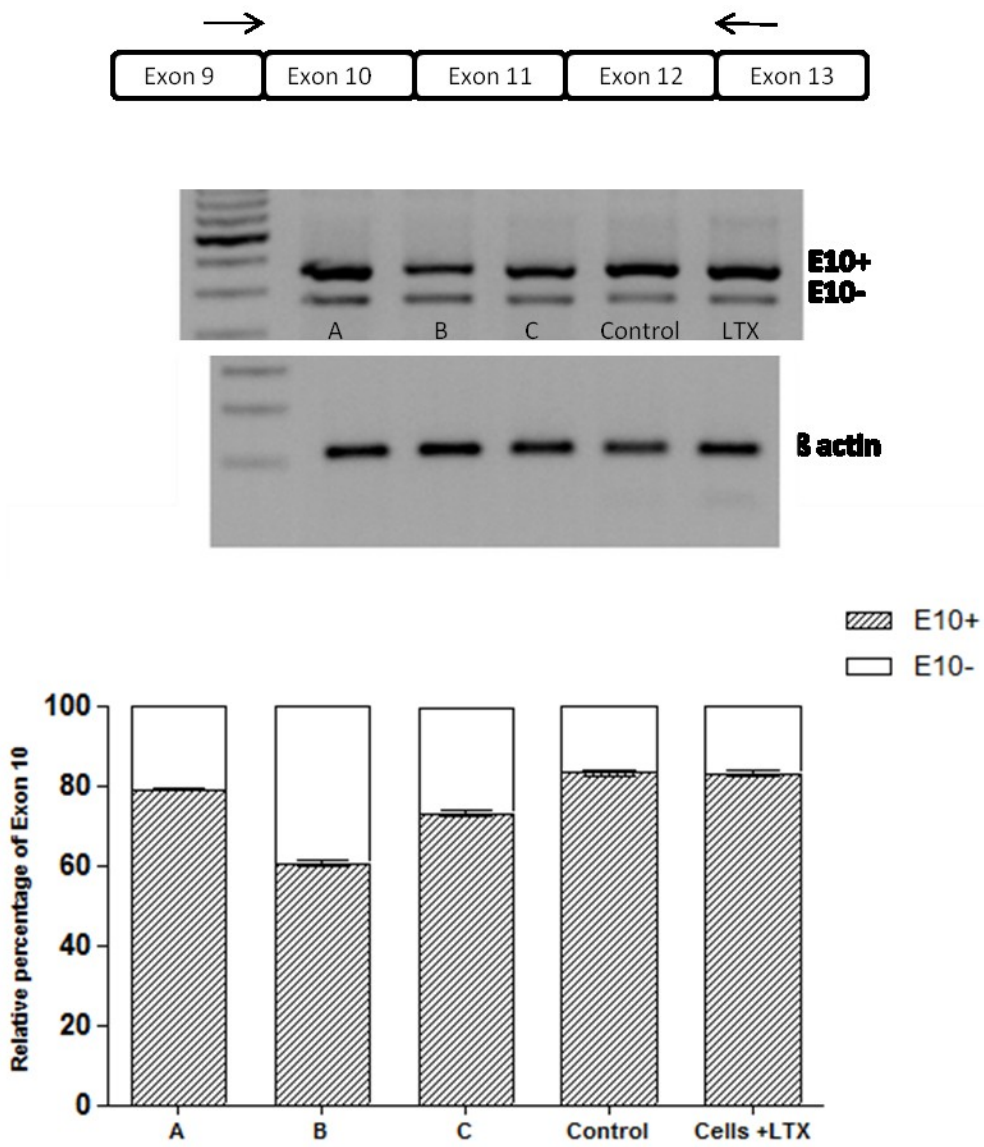Figure 8

Figure 9

Figure 10

Figure 11

WT PFLARE PLASMID

```
tagttattaa tagtaatcaa ttacggggtc attagttcat agcccatata tggagttccg      60
cgttacataa cttacggtaa atggcccgcc tggctgaccg cccaacgacc cccgcccatt     120
gacgtcaata atgacgtatg ttcccatagt aacgccaata gggactttcc attgacgtca     180
atgggtggag tatttacggt aaactgccca cttggcagta catcaagtgt atcatatgcc     240
aagtacgccc cctattgacg tcaatgacgg taaatggccc gcctggcatt atgcccagta     300
catgacctta tgggactttc ctacttggca gtacatctac gtattagtca tcgctattac     360
catggtgatg cggttttggc agtacatcaa tgggcgtgga tagcggtttg actcacgggg     420
atttccaagt ctccacccca ttgacgtcaa tgggagtttg ttttggcacc aaaatcaacg     480
ggactttcca aaatgtcgta caactccgc cccattgacg caaatgggcg gtaggcgtgt     540
acggtgggag gtctatataa gcagagctgg tttagtgaac cgtcagatcc gctagcgcta     600
ccggactcag atctaccatt ggtgcacctg actcctgagg agaagtctgc cgttactgcc     660
ctgtggggca aggtgaacgt ggaagagttg gtggtgaggc cctgggccac cagtaagtat     720
caaggttaca agacaggttt aaggagacca atagaaactg ggcatgtgga gacagagaag     780
actcttgggt ttctgaattc ctcatccttt tttctggcta ccaaaggtgc agataattaa     840
taagaagctg gatcttagca cgtccagtc caagtgtggc tcaaaggata atatcaaaca     900
cgtcccggga ggcggcagtg tgagtacctt cacacgtccc atgcgccgtg ctgtggcttg     960
aattattagg aagtggtgtg agtgcgtaca cttgcgagac actgcataga ataaatcctt    1020
ctggatccac catggtggct tagatccggg catgtggaga cagagaagac tgttgagttt    1080
gtgataagca ctgactctct ctgcctattg gtctattttc cctccctcag tggcggtcga    1140
ggacaaactc tacgcggact tgccagtacg cttcgtgagc aagggcgagg agctgttcac    1200
cggggtggtg cccatcctgg tcgagctgga cggcgacgta aacggccaca gttcagcgt    1260
gtccggcgag ggcgagggcg acgccaccta cggcaagctg accctgaagt tcatctgcac    1320
caccggcaag ctgcccgtgc cctggcccac cctcgtgacc accctgacct acggcgtgca    1380
gtgctttagc cgctaccccg accacctgaa gcagcacgac ttcttcaaga gtgcaatgcc    1440
cgaaggctac gtccaggagc gcaccatctt cttcaaggac gacggcaact acaagacccg    1500
cgccgaggtg aagttcgagg gcgacaccct ggtgaaccgc atcgagctga agggcatcga    1560
cttcaaggag gacggcaaca tcctggggca caagctggag tacaactaca acagccacaa    1620
cgtctatatc accgccgaca agcagaagaa cggcatcaag gtgaacttca gatccgcca    1680
caacatcgag gacggcagcg tgcagctcgc cgaccactac cagcagaaca cccccatcgg    1740
cgacggcccc gtgctgctgc cgacaacca ctacctgagc acccagtccg ccctgagcaa    1800
agaccccaac gagaagcgcg atcatatggt cctgctggag ttcgtgaccg ccgccgggat    1860
cactctcggc accgacgagc tgtacaagta accggtcgcc accatggtga caagggcga    1920
ggagaataac atggccatca tcaaggagtt catgcgcttc aaggtgcgca tggagggctc    1980
cgtgaacggc cacgagttcg agatcgaggg cgaggcgag ggccgcccct acgagggcac    2040
ccagaccgcc aagctgaagg tgaccaaggg tggcccctg cccttcgcct gggacatcct    2100
aacccccaac ttcacctacg gctccaaggc ctacgtgaag caccccgccg acatccccga    2160
ctacttgaag ctgtccttcc ccgagggctt caagtgggag cgcgtgatga acttcgagga    2220
```

Figure 12

```
cggcggcgtg gtgaccgtga cccaggactc ctccctgcag gacggcgagt tcatctacaa          2280

ggtgaagctg cgcggcacca acttcccctc cgacggcccc gtaatgcaga agaagaccat          2340

gggctgggag gcctcctccg agcggatgta ccccgaggac ggcgccctga agggcgagat          2400

caagatgagg ctgaagctga aggacggcgg ccactacgac gctgaggtca agaccaccta          2460

caaggccaag aagcccgtgc agctgcccgg cgcctacatc gtcggcatca agttggacat          2520

cacctcccac aacgaggact acaccatcgt ggaactgtac gaacgcgccg agggccgcca          2580

ctccaccggc ggcatggacg agctgtataa gtaagcggcc gcgactctag atcataatca          2640

gccataccac atttgtagag gttttacttg ctttaaaaaa cctcccacac ctccccctga          2700

acctgaaaca taaaatgaat gcaattgttg ttgttaactt gtttattgca gcttataatg          2760

gttacaaata aagcaatagc atcacaaatt tcacaaataa agcatttttt tcactgcatt          2820

ctagttgtgg tttgtccaaa ctcatcaatg tatcttaagg cgtaaattgt aagcgttaat          2880

attttgttaa aattcgcgtt aaatttttgt taaatcagct cattttttaa ccaataggcc          2940

gaaatcggca aaatccctta taaatcaaaa gaatagaccg agatagggtt gagtgttgtt          3000

ccagtttgga acaagagtcc actattaaag aacgtggact ccaacgtcaa agggcgaaaa          3060

accgtctatc agggcgatgg cccactacgt gaaccatcac cctaatcaag tttttttgggg         3120

tcgaggtgcc gtaaagcact aaatcggaac cctaaaggga gcccccgatt tagagcttga          3180

cggggaaagc cggcgaacgt ggcgagaaag gaagggaaga aagcgaaagg agcgggcgct          3240

agggcgctgg caagtgtagc ggtcacgctg cgcgtaacca ccacacccgc cgcgcttaat          3300

gcgccgctac agggcgcgtc aggtggcact tttcggggaa atgtgcgcgg aaccCctatt          3360

tgtttatttt tctaaataca ttcaaatatg tatccgctca tgagacaata accctgataa          3420

atgcttcaat aatattgaaa aaggaagagt cctgaggcgg aaagaaccag ctgtggaatg          3480

tgtgtcagtt agggtgtgga aagtccccag gctccccagc aggcagaagt atgcaaagca          3540

tgcatctcaa ttagtcagca accaggtgtg gaaagtcccc aggctcccca gcaggcagaa          3600

gtatgcaaag catgcatctc aattagtcag caaccatagt cccgcccta actccgccca          3660

tcccgcccct aactccgccc agttccgccc attctccgcc ccatggctga ctaattttttt        3720

ttatttatgc agaggccgag gccgcctcgg cctctgagct attccagaag tagtgaggag          3780

gctttttttgg aggcctaggc ttttgcaaag atcgatcaag agacaggatg aggatcgttt        3840

cgcatgattg aacaagatgg attgcacgca ggttctccgg ccgcttgggt ggagaggcta          3900

ttcggctatg actgggcaca acagacaatc ggctgctctg atgccgccgt gttccggctg          3960

tcagcgcagg ggcgcccggt tctttttgtc aagaccgacc tgtccggtgc cctgaatgaa          4020

ctgcaagacg aggcagcgcg gctatcgtgg ctggccacga cgggcgttcc ttgcgcagct          4080

gtgctcgacg ttgtcactga agcgggaagg gactggctgc tattgggcga agtgccgggg          4140

caggatctcc tgtcatctca ccttgctcct gccgagaaag tatccatcat ggctgatgca          4200

atgcggcggc tgcatacgct tgatccggct acctgcccat tcgaccacca agcgaaacat          4260

cgcatcgagc gagcacgtac tcggatggaa gccggtcttg tcgatcagga tgatctggac          4320

gaagagcatc aggggctcgc gccagccgaa ctgttcgcca ggctcaaggc gagcatgccc          4380

gacggcgagg atctcgtcgt gacccatggc gatgcctgct tgccgaatat catggtggaa          4440

aatggccgct tttctggatt catcgactgt ggccggctgg gtgtggcgga ccgctatcag          4500
```

Figure 12 – cont.

```
gacatagcgt tggctacccg tgatattgct gaagagcttg gcggcgaatg ggctgaccgc      4560
ttcctcgtgc tttacggtat cgccgctccc gattcgcagc gcatcgcctt ctatcgcctt      4620
cttgacgagt tcttctgagc gggactctgg ggttcgaaat gaccgaccaa gcgacgccca      4680
acctgccatc acgagatttc gattccaccg ccgccttcta tgaaaggttg ggcttcggaa      4740
tcgttttccg ggacgccggc tggatgatcc tccagcgcgg ggatctcatg ctggagttct      4800
tcgcccaccc taggggagg ctaactgaaa cacggaagga dacaataccg gaaggaaccc      4860
gcgctatgac ggcaataaaa agacagaata aaacgcacgg tgttgggtcg tttgttcata      4920
aacgcggggt tcggtcccag ggctggcact ctgtcgatac cccaccgaga ccccattggg      4980
gccaatacgc ccgcgtttct ccttttccc caccccaccc cccaagttcg ggtgaaggcc      5040
cagggctcgc agccaacgtc ggggcggcag gccctgccat agcctcaggt tactcatata      5100
tactttagat tgatttaaaa cttcattttt aatttaaaag gatctaggtg aagatccttt      5160
ttgataatct catgaccaaa atcccttaac gtgagttttc gttccactga gcgtcagacc      5220
ccgtagaaaa gatcaaagga tcttcttgag atcctttttt tctgcgcgta atctgctgct      5280
tgcaaacaaa aaaaccaccg ctaccagcgg tggtttgttt gccggatcaa gagctaccaa      5340
ctcttttttcc gaaggtaact ggcttcagca gagcgcagat accaaatact gtccttctag      5400
tgtagccgta gttaggccac cacttcaaga actctgtagc accgcctaca tacctcgctc      5460
tgctaatcct gttaccagtg ctgctgcca gtggcgataa gtcgtgtctt accgggttgg      5520
actcaagacg atagttaccg gataaggcgc agcggtcggg ctgaacgggg ggttcgtgca      5580
cacagcccag cttggagcga acgacctaca ccgaactgag atacctacag cgtgagctat      5640
gagaaagcgc cacgcttccc gaagggagaa aggcggacag gtatccggta agcggcaggg      5700
tcggaacagg agagcgcacg agggagcttc caggggaaa cgcctggtat ctttatagtc      5760
ctgtcgggtt cgccacctc tgacttgagc gtcgatttt gtgatgctcg tcaggggggc      5820
ggagcctatg gaaaaacgcc agcaacgcgg ccttttacg gttcctggcc ttttgctggc      5880
cttttgctca catgttcttt cctgcgttat cccctgattc tgtggataac cgtattaccg      5940
ccatgcat                                                                5948
```

Figure 12 – cont.

MUT PFLARE PLASMID

```
tagttattaa tagtaatcaa ttacggggtc attagttcat agcccatata tggagttccg      60
cgttacataa cttacggtaa atggcccgcc tggctgaccg cccaacgacc cccgcccatt     120
gacgtcaata atgacgtatg ttcccatagt aacgccaata gggactttcc attgacgtca     180
atgggtggag tatttacggt aaactgccca cttggcagta catcaagtgt atcatatgcc     240
aagtacgccc cctattgacg tcaatgacgg taaatggccc gcctggcatt atgcccagta     300
catgacctta tgggactttc ctacttggca gtacatctac gtattagtca tcgctattac     360
catggtgatg cggttttggc agtacatcaa tgggcgtgga tagcggtttg actcacgggg     420
atttccaagt ctccacccca ttgacgtcaa tgggagtttg ttttggcacc aaaatcaacg     480
ggactttcca aaatgtcgta acaactccgc cccattgacg caaatgggcg gtaggcgtgt     540
acggtgggag gtctatataa gcagagctgg tttagtgaac cgtcagatcc gctagcgcta     600
ccggactcag atctaccatt ggtgcacctg actcctgagg agaagtctgc cgttactgcc     660
ctgtggggca aggtgaacgt ggaagagttg gtggtgaggc cctgggccac cagtaagtat     720
caaggttaca agacaggttt aaggagacca atagaaactg ggcatgtgga gacagagaag     780
actcttgggt ttctgaattc ctcatccttt tttctggcta ccaaaggtgc agataattaa     840
gaagaagctg gatcttagca cgtccagtc caagtgtggc tcaaaggata atatcaaaca     900
cgtcccggga ggcggcagtg tgagtacctt cacacgtccc atgcgccgtg ctgtggcttg     960
aattattagg aagtggtgtg agtgcgtaca cttgcgagac actgcataga ataaatcctt    1020
ctggatccac catggtggct tagatccggg catgtggaga cagagaagac tgttgagttt    1080
gtgataagca ctgactctct ctgcctattg gtctattttc cctccctcag tggcggtcga    1140
ggacaaactc tacgcggact tgccagtacg cttcgtgagc aagggcgagg agctgttcac    1200
cggggtggtg cccatcctgg tcgagctgga cggcgacgta aacggccaca gttcagcgt     1260
gtccggcgag ggcgagggcg acgccaccta cggcaagctg accctgaagt tcatctgcac    1320
caccggcaag ctgcccgtgc cctggcccac cctcgtgacc accctgacct acggcgtgca    1380
gtgctttagc cgctacccccg accacctgaa gcagcacgac ttcttcaaga gtgcaatgcc    1440
cgaaggctac gtccaggagc gcaccatctt cttcaaggac gacggcaact acaagacccg    1500
cgccgaggtg aagttcgagg gcgacaccct ggtgaaccgc atcgagctga agggcatcga    1560
cttcaaggag gacggcaaca tcctggggca caagctggag tacaactaca cagccacaa     1620
cgtctatatc accgccgaca agcagaagaa cggcatcaag gtgaacttca gatccgcca     1680
caacatcgag gacggcagcg tgcagctcgc cgaccactac cagcagaaca cccccatcgg    1740
cgacggcccc gtgctgctgc ccgacaacca ctacctgagc acccagtccg ccctgagcaa    1800
agaccccaac gagaagcgcg atcatatggt cctgctggag ttcgtgaccg ccgccgggat    1860
cactctcggc accgacgagc tgtacaagta accggtcgcc accatggtga gcaagggcga    1920
ggagaataac atggccatca tcaaggagtt catgcgcttc aaggtgcgca tggagggctc    1980
cgtgaacggc cacgagttcg agatcgaggg cgagggcgag ggccgcccct acgagggcac    2040
ccagaccgcc aagctgaagg tgaccaaggg tggccccctg cccttcgcct gggacatcct    2100
aacccccaac ttcacctacg gctccaaggc ctacgtgaag caccccgccg acatccccga    2160
ctacttgaag ctgtccttcc ccgagggctt caagtgggag cgcgtgatga acttcgagga    2220
```

Figure 13

```
cggcggcgtg gtgaccgtga cccaggactc ctccctgcag gacggcgagt tcatctacaa    2280

ggtgaagctg cgcggcacca acttcccctc cgacggcccc gtaatgcaga agaagaccat    2340

gggctgggag gcctcctccg agcggatgta ccccgaggac ggcgccctga agggcgagat    2400

caagatgagg ctgaagctga aggacggcgg ccactacgac gctgaggtca agaccaccta    2460

caaggccaag aagcccgtgc agctgcccgg cgcctacatc gtcggcatca agttggacat    2520

cacctcccac aacgaggact acaccatcgt ggaactgtac gaacgcgccg agggccgcca    2580

ctccaccggc ggcatggacg agctgtataa gtaagcggcc gcgactctag atcataatca    2640

gccataccac atttgtagag gttttacttg ctttaaaaaa cctcccacac ctccccctga    2700

acctgaaaca taaaatgaat gcaattgttg ttgttaactt gtttattgca gcttataatg    2760

gttacaaata aagcaatagc atcacaaatt tcacaaataa agcatttttt tcactgcatt    2820

ctagttgtgg tttgtccaaa ctcatcaatg tatcttaagg cgtaaattgt aagcgttaat    2880

attttgttaa aattcgcgtt aaatttttgt taaatcagct cattttttaa ccaataggcc    2940

gaaatcggca aaatccctta taaatcaaaa gaatagaccg agatagggtt gagtgttgtt    3000

ccagtttgga acaagagtcc actattaaag aacgtggact ccaacgtcaa agggcgaaaa    3060

accgtctatc agggcgatgg cccactacgt gaaccatcac cctaatcaag ttttttgggg    3120

tcgaggtgcc gtaaagcact aaatcggaac cctaaaggga gcccccgatt tagagcttga    3180

cggggaaagc cggcgaacgt ggcgagaaag gaagggaaga aagcgaaagg agcgggcgct    3240

agggcgctgg caagtgtagc ggtcacgctg cgcgtaacca ccacacccgc cgcgcttaat    3300

gcgccgctac agggcgcgtc aggtggcact tttcggggaa atgtgcgcgg aacccctatt    3360

tgtttatttt tctaaataca ttcaaatatg tatccgctca tgagacaata accctgataa    3420

atgcttcaat aatattgaaa aaggaagagt cctgaggcgg aaagaaccag ctgtggaatg    3480

tgtgtcagtt agggtgtgga aagtccccag gctccccagc aggcagaagt atgcaaagca    3540

tgcatctcaa ttagtcagca accaggtgtg gaaagtcccc aggctcccca gcaggcagaa    3600

gtatgcaaag catgcatctc aattagtcag caaccatagt cccgccccta actccgccca    3660

tcccgcccct aactccgccc agttccgccc attctccgcc ccatggctga ctaatttttt    3720

ttatttatgc agaggccgag gccgcctcgg cctctgagct attccagaag tagtgaggag    3780

gcttttttgg aggcctaggc ttttgcaaag atcgatcaag agacaggatg aggatcgttt    3840

cgcatgattg aacaagatgg attgcacgca ggttctccgg ccgcttgggt ggagaggcta    3900

ttcggctatg actgggcaca acagacaatc ggctgctctg atgccgccgt gttccggctg    3960

tcagcgcagg ggcgcccggt tctttttgtc aagaccgacc tgtccggtgc cctgaatgaa    4020

ctgcaagacg aggcagcgcg gctatcgtgg ctggccacga cgggcgttcc ttgcgcagct    4080

gtgctcgacg ttgtcactga agcgggaagg gactggctgc tattgggcga agtgccgggg    4140

caggatctcc tgtcatctca ccttgctcct gccgagaaag tatccatcat ggctgatgca    4200

atgcggcggc tgcatacgct tgatccggct acctgcccat tcgaccacca agcgaaacat    4260

cgcatcgagc gagcacgtac tcggatggaa gccggtcttg tcgatcagga tgatctggac    4320

gaagagcatc aggggctcgc gccagccgaa ctgttcgcca ggctcaaggc gagcatgccc    4380

gacggcgagg atctcgtcgt gacccatggc gatgcctgct tgccgaatat catggtggaa    4440

aatggccgct tttctggatt catcgactgt ggccggctgg gtgtggcgga ccgctatcag    4500

gacatagcgt tggctacccg tgatattgct gaagagcttg gcggcgaatg ggctgaccgc    4560
```

Figure 13 – cont.

```
ttcctcgtgc tttacggtat cgccgctccc gattcgcagc gcatcgcctt ctatcgcctt    4620
cttgacgagt tcttctgagc gggactctgg ggttcgaaat gaccgaccaa gcgacgccca    4680
acctgccatc acgagatttc gattccaccg ccgccttcta tgaaaggttg ggcttcggaa    4740
tcgttttccg ggacgccggc tggatgatcc tccagcgcgg ggatctcatg ctggagttct    4800
tcgcccaccc tagggggagg ctaactgaaa cacggaagga gacaataccg gaaggaaccc    4860
gcgctatgac ggcaataaaa agacagaata aaacgcacgg tgttgggtcg tttgttcata    4920
aacgcggggt tcggtcccag ggctggcact ctgtcgatac cccaccgaga ccccattggg    4980
gccaatacgc ccgcgtttct tccttttccc caccccaccc cccaagttcg ggtgaaggcc    5040
cagggctcgc agccaacgtc ggggcggcag gccctgccat agcctcaggt tactcatata    5100
tactttagat tgatttaaaa cttcattttt aatttaaaag gatctaggtg aagatccttt    5160
ttgataatct catgaccaaa atcccttaac gtgagttttc gttccactga gcgtcagacc    5220
ccgtagaaaa gatcaaagga tcttcttgag atcctttttt tctgcgcgta atctgctgct    5280
tgcaaacaaa aaaaccaccg ctaccagcgg tggtttgttt gccggatcaa gagctaccaa    5340
ctctttttcc gaaggtaact ggcttcagca gagcgcagat accaaatact gtccttctag    5400
tgtagccgta gttaggccac cacttcaaga actctgtagc accgcctaca tacctcgctc    5460
tgctaatcct gttaccagtg ctgctgcca gtggcgataa gtcgtgtctt accgggttgg    5520
actcaagacg atagttaccg gataaggcgc agcggtcggg ctgaacgggg ggttcgtgca    5580
cacagcccag cttggagcga acgacctaca ccgaactgag atacctacag cgtgagctat    5640
gagaaagcgc cacgcttccc gaagggagaa aggcggacag gtatccggta agcggcaggg    5700
tcggaacagg agagcgcacg agggagcttc caggggggaaa cgcctggtat ctttatagtc    5760
ctgtcgggtt cgccacctc tgacttgagc gtcgattttt gtgatgctcg tcaggggggc    5820
ggagcctatg gaaaaacgcc agcaacgcgg cctttttacg gttcctggcc ttttgctggc    5880
cttttgctca catgttcttt cctgcgttat cccctgattc tgtggataac cgtattaccg    5940
```

Figure 13 – cont.

BUZZI, NOTARO & ANTONIELLI d'OULX

Consulenti in Proprietà Industriale ▪ European Patent, Trademark and Design Attorneys

Franco Buzzi
Giancarlo Notaro
Enrico Antonielli d'Oulx
Luciano Bosotti
Mauro Marchitelli
Livia Pasqualigo
Franco Gallarotti
Cristina Freyria Fava
Alessandra Romeo
Giorgio Crovini
Elisa Giraldi
Stefano Frontoni
Tassilo Meindl
Antonella Vitale
Davide Resmini
Paolo De Bonis
Roberta Cesa

Universita' degli Studi di Trento
Divisione Supporto alla Ricerca Scientifica
** ed al Trasferimento Tecnologico**
c.a.: Dr. Lino Giusti
Via Calepina 14
38122 Trento TN

31 marzo 2015

Ns. Rif.:   BIT18156-CF/ps

Ogg.: Domanda di brevetto per Invenzione Industriale
n. TO2015A000185 depositata in data 25 marzo 2015
dal titolo: "Terapia mediata da RNA di interferenza per malattie
neurodegenerative"

Vi trasmettiamo la documentazione relativa alla domanda in oggetto, depositata in data **25 marzo 2015** con il numero: **TO2015A000185.**

Dalla data di deposito decorre il periodo di priorità di 12 mesi entro il quale la domanda italiana potrà essere estesa all'estero beneficiando della data di deposito italiana.

Per il mantenimento del brevetto per la sua naturale durata di 20 anni dal deposito occorrerà versare le tasse annuali alle relative scadenze a partire dalla tassa relativa al quinto anno, dovuta entro il mese di **marzo 2019.**

Ci permettiamo di allegare la fattura per le nostre prestazioni, con preghiera di cortese rimessa a saldo.

Cordiali saluti.

Buzzi, Notaro & Antonielli d'Oulx

Cristina Freyria Fava

All.:   - documentazione di deposito
          - fattura (segue)